Engineering Doctorate
in Environmental Technology

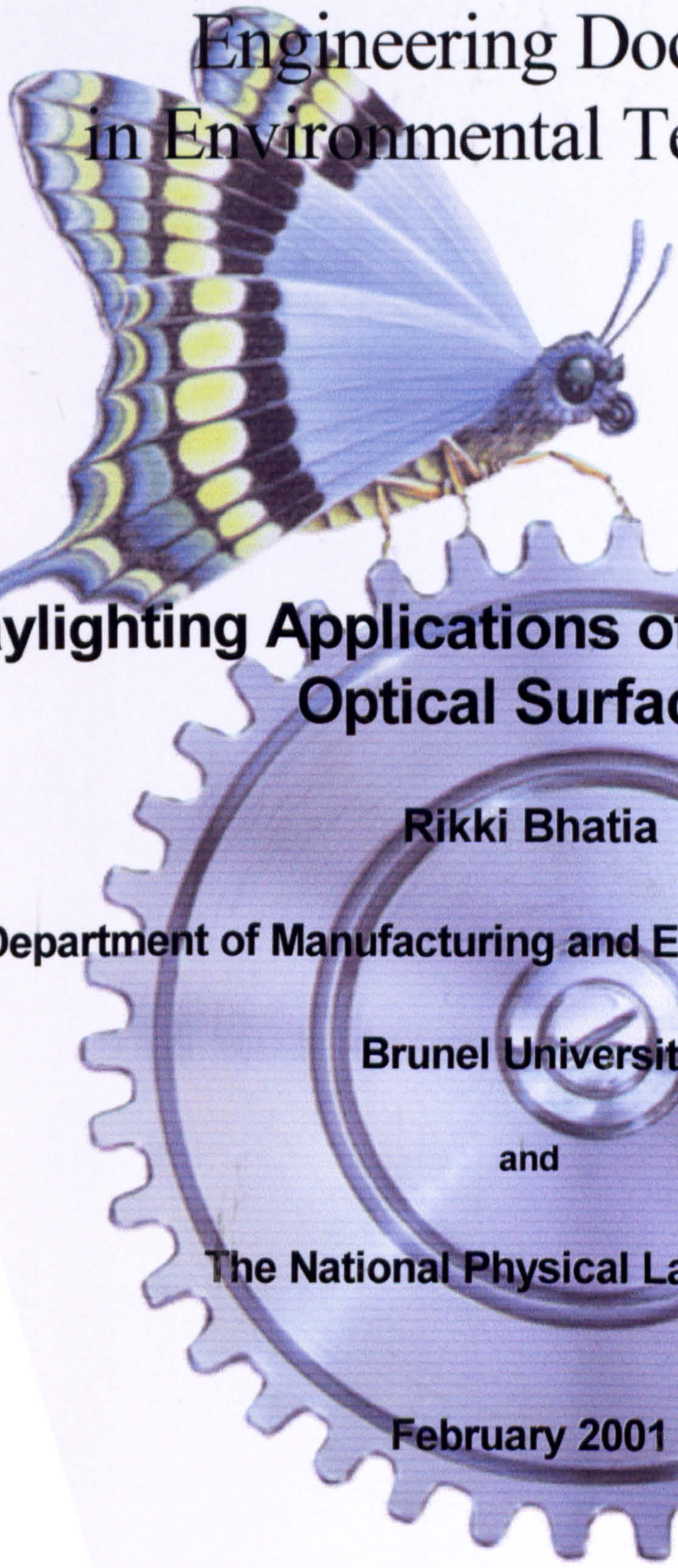

Daylighting Applications of Micro-Textured Optical Surfaces

Rikki Bhatia

Department of Manufacturing and Engineering Systems,

Brunel University

and

The National Physical Laboratory

February 2001

For the attention of candidates who have completed Part A

i) Attention is drawn to the fact that the copyright of a thesis rests with its author.

ii) A copy of a candidate's thesis is supplied to the Library on condition that anyone who consults it is understood to recognise that its copyright rests with its author and that no quotation from the thesis and no information derived from it may be published without the prior written consent of the author or the University, as appropriate.

Requests for such permission should be addressed in the first instance to the Head of Library Services.

Dedication

This thesis is dedicated to the memory of my mate Bart Burgess. A fellow St. Andrews Graduate, a bloody American and a great guy, he will be sadly missed by all who were lucky enough to know him.

Remember me when I am gone away,
Gone far away into the silent land;
When you can no more hold me by the hand,
Nor I half turn to go yet turning stay.
Remember me when no more day by day
You tell me of our future that you planned:
Only remember me; you understand
It will be late to counsel then or pray.
Yet if you should forget me for a while
And afterwards remember, do not grieve:
For if the darkness and corruption leave
A vestige of the thoughts that once I had,
Better by far you should forget and smile
Than that you should remember and be sad.

Remember, Christina Rossetti (1830- 94)

For all the beers and the good times my friend.

Abstract

Daylighting is the use of natural light to replace artificial light. In traditional rooms sunlight will only illuminate the area closest to the window due to the high solar angle. The rear of the room appears gloomy and occupants will use electric lighting even though there is sufficient daylight to illuminate the interior.

The first section of this thesis reports on the application of micro-prisms to glazing. Such systems could improve the penetration of the light and reduce the energy bill.

Fig 1: (Left): A traditional window. (Right) A window with the top third coated in microprisms.

The aim of the work is to develop suitable structures than can be easily and cheaply mass produced using an industrial UV embossing process. Whenever possible the requirements of this process dictate the physical characteristics of the microstructures.

The development process includes all the stages from design to full-scale testing of the prototypes in an office. Several different mechanical methods are used to produce prismatic arrays that conform to an initial design calculation. Each sample is evaluated in terms of its physical characteristics, its optical properties and finally its ability to improve illumination within a room. The latter aspect is determined, not only by measurement, but also the subjective assessment of occupants.

The second micro-textured surface to be examined is the microlens. Three systems are investigated:

- A controlled diffuser incorporating cylindrical lenses to improve the distribution of the daylight.
- An afocal pair of lenses to improve the penetration of daylight through beam-steering.
- An angular filter to exclude direct sunlight while admitting diffuse light.

Most of the research is concerned with the third system. On sunny days windows can cause sufficient glare that occupants will pull the venetian blinds. Not only will this exclude the direct sunlight but also the diffuse daylight, cause darkening of the room and leading to the use of artificial light. The angular filter or 'solar shade' uses microlenses to image the direct sunlight which can then be blocked by circular obturations. The diffuse sunlight is not focused and therefore transmitted so the room is not darkened.

The research is based on experimentation with small-scale systems and computer modelling to optimise the system. The results show potential improvements over new 'smart' windows although mechanical tolerances are high.

Preface

Criteria for a Doctorate in Environmental Technology (EngD)

To qualify for a doctorate the work must meet two fundamental criteria: it must have an environmental theme and provide a contribution to knowledge.

Environmental Themes

- The principal theme of this thesis is the investigation of daylighting devices. Daylighting is the use of natural light to illuminate an interior and thus reduce the use of artificial light and the energy bill. As the production of electricity will normally cause the emission of greenhouse gases (9%of Carbon dioxide emissions are due to lighting[i]) there is a strong environmental imperative for reducing electricity consumption
- The second theme of this thesis examines the potential to save energy by *excluding* sunlight. On sunny days, direct sunlight can cause glare discomfort for room occupants. Traditional solutions such as venetian blinds cause darkening of the room by excluding direct and diffuse illumination, resulting in the use of artificial lighting. This thesis investigates a transparent solar shade that excludes the direct but still admits the diffuse sunlight and could avoid such energy expenditure.

Contribution to knowledge

Most of the research in this thesis is aimed at exploiting existing industrial process and developing a daylighting system that could be cheaply mass-produced. There have been many innovative daylighting systems developed over the years but it would appear than few have reached commercial exploitation. If the bank of knowledge that has been generated by research is not used in the manufacture of a commercial system, then all that has been created is the environmental impact of the scientific investigation. By using the criteria for mass production as a starting point it is hoped to highlight a new approach to the manufacture of daylighting devices.

In addition there are several original aspects to the scientific investigations:

- The investigation of mechanical techniques for producing high spatial frequency (<100 μm period) saw-tooth structures, that can be used for daylighting when embossed in transparent polymers. The process includes:

1. Design.
2. Characterisation of physical properties.
3. Application to windows for evaluation as daylighting devices.

- The characterisation process involves reflection measurements from a relatively large area of the microtextured surface. The results determine if prior measurements on the physical characteristics of single features are representative of the whole array.
- Investigation into the use of microlenses to deviate direct sunlight.
- Investigation of microlenses with obturations as excluders of direct sunlight.

Introduction

Daylighting and Modern Environmental Issues

"Daylighting is the use of daylight to avoid or reduce the use of electric lighting in buildings"

A. Goetzberger.[ii]

Ideally all buildings would have the use of daylight as a fundamental design consideration. However, the convenience of electric lighting means that most buildings have failed to use natural light effectively. The aim of this research work is develop a system that can be applied to such buildings.

Environmentally orientated products or services can be thought of in two categories: clean technologies or clean-up technologies. The latter consists of the application of a device to a polluting system to reduce its environmental impact, for example a catalytic converter. The former involves avoiding the pollution in the first instance, for example cycling to work instead of using the car and its catalytic converter. In choosing a technology, the further up-stream the environmental impacts are considered (for example in the design rather than the use phase) the greater the savings that can be made.

Lighting and energy should be an integral part of the building design process: not an afterthought[iii] and should also address the concept of sustainability. Guzowski[iv] sets out the nine principles that should govern the application of daylighting to buildings:

Principle One: Take a Bioregional Approach
Daylighting design should include the local environment conditions such as the climate, sun path and sky conditions.
Principle Two: Do more with less
Daylighting can serve many purposes apart from lighting such as heating and electricity generation.
Principle Three: Design for Evolution, Flexibility and Adaptability.
By planning for the future, building obsolescence and waste can be reduced.
Principle Four: Shape form to guide flow
Using architectural design can influence the quantity and quality of daylight as well as its functionality.
Principle Five: Use technology that is appropriate dependable and durable
Priniciple Six: Take an integrated approach
Blending design, technology and mechanical equipment provides a more effective integrated daylighting system.
Principle Seven: Address Health and Well-being
Daylighting plays a strong role in the psychological well-being of the of building occupants by addressing complaints such as Seasonal Affective Disorder.
Principle Eight: Consider Quality of Life
The aesthetics of the lighting affect the experience of the occupants
Principle Nine: Reveal Processes to Educate.

Morrison[v] enthusiastically embraces the sustainable theme, though on a more superficial level. However, she emphasises that sustainable buildings need not cost money but sees it as an opportunity to resolve 'the historic conflict between economic progress and environmental safeguards'. Reducing the use of resources not only benefits the environment but it also reduces the financial cost to the purchaser.

Unfortunately, reducing the environmental impact of a building has not always been the prime concern of architects and many use lighting poorly. As there is a low turn-over of buildings in the UK there is not always the opportunity to redesign the structure to accommodate the new environmental concepts. Consequently there is a need for 'clean-up' daylighting that can be retro-fit to the glazing. The majority of this thesis addresses this whilst trying to provide new tools to be used in Principle six of the sustainable approach to daylighting.

Daylighting: Basic Principles

The use of solar energy by man is not a novel concept. It is believed by some that priestesses in ancient Mesopotamia ignited the temple fires by concentrating the sun's rays with polished golden vessels. Mythology even suggests that Archimedes (287-212 BC) used sunlight to burn an invading Roman fleet[vi]. The uses of natural light described in this paper are much more benign than those mentioned in legend, however it is easy to forget how much energy is available from sunlight and how much we waste. At present lighting accounts for up to 60% of the energy consumed in commercial buildings in the UK[vii] and is extremely inefficient. It is especially wasteful considering the large amount of unused natural light that is incident on the external glazing. Most modern windows allow the sunlight to merely illuminate the floor (see Fig 2) and as this has a low reflectance, only a small proportion subsequently lights the room. Daylighting techniques attempt to redistribute the sun's rays to produce an even illumination of the interior (see Fig 3).

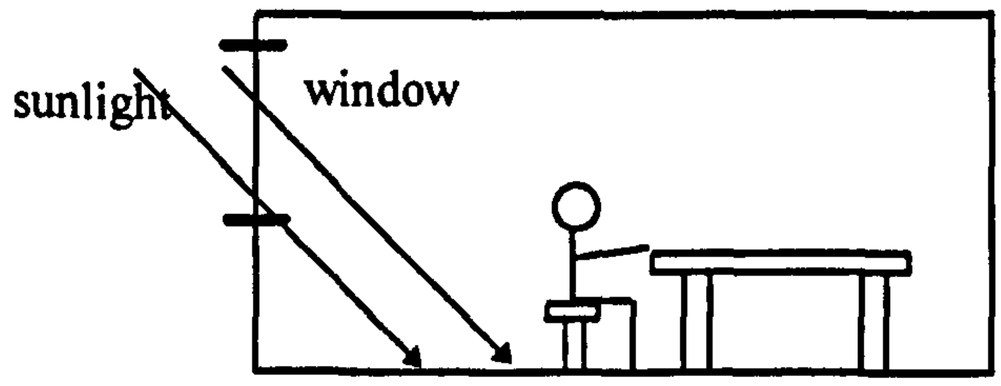

Fig 2:Traditional windows allow sunlight to merely illuminate floor closest to window.

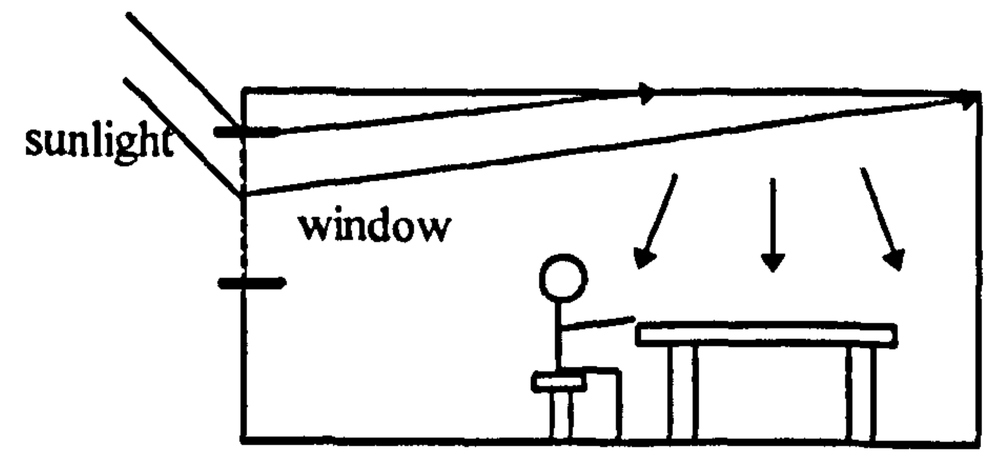

Fig 3: Daylighting systems re-distribute sunlight for a more even illumination.

With the increase in multi-story office blocks the need for daylighting devices is especially acute[viii] as the available area for collecting sunlight is small and many areas are remote from the apertures.

Daylighting is the cheapest and most efficient application of solar energy, requiring no conversion into another form. In addition, the logarithmic sensitivity of the eye means that major losses (say 50%) are hardly noticeable in a daylit room, whereas such inefficiency would by intolerable in other solar energy systems. The converse though is that light levels in the room should be ideally doubled to be appreciable to the observer.

Apart from the reduction of electricity for lighting, other less obvious advantages exist:

1) Reduction in cooling equipment

Artificial lighting acts as a source of heat as well as illumination and can lead to the use of cooling equipment during the summer months. Daylighting has a much higher luminous efficacy[ix] (that is light to heat ratio) than electric lighting which means that it can reduce this secondary load. The table below shows typical values[x]

Source	Luminous efficacy (lumens/watt)
Sunlight	102-116
Total daylight	110-134
White fluorescent lamp	63

2) Improvement of the working or living environment

Admission of natural light into the workplace can provide lighting similar to that experienced outdoors, and informal surveys of employees' opinions have shown that daylit areas are well liked. Moreover, it has been supposed that daylighting has been directly responsible for dramatic increases in productivity that have dwarfed the financial gains made from the energy savings. Already companies that have harnessed this source have seen some dramatic results. A case in point is "Building 157" constructed for Lockheed in 1987[xi]. In its first year of operation the building saved 50% in energy bills and also increased productivity by 15%, resulting in a further saving of $2 million. Considering that the cost of installation was $2 million, it can be seen that it is financially as well as environmentally sound. Equivalent energy savings are possible with merely controlled lighting[xii] because daylighting systems invariably need supplementary artificial light at certain times of the year. As a consequence the improved interior environment represents one of the strongest arguments for daylighting.

However there are certain unwanted effects caused by intense, direct sunlight and these are particularly problematic for south façades of buildings in the northern hemisphere:

1) Overheating of interior during summer.

During the winter, daylight can act as a passive source of heat, yet during the summer overheating can occur (despite its low luminous efficacy) and some form of shading is often required.

2) Glare[xiii] (high illumination in an otherwise low illumination field)

Direct sunlight can cause discomfort if it is not diffused, therefore some form of sun protection is often needed. Traditional methods of limitation (for example venetian blinds) cause complete darkening of the room and are therefore unsuitable.

Of the two forms of sunlight (direct and diffuse) direct solar radiation is the easiest to manipulate but its availability is limited. It forms a parallel beam of high intensity light, with an angle of incidence that varies with the movement of the sun. Consequently, many systems that utilise direct sunlight involve tracking systems that are complex and costly.

Using diffuse sunlight, which is more readily available, is more technically difficult because it cannot be concentrated nor can it be redirected by lenses. However, it is less likely to cause glare and as a result many daylighting techniques are designed to convert direct into diffuse sunlight (although a bright diffuse source can still produce significant discomfort). Often additional shading may be required in conjunction with the novel glazing system because even a ten-fold reduction in transmission can still cause problems with glare. This is a particularly significant issue because of the proliferation of VDU's[xiv] that are easily obscured by relatively low light levels.

Intuitively one would think that daylighting systems would increase the transmission of light into the room, however the addition of any optical component onto existing glazing significantly reduces the transmission[xv]. The increased losses are due to fresnel reflections, absorption and scatter. Fresnel reflections occur at the boundary between two media and increase significantly with the angle of illumination until total internal reflections occurs at the critical angle. Fresnel losses are particularly significant in the case of daylighting, where the source (that is the sun) can be at an oblique angle of incidence.

However, the occupant's perception of brightness is not based only on the light level. In fact the darkness, not the lightness, of the interior (and the contrast between the two) governs whether an individual will use artificial lighting. Consequently, attaining a more even illumination will reduce the energy bill. Simple measures such as painting the walls and ceiling white, or by shading the front of the room, can help to achieve this.

Another consideration is the view out of the window. Some surfaces such as a prismatic array, obscure or distort the view for the occupants and in many situations this would be unacceptable. As a result, in offices and homes such structures would only be cover the top part of the window. The percentage of the window that needs to be covered is described in the British Standard 'Lighting for Buildings: Part 2[xvi].' Yet there are many situations where the view is not important: for example high windows in factories and sports halls[xvii] or places where people do not linger, such as shopping centers. In these places it would be possible to cover the whole glazing with the microstructures.

In summary, the Building Research Establishment[xviii] has identified several situations where daylighting systems would be appropriate:

- *Visual requirements within the space are especially stringent, e.g. in a room with visual display units.*
- *There are large external obstructions outside.*

- *Much sunlight is available, typically a south-facing window wall in a sunny location.*
- *The space is too deep to give adequate uniformity of lighting with conventional windows.*
- *Conventional windows or rooflights would give unacceptable, gloomy areas within a space.*

The methods that are to be investigated for daylighting involve the use of microtextured optical surfaces (or more specifically micro-lenses and micro-prisms) with high spatial frequencies. The advantage of such structures is that they can be embossed in large volume and therefore cheaply. The company that would produce the any successful systems from this thesis would be Autotype UK, which has had a long-standing, working relationship with NPL. Their process requires that the dimensions of any surface features on the structure to be embossed, must be less that 100μm. In addition to be commercially viable the finished product must be cosmetically appealing and therefore a seamless continuous structure is required. To achieve this, any structure deemed suitable for commercial purposes, would be mechanically cut into a roller that is used as a master in the embossing process. Therefore, whenever possible, the small scale prototypes investigated in this thesis are manufactured using mechanical techniques.

Thesis Structure

There are two types of structure considered in this thesis: microprisms and microlenses. The former are considered in the first three chapters, with a conclusion at the end of the chapter 3. The final chapter discusses three possible systems employing micro-lenses and includes computer simulations as well as empirical results.

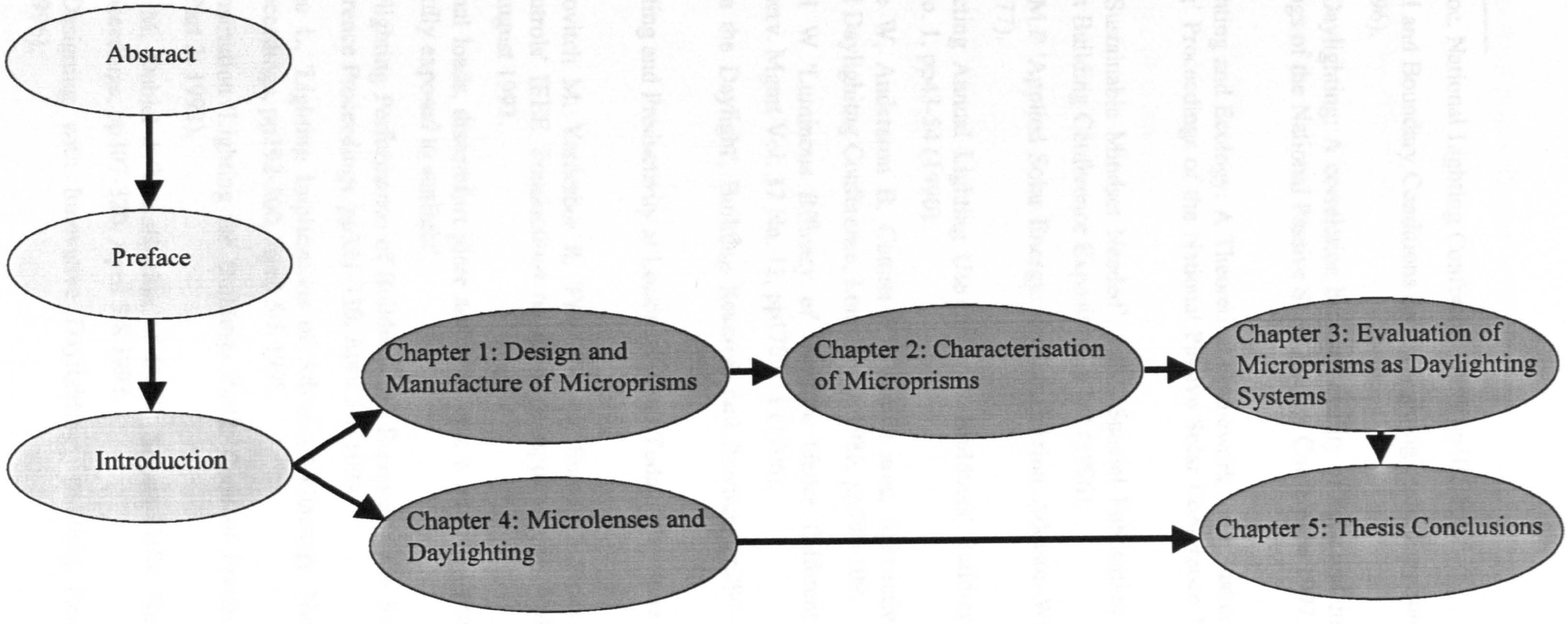

i Raynham P, 'Candle' Proc. National Lighting Conference 1998 pp102-109.

ii. Goetzberger A 'Optical and Boundary Conditions for Daylighting' Proc. EuroSun '96, Vol. 3, pp1230-1236 (1996).

iii Krug N, Energy and Daylighting: A correlation between quality of light and energy consciousness' Proceedings of the National Passive Solar Energy Conference 1997, vol. 22, pp 105 to end.

iv Guzowski M, 'Daylighting and Ecology: A Theoretical Framework for a Sustainable Approach to Daylighting' Proceedings of the National Passive Solar Conference 1996, vol. 2, 335 to end.

v Morrison D R 'New Sustainable Mindset Needed', NIST Special Publication 908: Third International Green Building Conference Exposition, p 1-3 (1996).

vi. Meinel A.B, Meinel M.P 'Applied Solar Energy: An Introduction' Addison-Wesley Publishing Company (1977).

vii. Littlefair P J 'Predicting Annual Lighting Use in Daylit Buildings' Building and Environment, Vol. 25, No. 1, pp43-54 (1990).

viii Howard T C, Place W, Andersson B, Couiter P 'Variable area, light-reflecting assemblies', International Daylighitng Conference, Long Beach 1986, pp306-309.

ix. Liam J C, Li D H W 'Luminous Efficacy of Daylight Under Different Sky Conditions' Energy Conserv. Mgmt Vol. 37 No. 12, pp1703-11 (1996).

x Ruck N C, 'Letting in the Daylight', Building Research and Practice, pp294- 300, Sept/Oct 986.

xi.Thayer B. M 'Daylighting and Productivity at Lockheed' Solar Today, May/June 1995 pp26-29.

xii.Rubinstein F, Siminovitch M, Verderber R, 'Fifty Percent Energy Savings with Automatic Lighting Controls' IEEE Transactions on Industry Applications, Vol. 29, No.4, pp768-773 July/ August 1993.

xiii. Boubekri M 'Thermal loads, discomfort glare and emotions: a multifold problem for designing windows fully exposed to sunlight'.

xiv. Fontoynont M 'Daylighting Performance of Buildings: 60 European Case Studies' National Lighting Conference Proceedings, pp321-330, April 5-8 1998.

xv. Littlefair P.J, Roche L, 'Lighting Implications of Advanced Glazings' National Lighting Conference Proceedings, pp292-300, April 5-8 1998.

xvi British Standards Institution 'Lighting for Buildings Part2: Code of Practice for Daylighting' (BS 8206: Part 2: 1992).

xvii Clemo A, Wilson M, Dubiel J 'Visualisation of Daylit Sports Halls' National Lighting Conference Proceedings, pp307-320, April 5-8 1998.

xviii Littlefair P. J, 'Designing with Innovative Daylighting', Building Research Establishment Report (1996).

1. The Design and Manufacture of Microprism Arrays

1.1 Introduction

The first structure to be investigated is the microprism. The application of microprisms to windows could increase the penetration of daylight into a room and provide an environmentally friendly way of improving lighting It may also form a commercially viable product. This chapter describes the first steps towards that goal. The first stage is to assess the work of others, before designing and manufacturing an original structure whose performance is assessed in the following chapter. Before addressing the design and manufacture of the structure, it is useful to describe the context in which the work is set.

1.1.1 Prisms and Sunlight: A Review

The use of prisms to re-direct sunlight is not a new idea. As early as the 1950's[i] prisms were installed in schools to improve the lit environment. Since then a series of geometries have been explored. N C Rodgers[ii] for example suggests using two prism arrays to re-direct the light and install them inside double glazing to maintain their cleanliness and therefore effectiveness (see Fig 1-1). Results show increases in the penetration of sunlight with solar altitude with the greatest improvement occurring during the summer months[iii].

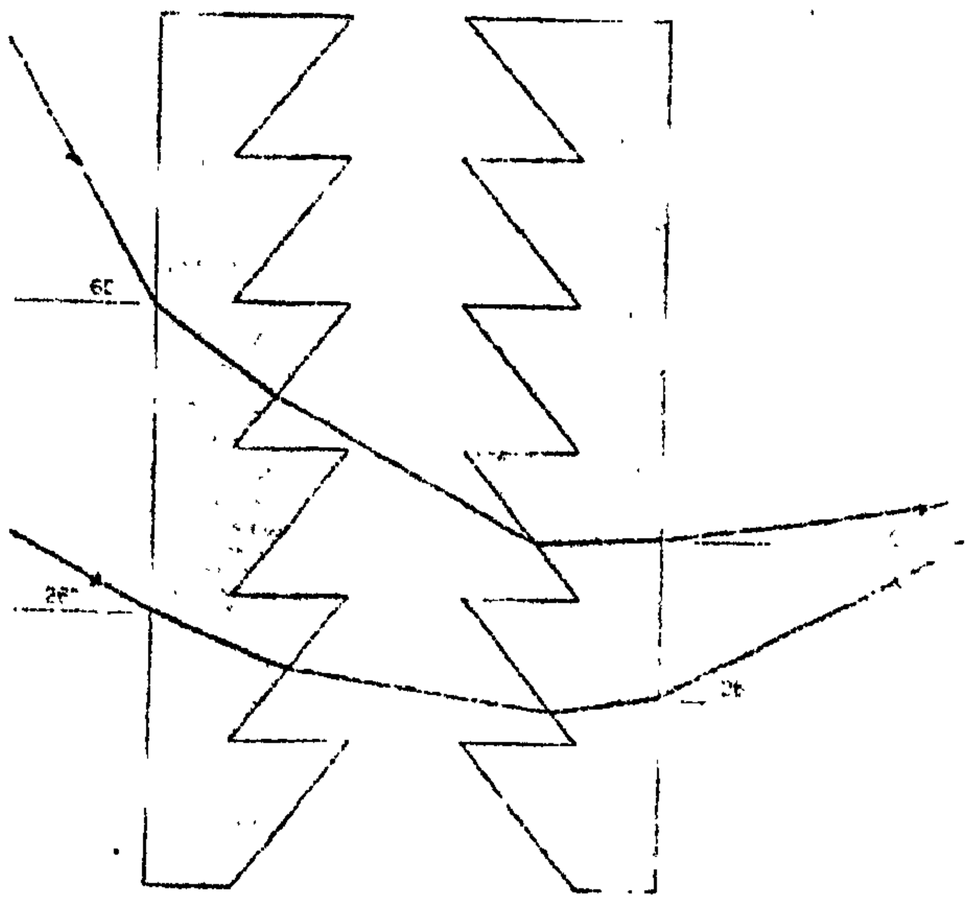

Fig 1-1: Re-directing direct sunlight with two prismatic arrays.

The use of a prismatic panel within double glazing is also advocated by Ruck[ivv] but with the glazing hinged to the frame (see Fig 1-2).

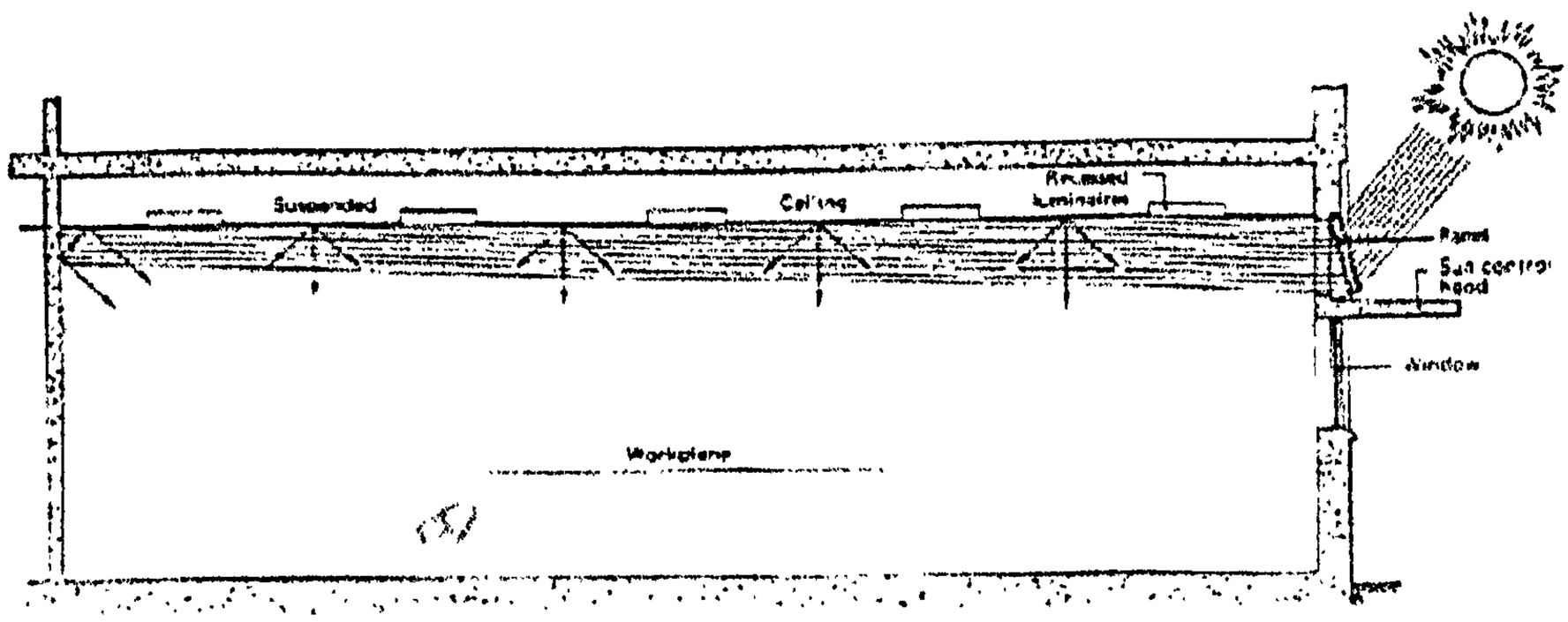

Fig 1-2: Beam sunlighting with hinged array

If the prism angles do not provide sufficient deviation of sunlight, then tilting the windows can compensate and glare can be reduced. Ruck reports that by covering only a small area of the glazing, light levels of 500 lux (the recommended[vi] illuminance for general offices) can be achieved at a depth of 10 metres from the window.

One of the most interesting devices that employs prisms is the 'Serraglaze' product[vii,viii]. It is manufactured by combining two arrays of prisms with sub-millimeter dimensions (see Fig 1-3).

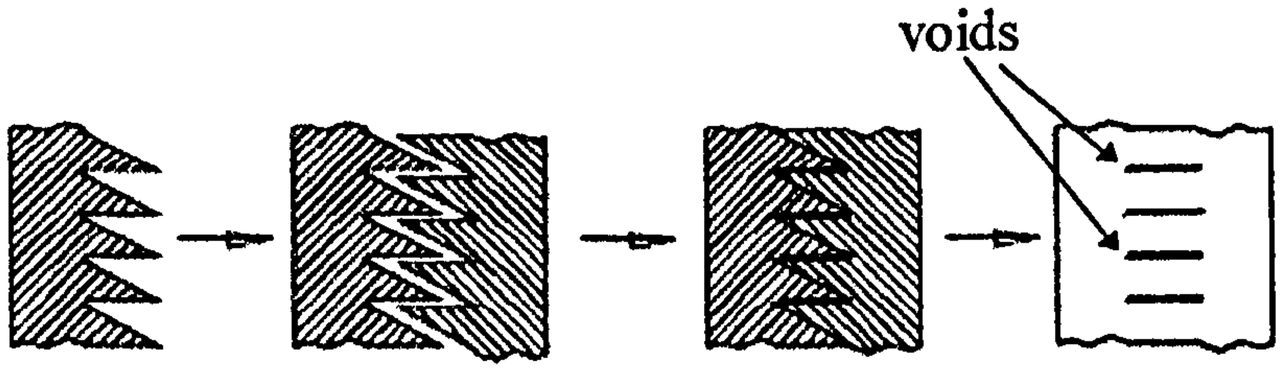

Fig 1-3: Production of Serraglaze.

The prisms do not match perfectly, and voids are left in the structure that are a few micrometers thick and 0.3 mm in length. Light from high solar altitudes is total internally reflected from these voids to the back of the room. However the view-out is not compromised as light at lower altitudes is transmitted between the gaps.

Prisms may only be useful for deviating sunlight into a room, but can also act as excluders during periods of very hot weather. In winter, it is useful to have a building heated by the sun, although during the summer excessive solar radiation may cause problems. Fenestration with seasonally dependent transmission properties would therefore be desirable. D. Christoffers[ix,x] has developed a seasonal shade using prismatic panes (see Fig 1-4) which utilise the variation in solar altitude.

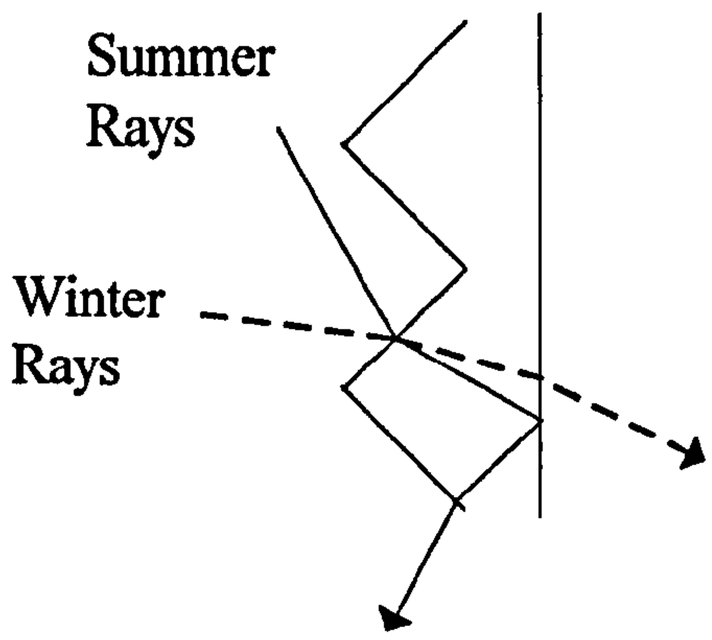

Fig 1-4: High altitude summer rays are totally internally reflected while low altitude rays are transmitted.

The prism angles are calculated so that during the summer the rays are totally internally reflected (because of their high angle of incidence) but during the winter, when the sun is lower, they are transmitted. The Building Research Establishment has also evaluated prisms as a daylighting device and as an excluder of direct sunlight[xi] (see Fig 1-5) in experimental rooms.

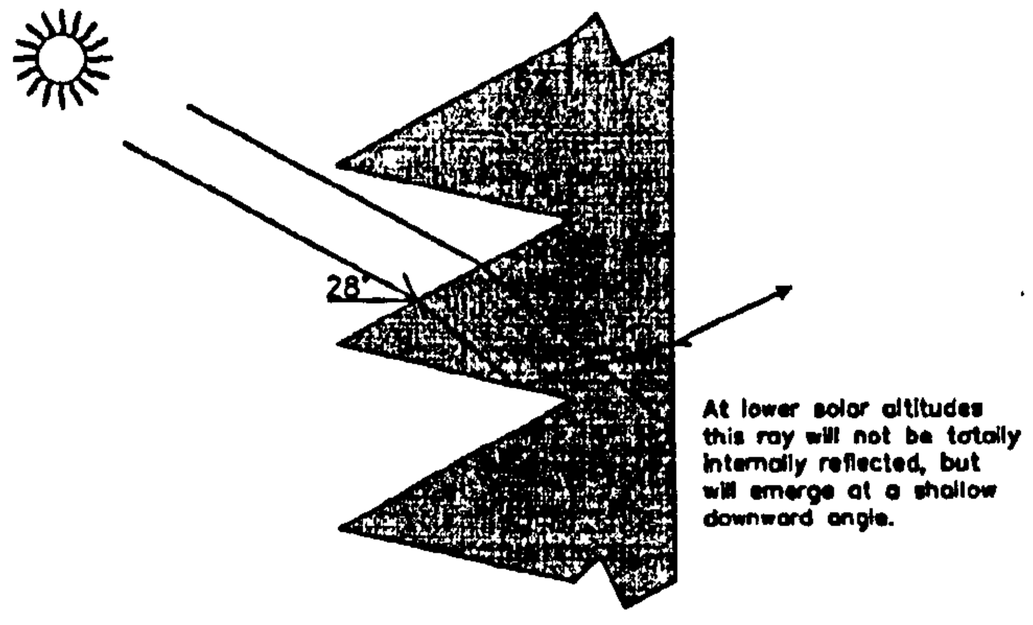

Fig 1-5: Prismatic excluder.

The film[xii] did provide some protection from direct sunlight in some areas but only modestly increased the light levels in others, especially at the back. It would probably also require additional glare protection from blinds.

Prismatic arrays generally obscure the view-out but I Edmonds[xiii] has produced an array of rectangular prisms that overcome this difficulty (see Fig 1-6). Occupants can still see out, but direct sunlight is transmitted deep into the room by total internal reflection. To account for variations in solar altitude, the window is tilted and, while this reduces the transparency, a clear view is still afforded.

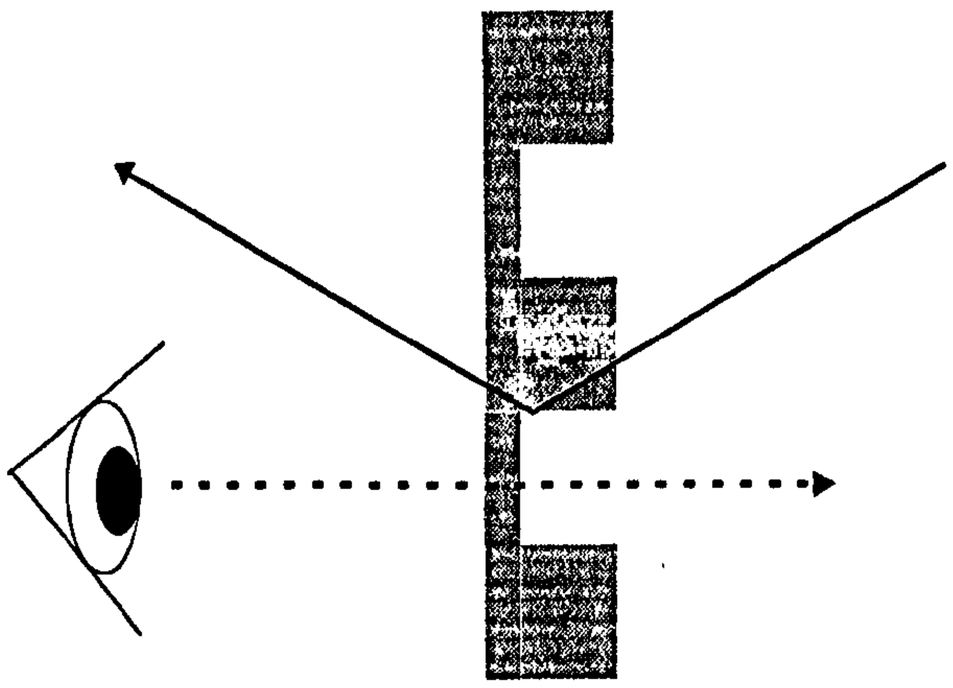

Fig 1-6: Deflection of light by rectangular prismatic array.

The main disadvantage of this system is the cost incurred in its production. The individual elements are cut from acrylic using a laser, which is initially expensive and also labour intensive (as it requires constant supervision) so the retail price is estimated at 4-5 times that of glass.

Prisms have been used in light pipes to transport daylight to poorly illuminated parts of a building. The light pipe system normally consists of three major components: a heliostat, a pipe and an emitter. From the roof the heliostat (which is a device that tracks the sun across the sky) collects solar rays and condenses them into a pipe. The light is then conveyed to another part of the building where it is distributed by a separate emitter. Originally the pipes consisted of a hollow metal tube containing a system of confocal lenses to maintain the concentration of the light. However, Whitehead et al[xiv] have developed a prismatic light guide that transports the light more efficiently using total internal reflection (see Fig 1-7). Furthermore, as the pipe is made of acrylic (and not metal) absorption losses are greatly reduced, so that the major reduction in transmission is as a result of light escaping from the guide. Hence there is no need for a separate emitter as the guide acts as its own light source.

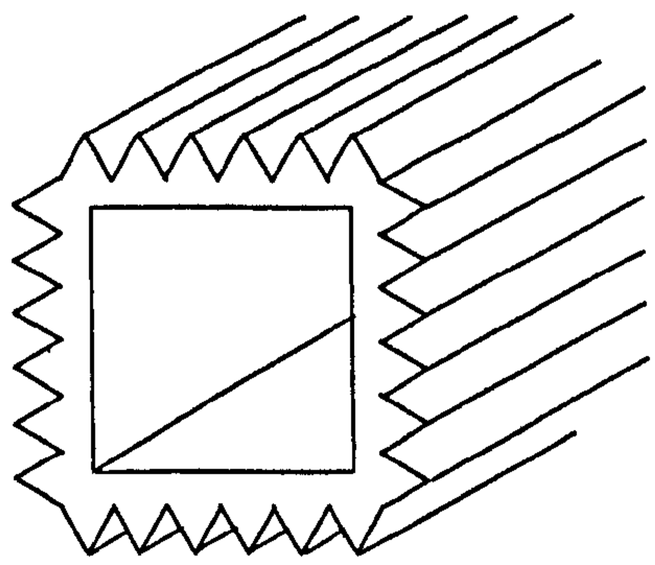

Fig 1-7: Prismatic light guide

It is desirable to be able to use a light pipe system without the expensive and complex heliostat, but this would not be practicable as (for low angles of solar elevation) the effective aperture of the pipe is very small. However, collection can be improved by the application of laser cut panels[xv] (Fig 1-6) that also reduce the number of reflection losses (see Fig 1-8). The result is that light levels are enhanced in the room beneath the pipe.

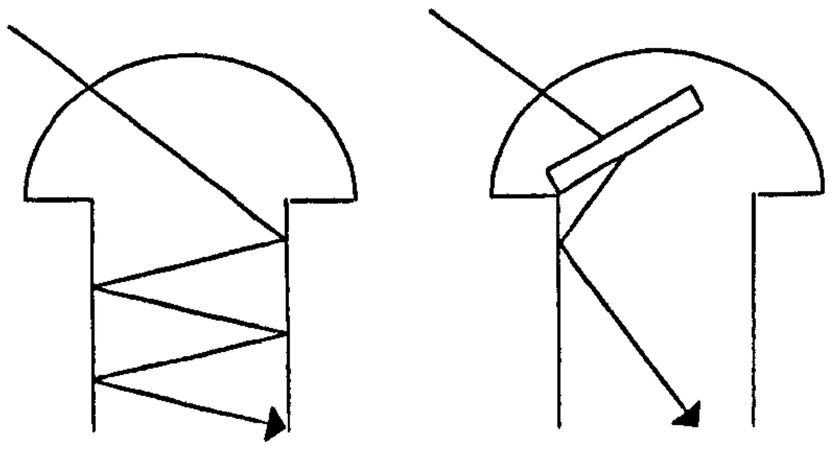

Fig 1-8: (Left) Low elevation light entering the light pipe suffers multiple reflections. (Right) Inserting the laser cut panel reduces reflections and therefore the losses.

Laser cut panel reduces the number of reflections. If the panes are fixed, then an improvement only occurs during the winter; but if made to track the sun, then a more constant interior illumination is possible during all the hours of daylight. Although significantly cheaper than the heliostat, the laser cut panels cannot match its performance.

Improving the transmission of daylight can also have benefits for agriculture. In the winter, the effectiveness of a greenhouse is limited by poor natural light levels, but in the summer overheating can occur, giving rise to crop damage. K. Kurata has demonstrated that by applying a fresnel prism† to a single span greenhouse[xvi] (see Fig 1-9), more favourable conditions can be achieved.

---

† A Fresnel prism is a flat sheet of transparent material, with one side cut as a saw-tooth profile. In fig.6, the whole of the south facing roof is the fresnel prism, consisting of an array of smaller prisms.

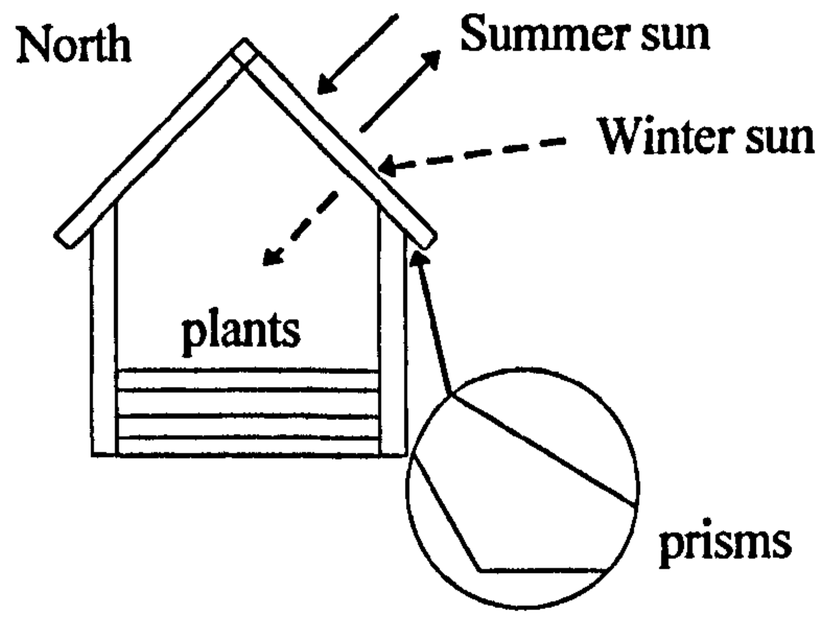

Fig 1-9: Fresnel prism applied to the south side of a greenhouse roof.

Winter conditions may also be improved by using the prisms in a venetian blind assembly as proposed by Critten[xvii] (see Fig 1-10). The system consists of a series of alternating tilted and vertical prismatic panes, to redistribute light that would otherwise pass straight through the greenhouse. Light incident on the tilted sections suffers total internal reflection and illuminates the southern half of the greenhouse; while the vertical sections deviate the light onto the northern half. It has been predicted that up to 25% light enhancement could be possible.

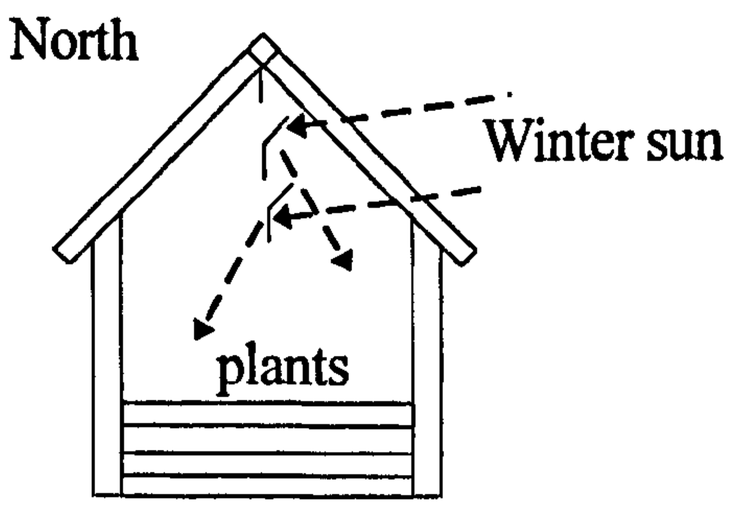

Fig 1-10: Venetian blind arrangement of prismatic panes.

The aim of the work described below is to produce a microprismatic structure, (period <100μm) that can be embossed onto thin (<250 μm) polycarbonate or melinex film. This could then be applied to new and existing glazing to improve the distribution of natural light in a room. Normally it is not desirable to exactly translate a specific daylighting system from one building to the next because changes in climate and facade orientation. However, as the retail price is expected to be less than £10/m^2 a cost/benefit analysis may justify the use of microprisms in a variety of situations.

1.2 Design of Microprism Structure

Rooms appear gloomy when the solar altitude is high and concentrated close to the window with little towards the rear. Examining the solar path for the latitude of the NPL site[xviii] shows that the solar altitude, θ varies between 0° and 60°. It was mentioned in the introduction that occupants are more likely to use electric lighting when the room is not evenly lit. An imbalance is most likely to occur at the higher altitudes, say between 40° and 60°. The design criteria therefore took an 'average' of 50° and calculated the prism angles such that light was deviated on to 10° above the horizontal and therefore to the back of the room. For this profile the angles of emergence were then calculated for light incident at 40° and 60° and the fresnel losses at each surface. Although there were concerns about glare, the prisms were considered to be controlled diffusers and may reduce the discomfort caused by solar illumination at angles other than 50°.

1.2.1 Calculation of Prism Angles

We assume for practical reasons that one face of the prism is vertical and that the prisms are on the inside of the window. Applying Snell's law to the first interface:

$$\theta_1 = \sin^{-1}[n_2(\sin 50)/ n_1] = 29.27°$$

if we assume a value of 1.567 (that of epoxy resin) for the refractive index of the prism.

By simple geometry the angle of incidence on the second surface θ_3 is given by:

$$\theta_3 = \theta - \theta_2$$

Where θ is the prism angle.

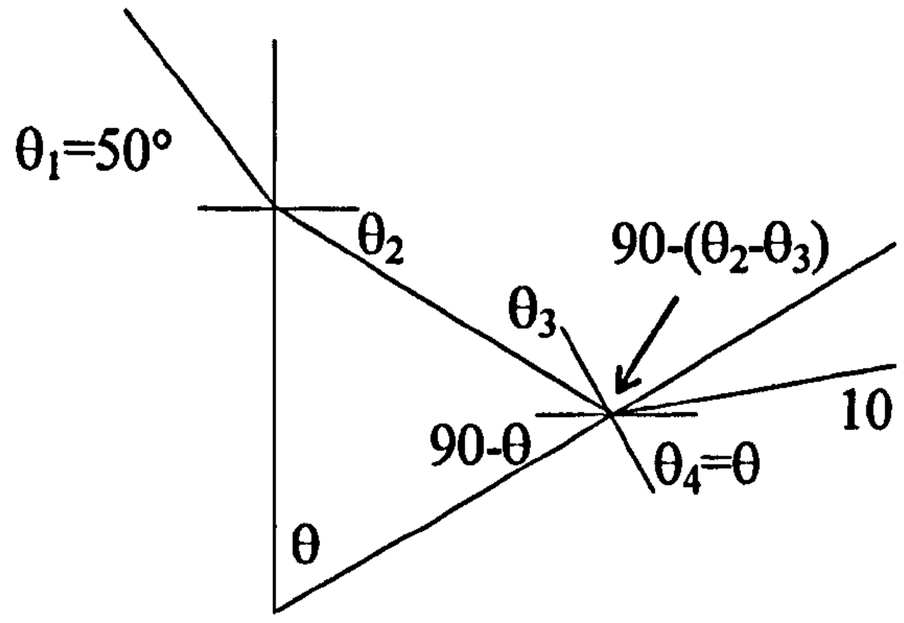

Fig 1-11: The geometry of the transmission of light through the prism

so by applying Snell's law

$$1.567 (\sin\theta - 29.27) = \sin(\theta + 10)$$

from which we derive that $\theta = 67.87°$:

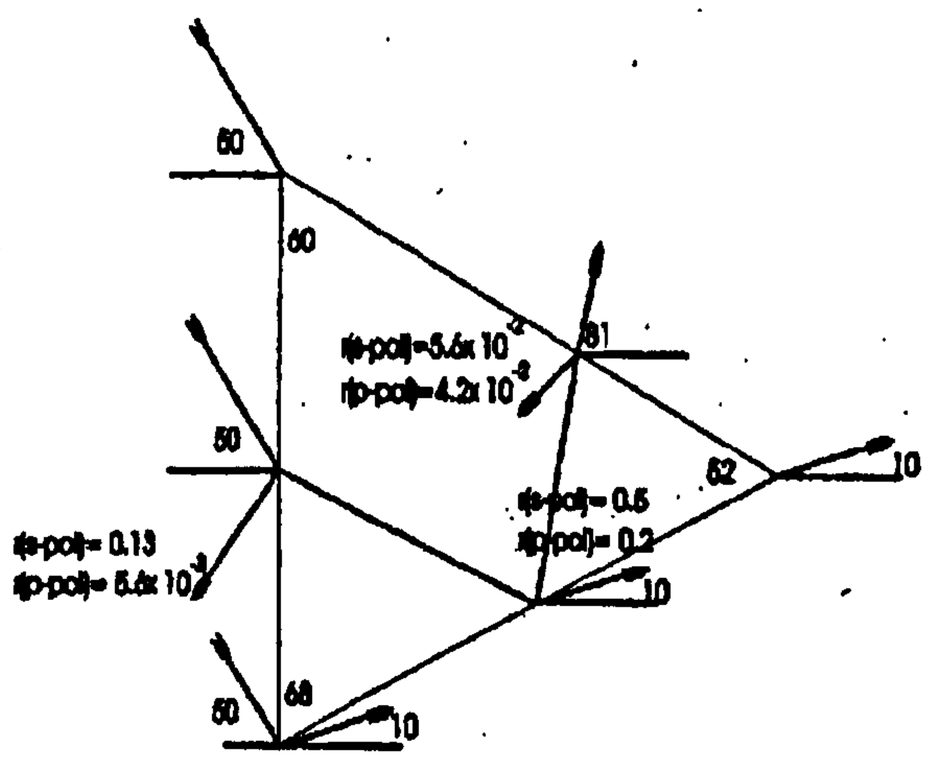

Fig 1-12: Reflection losses and transmission angles through the prism.

The upper angle in Fig 1-12 is simply the angle of emergence of the light at the first interface:

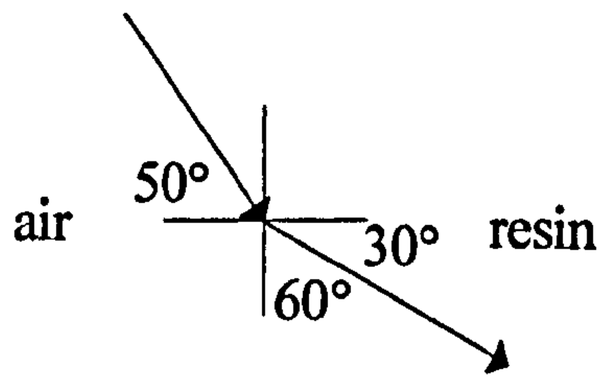

Thus all of the light illuminating the first surface follows the path shown in Fig 1-12.

Transmission Angles

The table below summarizes the transmission of light through the prism for light incident at 40°, 50° and 60°. The significance of the 'Area Illuminated' column is explained in Fig 1-13.

Angle of incidence	Area Illuminated	Transmission (%)	Total Transmission (%)	Total Transmission (%) (unpolarised)	Output Angle (relative to horizontal)
40°	13%	t_s=73	9.6	11.3	-10.5°
		t_p=98	13		-10.5°
	87%	t_s=87	76	79	85°
		t_p=94	82		85°
50°	100%	t_s=41	41	60	10°
		t_p=79	79		10°
		t_s=56	56	38	81°
		t_p=20	20		81°
60°	100%	t_s=66	66	83	-3.5°
		t_p=100	100		-3.5°

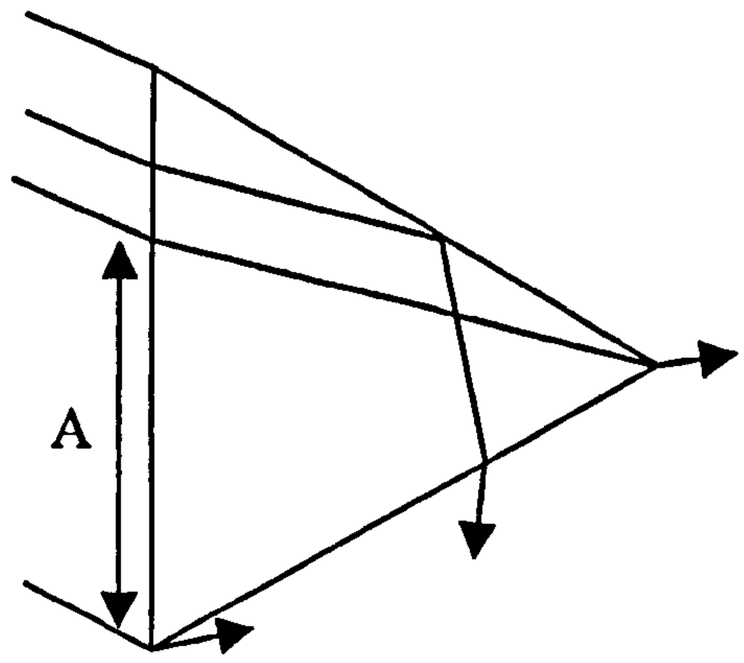

Fig 1-13: Area Illuminated A is the proportion of the first interface over which the transmission angle is constant for a given angle of incidence.

The angles of emergence for incident angles of 40° and 60° were also calculated using Snell's Law. The losses due to reflection at each interface were calculated according to the Fresnel formulae:

$$R_s = [\sin(\theta-\theta')/\sin(\theta+\theta')]^2 \qquad R_p = [\tan(\theta-\theta')/\tan(\theta+\theta')]^2$$

$$\text{and} \qquad t_s = 1-(R_s)^2 \qquad t_p = 1-(R_p)^2$$

The overall transmission factor is the product of the vignetting factor and the transmission factors at the two prism surfaces. The total transmission factor is then the product of the illuminated area and the transmission factor at each surface. Fig 1-14 shows the deviation of light by the prism array.

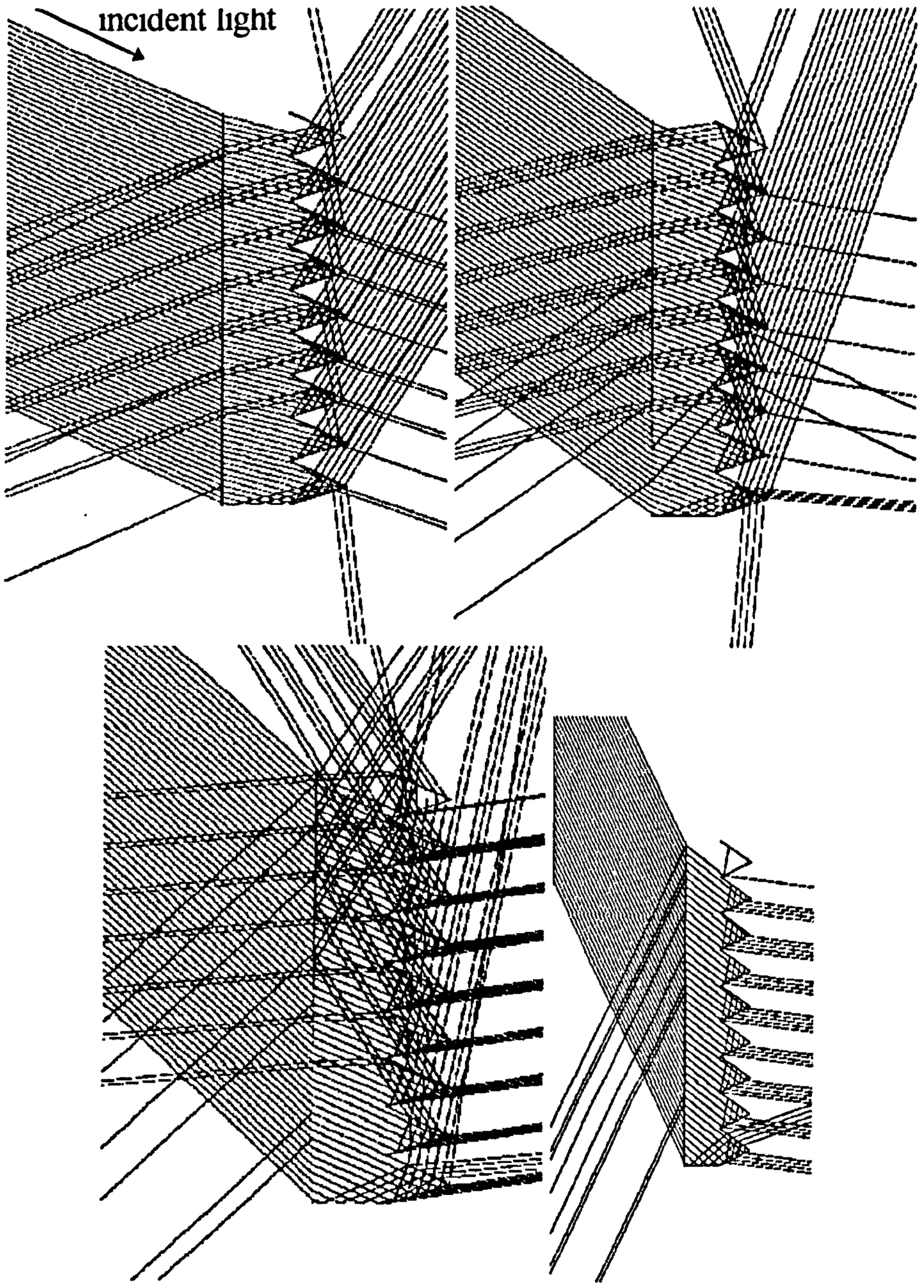

Fig 1-14: Deviation of light through the zone 3 prismatic array for light incident at (*clockwise from top left*) 30°, 40°, 50° and 60°.

The diagrams show that light is transmitted above the horizontal at 50° and just below at 60°. The latter may be tolerable for occupants in a room with high windows as the prisms will only cover the top third in practice, so as not to obscure the view. At 30° and 40° the light is inefficiently transmitted below the horizontal and therefore the prisms may provide glare protection at these solar altitudes.

When using prismatic structures for daylighting techniques, a source of concern is the dispersion and production of coloured bands against the wall or ceiling. The high spatial frequency of the micrprisms should produce sufficient diffusion to obscure most of the colour effectis. Some colouration may be still visible at the borders of the deviated light, but provided it is not projected on to the working plane, this should not cause significant discomfort[xix].

1.3 Commercially Available Microprisms

Microprismatic structures are already available from 3M however they are not designed for daylighting techniques but are used to enhance computer displays (see Appendix B). Samples of these structures have been obtained and their efficiency at deviating light measured using a collimated white light source and integrating sphere (see Fig 1-15). Shown below is data obtained from 3M's BEFII product

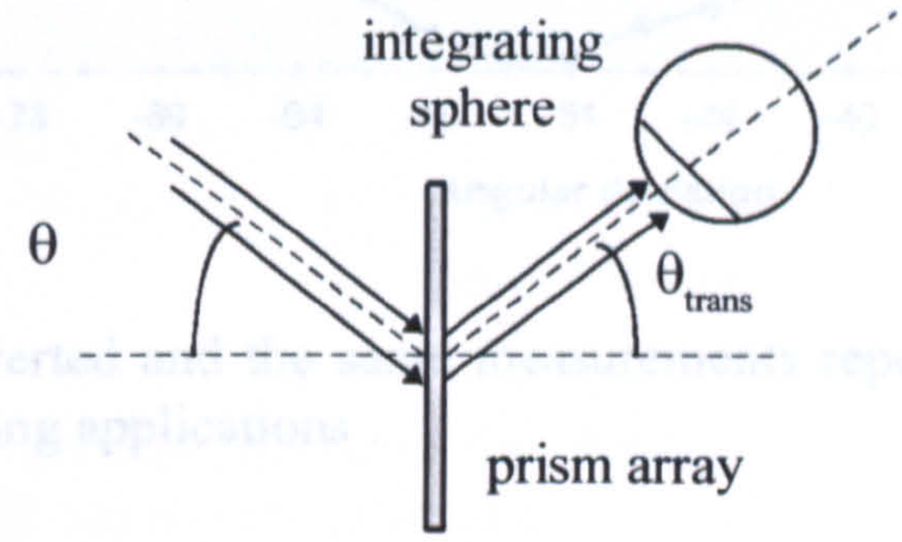

Fig 1-15: Measurement of transmission properties with collimated white light source.

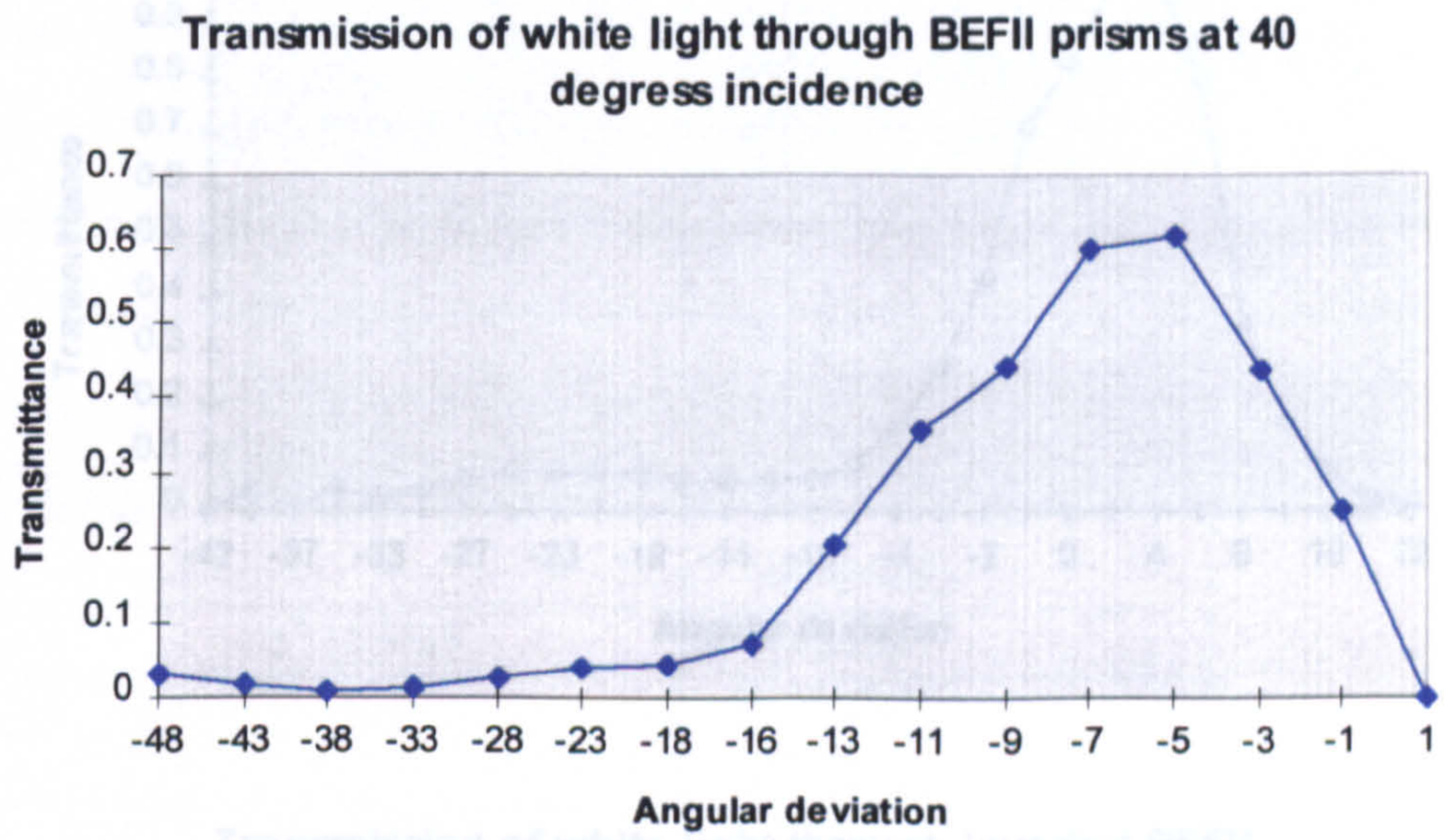

Transmission of white light through BEFII prisms at 50 degrees incidence

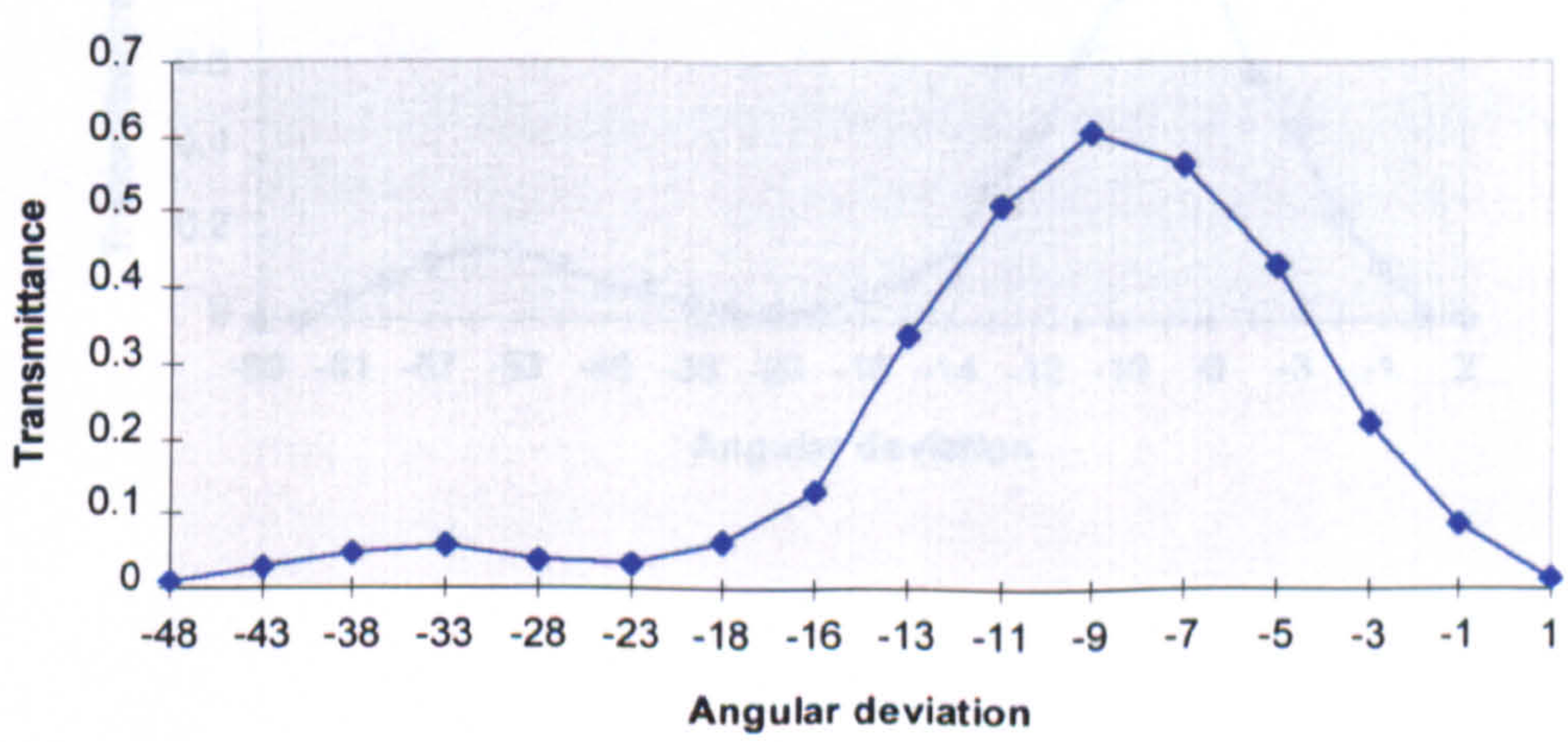

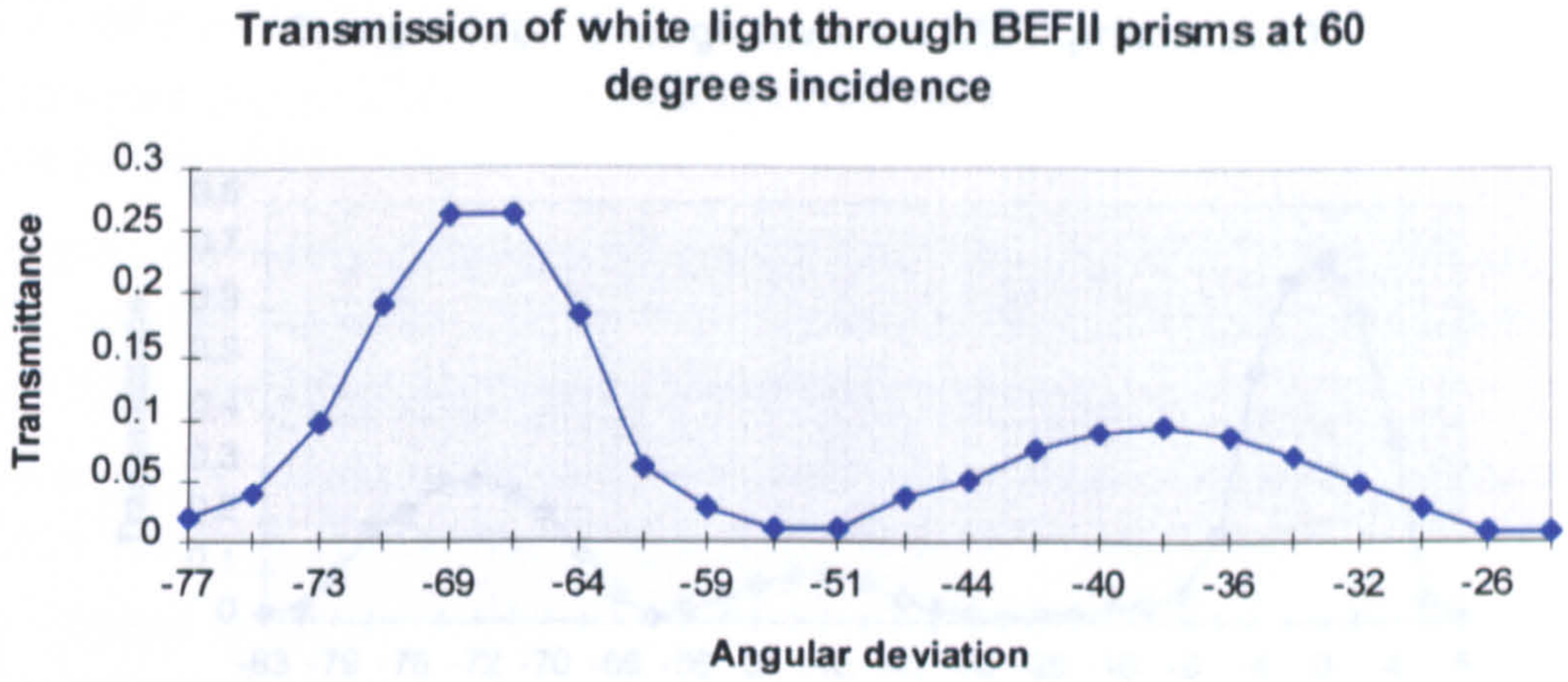

The array was then inverted and the same measurements repeated to determine the correct orientation for daylighting applications

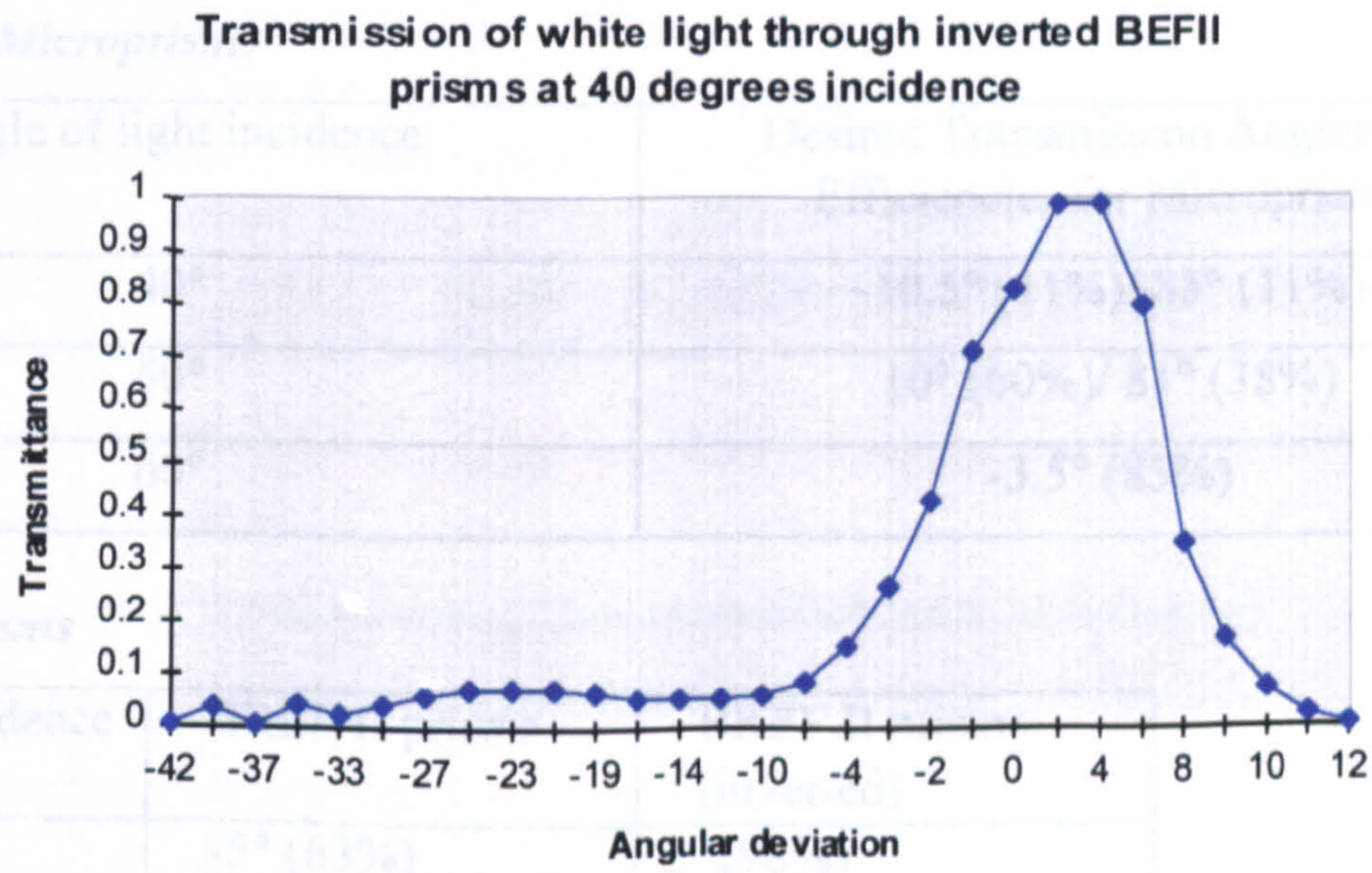

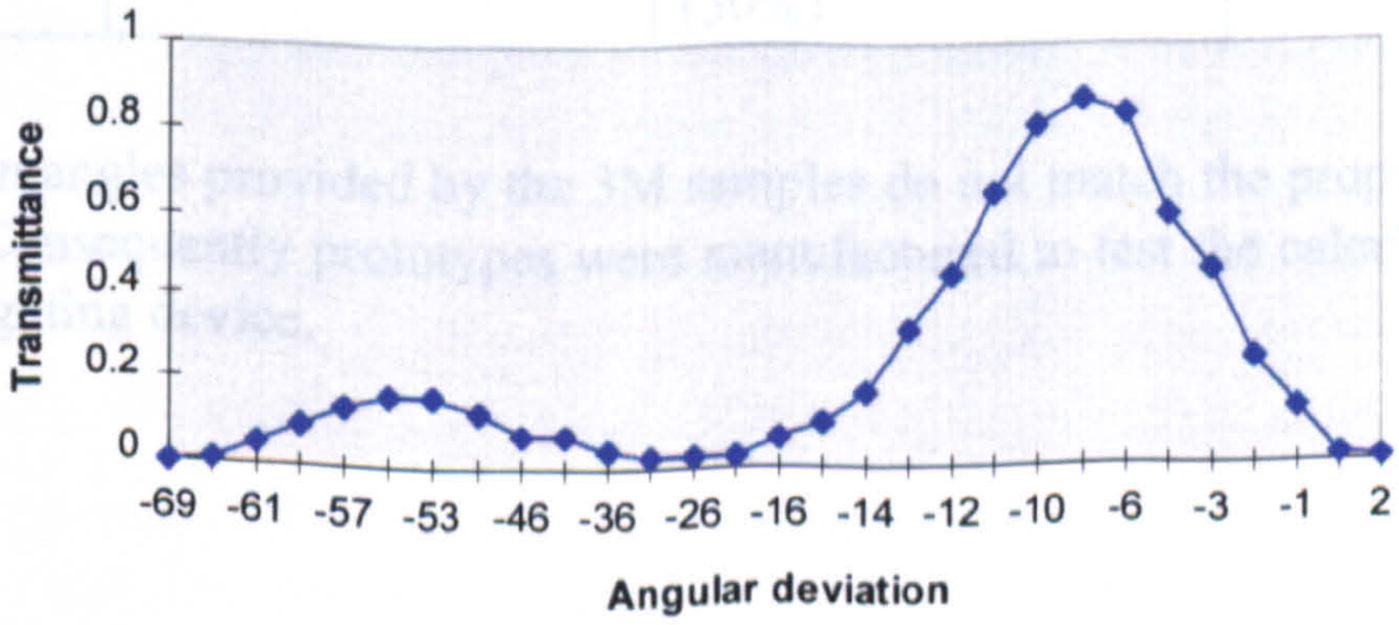

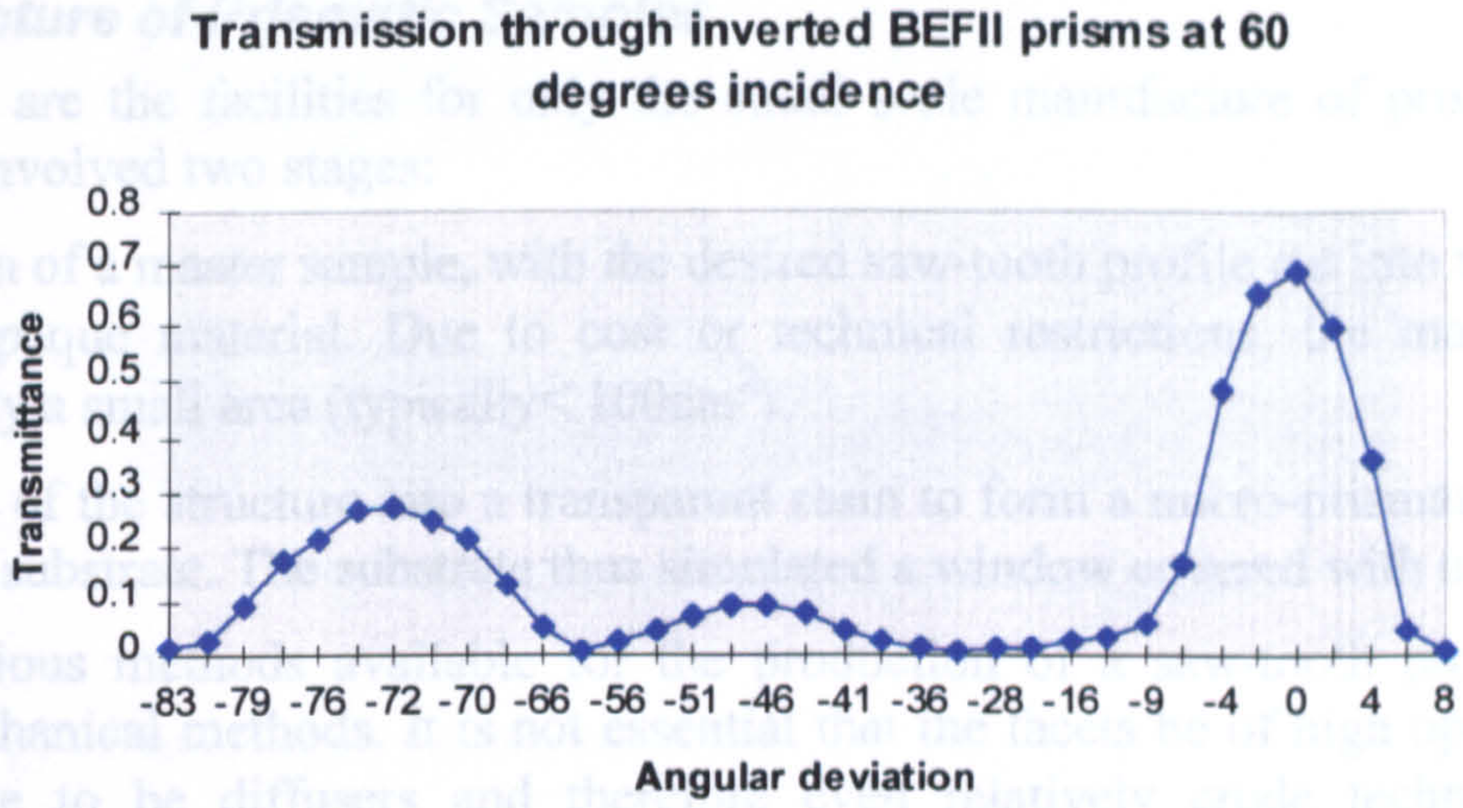

Given below is a comparison between the desired properties of the microprisms (as determined in this thesis) and the 3M products.

Daylighting Microprisms

Angle of light incidence	Desired Transmission Angles and Efficiencies for Microprisms
40°	-10.5° (11%)/ 85° (11%)
50°	10° (60%)/ 81° (38%)
60°	-3.5° (83%)

3M Microprisms

Angle of incidence	BREF II prisms	BREF II prisms (inverted)
40°	-5° (63%)	2° (98%)
50°	-9° (60%)	-8° (90%), -55° (20%)
60°	-68° (26%),	0° (69%) -58° (10%) -72° (30%)

The transmission angles provided by the 3M samples do not match the properties determined in section 1.2. Consequently prototypes were manufactured to test the calculated structure as a possible daylighting device.

1.4 Manufacture of Prismatic Samples

At NPL there are the facilities for only the small scale manufacture of prism arrays. The process used involved two stages:

1. The creation of a master sample, with the desired saw-tooth profile cut into the surface of a normally opaque material. Due to cost or technical restrictions, the masters normally covered only a small area (typically< 100cm^2).
2. Replication of the structure into a transparent resin to form a micro-prismatic surface on a transparent substrate. The substrate thus simulated a window covered with microprisms.

There are various methods available for the production of a saw-tooth profile, either by optical or mechanical methods. It is not essential that the facets be of high optical quality as the prisms are to be diffusers and therefore even relatively crude techniques may be acceptable.

1.4.1 Generation of Master Surfaces: Optical techniques[xx]

A saw-tooth profile can be produced by photosculpture in photoresist. A similar process is described in Chapter 5 for the production of microlenses. There are technical difficulties in using such a method to produce refractive prisms, primarily in achieving sharp edges to features. Diffractive optics though do not suffer the same rounding as the period of the structures is typically < 1μm For the sake of completeness, given below is a list of possible optical techniques that are used in photosculture:

1. **Direct laser writing.**
2. **Electron Beam writing**
3. **The LIGA process (Lithographie, Galvanotechnik und Abformung)**
4. **Optical Exposure through a Grating Slit Mask**
5. **Fourier Synthesis from Sinusoidal Interference Fringes**

The manufacture of master surfaces by any one of these methods would be expensive and complex and unrepresentative of the final mechanically-cut structure required for the embossing process. Consequently processes of the latter nature were pursued instead.

1.4.2 Generation of Master Surfaces: Mechanical techniques

There are basically two approaches to the mechanical production of prism-shaped grooves on a surface. Either a tool of the appropriate shape cuts or burnishes the groove in a single pass or a very fine tool carves out the desired shape in a large number of passes. These processes determine the shape of the prism. Described below are the processes that have been investigated.

The Merton Process[xxi]

A single helical groove is cut in one pass on the surface of a cylinder using a diamond tool of the appropriate shape. The process was developed and operated at NPL in the 1950s. Several gratings of this nature were available but none deviated the light sufficiently for daylighting purposes.

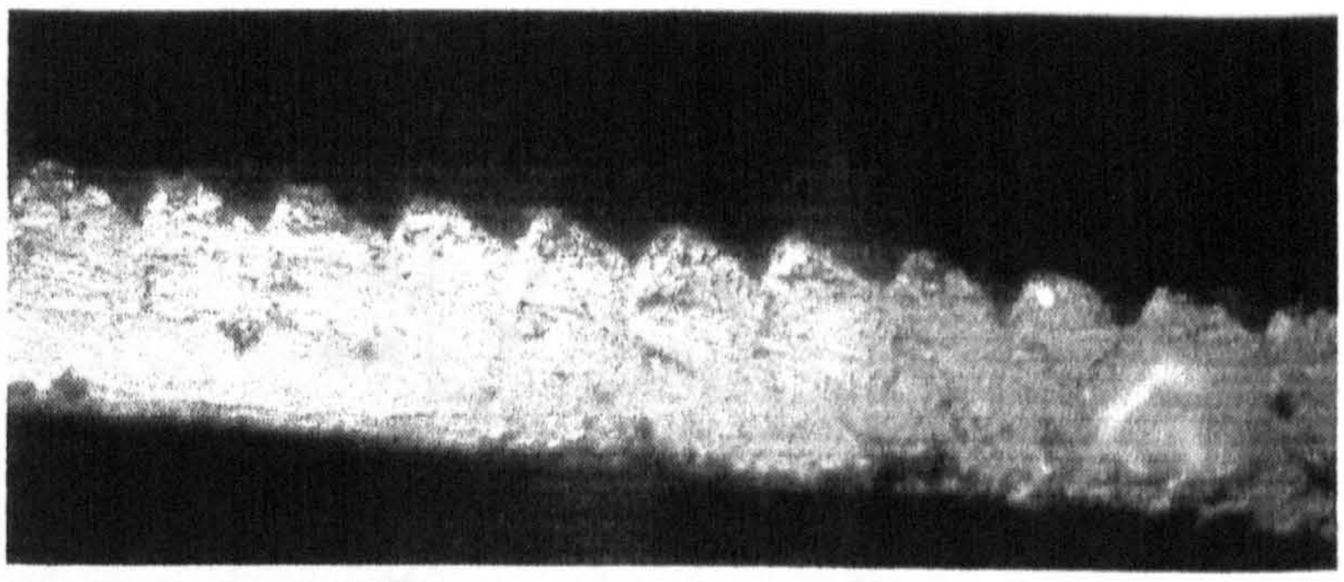

Fig 1-16: Merton Grating (30 μm pitch)

Flat samples generated on a shaping machine.

On discussion with the NPL workshop staff, it was decided that it would be possible to cut fine rulings into a flat surface, that on replication in transparent material would form a prismatic structure. Initially small-area prototypes (2.5 cm x 2.5 cm) were manufactured.

A fly cutting process was attempted in perspex and in delrin but was not successful because machines of sufficient quality were not available. Therefore grooves were cut using a shaping tool that was ground to the required profile (see Fig 1-17). The delrin proved to machine better than the perspex and resin replicas of the structure were made using the method described in section 1.5. Preliminary measurements showed that the prisms had a peak transmittance at approximately 10° for a source at 50° incidence. As this matched the design criteria, larger samples were manufactured (10cm x 30cm).

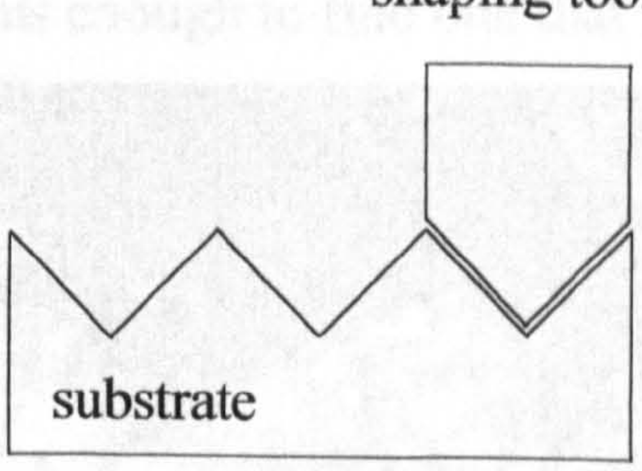

Fig 1-17: A shaping tool, ground to the correct profile is dragged along the substrate to form the groove profile.

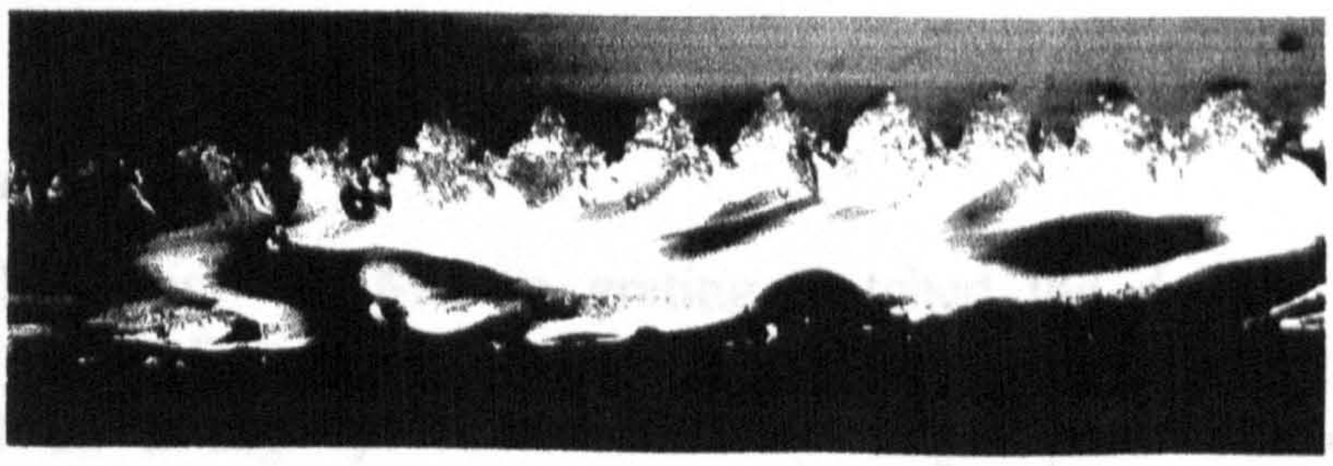

Fig 1-18: Grating cut with shaping tool (100 μm period).

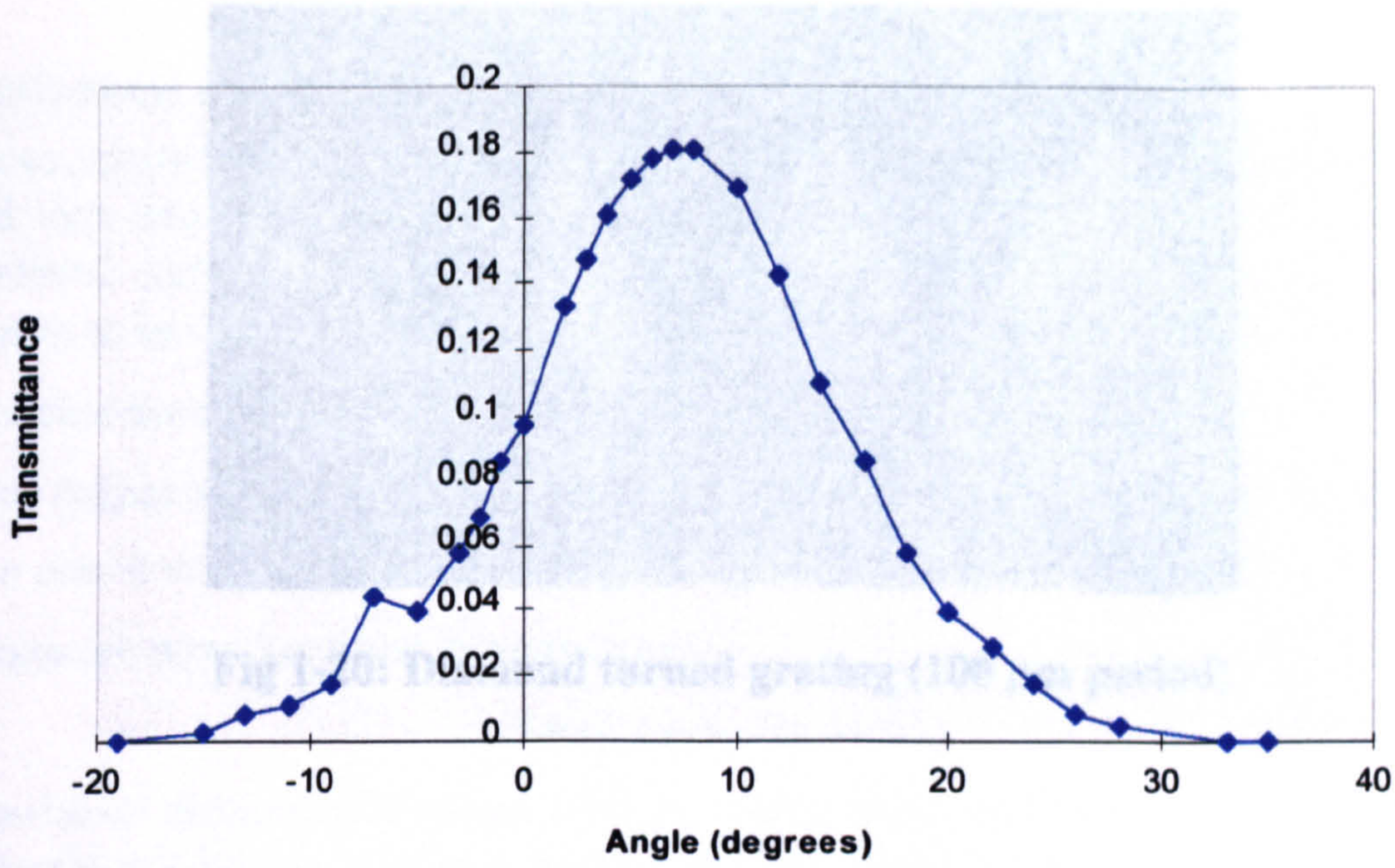

Graph 1-1: Transmission of white light through prisms created using shape cutter and source at 50°.

Echelle diffraction gratings

Echelle diffraction are efficiently blazed gratings that are produced on a ruling engine which is an extremely precise version of a workshop shaper. Consequently, the gratings are extremely expensive. However, a grating was already available at NPL and its performance assessed but we were not fortuitous enough to find one that matched our specifications.

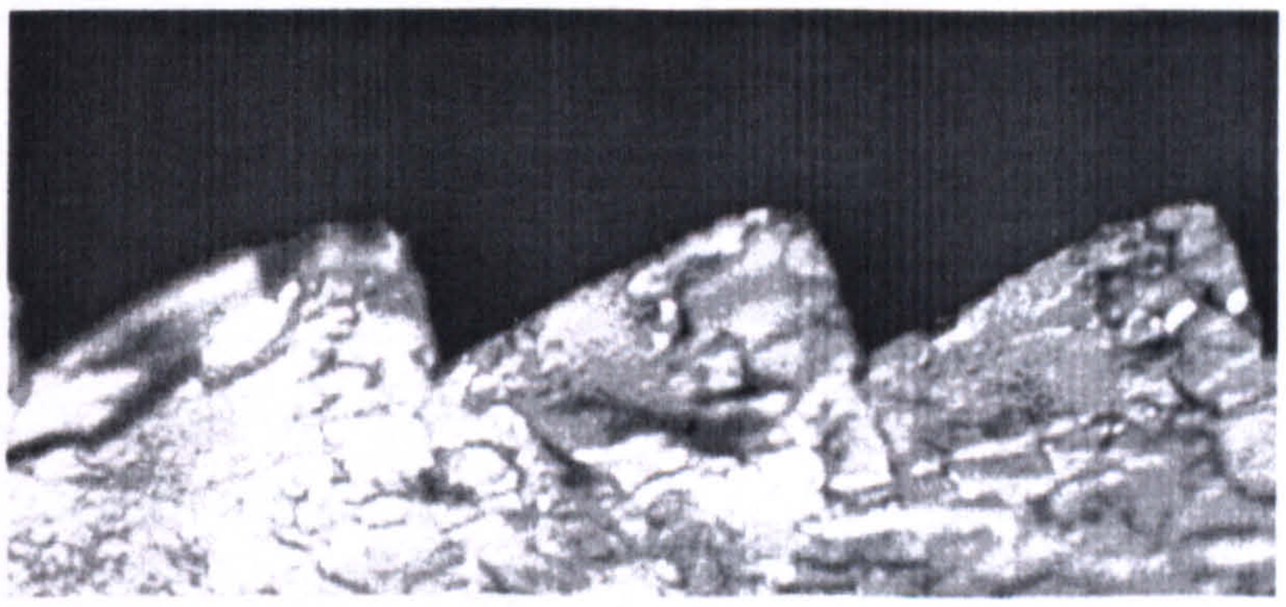

Fig 1-19: Echelle Grating (25 μm pitch)

Single point diamond turning

As neither the Echelle nor the Merton grating matched the desired specifications, an alternative, precisely-manufactured structure was sought. A sample was purchased that had been manufactured on a high precision lathe by single point diamond turning. The specifications for the structure were 50μm period and facet angles as described on in section 1.2.1. The manufacturing method involved cutting the structure into a rotating face-plate, resulting in concentric circular grooves. The face-plate was then divided into 4 equal squares containing grooves with 100mm radius of curvature. Unlike the structures cut by the shaping tool, the facets of these prisms are of high optical quality (see Fig 1-20) with sharp apexes.

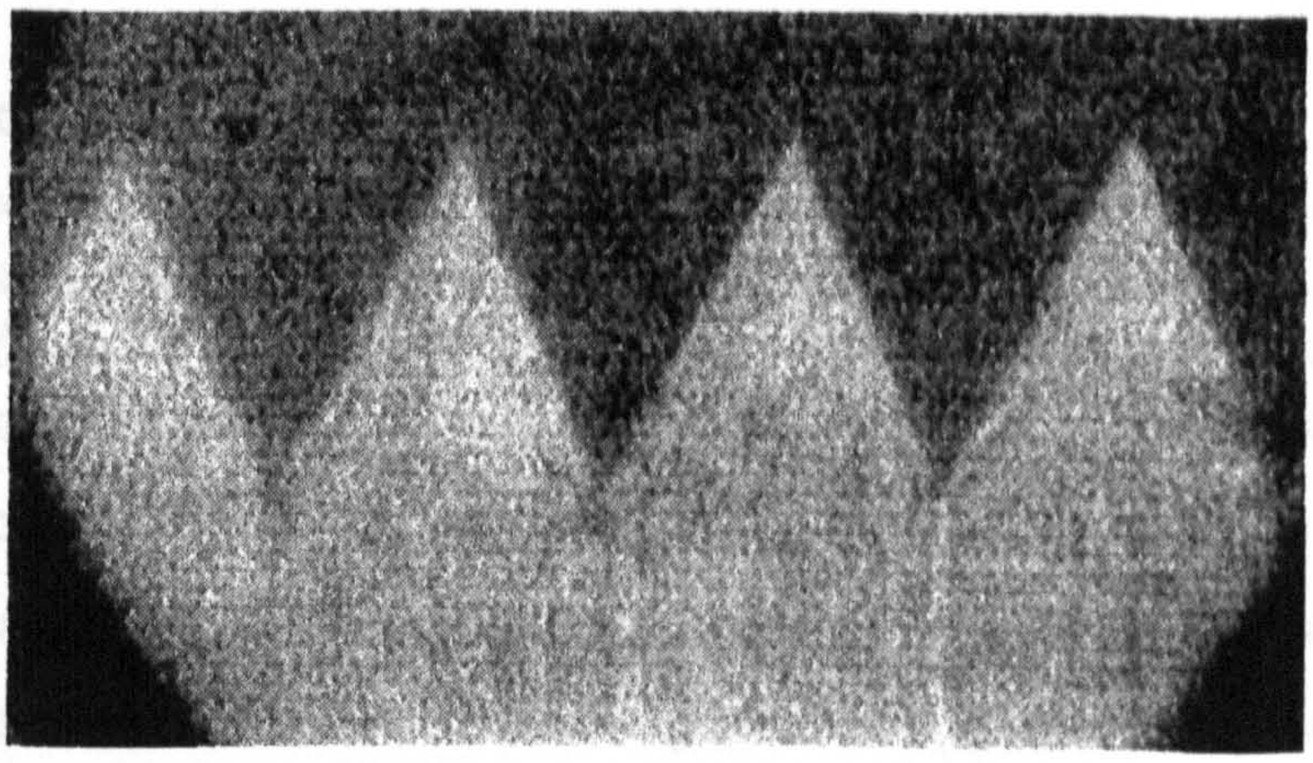

Fig 1-20: Diamond turned grating (100 μm period)

1.5 Replication of Micro-textured Surfaces

Most micro-textured surfaces are produced on opaque materials and therefore have to be replicated into transparent media for daylighting purposes. Furthermore, the production of micro-textured surfaces is technically demanding and therefore expensive, so small area masters have to be manufactured and many replicas combined to form a mosaic.

The replication process involves two stages:

1. A liquid rubber is applied to the original and hardened to produce a negative copy.
2. A resin cast is made of the rubber which is a positive copy of the original.

These stages are now described in more detail.

Stage 1 (see Fig 1-21)

A silicone-based elastomer is mixed with its curing agent and degassed. The mixing of the liquids should not be too vigorous because air becomes trapped in the liquid and leads to lengthy degassing times. The degassing process occurs in an evacuated bell jar that expands the bubbles in the liquid and bursts them (any bubbles left in the copy could produce imperfections in the profile). The elastomer is then poured directly onto the master (which is surrounded by a mould) and hardens at room temperature over 24 hours or at 90°C for one hour. Drying the liquid over a longer period produces a flatter back surface on the hardened rubber. Once solid, the rubber can be simply peeled from the master, giving a negative of the original profile. The process is very gentle and does not appear to harm the master at all.

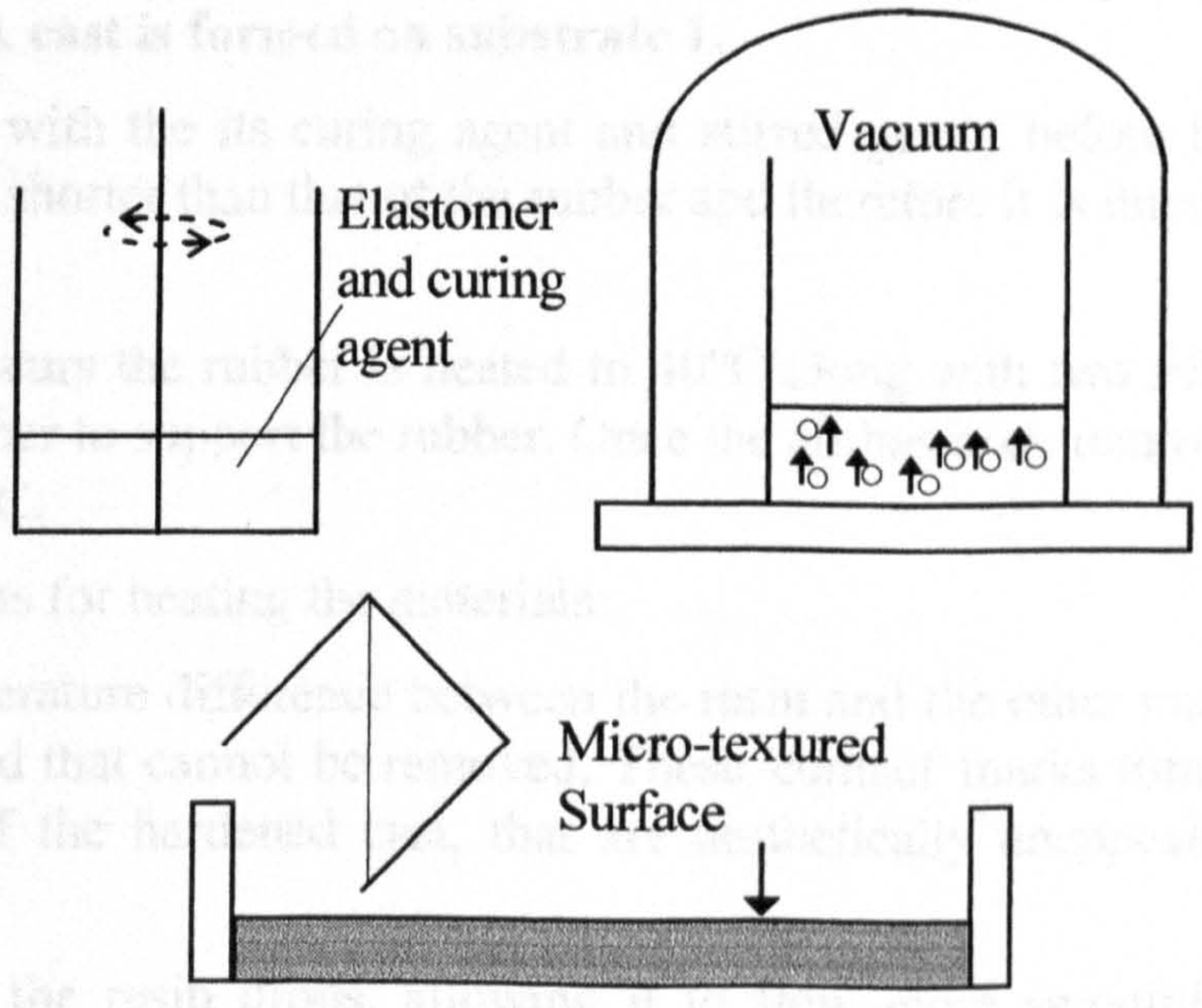

Fig 1-21: Stage 1. ***(Top Left)*** **The two liquids are mixed gently.** ***(Top Right)*** **The degassing process.** ***(Bottom)*** **Application of the elastomer.**

Stage 2 (see Fig 1-22)

The production of the resin cast creates more technical difficulties than the rubber, as it dries more quickly and is more prone to the retention of bubbles that disrupt the continuity of the structure.

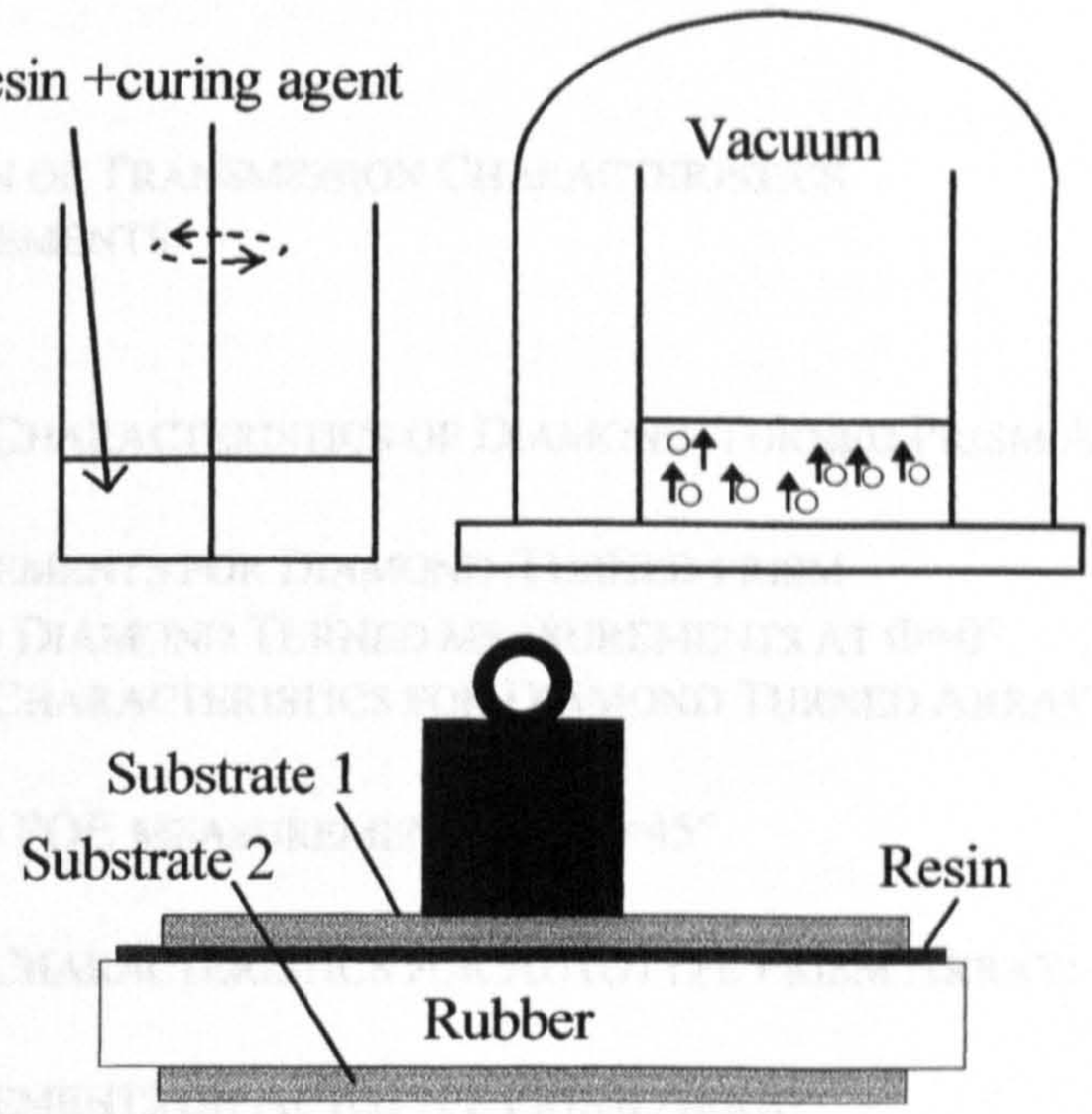

Fig 1-22: Stage2. ***(Top Left)*** **The two liquids are mixed gently.** ***(Top Right)*** **The degassing process.** ***(Bottom)*** **A cast is formed on substrate 1.**

The resin is mixed with the its curing agent and stirred gently before being degassed. The curing time is much shorter than that of the rubber and therefore it is important to trap as little air as possible.

Whilst degassing occurs the rubber is heated to 40°C along with two substrates: one for the resin cast and the other to support the rubber. Once the air has been removed from the resin, it is also heated to 40°C.

There are two reasons for heating the materials:

1. If there is a temperature difference between the resin and the other materials, tiny bubbles occur in the liquid that cannot be removed. These 'contact' marks form a web-like pattern on the surface of the hardened cast, that are aesthetically unappealing and disrupt the surface structure.
2. The viscosity of the resin drops, allowing it to flow more smoothly over the surface. However, the curing time reduces on heating so that once removed from the oven the remaining tasks must be completed rapidly.

Once everything is removed from the oven, the replication is carried out immediately. The first substrate is laid on a level surface, with the rubber on top and its profile facing upwards. The warm resin is then poured onto rubber and the final substrate is lowered onto the resin. The substrates should be slightly smaller than the rubber copy to avoid the meniscus left on the rubber upon drying, which would cause lifting between the substrates and rubber. The weight of the substrate pushes the resin over the rubber, but an extra mass is usually required to cover it completely. Most of the remaining bubbles should be ejected with the flow of the resin and any that are left squeezed out by applying extra pressure to the rubber. Unlike the

2. Characterisation of Prismatic Arrays

2.1 Introduction

The purpose of this section is to compare the transmission characteristics of the prism arrays to physical measurements on the saw-tooth structure. The former involves measurements on a goniophotometer and the latter using image analysis software in tandem with reflection measurements.

Three different samples were analyzed that had been embossed from the following masters:

- A diamond-turned array manufactured using single point diamond turning. Such a sample would be expected to have well-defined facet angles.
- An array purchased by Autotype. The master had been manufactured by cutting a saw-toothed structure into copper strips. As with the diamond-turned sample, this would be expected to have high quality facets.
- An array produced by shape-cutting into delrin. As the method of production was relatively crude, precise facet angles were not expected.

The shape-cut sample were expected to have lower transmission efficiencies at a given angle than the other arrays as their method of production was less precise.

2.2 Method

2.2.1 Determination of Transmission Characteristics

The facilities available at NPL for testing the samples are limited and therefore the following measurements were carried out in conjunction with the Fraunhofer Institute for Solar Energy. The first set of results were obtained using a goniophotometer (see Fig 2-1) to measure the bi-directional reflection/transmission function (BRTF). Fig 2-1 also shows the coordinate system that translates directly to the polar diagrams displaying the measurements.

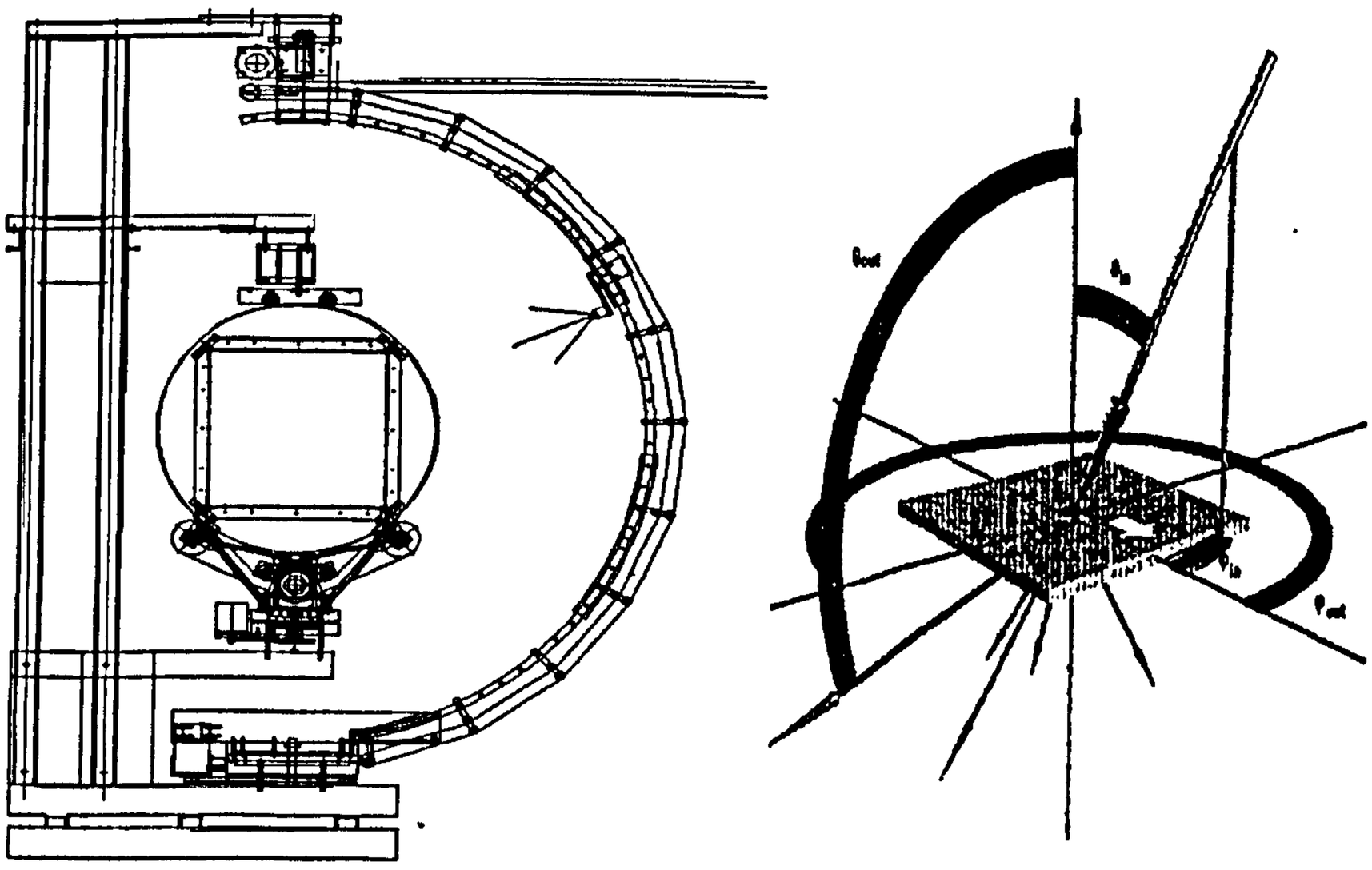

Fig 2-1: The goniophotometer (*right*) and its coordinate system.

The beam that is used to probe the sample and a typical polar plot are shown in Fig 2-2 and Fig 2-3 respectively.

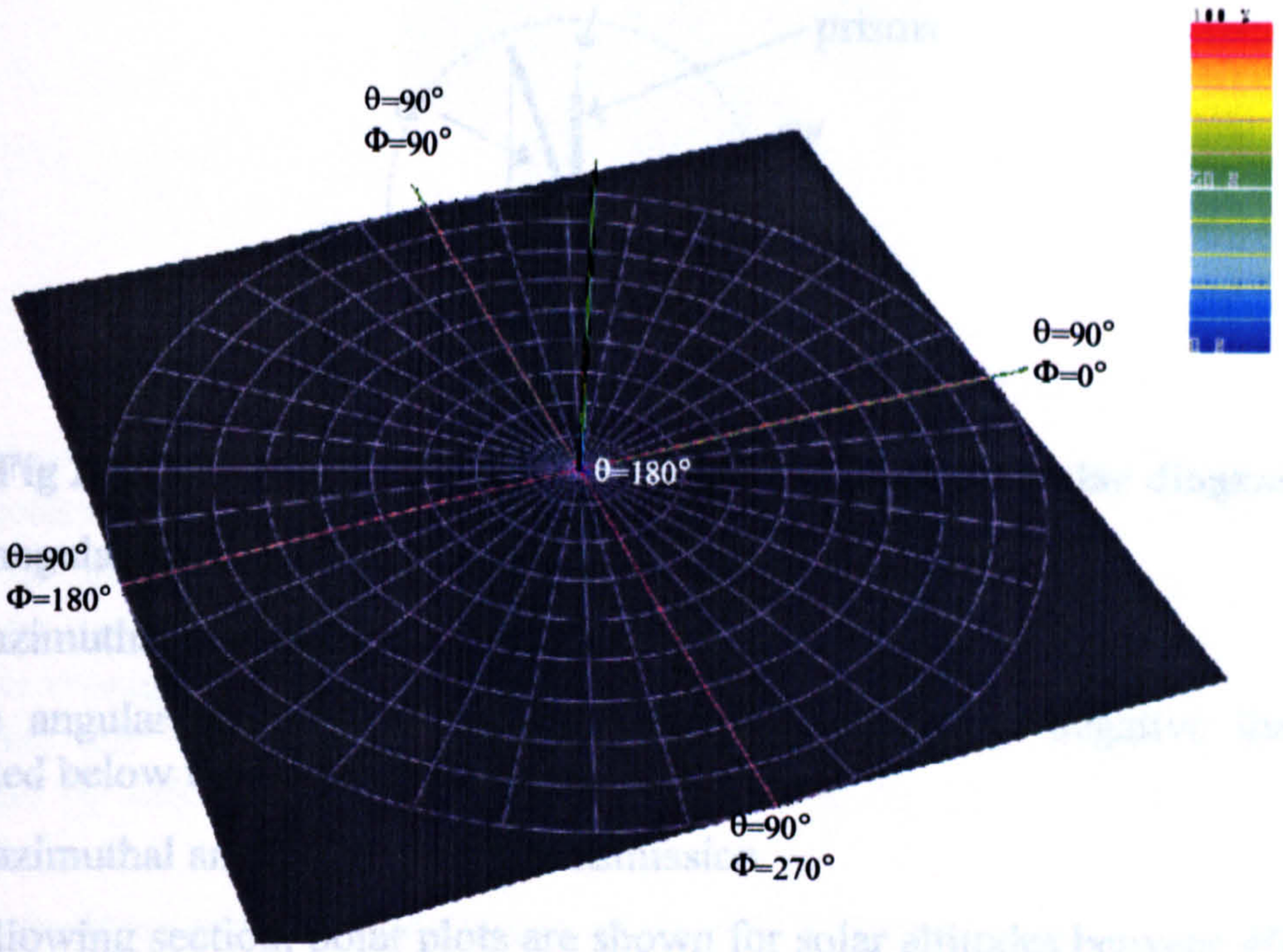

Fig 2-2: Reference beam without sample (used for all the structures) at θ=0°, Φ=0°.

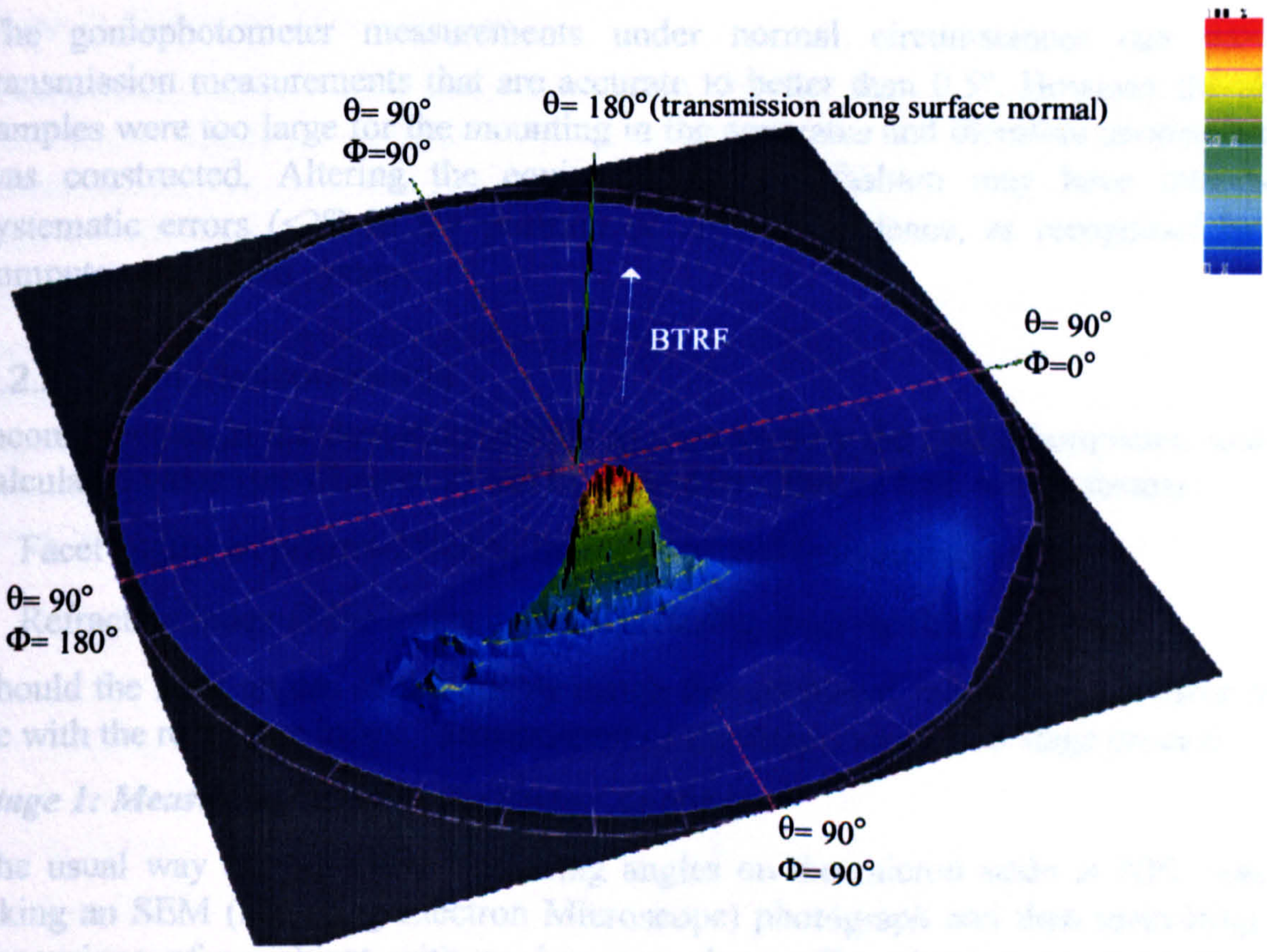

Fig 2-3: Polar diagram produced by the goniophotometer.

However, for this application, the polar plot is not the most useful output. A better performance indicator is to define a coordinate system in terms of the prism array, as it would be applied a window and this is shown in Fig 2-4.

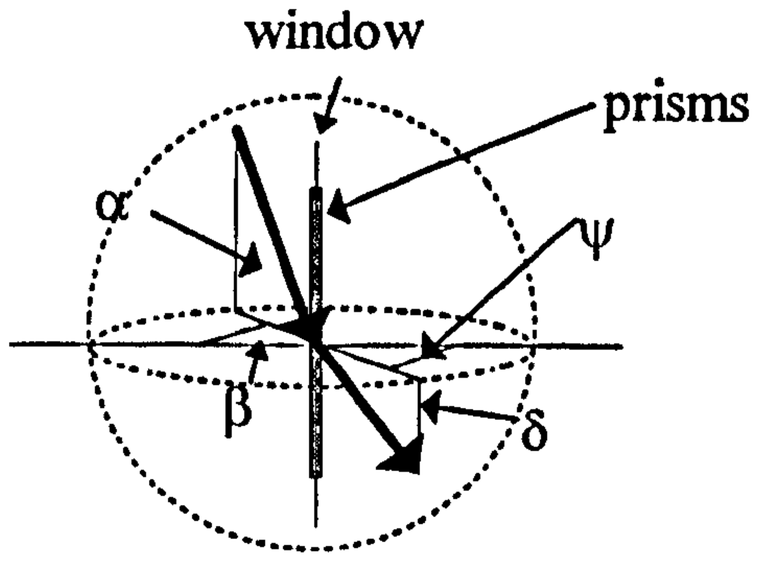

Fig 2-4: The coordinate system translated from the polar diagram

α is the angular altitude of the source

β is the azimuthal angle of the source

δ is the angular altitude of the peak transmission (when negative the light is transmitted below the horizontal)

ψ is the azimuthal angle of the peak transmission

In the following section, polar plots are shown for solar altitudes between 40° and 60° and azimuthal angles of 0° and 45°. Each has a diagram similar to that above to describe the effect for prisms applied to glazing.

Errors Associated with Goniophotometer Transmission Measurements

The goniophotometer measurements under normal circumstances can produce transmission measurements that are accurate to better than 0.5°. However the prism samples were too large for the mounting in the apparatus and therefore another holder was constructed. Altering the equipment in this fashion may have introduced systematic errors (<2°) in the position of normal incidence, as recognised by the computer-controlled system.

2.2.2 Facet Measurements

Inconsistencies in the deviation of light as measured by the goniophotometer, and the calculated value (see Chapter 2) can be caused by either or both of two factors:

- Facet angles on prisms differing from the desired (calculated) value.
- Refractive index of the prism material differing from the desired value.

Should the facet angles of the prisms match the calculated values then the error must lie with the refractive index. Measurement of the angles was a two-stage process.

Stage 1: Measurements with the Image Analyzer

The usual way of physically measuring angles on the micron scale at NPL was by taking an SEM (Scanning Electron Microscope) photograph and then measuring the dimensions of an object with an image analyzer. The photo is scanned into the computer then a straight line fitted to the facet. The computer measures the angle between the line and the horizontal. Fig 2-5 shows a typical photograph.

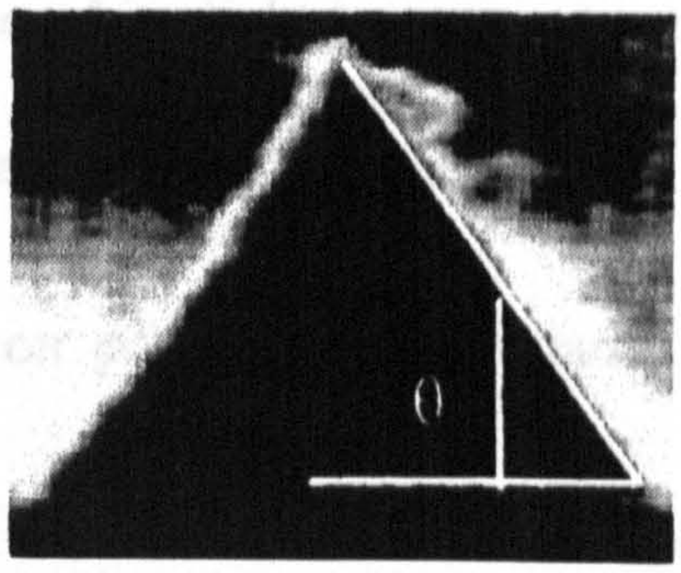

Fig 2-5: Facet angle measurements on SEM photographs.

Each measurement was performed 3 times and the average taken as the facet angle of that particular prism. To compensate for any image distortion each prism is rotated through 90° and photographed a second time. The same 3 measurements are then repeated on this second image of the same prism and averaged to give a second facet angle. The average of these 2 facet angels is taken to be the true angle of the prism. To characterise the whole array, all the prism angles are averaged and the error determined by calculating the standard deviation at the 95% confidence level (see Appendix A).

Errors Associated with Measurements on the SEM Photographs

Judging the 'best fit' of the horizontal line to the facet of the prism is the major source of systmatic error with this method, as it is subjective. However this would be no more than 1°.

Stage 2: Reflection Measurements

Measurement of the individual prisms can be a long process, especially if a statistically significant sample is required. Therefore, in the second part of the measurement process a relatively large area of the sample was illuminated and the angle of reflection measured.

The advantage of reflection over transmission measurements is that the results do not depend on the refractive index of the material. The angle of light reflected from a surface is dependent on the angle of incidence between the source and the surface normal. By reflecting a well-collimated beam of light off the facets of the prisms, the direction of the surface normal could be determined and therefore the facet angle. Using this method it is estimated that the facet angles could be determined to ±1°.

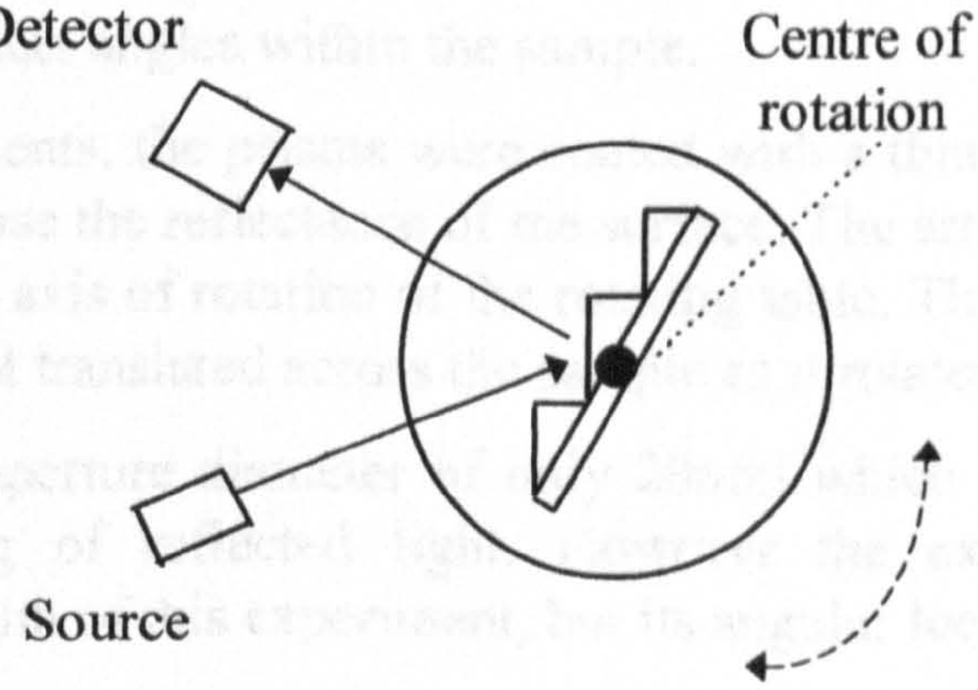

Fig 2-6: Measurement of prism angles by reflectance.

The angular divergence of the white light beam used was 0.02°, with a diameter of 11mm. Thus (11÷P) prisms are illuminated, where P is the period of the array measured in stage 1. It is assumed that the facet angle does not vary significantly along the length of one prism.

Prior to any measurements on prisms, the reflectance from a plane mirror was measured.

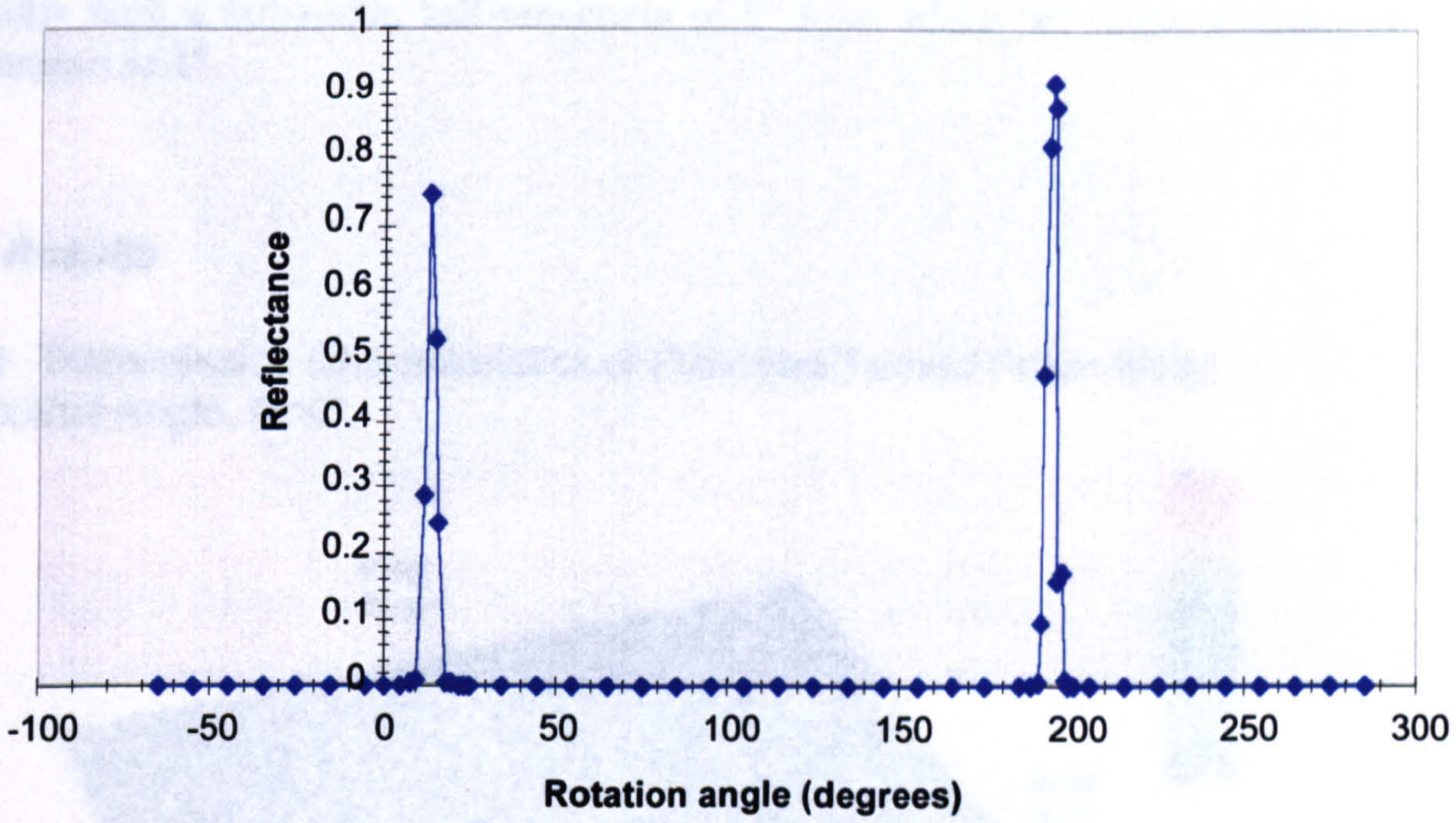

Graph 2-1: Reflectance versus angle of rotation for a plane mirror. Reflection from front surface at 14° and back surface at 194°.

The location of the reflection from the front surface gives the angular separation of the source and detector, which was 14°.

By using a well collimated of light, the spread of the reflectance angles may provide a gauge as to the range of the facet angles across the array. Graph 2-1 shows that the beam reflected from a flat surface forms a well-defined peak with a full-width, half maximum of approximately 3°. Any broadening of the curve on reflection from a prism sample could be either due to:

- Scatter from the surface.
- A range of prism facet angles within the sample.

Prior to the measurements, the prisms were coated with a thin layer (approx. 50 nm) of aluminium to increase the reflectance of the surface. The array, source and detector are all centered on the axis of rotation of the rotating table. This ensured that the area of illumination was not translated across the sample as it rotated.

The detector had an aperture diameter of only 20mm which meant there may have been some vignetting of reflected light. However the exact amplitude of the reflectance is not the aim of this experiment, but its angular location.

Each sample was measured in two different regions of the array to ensure that there were no variations in facet angle across the array.

Errors Associated with Reflection Measurements on the Prism Facets

Prior to measuring the angles of the prism facets, a back reflection from the array's base substrate was used to zero the rotation scale to an accuracy of 0.5°. The sample was then rotated by 180° and the facet angles measured.

The full width, half maximum of a peak reflection from a well-mirrored surface (see Graph 2-1) results in an accuracy of 0.5°. The reflections from the prism facets typically have a full-width, half-maximum of 8° from which the centre accuracy is determined to 1°.

2.3 Results

2.3.1 Transmission Characteristics of Diamond-Turned Prism Array: Azimuthal Angle, Φ=0°.

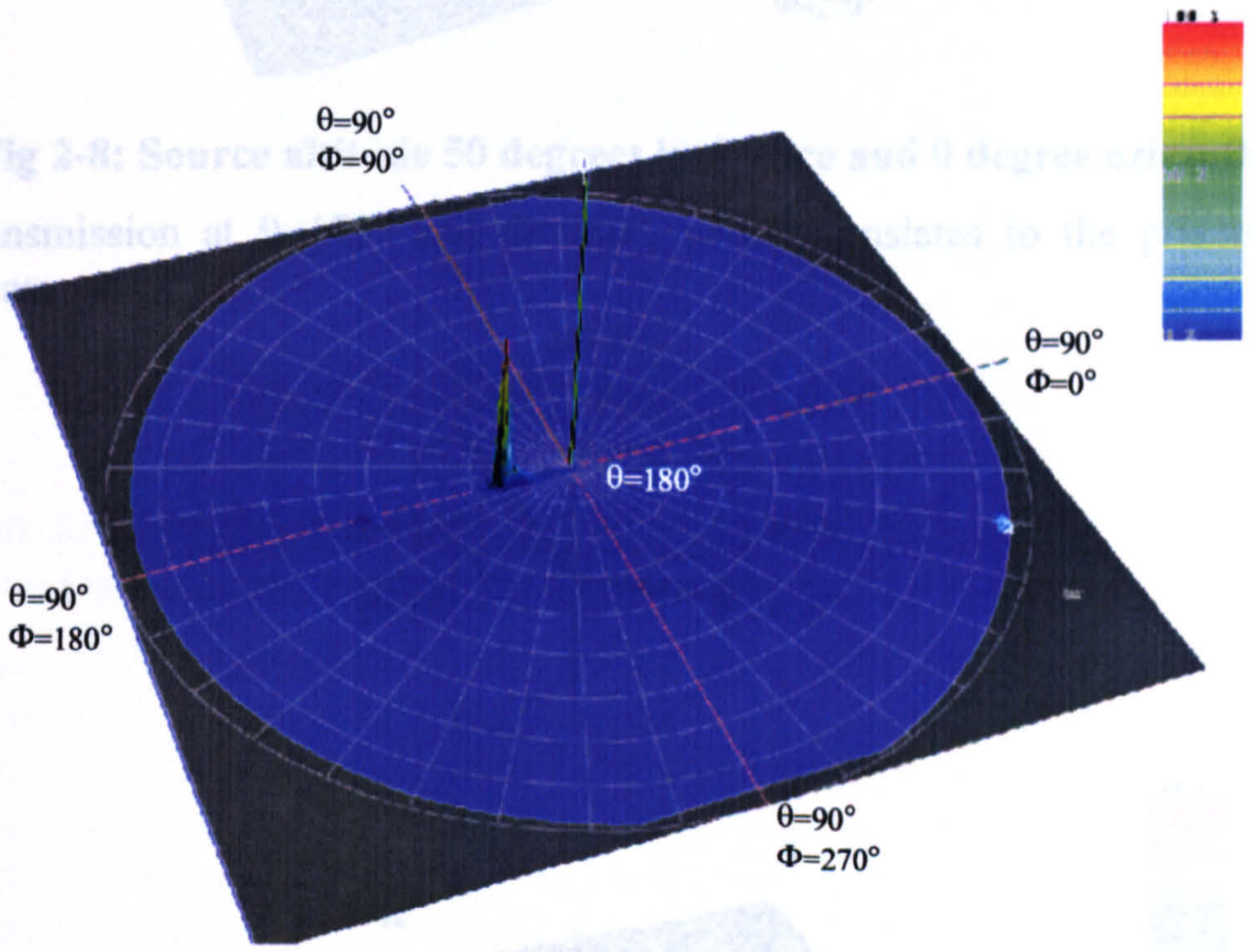

Fig 2-7: Solar altitude 40 degrees and 0 degree azimuth.

Peak transmission at θ=165° and Φ=180°, which translates to the prisms on the window as:

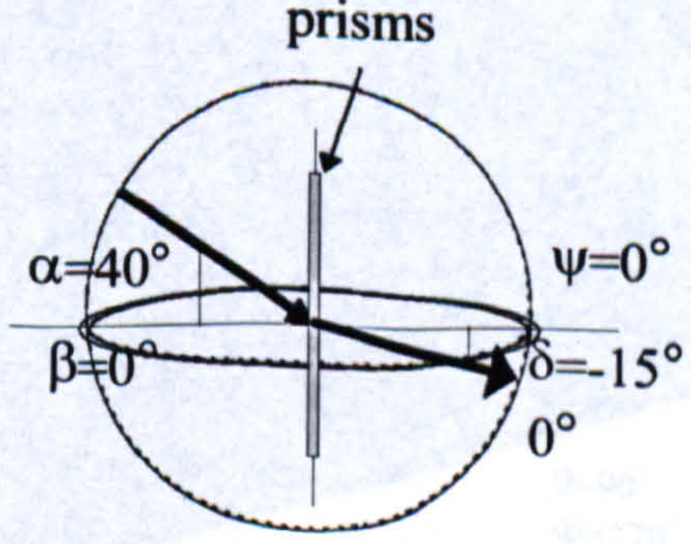

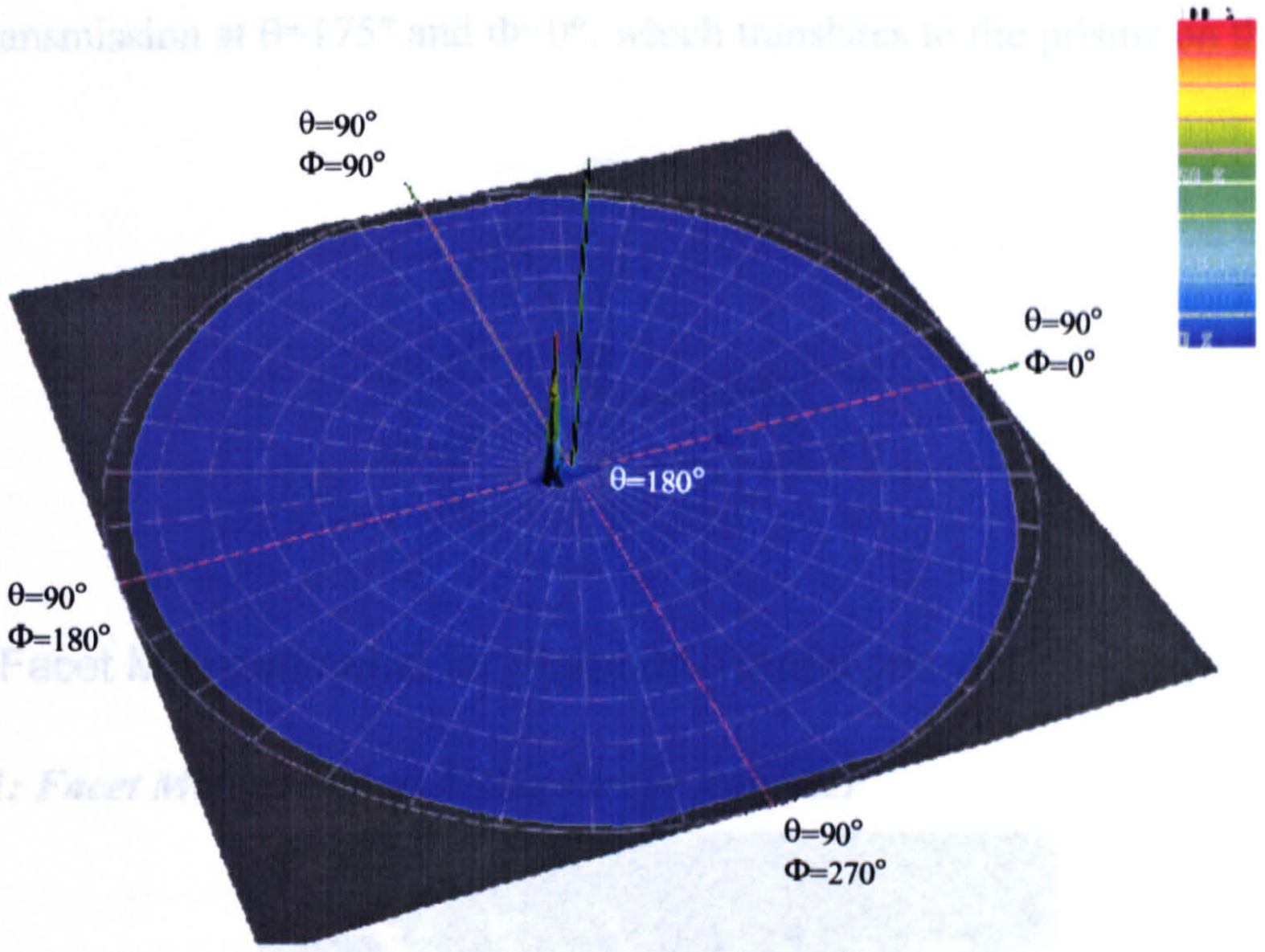

Fig 2-8: Source altitude 50 degrees incidence and 0 degree azimuth.

Peak transmission at θ=175° and Φ=180°, which translates to the prisms on the window as:

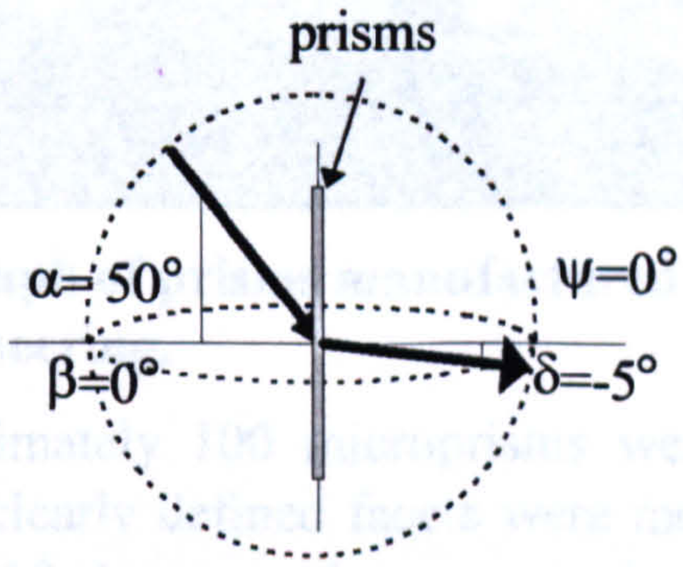

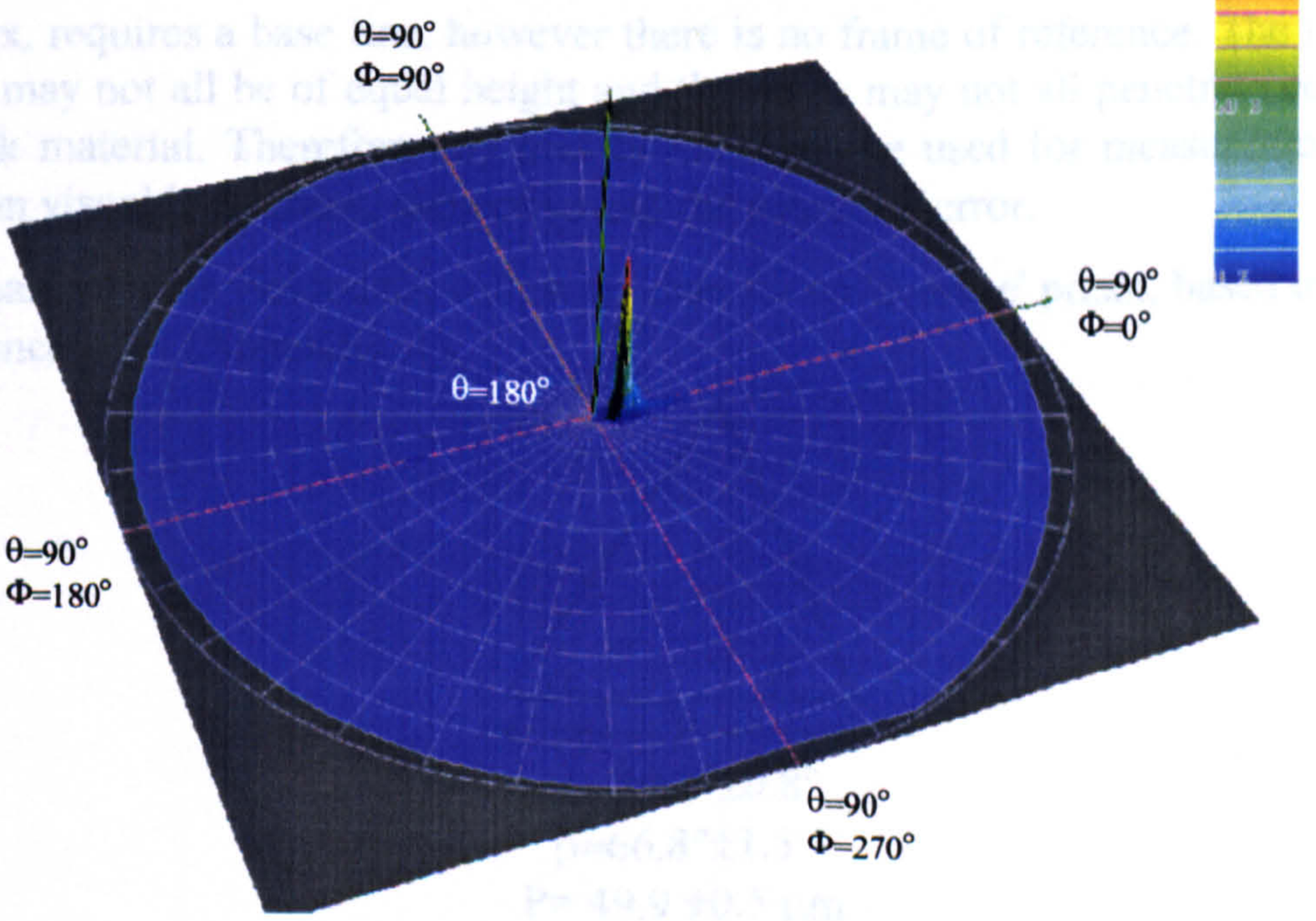

Fig 2-9: Source Altitude 60 degrees and 0 degree azimuth.

Peak transmission at θ=175° and Φ=0°, which translates to the prisms on the window as:

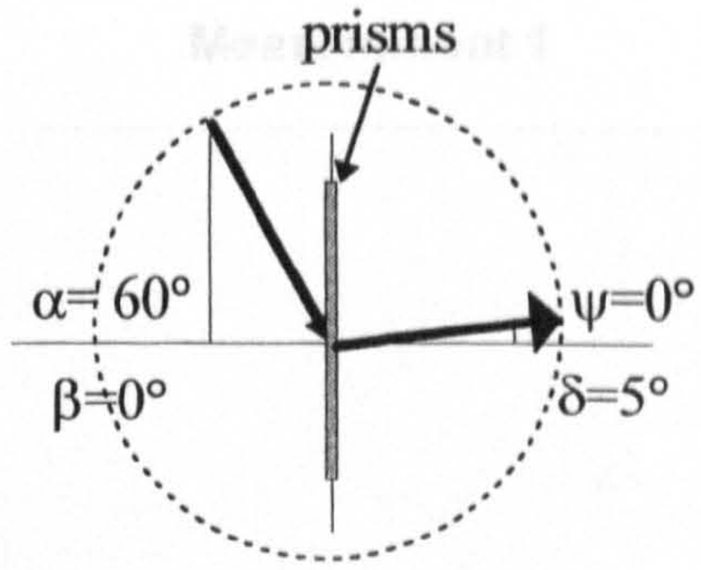

2.3.2 Facet Measurements for Diamond-Turned prism

Stage 1: Facet Measurements Using Image Analyser

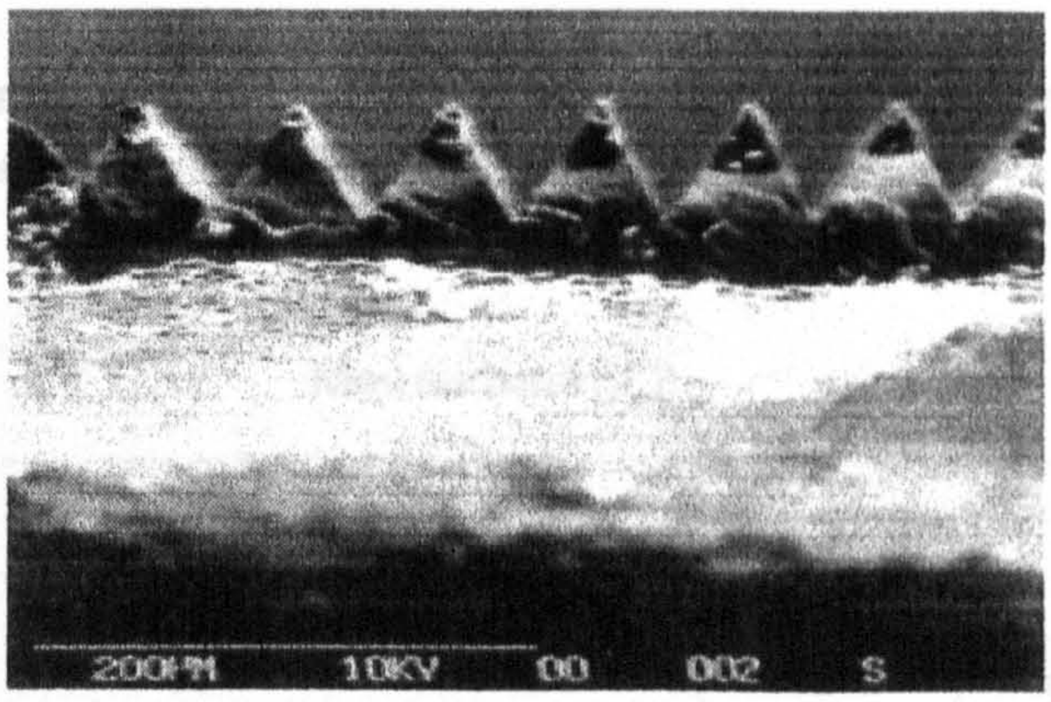

Fig 2-10: SEM photograph of prisms manufactured from a master created by Precision Optical Engineering.

Using the SEM approximately 100 microprisms were photographed. Of these 18 prisms with the mostly clearly defined facets were measured on the image analyzer. The photograph in Fig 2-10 shows another source of error in the measurement process and that is the definition of a horizontal. Measurement of the facet angles, other than the apex, requires a base line, however there is no frame of reference. The tops of the prisms may not all be of equal height and the bases may not all penetrate equally into the bulk material. Therefore any line 'horizontal' line used for measurement will be based on visual judgement, subjective and the source of error.

The measurements yielded the following data for an 'average' prism, based on the 95% confidence level (Appendix A):

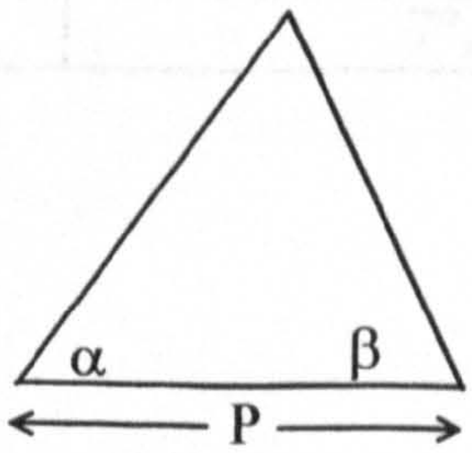

α= 59.1°±0.8°

β=66.8°±1.5°

P= 49.9 ±0.5 μm

Stage 2: Reflection Measurements

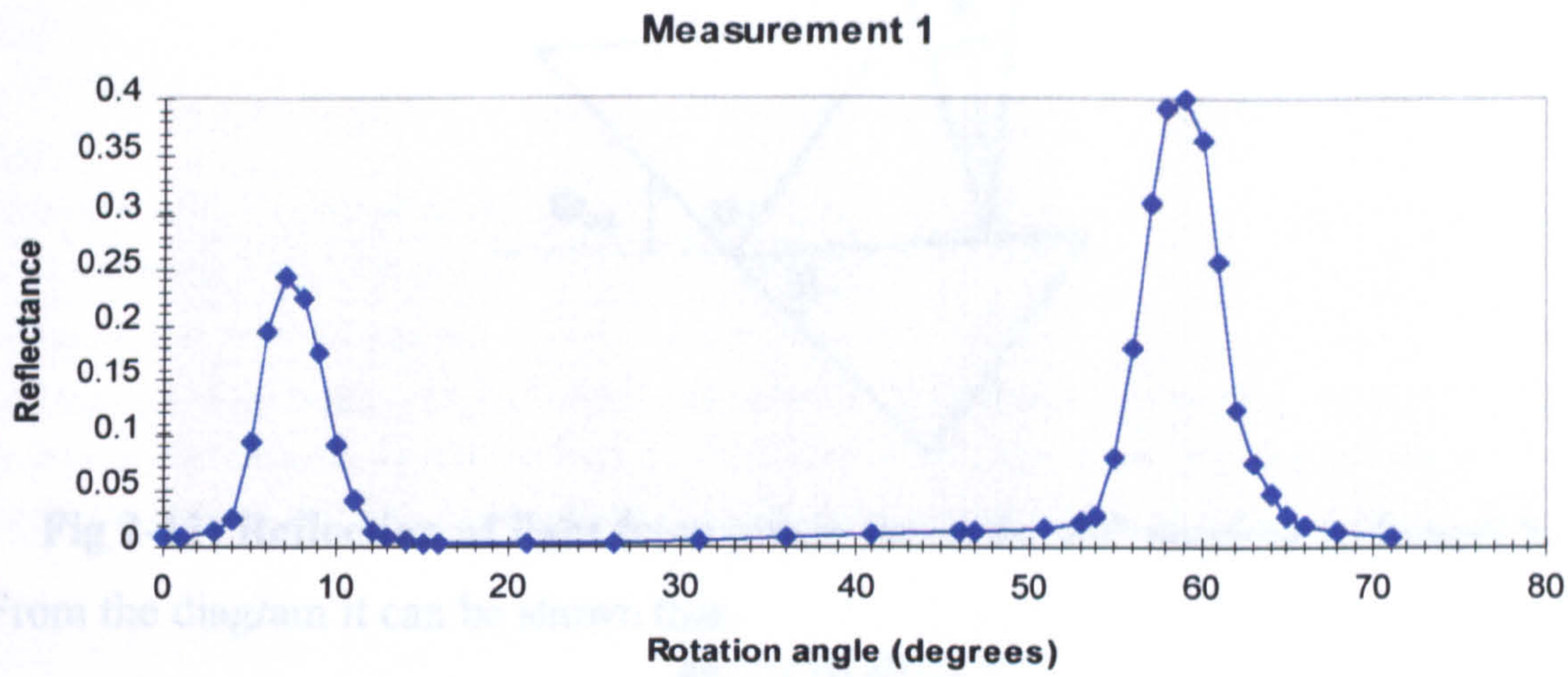

Graph 2-2: Reflectance versus rotation angle for prisms generated from POE master- measurement 1.

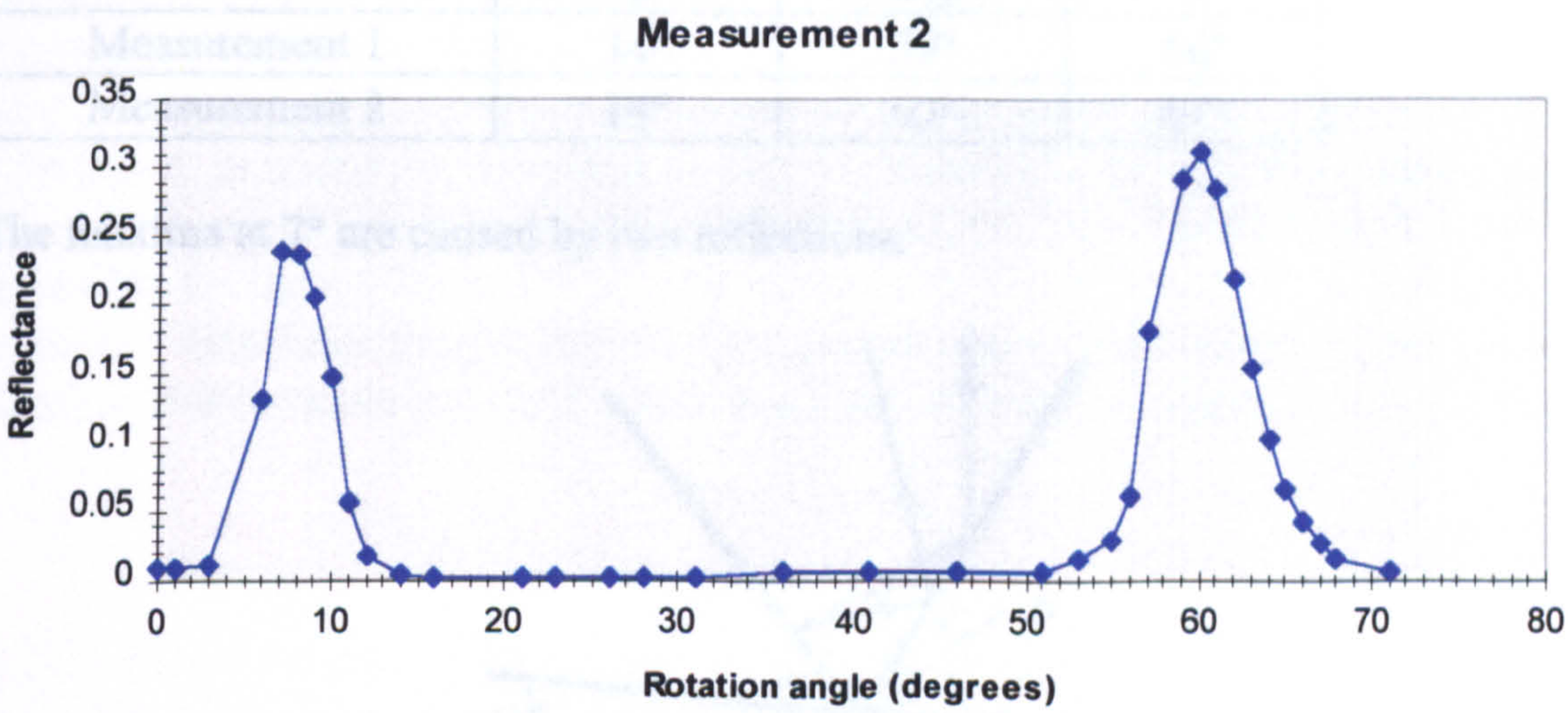

Graph 2-3: Reflectance versus rotation angle for prisms generated from POE master- measurement 2.

	Rotation Angle of Maxima
Measurement 1	7°, 59°
Measurement 2	7°, 60°

The peaks around 60° are the result of a single reflection as shown in Fig 2-11:

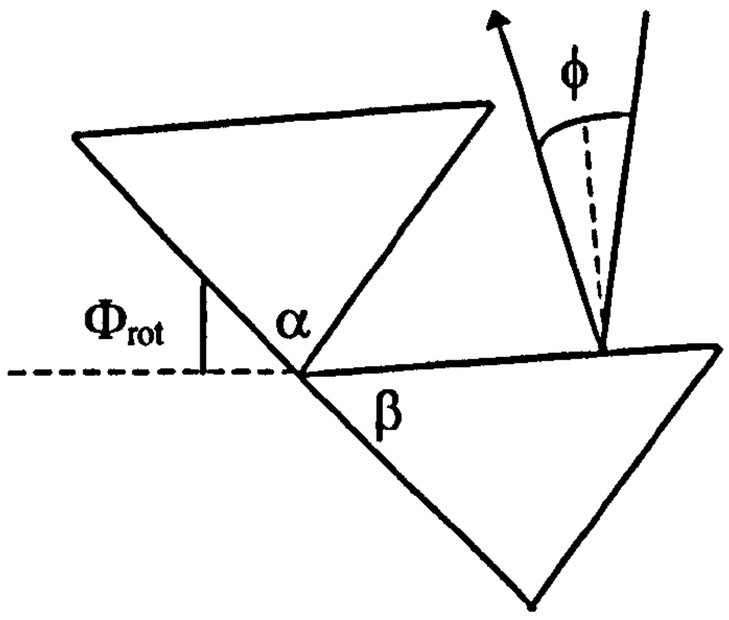

Fig 2-11: Reflection of light from prism facets for 60° maxima in Graph 2-3.

From the diagram it can be shown that:

$$\phi = 2 \times (\beta - \Phi_{rot})$$

where ϕ is the angular separation of the source/detector

β is the prism angle

Φ_{rot} is the rotation angle of the prism array

Therefore:

	ϕ	Φ_{rot}	β
Measurement 1	14°	59°	66°
Measurement 2	14°	60°	67°

The maxima at 7° are caused by two reflections.

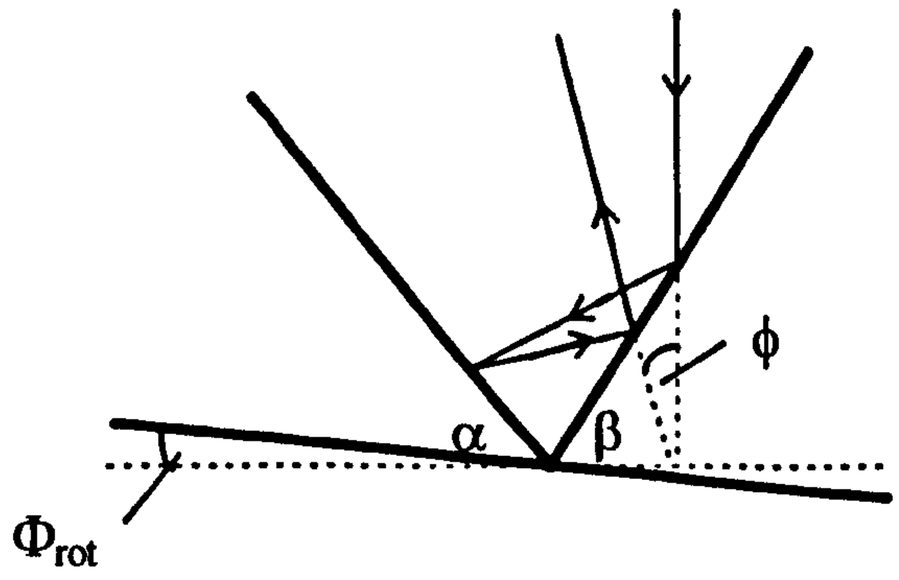

Fig 2-12: Reflection of light from prism facets for maxima at 7° in Graph 2-3.

From the diagram it can be shown that:

$$\phi = 2(\beta - \Phi_{rot}) - 2(\alpha + \Phi_{rot})$$

$$\therefore \phi = 2(\beta - \alpha) = 2\Phi_{rot}$$

These maxima only occur because the source/detector separation happens to be twice the difference between the prism angles.

Therefore:

	ϕ	Φ_{rot}	β	α
Measurement 1	14°	7°	66°	59°
Measurement 2	14°	7°	67°	60°

Using the same method

Comparison of results between stage 1 and stage 2 for POE prisms

	α	β
Stage 1		
Averaged over 18 prisms	59.1°±0.8°	66.8°±1.5°
Stage 2		
Measurement 1 (220 prisms)	59°±1°	66°±1°
Measurement 2 (220 prisms)	60°±1°	67°±1°
Averaged over 440 prisms	59.5°±1.4°	66.5±1.4°

The results for both stages show excellent agreement to within less than 0.5°. Therefore the results in stage 1 of the individually measured prisms are likely to be representative of the facets across the whole array.

2.3.3 Conclusion to Diamond Turned measurements at Φ=0°

	Calculated	Measured
α	60°	59.5°±1.4°
β	67.9°	66.5°±1.4°
Transmission angle at 40° incidence	δ= -10.5°/85°	δ= -15°
Transmission angle at 50° incidence	δ= 10.5°/81°	δ=10°
Transmission angle at 60° incidence	δ= -3.5°	δ= 5°

There is a clear difference between the calculated and measured values for the angles of deviation provided by the prisms. The measurements on the facet angle angles demonstrate consistency with the calculated angles and therefore could not be responsible for the variation. However it is more likely to be the result of reflections at the second interface being close to the critical angle and therefore total internal reflection. For the resin (n=1.567) to air boundary the critical angle is:

$$\sin \theta_c = (1/n)$$

$$\therefore \theta_c = 40°$$

Fig 2-13 shows the path of rays at 50° incidence and its proximity to the critical angle. Graph 2-4 shows the highly critical dependence of the transmission angle on the incident angle. The precise value of the prism refractive index was unknown, but estimated by the manufacturers to be between 1.53 and 1.58. Consequently the Graph describes transmission angles for several values of 'n' within this range.

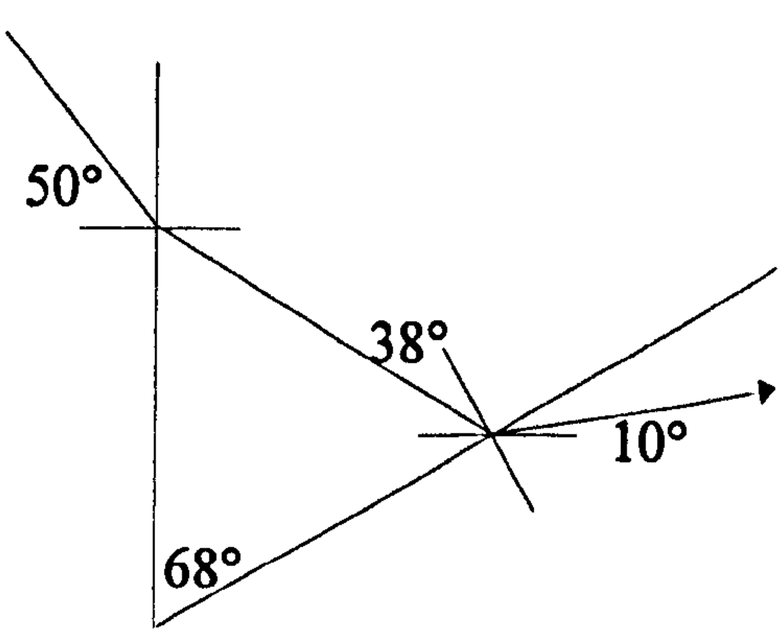

Fig 2-13: Path of a light ray through the prism. The angle of incidence at the second interface (38°) is close to the critical angle (40°).

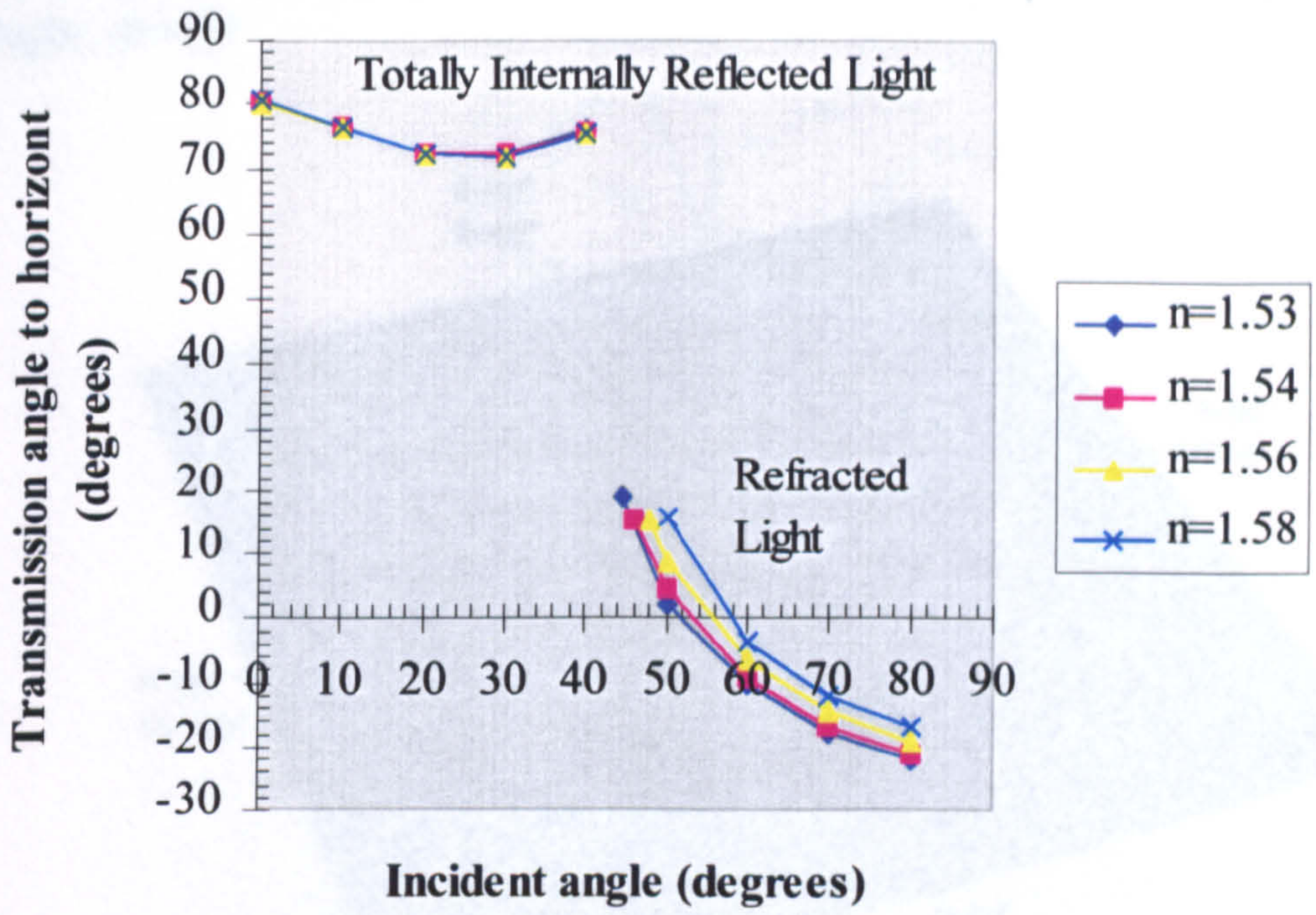

Graph 2-4: Variation in transmission angle with incident angle and refractive index for the prismatic structure. The discontinuity is a result of Total Internal Reflection at the prism/air boundary, which occurs for incident angles between 39° and 41° (depending on n). Light that has undergone Total Internal Reflection is transmitted through the top of the prism after suffering a further refraction at the prism/air boundary.

Graph 2-4 shows between 40° and 60°, a 1° variation in incidence produces a 10° variation in the transmission angle. Other possible sources of such variations that could have lead to inconsistencies between the measured and calculated values include:

- The positioning of the sample in the goniophotometer. Due to its relatively large size, the sample had to be situated in a specially constructed holder. As a consequence small inaccuracies in its angular position may have been introduced.
- The transparent perspex substrate on to which the prismatic structure was replicated and tested. The base substrate was ignored in the calculation of the paths through the prism. It would only introduce an error of approximately 1° in the angle of incidence on the first prism facet, however this has proved to be critical.

However as these errors do not entirely account for the variations, the problem must result from uncertainties in the value of the prisms' refractive index.

2.3.4 Transmission Characteristics for Diamond Turned Array: Azimuthal Angle, Φ=45°

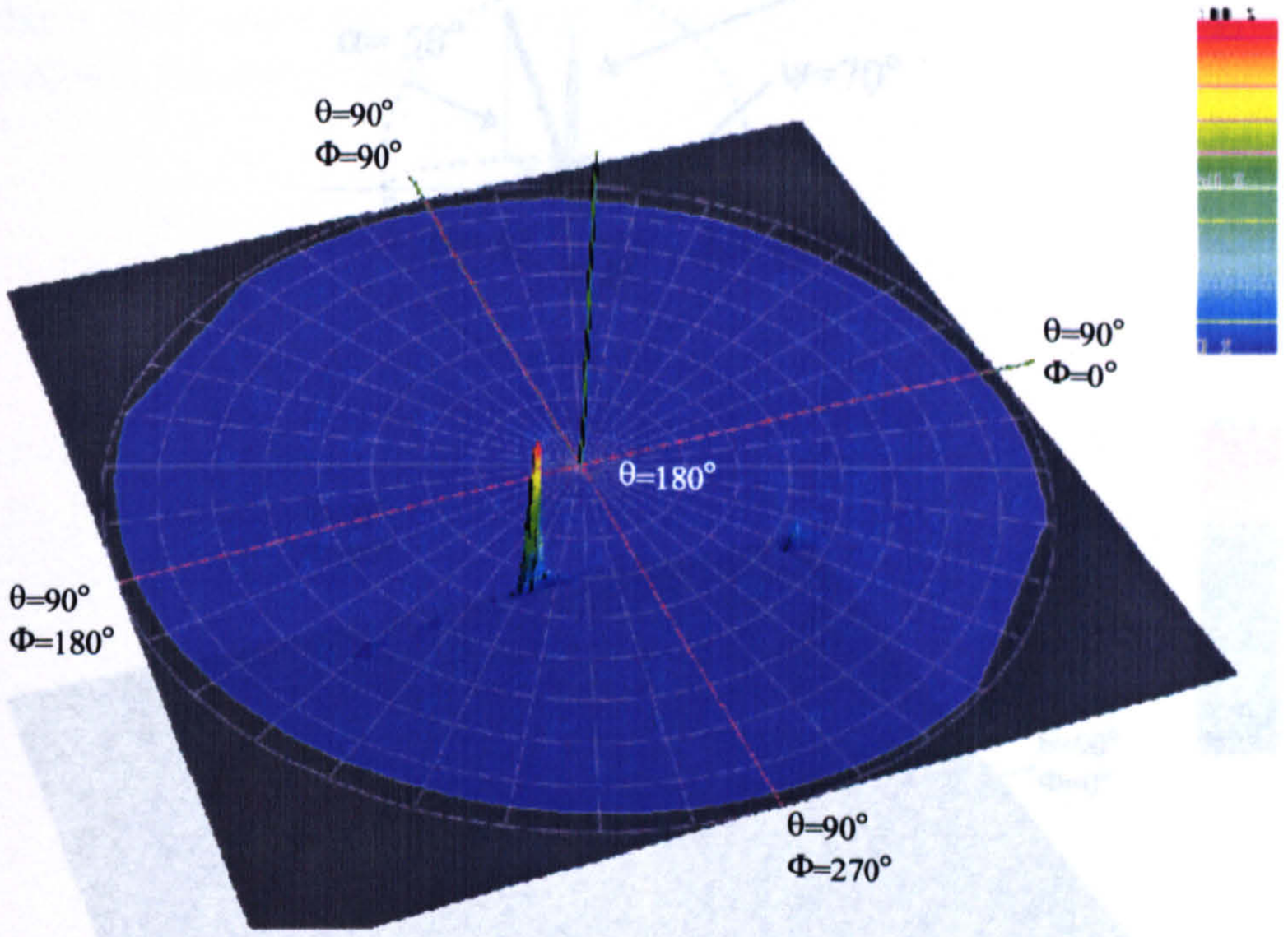

Fig 2-14: Source altitude 40 degrees and 45 degrees azimuth.

Peak transmission at θ=145° and Φ=230° and FWHM of approx. 5°

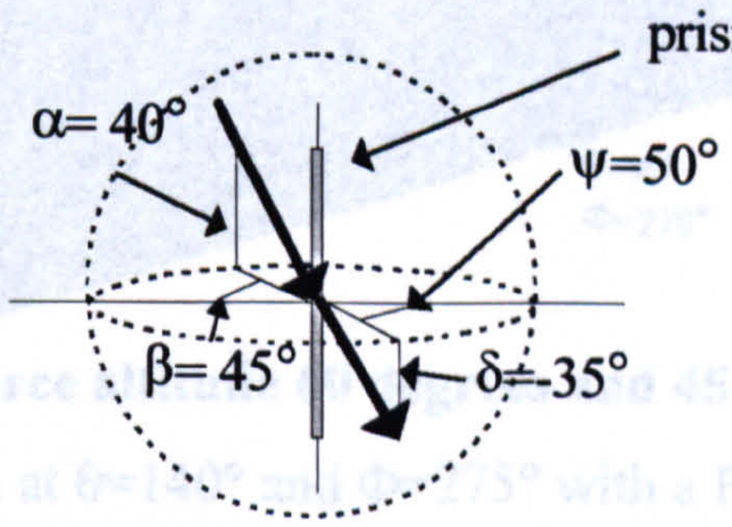

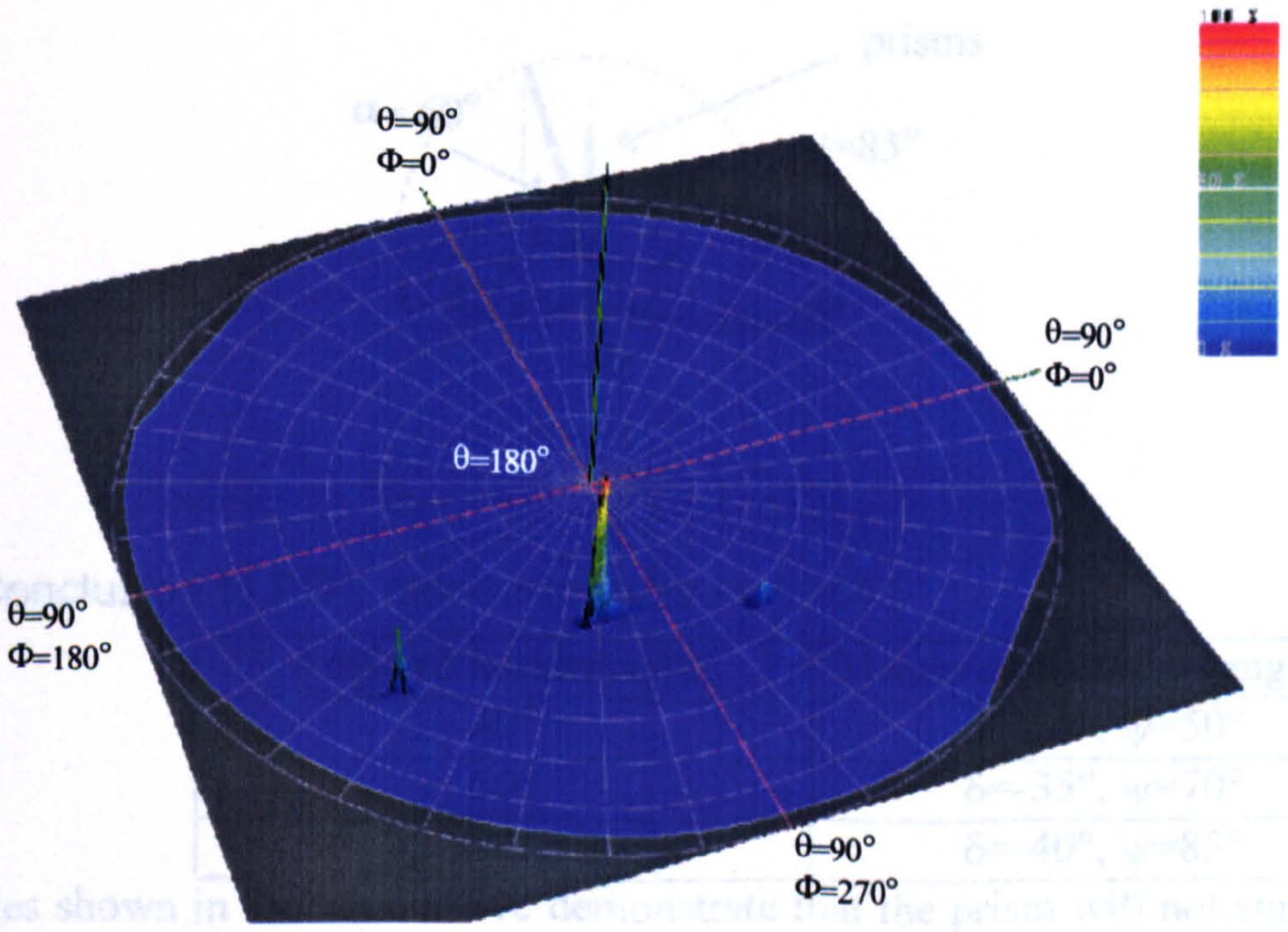

Fig 2-15: Source altitude 50 degrees and 45 degrees azimuth.

Peak transmission at θ=145° and Φ=250° with a FWHM of approx. 5°.

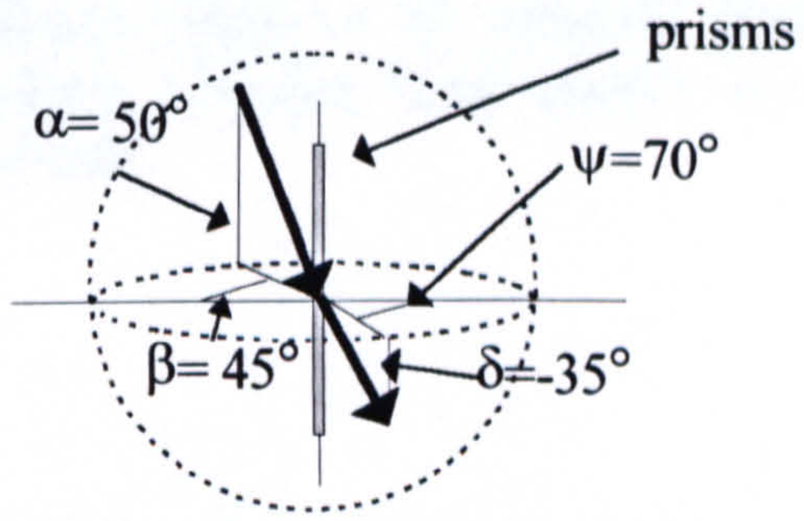

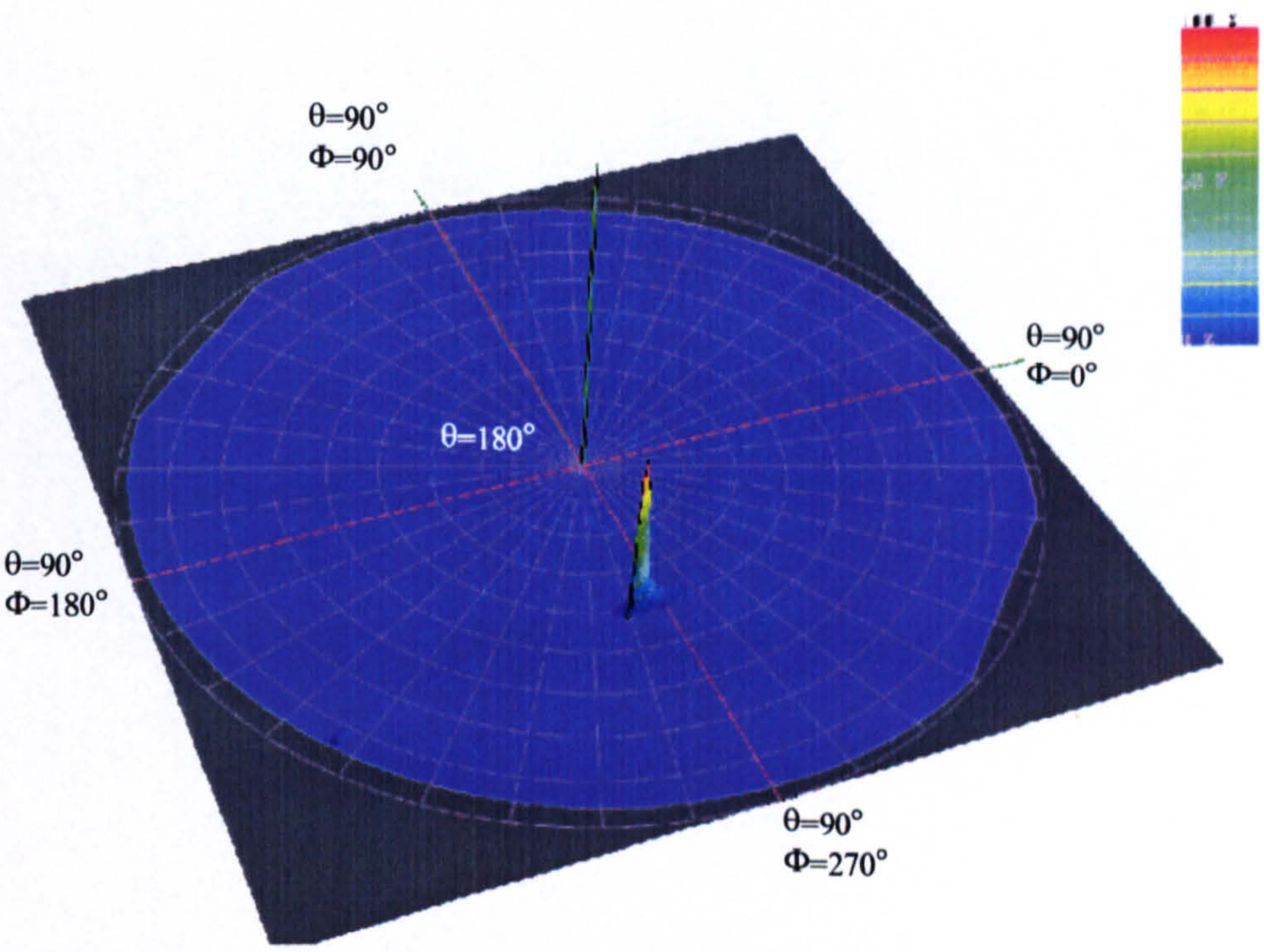

Fig 2-16: Source altitude 60 degrees and 45 degree azimuth.

Peak transmission at θ=140° and Φ=275° with a FWHM of approx. 5°.

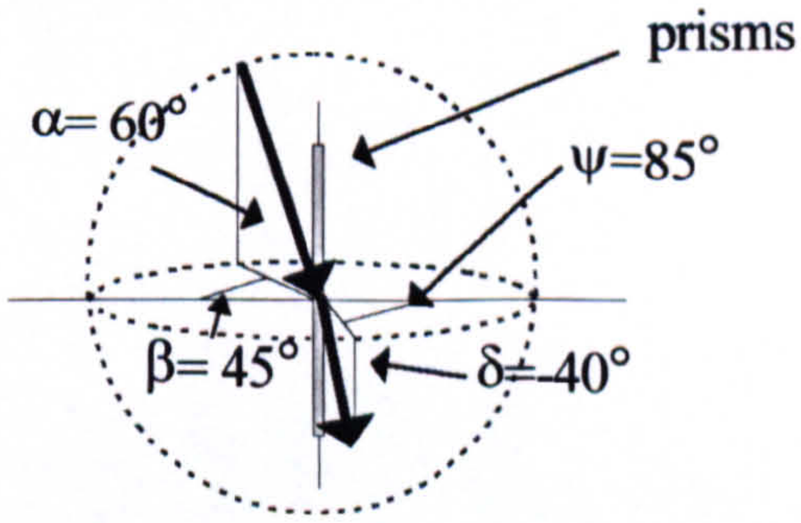

2.3.5 Conclusion to POE measurements at Φ=45°

Angle of incidence (θ)	Measured deviation angle
40°	δ=-35°, ψ=50°
50°	δ=-35°, ψ=70°
60°	δ=-40°, ψ=85°

The angles shown in the table above demonstrate that the prism will not significantly deviate the azimuthal component of the light. In the azimuthal plane light is only deviated by the change in refractive index and remains unaffected by the prism

This may be a serious limitation to the prism's performance as a daylighting system. Calculating the transmission angles at 45° azimuth through the prismatic structure would have been extremely complex. Consequently it is not possible to compare theoretical and measured data.

2.3.6 Transmission Characteristics for Autotype Prism Array: Azimuthal Angle, Φ=0°

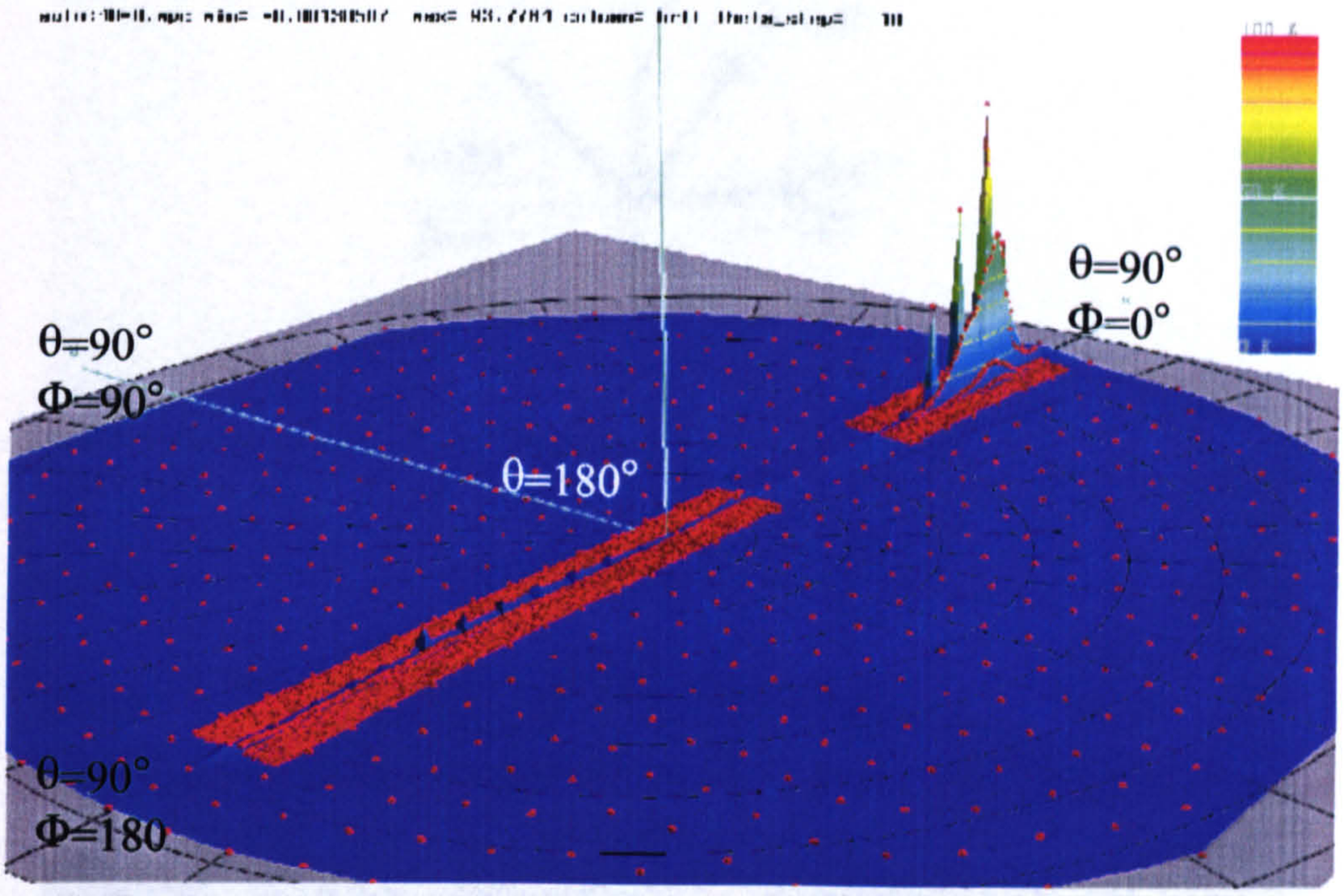

Fig 2-17: Solar altitude 40 degrees and 0 degree azimuth.

Peak transmission at θ=116° and Φ=0°which translates to the prisms on the window as:

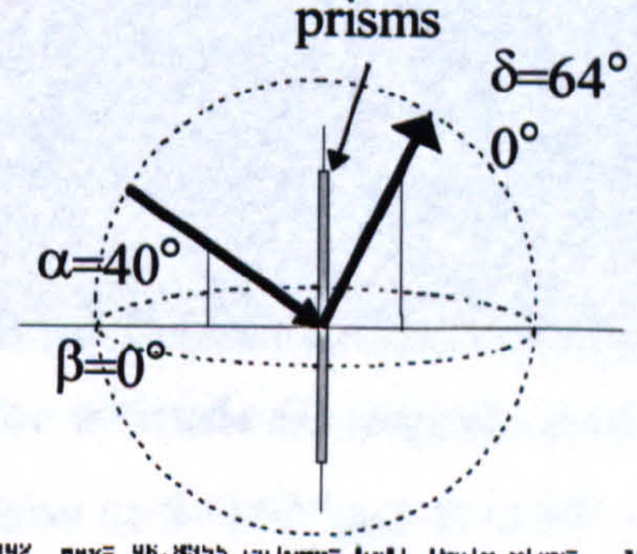

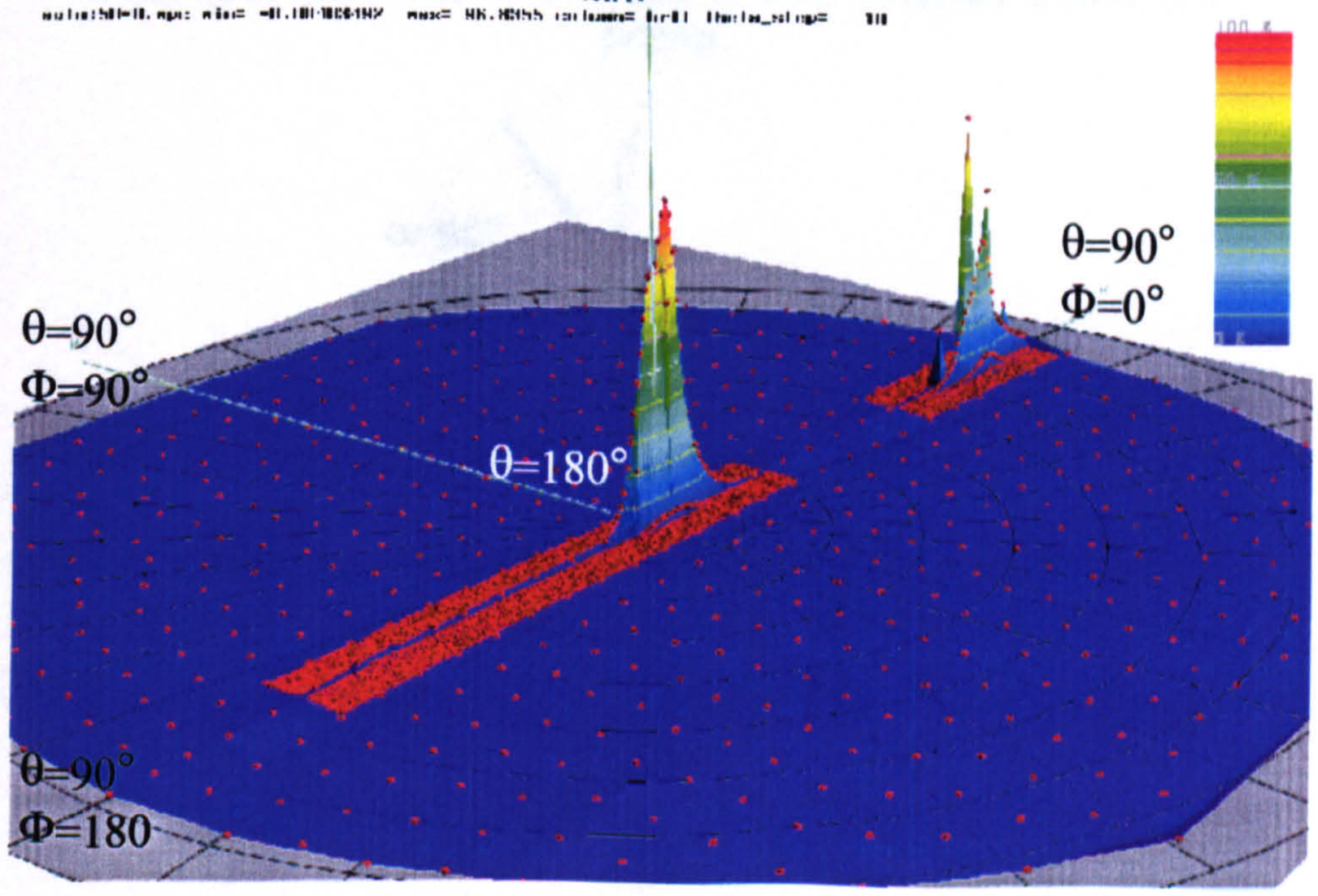

Fig 2-18: Solar altitude 50 degrees and 0 degree azimuth.

Peak transmission at θ=178°, 116°and Φ=0° which translates to the prisms on the window as:

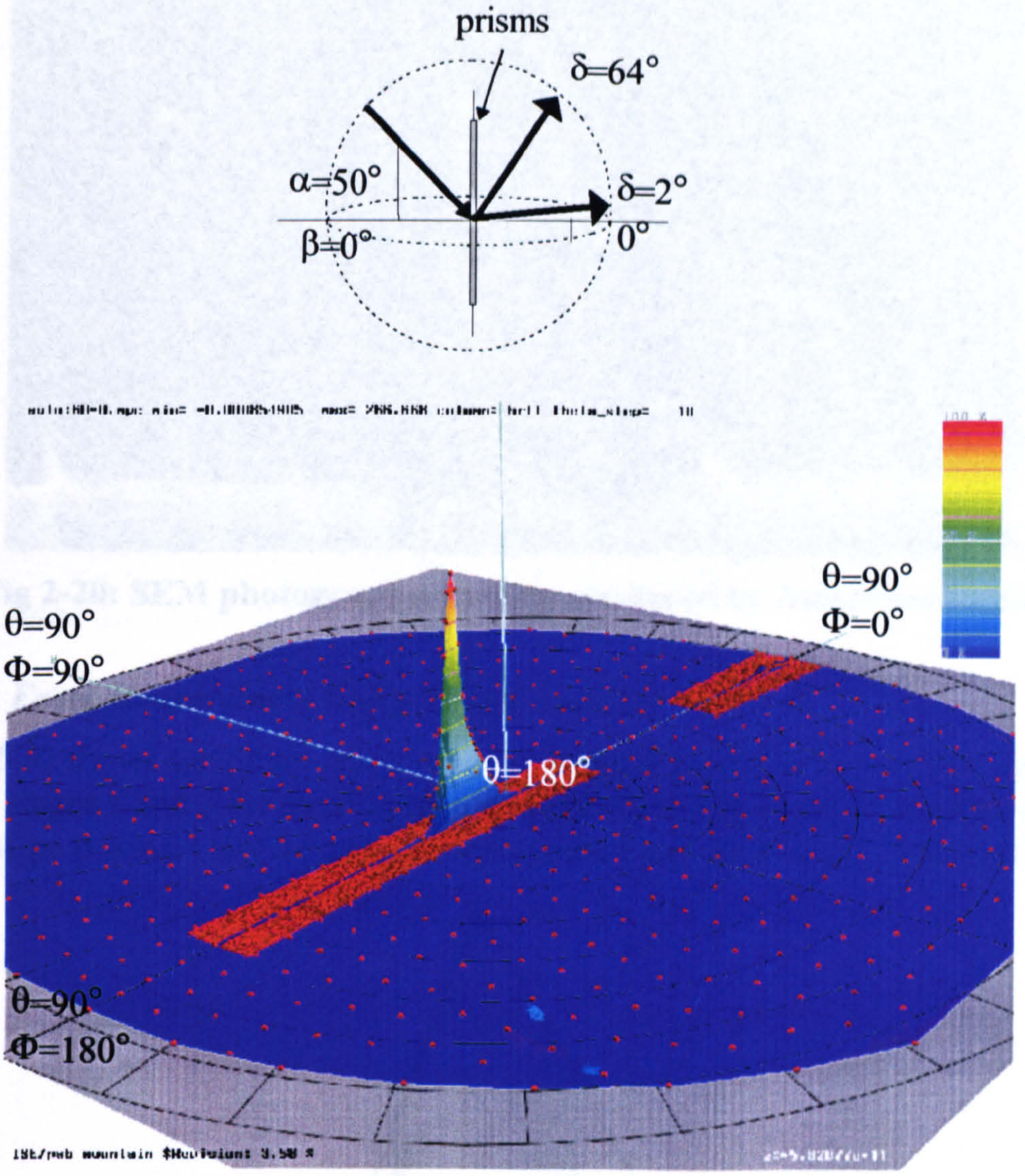

Fig 2-19: Solar altitude 60 degrees and 0 degree azimuth.

Peak transmission at θ=169°and Φ=180° with a FWHM of 5°.

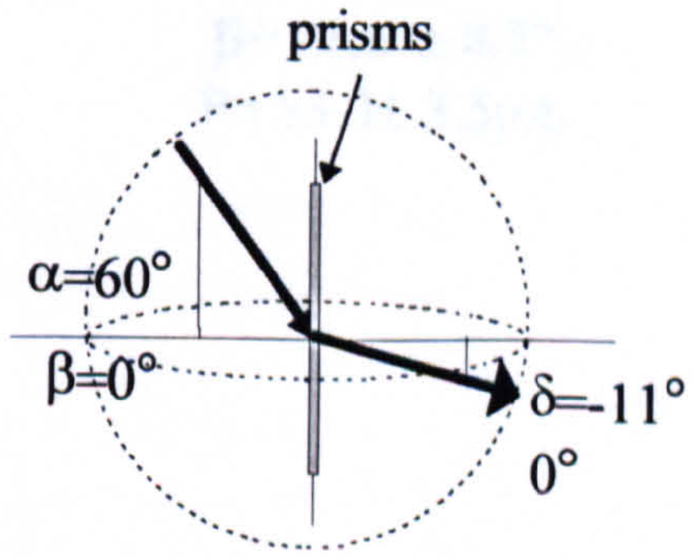

2.3.7 Facet Measurements on Autotype Prism Array

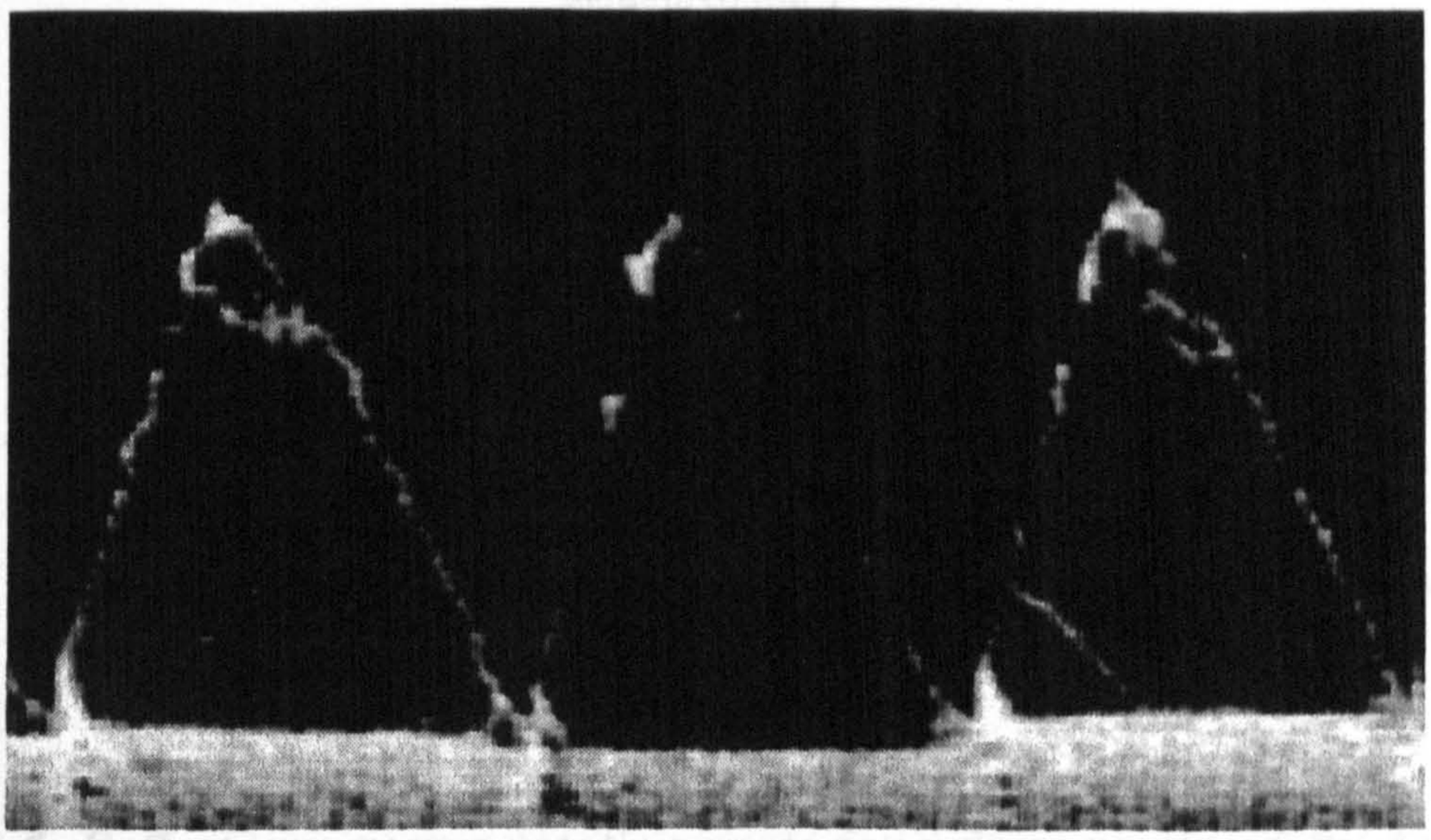

Fig 2-20: SEM photograph of prisms produced by Autotype sample.

Stage 1: Facet Measurement Using Image Analyser

As Fig 2-20 shows the prism facets are well-defined (and due to the close agreement between stages 1 and 2 for the POE sample) a much smaller sample was measured for the Autotype prisms. Only 4 prisms were measured and the average calculated:

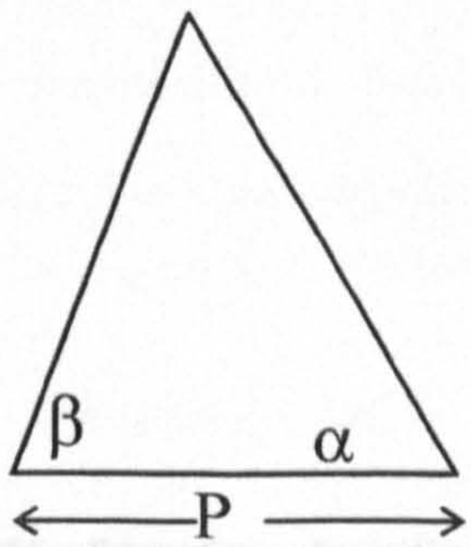

$\alpha = 61.3° \pm 0.9°$

$\beta = 71.6° \pm 0.7°$

$P = 53.0 \pm 3.5\mu m$

Stage 2: Reflection Measurements

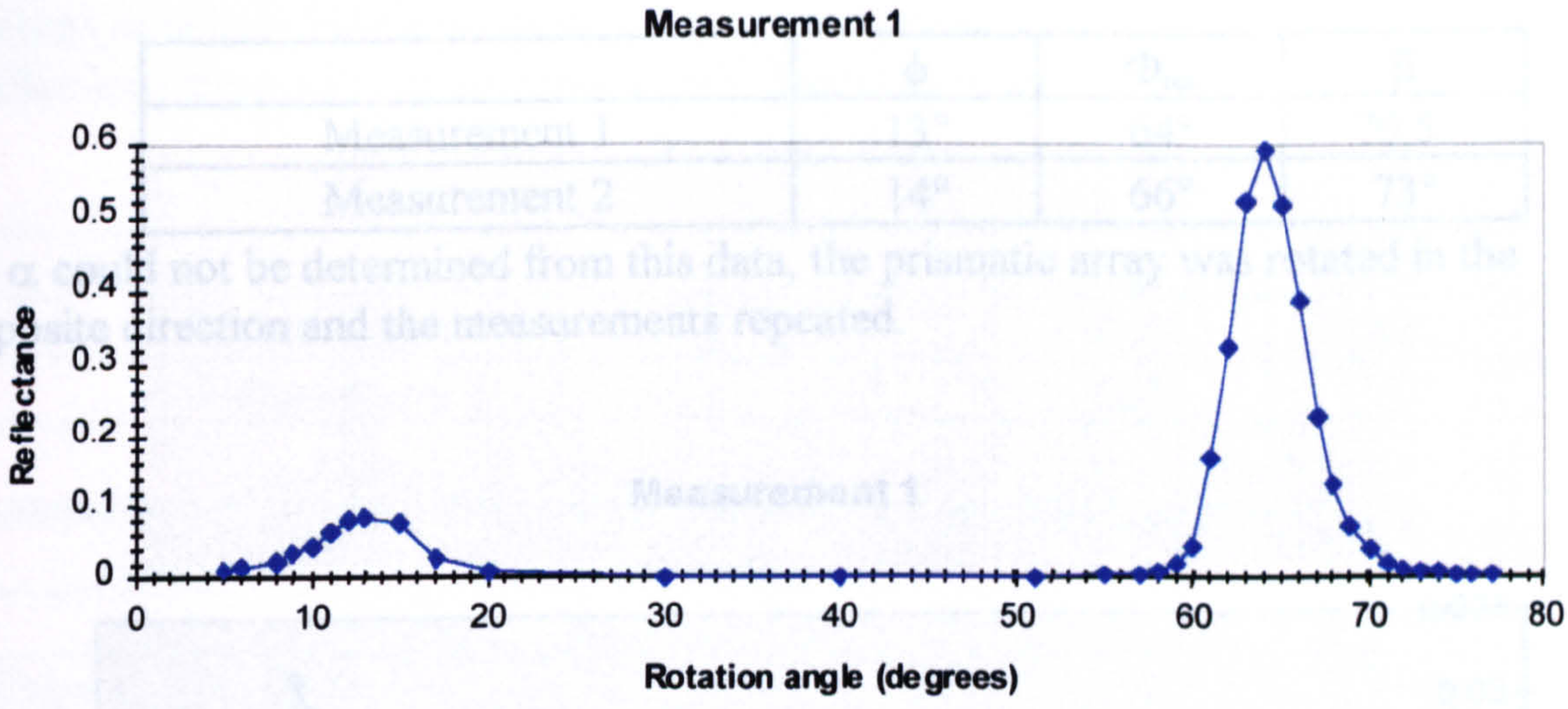

Graph 2-5: Reflectance versus rotation angle for prisms produced by Autotype- measurement 1. Source/detector separation = 13°.

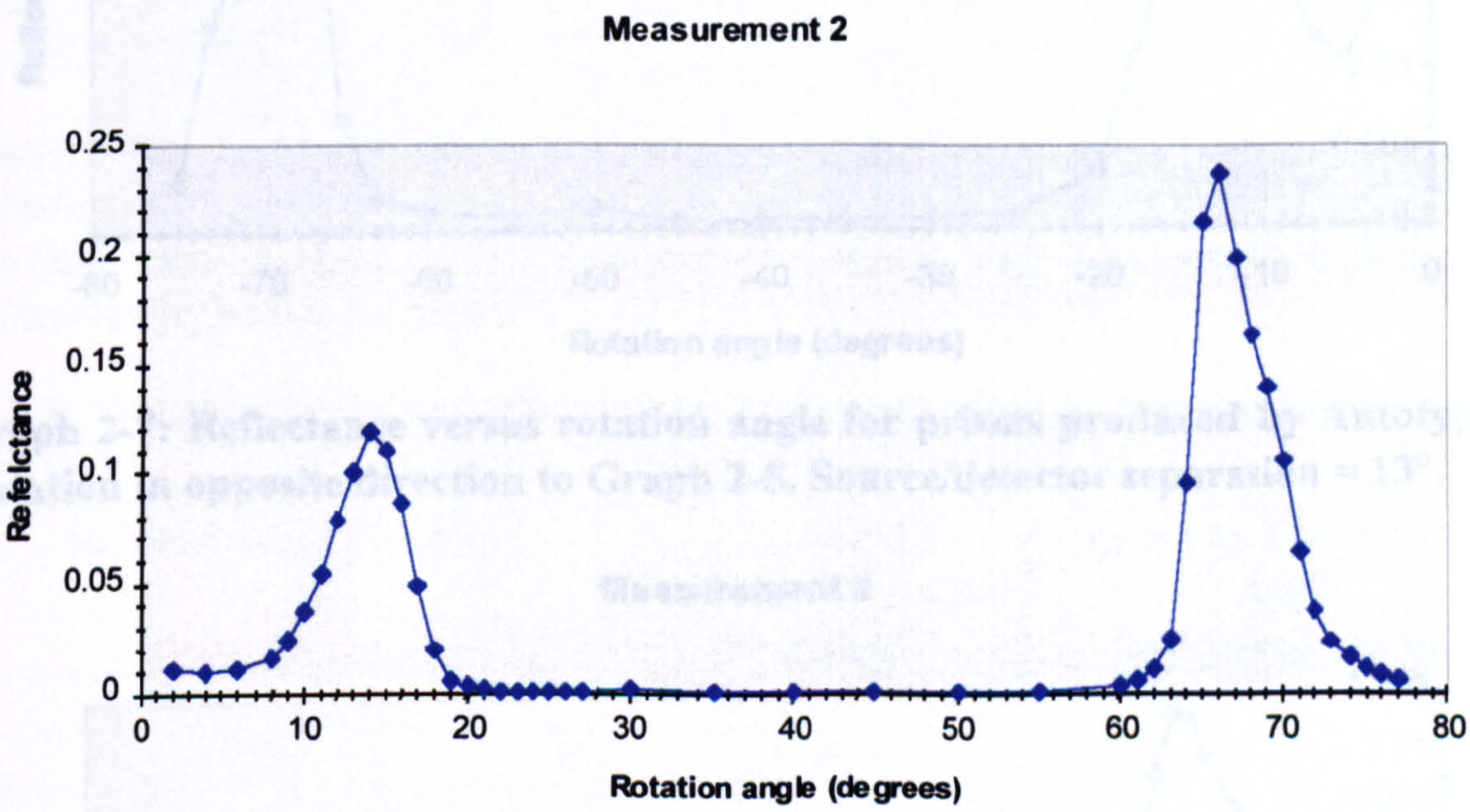

Graph 2-6: Reflectance versus rotation angle for prisms produced by Autotype- measurement 2. Source/detector separation = 14°.

	Rotation Angle of Maxima
Measurement 1	13°, 62°
Measurement 2	14°, 64°

The first maxima at around 14° is reflectance from a plane surface as it is equal to the source/detector separation determined using a plane mirror. Fig 2-20 shows that the prisms do not form a continuous structure and it is from the discontinuities that light is reflected.

The second maxima at around 64° can be used to derive β (as was shown with the diamond-turned sample) from the equation:

$$\phi = 2 \times (\beta - \Phi_{rot})$$

Therefore:

	ϕ	Φ_{rot}	β
Measurement 1	13°	64°	70.5°
Measurement 2	14°	66°	73°

As α could not be determined from this data, the prismatic array was rotated in the opposite direction and the measurements repeated.

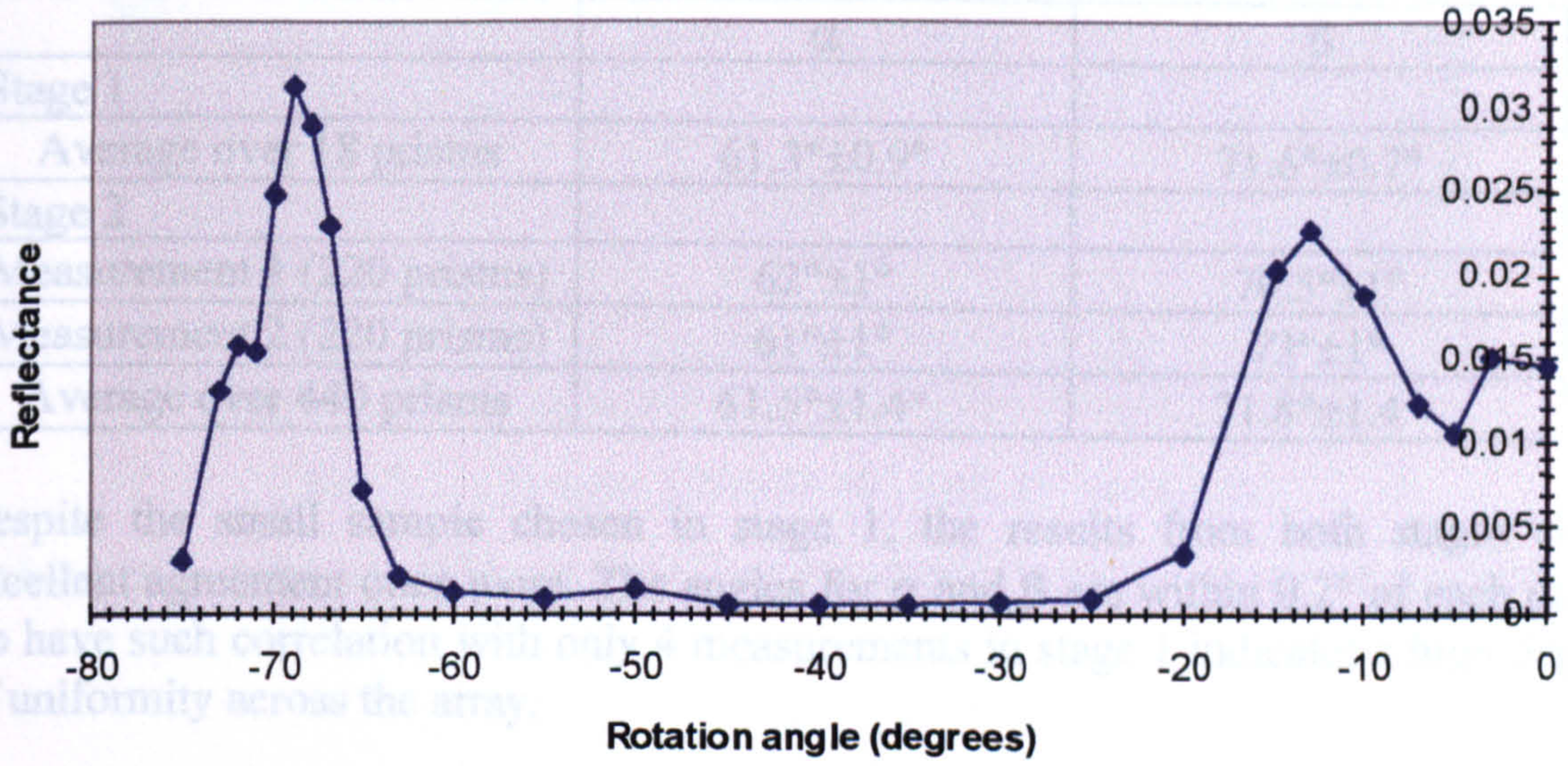

Graph 2-7: Reflectance versus rotation angle for prisms produced by Autotype. Rotation in opposite direction to Graph 2-5. Source/detector separation = 13°.

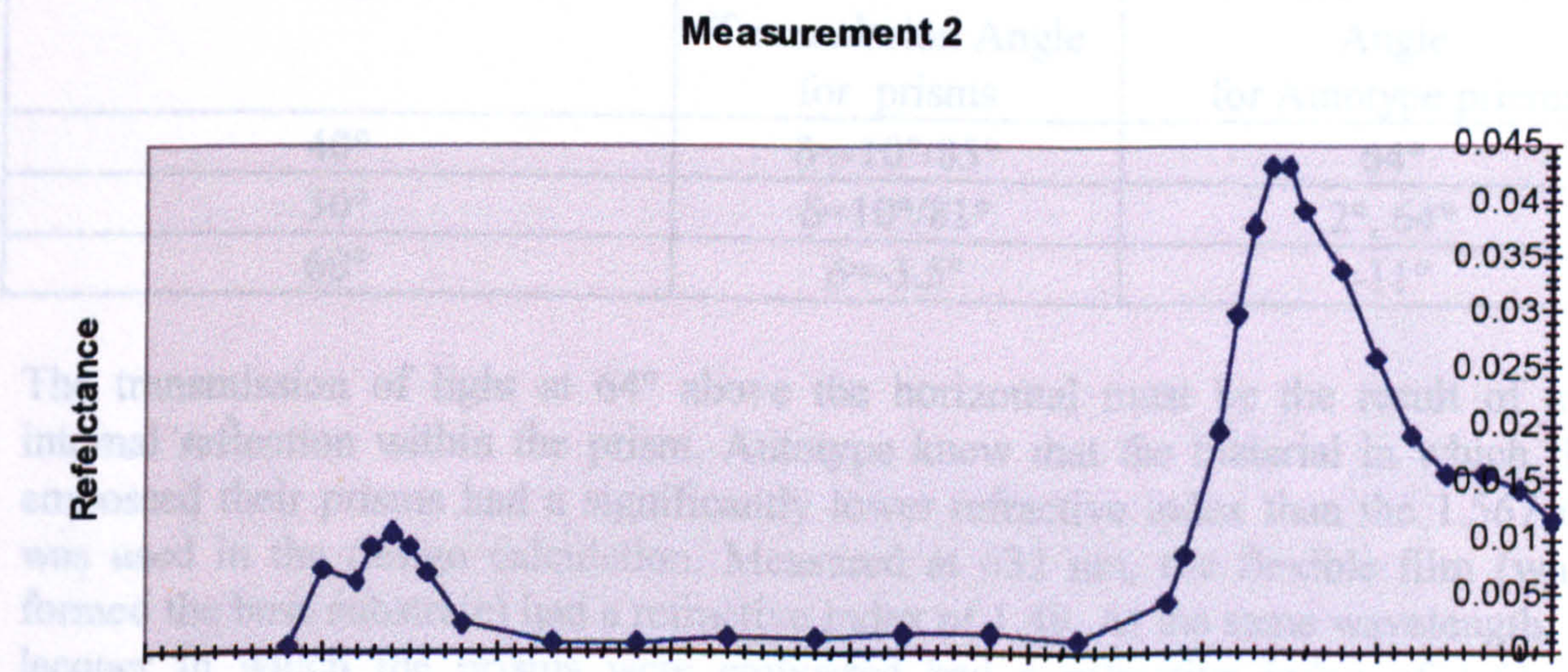

Graph 2-8: Reflectance versus rotation angle for prisms produced by Autotype. Rotation in opposite direction to Graph 2-6. Source/detector separation = 14°.

	Rotation Angle
Measurement 1	-13°,-69°
Measurement 2	-14°,-68°

At the first maxima at around -14° the light is reflected from the substrate between prisms as before. However, as the array has now been rotated in the opposite direction, reflections from α cause the second peak, therefore from:

$$\phi = 2 \times (\alpha - \Phi_{rot})$$

	ϕ	Φ_{rot}	α
Measurement 1	13°	64°	62°
Measurement 2	14°	66°	61°

Comparison of results between stage 1 and stage 2 for Autotype prisms

	α	β
Stage 1		
Average over 18 prisms	61.3°±0.9°	71.6°±0.7°
Stage 2		
Measurement 1 (220 prisms)	62°±1°	70.5°±1°
Measurement 2 (220 prisms)	61°±1°	73°±1°
Average over 440 prisms	61.5°±1.4°	71.8°±1.4°

Despite the small sample chosen in stage 1, the results from both stages show excellent agreement once more. The angles for α and β are within 0.2° of each other. To have such correlation with only 4 measurements in stage 1 indicates a high degree of uniformity across the array.

2.3.8 Conclusion to Goniophotometer Measurements on Autotype Prisms, Φ= 0°

Incident Angle (Φ=0°)	Calculated Transmission Angle for prisms	Measured Transmission Angle for Autotype prisms
40°	δ=-10°/85°	64°
50°	δ=10°/81°	2°, 64°
60°	δ=-3.5°	-11°

The transmission of light at 64° above the horizontal must be the result of total internal reflection within the prism. Autotype knew that the material in which they embossed their prisms had a significantly lower refractive index than the 1.567 that was used in the design calculation. Measured at 632 nm, the flexible film (which formed the base substrate) had a refractive index of 1.49. At the same wavelength, the lacquer in which the prisms were embossed had a refractive index of 1.51. To compensate for this reduction, the facet angles of the prisms were increased causing total internal reflection and higher transmission angles.

2.3.9 Transmission Characteristics for Autotype Prism Array: Azimuthal Angle Φ=45°

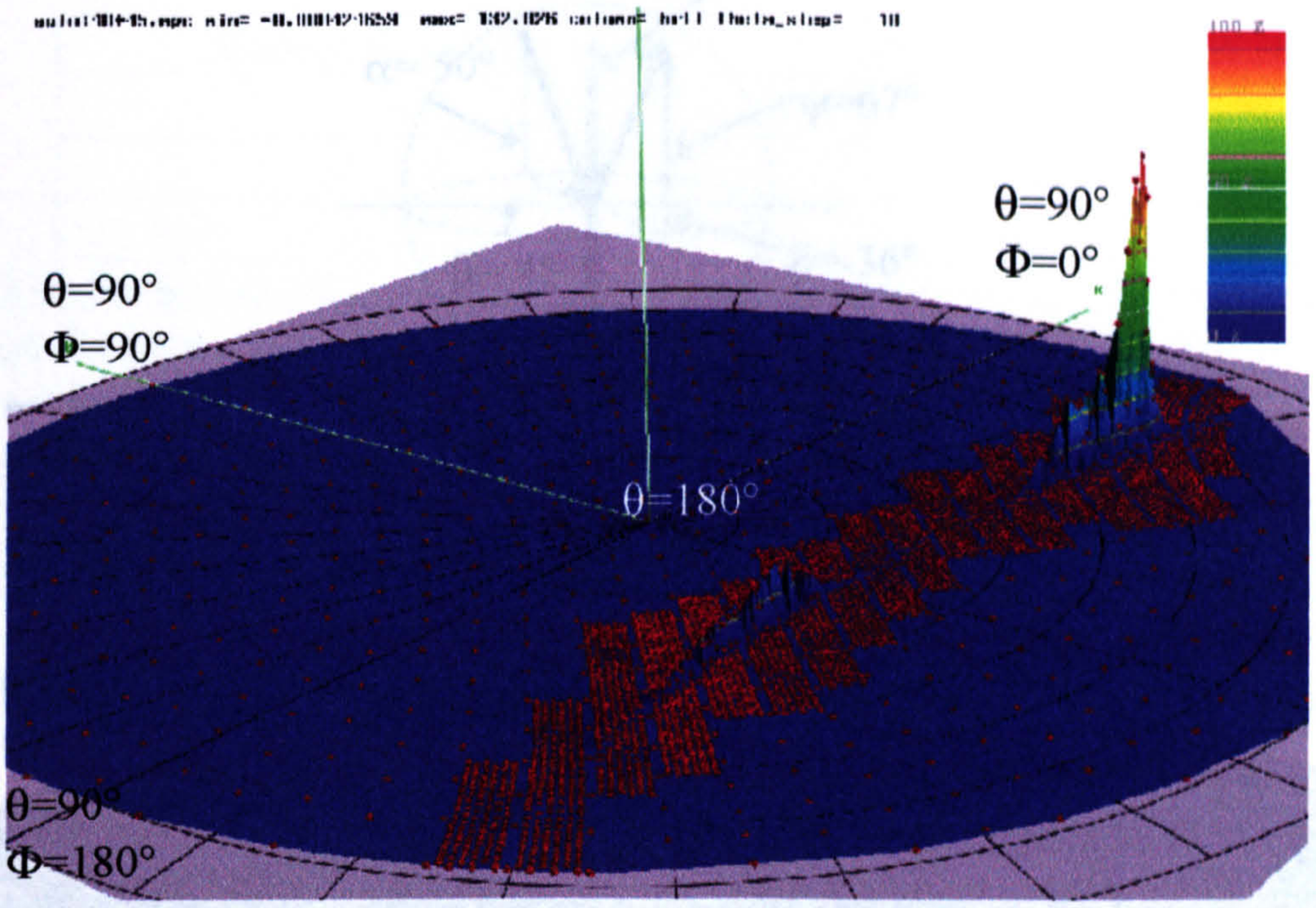

Fig 2-21: Source altitude 40° and 45° azimuth.

Peak transmission at θ=119° and Φ=32° which translates to the prisms on the window as:

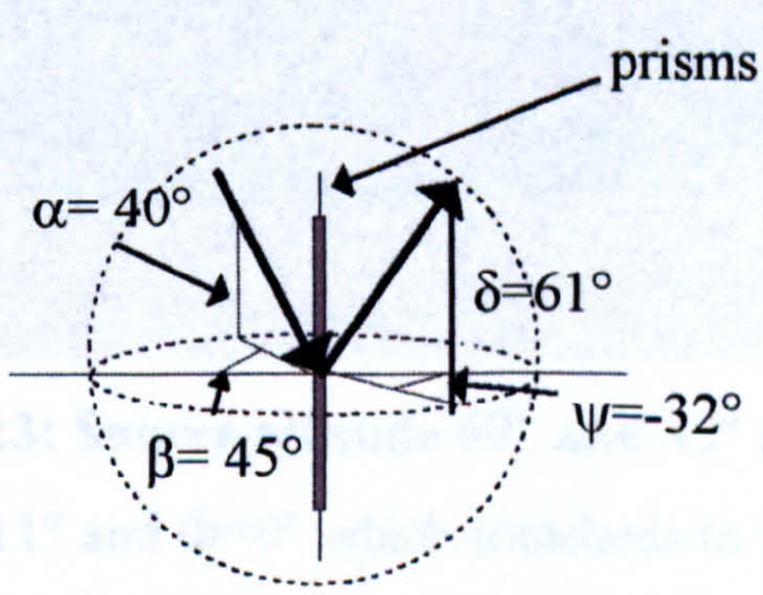

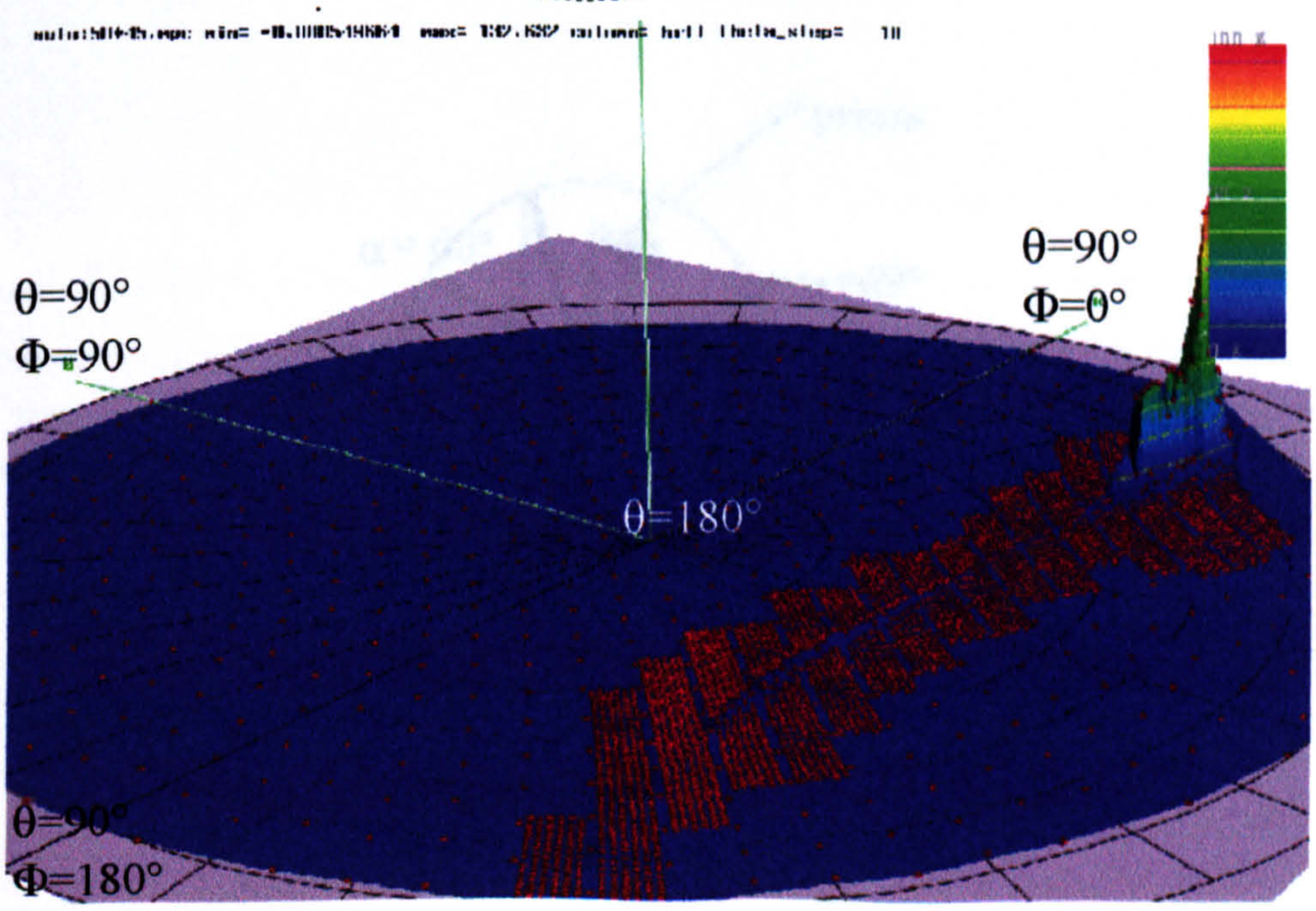

Fig 2-22: Source altitude 50° and 45° azimuth.

Peak transmission at θ=145° and Φ=230° which translates to the prisms on the window as:

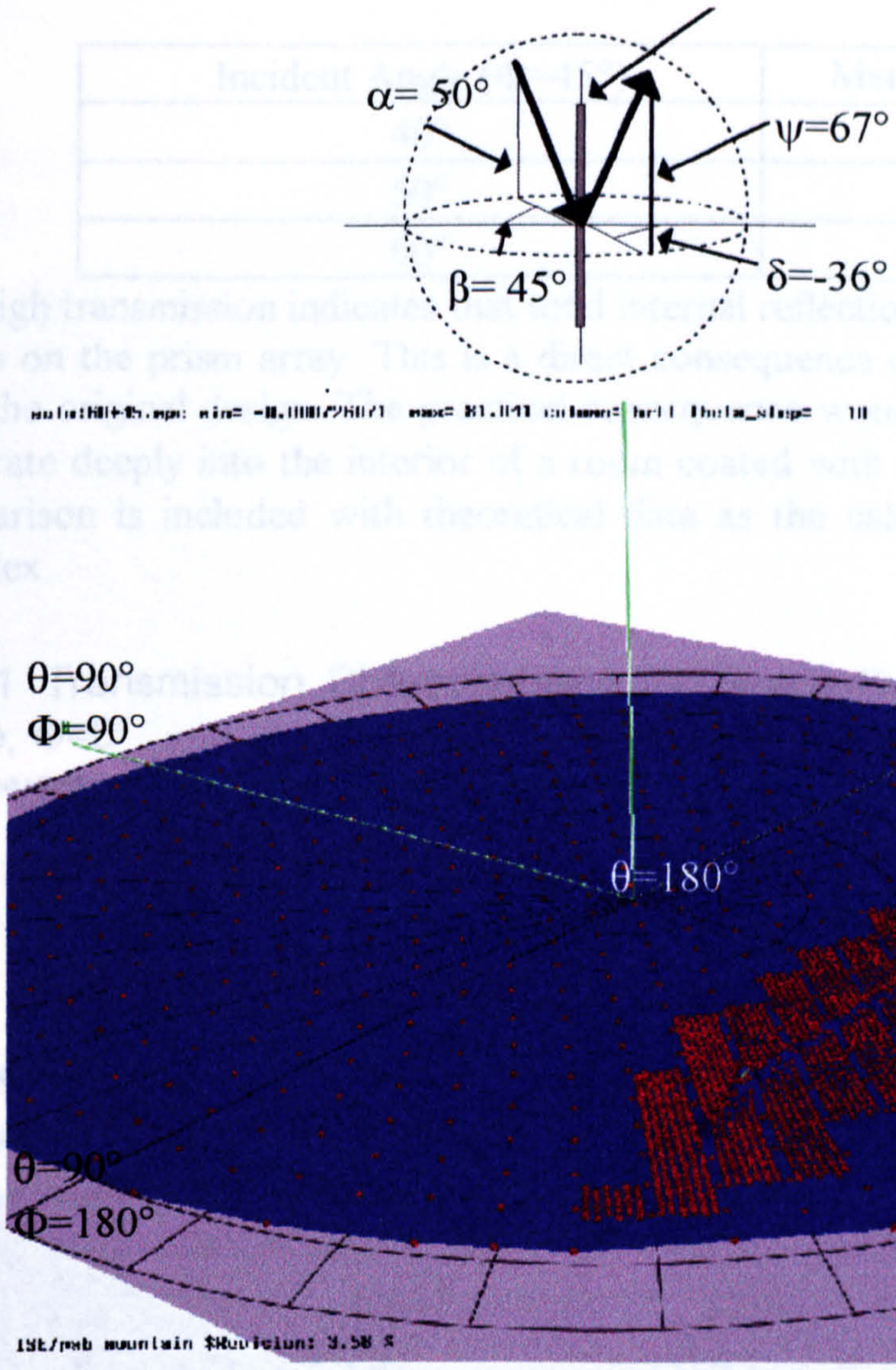

Fig 2-23: Source altitude 60° and 45° azimuth.

Peak transmission at θ=111° and Φ=0° which translates to the prisms on the window as:

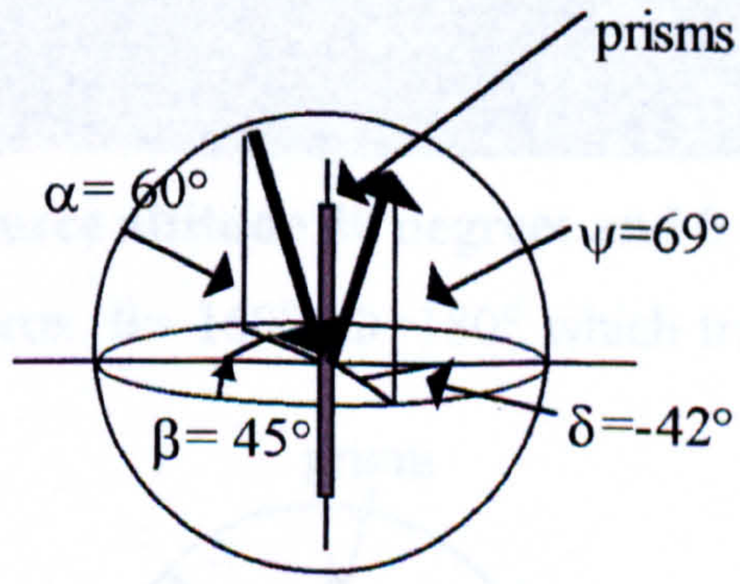

2.3.10 Conclusion to Transmission Measurements on Autotype Prisms, Φ= 45°

Incident Angle (Φ=45°)	Measured Transmission Angle
40°	δ=61° ψ=-32°
50°	δ=67° ψ=-36°
60°	δ=69° ψ=-42°

The high transmission indicates that total internal reflection occurs for all three incident angles on the prism array. This is a direct consequence of the increase in prism angle over the original design. The practical consequence would be that daylight would not penetrate deeply into the interior of a room coated with these prisms for Φ= 45°. No comparison is included with theoretical data as the calculation would be extremely complex.

2.3.11 Transmission Characteristics for Shape-Cut Prism Array: Azimuthal Angle, Φ=0°

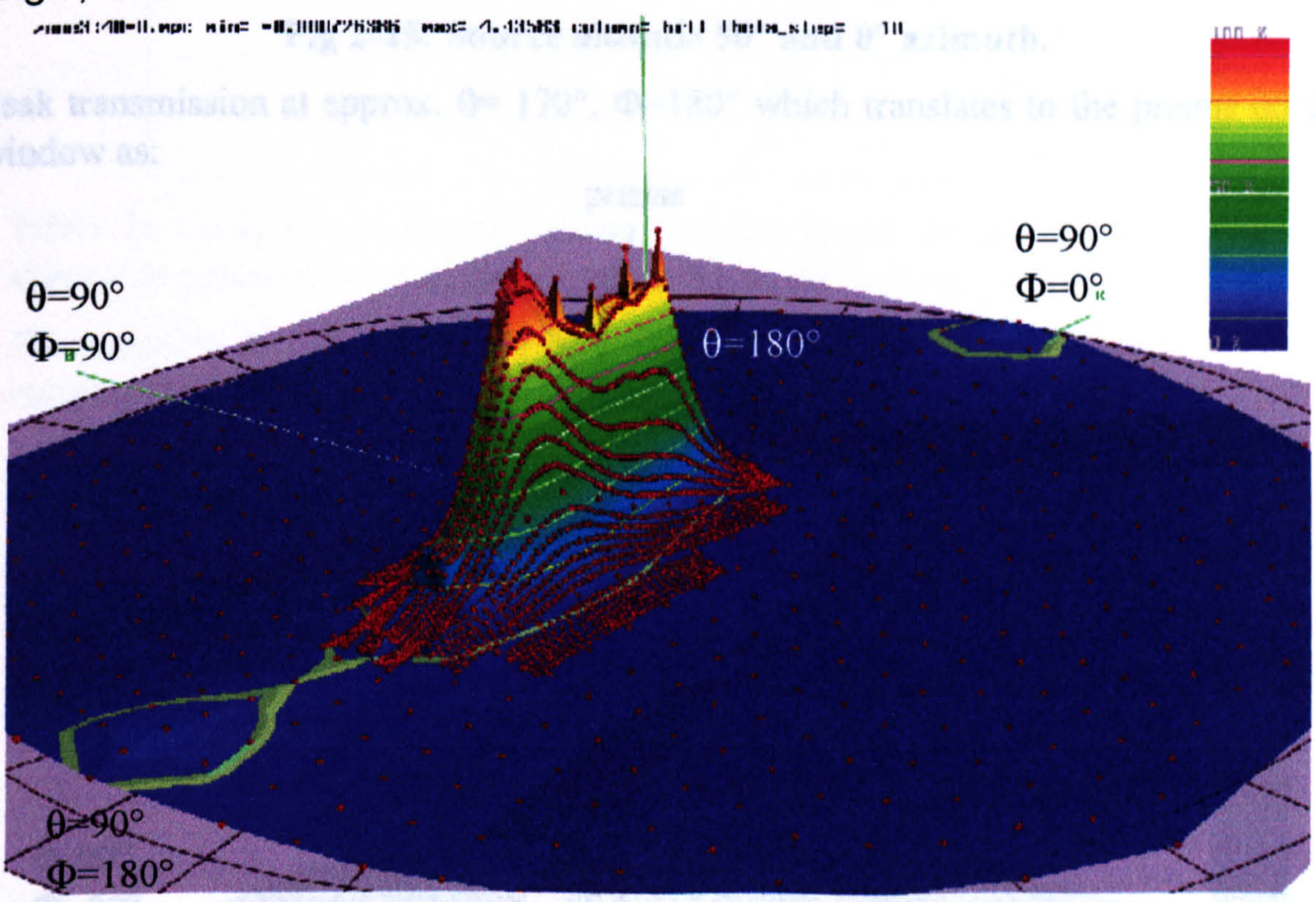

Fig 2-24: Source altitude 40 degrees and 0 degree azimuth.

Peak transmission at approx. θ= 160°, Φ=180° which translates to the prisms on the window as:

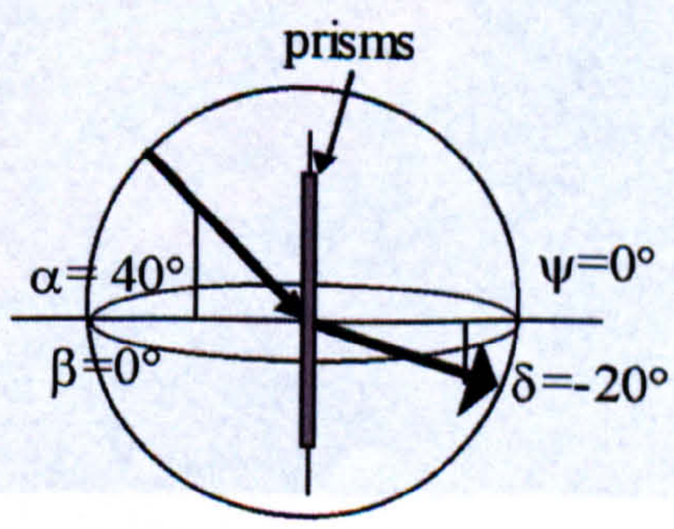

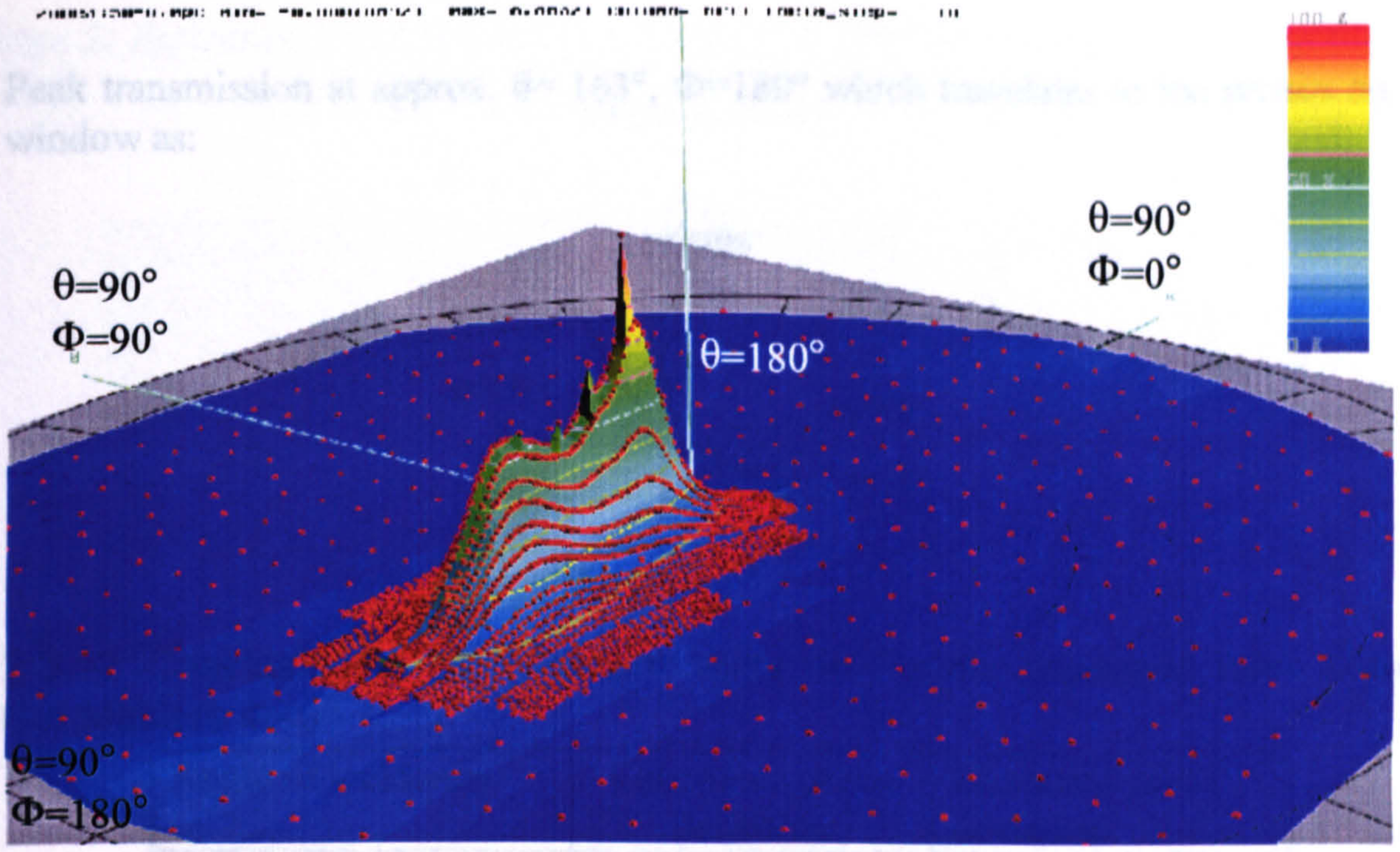

Fig 2-25: Source altitude 50° and 0° azimuth.

Peak transmission at approx. θ= 170°, Φ=180° which translates to the prisms on the window as:

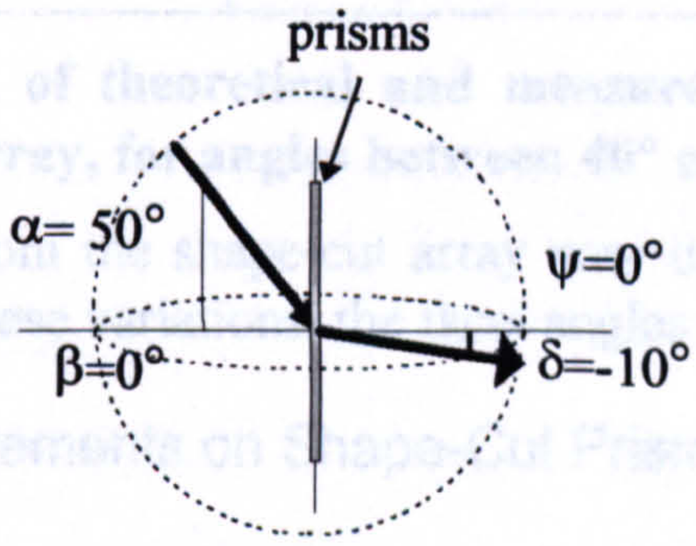

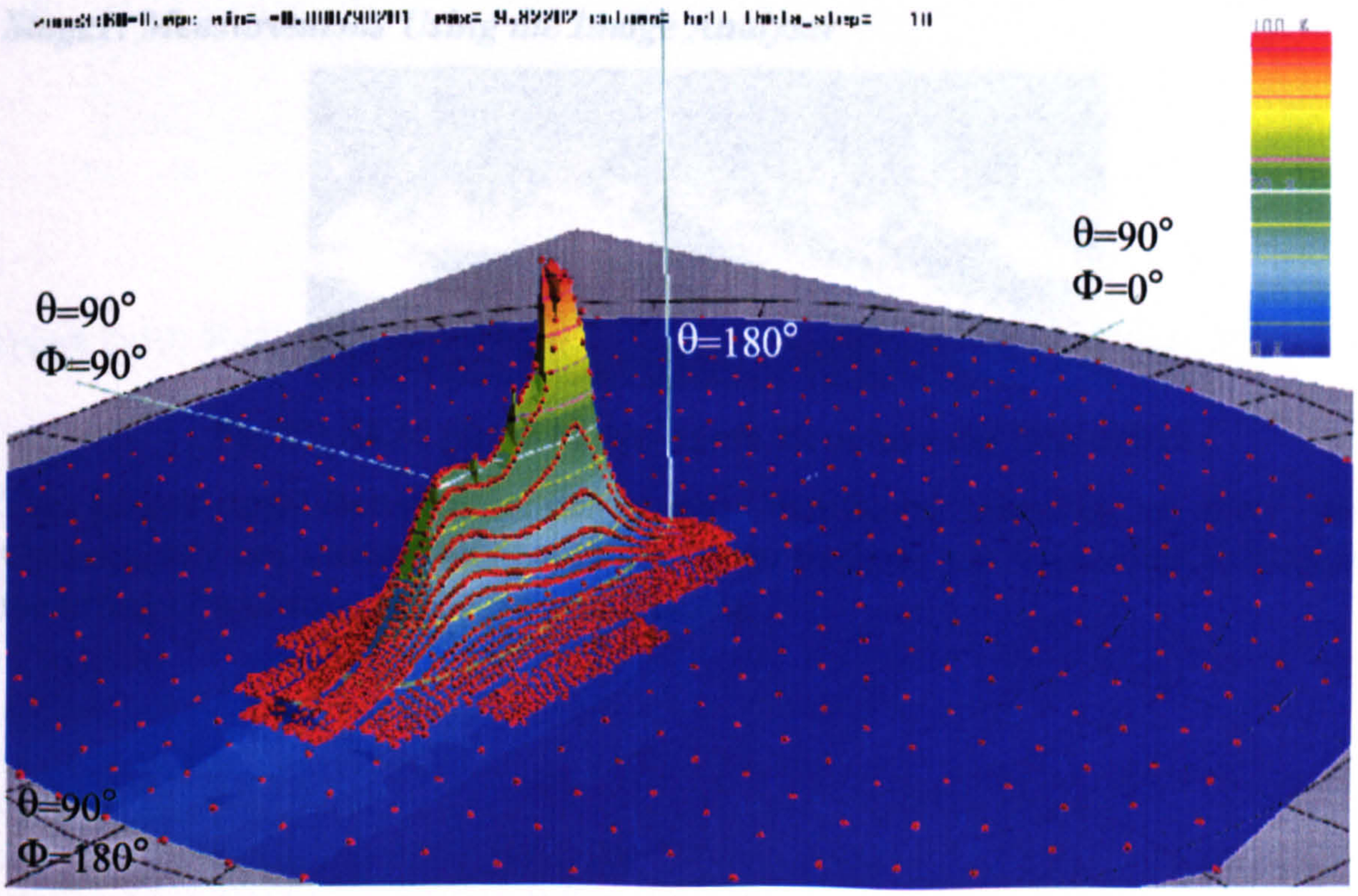

Fig 2-26: Source altitude 60 °and 0° azimuth.

Peak transmission at approx. θ= 163°, Φ=180° which translates to the prisms on the window as:

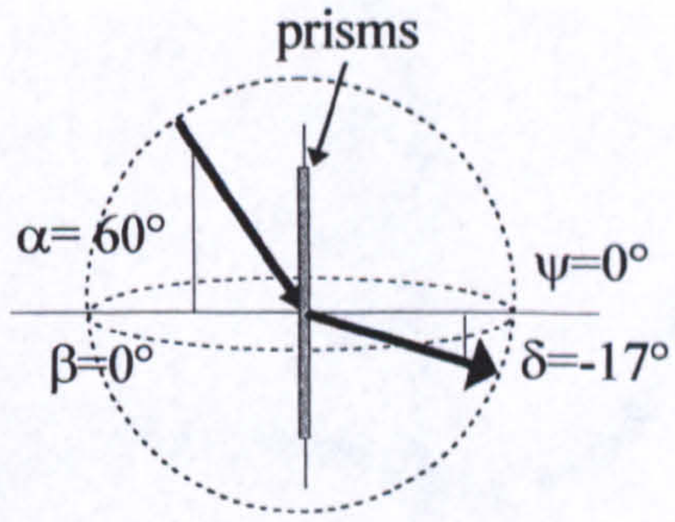

2.3.12 Conclusion to the Measurements on Prisms produced from Shape-Cut Masters Φ=0°

Angle of incidence	Calculated prism deviation	Measured prism deviation
40°	δ= -10.5°/85°	δ=-20°
50°	δ= 10.5°/81°	δ=-10°
60°	δ= -3.5°	δ=-17°

Table 1: Comparison of theoretical and measured deviation of light through shape-cut prismatic array, for angles between 40° and 60° altitude.

Transmission angles from the shape-cut array vary dramatically from the calculated values and to explain these variations, the facet angles must be examined.

2.3.13 Facet Measurements on Shape-Cut Prism Array

Stage1: Measurements Using the Image Analyser

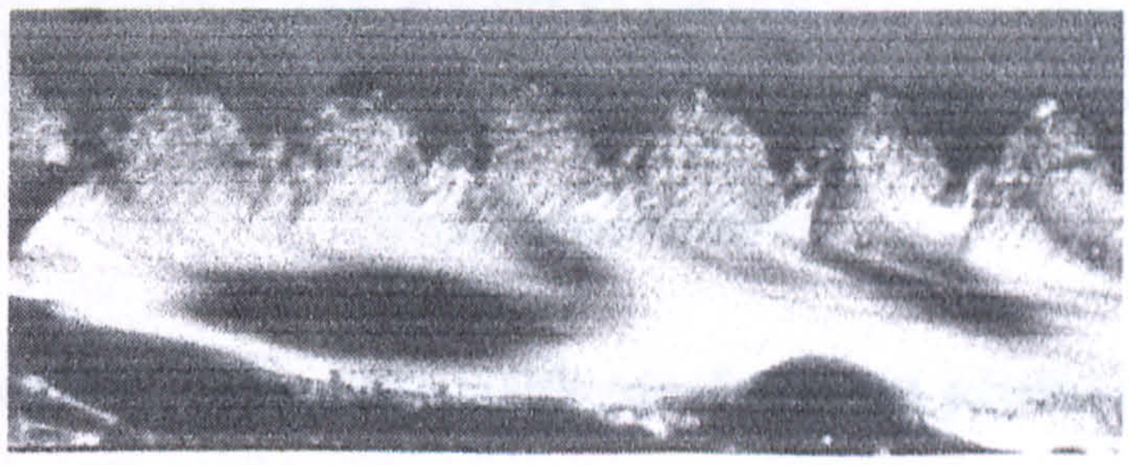

Fig 27: SEM photo of saw-tooth structure cut into delrin.

The prisms manufactured in delrin had significant rounding of their facets. Consequently any measurement with the image analyser was impossible as it requires the fitting of a straight line to the prism facets.

Stage 2: Reflection Measurements on Shape Cut Prismatic Array.

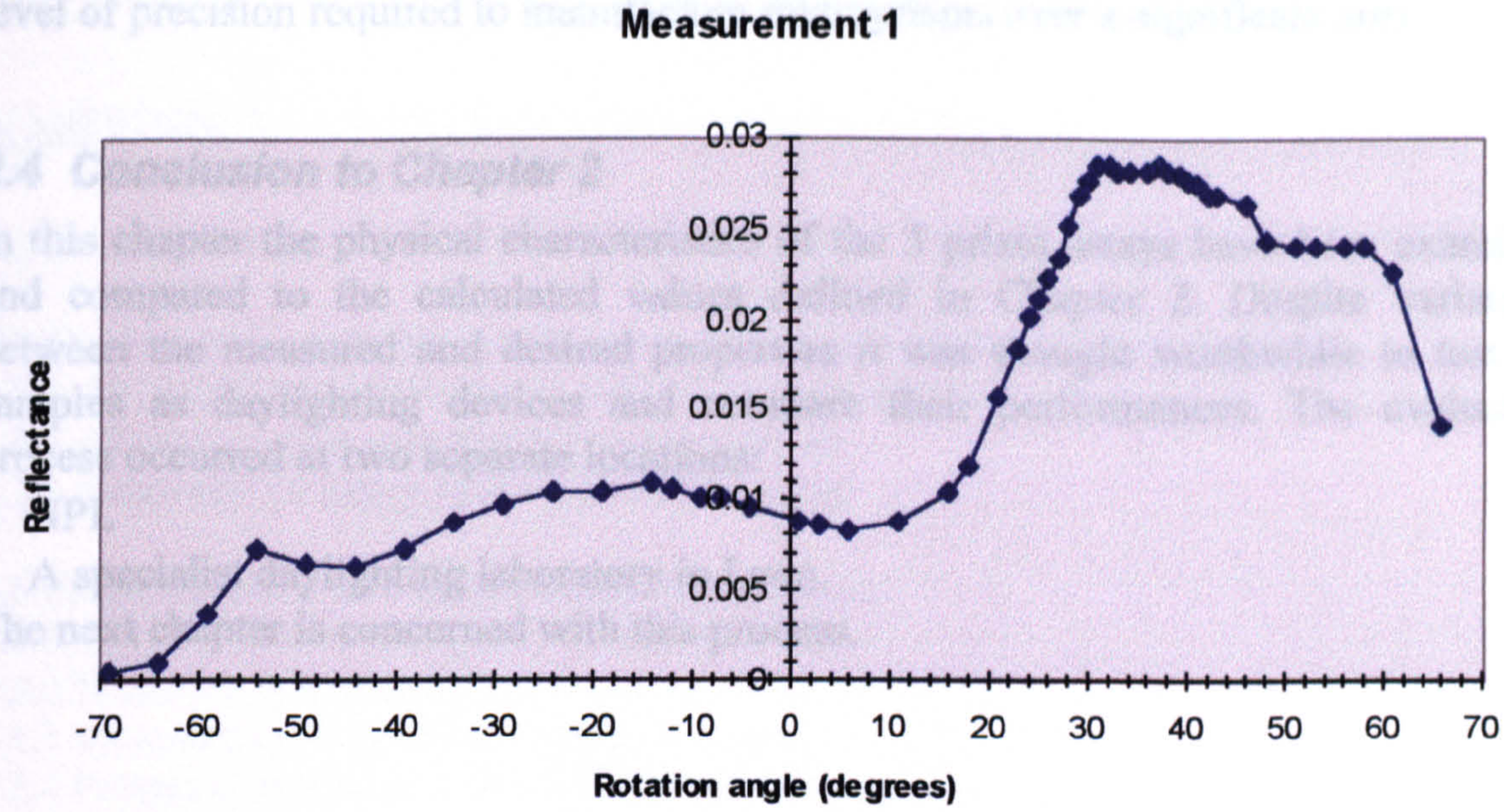

Graph 2-9: Reflectance vs. rotation angle for shape-cut prism- measurement 1.

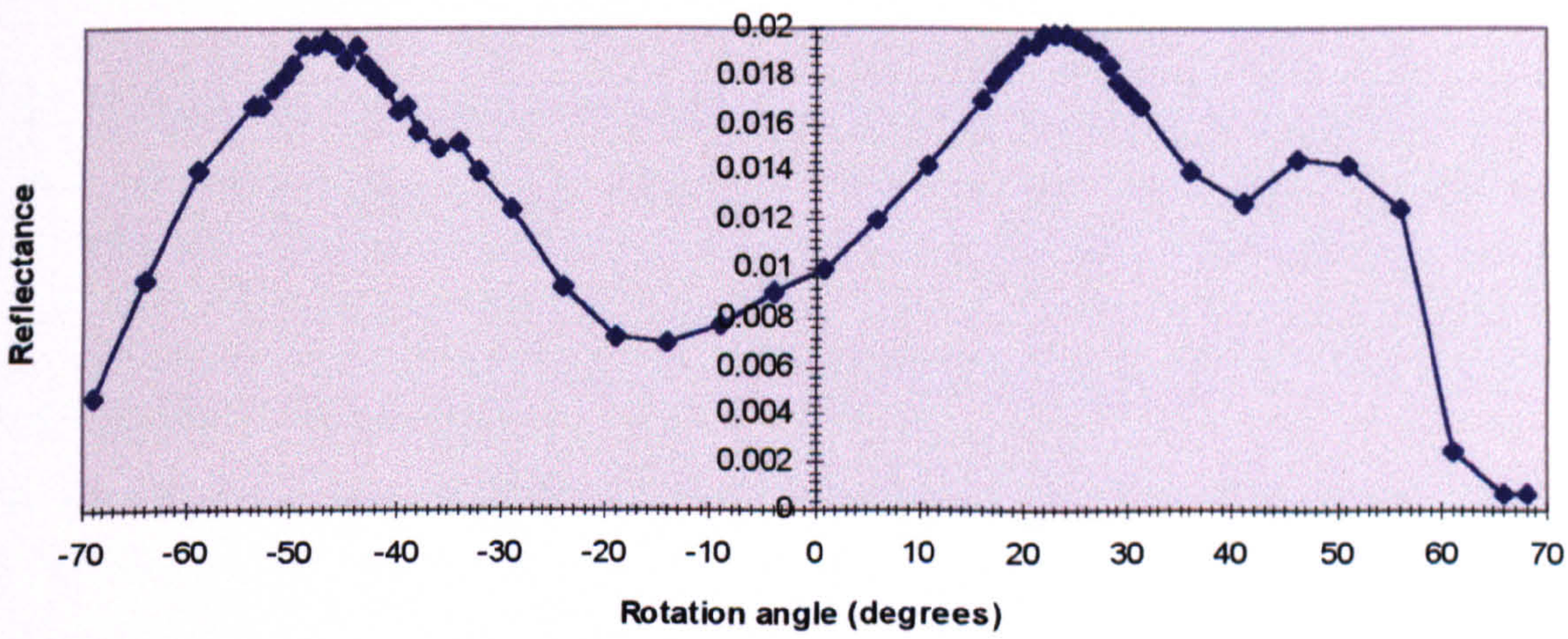

Graph 2-10: Reflectance vs. rotation angle for shape-cut prism- measurement 2.

2.3.14 Conclusions to Measurements on Shape- Cut Prisms.

Although the graphs for the shape-cut prisms show maxima and minima, their values on the y-axis indicate that the difference between the two is typically less than 1%. Furthermore measurements in different areas of the array yield different results as to the location of these points. The conclusion that can be drawn is that the saw-tooth structure varies significantly across the array. Rather than a series of prisms, the array can be considered to be simply a diffusing panel.

The decision to produce arrays of the prisms (10cm x 30cm) from delrin masters was based on the success of small scale prototypes (2.5cm x 2.5cm). It can therefore be concluded that the shape-cutting tool used to produce the prisms cannot maintain the level of precision required to manufacture microprisms over a significant area.

concluded that the shape-cutting tool used to produce the prisms cannot maintain the level of precision required to manufacture microprisms over a significant area.

2.4 Conclusion to Chapter 2

In this chapter the physical characteristics of the 3 prism arrays have been examined and compared to the calculated values defined in Chapter 2. Despite variations between the measured and desired properties it was thought worthwhile to test the samples as daylighting devices and compare their performances. The evaluation process occurred at two separate locations:

- NPL
- A specialist daylighting laboratory in Lyon.

The next chapter is concerned with this process.

3. Assessment of Microprism Arrays as Daylighting Systems

3.1 Introduction

The preceding discussion has been principally concerned with the optical properties of the prismatic arrays. However these measurements do not illustrate how the prisms will perform as daylighting systems. The purpose of this chapter is to test the prisms under celestial illumination and determine if the prisms would improve illumination within a room. As the eye's sensitivity functions on a logarithmic scale, illumination should be doubled to be perceptible, with the greatest improvement away from the window. Furthermore the production of glare should be minimised so as not to cause discomfort to the occupants.

The prisms were evaluated under both artificial and real skies. The advantage of an artificial sky is that it provides a stable luminous environment for comparing the different prismatic arrays. Its luminance distribution is based on the CIE overcast sky which is given by the equation:

$$L\gamma = Lz\,(1+2\sin\gamma)/3$$

where:

$L\gamma$ is the luminance at an angle of elevation γ above the horizon

Lz is luminance at the zenith

The real sky evaluation involved not only luminance and illuminance measurements but also a questionnaire to ascertain occupant opinions.

3.2 Evaluation of Prisms Under an Artificial Sky at the ENTPE[1]

Three prismatic samples were tested as elements in a composite window under artificial skies. The lower part of the window was traditional single glazing and upper part prisms with their apexes pointing to the interior. If the lower part of the window had been covered with the prisms the view out would have been obscured and proved unacceptable for occupants.

The model under the artificial sky had been constructed to a scale of 1:10. The dimensions as shown in Fig 3-1 the 'life size' room that it was designed to represent.

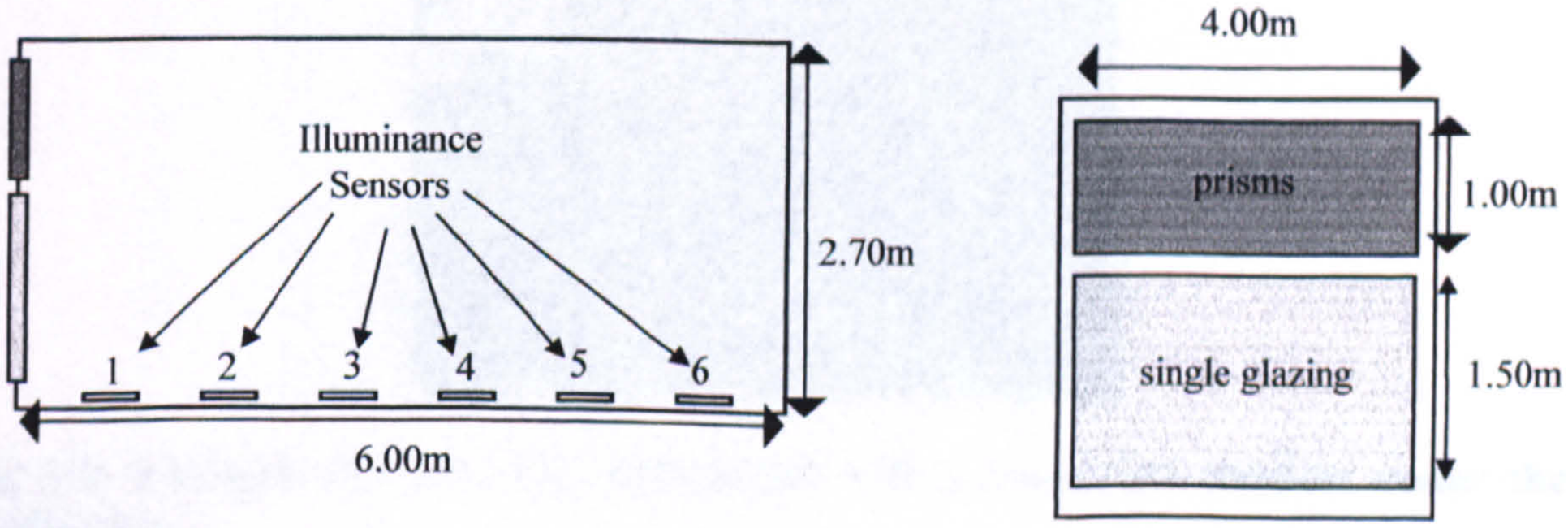

Fig 3-1: Life-size' dimensions of model room.

[1] Ecole Nationale Travaux Puplic de l'Etat

Reflectances of surfaces in model room:

Surface	Reflectance
ceiling	94%
wall	80%
floor	29%

The performances of the samples were determined by the calculation of a daylighting factor:

$$DF=E_{in}/E_{out} \times 100$$

E_{out} is the external illuminance (lux)

E_{in} is the illuminance inside the room (lux)

Such measurements can only be made in isotropic overcast conditions (simulated by the artificial sky) due to the variability in illuminance under clear sky conditions.

It is quite common for the view from a window to be blocked, for example by another building. Therefore the prisms were assessed with obstructions of various heights, as well as with a clear view.

Three types of prisms were tested:

- The shape- cut array, with poor quality facets.
- The diamond turned array.
- The Autotype array

In addition to the illuminance measurements 'fish-eye' photographs were taken of the interior of the rooms. The effect of the prisms can be clearly seen on the wall near the top of the composite window (see Fig 3-2).

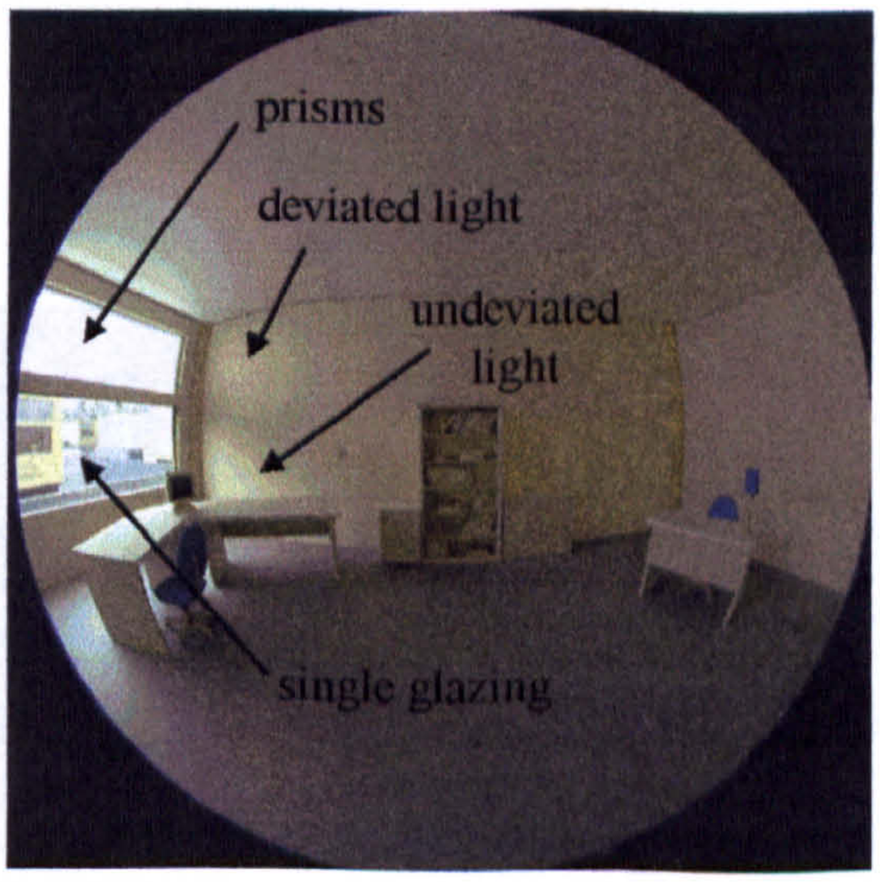

Fig 3-2: Example of a fish-eye photograph with a composite window under the artificial sky.

3.2.1 Artificial sky with clear view from window

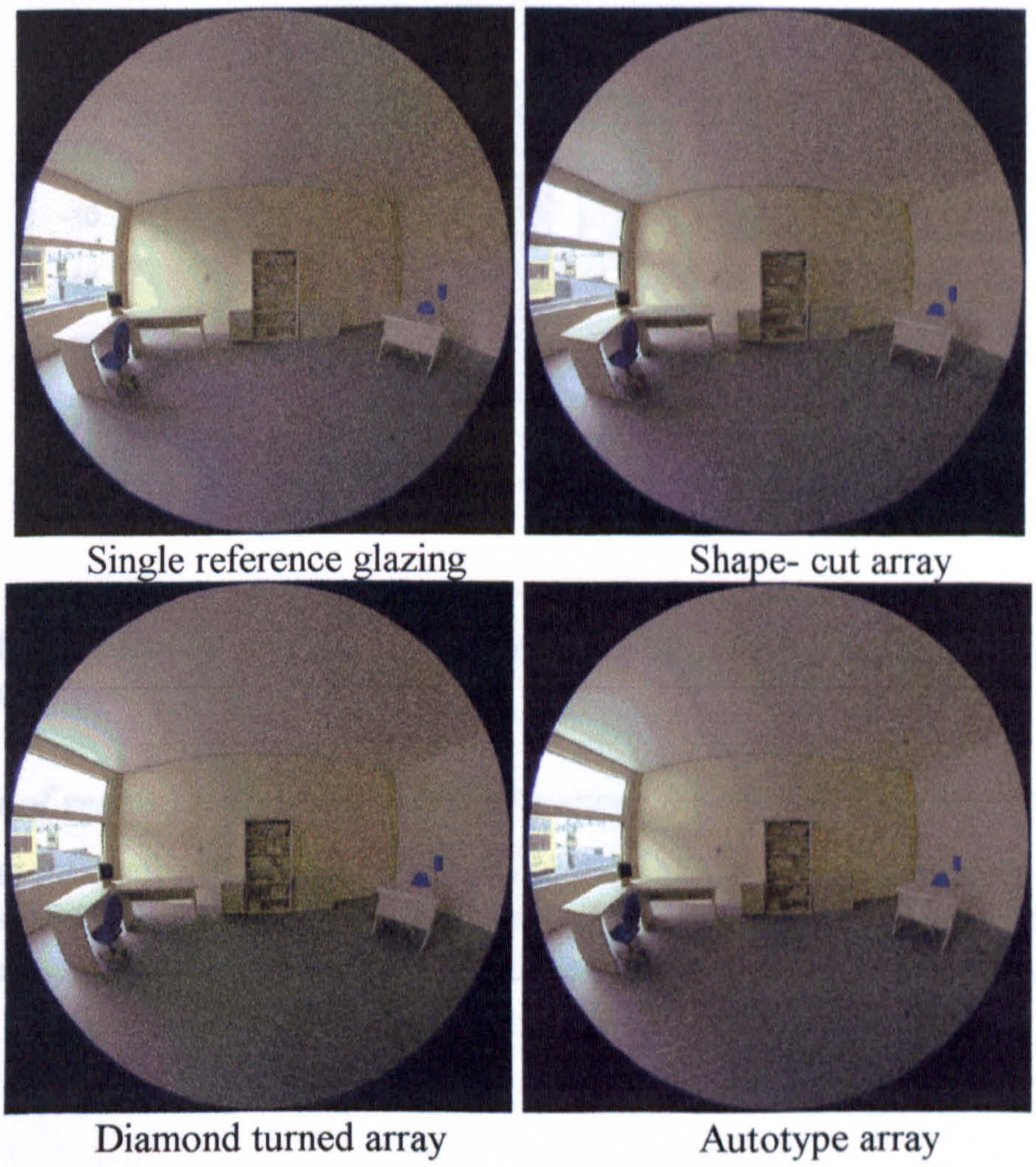

Fig 3-3: Photographs of model rooms with composite windows (exposure: f/11, 1/60s, 100 ASA).

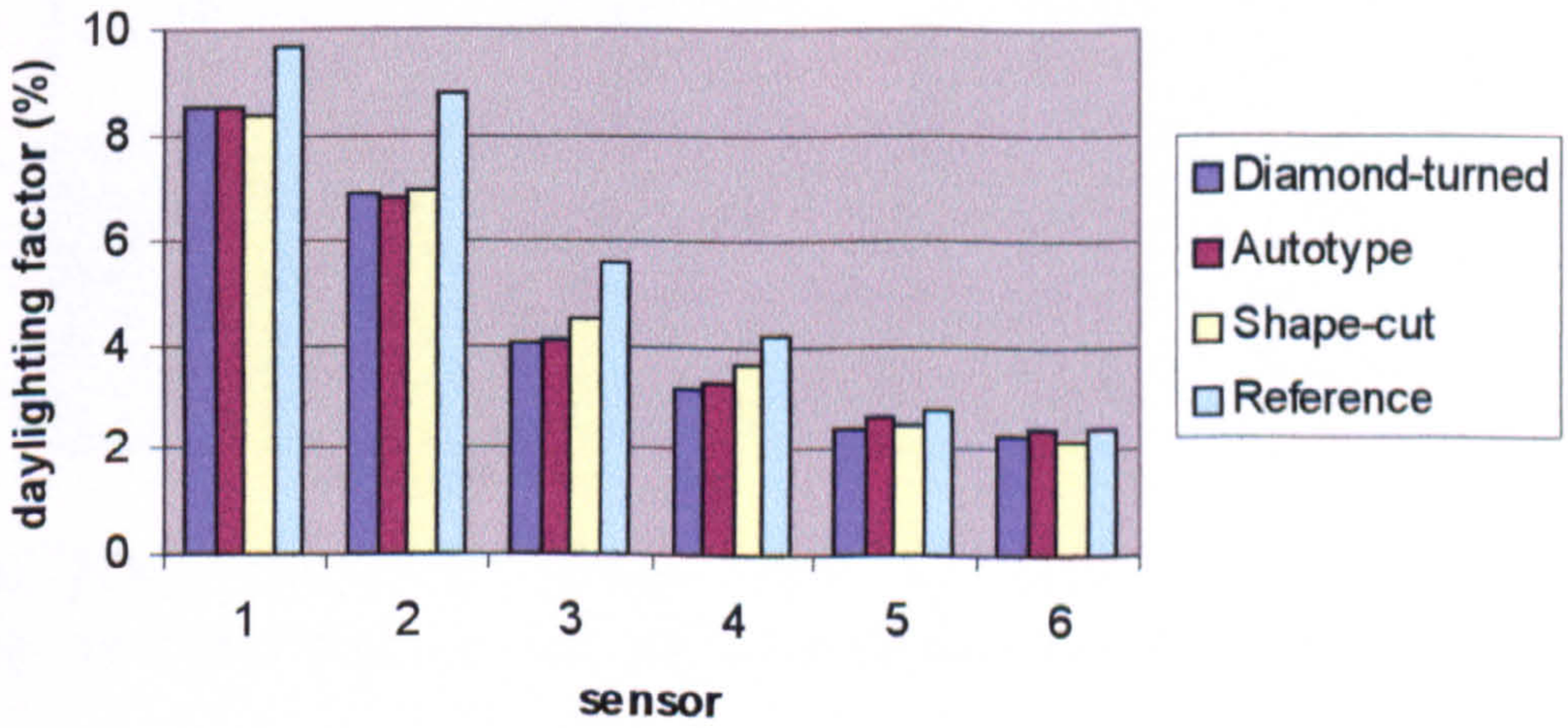

Graph 3-1: Daylighting factor measurements with no obstruction outside the window.

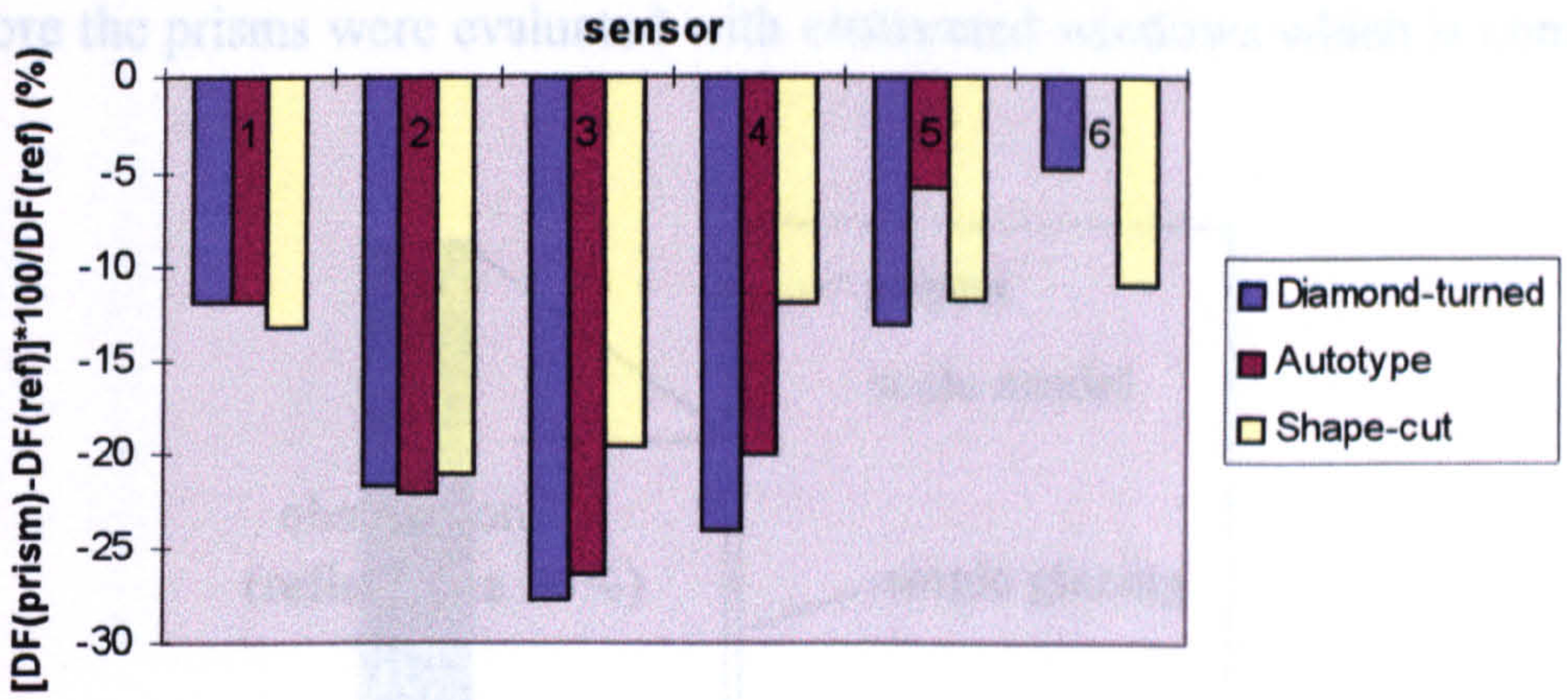

Graph 3-2: Percentage change in the daylighting factor for prismatic compared to reference glazing.

Discussion of results in comparison to reference glazing

None of the prismatic arrays improve the lighting within the interior. The delrin array reduces the illumination least in the centre of the room. At the back of room the Autotype array performs the best, but still does not improve over the reference glazing.

3.2.2 Artificial sky and obstructed windows

The use of daylighting devices must consider the site-layout of the urban environment[i] and therefore the prisms were evaluated with obstructed windows which is common in the city.

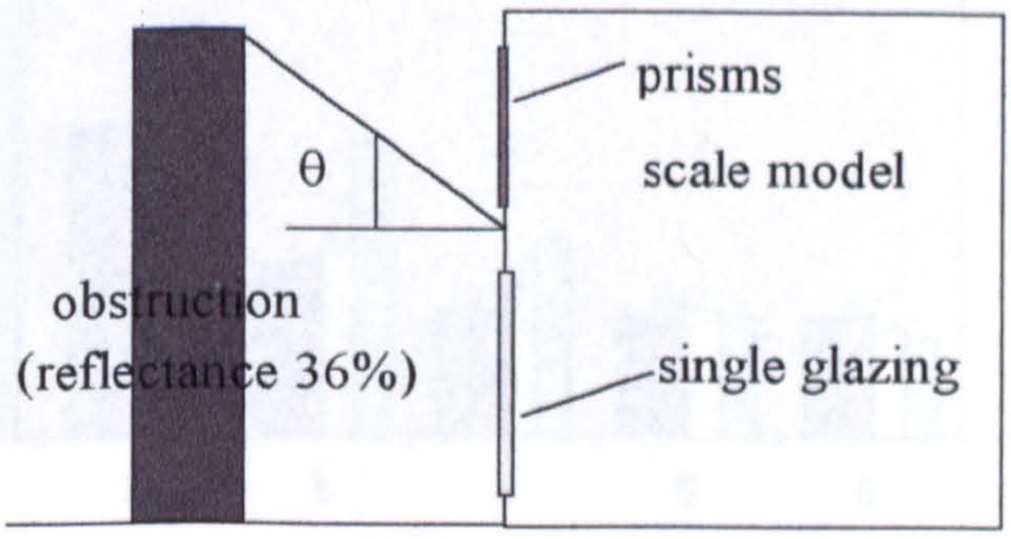

θ= obstruction angle

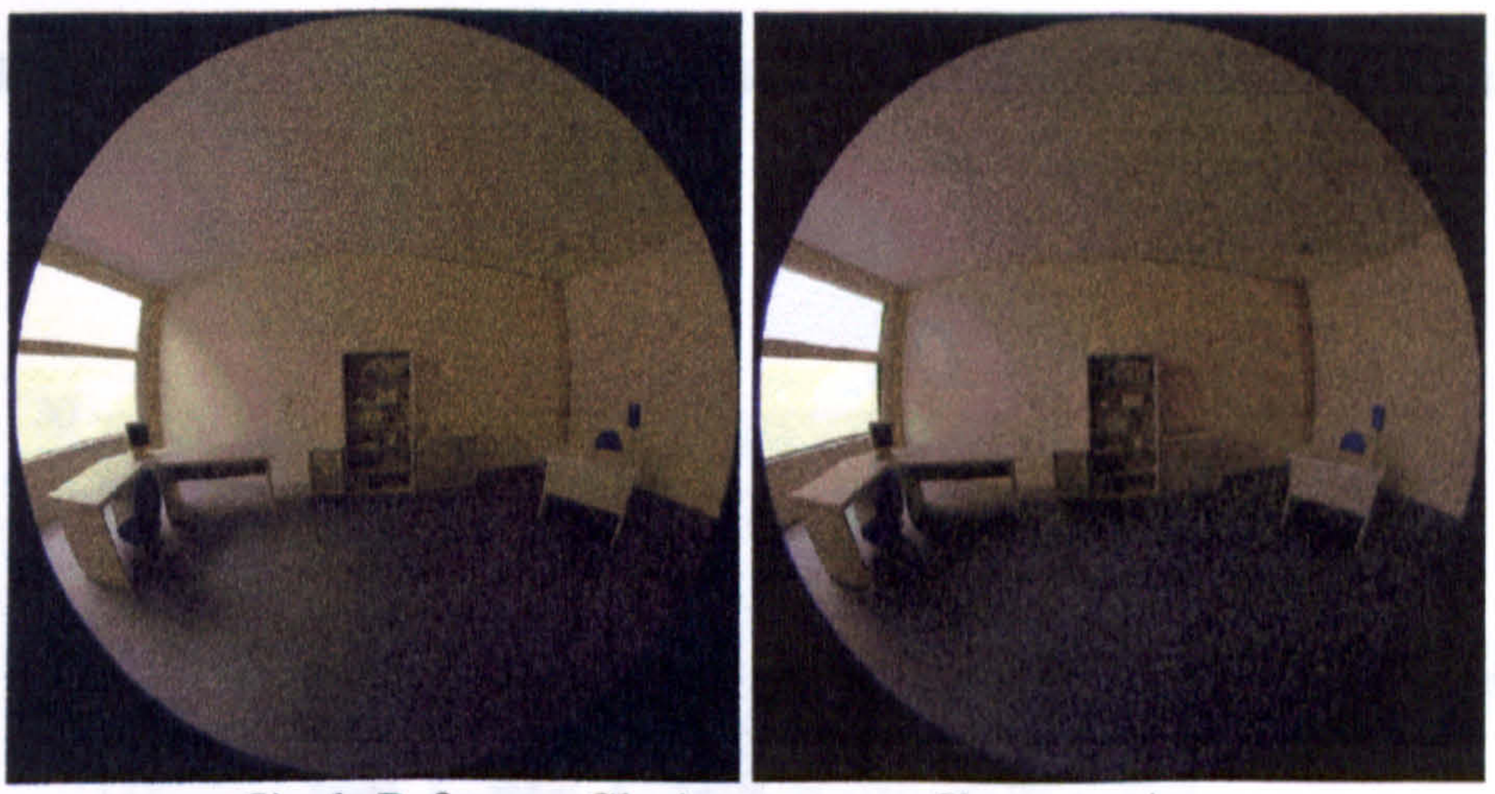

Single Reference Glazing | Shape-cut Array

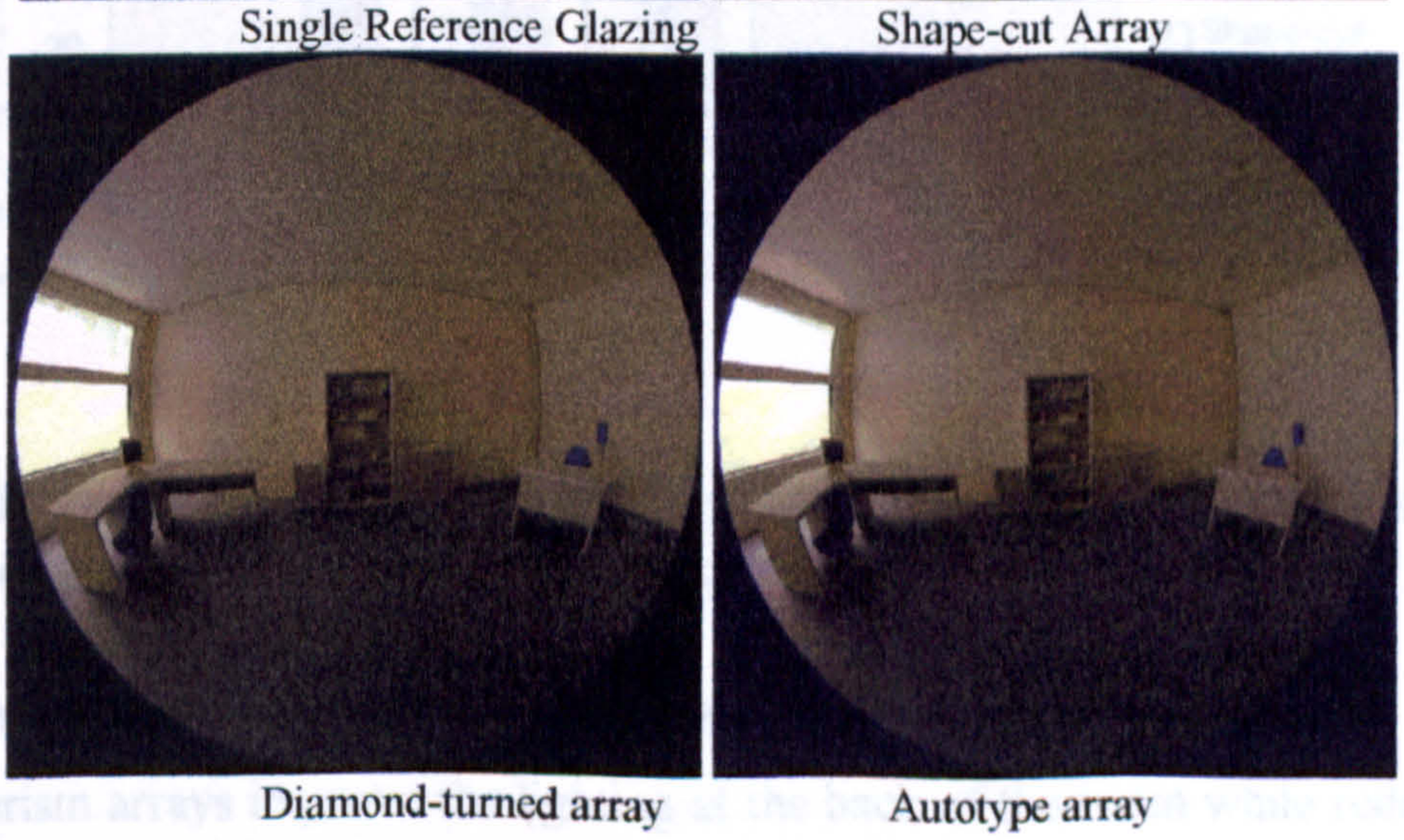

Diamond-turned array | Autotype array

Fig 3-4: ***(Top)*** **Schematic representation of obstructed window.** ***(Bottom)*** **Photographs of model rooms with 40° obstruction (exposure f11, 1/60s, 100 ASA).**

20° Obstruction

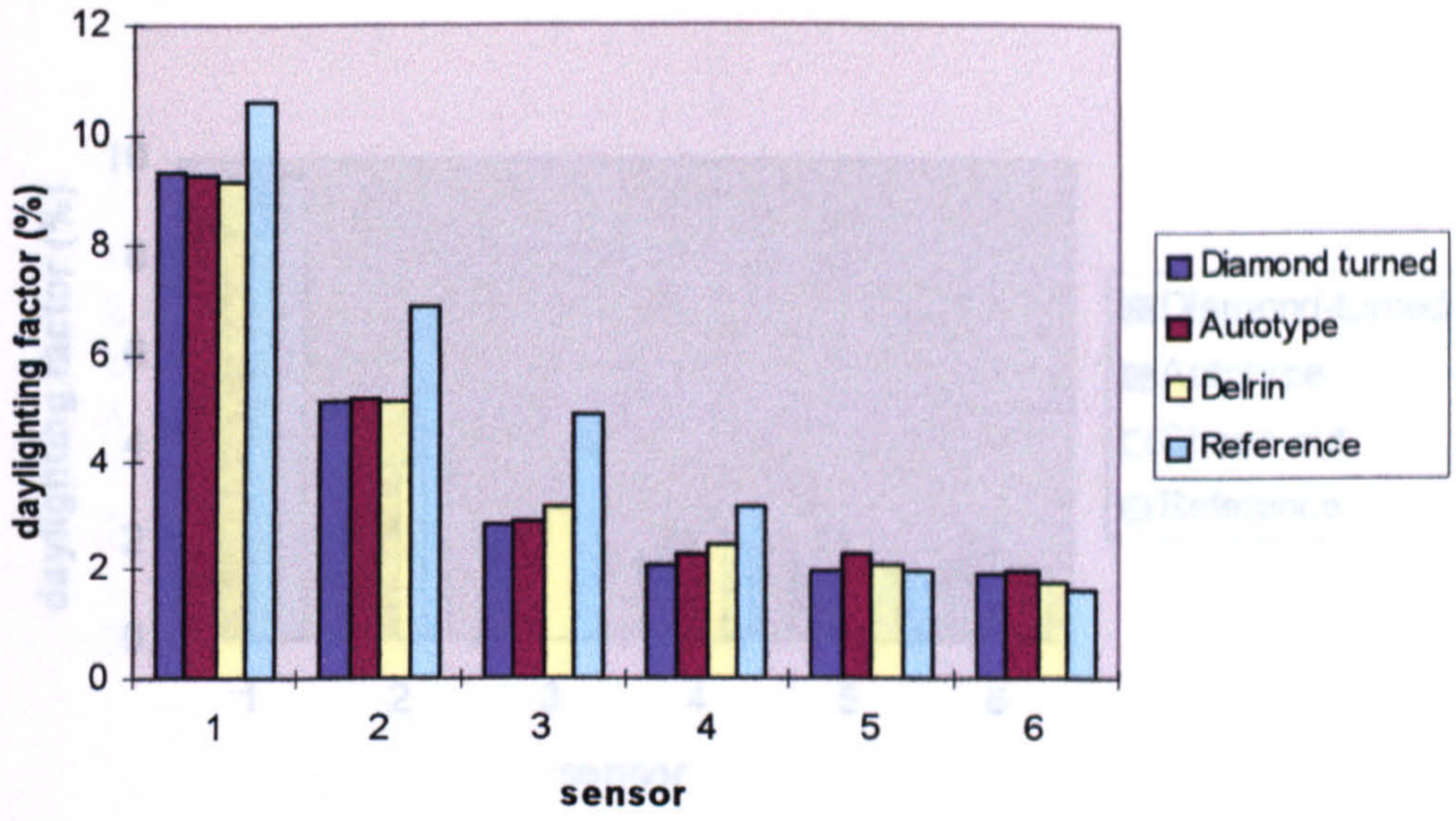

Graph 3-3: Daylighting factor measurements with 20° obstruction outside the window.

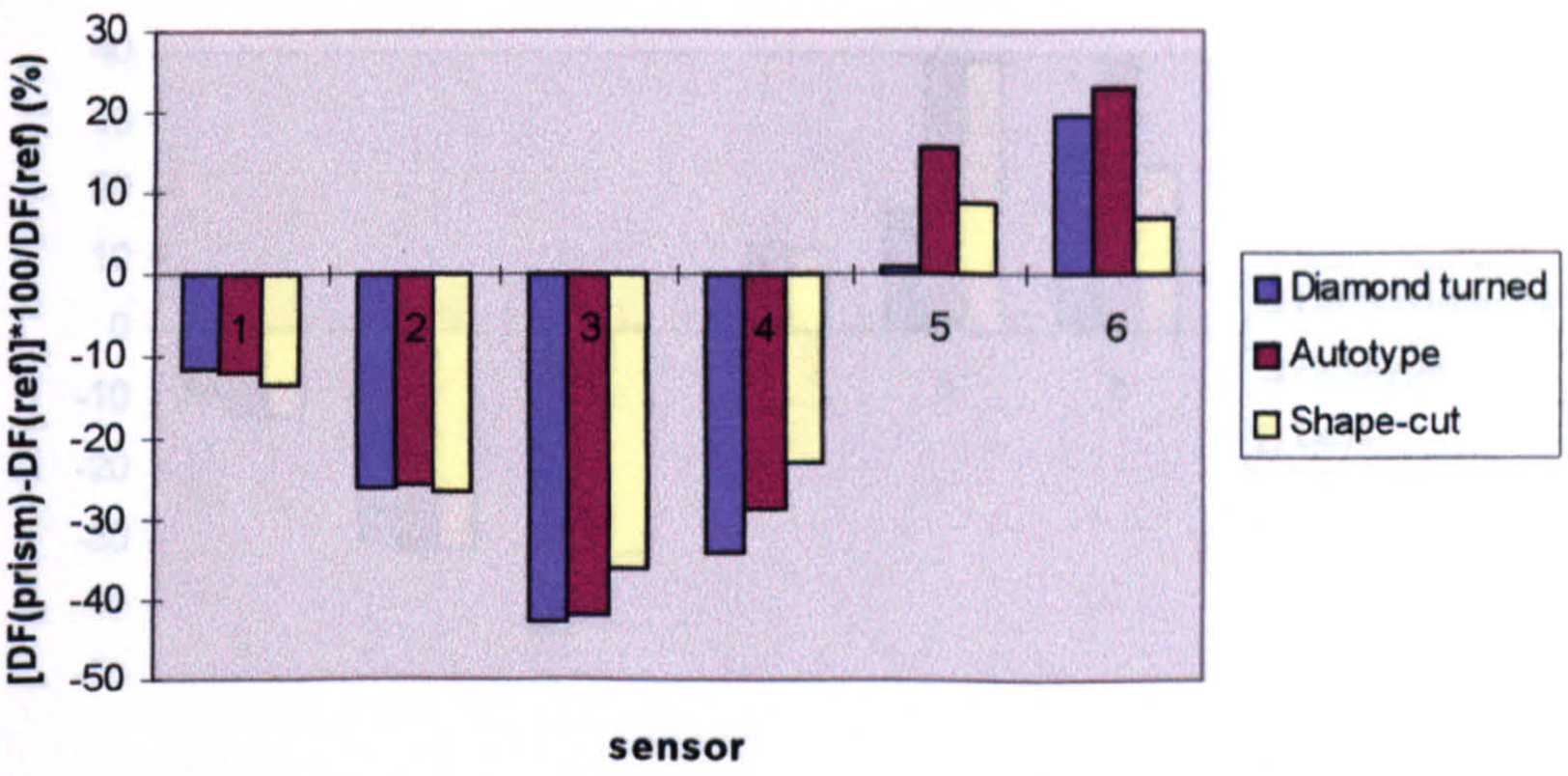

Graph 3-4: Percentage change in the daylighting factor for prismatic compared to reference glazing with 20° obstruction.

Discussion of results in comparison to reference glazing

All three prism arrays improve the lighting at the back of the room while reducing it at the front and centre. The greatest decrease occurs at sensor 3, where the illumination is reduced by up to 40%. The greatest increase occurs at the back where the illumination is improved by around 20%.

30° Obstruction

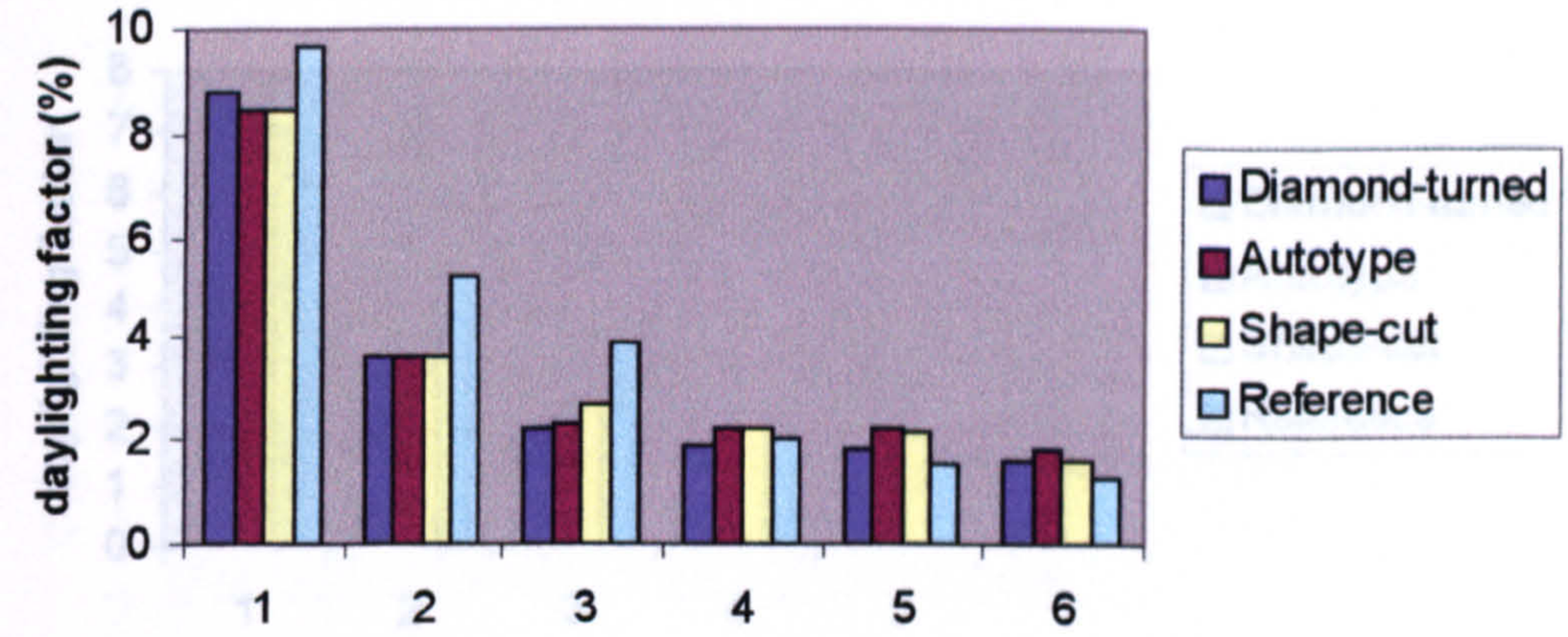

Graph 3-5: Daylighting factor measurements with 30° obstruction outside the window.

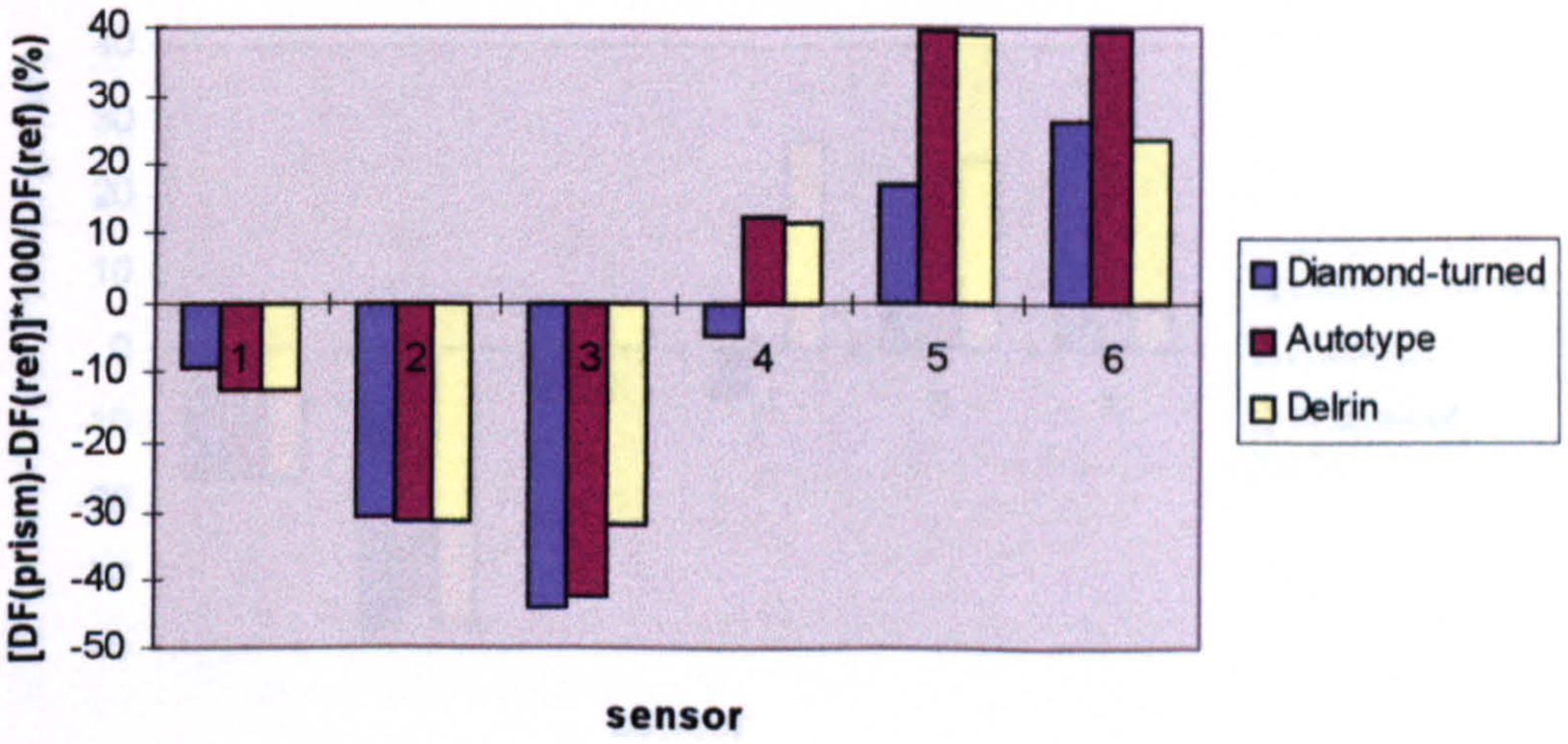

Graph 3-6: Percentage change in the daylighting factor for prismatic compared to reference glazing with 30° obstruction.

Discussion of results in comparison to reference glazing

The greatest improvement over the traditional glazing is provided by the Autotype prism which increases illumination at the back of the room by 40%. Near the centre the illumination is decreased by between 30 and 40% by the prisms.

40° Obstruction

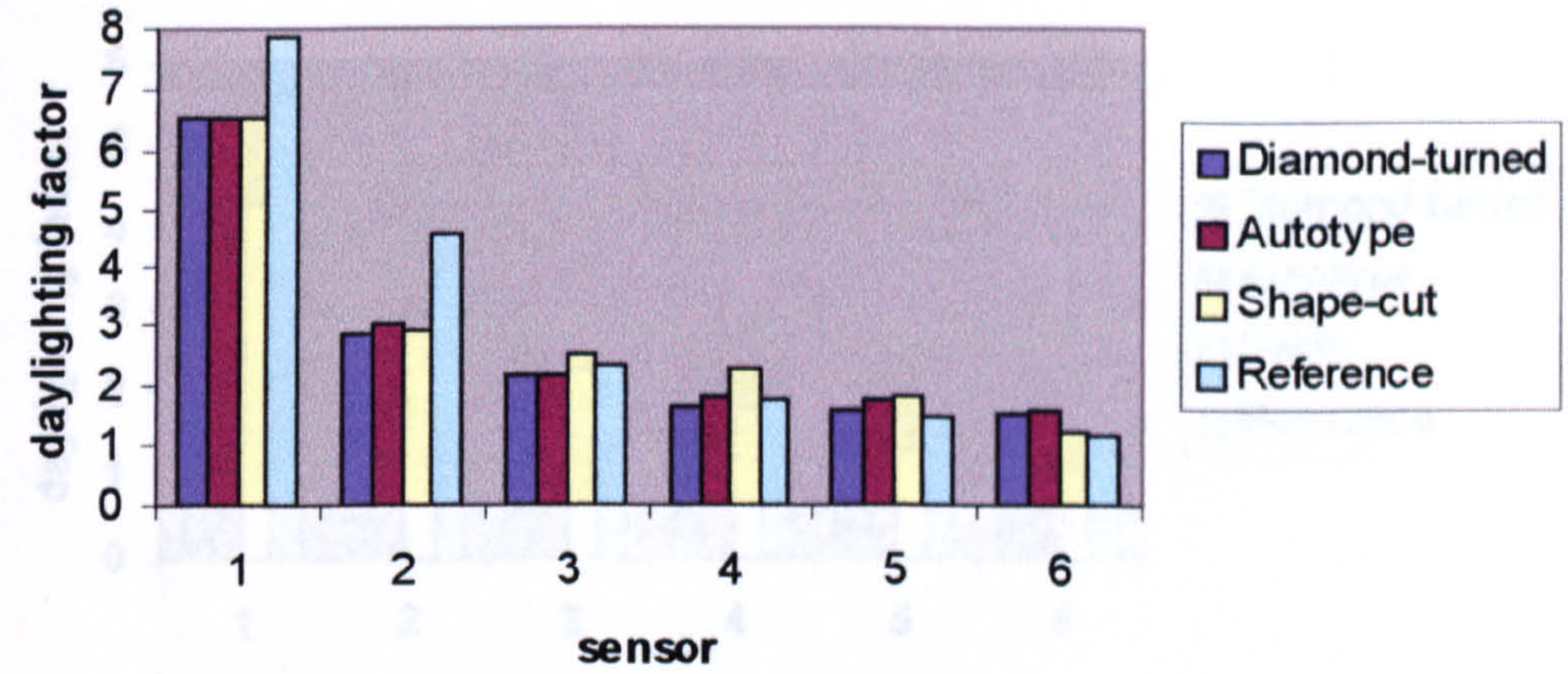

Graph 3-7: Daylighting factor measurements with 40° obstruction outside the window.

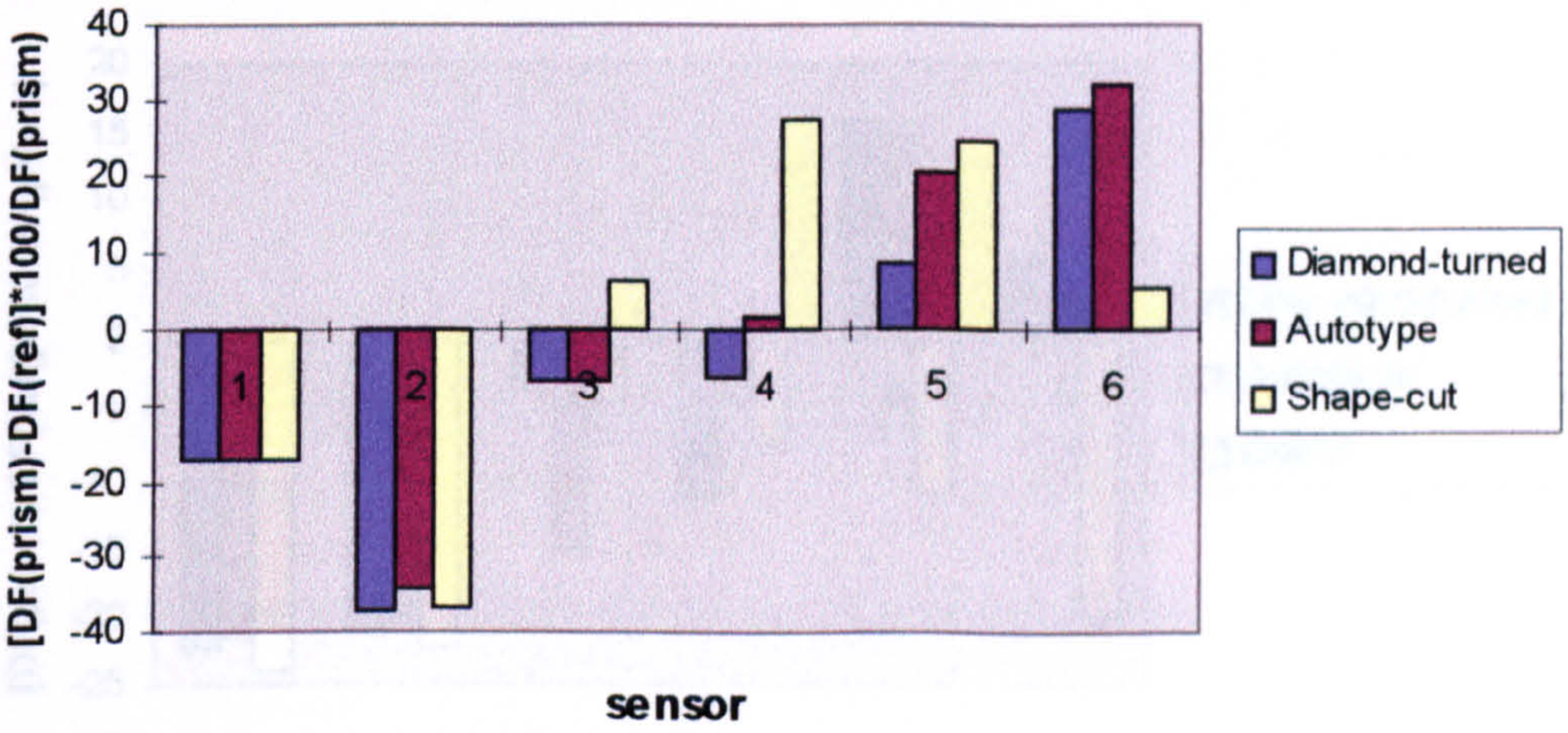

Graph 3-8: Percentage change in the daylighting factor for prismatic compared to reference glazing with 40° obstruction.

Discussion of results based on comparison with reference glazing

The improvement at the back of the room is now less than 40% for all the arrays, but once again the Autotype array shows the greatest improvement. The greatest reduction occurs closer to the window now at sensor two and is around 35%.

50° Obstruction

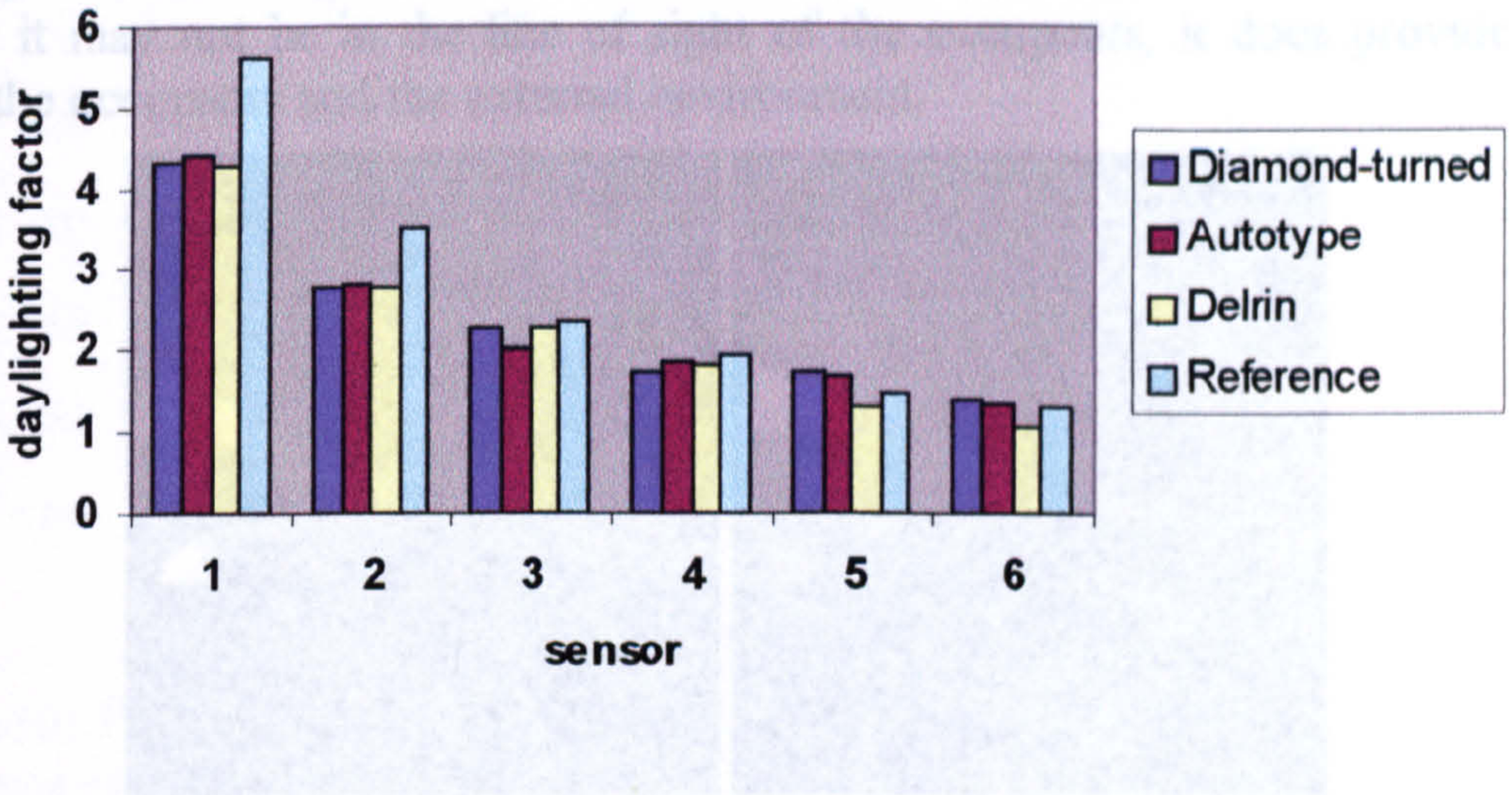

Graph 3-9: Daylighting factor measurements with 50° obstruction outside the window.

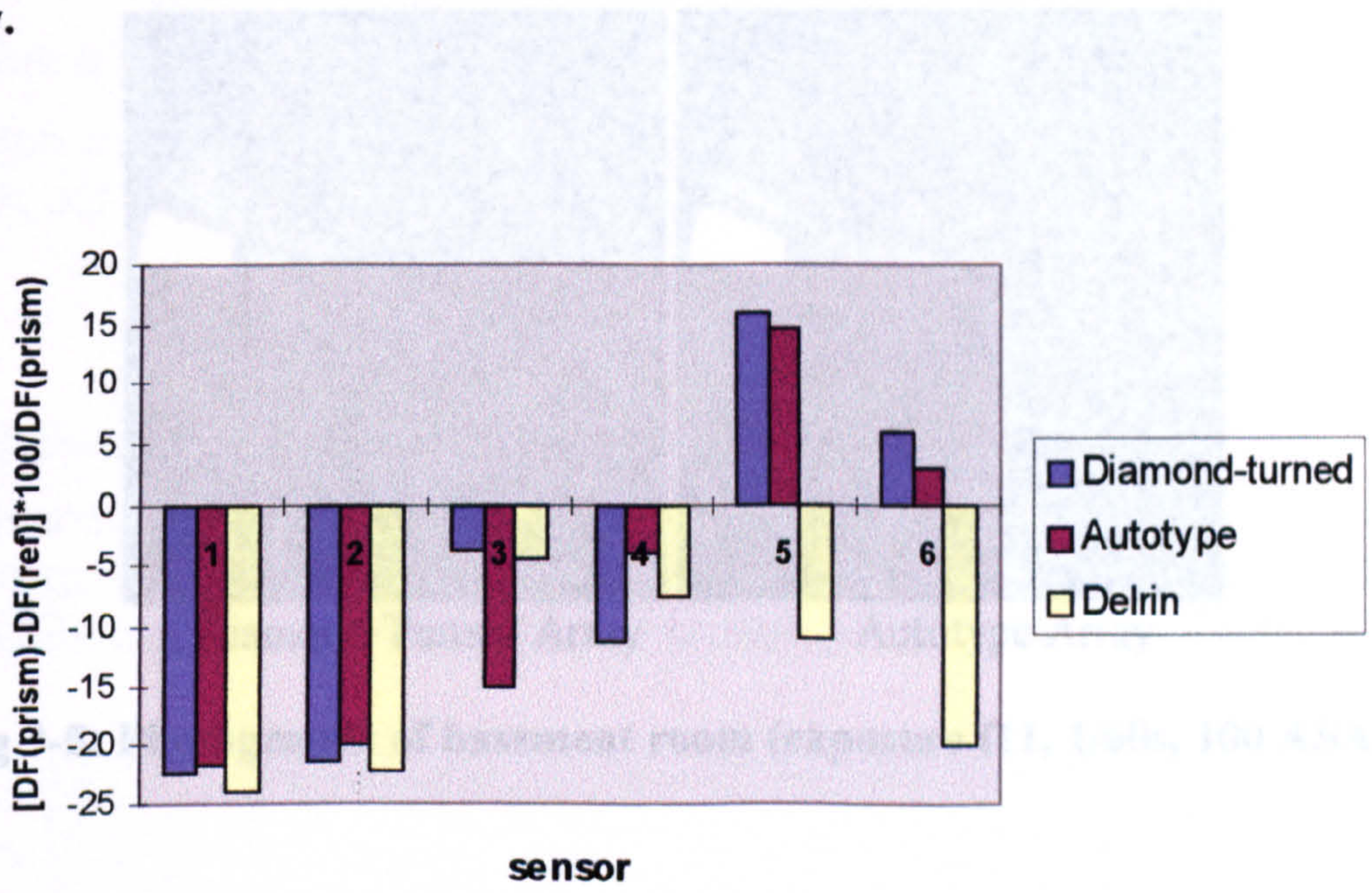

Graph 3-10: Percentage change in the daylighting factor for prismatic compared to reference glazing with 50° obstruction.

Discussion of results based on comparison with reference glazing

With a 50° obstruction the delrin array reduces the illumination through the interior of the room. The remaining two arrays give some improvement, but there is little at the rear and less than 20% at the fifth sensor.

Basement Room

The lower part of the glazing was completely blocked with the same material as the walls to simulate a basement room. In such rooms supplementary lighting may be in frequent use due to the small area of glazing. Covering this area with prisms while interesting, may not be practicable in reality because it obscures the view completely. Although it may not be in the line of sight of the occupants, it does provide a link between the occupants and the external environment.

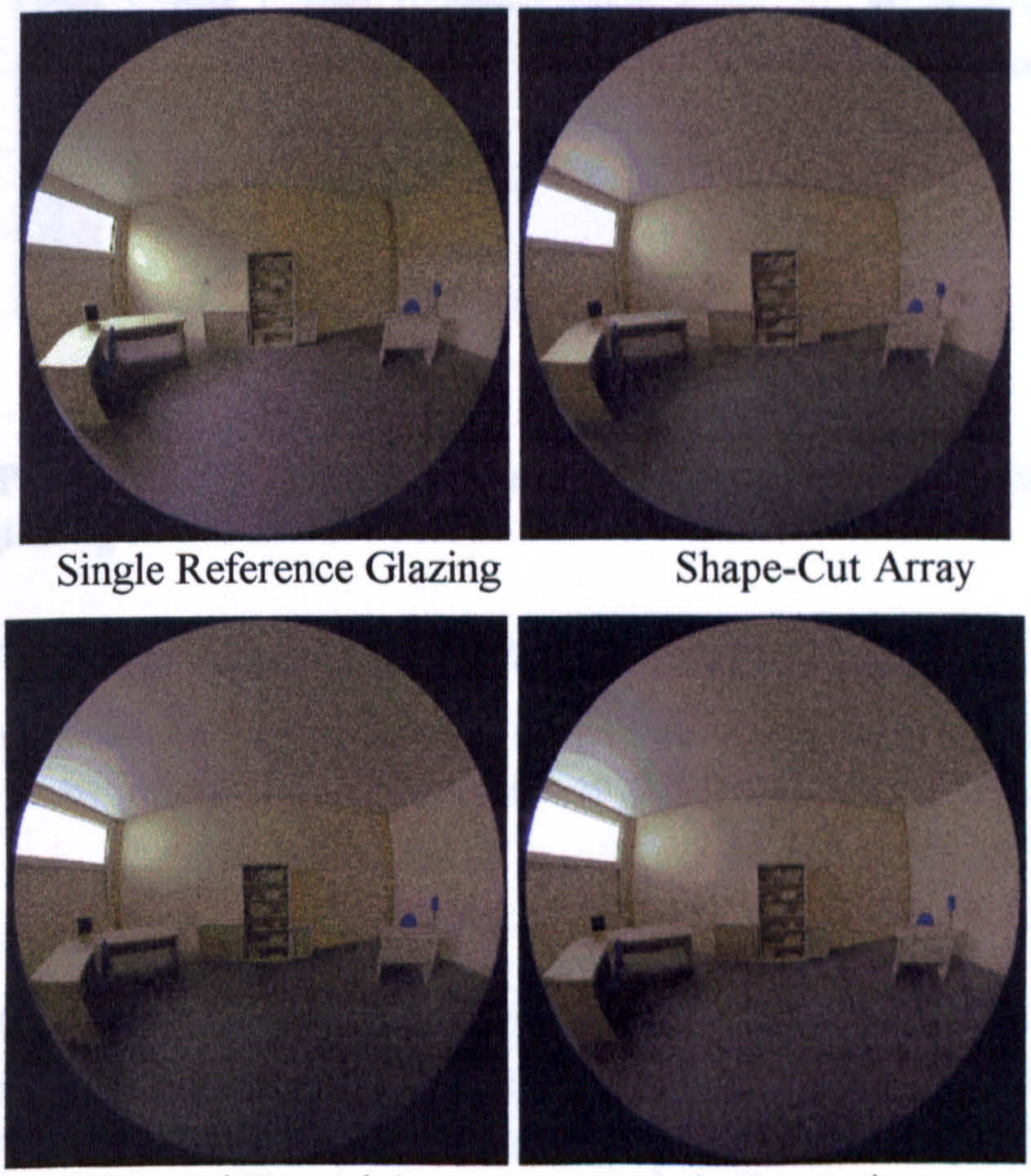

Single Reference Glazing | Shape-Cut Array

Diamond Turned Array | Autotype Array

Fig 3-5: Photographs of basement room (exposure f11, 1/60s, 100 ASA).

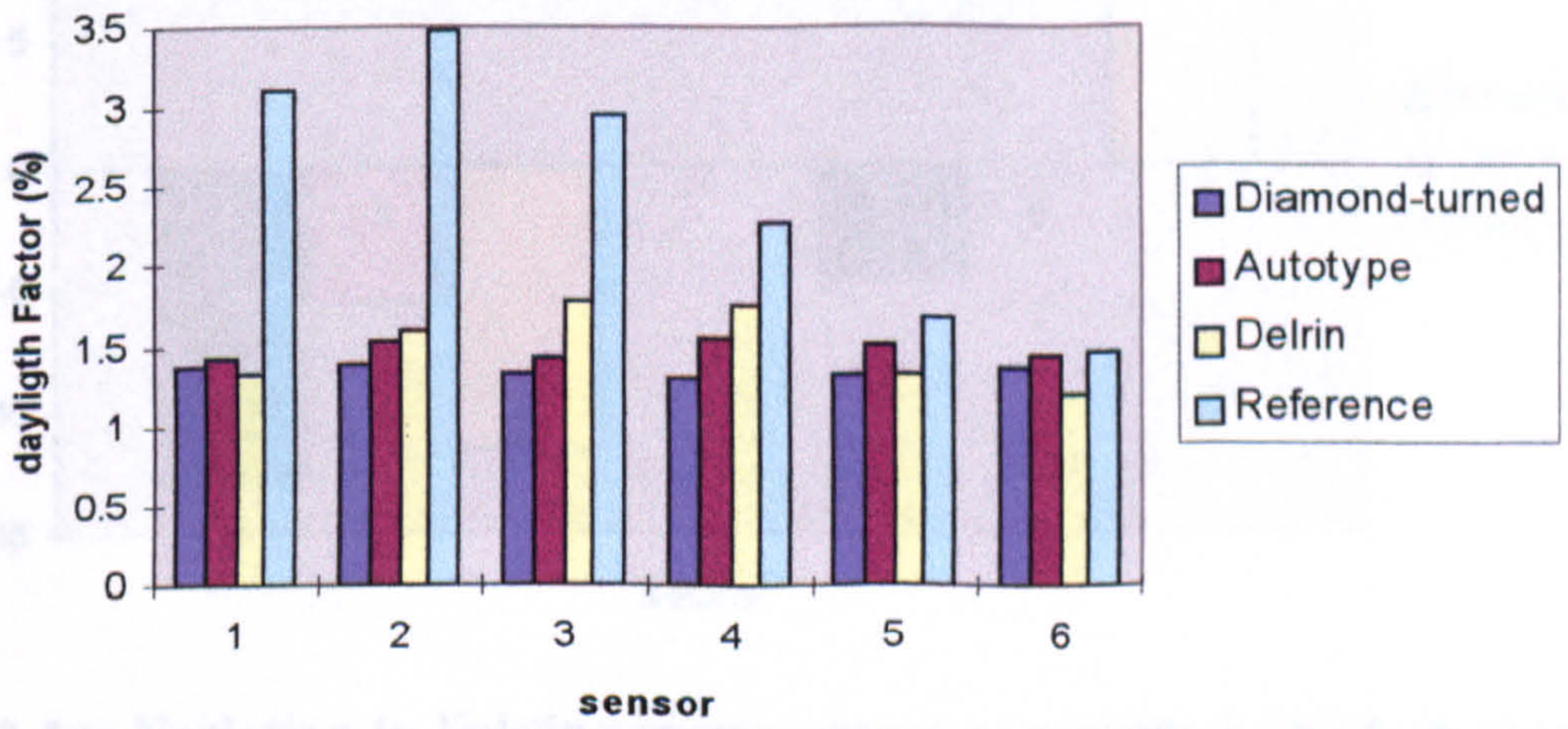

Graph 3-11: Daylighting factor measurements in basement room.

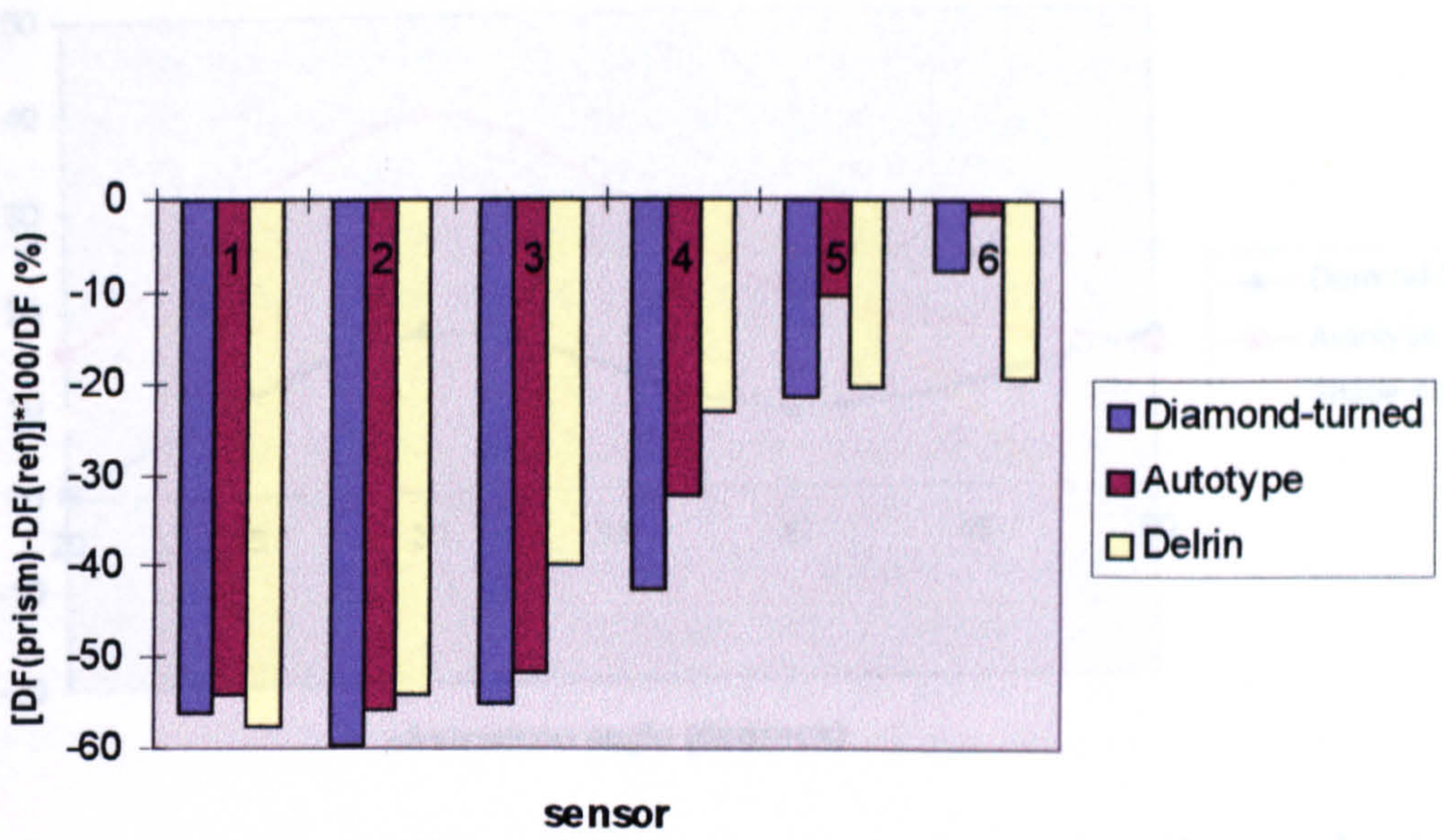

Graph 3-12: Percentage change in the daylighting factor for prismatic compared to reference glazing in basement room.

Discussion of results in comparison to reference glazing

All 3 prism arrays reduce the illumination in the interior of the room. At the rear the reduction can be by less than 10% but closer to the window this increases to around 60%.

3.2.3 Summary of results for artificial skies

To create even illumination within a room the lighting should be increased at the back, at the expense of lighting close to the window. The critical performance indicators in this experiment are therefore the back two sensors (see Graph 3-13 to Graph 3-16).

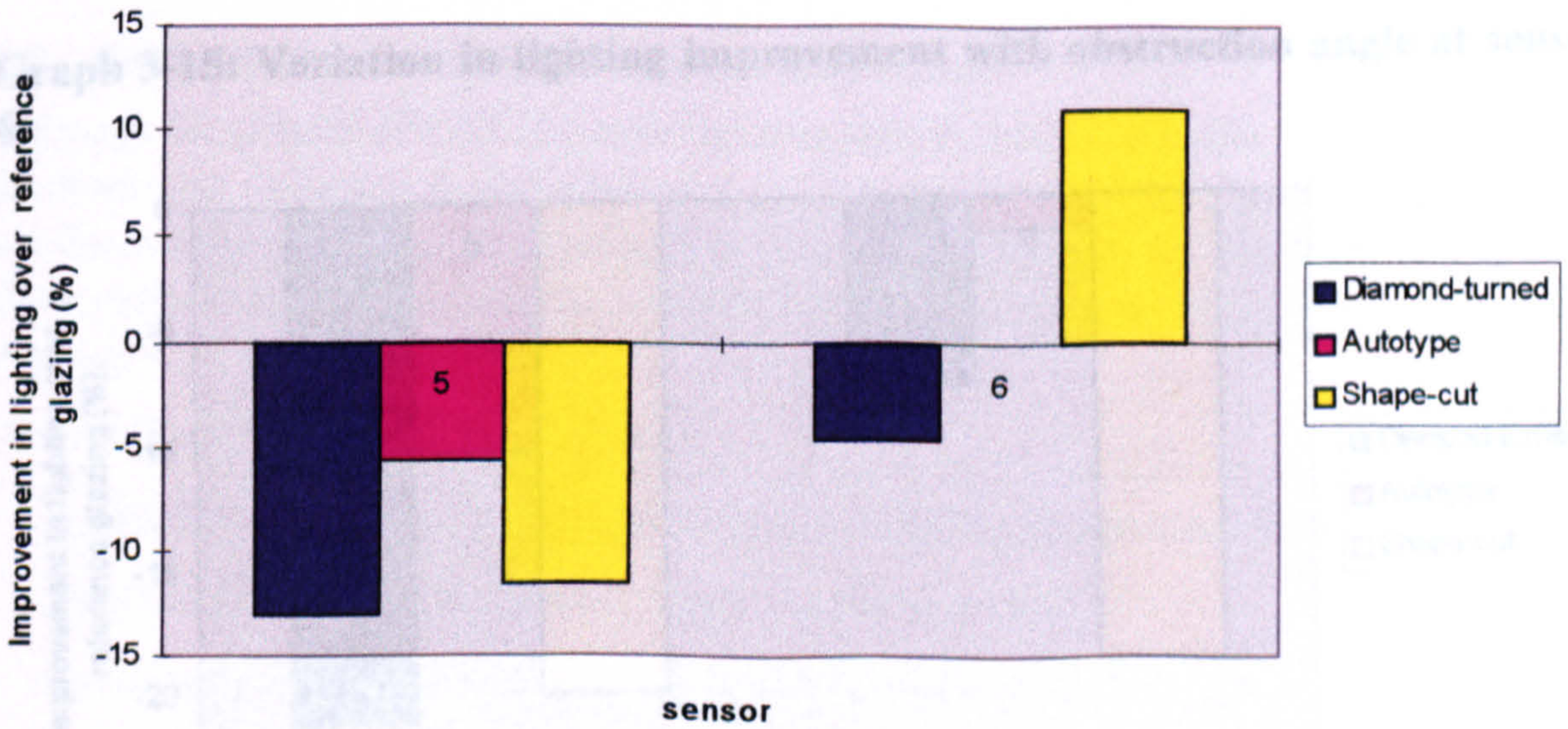

Graph 3-13: Variation in lighting improvement at sensors 5 and 6 in room with unobstructed window.

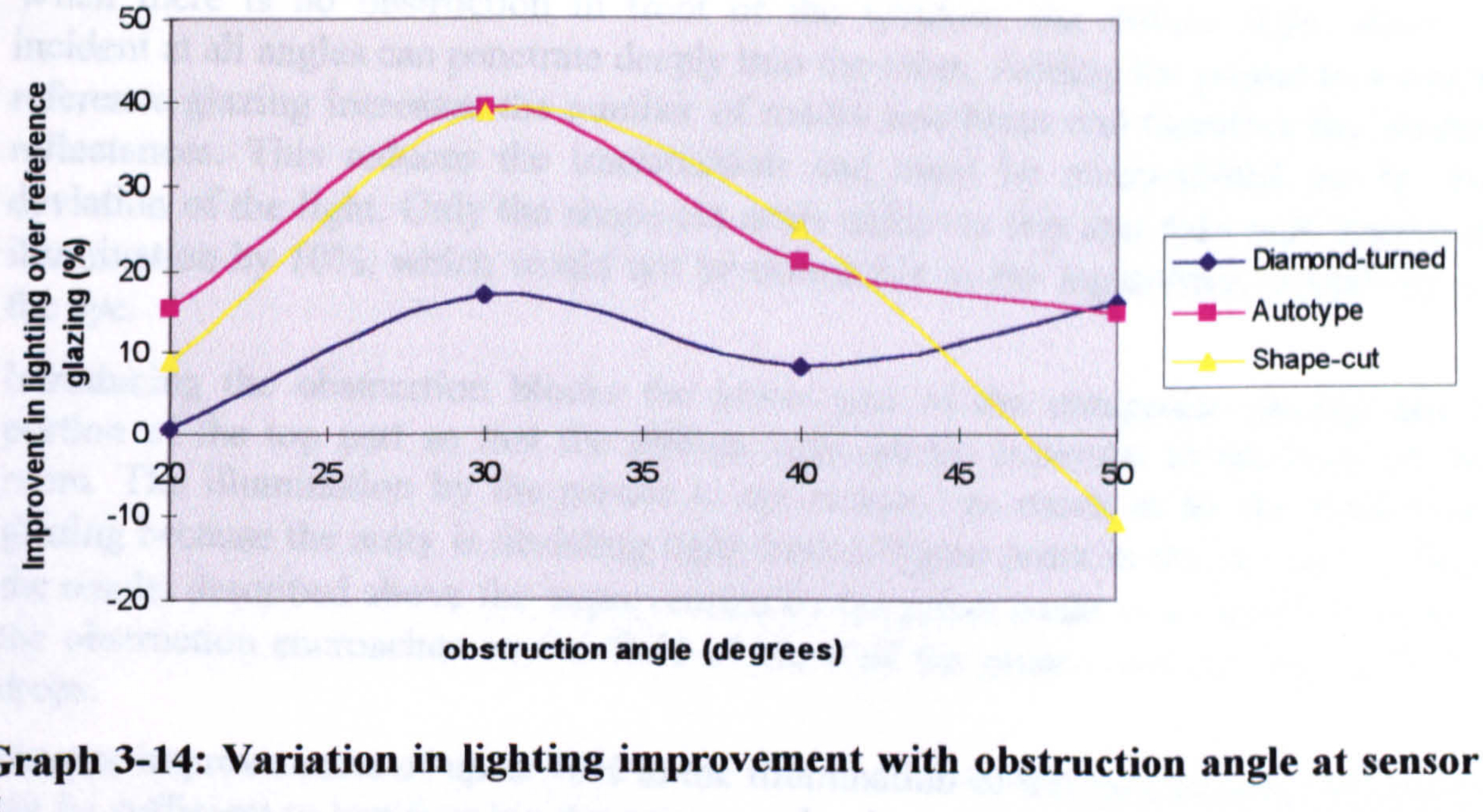

Graph 3-14: Variation in lighting improvement with obstruction angle at sensor 5.

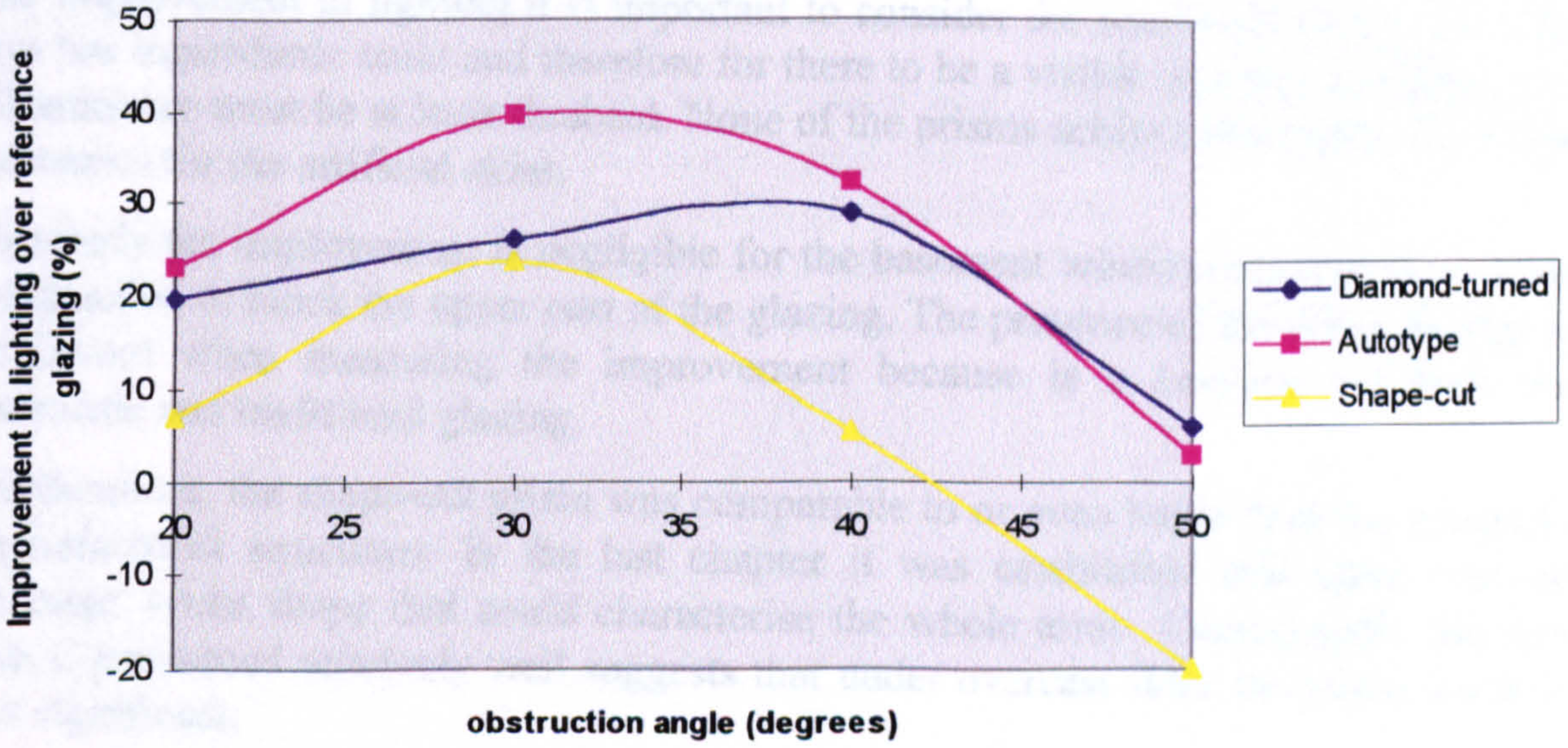

Graph 3-15: Variation in lighting improvement with obstruction angle at sensor 6.

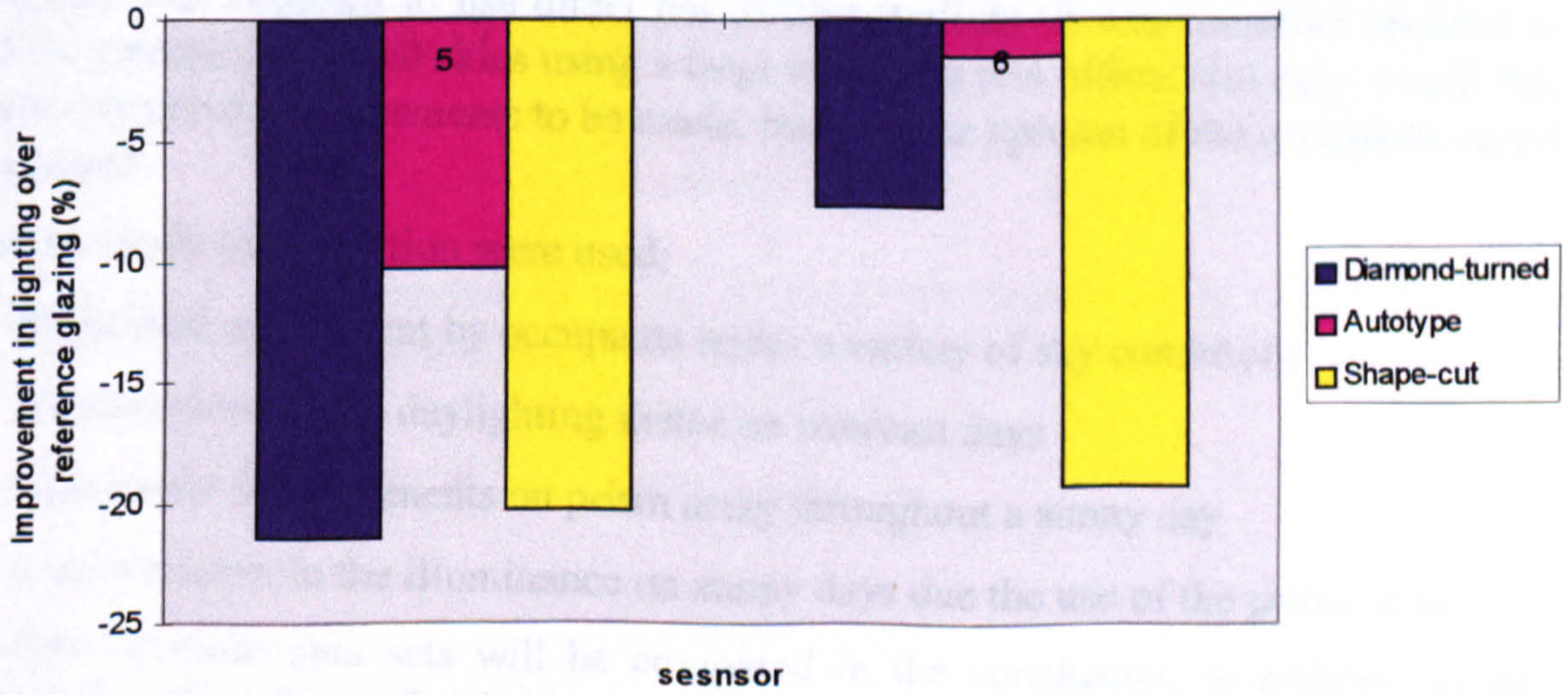

Graph 3-16: Lighting improvement at sensors 5 & 6 in basement room.

When there is no obstruction in front of the window, the diffuse light which is incident at all angles can penetrate deeply into the room. Adding the prisms to a single reference glazing increases the number of media interfaces and therefore the fresnel reflectances. This reduces the transmission and must be compensated for by the deviation of the light. Only the shape-cut array achieves this and then only improves illumination by 10%, which would not be noticeable to the logarithmic sensitivity of the eye.

Introducing the obstruction blocks the lower part of the composite glazing and a portion of the top part so that the diffuse light cannot penetrate to the back of the room. The illumination by the prisms is not reduced as much as by the traditional glazing because the array is deviating light from a higher point in the sky vault. From the results described above the improvement by the prism peaks at around 30°, before the obstruction encroaches on the 'field of view' of the prisms and the improvement drops.

Despite improvements of up to 40% in the illumination of the interior this still would not be sufficient to justify using the prisms under these sky conditions. When gauging the improvement in lighting it is important to consider the sensitivity of the eye. The eye has logarithmic scale and therefore for there to be a visible increase in lighting the illuminance must be at least doubled. None of the prisms achieve this under any of the scenarios for the artificial skies.

Similarly the improvement is negligible for the basement window because there is no obstruction to block the upper part of the glazing. The presence of the lower glazing is irrelevant when measuring the improvement because is a constant for both the primsatic and traditional glazing.

Furthermore, the shape-cut prism was comparable to or even better than the precisely manufactured structures. In the last chapter it was established that there was no 'average' prism shape that could characterise the whole array. Consequently the fact that it performed relatively well suggests that under overcast skies the prism angle is not significant.

3.3 Performance of Prisms under Real Skies

Although the prisms did not improve lighting significantly under the artificial sky, the structure was designed to use direct not diffuse sunlight. It was therefore decided to test the prisms under real skies using a large array in a real office. Not only would this allow extensive measurements to be made, but also the opinion of the occupants could be gauged.

Four methods of evaluation were used:

- Subjective assessment by occupants under a variety of sky conditions
- Measurement of the daylighting factor on overcast days
- Luminance measurements on prism array throughout a sunny day
- Improvements in the illuminance on sunny days due the use of the prism array

All four of these data sets will be compared in the conclusion, in addition to the information from the artificial skies.

The Prism Array

A large-scale test of the prisms was performed in an office at NPL. One third of a large window (60 cm x 40cm) was to be covered with a mosaic of the prisms on a perspex sheet. The choice of the prism from the three tested was limited. The masters for the Autotype array had been destroyed by the company. The master of the shape cut array did not have the required facet angle. The only possibility was the diamond-turned prism which had a master array of area 7.5cm x 7.5 cm. To fill one third of the window would require at least 150 copies to be manufactured using the process described in Chapter 2. The process usually involves producing a resin replica on perspex substrates but gluing the separate pieces together would form quite a fragile structure. In addition the adhesive may cover some of the prismatic structure. An alternative method was tried of replicating the resin copy onto a flexible melinex film (similar to acetate). Poor adhesion of the resin to the film though meant that an alternative method had to be sought.

The masters were instead sent to OpSec, a company that produces nickel shims for the Autotype process. These metalised copies were then used to emboss a roll of transparent prism replicas on flexible film that could cover the window.

It had hoped that the prisms would be embossed into a material of similar refractive index as that used in the design calculation (page 1-8). However the Autotype, lacquer has a lower refractive index (1.51 at 632nm) than the 1.567 (at 587nm) used in the design calculation. Graph 3-17, Graph 3-18 and Graph 3-19 show the effect on the deviation angles of a collimated white light source as shown on page 1-12.

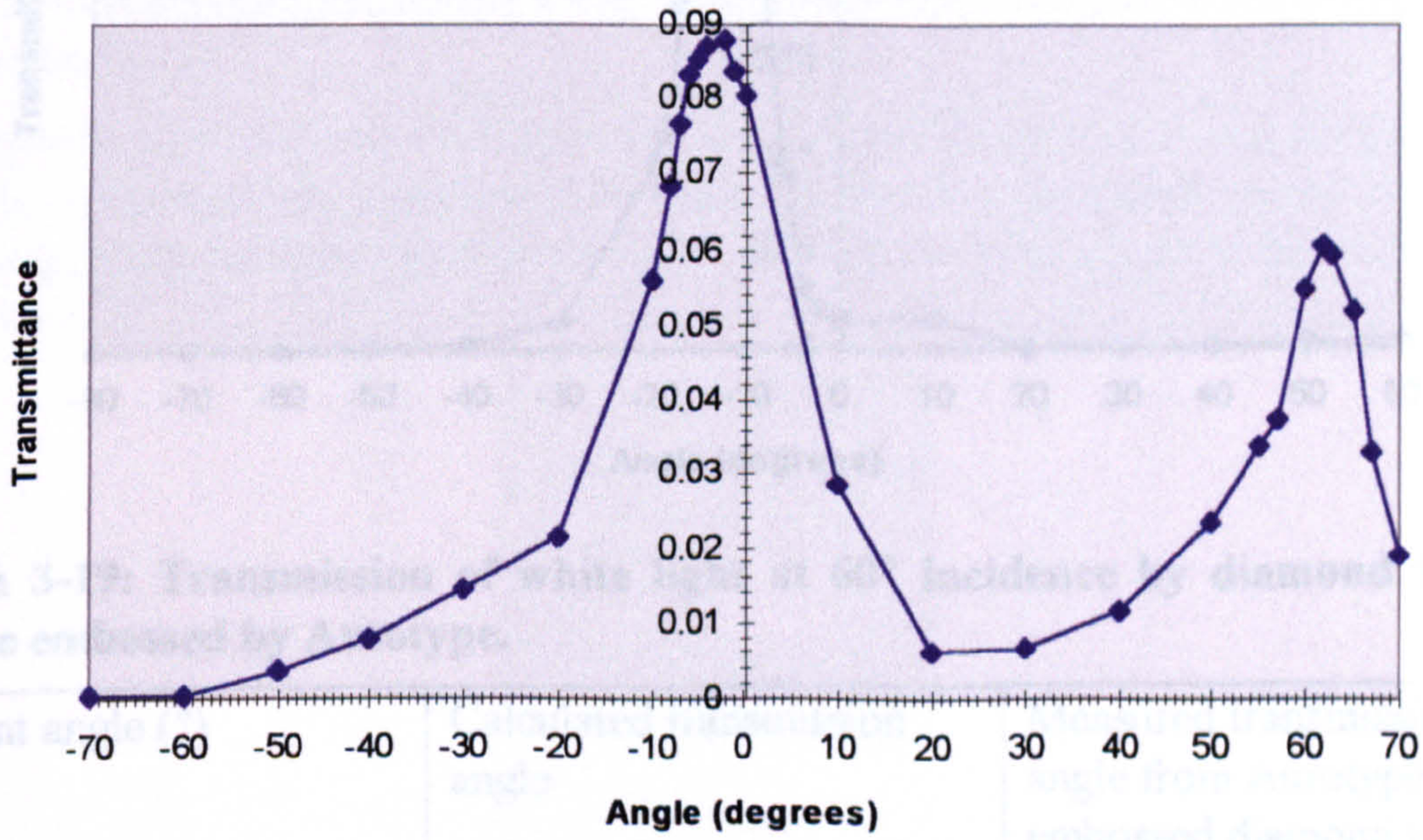

Graph 3-17: Transmission of white light at 40° incidence by diamond turned sample embossed by Autotype.

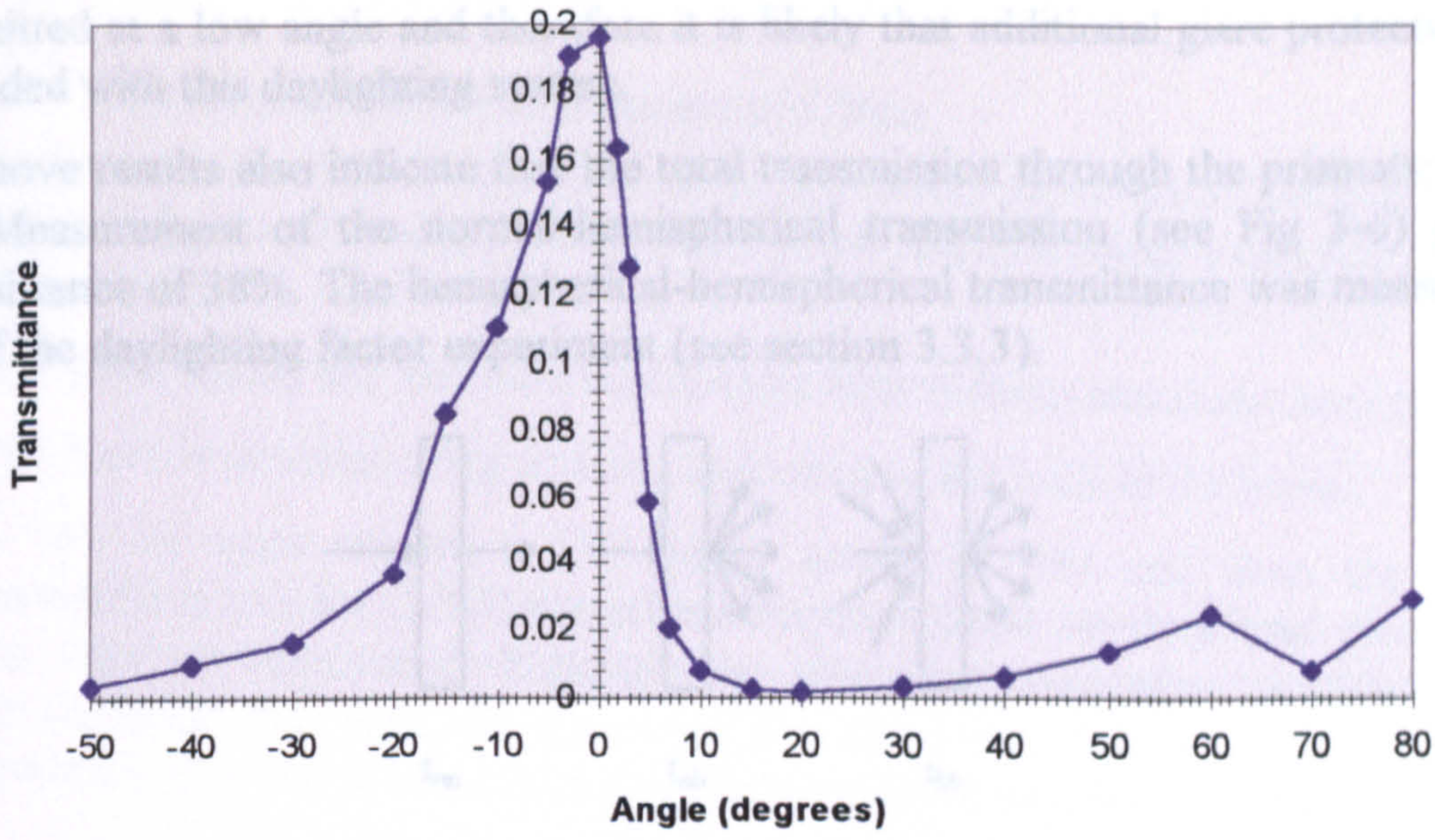

Graph 3-18: Transmission of white light at 50° incidence by diamond turned sample embossed by Autotype.

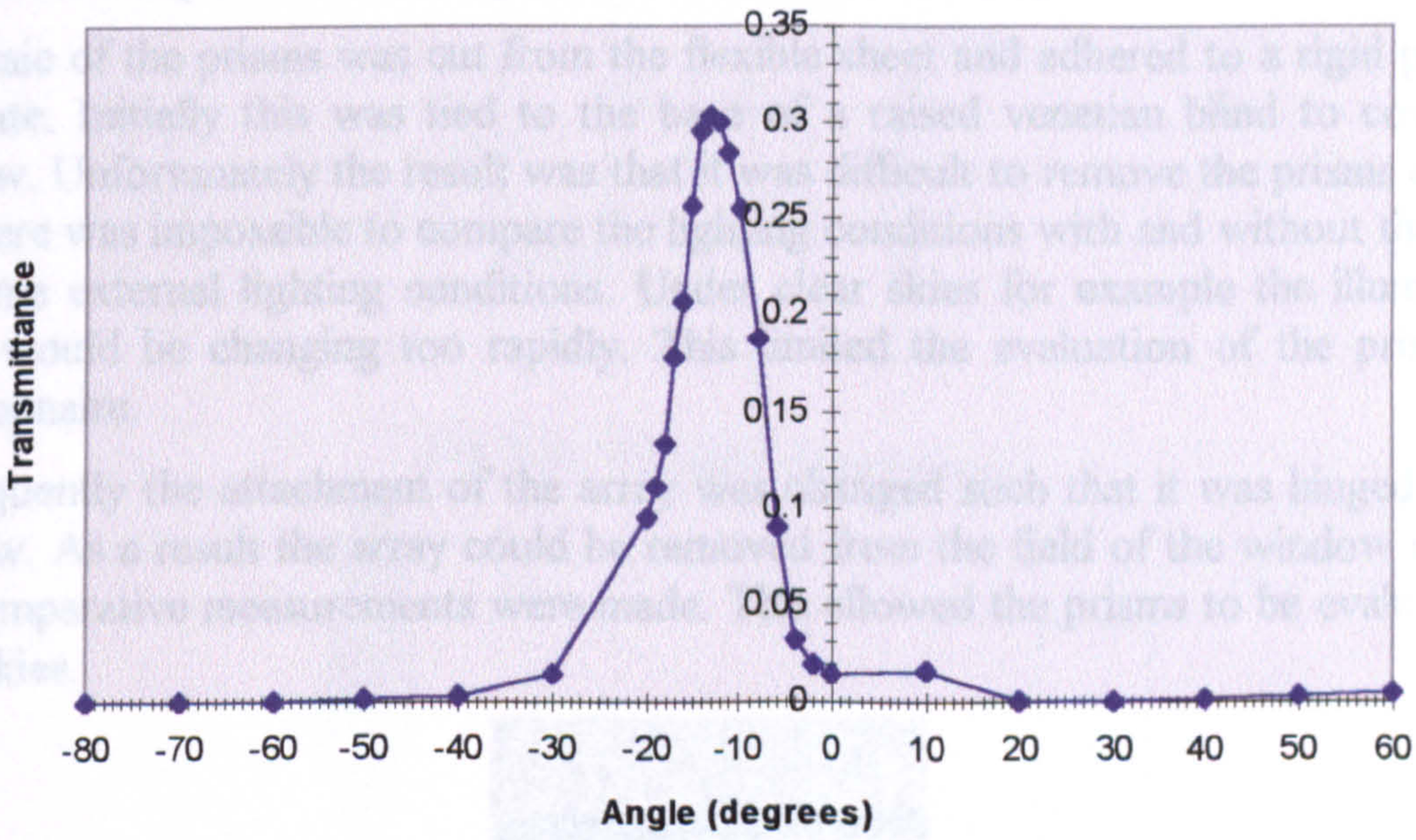

Graph 3-19: Transmission of white light at 60° incidence by diamond turned sample embossed by Autotype.

Incident angle (°)	Calculated transmission angle	Measured transmission angle from Autotype-embossed diamond turned sample
40°	-10.5°	-5°
	85°	63°
50°	10°	0°
	81°	
60°	-3.5°	-14°

The transmission angle below the horizontal at 40° is not as low as the calculated value and therefore represents an improvement. At 50°, the transmission angle is not as high as the original design, but still not below the horizontal. At 60° though the light is

transmitted at a low angle and therefore it is likely that additional glare protection will be needed with this daylighting system.

The above results also indicate that the total transmission through the prismatic film is low. Measurement of the normal-hemispherical transmission (see Fig 3-6) gave a transmittance of 38%. The hemispherical-hemispherical transmittance was measured as part of the daylighting factor experiment (see section 3.3.3).

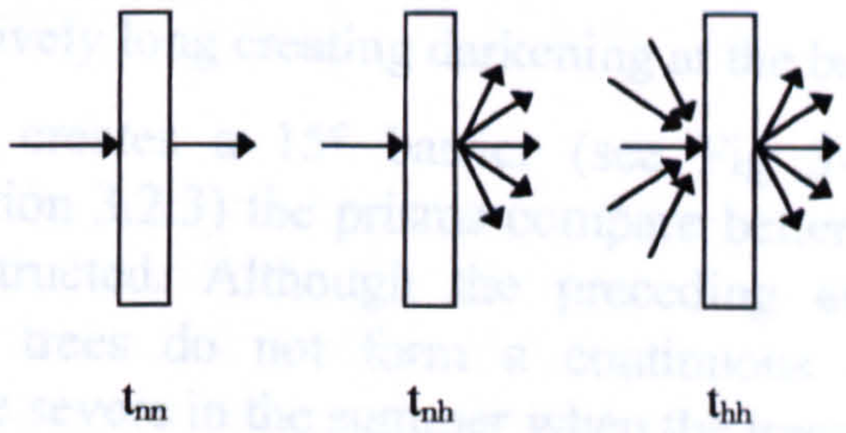

Fig 3-6: Characteristics of glazing (diagram from Fontoynont and Berruto, 1998): normal-normal transmittance (t_{nn}), normal-hemispherical transmittance (t_{nh}) and hemispherical- hemispherical transmittance (t_{hh}).

A mosaic of the prisms was cut from the flexible sheet and adhered to a rigid perpsex substrate. Initially this was tied to the base of a raised venetian blind to cover the window. Unfortunately the result was that it was difficult to remove the prisms quickly and there was impossible to compare the lighting conditions with and without the array for some external lighting conditions. Under clear skies for example the illuminance levels would be changing too rapidly. This limited the evaluation of the prisms by questionnaire.

Subsequently the attachment of the array was changed such that it was hinged to the window. As a result the array could be removed from the field of the window quickly and comparative measurements were made. This allowed the prisms to be evaluated in clear skies.

Fig 3-7: Prism array over an office window at NPL (exposure: f11, 1/60s, 100 ASA).

3.3.1 Test Location and Dimensions of Office

The room is part of the National Physical Laboratory complex at Teddington and is situated on the 1st floor of a 3 story office block. This particular room was chosen for several reasons:

- It is south facing and therefore experiences both indirect and direct sunlight.
- The room is relatively long creating darkening at the back of the room.
- A row of trees creates a 15° barrier (see Fig 3-9) and from the previous experiments (section 3.2.3) the prisms compare better to traditional glazing when the view is obstructed. Although the preceding evaluation considered lower obstructions, the trees do not form a continuous wall. The obstruction will obviously be more severe in the summer when the trees are covered in leaves.

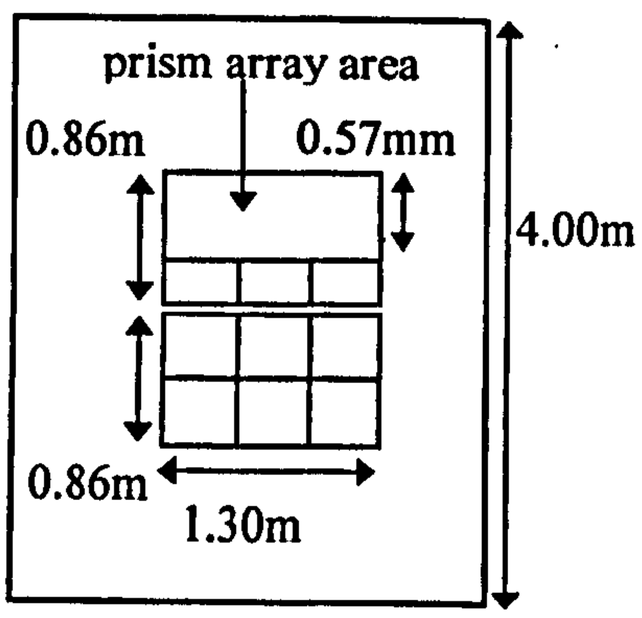

Fig 3-8: Window dimensions.

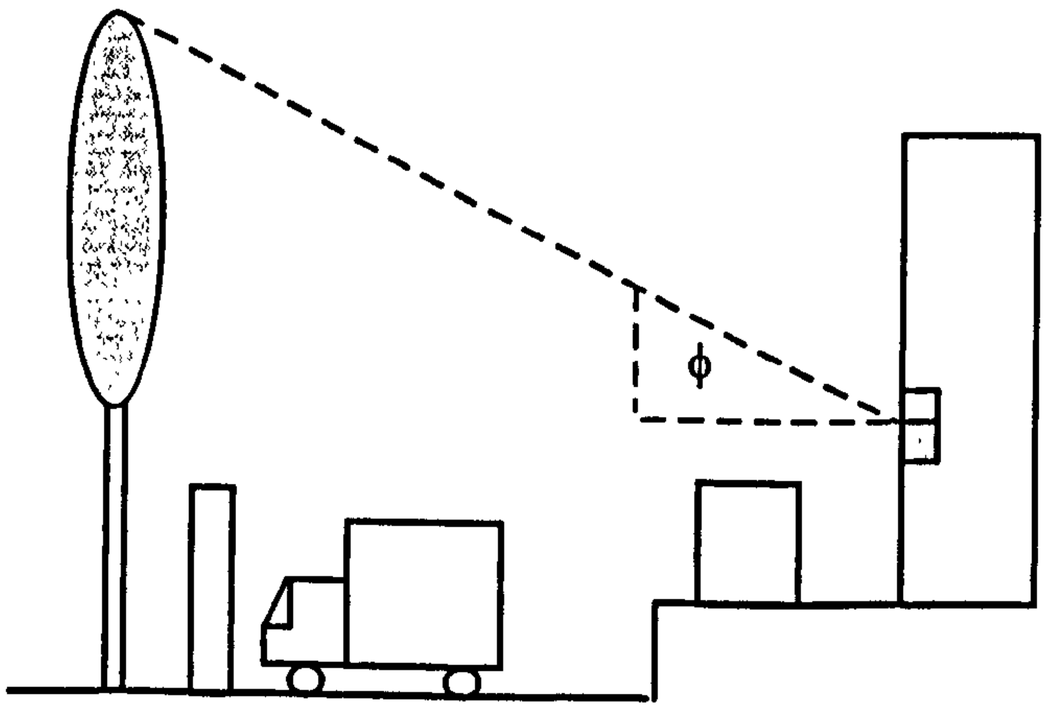

Fig 3-9: Obstructions in front of office window. ϕ≈ 15°.

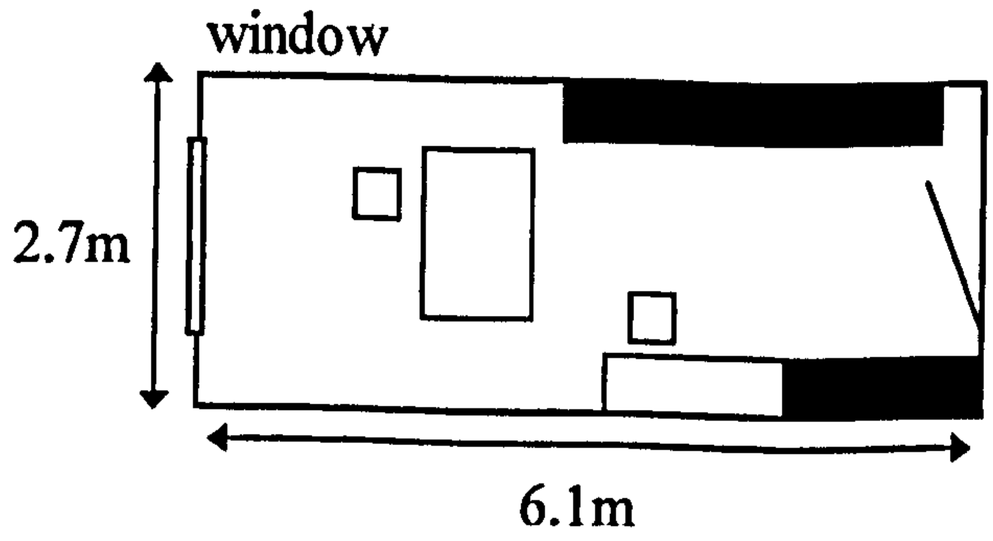

Fig 3-10: Plan View of office.

3.3.2 Subjective Assessment of Lighting

The aim was to evaluate people's opinions as to the use of microprisms as a daylighting system. The experiment focused not only on the ambient lighting but also for performing tasks. On suitable days the daylighting factor was also assessed for the prismatic array and contrasted with the traditional glazing.

Data was gathered between the beginning of March and the beginning of June.

a) Method

An array of prisms was adhered to a sheet of perspex and hung over the window. Subjects then entered the office and completed a questionnaire about the lighting quality in the room. One major feature of the questioning was the problem of glare. Discomfort from intense daylight directed at occupants' eyes could be a major disadvantage of this system.

On certain overcast days, under relatively isotropic skies, the perspex sheet with the prisms was removed and replaced with a plain, uncoated sheet. The subjects were then asked to complete a second identical questionnaire and the two sets of responses compared.

On overcast days the lit environment was also characterised using the daylighting factor; both with and without the prisms. Each of these stages will now be considered in more detail.

b) Questionnaire

Participants were asked to complete the following questionnaire. Texts were placed at positions 1, 2 and 3 in Fig 3-11 for subjects to read and gauge the adequacy of task lighting. Each was written with Times New Roman, 12 point font on plain paper.

Daylighting Performance of Prisms in an Office

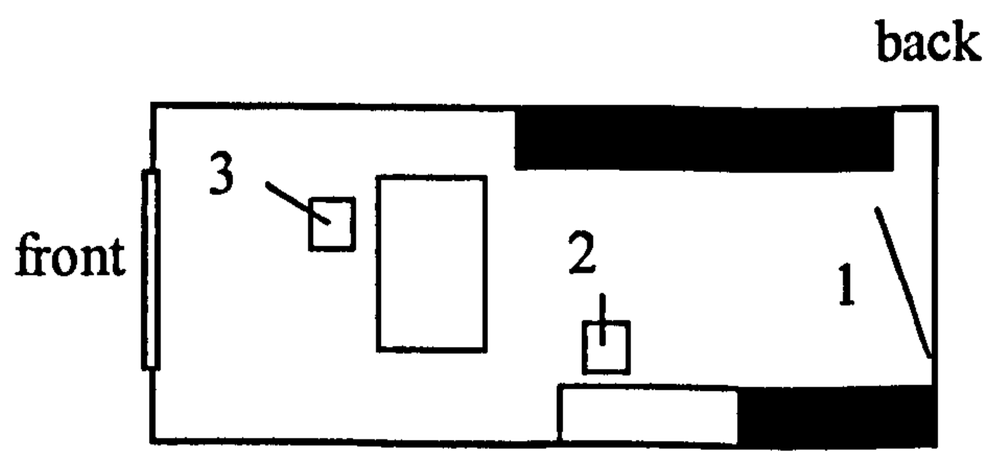

Fig 3-11: Plan view of office

Position 1

First impression:

Would you need to switch the light on if you were working in this office?

Would you need to pull the blinds if you were working in this office?

Could you rate the following statements:

1= strongly agree 5= strongly disagree

The room is evenly lit	1	2	3	4	5
The front of the room is too dark	1	2	3	4	5
The front of the room is too bright	1	2	3	4	5
The back of the room is too dark	1	2	3	4	5
The back of the room is too bright	1	2	3	4	5

The section of the window containing the prisms is a source of glare yes/no
If yes, how would you rate the glare?

Very strong Very weak
1 2 3 4 5

The section of the window without the prisms is a source of glare yes/no
If yes, how would you rate the glare?

Very strong Very weak
1 2 3 4 5

Position 2

Please sit down and read the text at position 2.
Could you rate the following statements
1= strongly agree 5= strongly disagree

I find it easy to read the words	1	2	3	4	5
I have to strain my eyes to read	1	2	3	4	5
Under these conditions I would normally turn on the light to read	1	2	3	4	5

Position 3

Please sit down and read the text at position 3.
Could you rate the following statements
1= strongly agree 5= strongly disagree

I find it easy to read the words	1	2	3	4	5
I have to strain my eyes to read	1	2	3	4	5
Under these conditions I would normally turn on the light to read.	1	2	3	4	5

Other Comments

Would you care to make any other comments about lighting in the room?

Thank you for taking the time to complete this questionnaire

Subjects were asked to complete the questionnaire three times during the day. The timing of the assessments are crucial because of light switching behaviour[ii]. Most

people will enter the office at around 9.00 a.m. and decide whether or not to turn on the light. If the decision is yes, then the light will often remain on for the rest of the day. The first assessment therefore occurred between 9 and 9.30am. The second assessment occurred between 1.00pm and 1.30pm which is solar noon and is the most likely time that glare problems will occur. It also coincides with the time NPL staff return from lunch and could be another occasion when a decision is made as to the lighting conditions. The final assessment took place between 4.30 and 5pm, which was when the light started to fade (during winter) and supplementary lighting could be required.

Before each questionnaire was completed the sky conditions as viewed through the office window were noted.

c) Results of Questionnaire (all times are British Summer Time)

The results are divided into 3 separate categories, based on the time that the questionnaire was completed. Each category is divided into 3 sub-categories based on the sky conditions: clear, broken cloud and overcast. The responses to the questionnaire are given in Appendix D, but their interpretation is documented below.

Time 9:00 am, Sky: Clear Completed Questionnaires: 3

The sample is rather limited for these conditions as clear skies at 9.00am in Britain are not a common phenomenon. All the participants agreed that the room was well-lit and did not need supplementary lighting or glare protection. There were no problems reading any of the texts and the room was perceived as being evenly lit. No 'Other Comments' were provided.

Time 9:00 am, Sky: Broken Cloud Completed Questionnaires: 9

Although this category includes a wide range of sky conditions, there would appear to be reasonable agreement between the participants on their first impressions. Only one person wanted to switch the light on and no glare protection was needed. Despite the former there was some debate as to the uniformity of the illumination. Yet even when the respondents did not feel the room was evenly lit, they would not have turned on the light and could read printed words with ease.

Other Comments:

"Generally the lighting conditions within the room were uniform. However a slight light gradient was in evidence, stemming from the windows."

"Need more light at the back of the room whilst sitting at position 3."

Time: 9.00 am Sky: Overcast Completed Questionnaires: 13

Opinion was divided as to whether the supplementary lighting was required under these conditions. There was also no strong indication of the uniformity of the lighting. although it did not seem to be sufficient at the back of the room. There was little difficulty in reading the words although some people still wanted supplementary lighting for this task.

Other comments:

"The backlighting at position 3 caused a shadow that might mean I'd turn the light on."

"There are shadows cast over the text when in position 3. I would turn on the light to mitigate this."

"Observers shadow affects visibility at position 3."

"Room lighting was even. Working in my own shadow at position 3."

Time: 1.00pm, Sky: Clear, Completed Questionnaires: 6

Only one person out of six felt the need to use the lights, but the majority also would have wanted to pull the blinds. The glare was nearly always felt to be very strong and this probably contributed to contributed to the opinion that the room was not evenly lit. The lighting though seemed to be sufficient for people to be able to read comfortably.

Other comments:

"If you could get rid of the glare, the room would be evenly lit."

"The day is sunny at this time but the back of the room is better illuminated than I would expect with a conventional window and the room is brighter and cheerier. Greater deviation of light would improve this impression."

Time: 1.00pm, Sky: Broken Cloud, Completed Questionnaires: 10

In the majority of case extra lighting was not needed, but glare was a problem. There was a more diverse range of glare ratings than for the clear skies but the it could still be very strong. The range of possible sky conditions within this category is reflected in some of the standard deviations. For example, the responses as to whether people need to turn the light on to read or considered the lighting to be uniform were quite diverse.

Other comments:

"Much brighter than the morning test."

"If I was going to be in the room for only a short while, I probably wouldn't need the light. However if I was going to be in the room for longer periods then I would need to turn it on."

Time 1.00 p.m., Sky: Overcast, Completed Questionnaires: 7

In all cases supplementary lighting would be needed on entering the room. The room was not perceived as being well lit and the back of the room considered to be too dark.

However occupants did not find the task of reading difficult, although would have liked extra lighting at positions 1 and 2.

Other Comments:

"Shadow from back illumination is irritating at position 3."

"The lighting is much better at position 3."

Time 4.00 p.m., Sky: Clear, Completed Questionnaires: 4

The majority of respondents did not think that extra lighting was required and the room considered to be reasonably evenly lit. However it was undecided whether the back of the room was too dark. Although the skies were clear, no problems were reported with glare.

Most people did not need to turn on the light to help them read and did not have to strain their eyes to read.

Other comments:

"Room is more evenly lit than at lunchtime but overall levels are lower. Prisms showing less obvious beneficial effect now, though blue sky evident from back of room which would not have been seen without the prisms."

Time: 4.00 p.m., Sky: Broken Cloud, Completed Questionnaires: 5

Nobody wanted to turn the lights under these conditions or to pull the blinds. The room was considered to be quite evenly lit. Only one instance of glare was noted and then it was very weak. The lighting seemed generally sufficient for reading, but there were occasions when extra may be needed at the back of the room.

Other Comments:

"My body made little or no shadow at position 3 despite the back lighting."

Time: 4.00 p.m., Sky: Overcast, Completed Questionnaires: 7

Most of the respondents said that they would turn the light on and that the room was not evenly lit. Furthermore they all agreed that the back of the room was too dark but opinion was split over whether the front was too dark as well. Although all but one subject, thought that they could read text reasonably well, most would have liked extra lighting.

Other Comments:

"Diffuse lighting."

In addition to the responses for the prisms on the window, subjects were also asked to complete questionnaires when the prism were removed. The two sets of results could then be compared. However due to the time needed to remove the prisms this test could only be performed on overcast days when the luminous environment was stable. Alternative methods are used in section 3.3.4 to evaluate the improvement by the prisms under sunny skies.

Comparison of lighting conditions, with and without prisms. Completed questionnaires: 4

Only on one occasion were the prisms considered to have improved the lighting sufficiently to turn off the lights. The room was believed to be more evenly lit with the prisms, but the back still regarded as too dark. The addition of the prisms did not significantly alter people's decision on the need for supplementary lighting when they were reading.

Other Comments:

"*Shadows are more obvious without prisms (especially at the back of the room). Might turn on light to remove them depending on where I was sitting.*"

With and without prisms: *"I would need to turn on the lights if I were to do precise mechanics or soldering."*

Without prisms*: "I would turn on the light in position 3 to minimise shadows"*

With prisms: *"Effect of shadows is reduced"*

The results from these questionnaires will be integrated in the final conclusion at the end of the chapter

3.3.3 Measurement of Daylighting Factor[iii]

The daylighting factor (see section 3.2) provides a measure of the variation of interior illumination with the outdoor lighting. In this experiment to is used to characterise the whole of an office, not just the central portion as with the artificial sky.

a) Method

As a commercial product the prisms would be located within the panes of a double glazed unit and therefore should be compared to traditional double glazing. Consequently a clear perspex sheet was placed in front of the single glazed window as the basis for comparison.

The illuminance metres used were not calibrated to an absolute standard and therefore it was necessary to construct a reference standard to ensure that the they were consistent with each other[iv]. The simplest way to achieve this was with a light box (see Fig 3-12) with a white, diffusing interior.

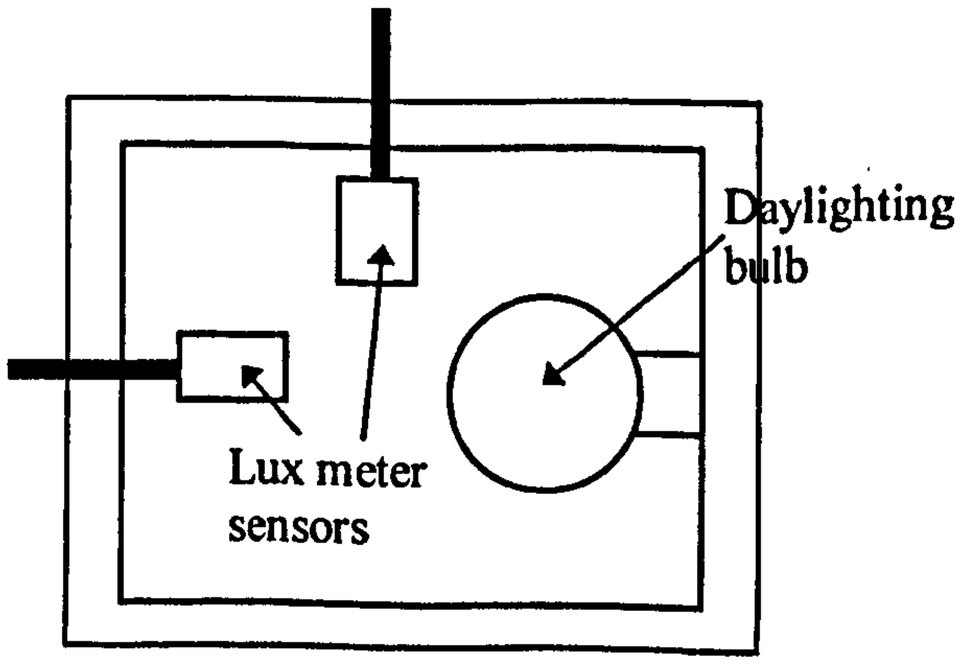

Fig 3-12: Light box as reference standard for calibrating luxmeters

The power source for the box was from the mains (as opposed to batteries) so that the power level did not deteriorate. Before a calibration the box was switched on for 30 minutes so that it reached its steady state level. The luxmeter sensors were then clamped into place (the same place for every calibration) and two readings taken. A conversion factor was then derived to ensure consistency between the two devices. Prolonged use of the bulb could cause clouding of its interior and therefore it was switched off immediately after the procedure. One of the luxmeters was taken outside but the other device remained in the office. Contact between the operators was maintained by mobile phone and measurements recorded simultaneously .To characterise the room completely the office was divided into a grid (Fig 3-13) and measurements taken at the height of the working plane (0.77m, the height of a desk).

In addition reflection measurements were carried out on all the horizontal planes within the interior. A surface of known reflectance was placed on a plane and the two luminances measured.

The reflectance of the plane was then given by:

$$\rho_p = (L_p/L_s)*\rho_s$$

where ρ_s is the known reflectance

ρ_p is the unknown reflectance

L_s and L_p are the respective measured luminances

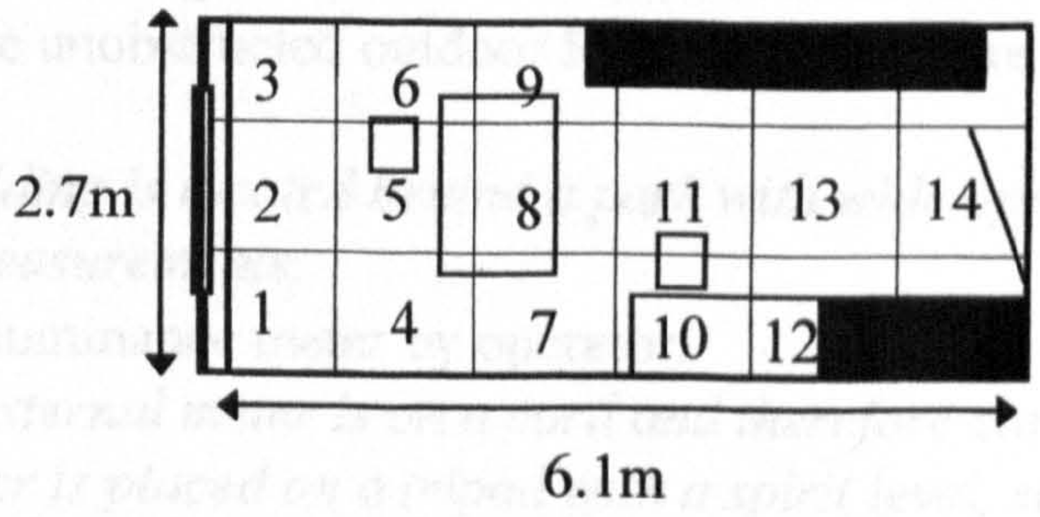

Fig 3-13: Office divided into grid for luminance measurements.

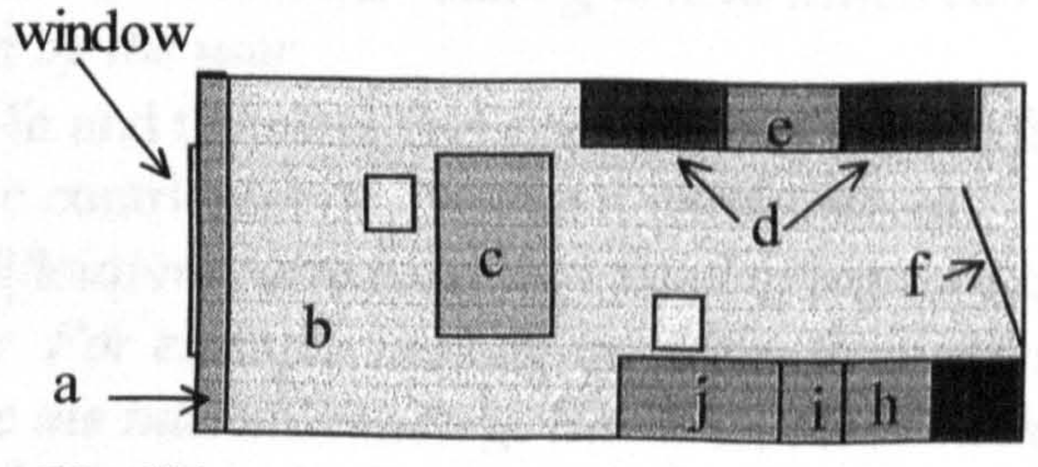

a	Wooden ledge 70±6%	g	Dark green filing cabinet 9±1%
b	Floor 14±1%	h	Brown filing cabinet 16±1%
c	Desk 18±1%	i	Dark brown filing cabinet 7±1%
d	2 Dark wooden cupboards 5±1%	j	Chest of drawers 24±1%
e	Dark metallic cupboard 16±2%	k	Wall 70±6%%
f	Door 33±1%	l	Ceiling 88±4%

Fig 3-14: Reflectances of surfaces within the office. Values are based on six measurements across a given surface with the error being the standard deviation of the mean at the 95% confidence level.

When measuring the daylighting factor, an important characteristic of the glazing is its hemispherical-hemispherical transmittance (see Fig 3-6). It was determined by measuring the illuminance either side of the glazing, for both the coated and uncoated window, then calculating the attenuation. As the prisms were attached to a perspex sheet and hung over the single glazing, the system simulated the losses in a double glazed unit. The average of three measurements gave a hemispherical-hemispherical transmittance of 65% for the traditional double glazing and 57% for the prisms in the double glazing. The total illumination of the interior was therefore not significantly reduced by the addition of the prisms.

b) Limitations of Daylighting Factor[v]

The daylighting factor is recommended by the British Standards Institution as a reasonable measure of the natural lighting conditions within a room. However doubts have been raised as to its validity[vi] on the following grounds:

1. It cannot be used in direct sunlight conditions

Alternative methods are used in section 3.3.5.

2. Variances in measured values.

In addition to the real sky measurements, the performance was measured under artificial skies.

3. A lack of correlation with occupants' opinions.

Occupant opinions have been sought as well and both will be taken into account when assessing the prisms' performance.

4. Difficulties in performing the measurements, of which there are three:

- Finding a suitable unobstructed outdoor location to measure the exterior illumination.

Fortunately the building is located behind a park with wide open spaces which are ideal for these measurements.

- Shading of the illuminance meter by operator.

The sensor for the external meter is on a cord and therefore can be remote to the user. The internal meter is placed on a tripod with a spirit level, so that it can be leveled and the operator can crouch under the detector. To take a measurement the operator presses a button and the reading is held which can then be removed from tripod and viewed by the user.

- The room is side-lit and therefore there are areas of the sky that do not illuminate the interior but are contributors the external measurement.

A number of modifications have been suggested to improve the accuracy of the daylighting factor. For example shading the meter from external illumination that does not influence the internal reading. However, these methods are not without errors as well and therefore the British Standard[vii] was followed as described above.

c) Results of Daylighting Factor Measurements

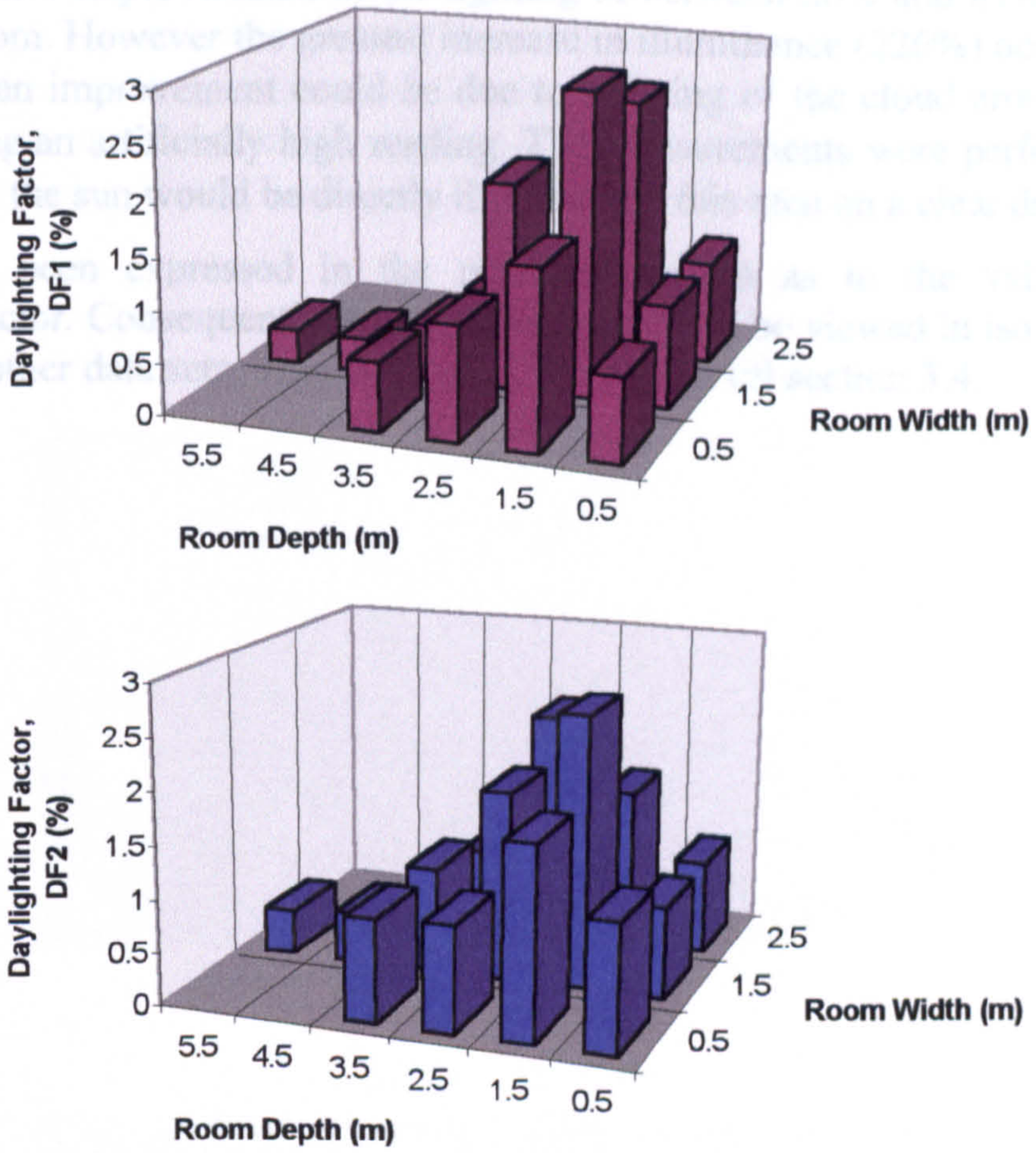

Graph 3-20: Daylighting factor measurements at working plane: (top) traditional glazing (bottom) with prismatic glazing.

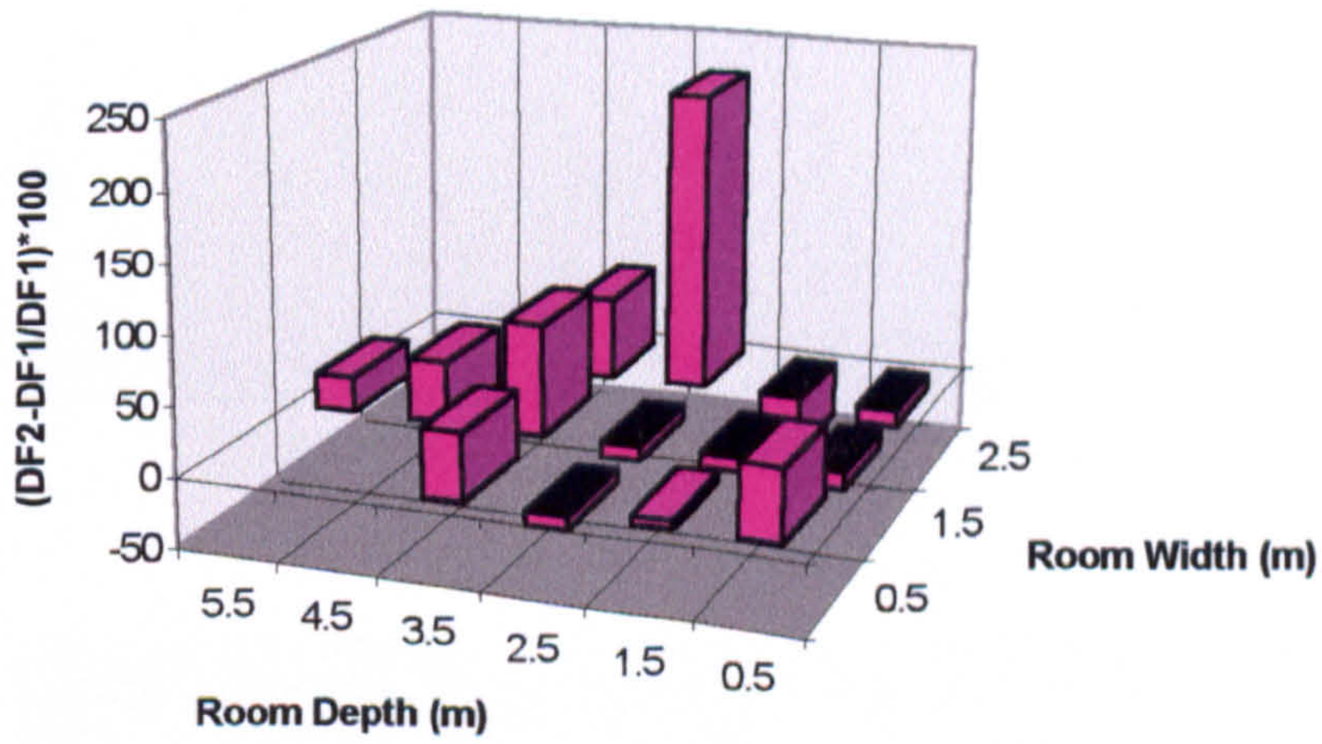

Graph 3-21: Change in daylighting factor at h=0.77m for prismatic glazing

d) Discussion of Daylighting Factor Results

The results show improvements in the lighting of between 26% and 81% in the back half of the room. However the greatest increase in illuminance (226%) occurs near the centre. Such an improvement could be due to thinning of the cloud around the solar disk producing an artificially high reading. The measurements were performed in the afternoon and the sun would be directly illuminating this area on a clear day.

Doubts have been expressed in the previous section as to the validity of the daylighting factor. Consequently these results should not be viewed in isolation, but in tandem with other data sets. This discussion is reserved till section 3.4.

3.3.4 Prisms under Clear Skies in Model Rooms

The performance of the prisms during sunny periods is vital to their acceptance by the occupants of a room. Deviation of strong sunlight into the interior can make the environment intolerable and the dispersion of colours can cause discomfort. The following photographs (Fig 3-15) give a qualitative impression of the glare caused by the prisms.

Single Reference Glazing

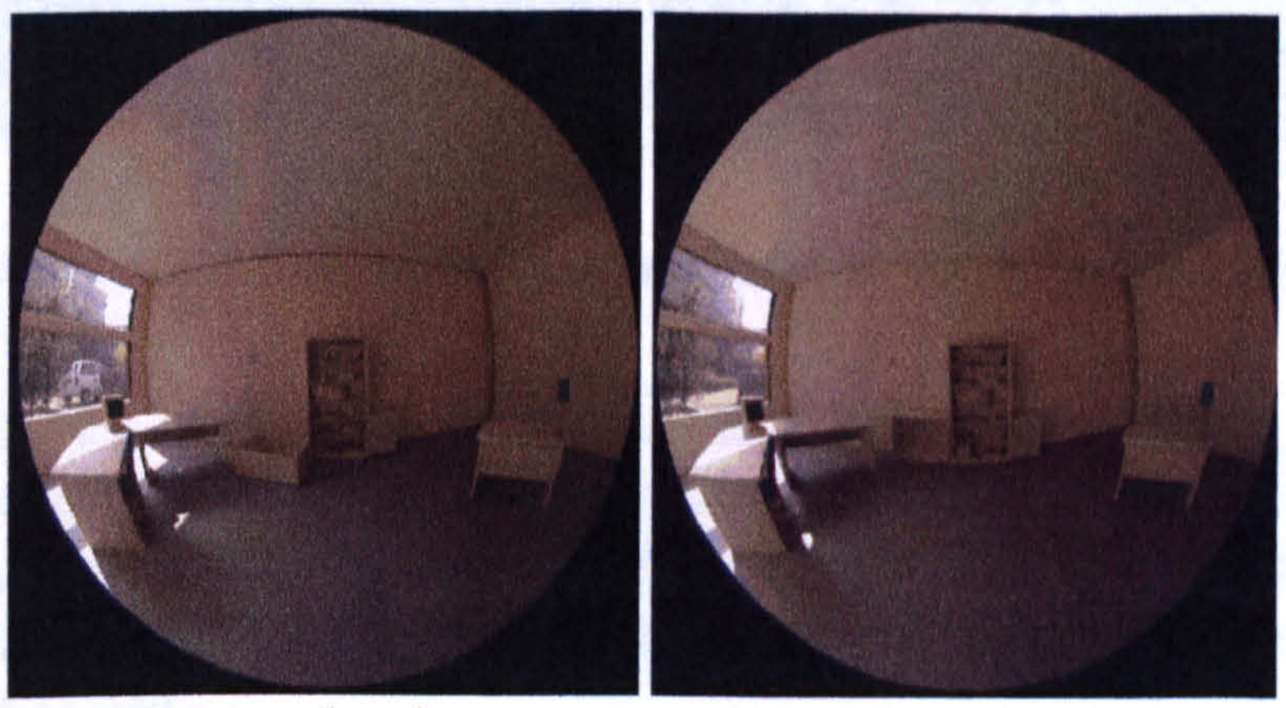

12.30 solar time 13.30 solar time

Shape-Cut Array

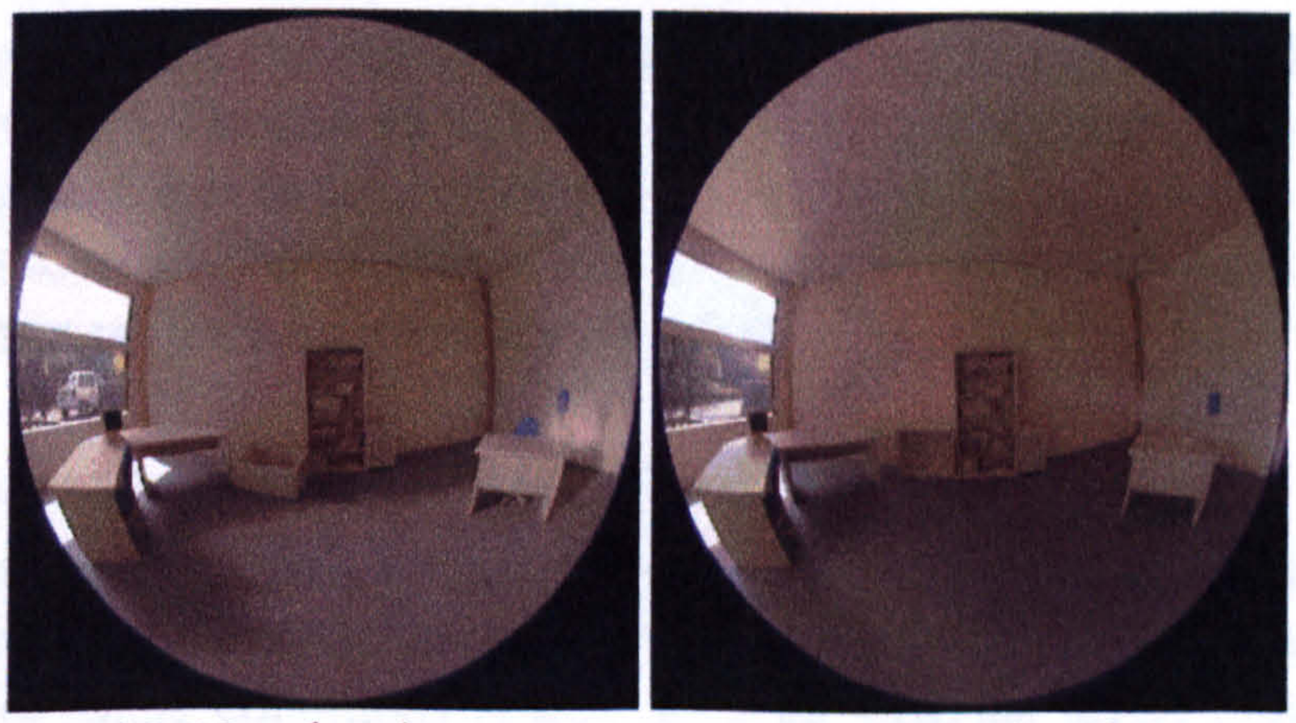

12.30 solar time 13: 30 solar time

Diamond Turned Array

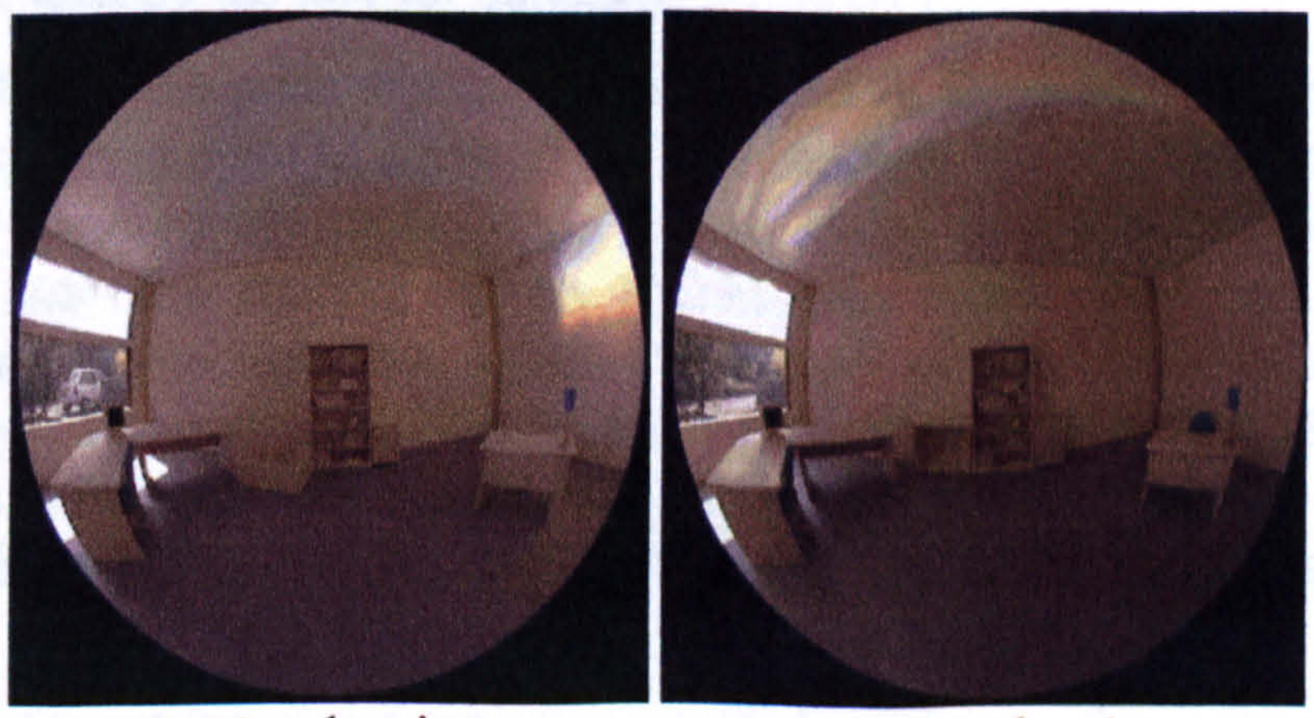

12.30 solar time 13.30 solar time

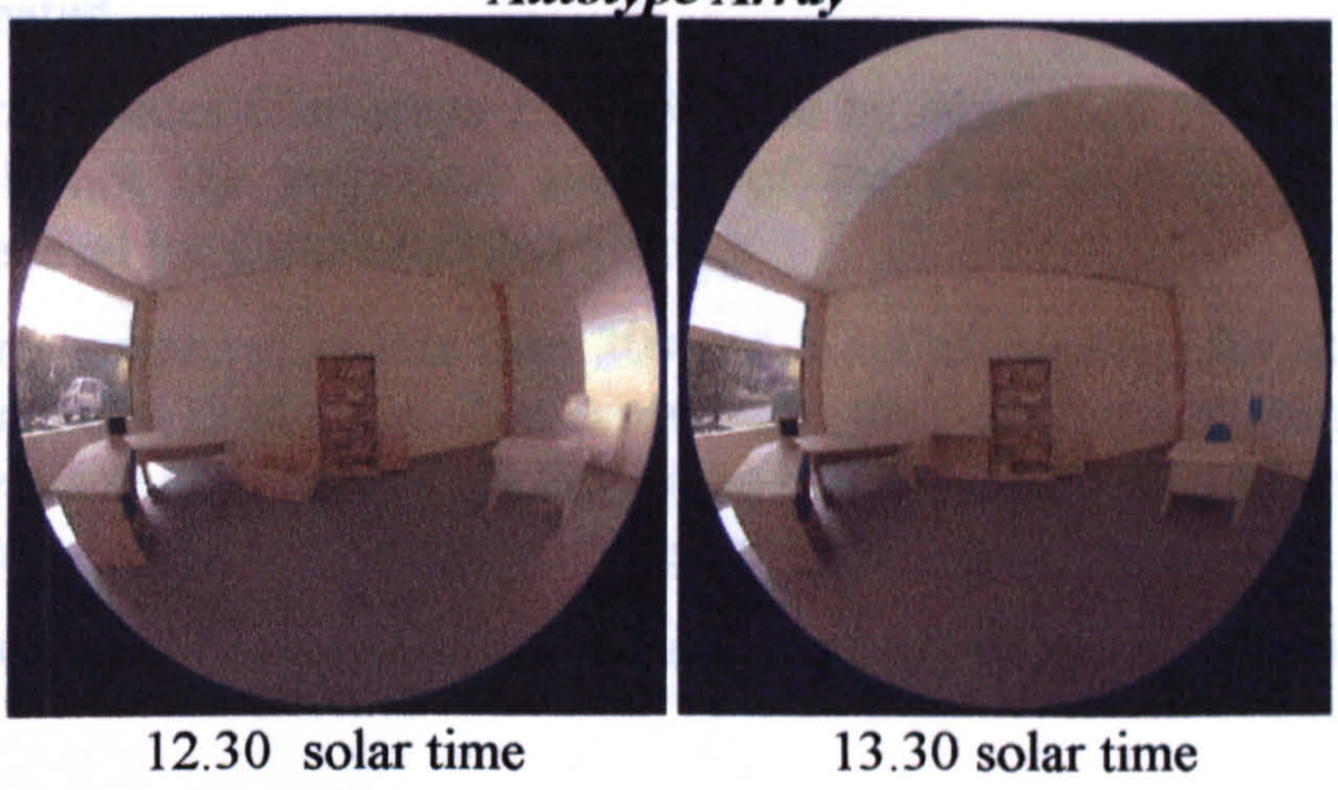

Fig 3-15: Prismatic samples under sunny conditions in model rooms (exposure f11, 1/60s, 100 ASA).

The single reference glazing shows the window as a bright source, but no direct sunlight is transmitted to the back of the room. The diamond turned array however, produces strong glare at 12.30, which is transmitted to the back of the room and some dispersion is visible. At 13.30 the light is transmitted to the ceiling but the array still seems to be very bright.

The Autotype array performs in a similar way but at 12.30 it appears that the light would be transmitted at anyone working at the desk.

Of the three arrays, only the shape-cut array seems not to transmit light efficiently to the back of the room. Despite its diffusion the glazing still produces significant glare. Therefore the prisms' role as a controlled diffuser cannot be relied upon to reduce glare and extra protection will be needed. A more quantitative method will now be used to establish the prism performance under sunny skies.

3.3.5 Prisms under Clear Skies in Office at NPL

Although the prisms had been examined under overcast skies, no quantitative results had been obtained for the array under sunny conditions. The problem with performing measurements in sunny conditions is that the light external levels change on a short time scale. Measuring the daylighting factor would therefore be meaningless. However within the office the illuminance values were found to be relatively stable due to diffusion of the light by the interior surfaces.

For this experiment the prismatic array was hinged to the window frame such that it could be easily swung open to show the lit environment without the modified glazing. The procedure required two participants: one to swing open the prismatic glazing and the other to note the reading on an illuminance meter. For each reading both participants were below the level of the meter (which was on a levelled tripod) to prevent shading of its aperture. The measurements were performed at the level of the working plane within the office (0.77m) and readings taken at each of the points described by the grid shown in Fig 3-13. The procedure for accumulating the data was as follows:

1. Illuminance measured at a point on the grid, without the prisms covering the window.

2. Illuminance measured at same point with prisms over the window
3. Step 1 repeated
4. If illuminance values from steps 1 and 3 differ by more than 5% then procedure is repeated. If not the numerical average of the two readings is taken as the illuminance level for the unmodified glazing.

Steps 1-3 were completed in less than 20s and 1 set of readings for the whole room lasted approximately 15 minutes. The experiment was performed at 9am, 11am, noon, 1pm, 2pm, 3pm and 4pm on a sunny day in the middle of July. For all six data sets the average variation between the readings taken in stage 1 and 3 was 1.5±0.3%.

The results are displayed in sets of three graphs with the room orientated as shown in

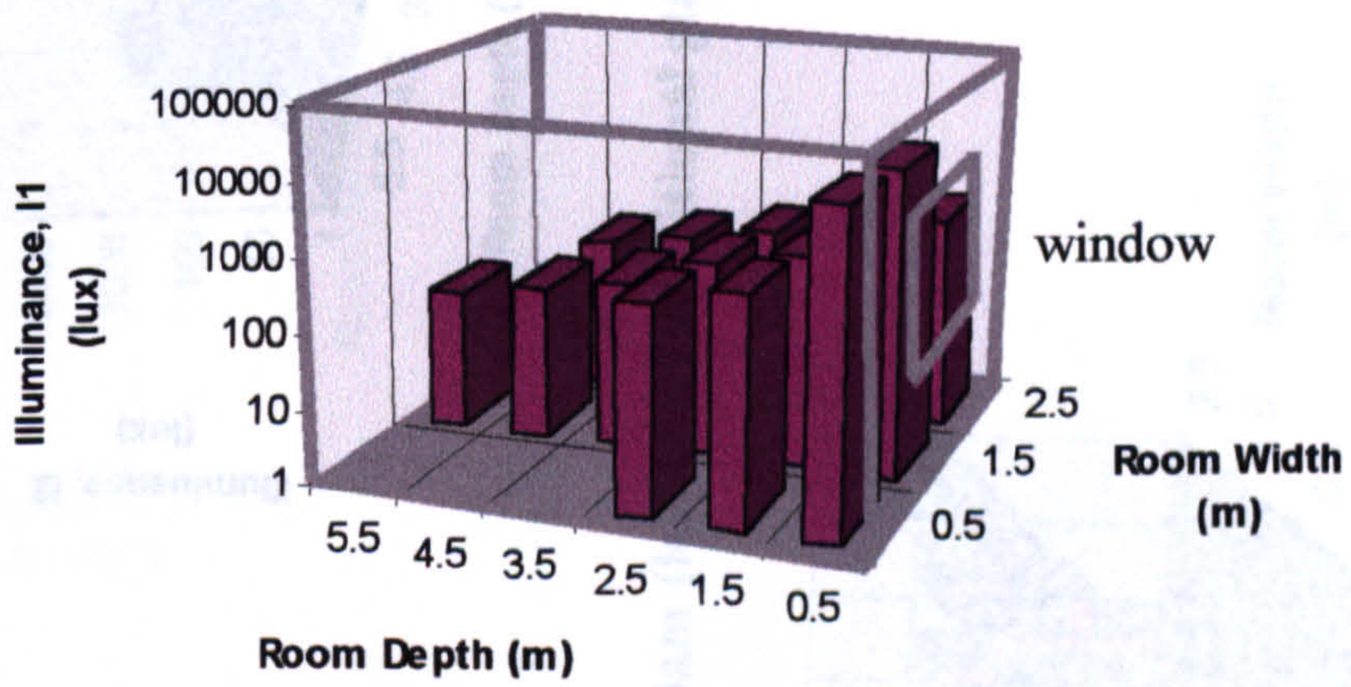

Fig 3-16: Orientation of room for Illuminance graphs.

The first two illustrate the illumination distribution in the rooms with and without the prisms. The y-axis has a logarithmic scale to coincide with the visual perception of occupants.

The third graph details the improvement in illumination as a result of the prisms.

a) Results (all times are British Summer Time)

9.00 am

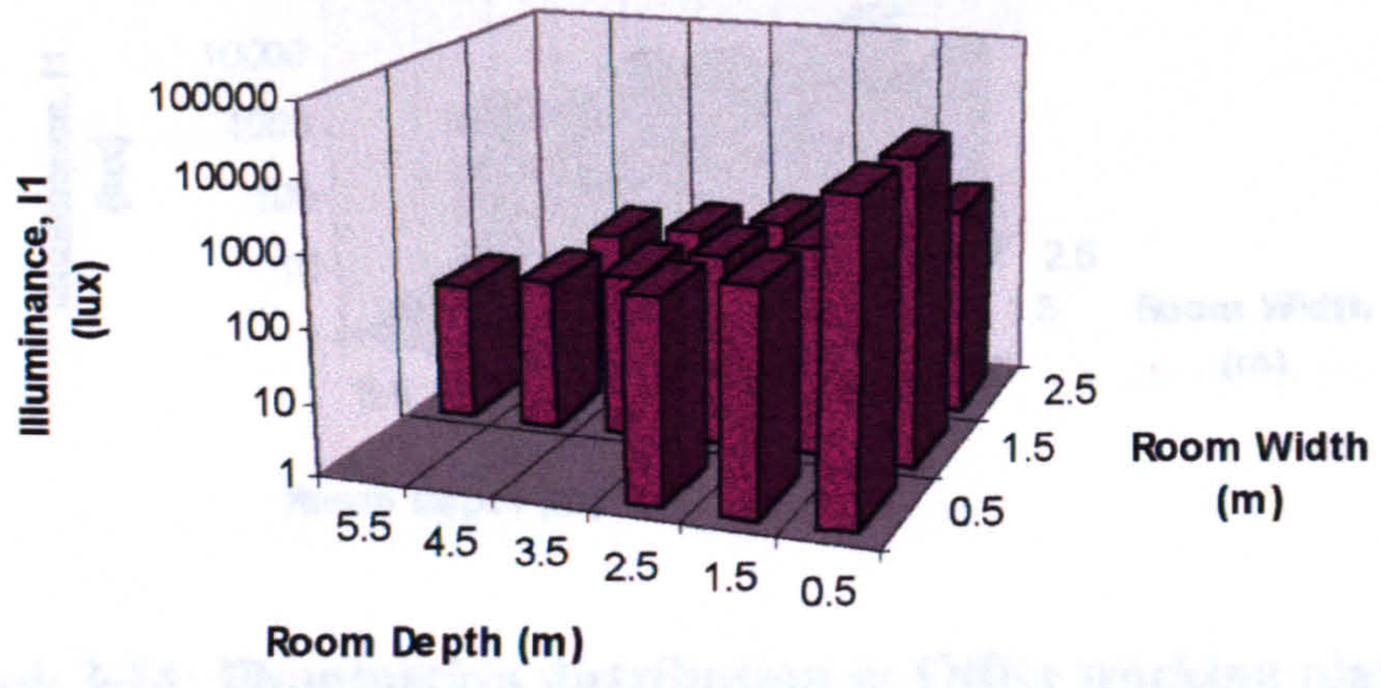

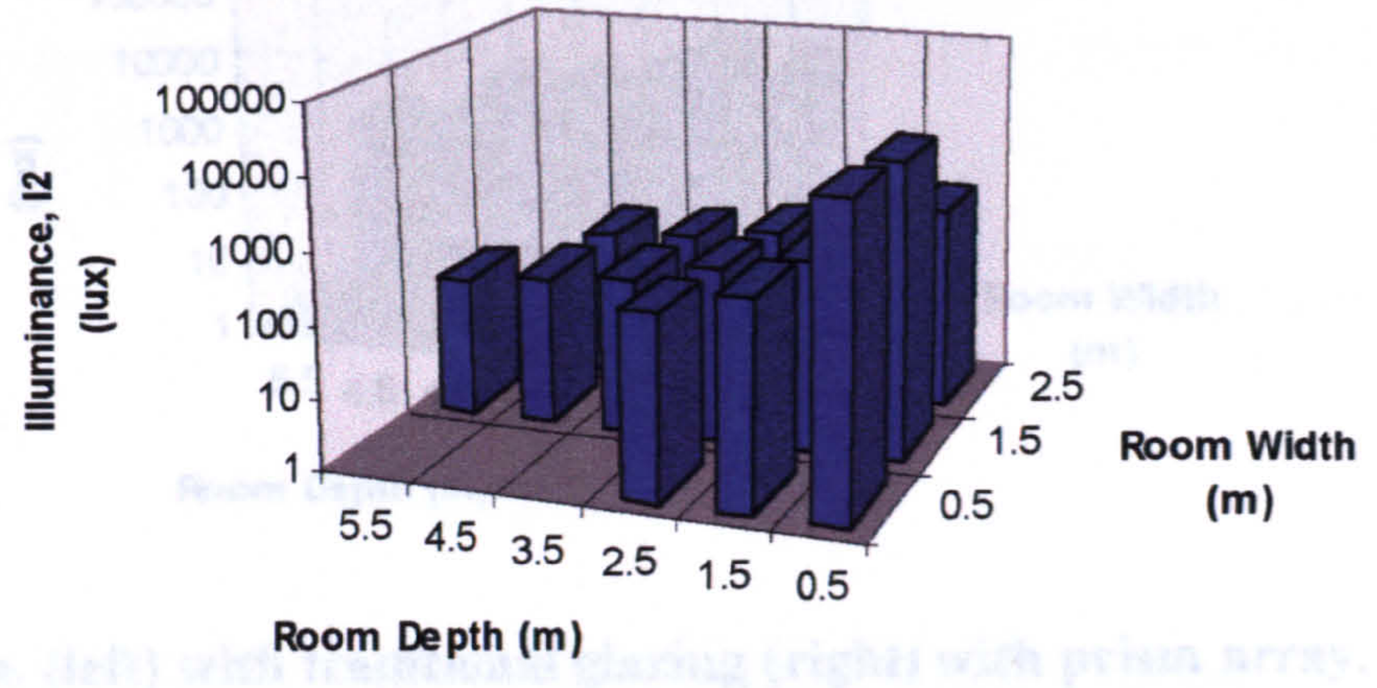

Graph 3-22: Illumination distribution in Office working plane at 9.00am (left) with traditional glazing (right) with prism array.

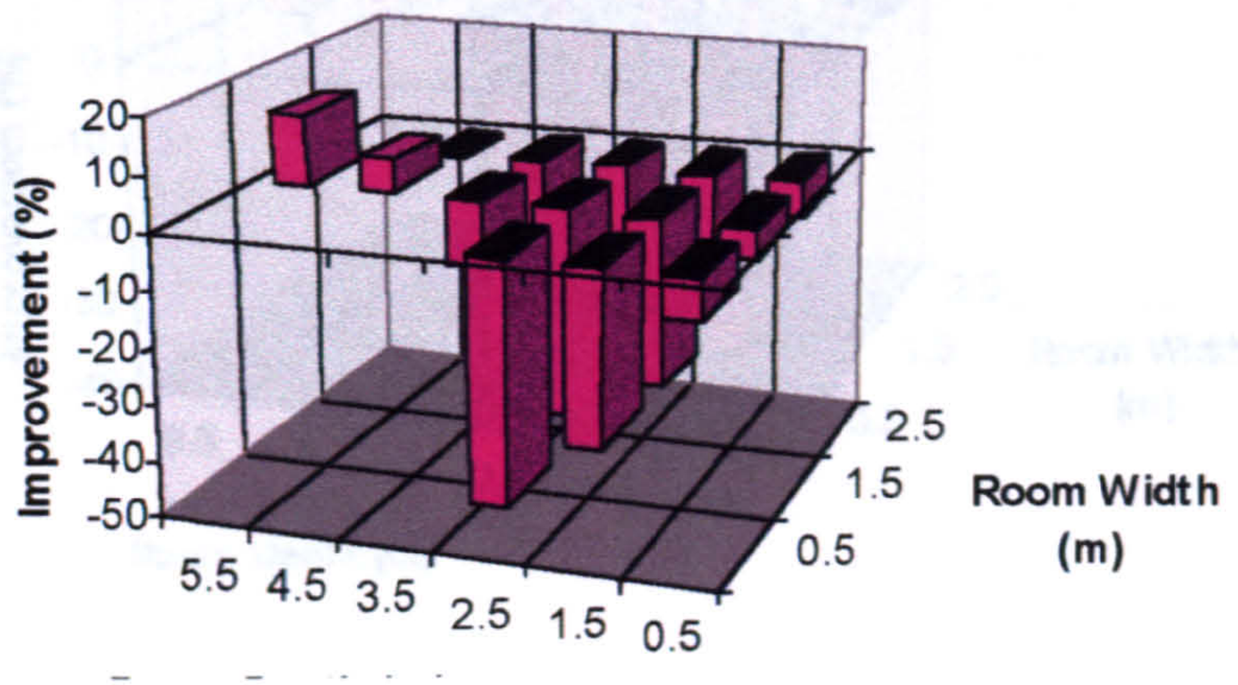

Graph 3-23: Change in illumination due to prismatic glazing at 9.00am.

11.00am

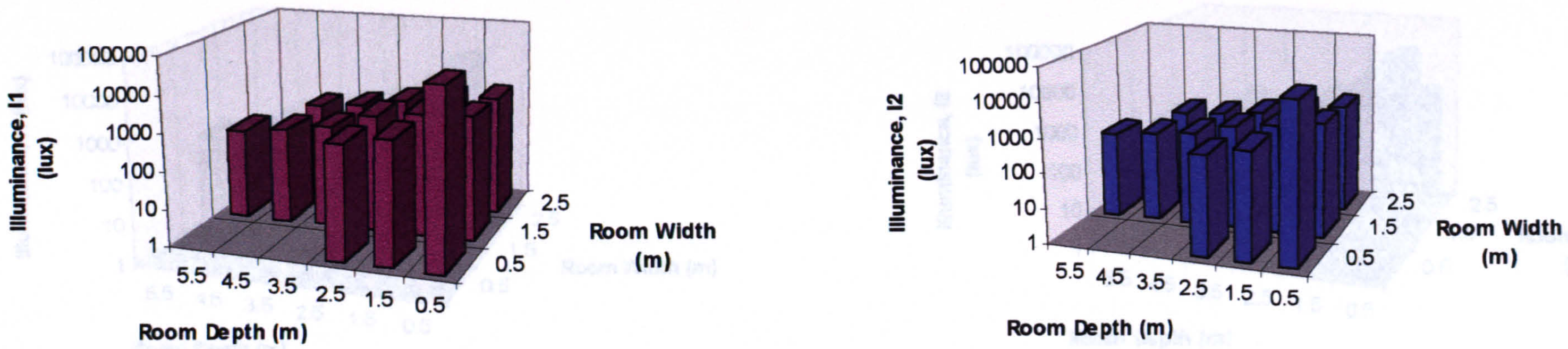

Graph 3-24: Illumination distribution in Office working plane at 11.00 a.m. (left) with traditional glazing (right) with prism array.

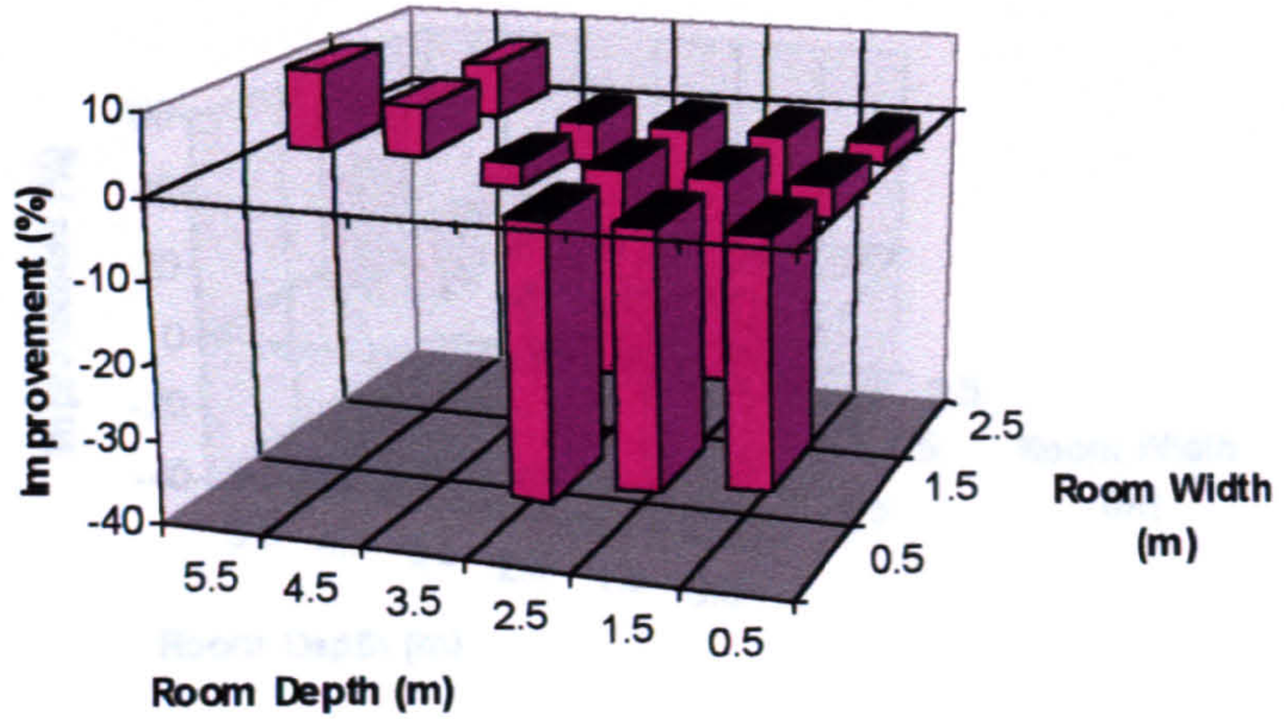

Graph 3-25: Change in illumination due to prismatic glazing at 11.00 a.m.

Noon

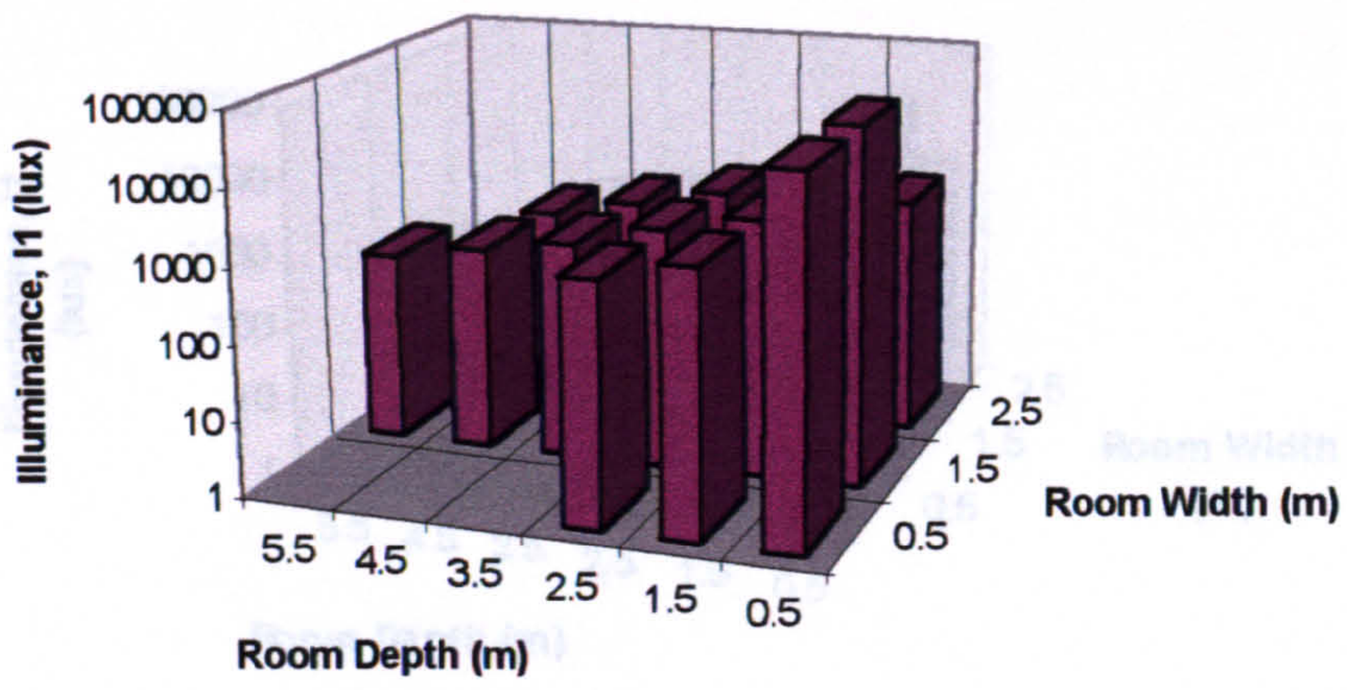

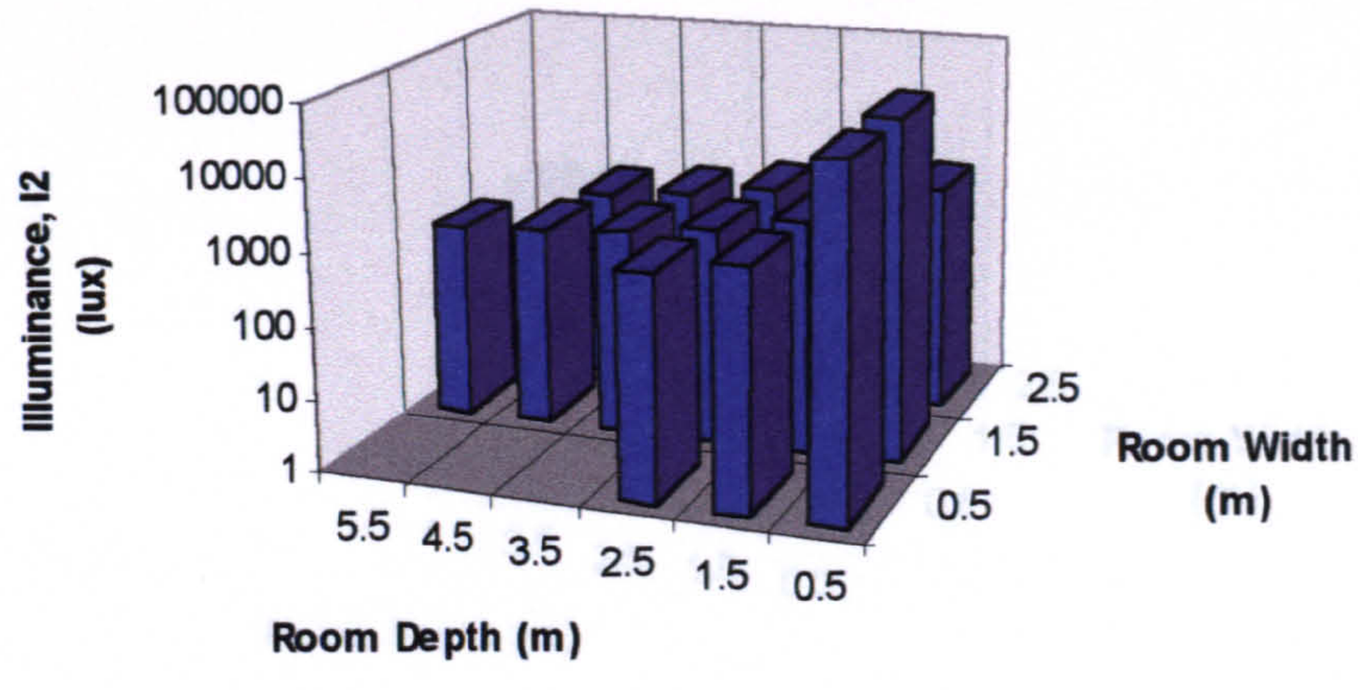

Graph 3-26: Illumination distribution in Office working plane at Noon (left) with traditional glazing (right) with prism array.

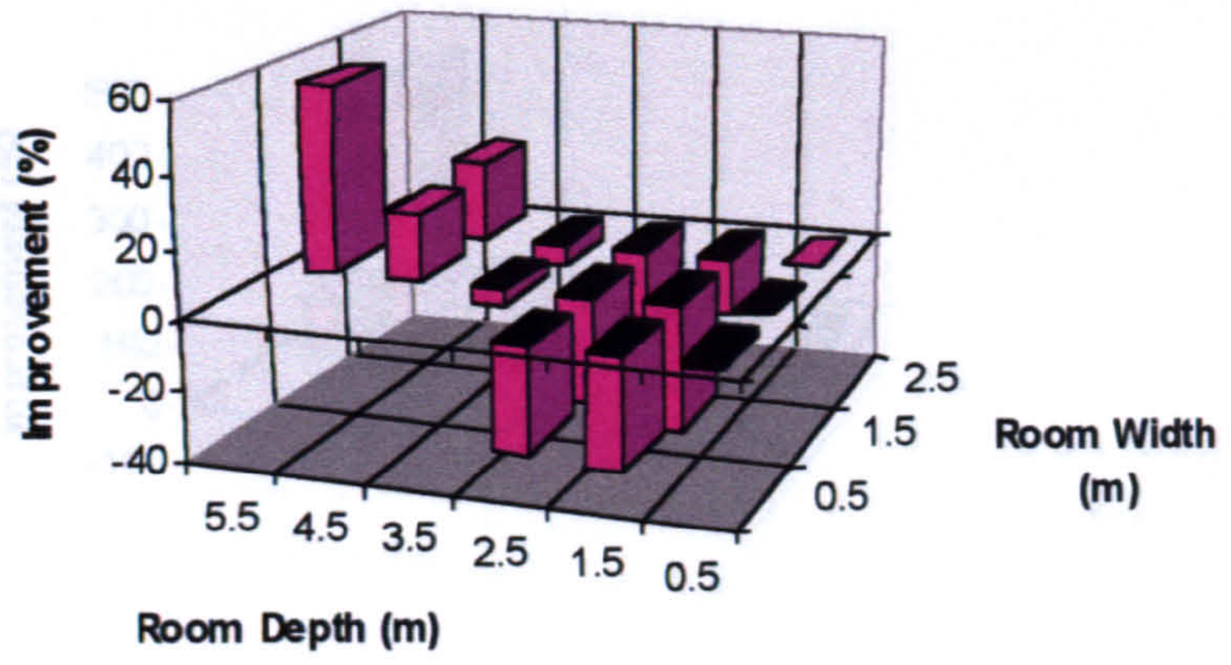

Graph 3-27: Change in illumination due to prismatic glazing at noon.

1.00 p.m.

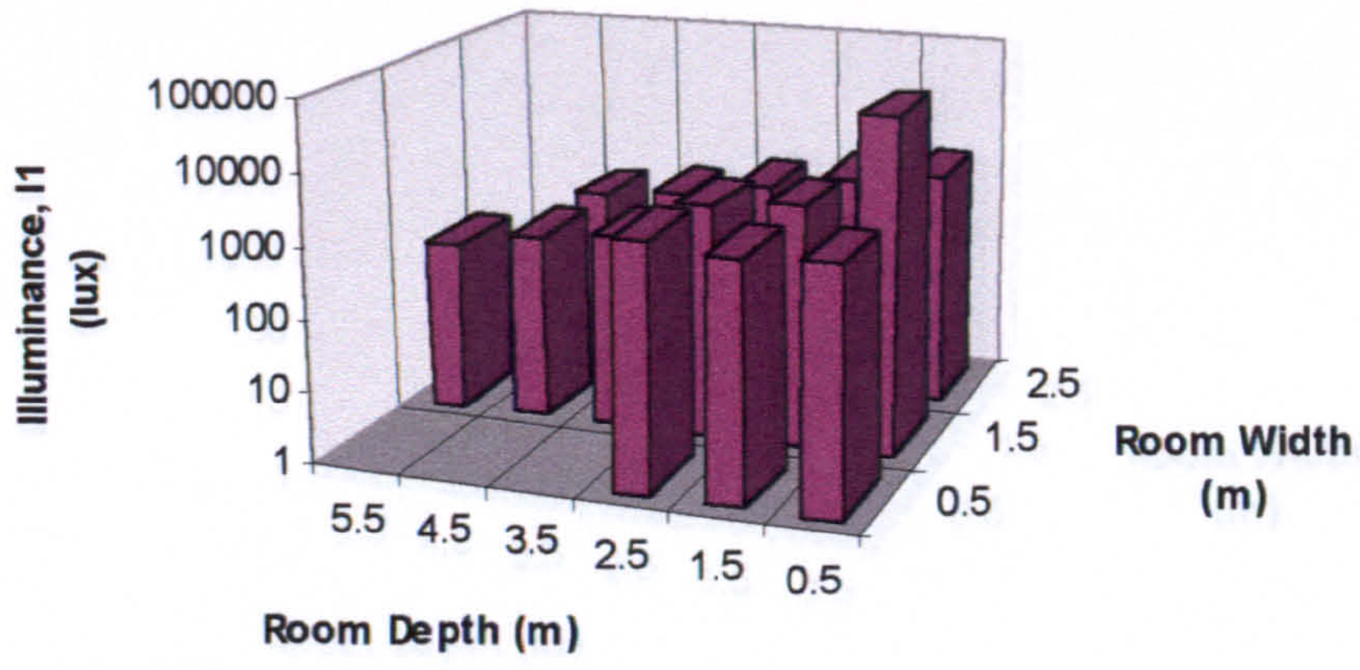

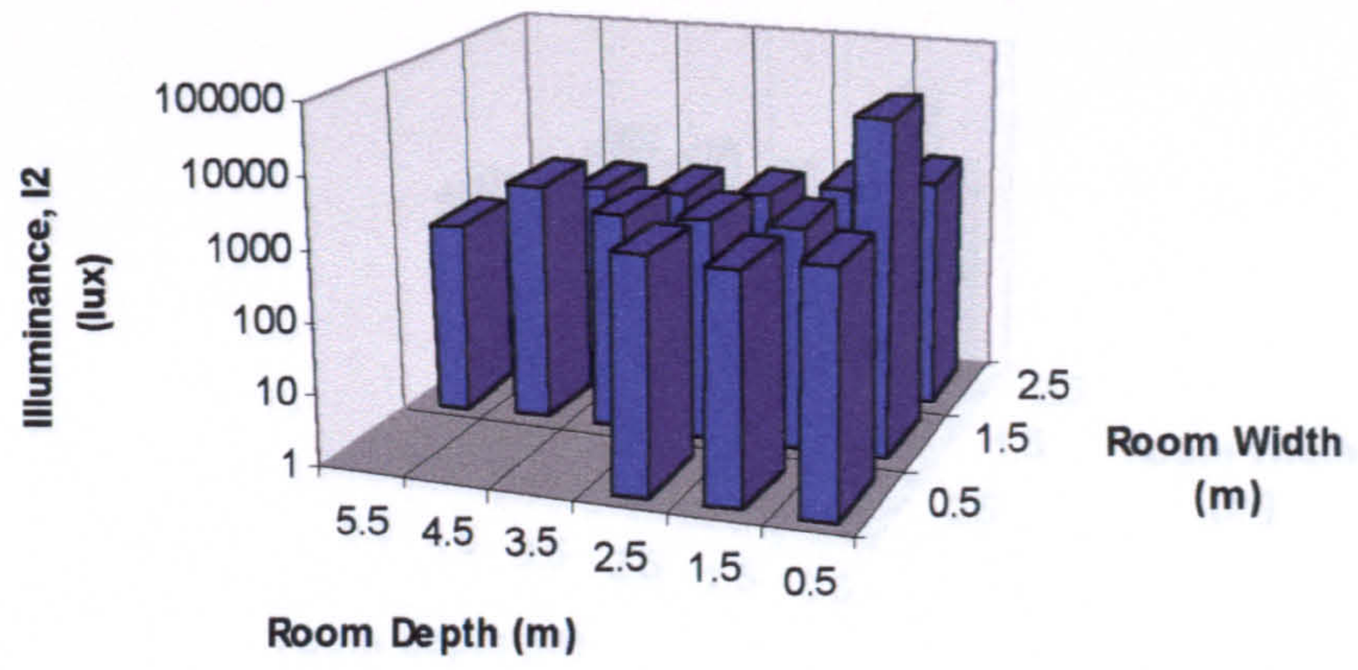

Graph 3-28: Illumination distribution in Office working plane at 1.00 p.m. (left) with traditional glazing (right) with prism array.

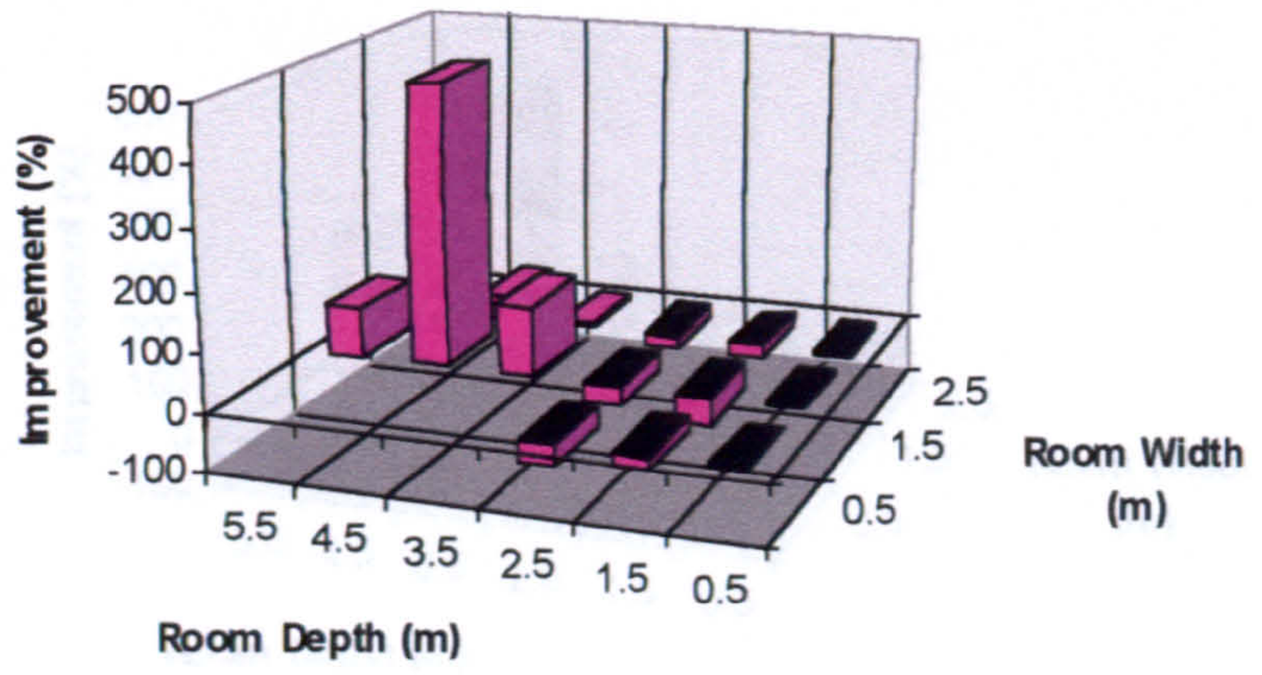

Graph 3-29: Change in illumination due to prismatic glazing at 1.00pm.

2.00pm

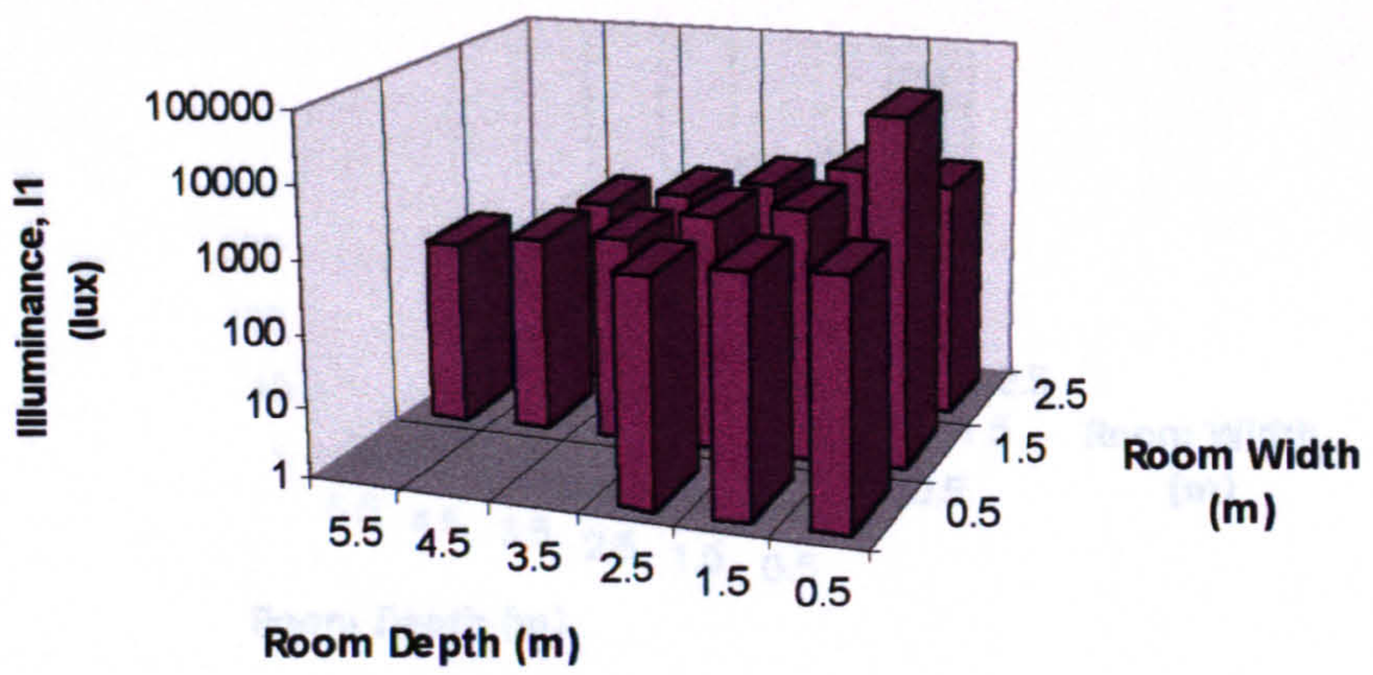

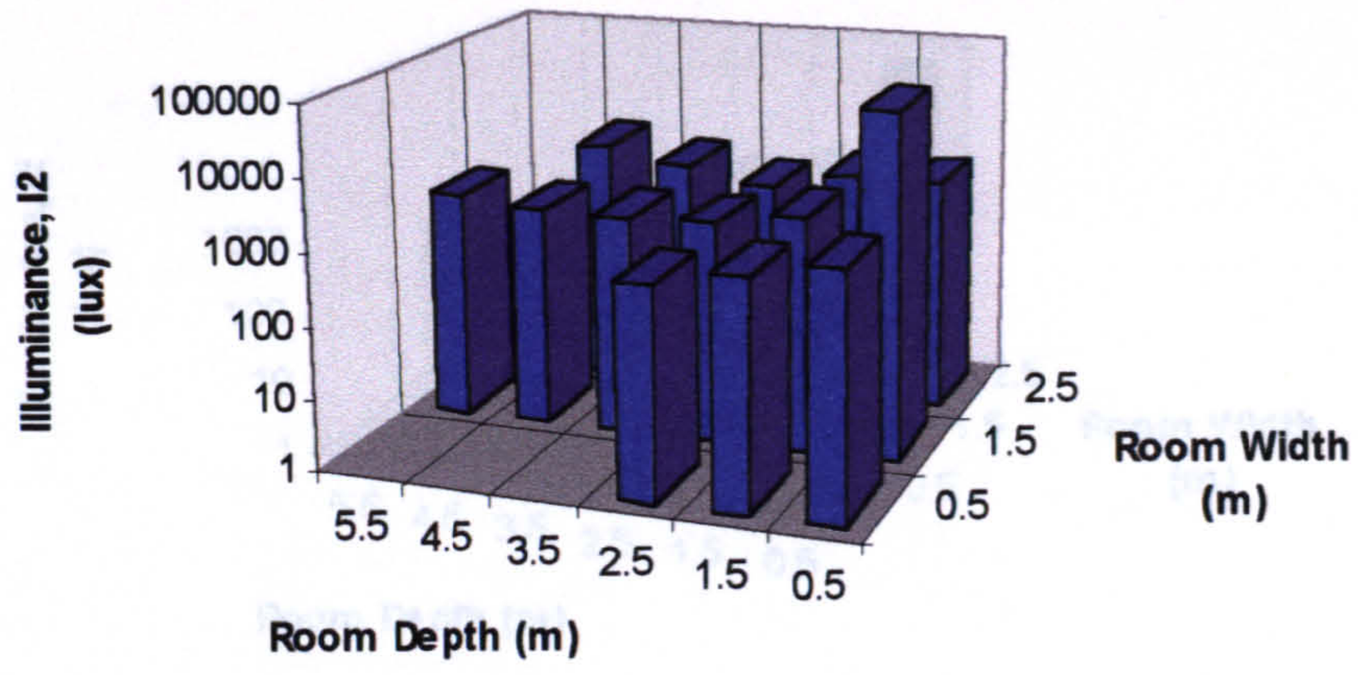

Graph 3-30: Illumination distribution in Office working plane at 2.00 p.m. (left) with traditional glazing (right) with prism array.

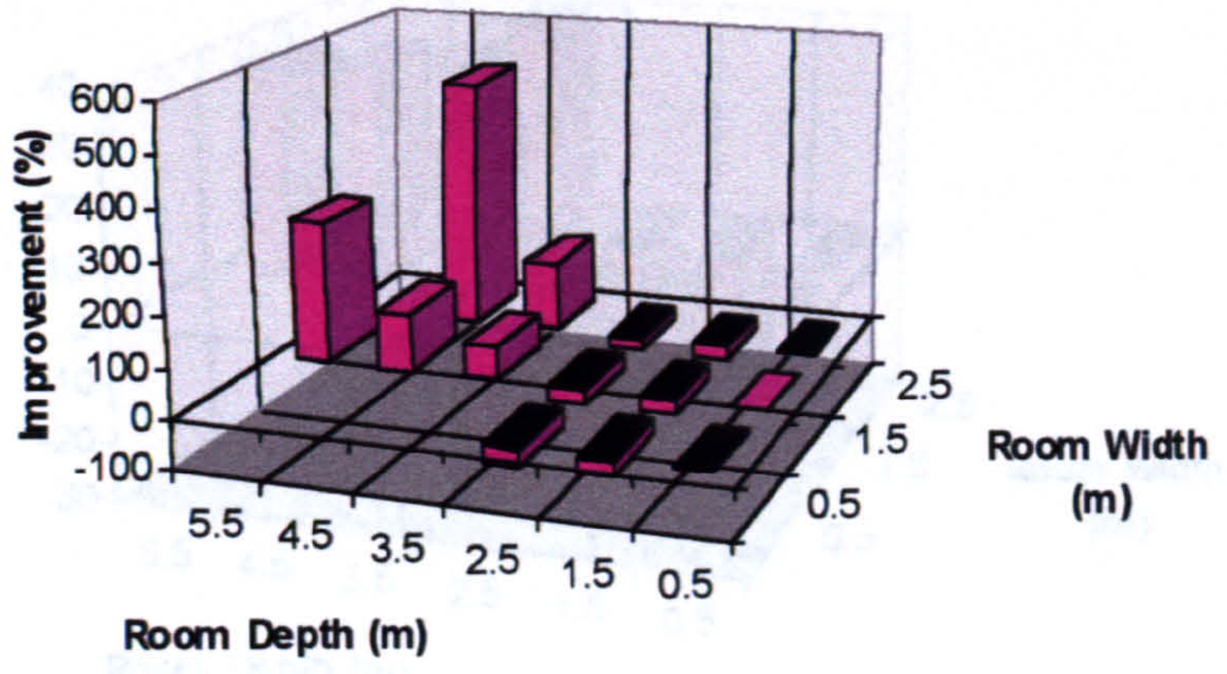

Graph 3-31: Change in illumination due to prismatic glazing at 2.00 p.m.

3.00pm

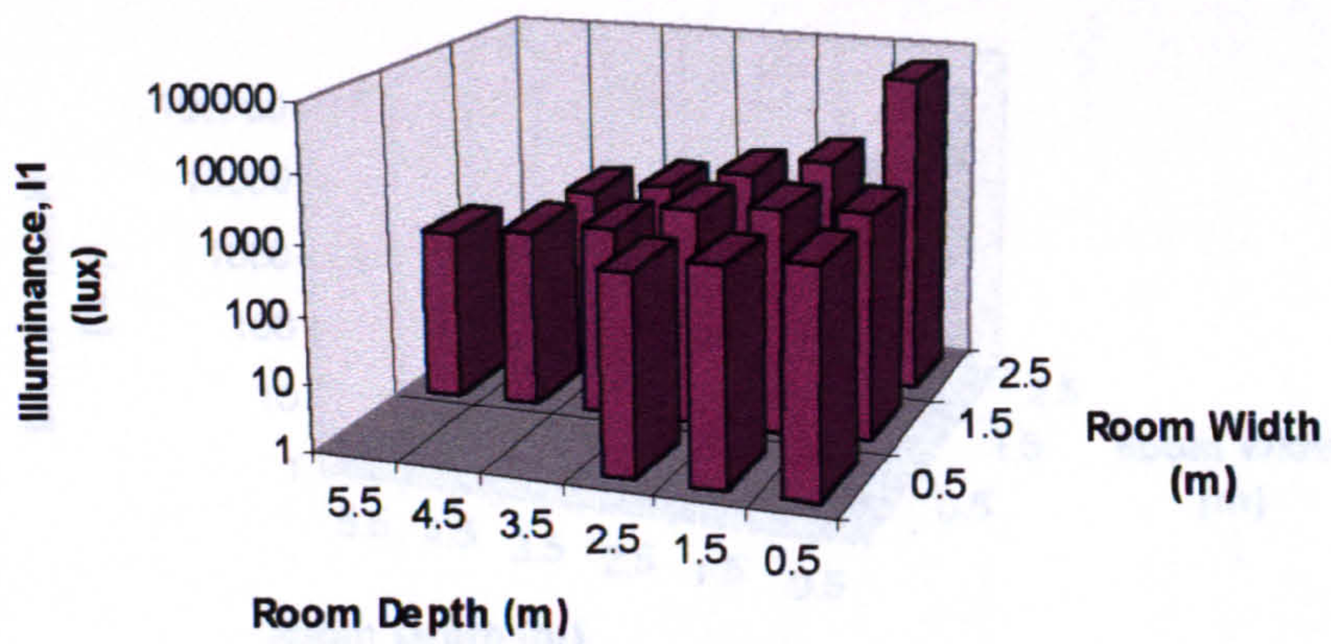

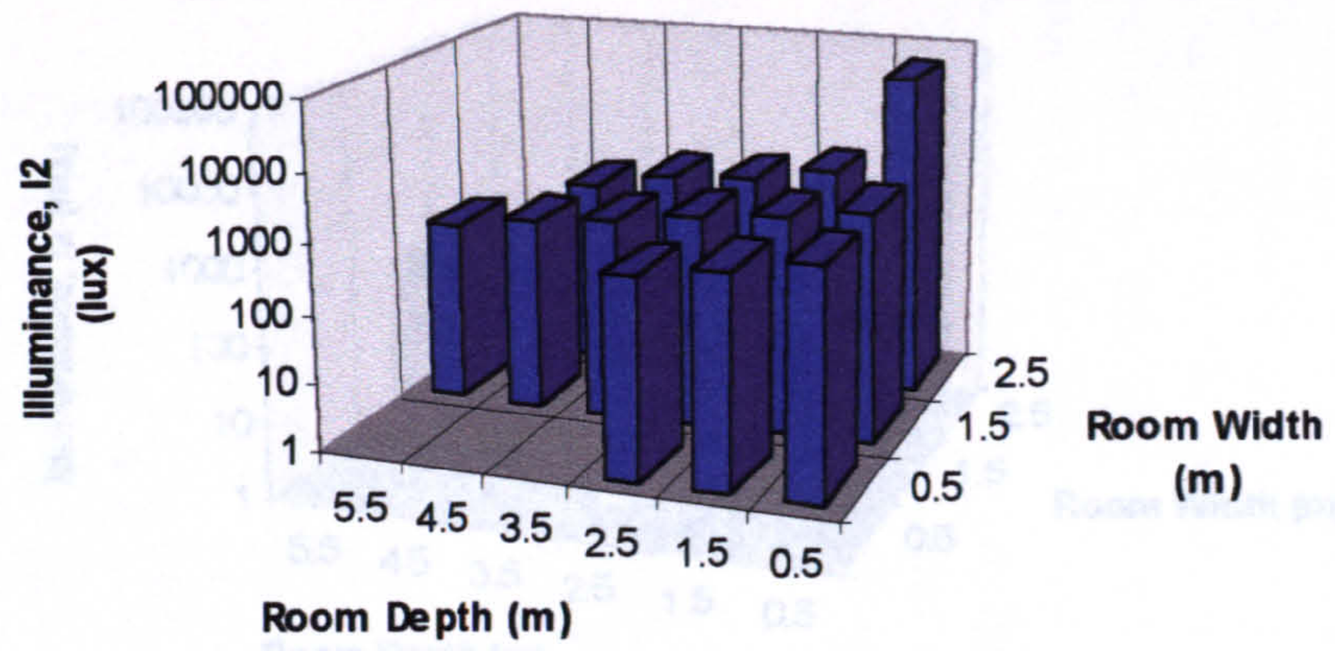

Graph 3-32: Illumination distribution in Office working plane at 3.00 p.m. (left) with traditional glazing (right) with prism array.

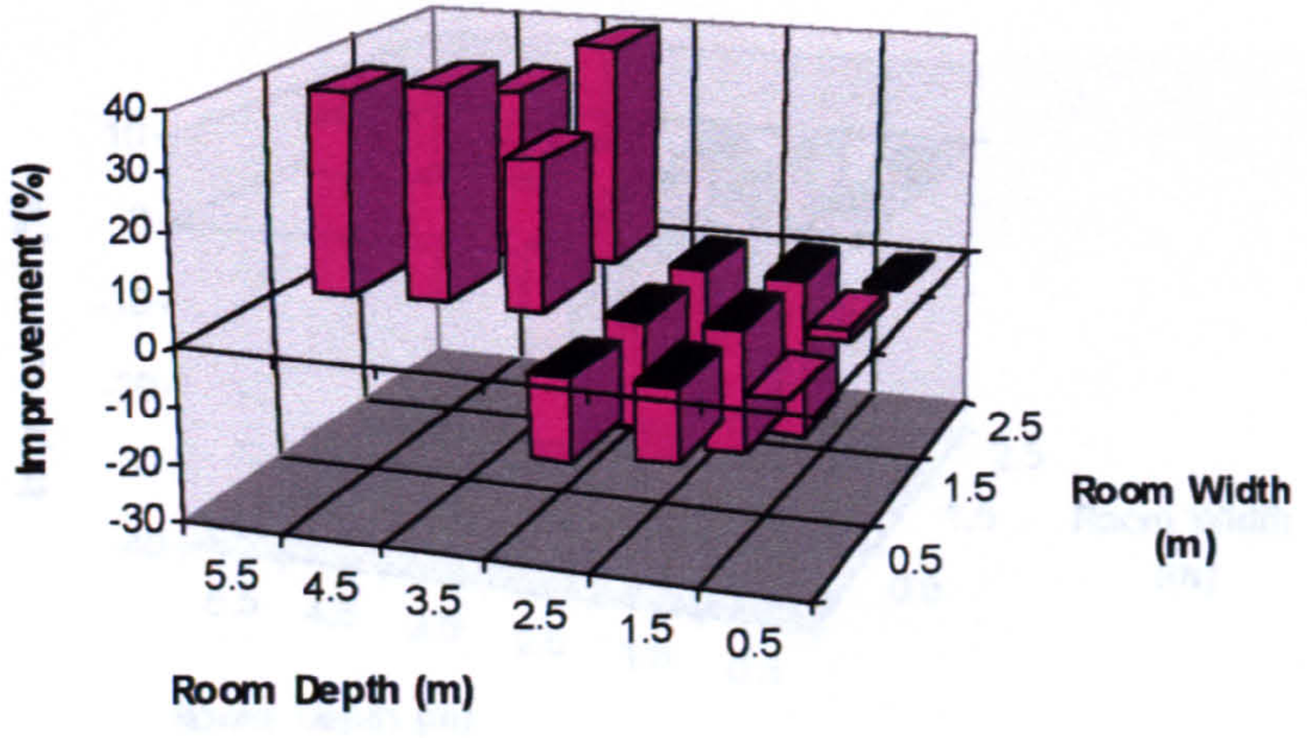

Graph 3-33: Change in illumination due to prismatic glazing at 3.00 p.m.

4.00 p.m.

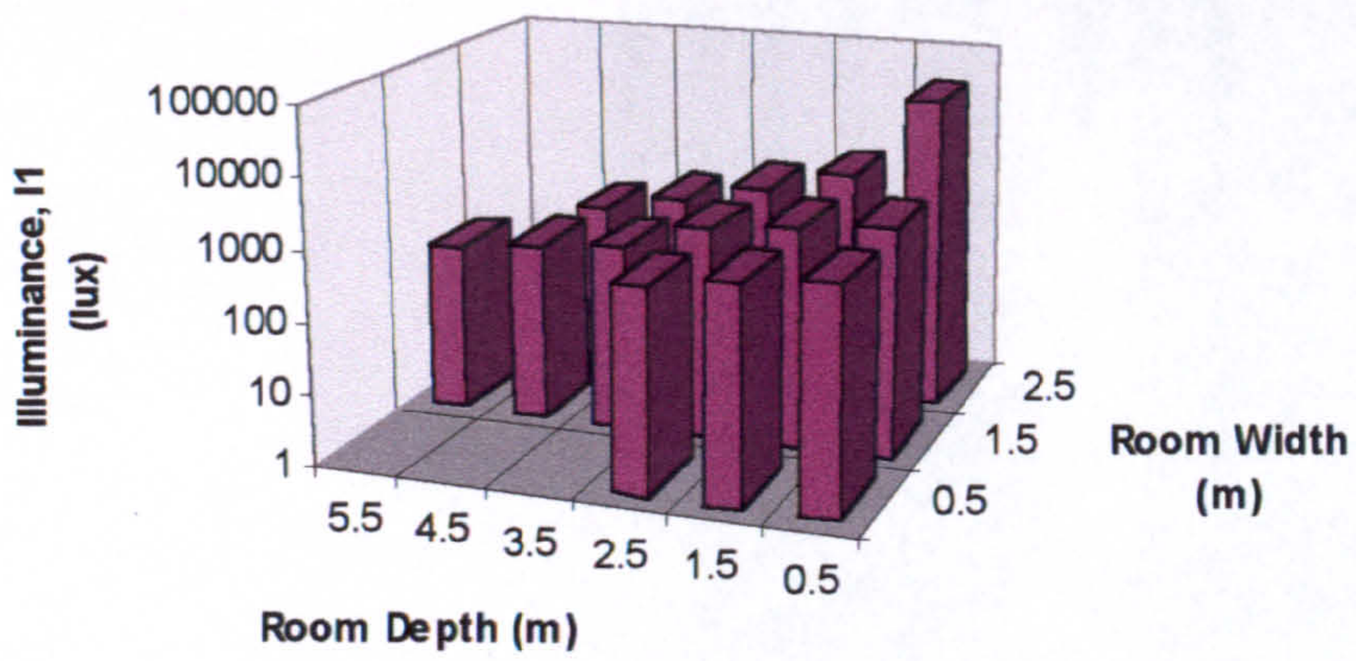

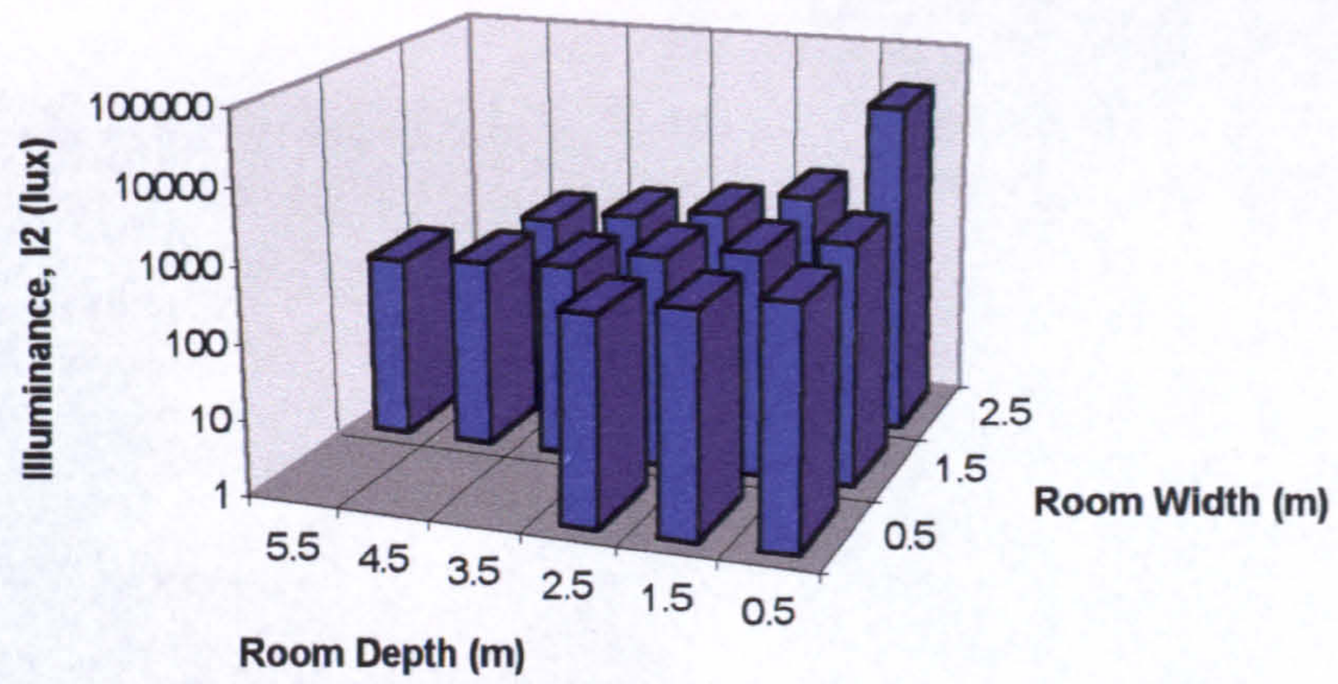

Graph 3-34: Illumination distribution in Office working plane at 4.00 p.m. (left) with traditional glazing (right) with prism array.

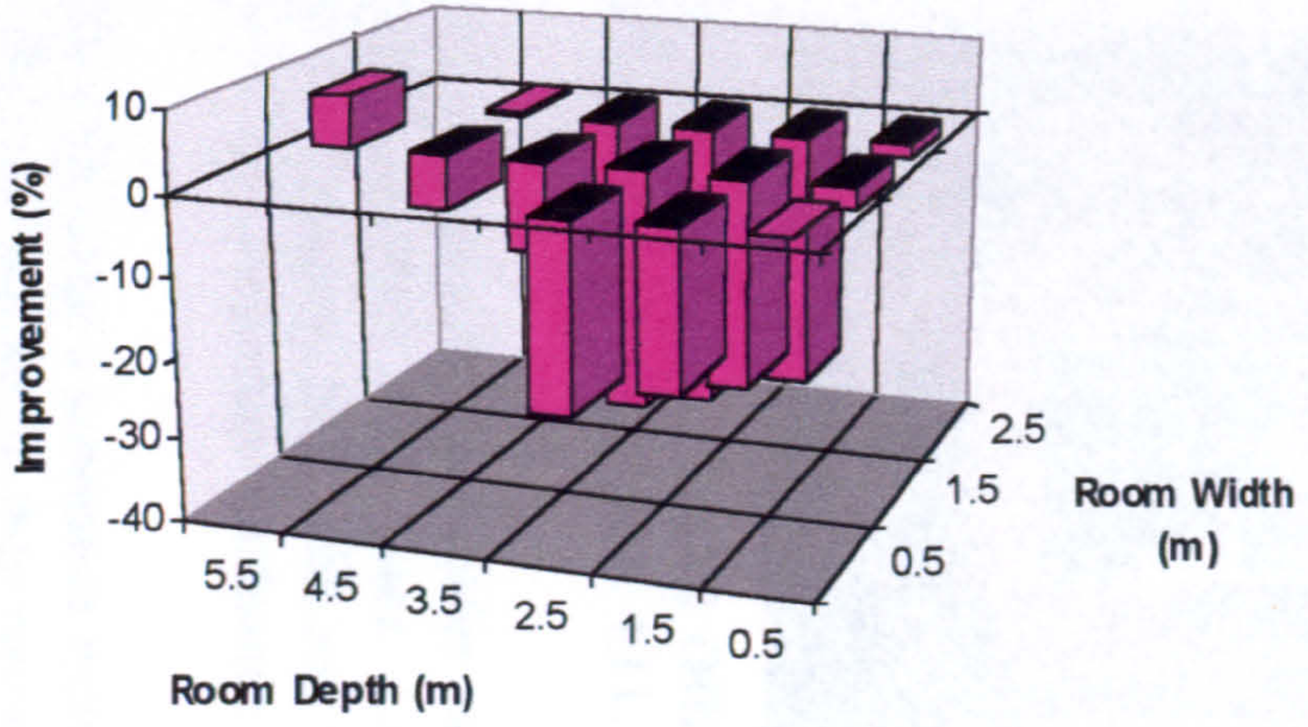

Graph 3-35: Change in illumination due to prismatic glazing at 4.00 p.m.

b) Discussion of Results

All the results from 9.00am till 4.00 p.m. show an increase in illumination at the back of the room and a decrease at the front. There is a consistent pattern in the illumination changes due to the prism. This suggests that measures taken to counteract the variability in the light levels were successful. The illumination distributions are dominated by the area closest to the window, with measurements up to 60,000 lux. The increases at the back of the room were modest until the early afternoon when up to 500% increases in the light levels were recorded. Such large increases appeared to be by direct illumination from the prisms and the light was not diffused by the ceiling.

3.3.6 Glare

Fig 3-17: (Left) Prisms on office window at solar noon. (Right) Office window without prisms at solar noon. Exposure for both photographs: f/11, 1/60s, 100 ASA.

From the questionnaire results and from the measurements made under sunny skies it was evident that the prisms would cause discomfort from glare. Consequently luminance measurements were performed on the window, both with and without the prisms covering the aperture. In each case the maximum luminance value was measured.

The readings were taken from the back of the field using a luminance meter with a 3° field. Firstly the luminance of the prismatic film was measured, then removed and the procedure repeated for the uncoated window. The time between the two measurements was minimised by using two participants: one at the front of the room to remove the prisms and the other at the back taking the readings. The results are shown in Graph 3-36.

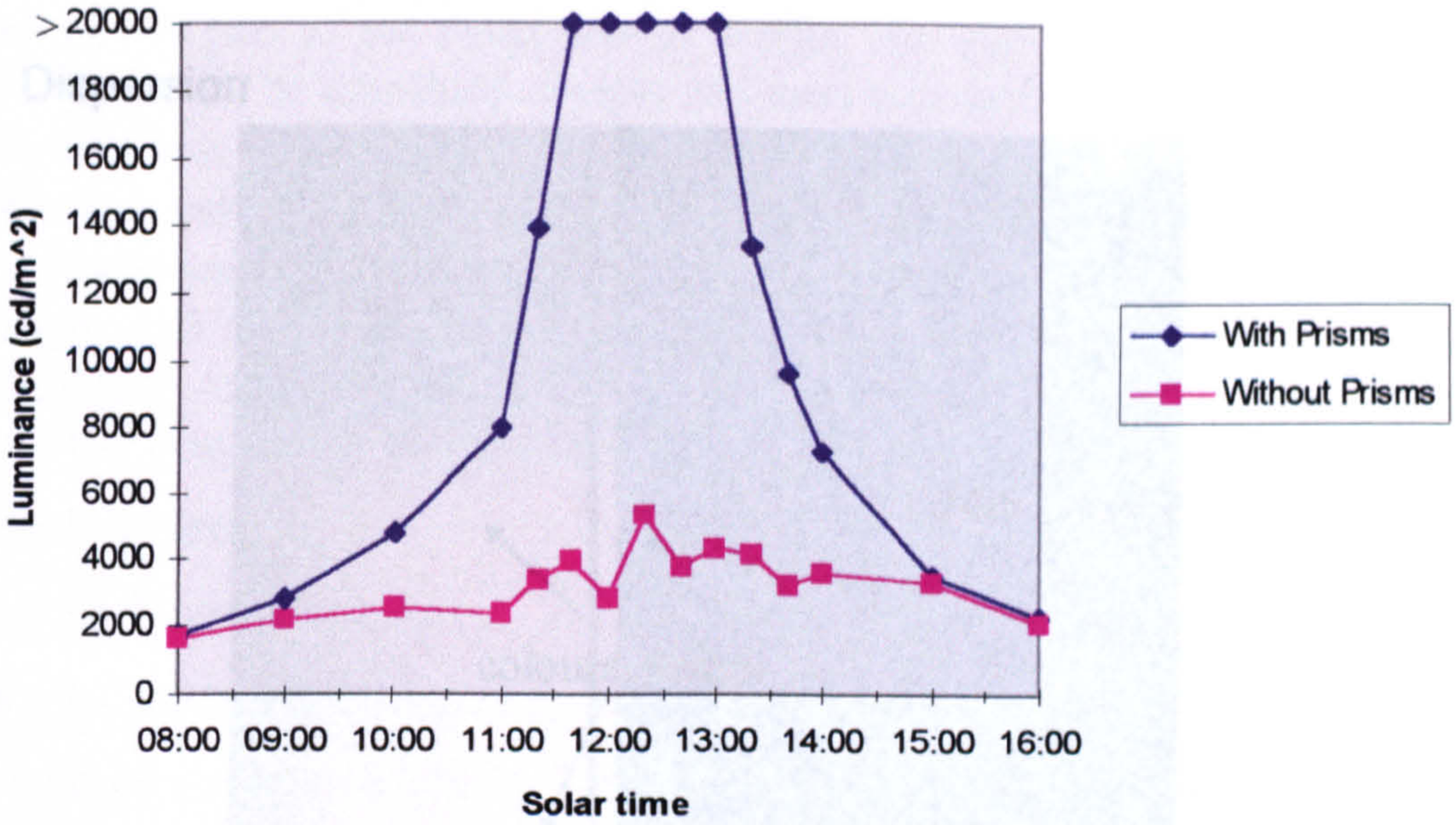

Graph 3-36: Maximum luminance measurements for the traditional and prismatic glazing.

As the experiment was conducted in late August, the trees in front of the window (see section 3.3.1) caused a significant barrier to the view. Therefore the highest readings for the uncoated window were between the branches. For the prismatic glazing the highest readings were governed by the solar position. The result is that the glare produced by the window without the prisms remains relatively constant, whereas the luminance values for the prismatic glazing change significantly throughout the day.

The upper limit for the luminance meter was 20,000 cd/m^2 and this was exceeded between 11:40 and 12:20. During that time period the luminance values for the prisms were at least three times that of the traditional window, causing significant glare discomfort. However, significant brightening was noticed from 11:00 and continued until 14:00.

3.3.7 Dispersion

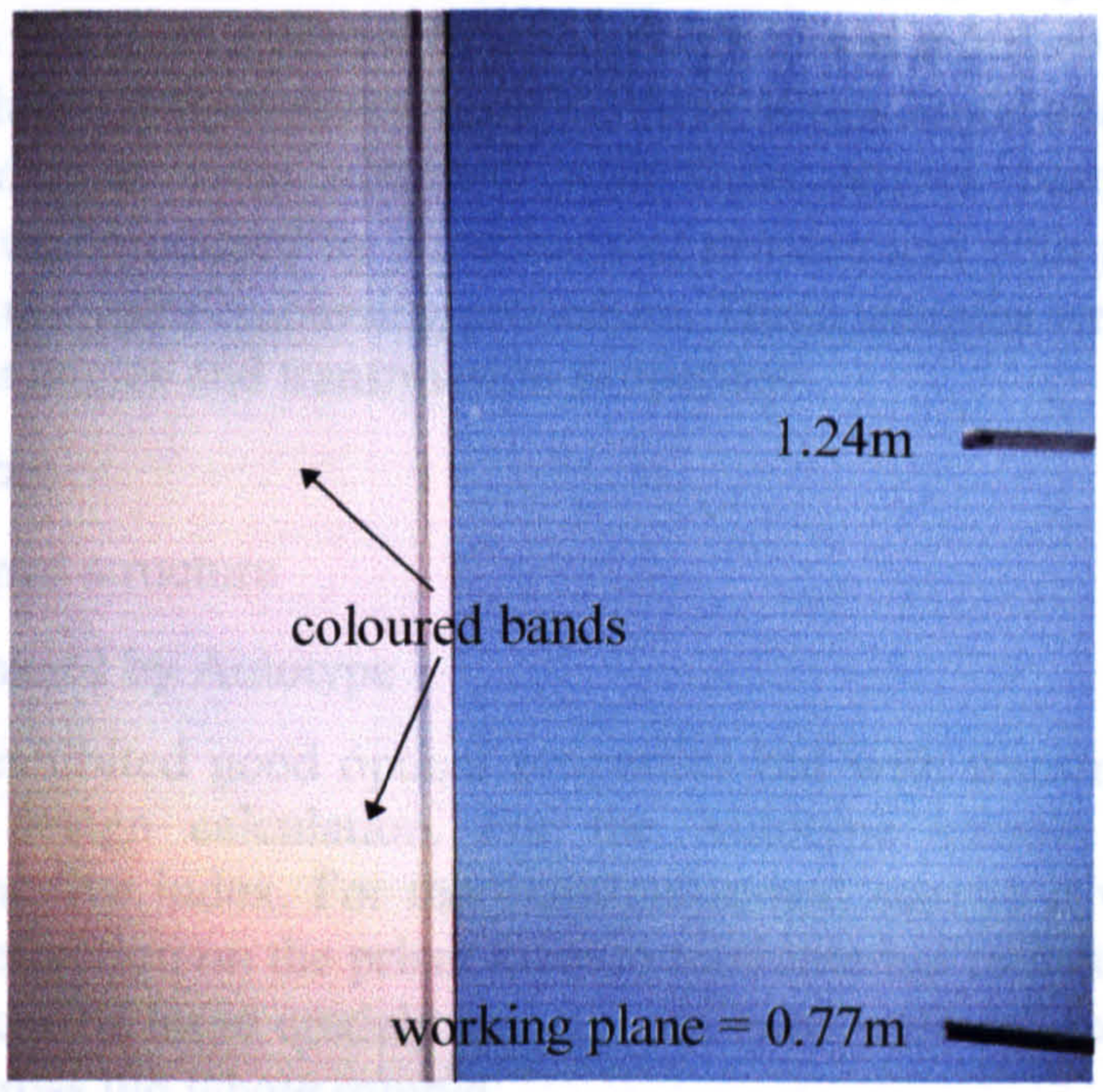

Fig 3-18: Dispersion of light transmitted through prism array in office.

Fig 3-18 shows the chromatic effects of the prisms at solar noon. The colours were only visible around this time and located at the working plane at the rear of the room. Although this is undesirable, no dispersion was evident on any of the working surfaces. Diffraction could be used to negate this effect in future systems, as it causes the spreading of light in the opposite sense to refraction. By choosing the period of the array such that the two phenomena are equal, it may be possible to eliminate dispersion.

In addition patterns were noticed on the west wall (see Fig 3-19) at around 11:00 am solar time, but would be too high to trouble occupants.

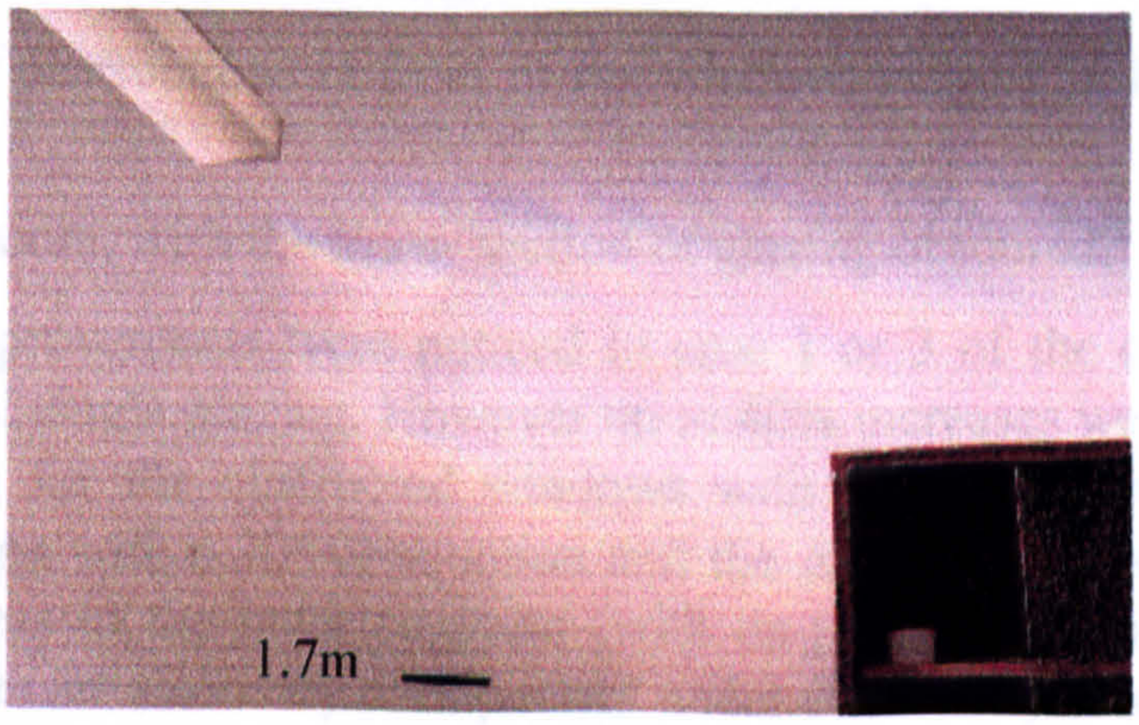

Fig 3-19: Speckle patterns produced by the prisms on the west wall.

3.4 Conclusion to Microprisms

The aim of this part of the thesis was to design, test and evaluate a microprismatic structure that could be embossed cheaply and used as a daylighting system. The design of the system was based on a simple calculation that used a 50° solar elevation angle as an 'average' value and transmitted light incident at this angle above the horizontal, several master samples were obtained with facet angles based on the design calculation. Each was produced by a mechanical process and with period< 100μm, to be applicable to Autotype's embossing procedure. Three samples were characterised in terms of their facet angles and transmission properties:

- A shape cut-array
- A diamond-turned structure
- A sample purchased by Autotype

The second two exhibited good optical properties but with transmission angles that varied from the design calculation. For the Autotype sample this was due to differences in refractive index. For the diamond-turned sample it was caused by the proximity of the refraction on the prism facet to total internal reflection. The shape cut array was manufactured more crudely and did not have well-defined facet angles that were consistent across the whole sample.

Despite differences between the theoretical and measured transmission angles all three were evaluated as possible daylighting systems. The testing occurred in two locations:

1. At the ENTPE in Lyon with small (10cm x 40 cm) samples in model rooms.
2. At the NPL in Teddington by covering an office window with a large (60cm x 40cm) array.

At the ENTPE is an artificial sky that allowed the measurement of the daylighting factor under very stable lighting conditions. Each sample was tested as part of a composite window under three different sets of conditions:

1. In a room with an unobstructed view.
2. In a room with obstructions in front of the window, varying in height from 20° to 50°.
3. In a basement room, with the lower section of glazing obscured.

No significant improvements were noticed in case 1 or 3 of the composite window over the traditional single glazing. However up to 40% increases were measured at the back of the room for the obstructed windows with the prism arrays. The greatest improvements being with a 30° obstruction and the Autotype and shape-cut samples. The relative success of the latter suggests (with its poor quality structure) indicates that the facet angles are relatively unimportant under diffuse sky conditions.

The large scale tests at NPL occurred in a south-facing office. The prism array consisted of the diamond-turned sample but embossed by Autotype in a lower refractive index than the original design. Although the transmission angles were lowered, the prisms were still thought to be useful as a possible daylighting system.

The evaluation included three stages:

- Subjective assessment by occupants at 9 a.m., 1 p.m. and 4 p.m.

- Measurement of the daylighting factor throughout the interior
- Evaluation of the prisms under sunny skies including illuminance measurements

People entering the office at 9 am with clear sky conditions did not need to turn on the light. However illuminance measurements at this time showed that there was little (15%) improvement due to the prism array at the back of the room but up to 50% reduction in the front half (see Graph 3-23).

At 1pm under the same sky conditions significant improvements in the lighting levels were measured. Increases of over 400% were noted close to the rear of the room (Graph 3-29).Yet respondents to the questionnaire stated that at this time the glare was very strong and luminance measurements showed values of over 20,000 cd/m^2 (Graph 3-36). In comparison an overcast day generates window luminances[viii] of 2000-6000 cd/m^2. As the prism reading was over 90 times the luminance of the traditional glazing, the improvement can be attributed to direct beam lighting without diffusion. As such glare protection would be needed between 11:00 and 14:00 at the very least.

At 4pm with a clear sky, most of the respondents did not want to turn the light on as they entered the room and it was viewed to be quite evenly lit. Illuminance measurements showed that there was less than 10% improvement in levels at the back of the room and up to 30% reduction near the centre (Graph 3-35).

Under overcast skies most respondents would have turned on the main electric light and needed lighting to read. The back of the room was generally considered too dark and the interior as a whole, not uniformly lit. Daylighting factor measurements (Graph 3-21) under these skies showed greater improvements than the same measurements under the artificial skies. Light levels at the rear of the room were increased by up to 100%. Near the centre improvements of over 200% were recorded. These results show greater improvements in lighting than those measured under artificial skies but should be taken with caution. The artificial skies do provide a more stable luminous environment to measure the daylighting factor and should be more reliable. However, direct comparison is difficult because the obstruction provided by the trees in front of the window was less than any used in the model rooms. In addition when questionnaire respondents were asked to compare the prismatic to the traditional glazing, there was no significant improvement was perceived.

To be an effective daylighting system, the prisms would have to at increase light levels at the back of the room by at least 100%, and minimise glare. The micro-prismatic film described in this thesis does not achieve this principally because it does not deviate the light sufficiently. Serraglaze, a micro-structured daylighting system (see section 2-1) is reported to increase internal illuminances at the rear of a room, of 50% to 1000%, depending on the ambient lighting conditions[ix]. As the redirection of the light is dependent on reflection not refraction then it is also less likely to cause glare, as the deviation angle will be greater. However because the manufacturing process would be more complex, 'Serraglaze' would probably be more expensive than the embossed prism described in this thesis.

i Littlefair P. J, 'Passive Solar Urban Design: Ensuring the Penetration of Solar Energy into the City', Renewable and Sustainable and Energy Reviews, September 1989, vol. 2, part 3, pp 303-326.

ii Hunt DRG 'Predicting Lighting Use- a Method Based on Observed Patterns of Behaviour,' Lighting Research and Technology, 12 (1) pp 7-14 (1980).

iii Fontoynont M, Berrutto V 'Daylighting Performance of Buildings: Monitoring Procedure' Conf. Proc Daylighting '98 pp 63-70, (1998).

iv Littlefair P J, Aizlewood M E, 'Measuring Daylight in Real Buildings', Proc. CIBSE National Lighting Conference, Bath, March 1996, pp112-125.

v Love A. J. 'The Evolution of Performance Indicators for the Evaluation of Daylighting Systems,' Conference Record of IEEE Industry APPA Soc., Annual Meeting Houston, USA 4-9 October 1992. IEE, NY, USA Vol. 2 pp 1830-1836.

vi Lynes J. A, 'Principles of Natural Lighting', Elsevier, London, pp77-8, (1968).

vii Bsi "Lighting for Buildings, Part 2: Code of Practice for Daylighting", BS8206: Part2 (1992).

viii Ed. Baker N, Fanchiotti, Steemers K, 'Daylighting in Architecture: A European Reference Book.', James and James, (1993).

ix Sample I, 'Let the Sun Shine In', New Scientist, No2249, 29 July 2000, p17.

4. Microlenses in Daylighting

4.1 Introduction to Microlenses in Daylighting

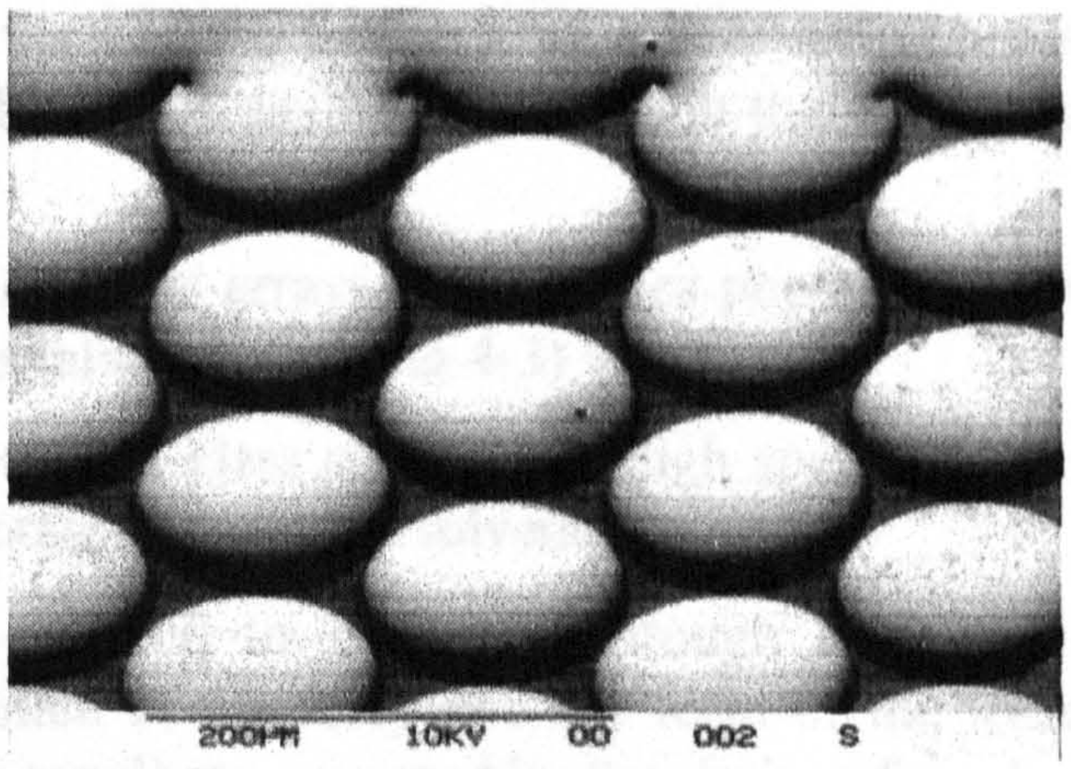

Fig 4-1: SEM photograph of 100 µm period array of spherical lenses.

At NPL the facilities exist for the manufacture of microlens arrays as shown in Fig 4-1. The lenses have short focal lengths so that small movements of the array can cause significant deviations in the light (see Fig 4-2). Such a property may be useful in devices that actively track the sun.

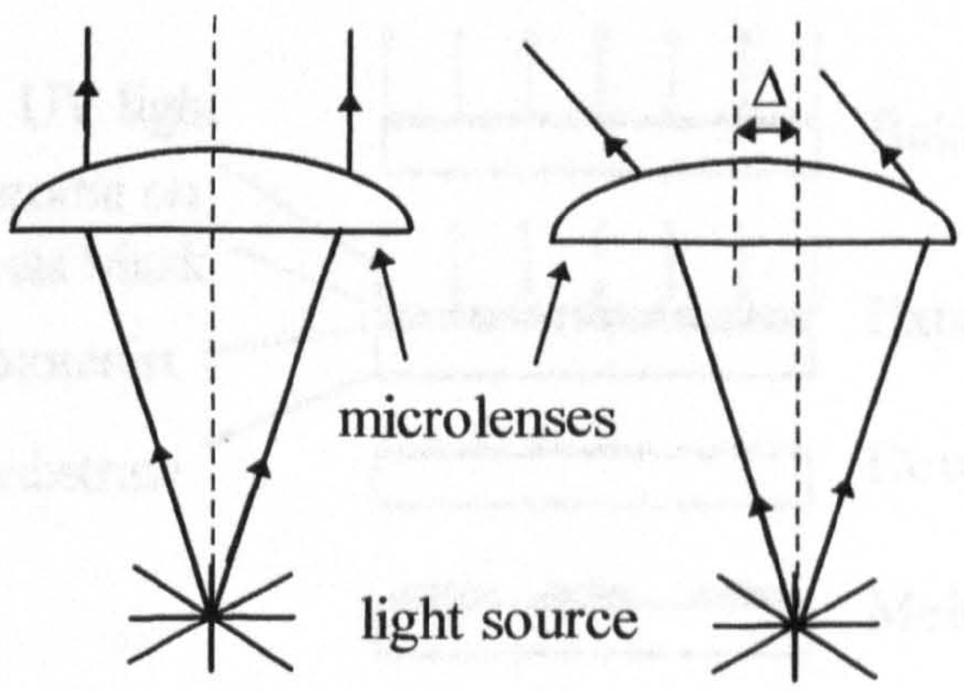

Fig 4-2: Deviation of illumination by microlenses where the displacement Δ is a fraction of the lens period.

Furthermore the lenses could be replicated cheaply and in large quantities by the same UV embossing procedure that would be used for the prisms.

Three microlens systems were explored as having potential daylighting applications. They were:

- Cylindrical microlenses as diffusers
- Afocal pairs of microlenses for beam-steering
- Microlenses as part of a solar shade

The first two systems were intended to improve the penetration of solar radiation and the third to exclude intense sunlight. Each will now be described in turn. However only the solar shade system was investigated in any depth at NPL (for reasons to be explained) and this is reflected in the brevity of the description of the first two systems.

4.1.1 Cylindrical Microlens Diffuser

It was suggested by the ENTPE that coating a window with cylindrical microlenses may cause a redistribution of daylight incident on the window and improve interior illumination.

The production of microlens arrays at NPL uses photolithographic techniques[i]. The key stages in their manufacture (see Fig 4-3) are:

1. Photoresist is spun on a glass substrate at high speeds to produce a flat coating. Baking then evaporates any excess solvent.
2. The substrate is exposed to UV light through a mask, to form 'islands' of photoresist. The pitch of the array and the form of the lenses (that is spherical, cylindrical or hexagonal) are governed by the choice of mask.
3. The resist array is immersed in developer, before being washed and dried.
4. On further baking of the substrate, the islands of photoresist are melted and drawn into lenses by surface tension.

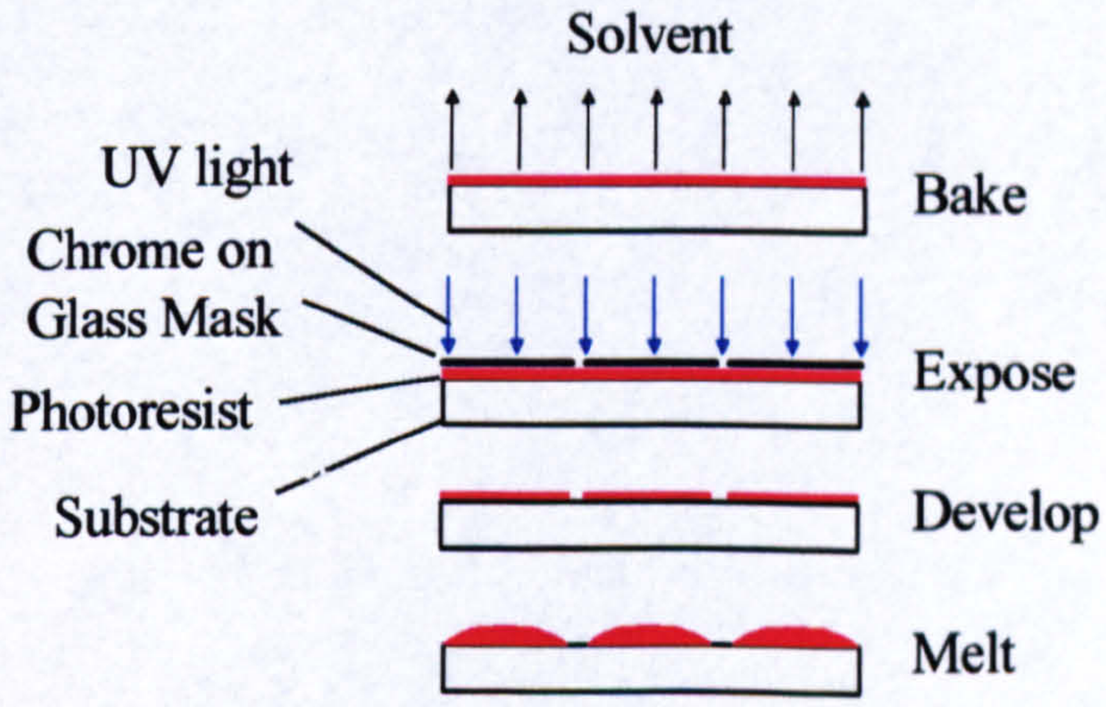

Fig 4-3: Manufacture of microlenses.

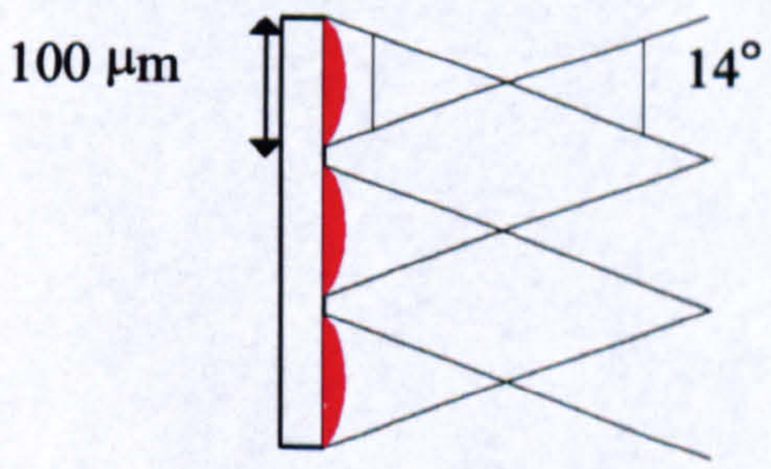

Fig 4-4: Specifications for the cylindrical microlens diffuser.

On consultation with the ENTPE it was decided that the diffuser should have an angular spread of approx. 14°.The lowest spatial frequency that Autotype would be able to manufacture (should the system be successful) is 100 μm, so this dictated the choice of mask used to make the lenses. In order to form such lenses, it is necessary to calculate the thickness of the resist coating.

By simple trigonometry (from Fig 4-4) the focal length (f) is 407 μm and the radius of the curvature (R) given by:

$$R = f/(n-1) = 224\ \mu m$$

(for n= 1.55, the refractive index of the resin replicas that will be used in the diffuser)

Therefore the height of the lens is:

$$h = R-(R^2-r^2)^{1/2} = 5.65\ \mu m$$

For the thickness of resist (T_{cyl}):

$$T_{cyl} = \tfrac{1}{2}\,[(R^2/r)\,\sin^{-1}\,(r/R)-R+h] = 3.8\ \mu m$$

Forming lenses with this relatively thin coating is difficult as the surface tension is insufficient to draw the photoresist into hemisphere. It was found that by exposing the substrate for a further period after the development process, this problem could be overcome. Fig 4-5 shows a comparison of lens profiles formed with and without the extra exposure time and Fig 4-6 the final lenses

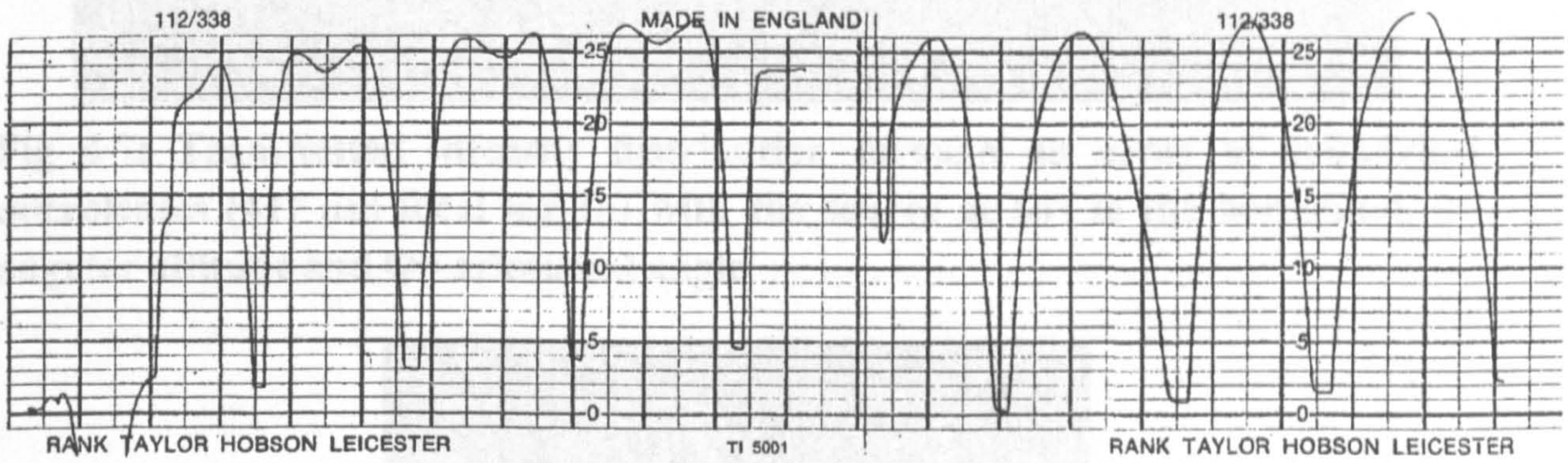

Fig 4-5: Cross-section of a microlens array traced using a Talystep. (*Left*) Lenses fail to form due to thin coating. (*Right*) Post-development exposure improves the lenses (100 μm period and height 6 μm).

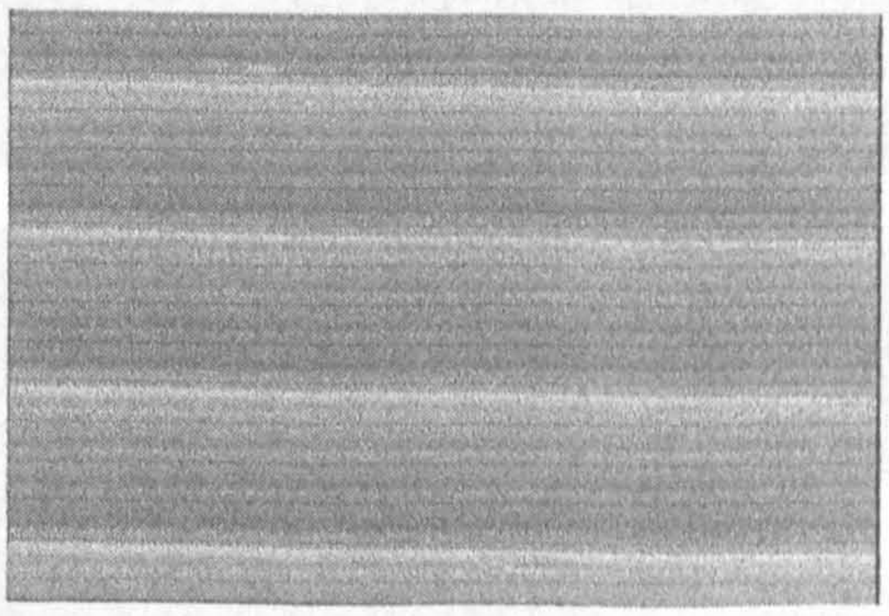

Fig 4-6: Photograph of cylindrical microlenses (through scanning electron microscope) with 100 μm period and 417 μm focal length (approx. x100 mag on printed page)

Conclusion to Cylindrical Microlens Diffuser

Taking the solar position to be 50°, Fig 4-7 shows the transmitted intensity distribution through the array (see Chapter 3 for explanation of polar plots). Light is transmitted between 30° and 50° below the horizontal which does not represent a significant deviation of the incident radiation.

Fig 4-8 compares the diffuser to traditional glazing. Measurements performed by the ENTPE showed there was insufficient improvement in the illumination, so the system was not investigated further.

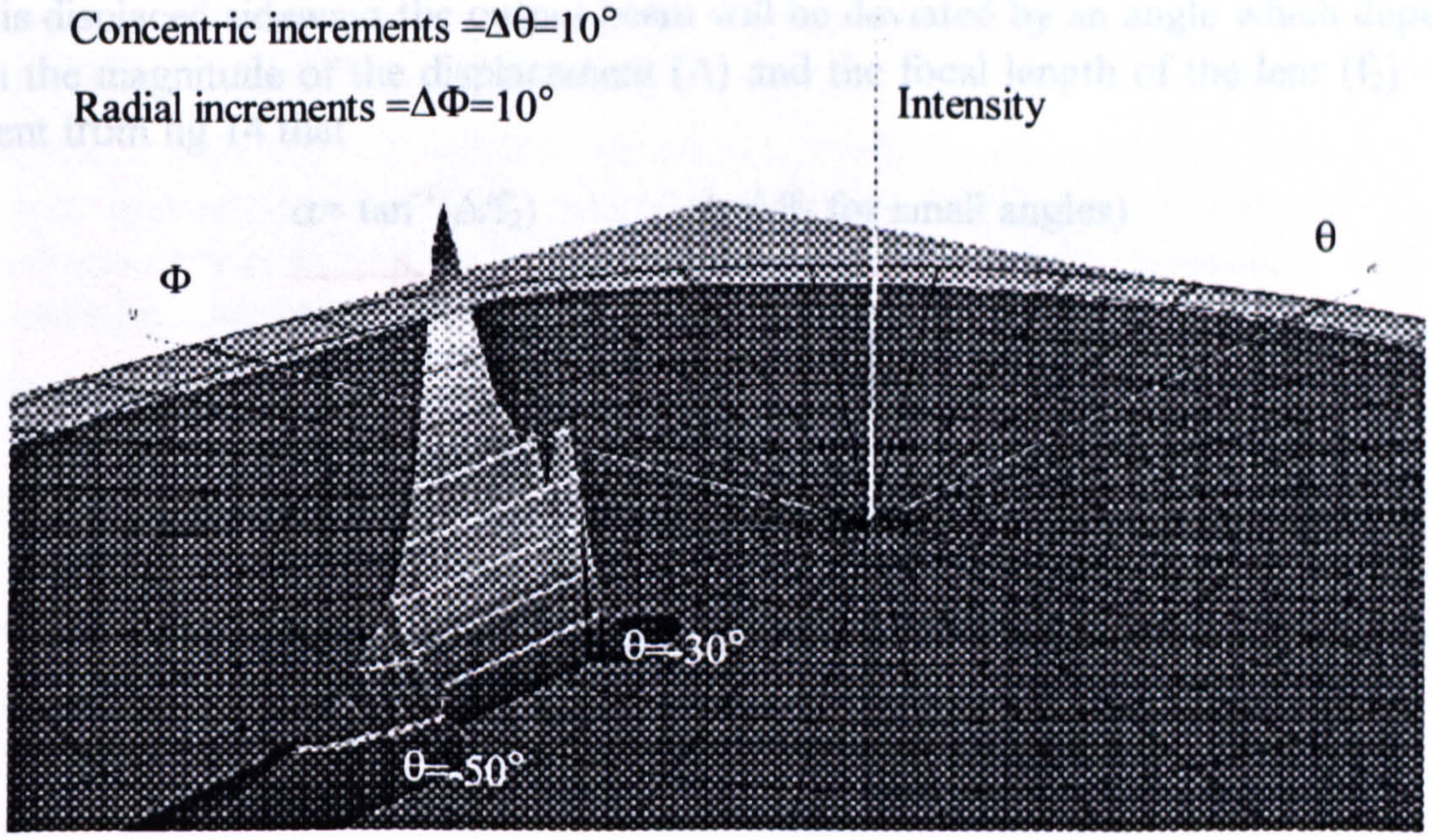

Fig 4-7: Transmitted intensity distribution through an array of cylindrical microlenses (417 μm focal length) with the source at 50° to the horizontal. θ= angular altitude and Φ= azimuthal angle

Fig 4-8: Reference single glazing (*left*) and cylindrical microlenses (*right*) under a global artificial sky.

focus by the first lens and recollimated by the second. If the optical axes of the two lenses are coincident, and if the light is incident parallel to the common axis, the direction of the out-going bundle of rays will be unchanged. If, however, the second lens is displaced sideways the output beam will be deviated by an angle which depends upon the magnitude of the displacement (Δ) and the focal length of the lens (f_2). It is evident from fig 14 that

$\alpha = \tan^{-1}(\Delta/f_2)$ $(=\Delta/f_2$ for small angles)

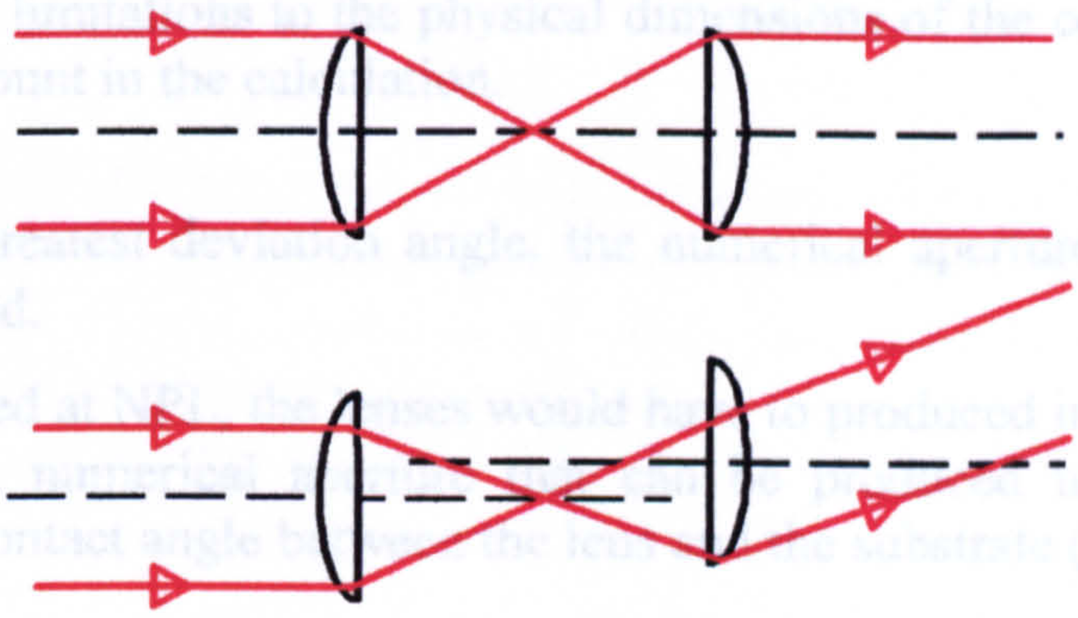

Fig 4-9: The use of an afocal pair of lenses to deviate a beam of light.

It was proposed to cover each internal face of a double glazed window with an array of spherical microlenses. The separation of the panes would be such that the system would be afocal and small displacements of the one pane relative to the other would allow beam-steering in the vertical and lateral planes. The system would then be able to track the sun and deviate the light deeper into the room.

Goltsos[ii] has performed beam steering with a Galilean telescope arrangement for light at normal incidence (see Fig 4-10). The Galilean arrangement makes the system more compact and reduces the aberrations in the system.

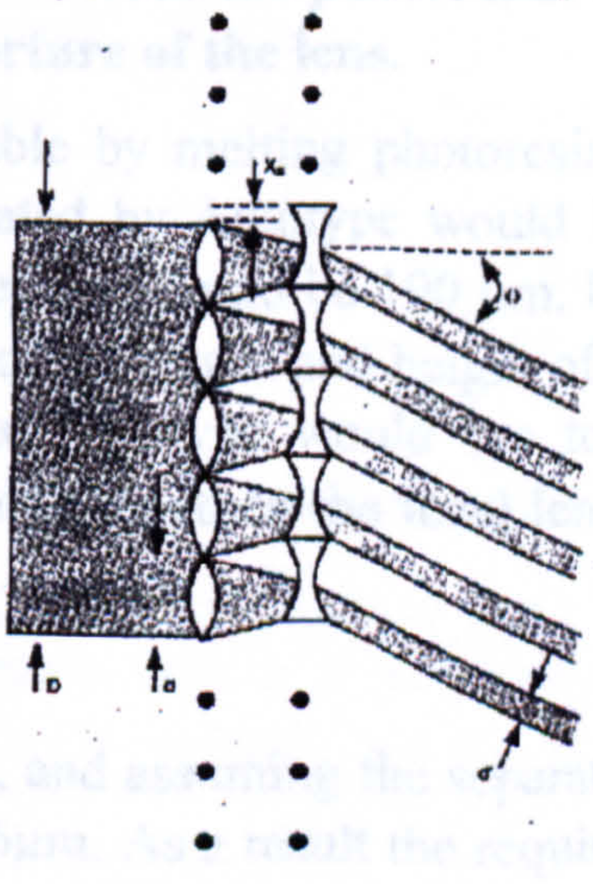

Fig 4-10: Galilean telescope arrangement for beam steering. Negative lens array is translated by x_s to deflect light through angle θ.

The light was deflected over an 11° field for lateral displacements of $\pm$ 100μm. If a similar system (but using positive lenses) is going to be applied to daylighting then a much greater angle of deviation would be required. The possibility was explored using

The light was deflected over an 11° field for lateral displacements of ± 100μm. If a similar system (but using positive lenses) is going to be applied to daylighting then a much greater angle of deviation would be required. The possibility was explored using ray-tracing software. The proceeding discussion is directed at calculating the parameters for the system.

To cover a large area of window, the lenses would be embossed by Autotype from masters manufactured at NPL and electroformed by OpSec. Using this process introduces certain limitations to the physical dimensions of the components and these are taken into account in the calculation.

Calculation of f2

To produce the greatest deviation angle, the numerical aperture of the second lens must be maximised.

To be manufactured at NPL, the lenses would have to produced in photoresist (see Fig 4-3). The highest numerical aperture that can be produced using this method is governed by the contact angle between the lens and the substrate (see Fig 4-11).

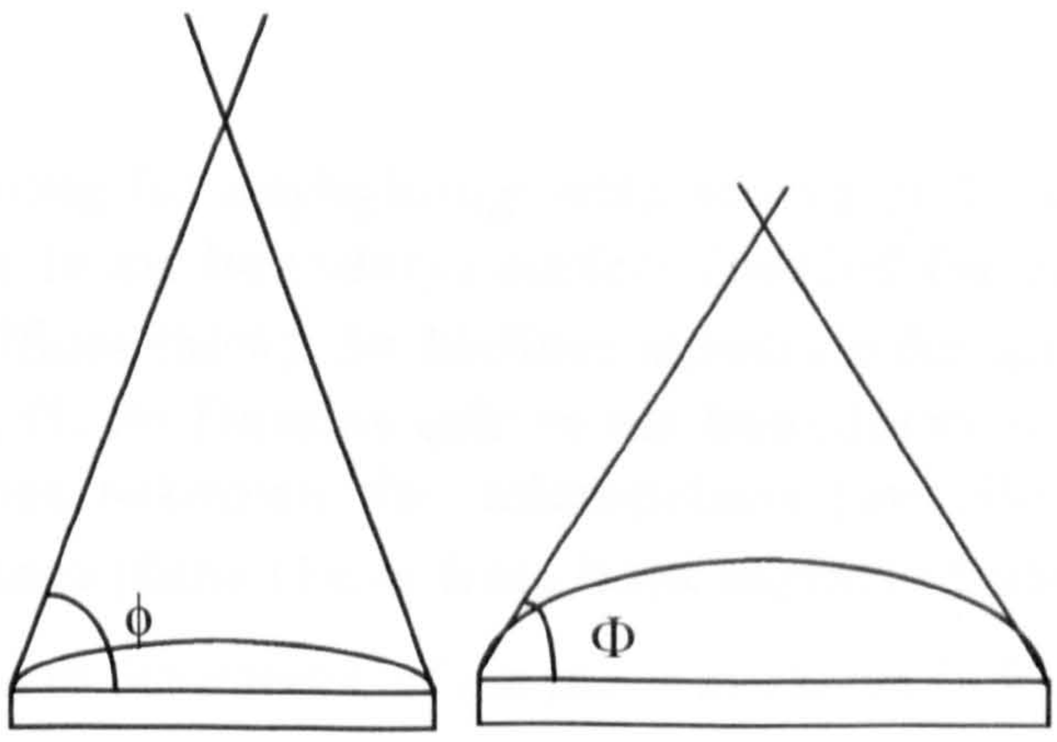

Fig 4-11: The contact angles between the photoresist lens and glass plate ϕ and Φ, govern the numerical aperture of the lens.

The lowest f-number achievable by melting photoresist is f1. The largest diameter structure that could be replicated by Autotype would be 100 μm therefore from f-no.=f/d, the focal length of the lens should be 100 μm. Using the equations in section 4.1.1 the values for its radius of curvature and height of the lens are 62μm and 25μm respectively. The material that Autotype would use to emboss the structure has a refractive index of 1.5 and would lengthen the focal length of the lens from 100[1] μm to 124 μm.

Calculation of f1

If the lenses were to be afocal, and assuming the separation of double glazing to be 6 mm, f1 would have to be 5876μm. As a result the required thickness of photoresist is calculated to be 0.5μm. Such a layer would be too thin for lenses to form and therefore this system requires that the panes be moved closer together. Lenses have been formed though with 100 μm period and 400μm focal length from a coating

[1] Typical refractive index of photoresist, n=1.62.

thickness of 5.5μm. For the purposes of this simulation these will suffice. Once embossed in polyester their focal length increases to 480μm.

The final system is shown in Fig 4-12. In practice the panes of glass would be approximately 4mm thick, but for the purposes of clarity they are modelled by sheets of comparable thickness (125μm) to the lens dimensions.

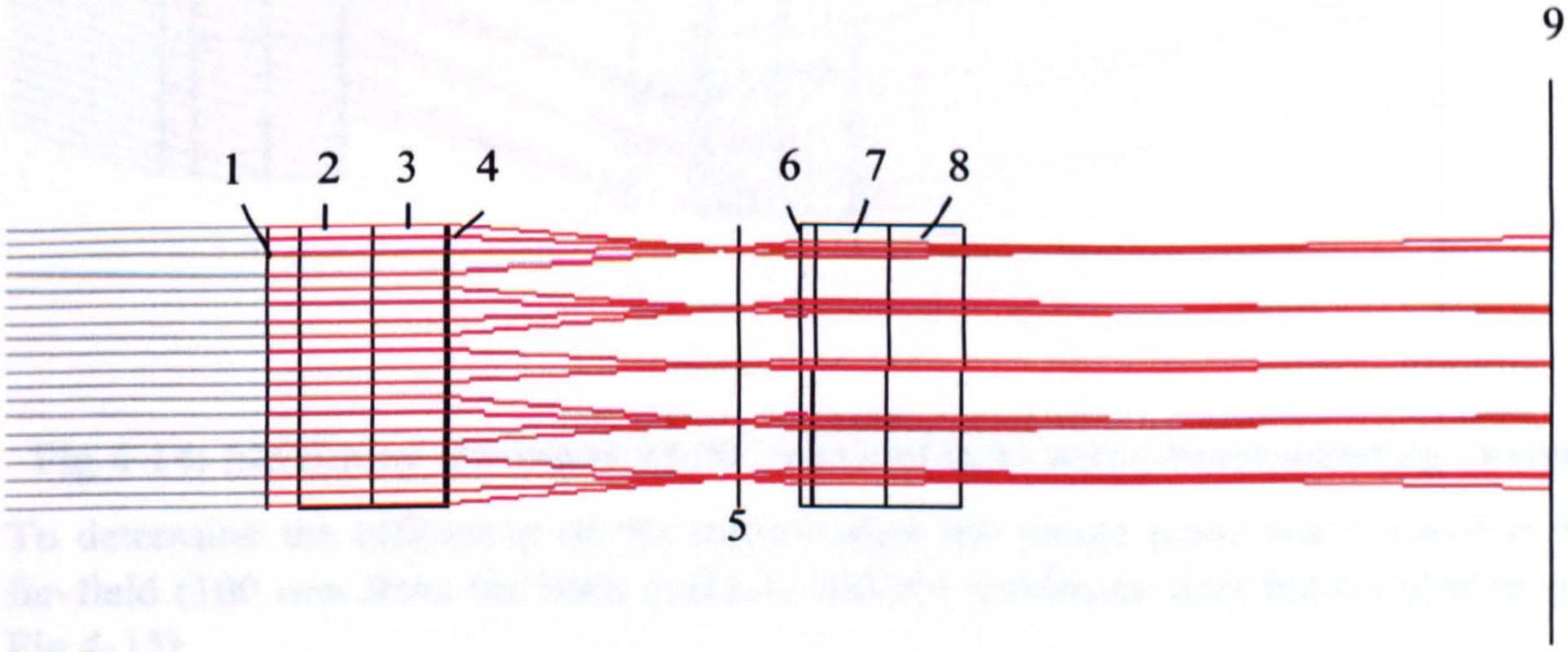

Fig 4-12: 'Beamsteering for daylighting' with source at 0° (described in section 4.3). 1= Dummy (air to air boundary) surface (needed for raytracing purposes) 2= Window pane (125μm thick). 3= Melinex substrate for microprisms (n=1.49). 4= Microlens array, f1. 5= Dummy (air to air boundary) surface. 6= Microlens array, f2. 7= Melinex substrate for microprisms (n=1.49). 8= Window pane (125μm thick). 9. Image plane (1mm from back surface of window pane).

The lenses are adhered to the interior of the panes as shown in Fig 4-13.

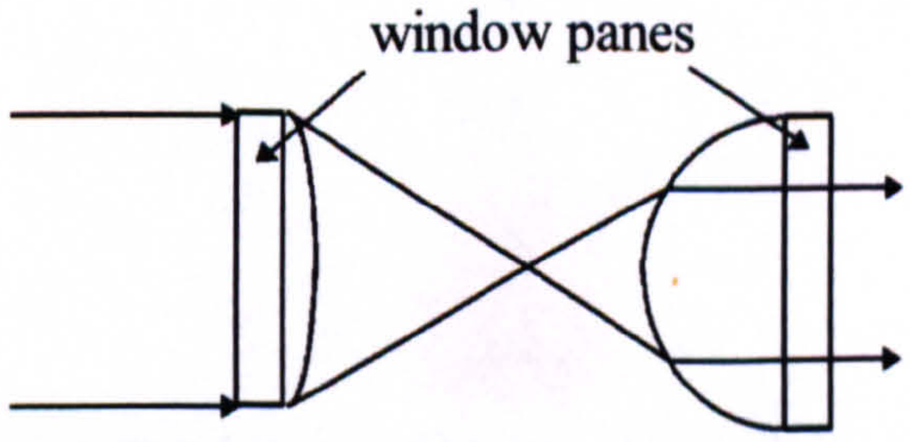

Fig 4-13: Arrangement of lenses within window.

The curved surface of the first lens is facing away from the collimated beam and thus would introduce more aberrations than if it were reversed. However placing the lenses on the internal faces of the window would mean that cleaning the system would not be necessary.

Varying the angle of incidence on the first surface simulated the changing solar position. In response the second array was displaced laterally to deviate the light above the horizontal. The greatest incident angle for which this was achieved was 20° (see Fig 4-14).

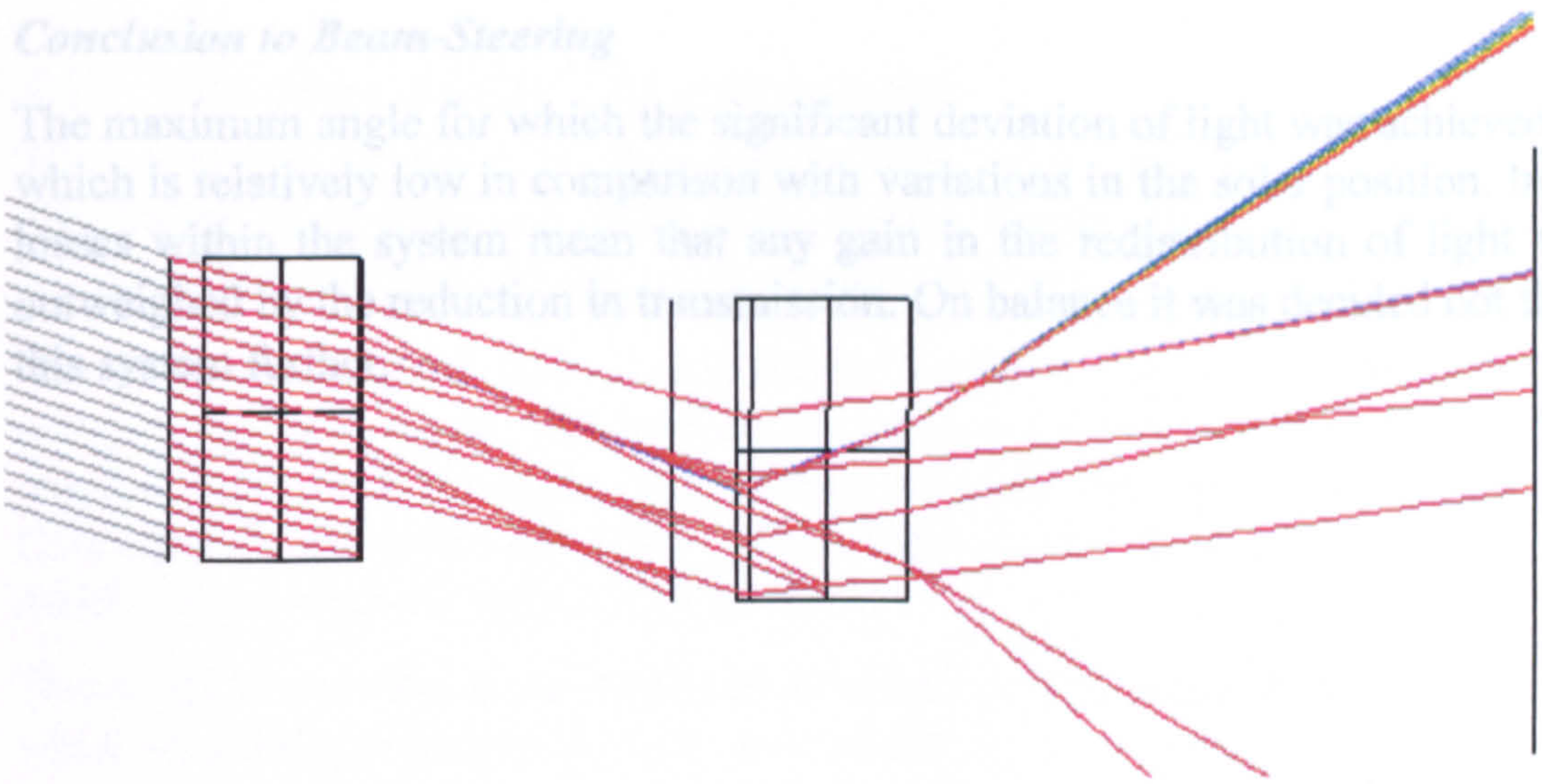

Fig 4-14: Maximum deviation of 20° incident light using beam-steering device.

To determine the efficiency of the transmission the image plane was located in the far-field (100 mm from the back surface) and the irradiance distribution plotted (see Fig 4-15).

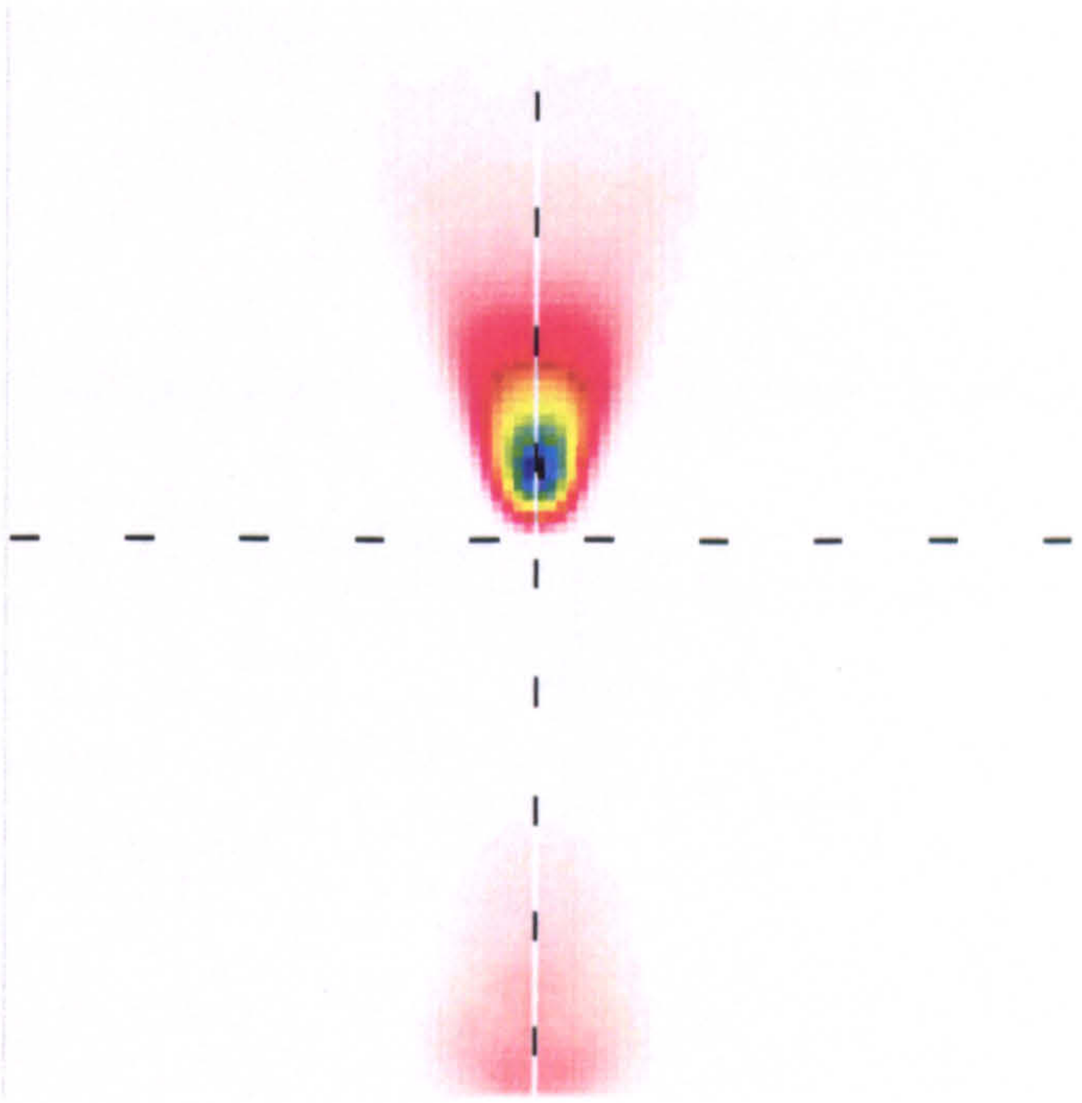

Fig 4-15: Irradiance distribution 100 mm from back surface of the window.

Of the transmitted light, 89% is above the horizontal and 11% below. The peak efficiency occurs at approximately 10° above the horizontal. Although similar efficiencies may have been possible at slightly higher incident angles, it was not thought that these improvements would have been significant. Although the system may seem relatively efficient, the light transmitted above the horizontal represents only 15% of the light incident on the first surface. This is illustrated in Fig 4-14 where much of the light is vignetted.

Conclusion to Beam-Steering

The maximum angle for which the significant deviation of light was achieved was 20° which is relatively low in comparison with variations in the solar position. In addition losses within the system mean that any gain in the redistribution of light would be outweighed by the reduction in transmission. On balance it was decided not the pursue this system further.

4.2 *The Solar Shade[2]: An Introduction*

The preceding sections of this thesis have been dominated by improving the distribution of daylight within the room to save energy. Ironically, the remainder will be concerned with saving energy by excluding sunlight.

On sunny days, glare from south facing windows can cause discomfort for the occupants of the room. The traditional solution of fitting a venetian blind to the window, not only excludes the intense sunlight but also the diffuse daylight. Consequently on days when there is the most natural light the room is completely darkened and artificial light is still used.

The simplest solution is the extended awning[iii] or light shelf. Both afford a view-out while providing protection from direct sunlight.

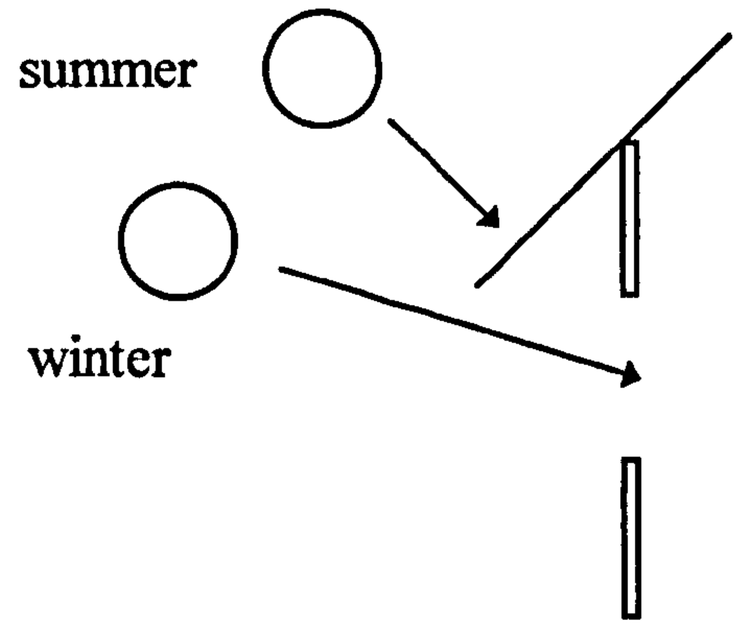

Fig 4-16: Roof awnings can prevent overheating during summer

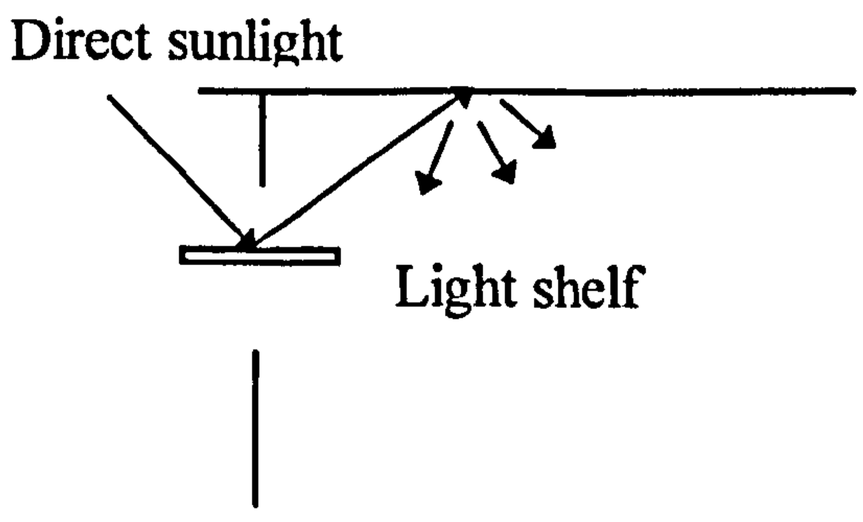

Fig 4-17: Light shelves can be used to prevent overheating by direct sunlight.

Tests[iv] on the light shelf showed that it shaded the front of the room during the spring and the summer while improving the overall uniformity of lighting even with overcast skies. Computer simulation[v] showed that while the shelf provided effective shading spring and summer, it could not provide total protection and allowed the emission of direct sunlight at low altitudes. As a consequence blinds would be needed in addition to the light shelf.

Some solutions to the problem of glare are based on the venetian blinds Automating their movement can take control away from the user and optimise their operation. By closing the blinds sufficiently to prevent glare but without excluding all the light energy savings can be made. Lee et al[vi] have compared such a system to a static venetian blind system set at a range of different angles in two adjacent offices. The

---

[2] The discussion in this section excludes prismatic solar shades, which are described in Chapter 2.

rooms were south-facing with large windows in a sunny, moderate climate. The resultant daily energy savings for the venetian blind were between 22% and 86%. In addition a saving on the cooling load of 28±5% was achieved. The relative contribution of the lighting reduction and the cooling reduction was dependent on the angle of the slats in the blind. If set horizontally, less artificial light was required but the cooling load was greater. At higher tilt angles the reverse was true.

A transparent solar shade however would be able to reduce the cooling load and the lighting demand. Thin films that act as such a shade are described by Smith[vii] et al. Unlike the blinds thin films are spectrally as well as directionally sensitive[viii]. They are manufactured by the vacuum deposition directly onto the window glass of metal or their oxides. The metals are deposited at oblique angles on the substrate and line up in rows in rows normal to the tilt (the gap between the rows being filled with either void or insulator). Light that is parallel to the to the rows is transmitted whereas light in the opposite direction is absorbed.

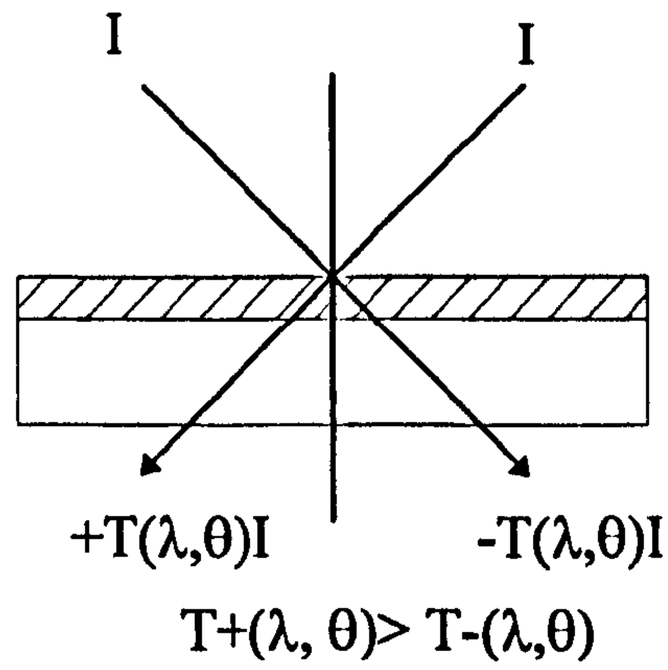

Fig 4-18: Performance of thin films is dependant not only on angle of incidence but also wavelength.

The target values for their performance are given below.

Performance issues	Preferences
Visible Angular Selectivity	Transmittance of diffuse daylight > 0.55 Transmittance of direct sunlight< 0.2
Solar Heat Gain	Transmittance of solar radiation < 0.15 Absorption of solar radiation should be as small as possible and reflectance of solar radiation as high as possible
Thermal Efficiency	low U-value and high IR reflectance.

As with controlled venetian blinds, the author emphasises the need for control of thermal as well as well as visible radiation. The figures in the preferences column are based upon what has been achieved, not upon what is desirable. No direct sunlight is required to light a room as north, east and west facing facades can provide sufficient illumination on sunny days, therefore the transmittance of direct sunlight would be zero,

A commercial thin film ('Llumar' window film, see Appendix C) is available. The manufacturers claim that it reduces UV transmission by 99%, solar energy by 79% and controls glare. However no figures are stated on the attenuation of direct sunlight.

More complex are the switchable, electrochromic and gasochromic[ix] and thermotropic glazing. All of these have useful thermal properties but for the purposes of this thesis, it is the visible properties that will be described. Electrochromic windows are based on the reversible formation of lithium tungsten bronze[x], and a typical window is shown in Fig 4-19. Initially the window is transparent, but the application of 1.5v across the cell causes the discharge of Li^+ ions which dissolve in the WO_3. The result is the formation of blue lithium tungsten bronze the visible transmission is reduced to approximately 15%.

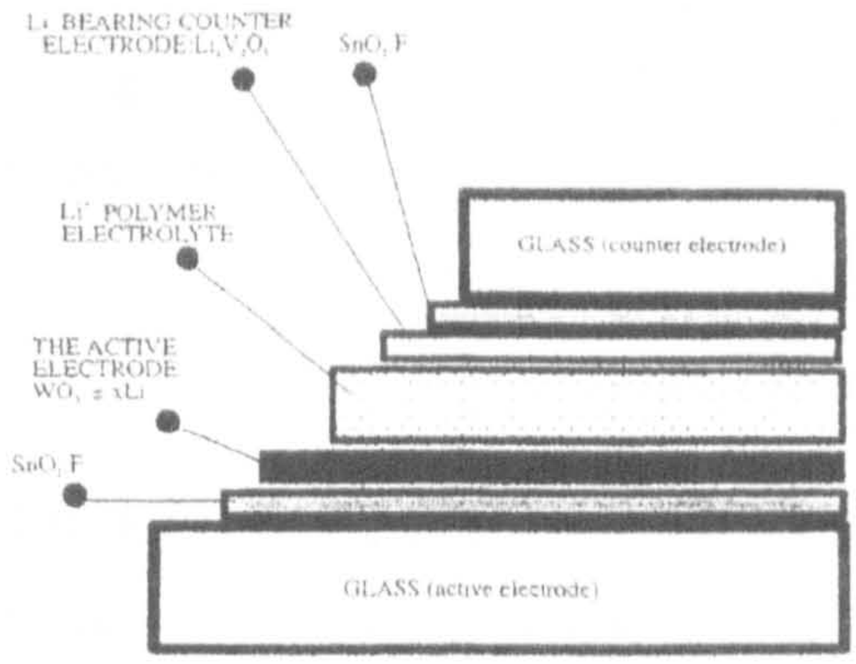

Fig 4-19: Structure of a typical electrochromic window.

Gasochromic[xi] glazing can be switched actively to any external parameter. A gasochromic window is covered with a layer of transparent tungsten oxide (WO_3). A temperature sensor (for example) triggers the release of highly diluted hydrogen that colours the WO_3 by the reaction:

$$xH+WO_3(\text{transparent})\rightarrow H_xWO_3(\text{blue})$$

As a result, the transmission of visible light falls to 18%.

In contrast thermotropic[xi] windows change automatically at a fixed temperature determined by the glazing material.

Fig 4-20: Operating principle for a thermotropic window. (Left) Clear state at low temperature. (Right) Scattering state at high temperature.

Between the two panes is a mixture of at least two materials with different refractive indices. At low temperature the mixture is homogenous and transparent. However, as the temperature increases, the two components separate and incident radiation is

scattered, most being reflected. Examples of thermotropic materials include hydrogels and polymer blends. Visually, the window becomes milky white on switching and incident illumination is scattered with a normal-to-hemispherical visible transmittance of 19%.

Concerning glare, the problem with these 'smart' windows is that they reduce both direct and scattered sunlight equally. In contrast, the transparent solar shade in this chapter is concerned with excluding direct visible sunlight but not diffuse sunlight, like the thin films. The basic system is shown in Fig 4-21.

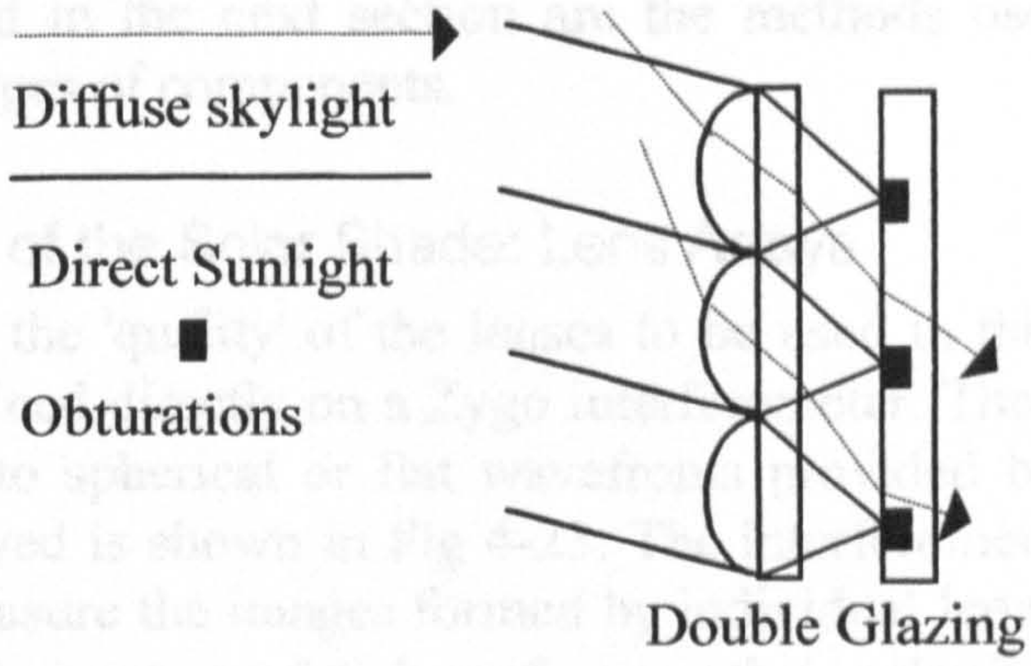

Fig 4-21: The proposed solar shade.

Direct sunlight has a well-defined angle of incidence, which is focused by the lenses onto an array of obturations and is blocked. Diffuse skylight however is not well focused by the array and is transmitted. Consequently solar protection is achieved without darkening the room. The lens and obturation arrays on glass and perpsex sheets would form the panes of double glazing with the separating air gap governed by the focal length of the lens. By translating the position of the lenses in the x and y direction with respect to the obturations the sun could be tracked and a shade provided for all solar positions. The ideal performance for the shade is shown in Fig 4-22

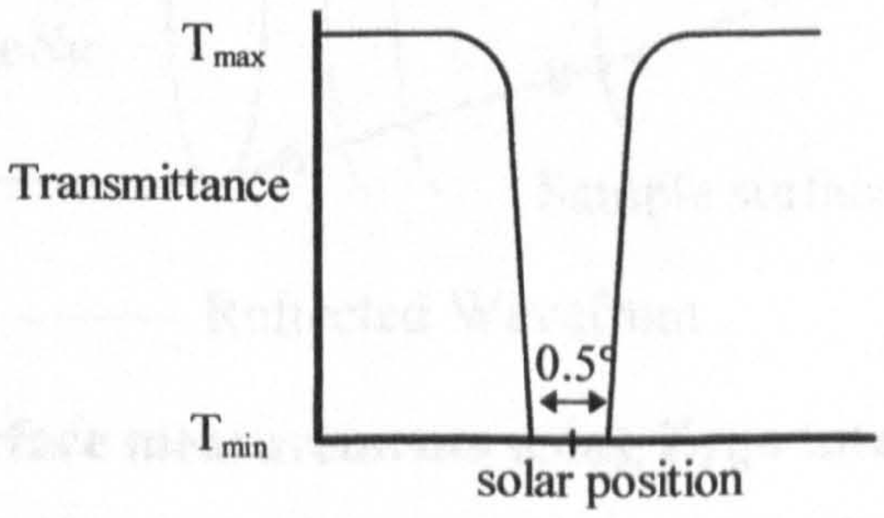

Fig 4-22: Transmission curve for an idealised solar shade (solar diameter 0.5°).

Ideally T_{max} would be close to 80% (allowing for 4% fresnel losses on each surface) although Boyce[xii] et al. have established that the minimum acceptable transmittance of glazing could be as low as 25% to 38%. Research into glare[xiii] is dominated by the quantification of diffuse daylight glare which depends on location specific features such as window size and background illumination. It is difficult therefore to establish a non-zero value should total exclusion prove too technically demanding. For the purpose of this thesis a goal will be set of less than 5% as a drive to optimise the system.

It was hoped originally that the lenses employed would be microlenses[xiv]. However as the translation required would be related to the pitch of the lenses it was thought that

such small movements would not be easily achieved. Consequently lenses with millimetre periods were sought. This would also mean that the lenses would be easier to clean and allow the array to be located on the exterior of the glazing. Thus parallel light would be incident on the curved surface and, introduce fewer aberrations than if the lens were reversed.

In developing the solar shade the first task was to obtain the two main components of the system: an obturation array and a lens array. Several lens arrays on plastic sheets were available in the laboratory for use in the system, as well as two different forms of obturations. Described in the next section are the methods used for assessing and manufacturing both types of components.

4.2.1 Components of the Solar Shade: Lens Arrays

In order to determine the 'quality' of the lenses to be used in the solar shade system, the arrays were examined directly on a Zygo interferometer. The system can compare reflected wavefronts to spherical or flat wavefronts provided by the interferometer. The technique employed is shown in Fig 4-23. The interferometer can either be used in transmission to measure the images formed by individual lenses, or in reflection to measure the radius of curvature of their surfaces or their sphericity. The latter will be described first.

An interference pattern is formed from the combination of reflections from the surface under investigation and the reference surface in the Zygo lens.

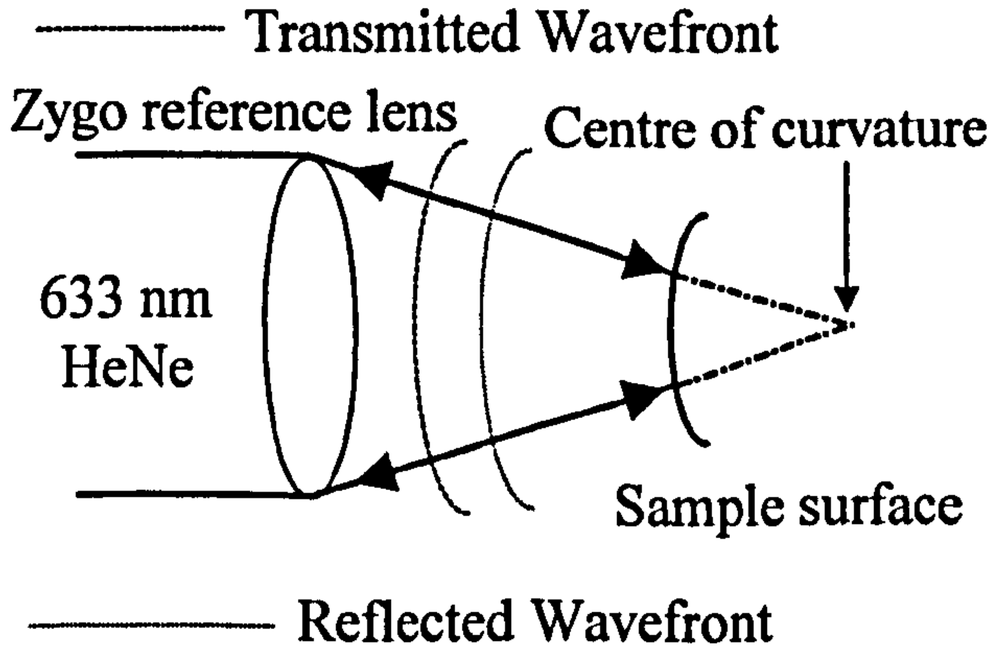

Fig 4-23: Surface measurements using Zygo interferometer.

The sphericity of the wavefront provides a measure of the lens quality and therefore the image.

Alternatively the image quality can be assessed by using the interferometer in transmission. To demonstrate the aberrations in images formed by the solar shade, the lenses were tested using this second method (see Fig 4-24).

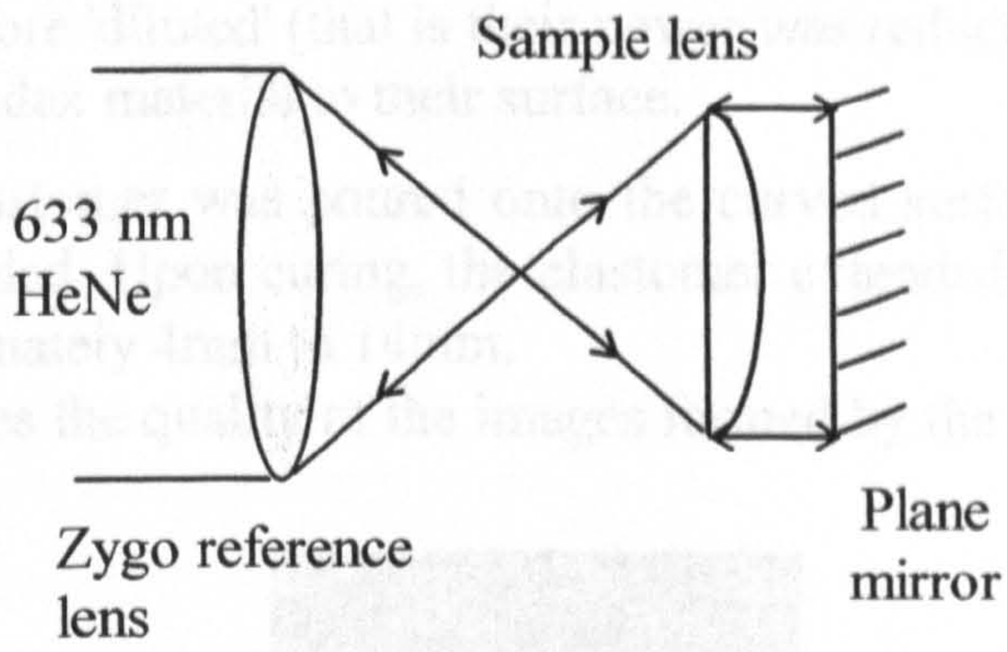

Fig 4-24: Measurement of image quality using Zygo interferometer.

The laser light is reflected back through the lens and brought to a focus which is reflected back to the Zygo and compared to the spherical wavefront. Perfectly spherical lenses that create straight fringes in reflection, produce curves of the shape shown in Fig 4-25 in transmission and demonstrate spherical aberration. To quantitatively determine the spherical aberration, the interferometer is adjusted such that the minimum number of fringes are visible. The number of fringes are then counted that intersect an imaginary line drawn across the centre of the aperture. In Fig 4-25 only one fringe is crossed by the line, therefore the spherical aberration is 1x $\lambda/2$= 317 nm, and would be adequate for use in the solar shade system.

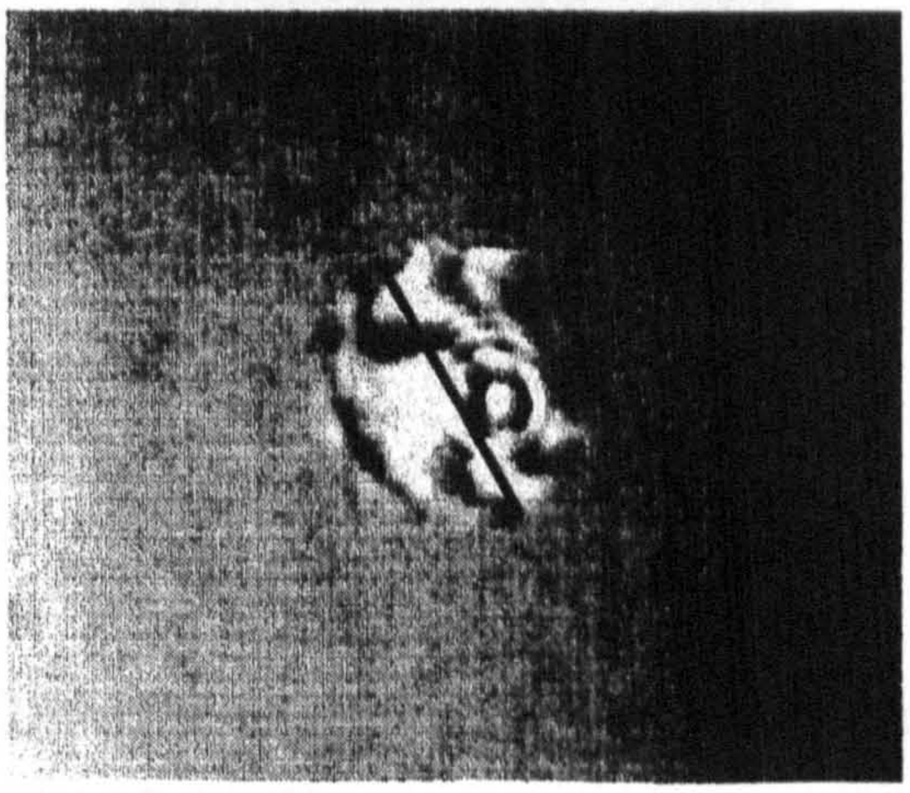

Fig 4-25: Spherical aberration fringes. A transverse line across the aperture crosses only 1 fringe and therefore has a wavefront aberration of only 317nm.

The interferometer was used to examine 3 different lens arrays:

I. 2.6 mm period plano-convex lenses

II. 10 mm period plano-convex lenses

III. 850 μm period plano-convex lenses

a) 2.6mm Plano- Convex Lens Array

The 2.6 mm lenses were manufactured to be diffusers and as such are not required to produce high quality images. It could be seen visually that they would not be of a sufficiently high standard for use in the system. In addition the image plane was located at the back surface of the lens. For the solar shade this would be unacceptable as the obturation array would have to be in contact with the lens, hindering movement.

The array was therefore 'diluted' (that is their power was reduced) with the application of a low refractive index material to their surface.

A liquid silicone elastomer was poured onto the curved surface of the lenses and a glass cover-slip applied. Upon curing, the elastomer extended the focal length of the lenses from approximately 4mm to 14mm.
Fig 4-26 demonstrates the quality of the images formed by the reduced-power 2.6 mm lenses.

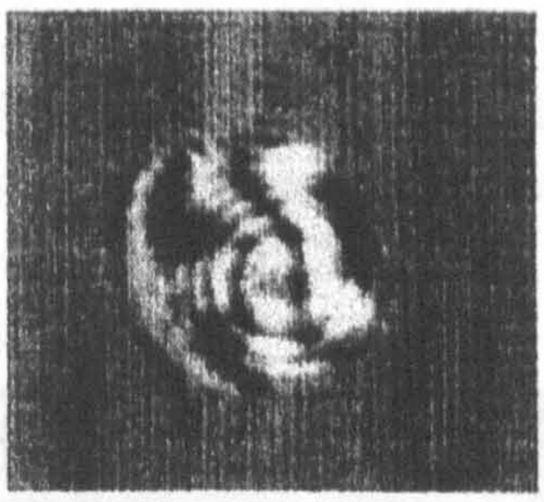

Fig 4-26: Interferogram of an image formed by a reduced-power, 2.6 mm lens, with radius of curvature of 1.3 mm

The interference patterns have only one fringe of spherical aberration or 317 nm which suggests quite a tightly focused image. However, fringe patterns produced by the surface of the lens (see Fig 4-27) indicate another problem.

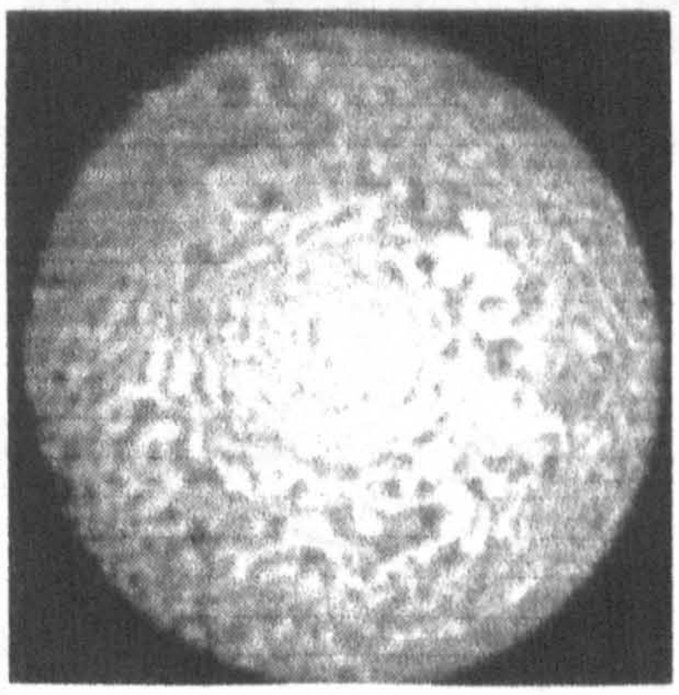

Fig 4-27: Interferogram of the surface of a 2.6 mm lens

The high spatial frequency of the fringe pattern suggests that the surface has a poor finish and is pitted and scratched. Fig 4-28 shows these surface scratches through a x4 microscope objective.

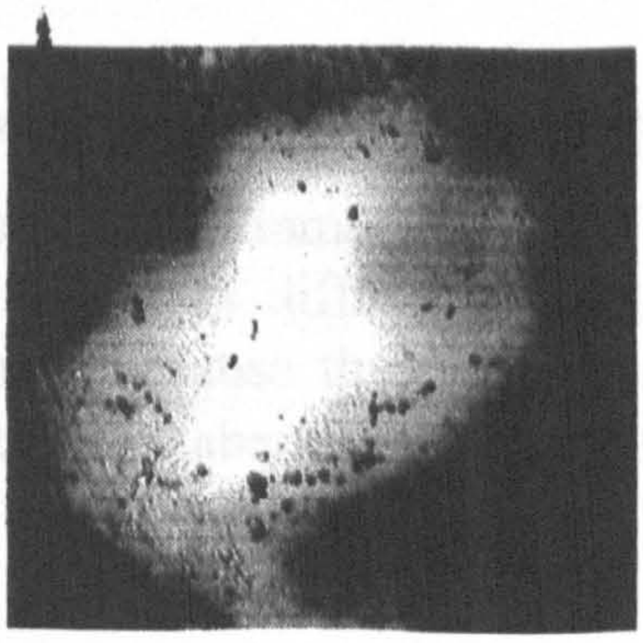

Fig 4-28: Surface of 2.6mm lens (x 20 mag).

The imperfections could cause the scattering of light over a relatively large area, but may not seriously affect the quality of the images. The scratches may not necessarily be cause by mistreatment of the array, but could be produced as part of the

manufacturing process. The lenses were embossed in PMMA and it would certainly be preferable from an optical quality perspective to have glass lenses instead. However glass lenses would be heavier than a perspex array and make their translation in a solar shade more difficult.

Two other lens arrays were examined to see if they would be more suitable for the system

b) 10 mm Plano-Convex Lens Array

The photograph below (Fig 4-29) shows the fringe pattern from the surface of a 10 mm lens in the array. The highly irregular fringe pattern demonstrates that the shape of the lens is far from spherical. The dark areas on the lens (where no fringe pattern is present) show that not all the light is reflected back to the interferometer (see Fig 4-29) and indicate an extremely poor lens.

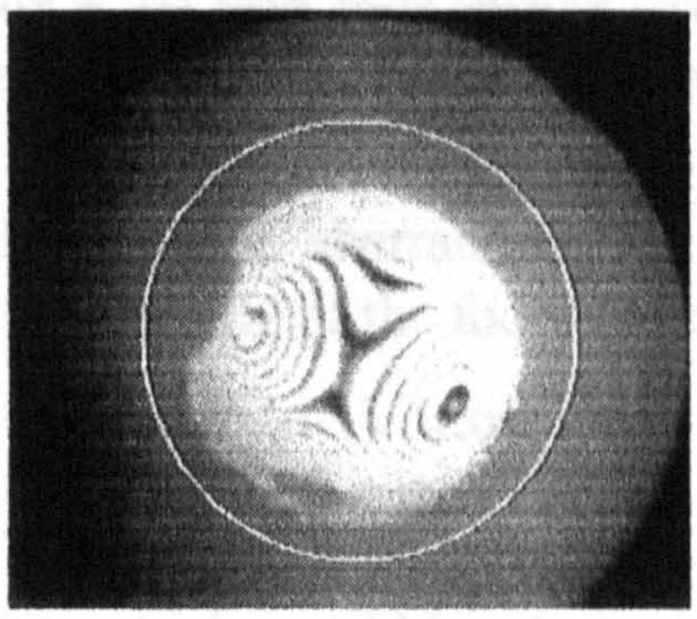

Fig 4-29: Interferogram from a 10mm diameter lenses with a radius of curvature of 27.9 mm

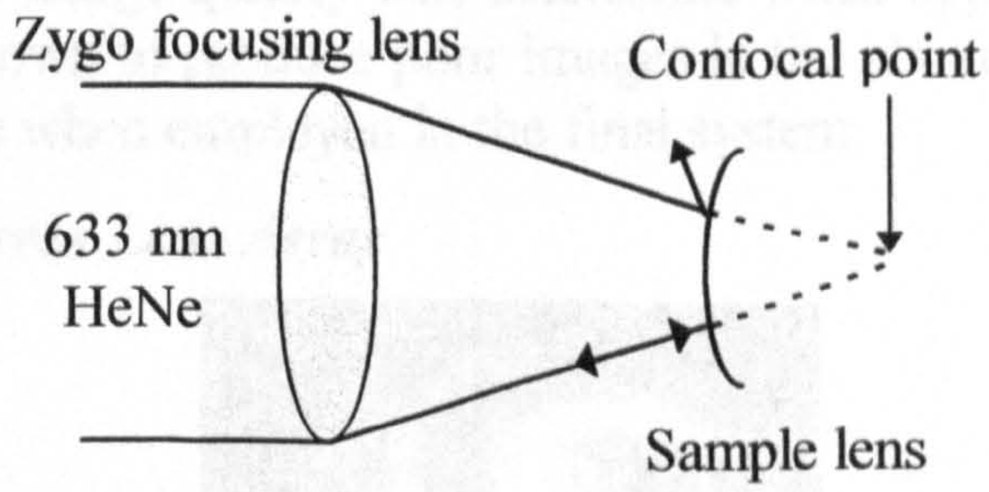

Fig 4-30: Imperfections in lenses scatter light away from interferometer.

The aberrations in these lenses differ dramatically from geometrical aberrations in the pictures of the 2.6 mm lenses. It is difficult to obtain a value for the radius of curvature of the 10 mm lenses because they depart so far from sphericity. A more quantitative feeling for the resultant aberrations can be obtained by changing the focus on the interferometer. Fig 4-31 shows interferograms both sides of the focus of the lens.

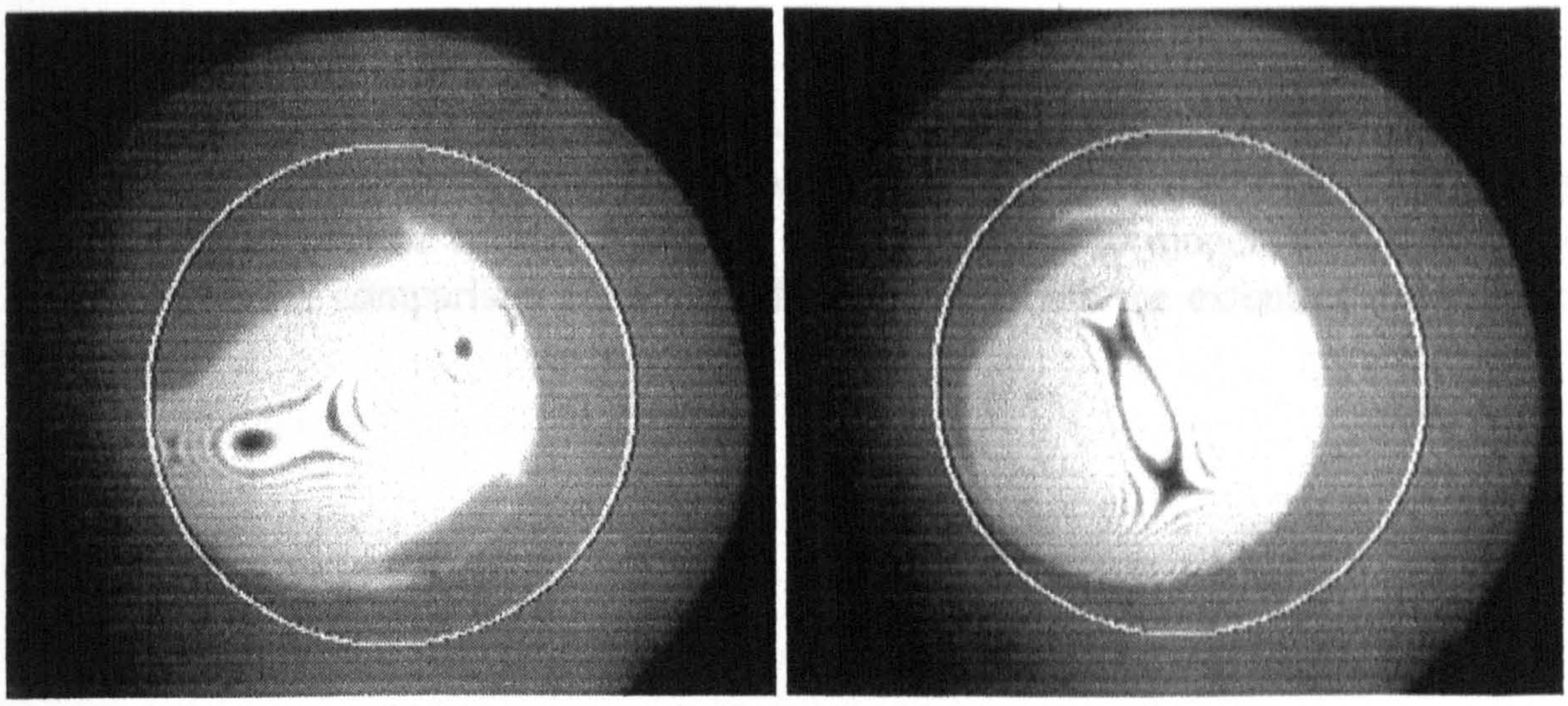

Fig 4-31: Fringe patterns for a 10 mm lens either side of the best focus. Left: radius of curvature = 27.6 mm; Right: radius of curvature = 27.0 mm.

The photographs in Fig 4-31 show an elongated fringe pattern which means that astigmatism is the most dominant of the aberrations. The difference in the radius of curvature (0.6 mm) implies a lengthening of the focus (Δf):

$$1/\Delta f = (n-1)/\Delta r.o.c$$
$$= 1.2 \text{ mm}$$

Such a highly aberrated lens would be inappropriate for the solar shade because it would require a large obturation which would block the indirect as well as the direct sunlight. A preferable system would have less than 1 μm of aberration or 3 fringes. The reason for demanding such a high quality lens is that the system will have work off-axis due to the high solar altitude. The measurements by the interferometer are on-axis and therefore the image quality will deteriorate when applied to the solar shade. Should the lens be shown to produce poor images in the above experiments then it is unlikely to be suitable when employed in the final system.

c) 850 μm Plano-Convex Lens Array

Fig 4-32: Interferograms from the surface of 850 μm period microlenses with a radius of curvature of 0.76 mm.

The interferograms show a surface that has a maximum aberration of 2 fringes or 633nm. However, using a 850μm period array would introduce significant technical difficulties when mechanically scanning the array to tack the sun across the sky. Movement would have to be limited to less that 850μm across the whole window and this would be unrealistic in most weather conditions.

Conclusion

It was decided that the 2.6mm reduced-power lens array was the best array out of those available for use in the solar shade despite its poor quality surface and the scattering that may be caused. However, it was intended to model the system on the computer and a comparison of the results would indicate the extent of the problem.

4.2.2 Components of the Solar Shade: Obturation Arrays

a) Manufacture of the Obturation Arrays

Six arrays of obturations were available for use in the solar shade (see Fig 4-33): large, medium and fine circular mirrors and black spots formed from photographic film ('photo-stops').

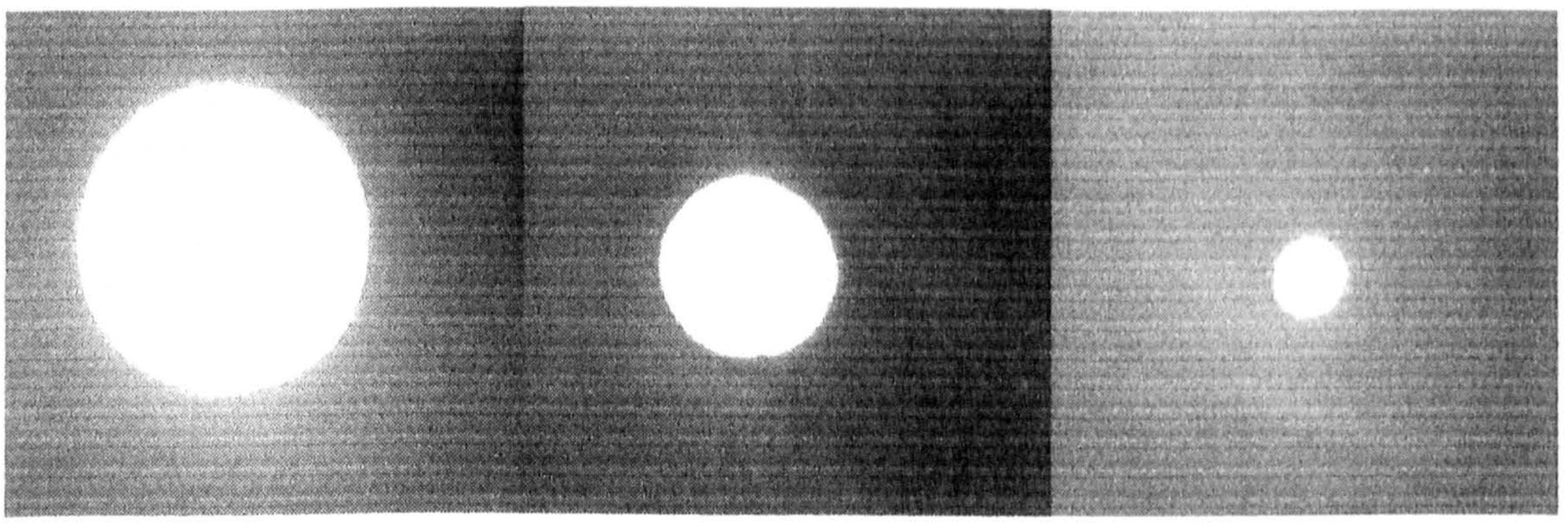

Fig 4-33: Circular mirror obturations viewed with x10 objective.

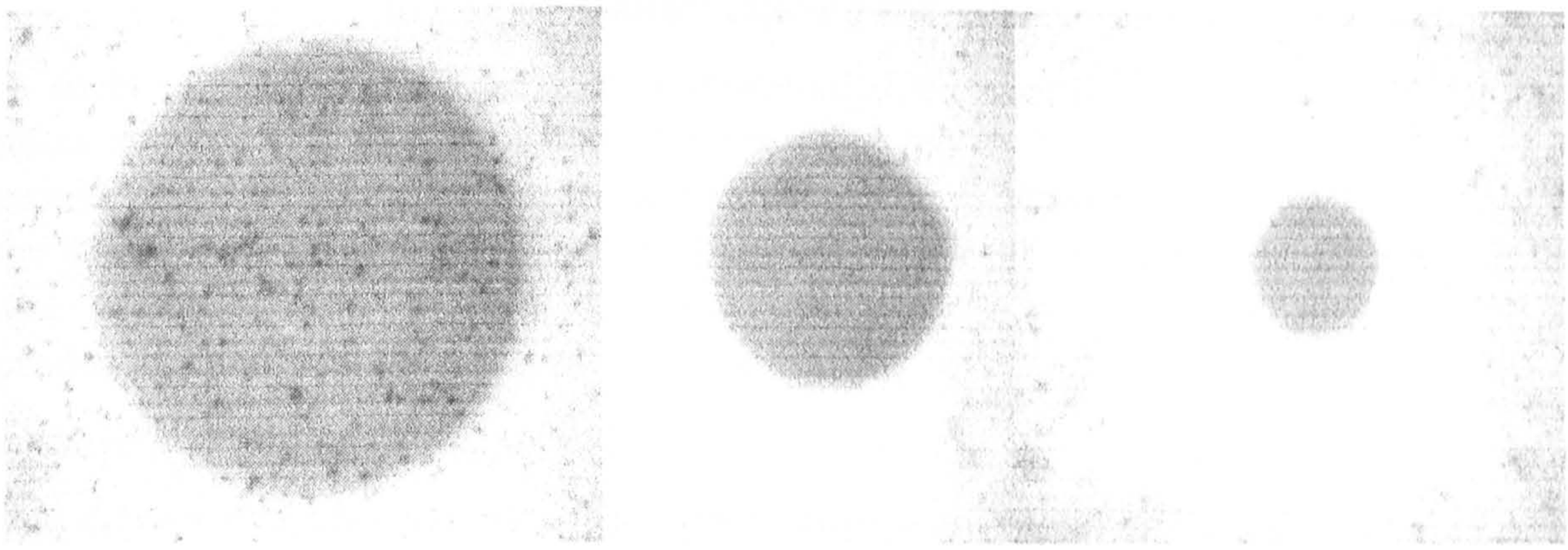

Fig 4-34: Obturations produced photographically and viewed with x10 objective.

The production of the mirrored obturations is a four a stage process shown diagrammatically in Fig 4-35 and described below:

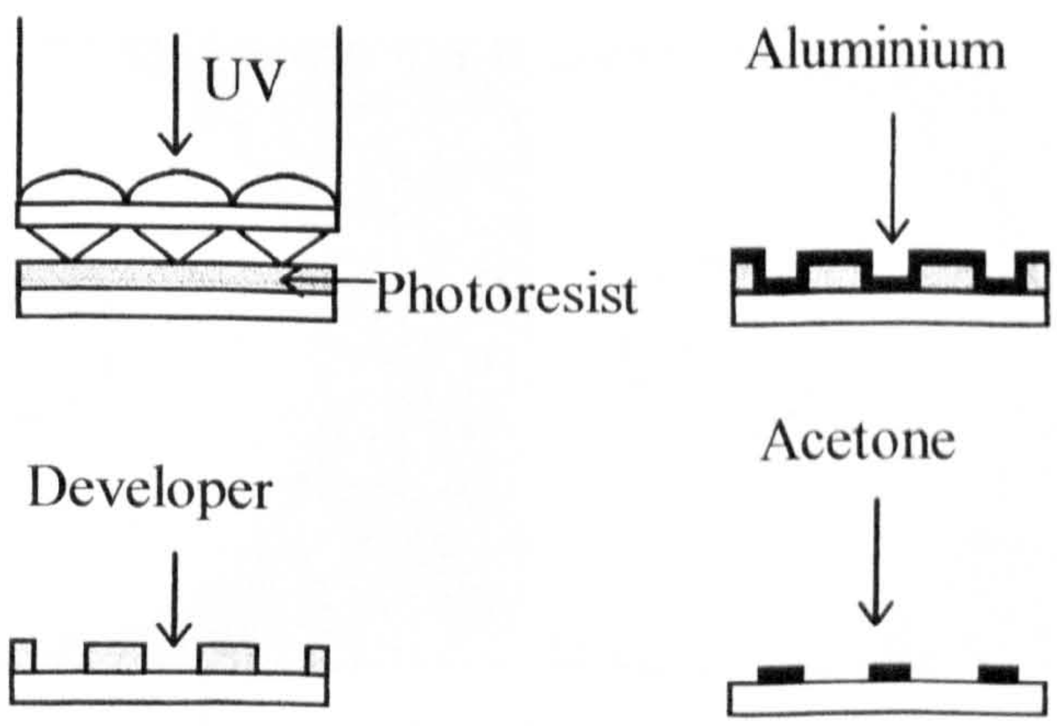

Fig 4-35: Production of mirrored obturations.

Stage 1: A substrate coated with photoresist is exposed to UV light from a mercury lamp *through the same array of microlenses that will form the solar shade.* This

ensures that the resultant stops will be coincident with the images of the source, when the lenses are tested in the shade. The diameter of an aperture in front of the mercury lamp is varied to produce a range of image sizes in the photoresist.
Stage 2: Developer is applied to the substrate, removing areas exposed to the UV light.
Stage 3: Substrate is coated with aluminium.
Stage 4: Substrate is washed with acetone removing coated photoresist. The remaining areas of aluminium are in the shape of the images produced by the lenses.

The arrangement used to produce the 'photostops' is shown in Fig 4-36.

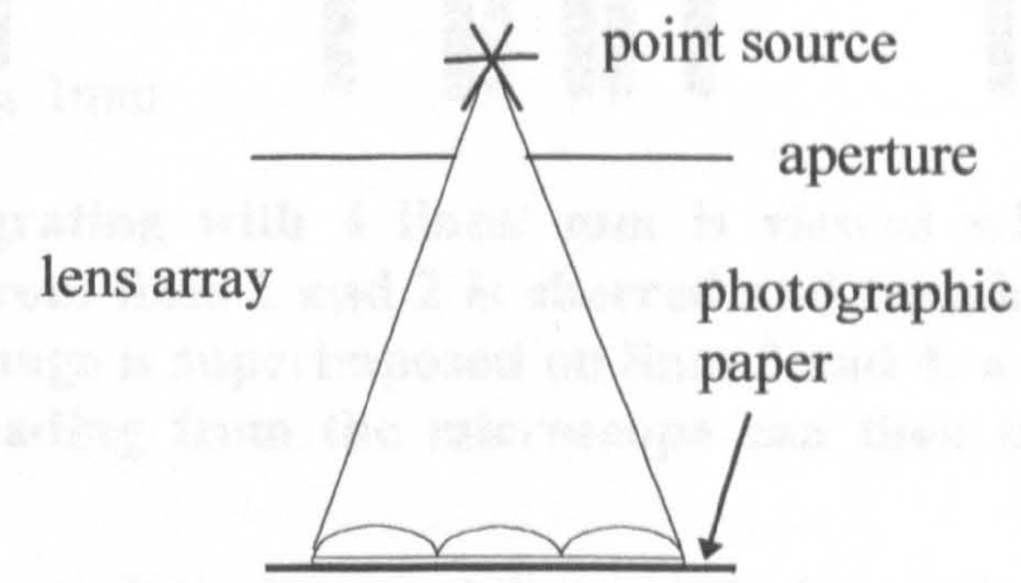

Fig 4-36: Manufacturing the 'photostops'.

A sheet of photographic paper was illuminated through the 2.6mm lens array by a point source. The interstitial area between the lenses was painted with ebonide to ensure that only the point images were transmitted. The paper was then developed to form an array of obturations, and photocopied onto transparent acetate. By varying the size of the aperture in front of the source a range of obturation sizes could be produced, each with the same pitch as the lenses.

b) Measurement of Obturation Arrays

The diameter of the mirrors and the photostops were measured using a Vickers M40 sheering microscope. It operates by splitting the primary image into two identical parts that are initially superimposed. By manually sheering one image so the two are distinct but touching (see Fig 4-37), the diameter of the object can be determined by the images' relative displacement.

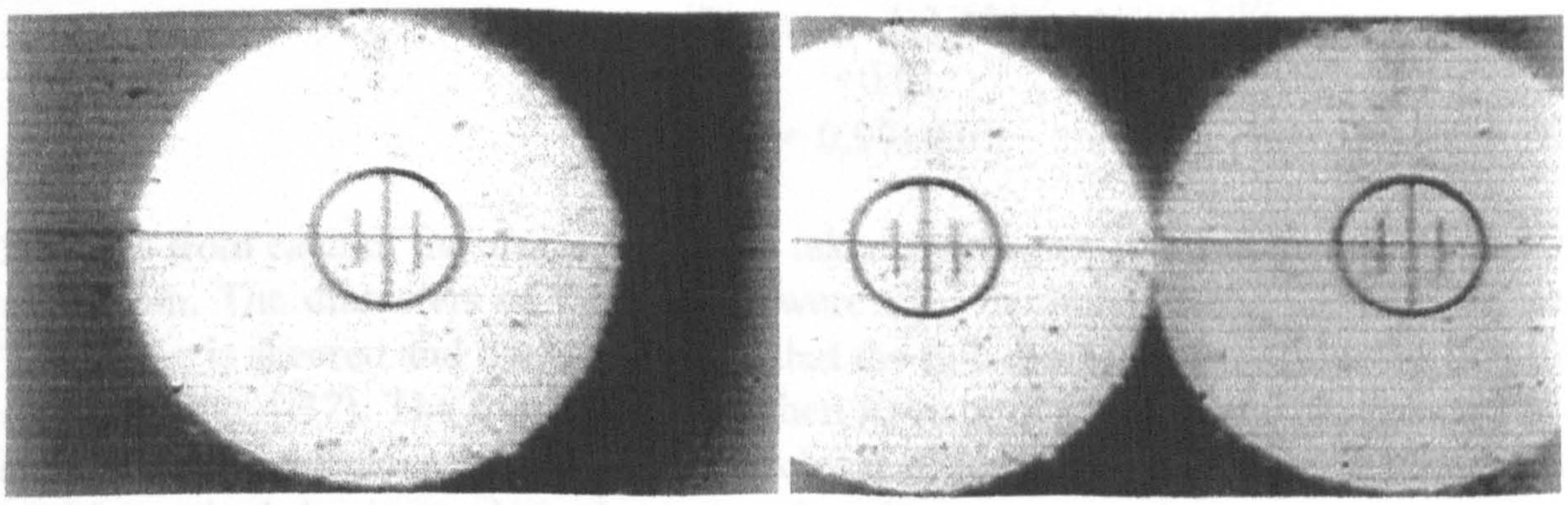

Fig 4-37: Image splitting using the sheering microscope.(*Left*) Two images of the same object are superimpose. (*Right*) Images are distinct but just touching.

Before measuring the obturations, the error in taking a reading had to be determined. The image of a grating with 4 lines/mm was sheered and translated by 500 micrometers (see Fig 4-38).

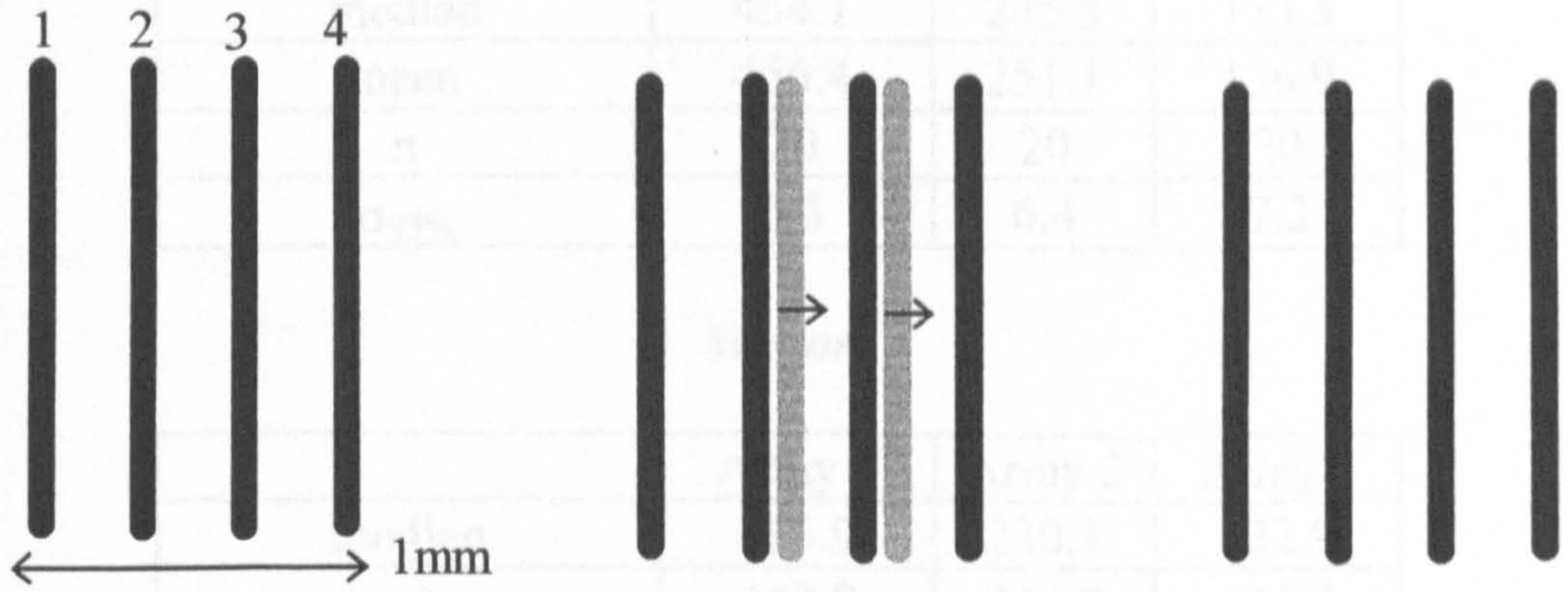

Fig 4-38: (Left) A grating with 4 lines/ mm is viewed with a x10 objective. (Centre)The image from lines 1 and 2 is sheered and translated towards lines 3 and 4. (Right) The image is superimposed on lines 3 and 4: a displacement of 500 micrometers. The reading from the microscope can then be compared to this displacement.

The procedure was repeated six times and the statistical analysis (see Appendix A) of the measurements is given below.

median	495.8
mean	497.0
n	6
$\sigma_{95\%}$	3.5

Consequently at the 95% confidence level the images of the grating were translated 497±3 μm. The grating however has a known period of 4lines/mm and therefore during the calibration the lines were translated 500±4 micrometers. To compensate for the discrepancy between this value and the measured value, a conversion factor was calculated.

$$\begin{aligned} CF &= 497/500 \\ &= 0.99 \\ CF\ error &= [(3/497)^2 + 4/500)^2]^{1/2} \\ &= 0.01 \\ \therefore CF &= 0.99 \pm 0.01 \end{aligned}$$

Samples from each of the arrays were then taken and twenty obturations were selected at random. The diameters of these stops were then measured using the microscope. The image is sheered and translated, such that the two components are side by side (as shown in Fig 4-37). The translation will then have been equal to the diameter of the stop. In reality the stops are not perfect circles and this is one of the major limitations of this method. In comparison the conversion factor was so close to one that it was negligible and ignored. Given below is the statistical data provided by the measurements of the six arrays.

Photostops

	Array 1	Array 2	Array 3
median	454.1	245.5	133.8
mean	456.4	251.1	136.9
n	20	20	20
$\sigma_{95\%}$	6.3	6.4	7.2

Mirrors

	Array 1	Array 2	Array 3
median	435.9	230.1	132.9
mean	442.8	234.2	136.2
n	20	20	20
$\sigma_{95\%}$	7.3	8.4	4.1

The arrays were then taken to consist of obturations with diameters equal to the median value. The median was selected over the mean as an 'average' because it is less perturbed by an atypical measurement.

All six obturation arrays were used in tandem with the reduced-power lens array to test the solar shade.

4.2.3 Empirical Assessment of Solar Shade's Performance

Simulating the performance of the solar shade required a white light source of the same angular size as the sun. In the first instance this was provided by collimating a 1mm diameter optical fibre with a 100mm focal length lens to give an angular subtense of 0.5°. Fig 4-39 shows the arrangement with the lens array and obturations. The illuminated part of the array was approximately 26mm in diameter, covering around 100 lenses.

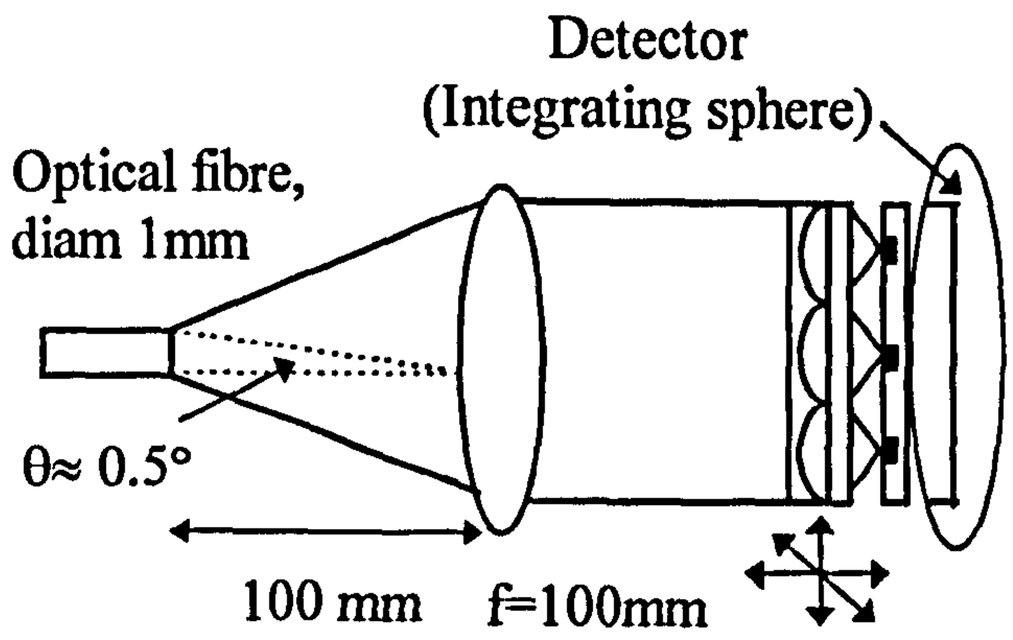

Fig 4-39: Transmission measurements with reduced-power lens array.

For the source at normal incidence, the lenses were translated with respect to the obturations such that the light measured by the detector was at a minimum (Tr_{min}). That is, the lenses focused the illumination on to the stops.

The system and detector were then rotated by small angle κ, such that the illumination was no longer blocked by the stops, giving Tr_{max}. Thus the attenuation by the array is:

$$A=Tr_{min}/Tr_{max}.$$

It will be appreciated that this equation ignores any fresnel reflections which increase with the angle of incidence. Tr_{max} would therefore be slightly greater if corrected for reflections from each surface boundary.

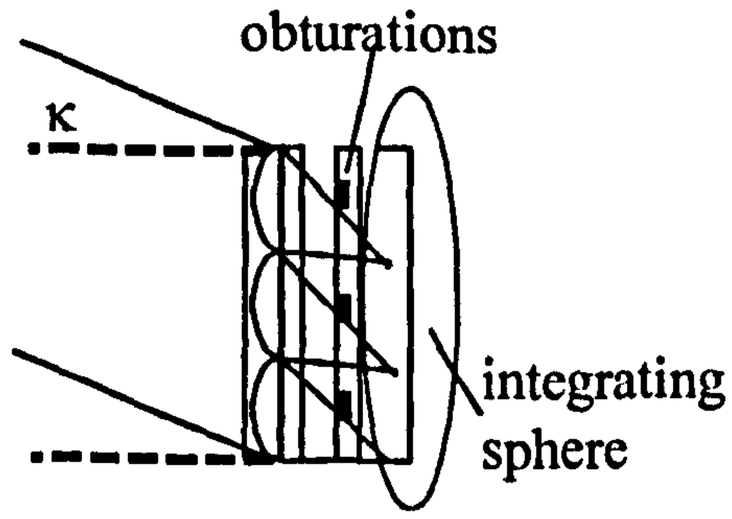

Fig 4-40: Rotation of array and detector by small angle κ.

Although it could said to be unrealistic to have the source at 0°, this was thought to be the angle at which Tr_{min} would be lowest. As the incident angle increases, so do the aberrations in the images and less light would be blocked by the aperture. Consequently it was logical to start with the source at normal incidence, before trying to attenuate the light at higher angles. The results are shown in Graph 4-1 for all six obturations.

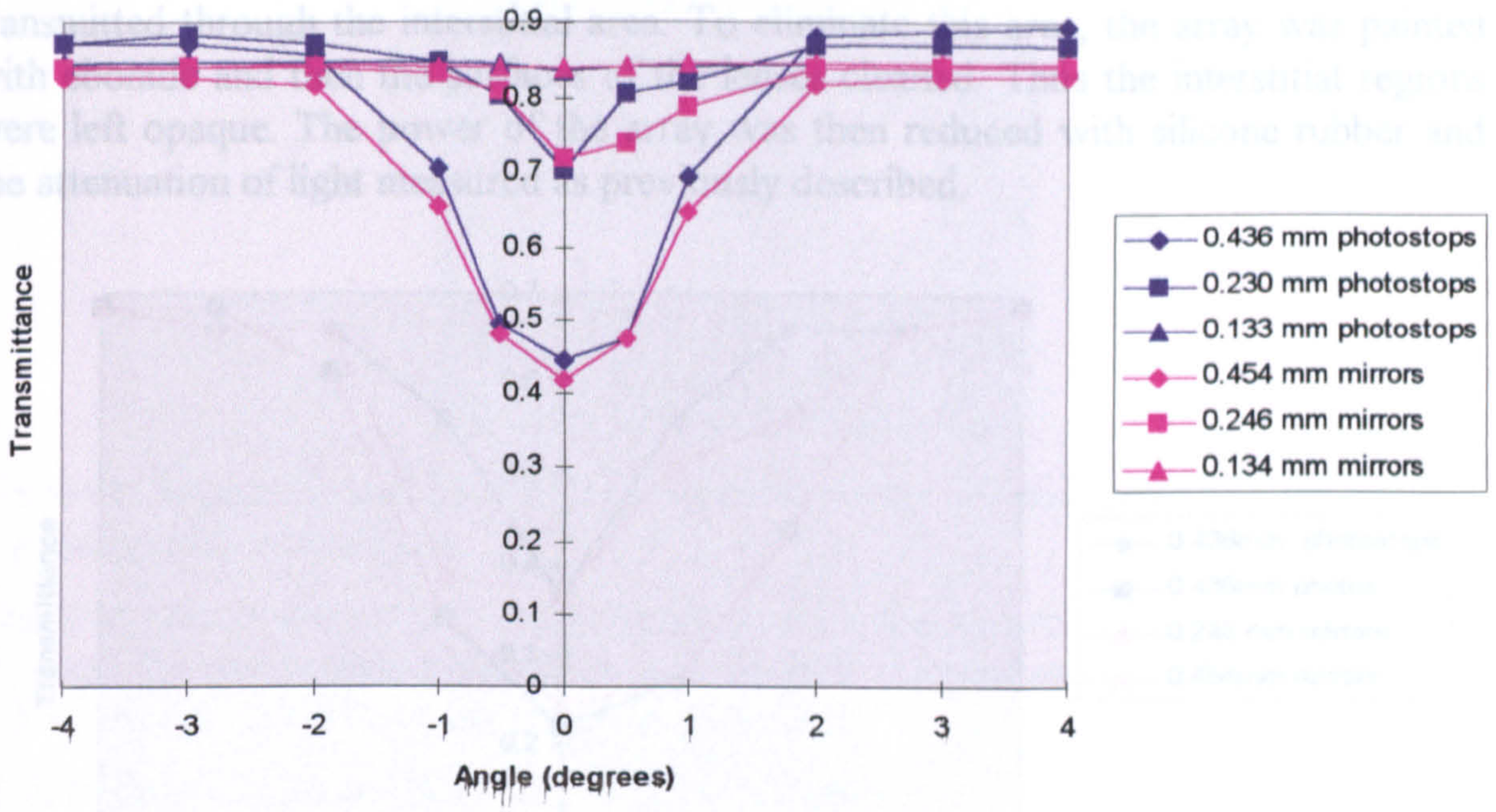

Graph 4-1: Comparison of transmission measurements through photographic and mirrored obturations in solar shade.

The lowest Tr_{min} was achieved with the 0.454mm mirrors, yet the value was still over 40% and far from the 5% target.

In order to reduce the transmission the origin of the unattenuated light had to be determined. There were three possible regions through which the light could have been transmitted:

a. The interstitial areas between lenses in the array.

b. Through the centre of the obturations.

c. Around the obturations.

In order to locate the source of the light, each of these possibilities were explored in turn.

The smallest mirrored and photographic obturations were no longer be used after this experiment, as the reduction in illumination provided by both was found to be negligible.

a) *Transmission through the Interstitial Area*

Spherical lenses in a hexagonally packed array do not mesh perfectly so light can be transmitted through the interstitial area. To eliminate this area, the array was painted with ebonide and then the surfaces of the lenses cleaned. Thus the interstitial regions were left opaque. The power of the array was then reduced with silicone rubber and the attenuation of light measured as previously described.

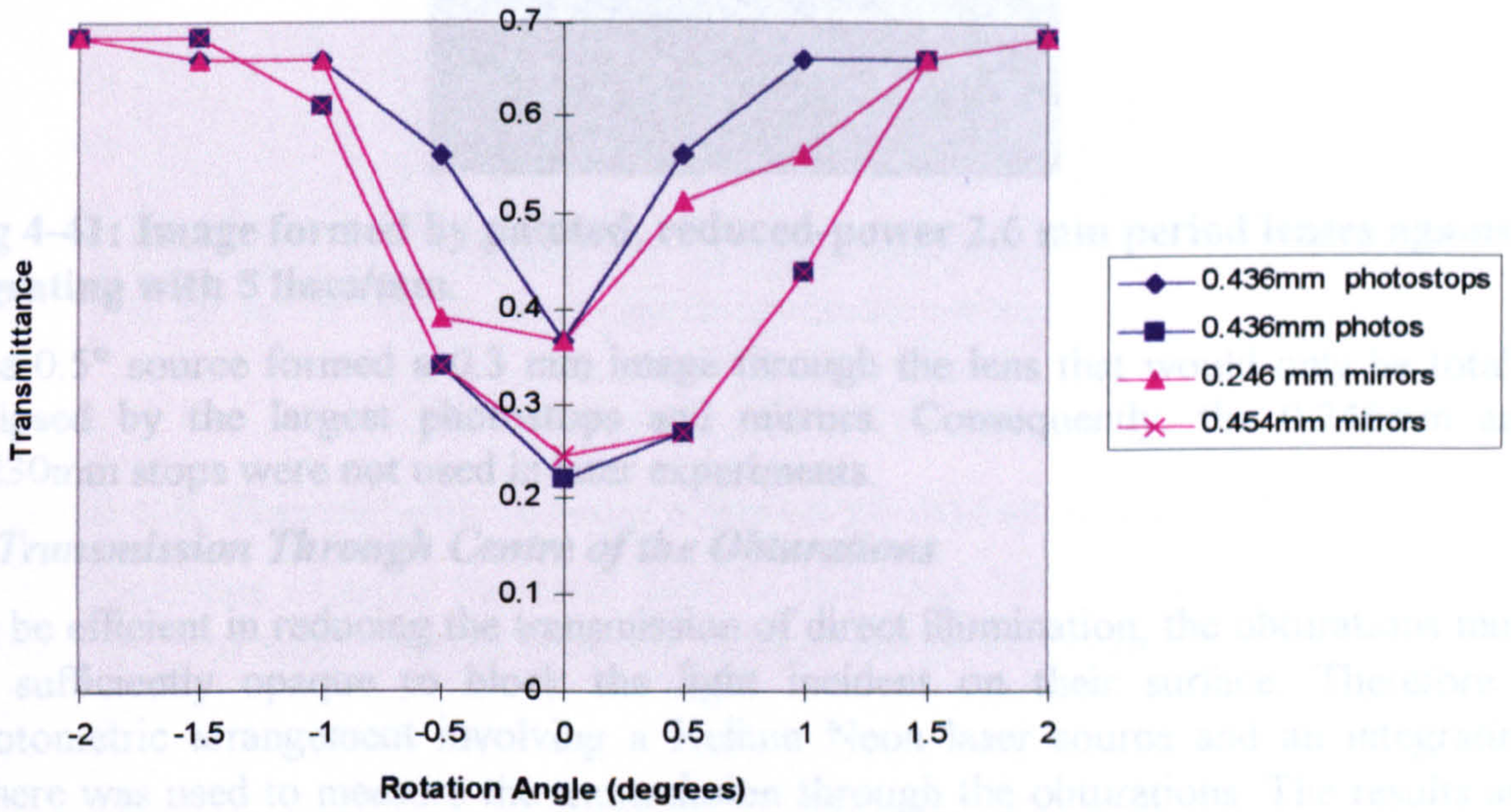

Graph 4-2: Transmission measurements with the painted array

The painting of the array significantly reduced the min transmission (Tr_{min}) through the system. It also reduces Tr_{max} and therefore the amount of diffuse light that the solar shade would allow into a room. The table below compares these values for both the painted and unpainted arrays, as well as showing the attenuation (A) by the obturation array.

unpainted array	*0.436 mm photostops*	*0.230 mm photostops*	0.454 *mm mirrors*	0.246 *mm mirrors*
Tr_{min}	0.44	0.70	0.41	0.72
Tr_{max}	0.89	0.88	0.82	0.84
$A = Tr_{min} / Tr_{max}$	0.49	0.80	0.51	0.86
painted array				
Tr_{min}	0.22	0.37	0.24	0.37
Tr_{max}	0.68	0.68	0.68	0.68
$A = Tr_{min} / Tr_{max}$	0.32	0.54	0.35	0.54

As the lenses with the opaque interstitial areas improved on previous measurements by reducing the transmitted light, they were used in all subsequent experiments. The

covering of the interstitial areas also meant that a clear picture could be taken of the images formed by the lens (see Fig 4-41).

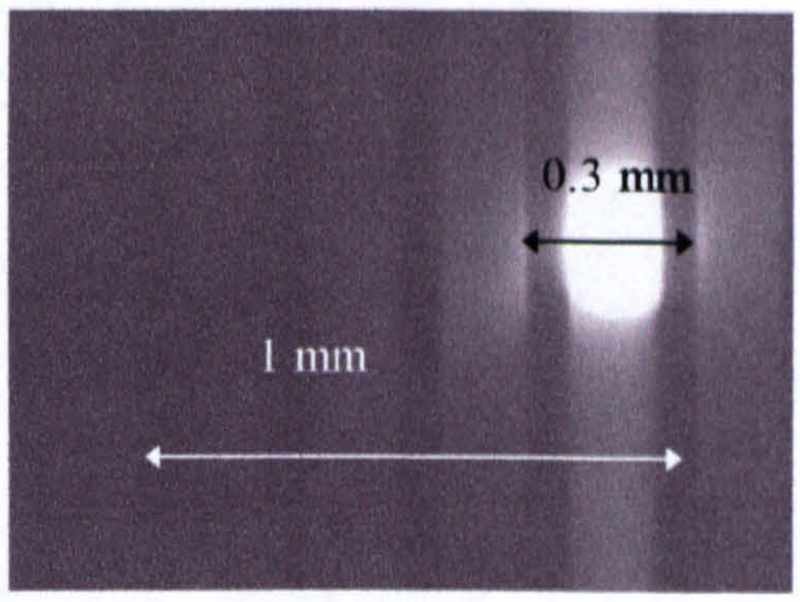

Fig 4-41: Image formed by painted, reduced-power 2.6 mm period lenses against a grating with 5 lines/mm.

The 0.5° source formed a 0.3 mm image through the lens that would only be totally eclipsed by the largest photostops and mirrors. Consequently, the 0.246mm and 0.230mm stops were not used in later experiments.

c) Transmission Through Centre of the Obturations

To be efficient in reducing the transmission of direct illumination, the obturations must be sufficiently opaque to block the light incident on their surface. Therefore a photometric arrangement involving a Helium Neon laser source and an integrating sphere was used to measure the transmission through the obturations. The results are shown in Graph 4-3 & Graph 4-4.

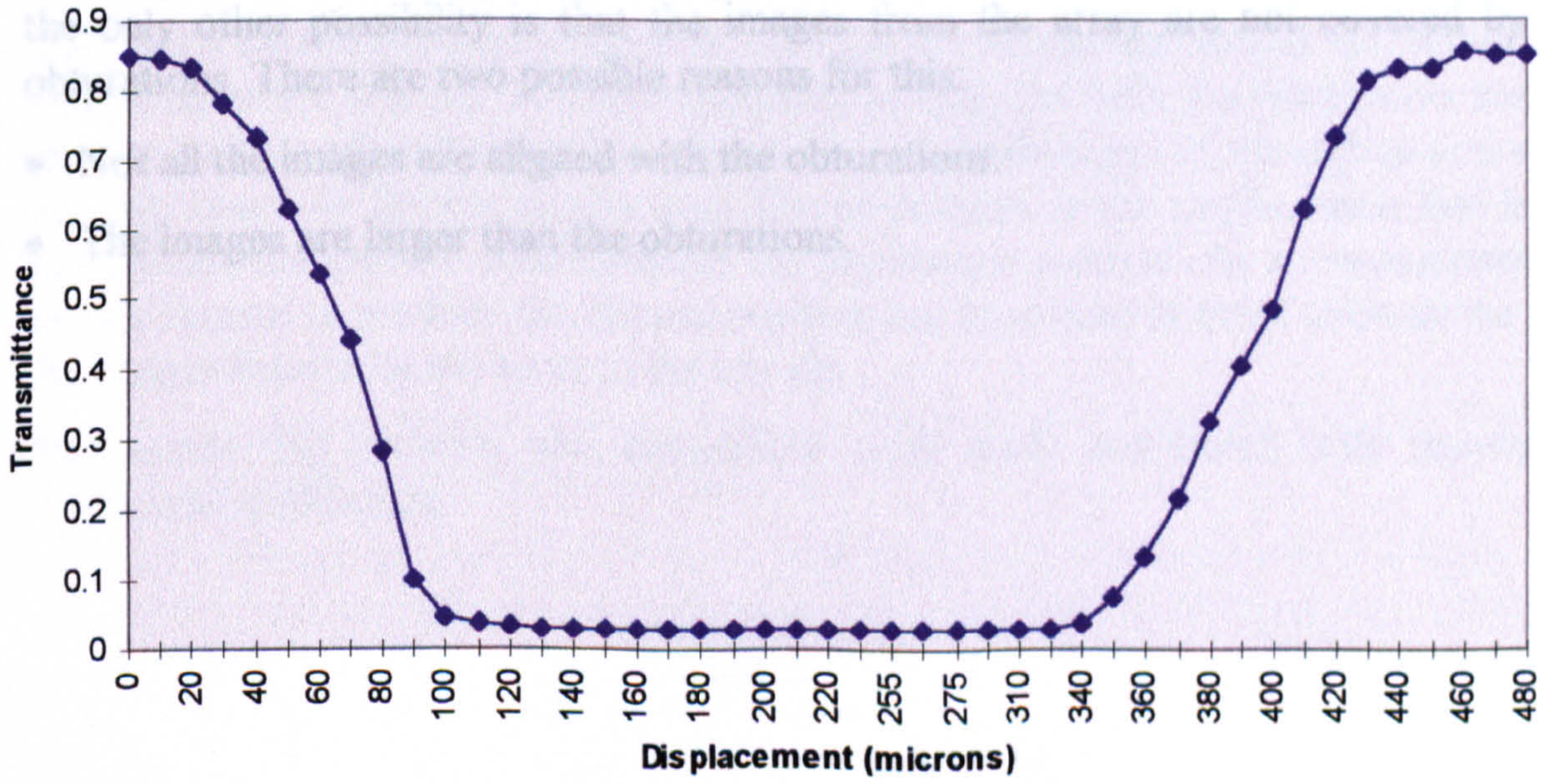

Graph 4-3: Transmission measurement through a typical mirror in the 0.454 mm array.

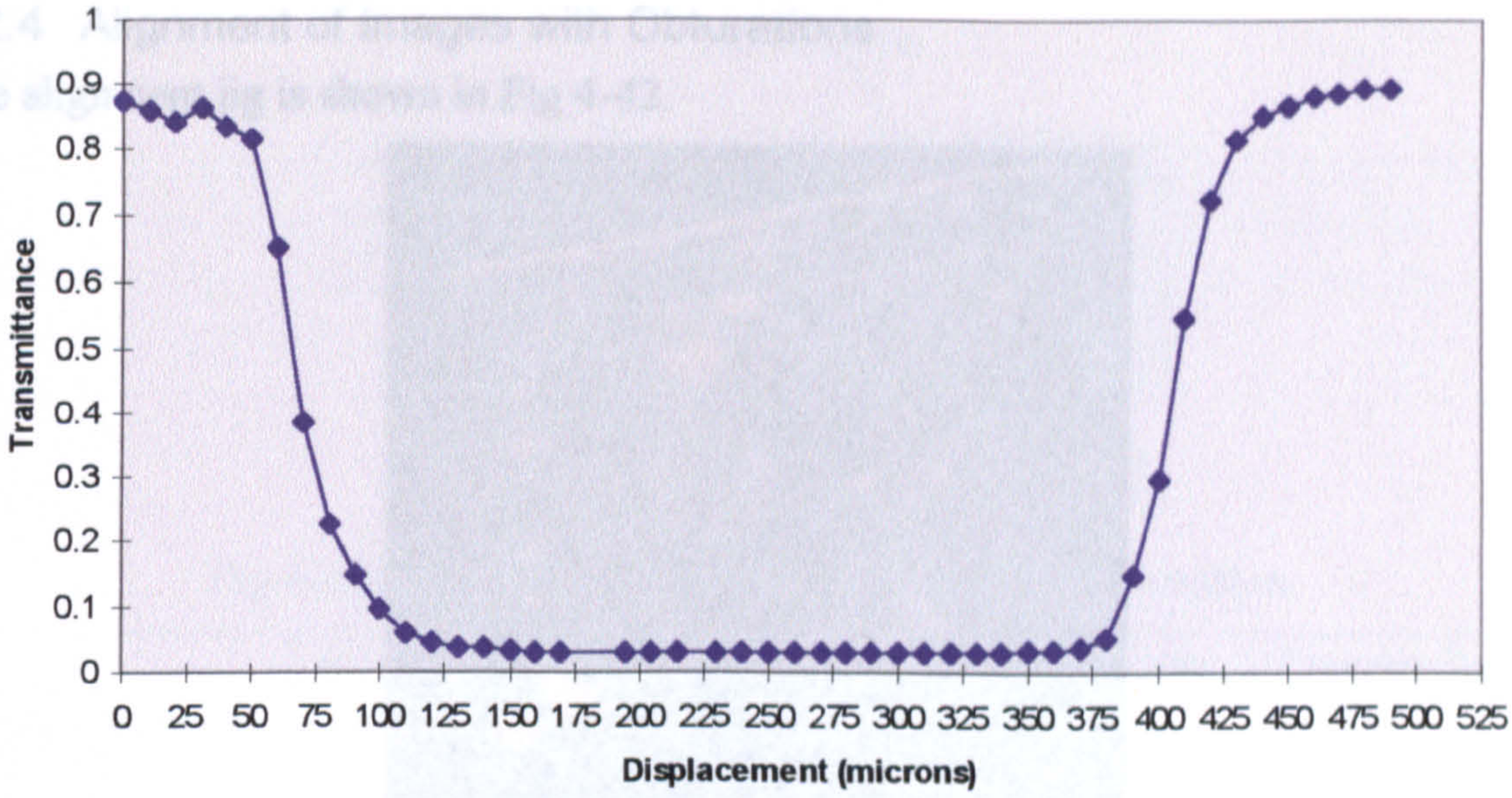

Graph 4-4: Transmission through a typical photostop in the 0.436 mm array.

Both obturations reduced the laser light to less than 3%. It was safe therefore to assume that the stops were sufficiently opaque not to be a major contributor to the high Tr_{min} values described previously. However, the parity between the measurements with the laser demonstrates that there is little difference between the two types of stop. Therefore, as it was more convenient to produce mirrors in the laboratory, all subsequent experiments used mirrors as the obturations.

d) Transmittance around Obturations

If the interstitial light has been eliminated and the obturations are sufficiently opaque, the only other possibility is that the images from the array are not covered by the obturations. There are two possible reasons for this:

- Not all the images are aligned with the obturations.
- The images are larger than the obturations.

4.2.4 Alignment of Images with Obturations

The alignment jig is shown in Fig 4-42.

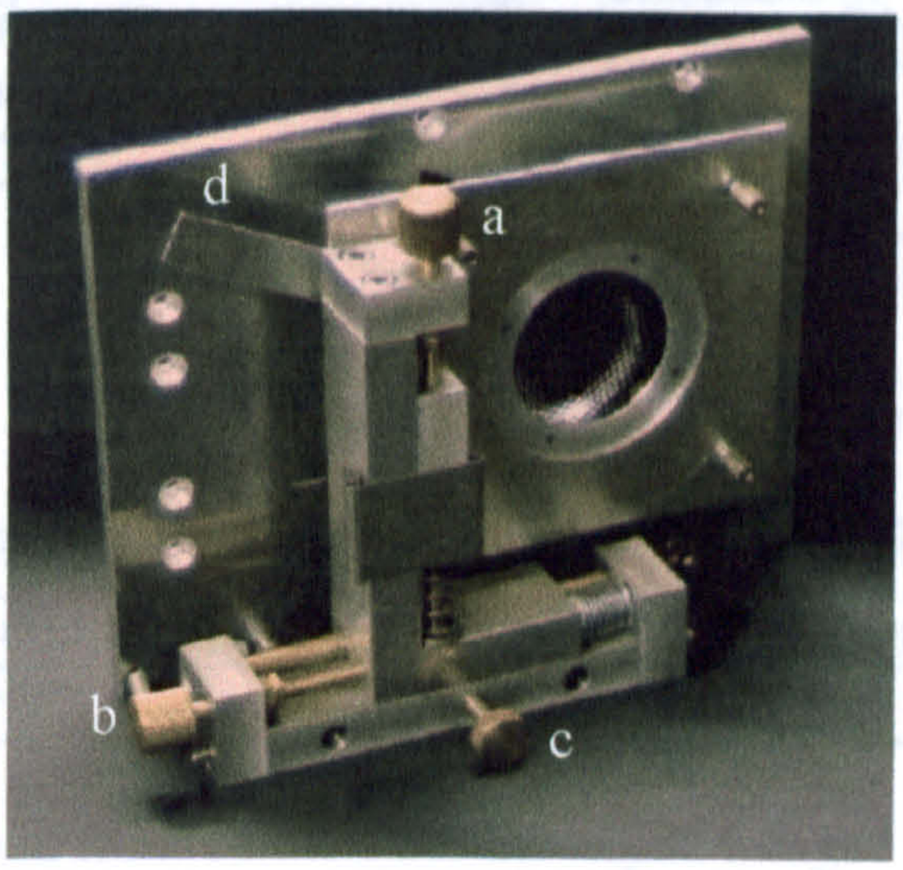

Fig 4-42: Alignment jig for lens and obturation arrays. Fine linear adjustment with screw-threads (a), (b) and (c). Coarse rotational adjustment with lever (d).

Translation in the x, y and z direction is achieved with sub-millimetre precision with fine screw-threads. Rotational alignment is also possible however this is more coarse (millimetre precision). The finer controls should be sufficient to ensure that the 2.6 mm period lens array is coincident with the obturations, certainly for the larger diameter obturations.

Initially it was thought that the spatial distribution of the obturations within their array may not have been the same as the spatial distribution of the lenses and therefore the two would not be perfectly coincident. Such a problem would occur because of differences between the collimation of the light in the manufacture of the obturations compared to the test rig. The manufacturing process for both the photostops and the mirrors used a well-collimated source, whereas the collimation of the source in the test rig only uses a f= 100mm singlet lens. The aberrations in the singlet mean that it will not provide comparable collimation to the production method. As a consequence the images formed to produce the obturations may not have been in exact coincidence with the images formed by the array in the test rig.

To counter this problem new obturations were made and tested with sources of comparable collimation.

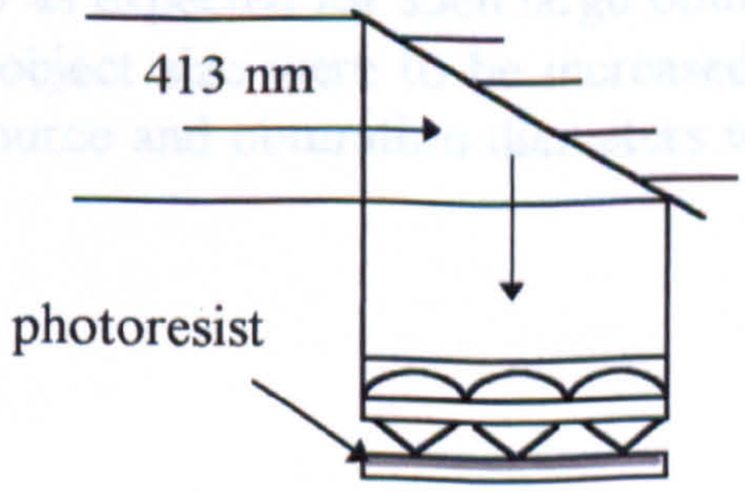

Fig 4-43: Formation of obturations with Krypton Laser

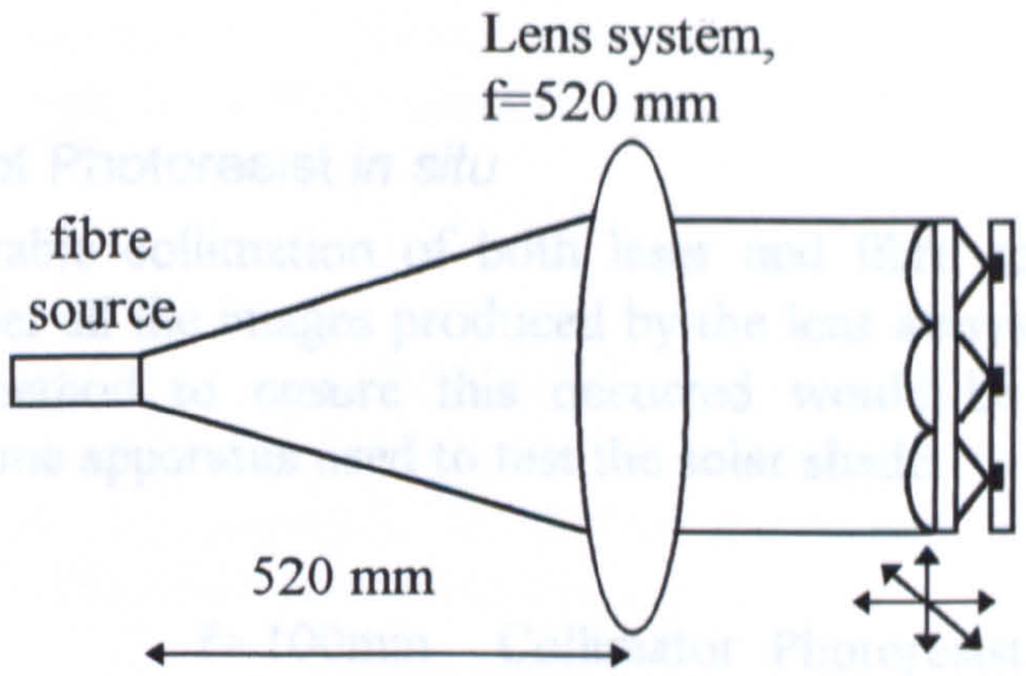

Fig 4-44: Modified test rig with improved collimation.

	f=100mm singlet lens	f=520mm lens system	Krypton laser
Divergence angle	≈1°	≈0.5°	≈0.5°

By opening an aperture in front of the laser the object imaged by the lens array could be enlarged to increase the diameter of the image formed in the photoresist. The result were 720μm obturations. In addition, by increasing the focal length of the lens system to 520mm, the angular size of images formed by the test rig were reduced to 0.1°. Although unrealistic for fabrication of the solar shade the result should indicate if complete elimination of the transmitted light is possible. The results are shown in Graph 4-5.

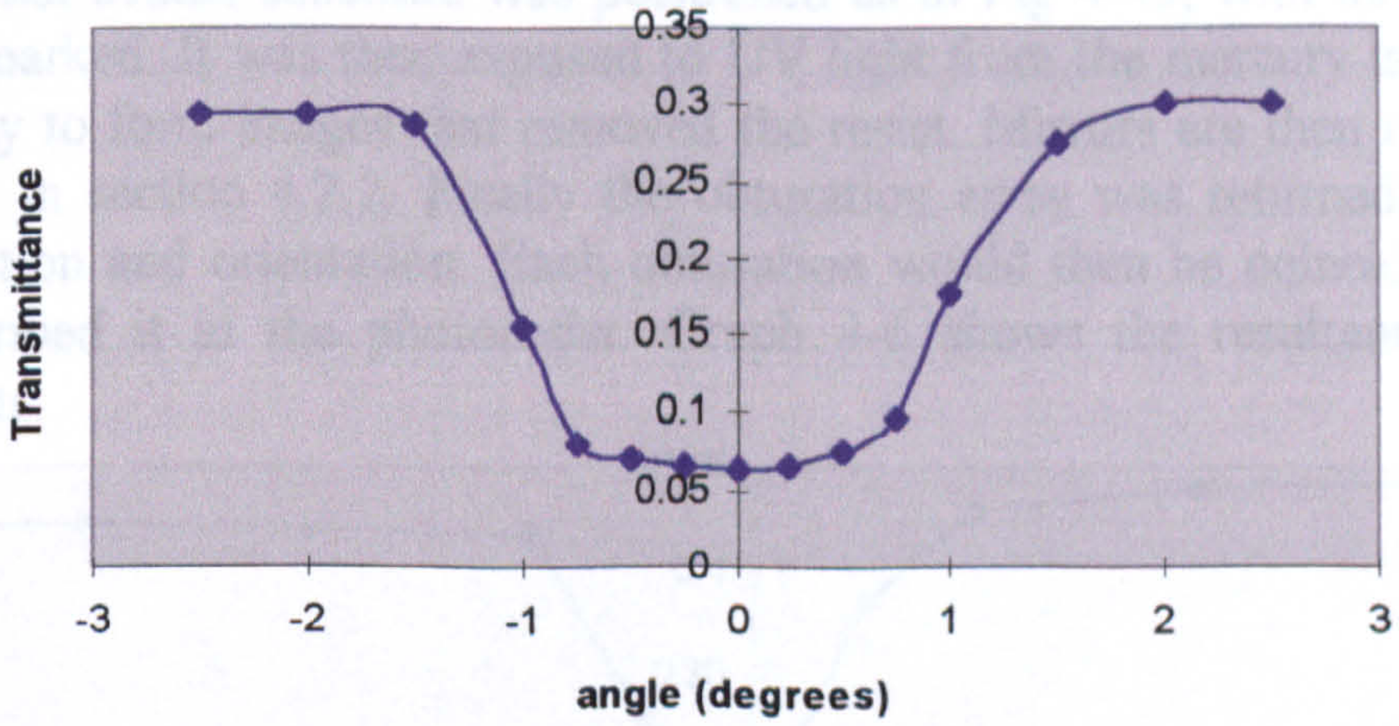

Graph 4-5: Transmission through approx. 200 lenses in solar shade with 720 μm obturations (100% transmission= 1mW).

Tr_{min} was reduced to 6% which is close to the target to prevent glare on a sunny day. However it was not as low as expected for such large obturations and was unlikely to remain below 10% if the object size were to be increased back to 0.5°. It had been hoped that changing the source and obturation diameters would have reduced Tr_{min} to zero.

4.2.5 Exposure of Photoresist *in situ*

Despite the comparable collimation of both laser and fibre source, there was still concern as to whether all the images produced by the lens arrays were incident on the obturations. One method to ensure this occurred would be to manufacture the obturations in the same apparatus used to test the solar shade.

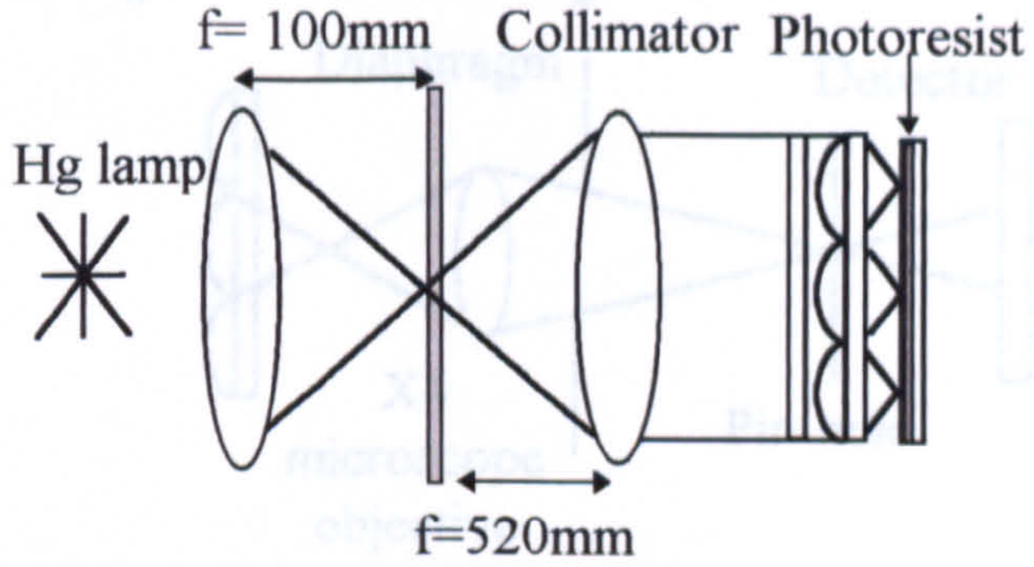

Fig 4-45: Exposure of photoresist 'in situ' to form obturations. The diaphragm in front of the silica lens controlled the object size for the lens array, which was reduced to 5mm giving an angular subtense of 0.5°.

The photoresist coated substrate was positioned as in Fig 4-45, with its location and orientation marked. It was then exposed to UV light from the mercury lamp, through the lens array to form images that removed the resist. Mirrors are then manufactured as described in section 4.2.2. Finally the obturation array was returned to its exact original position and orientation. Each obturation would then be coincident with the lens that formed it in the photoresist. Graph 4-6 shows the resultant attenuation measurements.

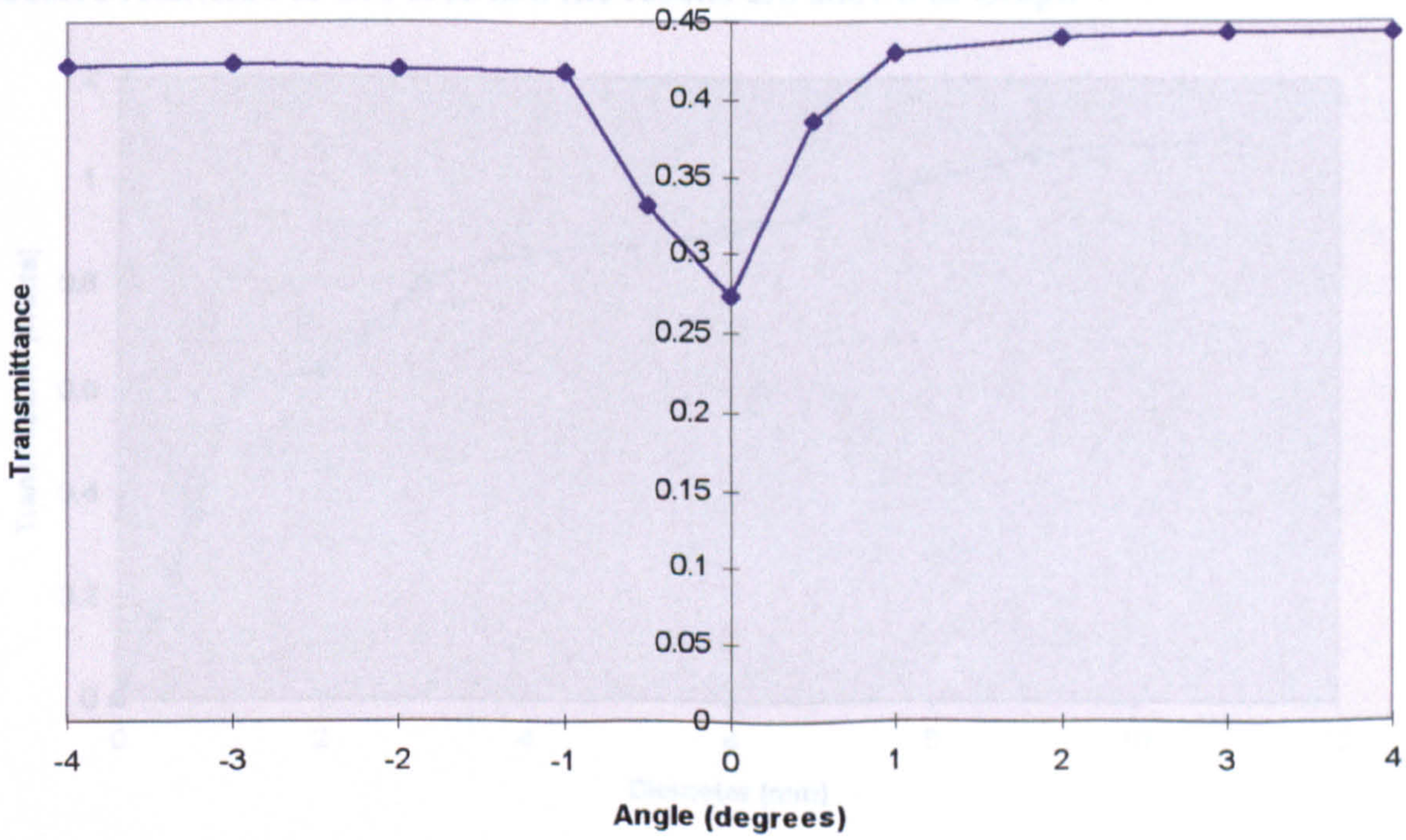

Graph 4-6: Transmission measurements on solar shade with approx. 300 micrometer diameter obturations and mercury lamp source.

Unfortunately transmission measurements with these obturations still produced a Tr_{min} of 27% which is too high. In order to identify the source of the transmitted light, it was decided to re-examine the image size.

4.2.6 Image size

Fig 3-21 shows the apparent image size of a 0.5° diameter object through the lens array. However the visual perception may be misleading, especially if the edges of the image are very diffuse. Consequently the power distribution of a typical image was measured, using the arrangement shown in Fig 4-46.

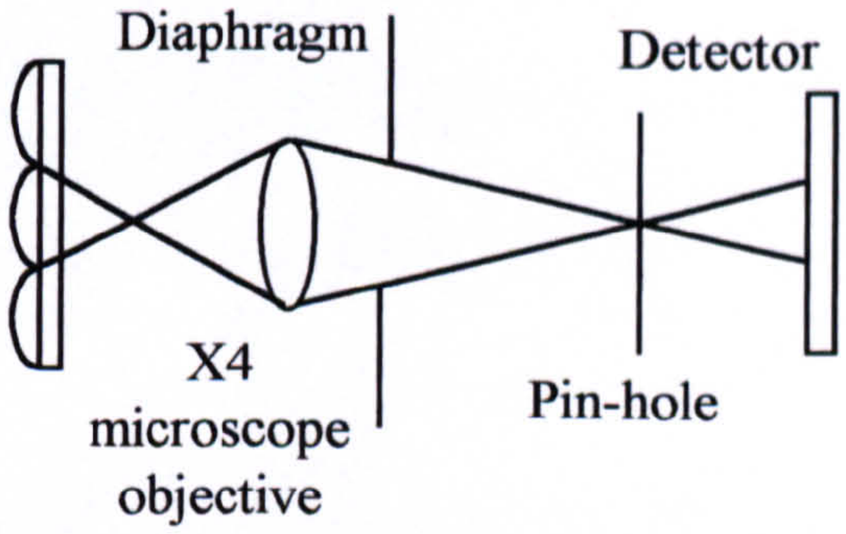

Fig 4-46: Selection of single image to determine power distribution.

A microscope objective was used to project an area of the image array onto the same plane as a pinhole. Next a diaphragm reduced the field size so that only single image was visible. Visually this image appeared to be approximately 1mm in diameter. The pinhole was then translated such that the maximum transmission measured. At this point the centre of the pinhole was taken to be at the centre of the image. By incrementally increasing the size of the pinhole the power distribution was determined across the image. The unmagnified image size was approximately 0.3 mm, but a magnification of X4 gave the projected image a 1.2 mm diameter and a unit cell diameter (the diameter of a lens in the image plane) of 10.4mm. Measurements were therefore restricted to this area and the results are shown in Graph 4-7.

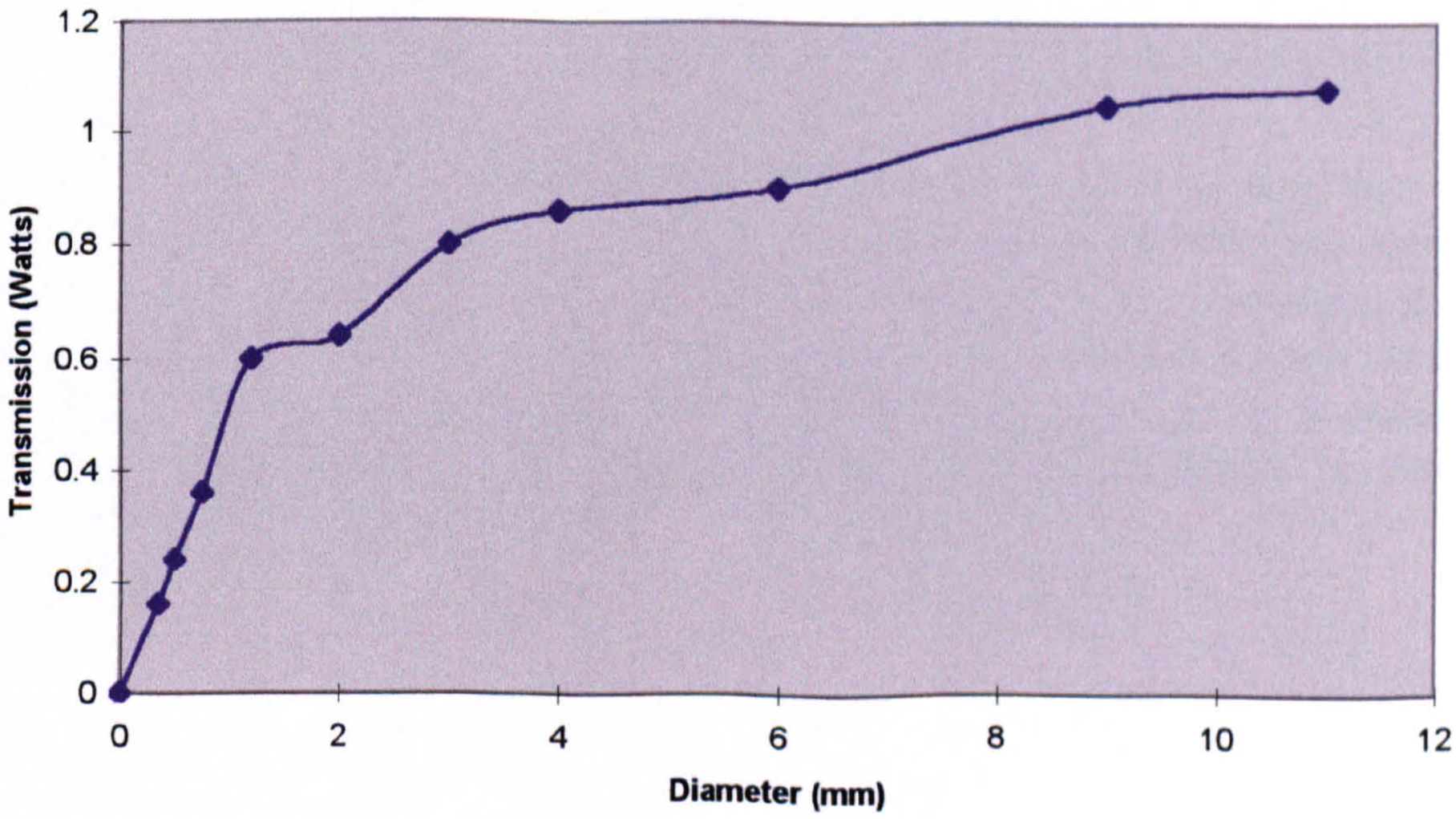

Graph 4-7: Transmission distribution through pin-hole in magnified image with visible size of approximately 1 mm.

Graph 4-7 shows that even if the visible image were totally obscured it would only reduce the transmitted light by 50%. That is:

$$Tr_{(min)} / Tr_{(max)} = 0.5$$

This measurement demonstrates that the illuminance is spread over a much larger area than the visible image indicates. This result indicates that the images are too diffuse to be effectively blocked by the obturations. The aberrations introduced by the spherical lens array may be too great to make the system effective as a solar shade. To examine the theoretical limit of the system with the spherical lenses the solar shade was modelled using a software package.

4.3 Modelling a Reduced-Power Array of Spherical Lenses

The work so far has shown that the solar shade would not provide sufficient attenuation of direct sunlight. To determine if the system was theoretically possible, it was decided to model the system on the SOLSTIS raytracing system. Fig 3.26 shows the unit cell lens system that was used to construct the array.

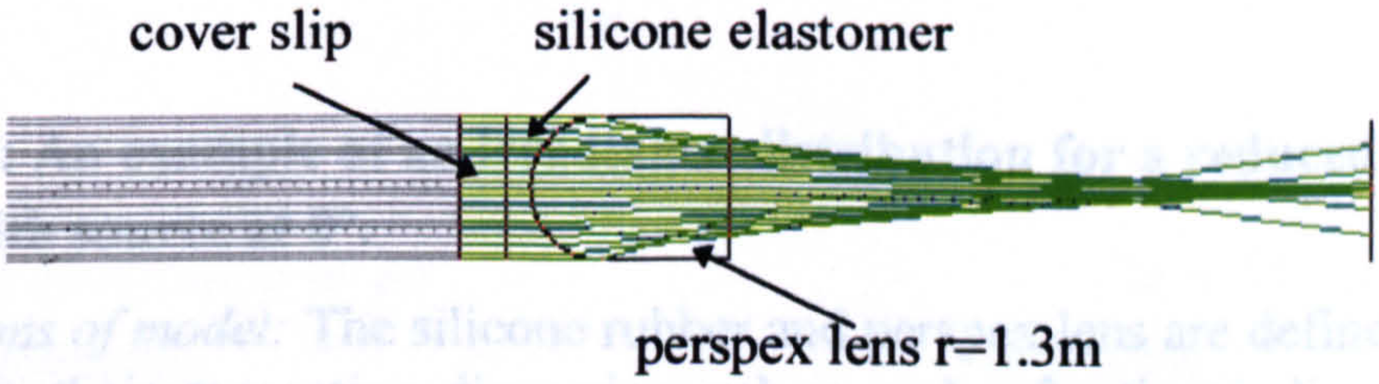

Fig 4-47: Lens System for solar shade (without obturation) in a monochromatic (550 nm) light source. Image plane lies at best focus, determined by tracing spherical wavefront through lens.

Comparison between experimental and empirical data was on the basis of the irradiance distribution. The source in all the simulations was based on the sun. Thus for all the proceeding irradiance plots, it is a blackbody radiator in the visible spectrum ($400nm \leq \lambda \leq 750nm$) with a colour temperature of 5400K[3], a Gaussian luminance distribution and an angular size of 0.5°.

The simulated array has a period of 2.6mm which is equivalent to the diameter of the lenses and therefore the lenses cover the whole of the array. However, there are discontinuities between two adjacent apertures created by the array effect. The software only calculates the paths of rays that pass through lenses and eliminates the rays from source that are incident on the interstitial areas. The irradiance plot effectively models the system employing the lens array with the opaque interstitial areas.

The accuracy of the irradiance distribution is determined by the number of rays that propagate through the system. The calculation is based on the Monte-Carlo method which suffers from statistical noise. A thorough analysis of the technique is not relevant to this thesis but a brief mention of the error source involved is applicable. In each of the following irradiance calculations 10^6 rays were used, giving a statistical error $\approx$ 1%. This error was reduced still further with the software's smoothing operator, so that the final value was 0.1%.

[3] Correlated colour temp for zenith Sun through atmosphere (G.W.C Kaye and T.H. Laby, 'Table of Chemical and Physical Constants, p79).

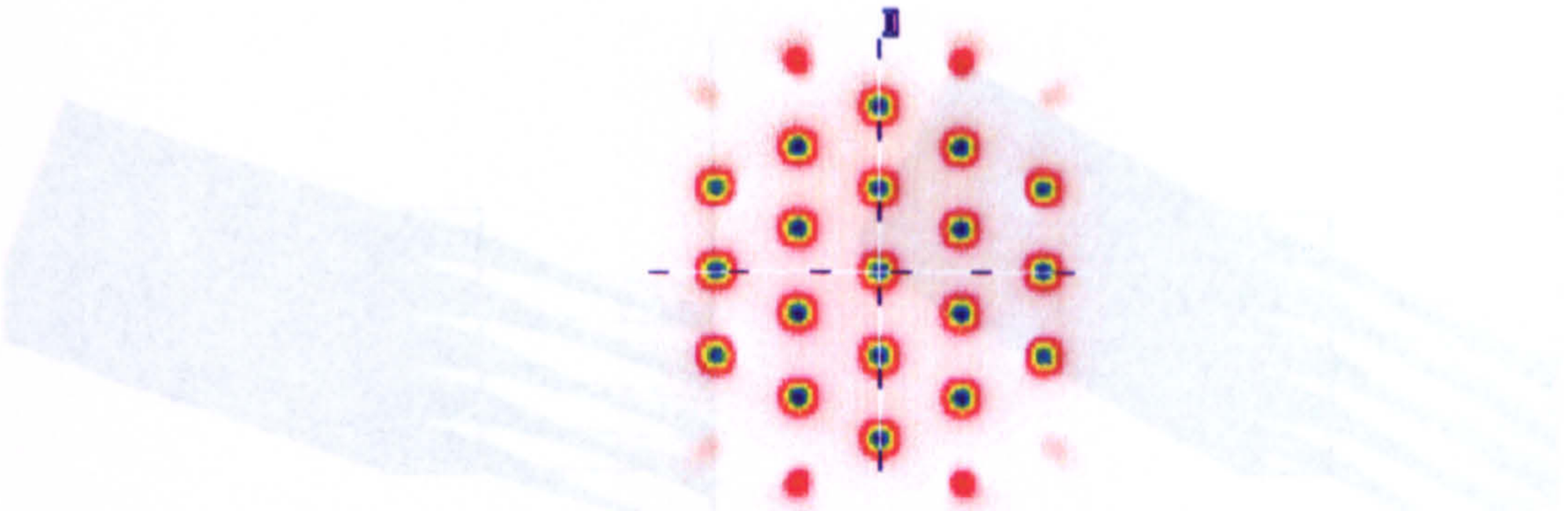

Fig 4-48: An example of an irradiance distribution for a reduced-power lens array with source at 0°.

Limitations of model: The silicone rubber and perspex lens are defined in the software purely by their respective dispersion values and refractive indices. No account is taken of imperfections in the bulk material that make plastics poorer optical materials than glasses. Nor are surface scratches which, in reality, are prevalent across the whole array (see section 4.2.1). A more accurate model would contain a diffuser and increase the scatter of light in the image plane. These limitations aside, the model should still provide a good theoretical guide as to the maximum of attenuation of direct sunlight that is possible with the solar shade.

The most important difference though between the theoretical calculations and the practical measurements is the treatment of fresnel reflections. These are not included in the simulation and were calculated independently.

4.3.1 Raytracing with the Reduced Power Lens Array

The following diagrams (Fig 4-49-Fig 4-57) depict the path of rays through an array of lenses, with their power reduced as described previously. As with the lens array chosen for the experiments, it is hexagonally close packed with a period of 2.6mm. The source is at infinity and, for clarity is emitting monochromatic (550 nm), visible radiation. No obturations are included in the system. The source elevation angle is varied from 0° to 80° to simulate the changing solar position. This is sufficient to cover the range of the solar altitude for latitudes > 32°.

Fig 4-49: Source at 0°.

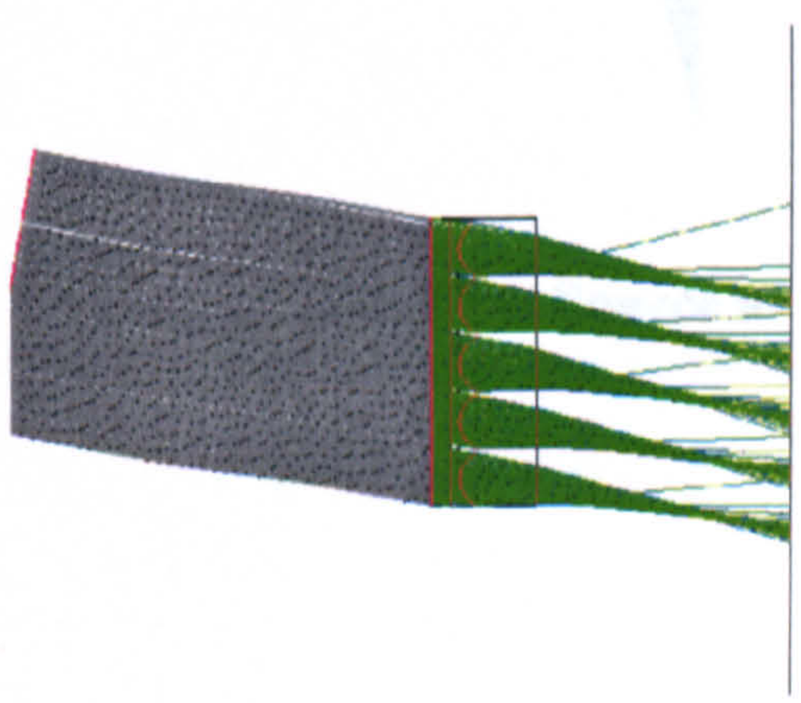

Fig 4-50: Source at 10°.

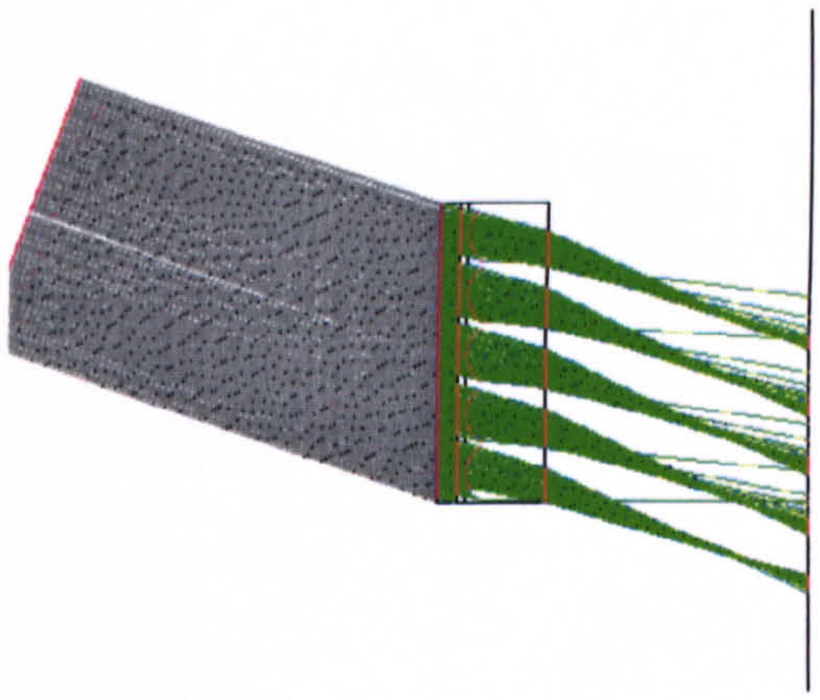

Fig 4-51: Source at 20°.

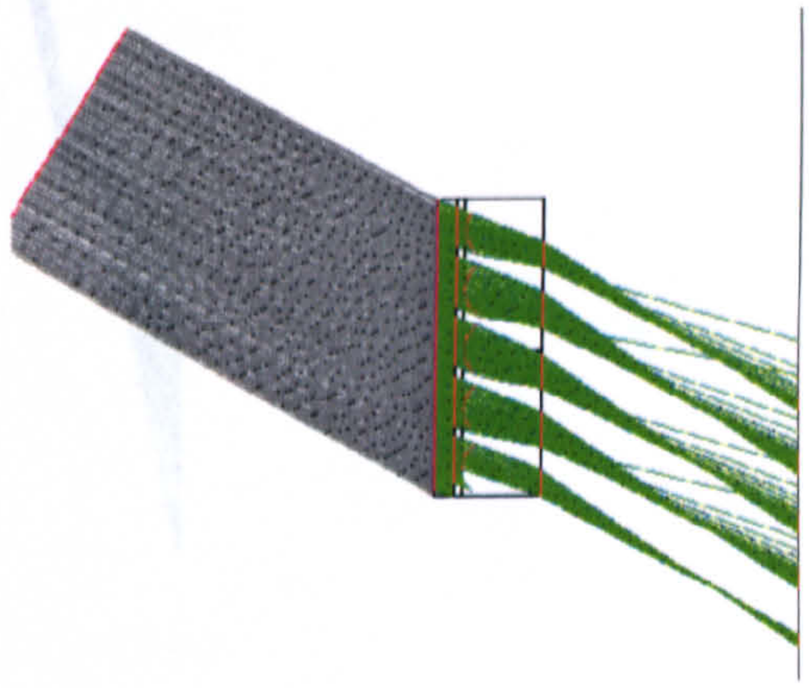

Fig 4-52: Source at 30°.

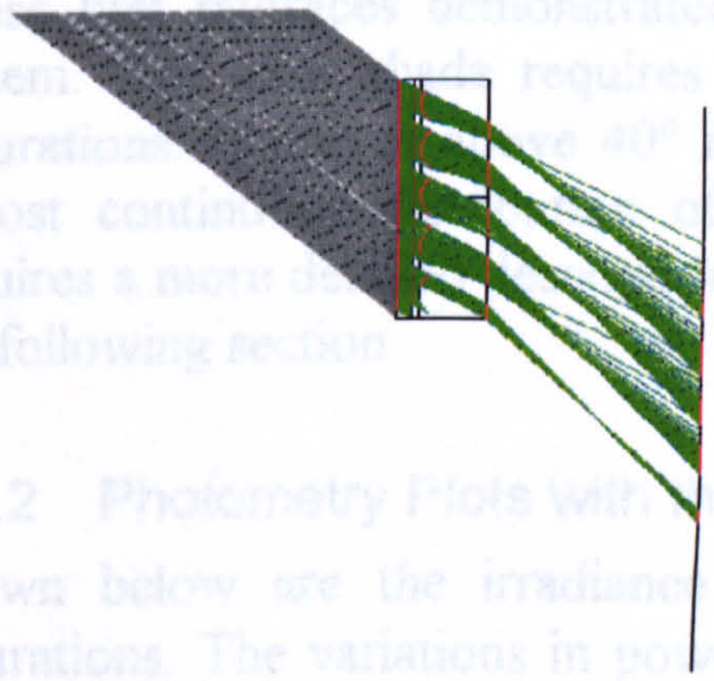

Fig 4-53: Source at 40°.

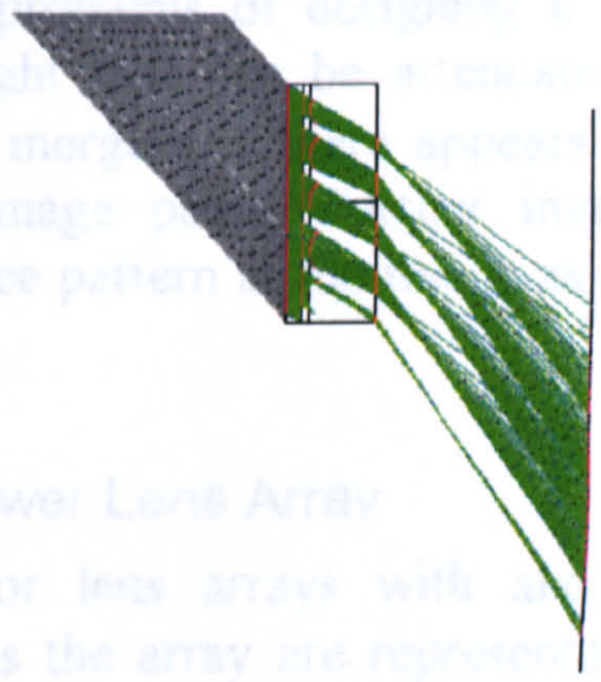

Fig 4-54: Source at 50°.

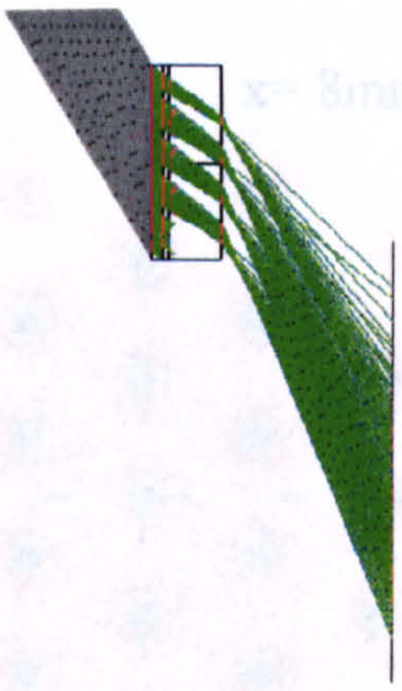

Fig 4-55: Source at 60°.

Fig 4-56: Source at 70°

Fig 4-57: Source at 80°.

These first raytraces demonstrated some of the problems of designing a lenticular system. The solar shade requires well-focused light that can be attenuated by the obturations. However above 40° adjacent images merge and there appears to be an almost continuous distribution of light at the image plane. Further investigation requires a more detailed description of the irradiance pattern at the focus, as shown in the following section

4.3.2 Photometry Plots with the Reduced Power Lens Array

Shown below are the irradiance distributions for lens arrays with and without obturations. The variations in power density across the array are represented by the variation in colour: the highest power densities represented by the darkest colours. The flux values represent the total irradiance contained within the plot.

a) Irradiance Distributions without Obturations at the Focus of the Array

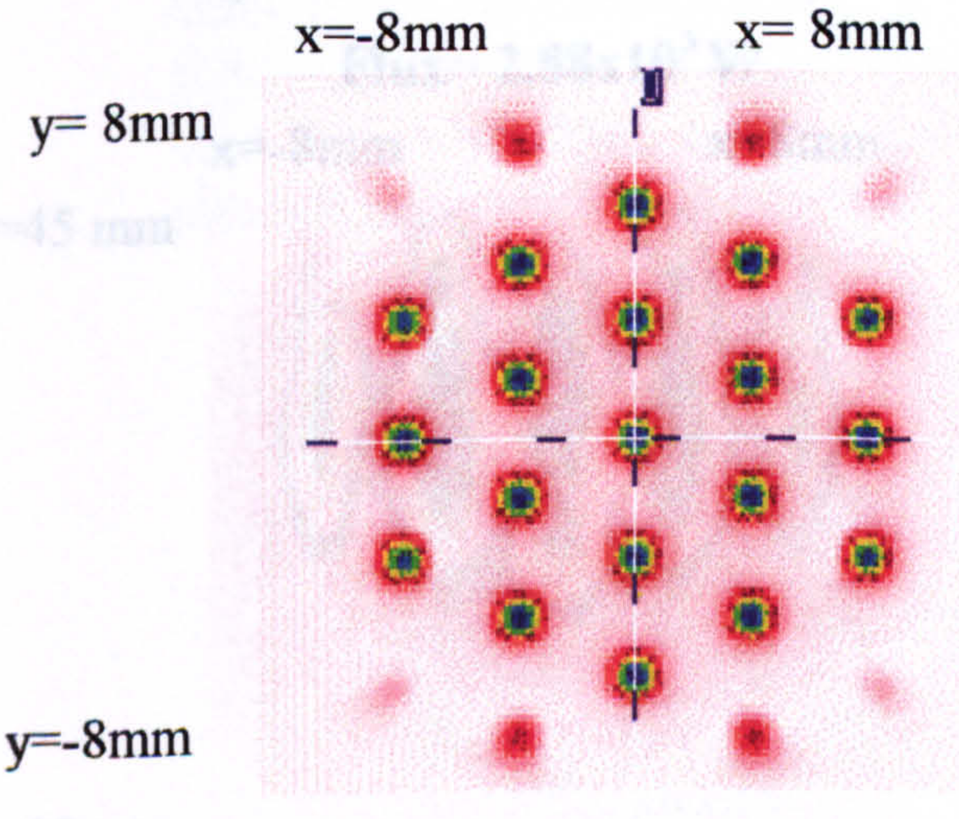

Fig 4-58: Source at 0 degrees.

Flux= 6.10×10^3 W

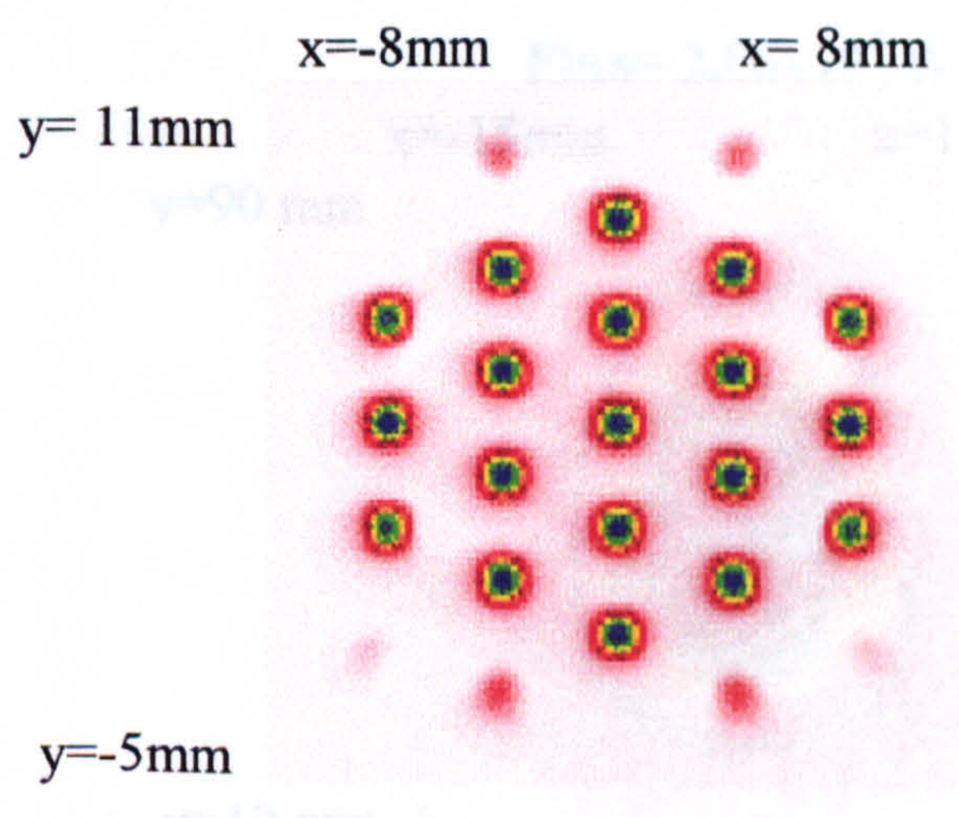

Fig 4-59: Source at 10 degrees.

Flux= 5.37×10^3 W

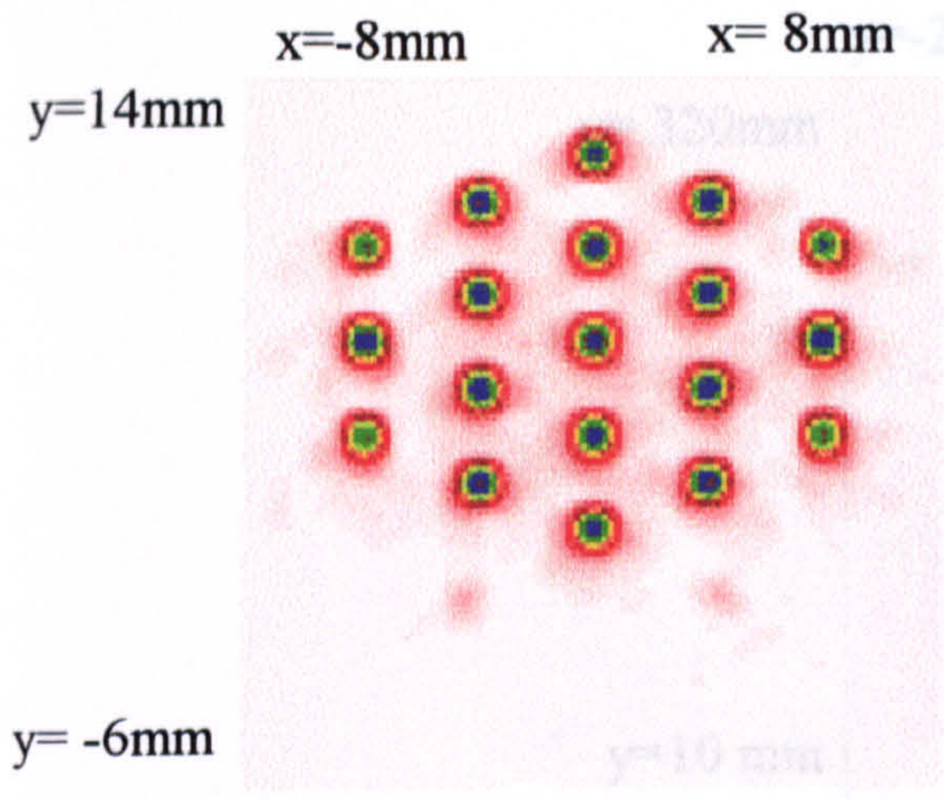

Fig 4-60: Source at 20 degrees.

Flux= 4.54×10^3 W

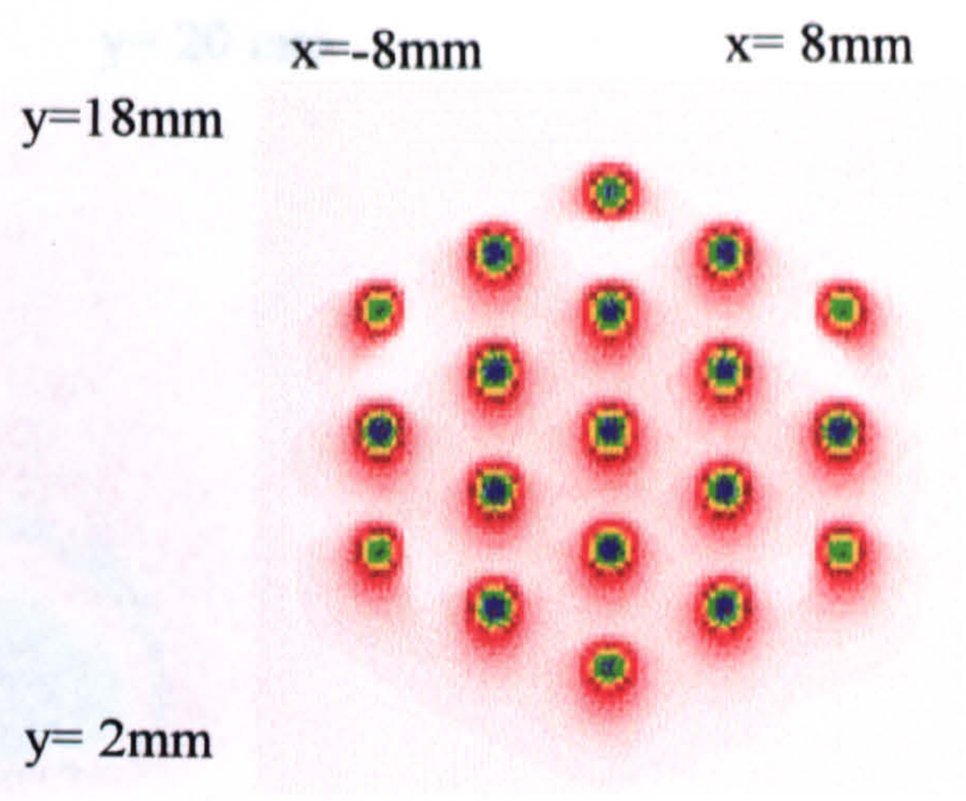

Fig 4-61: Source at 30 degrees.

Flux= 3.72×10^3 W

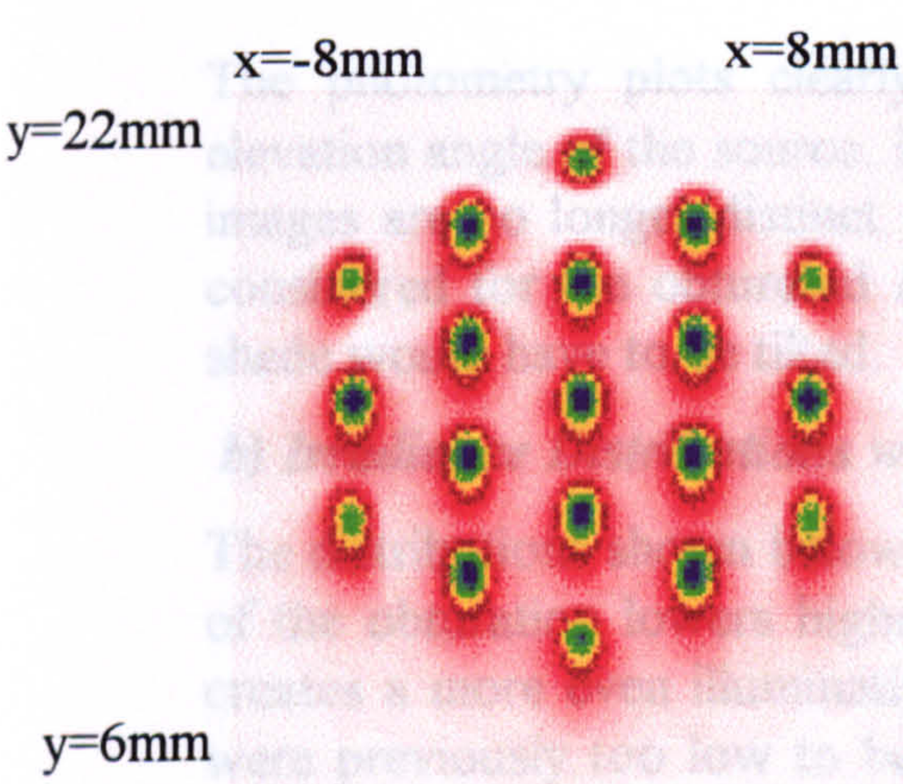

Fig 4-62: Source at 40 degrees.

Flux= 2.88×10^3 W

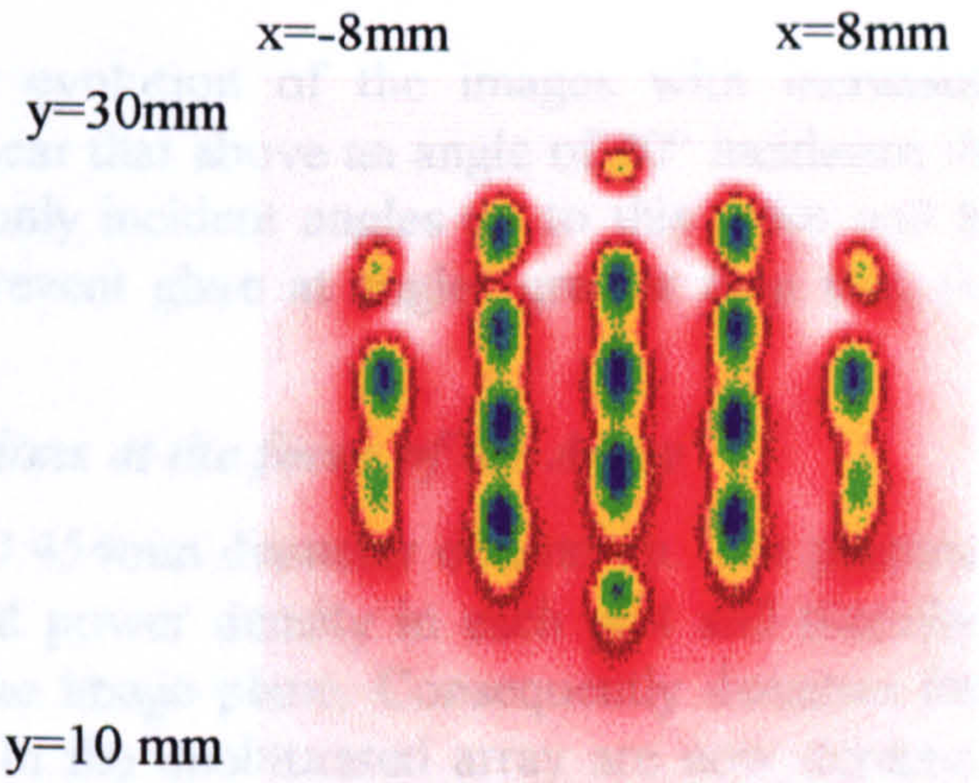

Fig 4-63: Source at 50 degrees.

Flux= 2.06×10^3 W

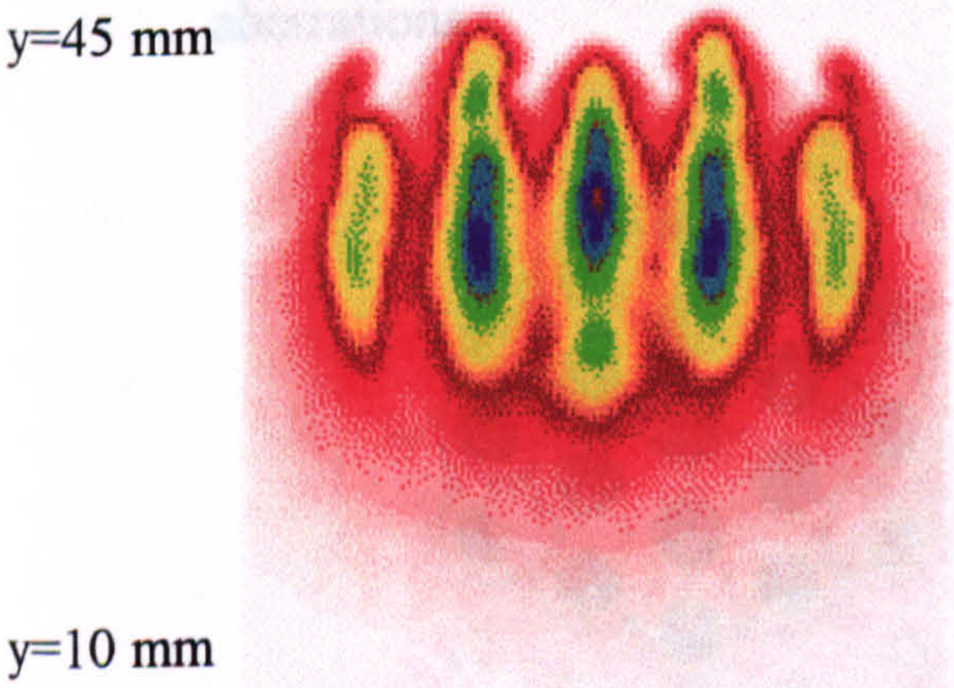

Fig 4-64: Source at 60 degrees.

Flux= 1.38×10^3 W

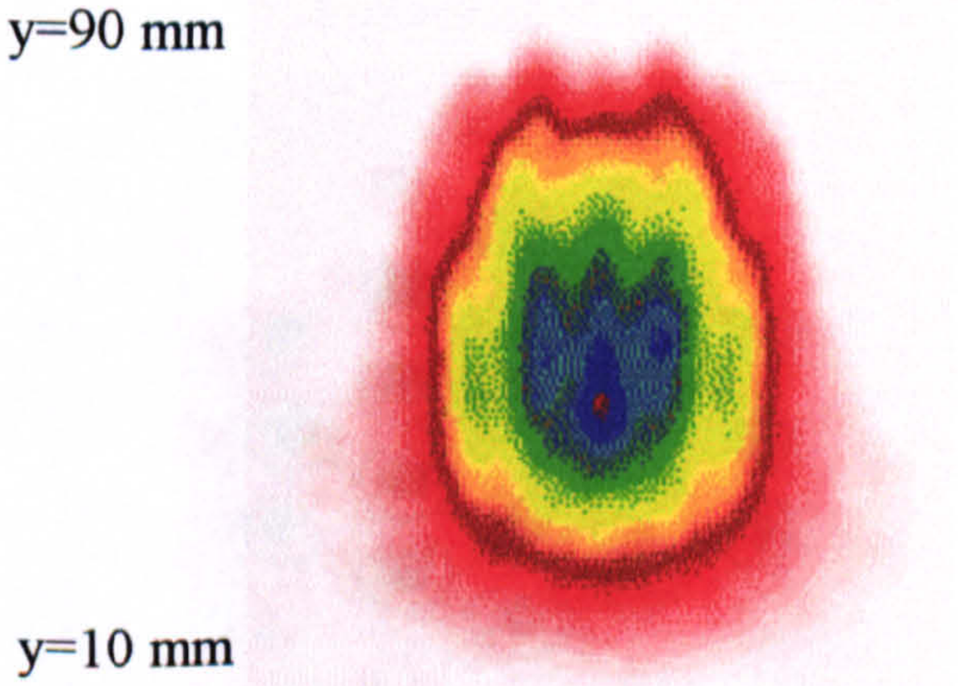

Fig 4-65: Source at 70 degrees.

Flux= 833 W

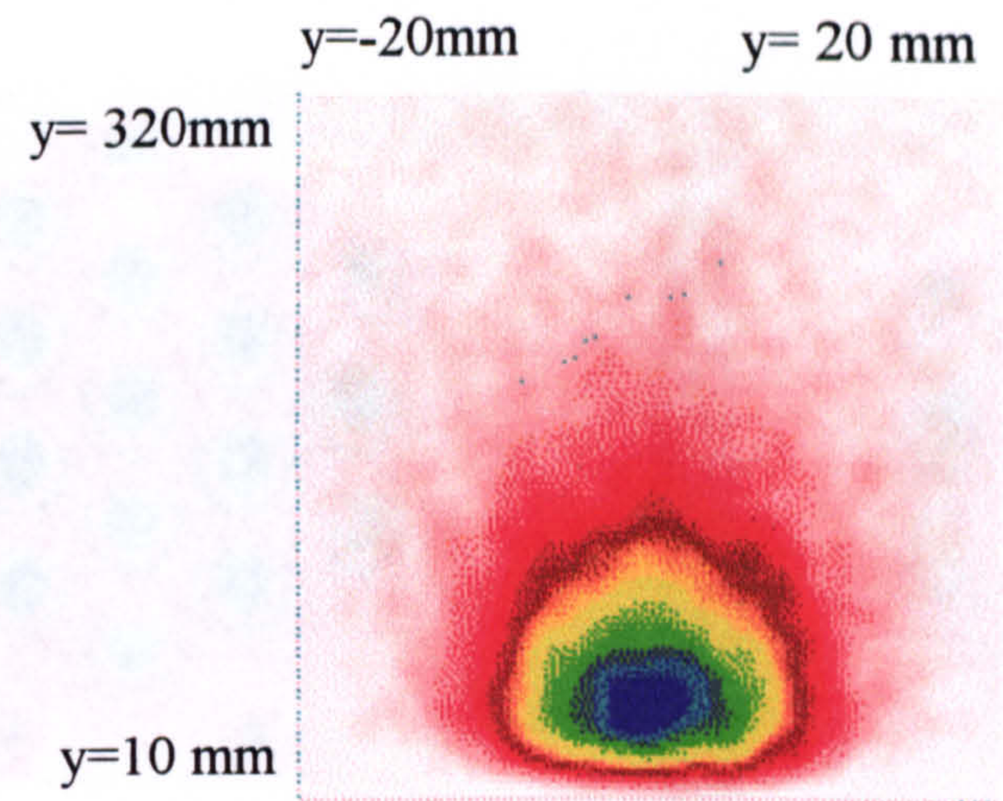

Fig 4-66: Source at 80 degrees.

Flux= 216 W

The photometry plots clearly show the evolution of the images with increasing elevation angle of the source. it would appear that above an angle of 40° incidence the images are no longer distinct. Therefore only incident angles up to this point will be considered for the obturated array. To prevent glare at angles greater than this, the shade would have to be tilted.

b) Irradiance Distributions with Obturations at the focus of the Array

The distributions shown below all used a 0.454mm diameter obturation. The presence of the obturation lowers highest measured power density in each plot and therefore creates a more even illumination across the image plane. Consequently densities that were previously too low to be measured in the unobturated array are now depicted. Therefore although there may appear to be a higher irradiance with the obturations, because the distributions appear more colourful this is not actually the case. The following diagrams therefore show the irradiance distributions to a higher resolution than the unobturated arrays and are indicative of poorly focused light resulting from aberrations.

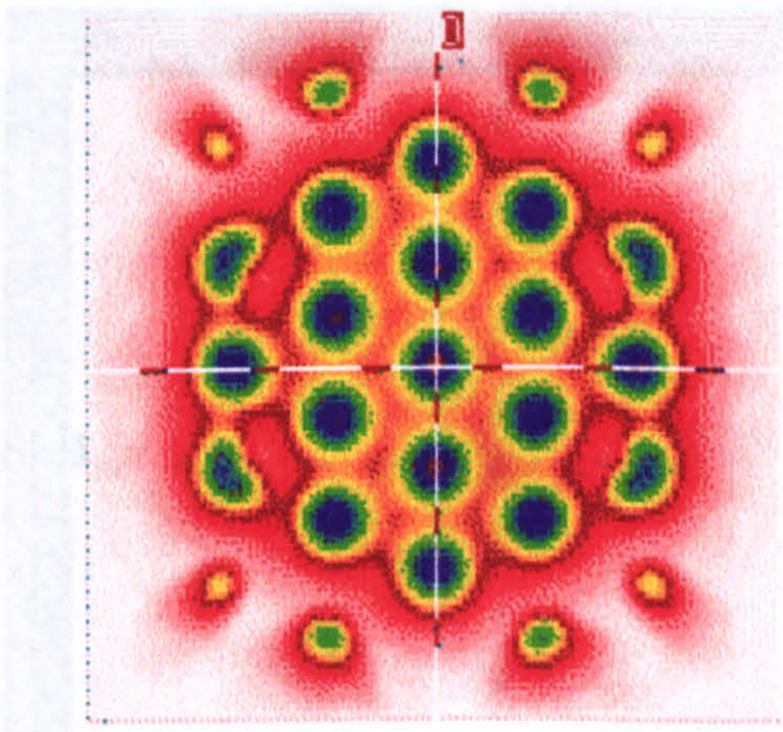

Fig 4-67: Source at 0 degrees

Flux= 2.23×10^3W

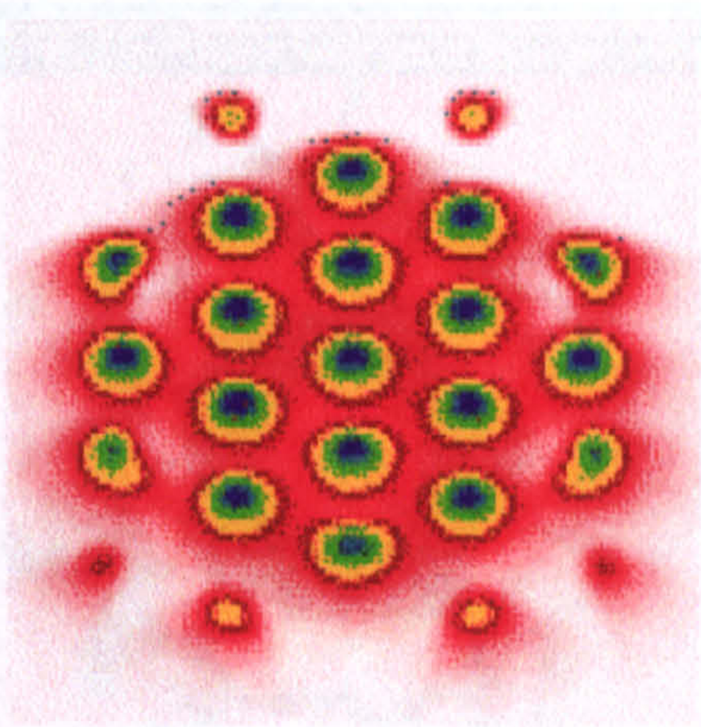

Fig 4-68: Source at 10 degrees

Flux= 2.15×10^3W

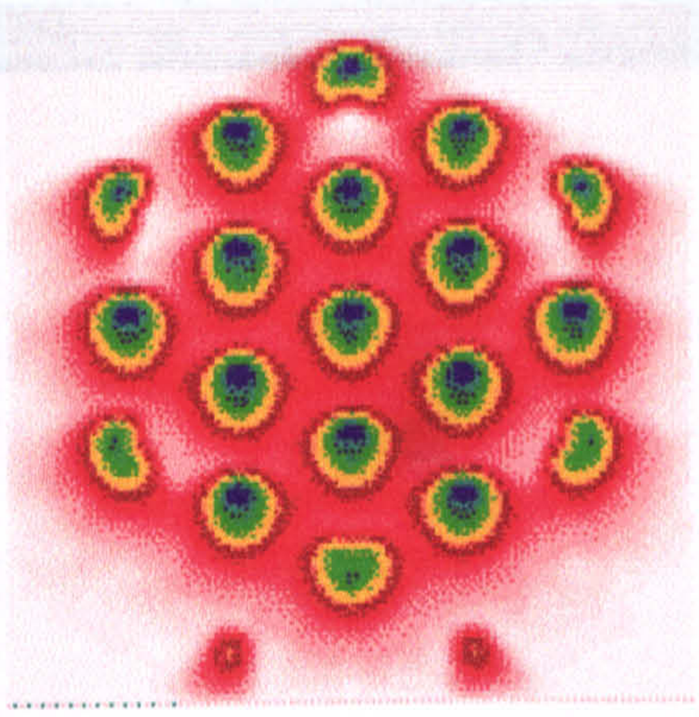

Fig 4-69: Source at 20 degrees

Flux= 1.49 x10^{3}W

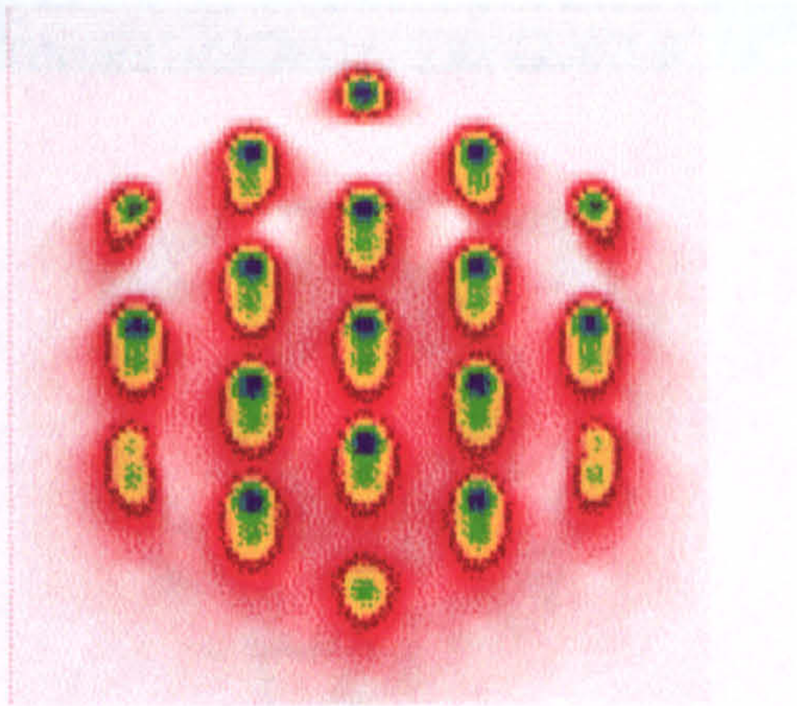

Fig 4-70: Source at 30 degrees

Flux= 1.86 x10^{3}W

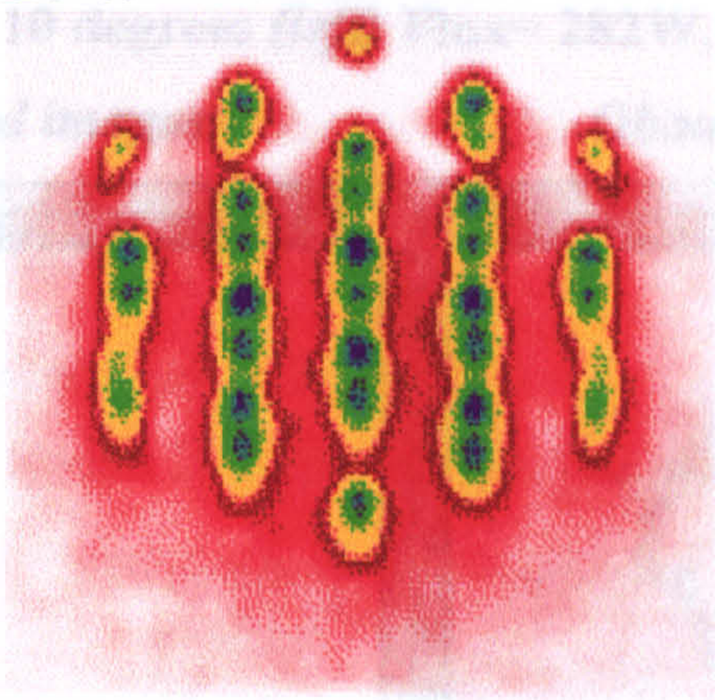

Fig 4-71: Source at 40 degrees.

Flux= 1.98 x10^{3}W

The resolution of the display is too poor to visually depict the obturations for the whole array, therefore individual images in the array must be examined. The diagrams below show the central obturation against the background of the focused light.

Unobturated images

Obturated images

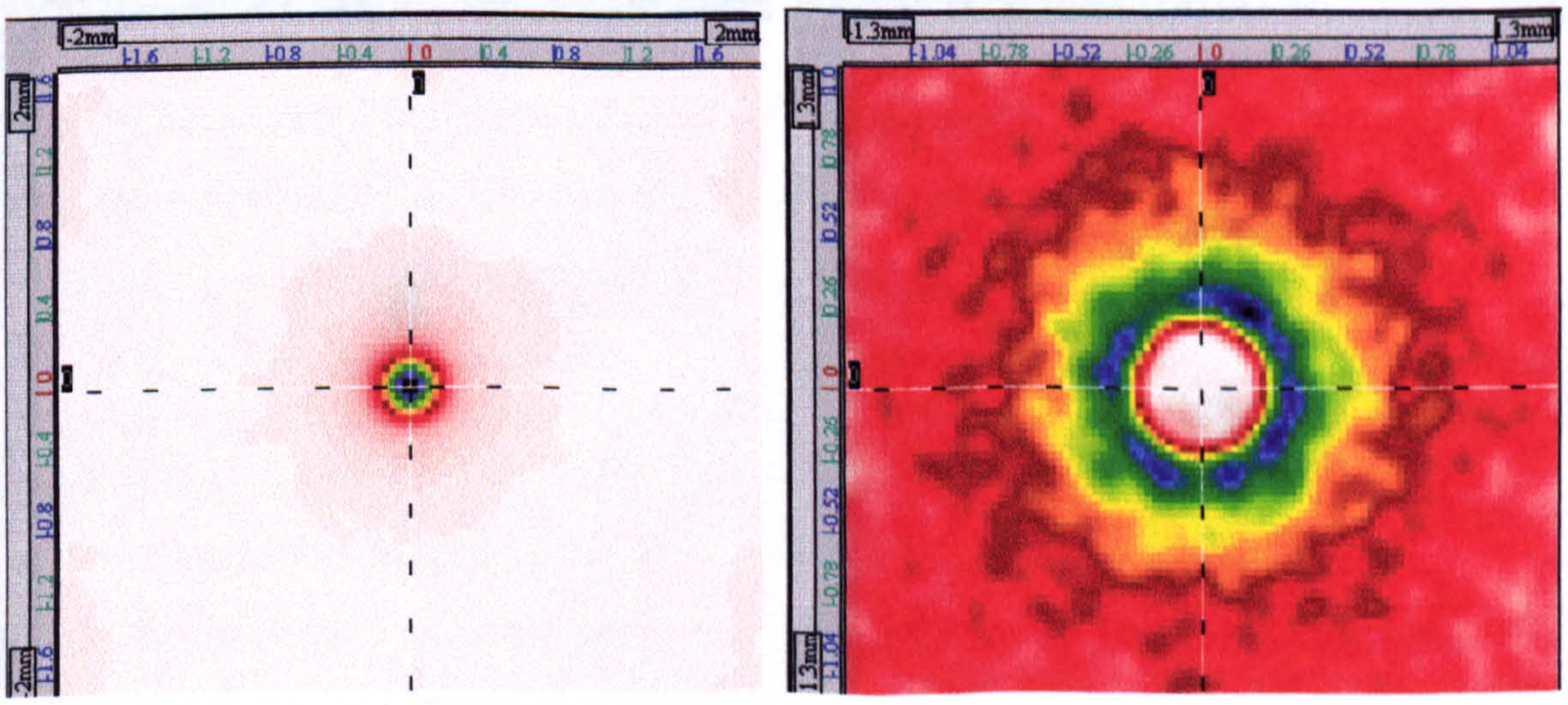

Fig 4-72: Source at 0 degrees *(left)* Flux= 320W, *(right)* Flux= 117W.

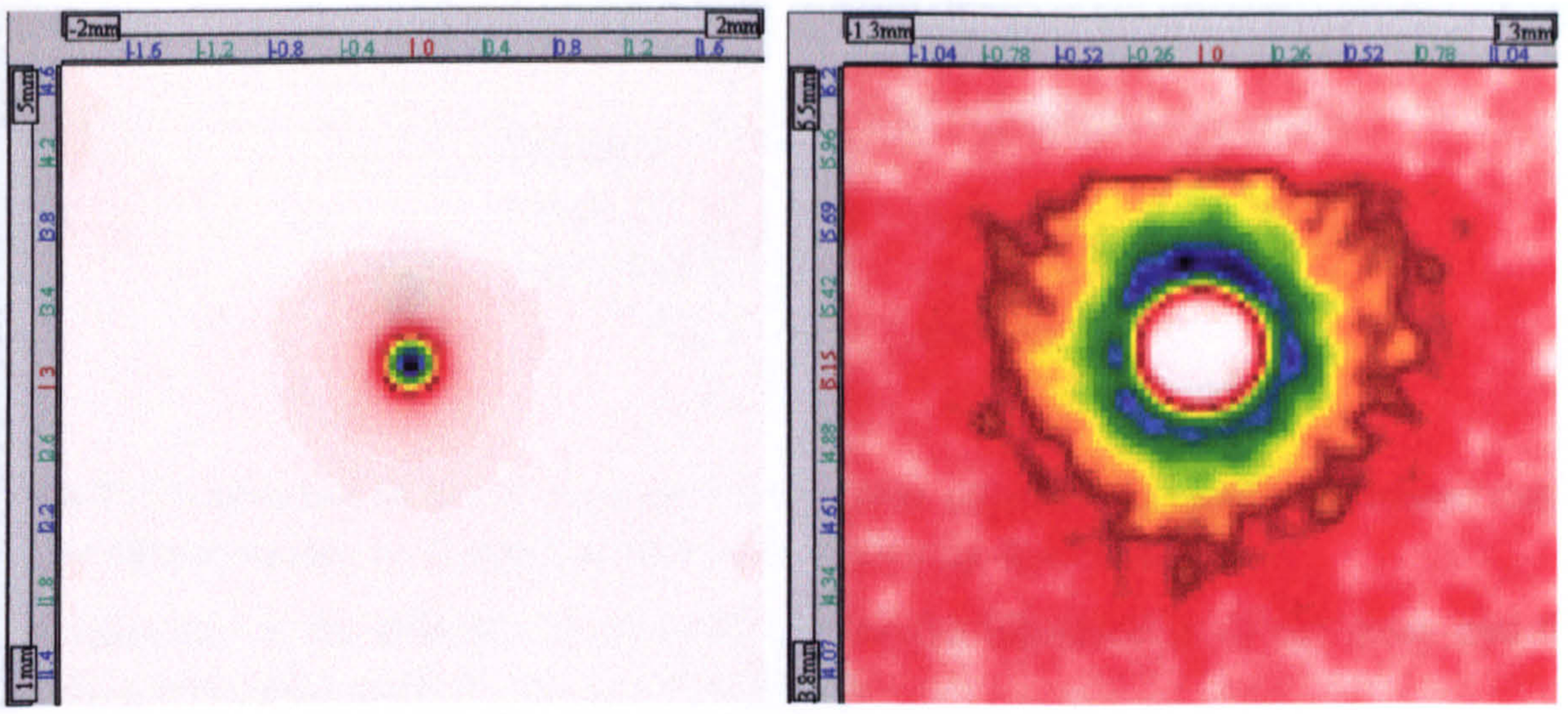

Fig 4-73: Source at 10 degrees *(left)* Flux= 282W, *(right)* Flux= 113W.

Unobturated images ***Obturated images***

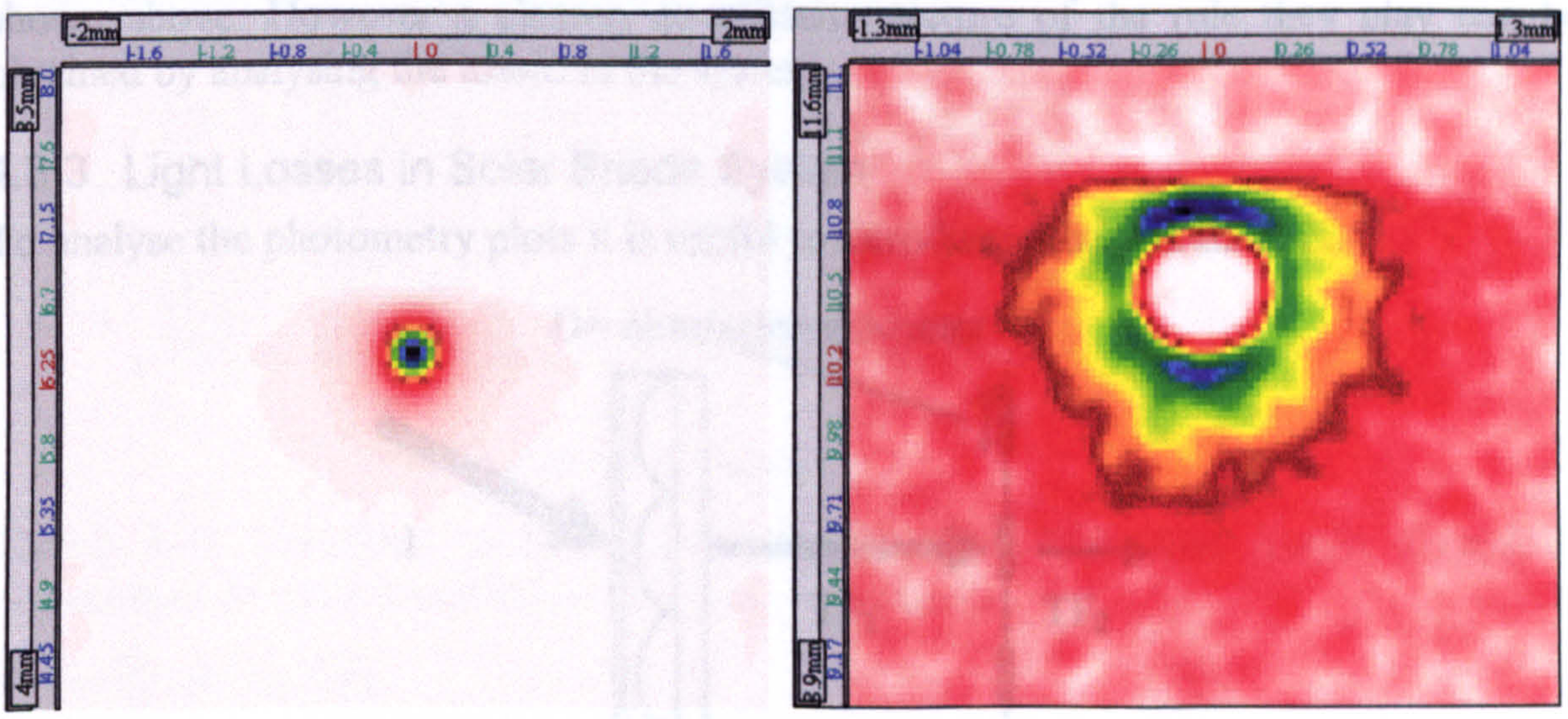

Fig 4-74: Source at 20 degrees *(left)* Flux= 238W, *(right)* Flux= 78W.

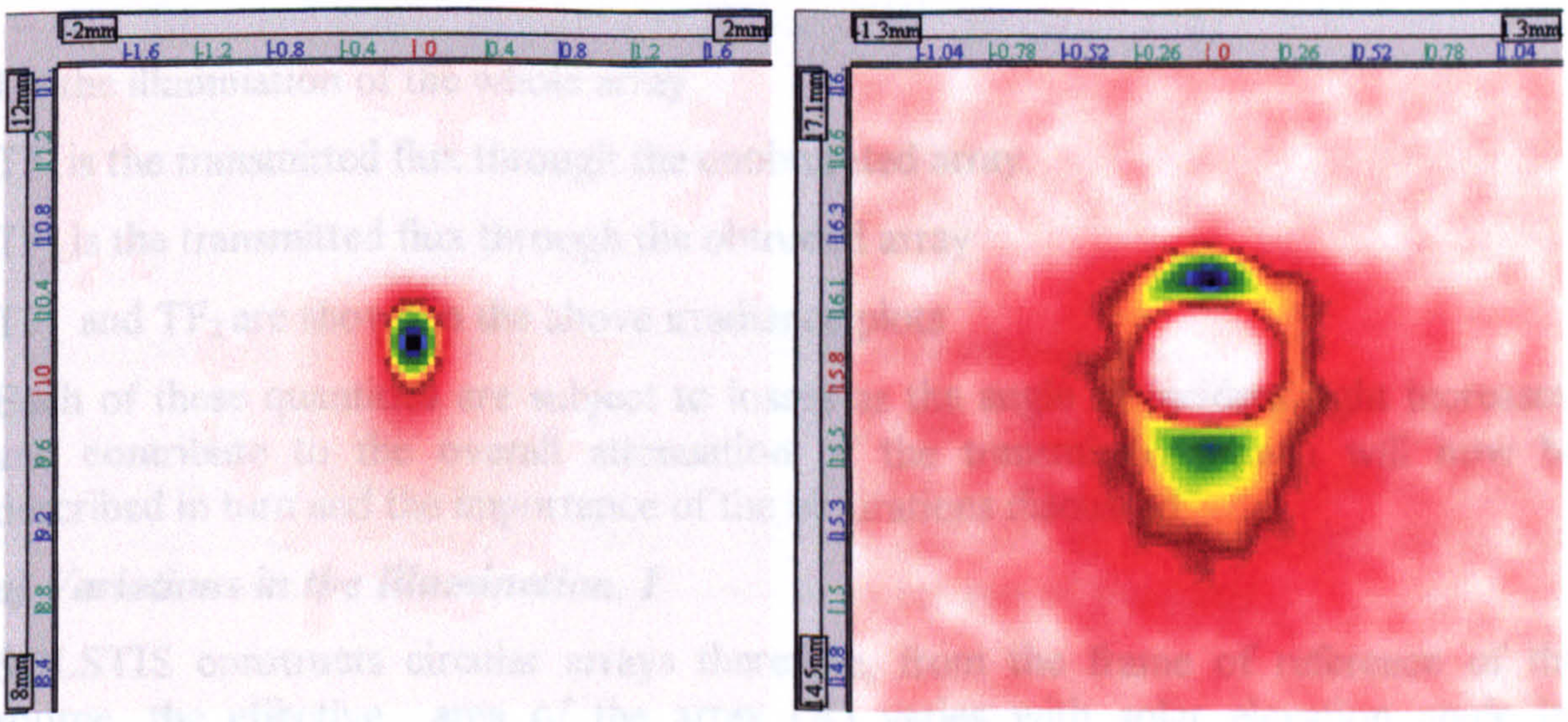

Fig 4-75: Source at 30 degrees*(left)* Flux= 196W, *(right)* Flux= 97W.

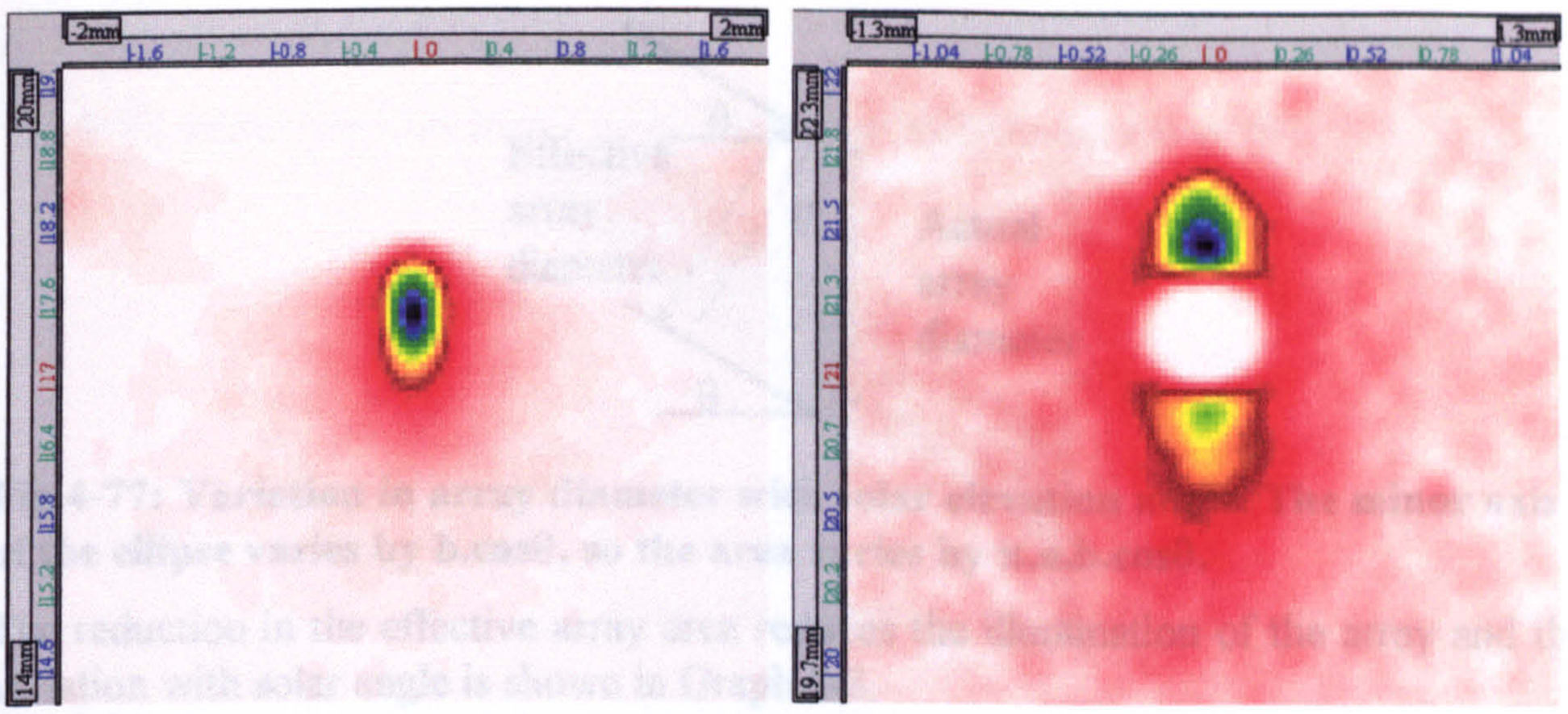

Fig 4-76: Source at 40 degrees *(left)* Flux= 151W, *(right)* Flux= 104W.

The diameter of the image is clearly much greater than the 0.454 mm obturations shown above. However a clearer, quantitative picture of the role they play can be obtained by analysing the losses in the system.

4.3.3 Light Losses in Solar Shade System

To analyse the photometry plots it is useful to introduce other parameters:

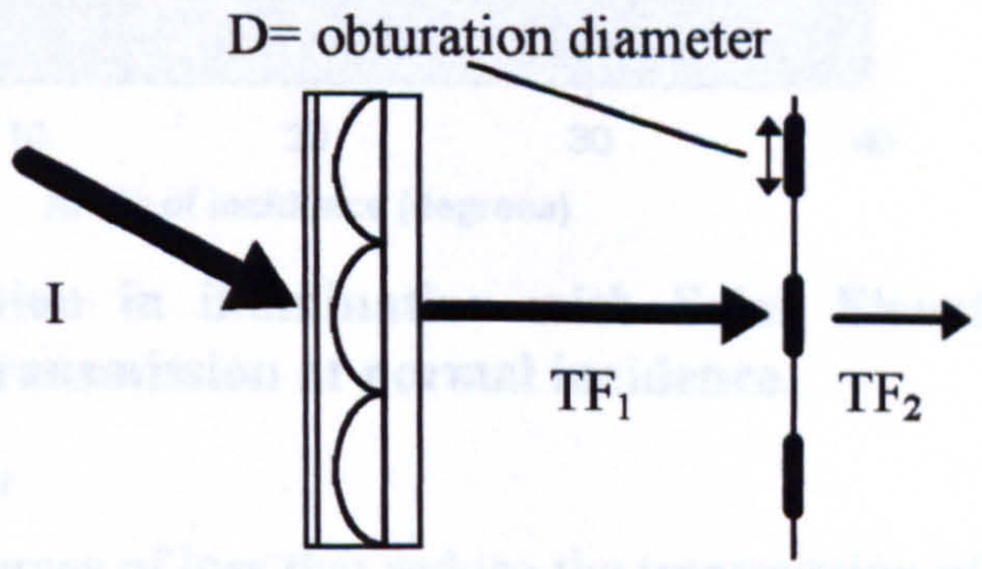

I is the illumination of the whole array

TF_1 is the transmitted flux through the unobturated array.

TF_2 is the transmitted flux through the obtruded array

TF_1 and TF_2 are shown in the above irradiance plots

Each of these quantities are subject to losses as the angle of incident light increases, and contribute to the overall attenuation of the transmission. Each will now be described in turn and the importance of the obturations discussed.

a) Variations in the Illumination, I

SOLSTIS constructs circular arrays therefore, from the frame of reference of the source, the effective area of the array (A) varies with solar elevation angle by $\pi.a.b.\cos\theta$ (see Fig 4-77).

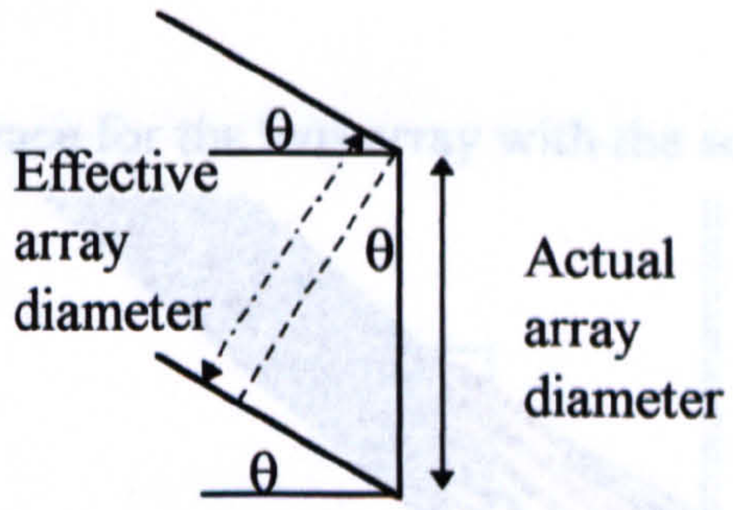

Fig 4-77: Variation in array diameter with solar elevation angle. The minor axis of the ellipse varies by b.cosθ, so the area varies by π.a.b.cosθ.

The reduction in the effective array area reduces the illumination of the array and the variation with solar angle is shown in Graph 4-8.

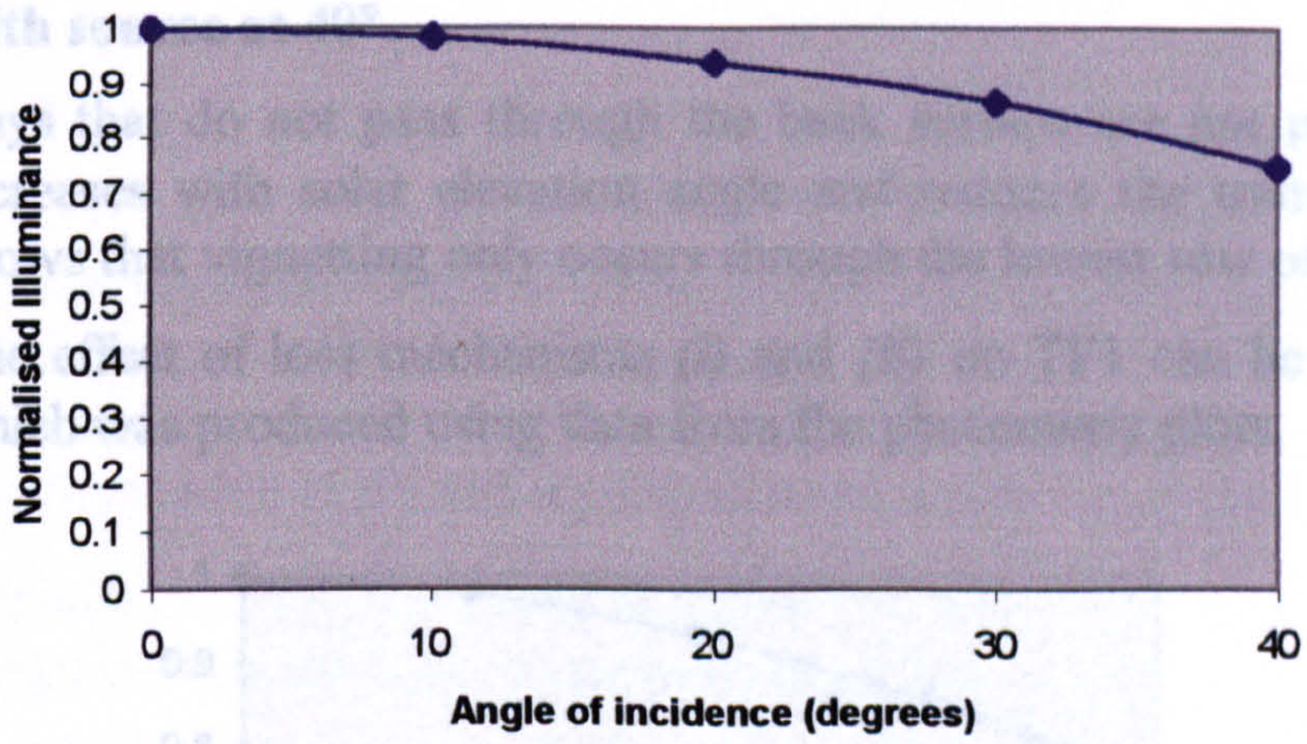

Graph 4-8: Variation in illumination with Solar Elevation Angle. Graph is normalised to the transmission at normal incidence.

b) Variations in TF_1

There are 3 main sources of loss that reduce the transmission of light through the array

i. Reduction of effective size of lens apertures with elevation angle.

ii. Vignetting

iii. Fresnel reflections.

Each will now be described in detail.

i) Reduction of effective size of lens apertures with elevation angle.

The lenses do not form a continuous structure across the whole array and losses occur between two adjacent apertures. This is equivalent to the opaque area of the array in the practical experiments. The effective aperture provided by each lens also varies with the source elevation angle in the same manner as the size of the array.

ii) Vignetting

Fig 4-78 shows the a ray trace for the lens array with the source at 40°.

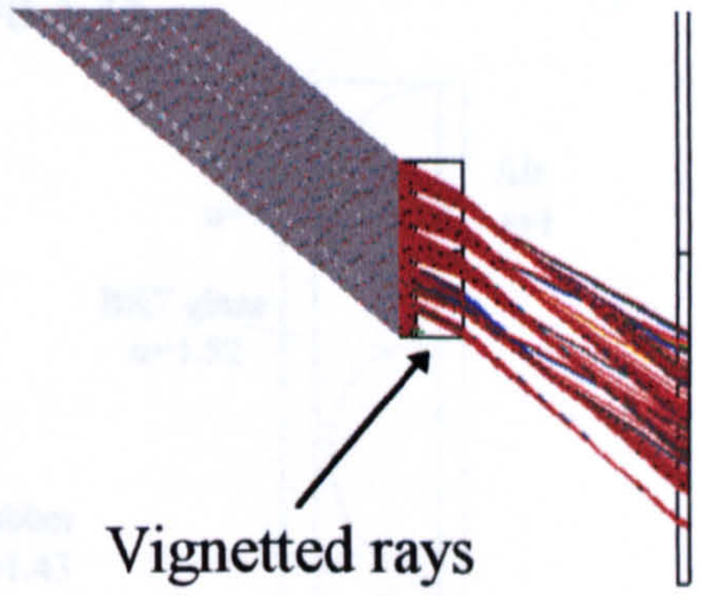

Fig 4-78: Ray trace through power-reduced lens array in polychromatic light with source at 40°.

Rays that do not pass through the back surface are not propagated. This vignetting increases with solar elevation angle and reduces the transmission. At 40° Fig 4-78 shows that vignetting only occurs through the lowest row of lenses.

The effect of loss mechanisms ***(i)*** and ***(ii)*** on TF1 can be deduced from Graph 4-9, which was produced using data from the photometry plots.

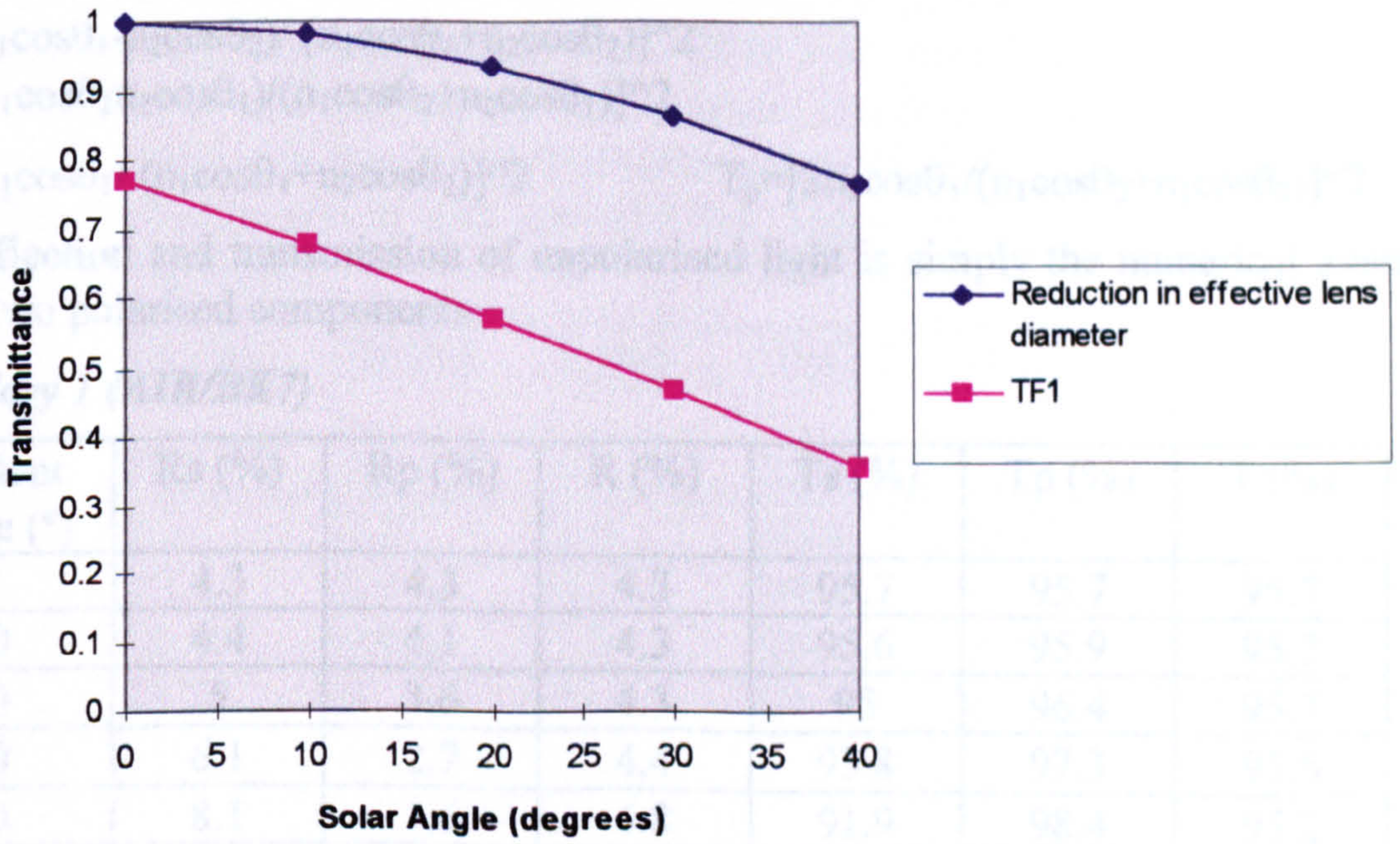

Graph 4-9: Variation in TF_1 and transmittance through the aperture of a single lens, with the solar elevation angle. Array diameter= 13mm, containing 19 lenses.

Graph 4-9 shows significant losses without the use of the obturations. At normal incidence there is a 23% reduction in the illumination which is attributable to the exclusion of light by the opaque interstitial area. If there were no vignetting, TF_1 would decrease at the same rate as the effective lens aperture. However its increased rate of decline TF_1 shows that vignetting has a significant role in the reduction of light transmitted through the lens array. At 40° TF_1 has fallen to less than half its value at normal incidence, leaving the obturations significantly less light to exclude to prevent glare.

(iii) Fresnel Reflections

There are seven changes of media within the reduced-power lens system that affect TF_1 and these are shown in fig 3.58.

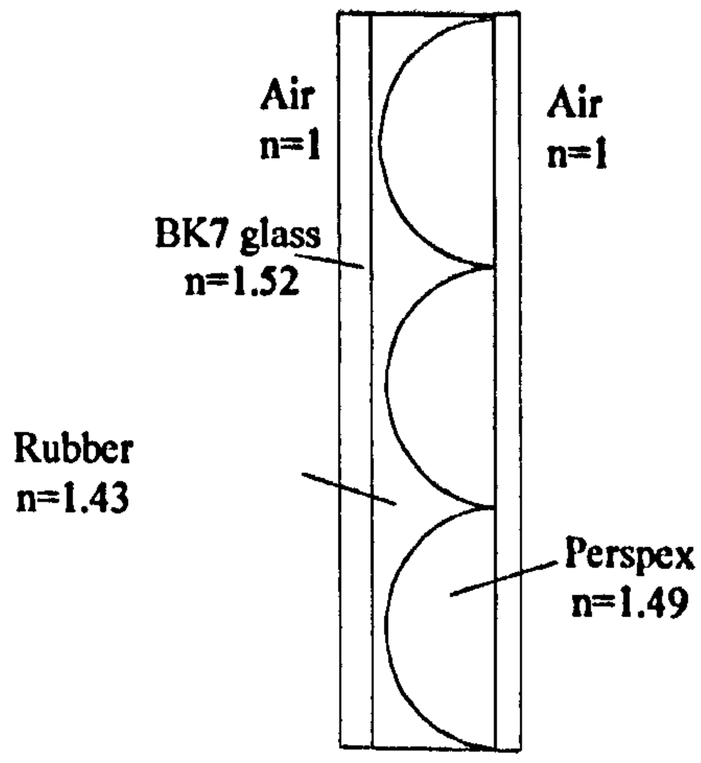

Fig 4-79: Reduced- power lens array.

Fresnel reflections occur at the boundary between two media and vary with the angle of incidence. Unfortunately they are not calculated by SOLSTIS and therefore must be calculated independently. The fresnel reflectance coefficients due to the change in refractive index at a plane air/dielectric boundary are given by the equations[xv]:

$R_s=[(n_1\cos\theta_1-n_2\cos\theta_2)/(n_1\cos\theta_1+n_2\cos\theta_2)]^2$

$R_p=[(n_1\cos\theta_2 n_2\cos\theta_1)/(n_1\cos\theta_2+n_2\cos\theta_1)]^2$

$T_s=[2n_1\cos\theta_1/(n_1\cos\theta_1+n_2\cos\theta_2)]^2$ $\quad$ $T_p=[2n_1\cos\theta_1/(n_1\cos\theta_2+n_1\cos\theta_2)]^2$

The reflection and transmission of unpolarised light is simply the numerical average of the two polarised components

Boundary 1 (AIR/BK7)

Incident Angle (°)	Rs (%)	Rp (%)	R (%)	Ts (%)	Tp (%)	T (%)
0	4.3	4.3	4.3	95.7	95.7	95.7
10	4.4	4.1	4.3	95.6	95.9	95.7
20	5	3.6	4.3	95	96.4	95.7
30	6.1	2.7	4.4	93.8	97.3	95.6
40	8.1	1.6	4.8	91.9	98.4	95.2

Boundary 2 (BK7/Rubber)

Incident Angle (°)	Rs (%)	Rp (%)	R (%)	Ts (%)	Tp (%)	T (%)
0	0.2	0.2	0.2	99.8	99.8	99.8
10	0.2	0.2	0.2	99.8	99.8	99.8
20	0.2	0.2	0.2	99.8	99.8	99.8
30	0.3	0.1	0.2	99.7	99.9	99.7
40	0.3	0.1	0.2	99.7	99.9	99.8

Boundary 3 (Rubber/Perspex)

The third boundary is curved and therefore the surface normal varies between 0° and 90° for any given incident angle. However as the refractive indices are very similar, the fresnel reflections do not vary significantly across the surface.

Incident Angle (°)	Rs (%)	Rp (%)	R (%)	Ts (%)	Tp (%)	T (%)
0	0	0	0	100	100	100
10	0	0	0	100	100	100
20	0	0	0	100	100	100
30	0	0	0	99.9	100	100
40	0	0	0	99.9	100	99.9
50	0.2	0	0.1	99.8	100	99.9
60	0.5	0.1	0.3	99.5	99.8	99.6
70	1.8	0.9	1.4	98.1	99.1	98.6
80	10.5	8.2	9.4	89.5	91.8	90.6

The fresnel reflectances are not significant until the incident angle> 70° with respect to the normal. By area, this means that there are no significant reflections for 93% of the lens surface. Consequently it is reasonable to approximate this surface to plane boundary and ignore these losses.

Boundary 4 (Perspex/Air)

At the fourth interface the light has been focused by the perspex lenses with a low numerical aperture. The ray-traces in figs 3-28 to 3-36 show that between for incident angles between 0° and 40° on the first surface, the rays are incident on the back surface of the lens at angles < 40°. The table below shows the losses over this range. As a first approximation it was assumed that losses were constant at 4% at this interface (see Fig 4-83).

Incident Angle (°)	Rs (%)	Rp (%)	R (%)	Ts (%)	Tp (%)	T (%)
0	3.9	3.9	3.9	96.1	96.1	96.1
10	4.2	3.5	3.9	95.8	96.5	96.1
20	5.7	2.4	4.1	94.3	97.6	96
30	10.1	0.4	5.3	89.9	99.5	94.7
40	35.7	8	21.8	64	92	78

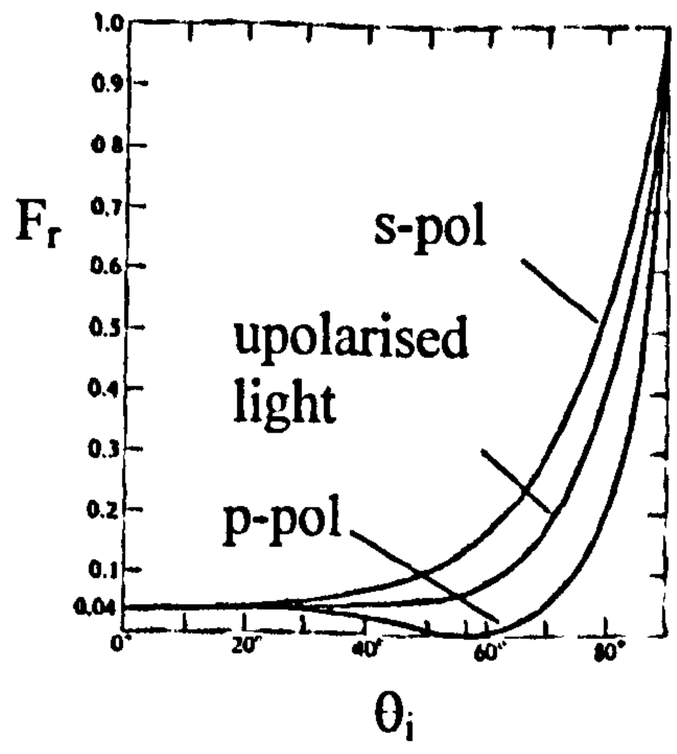

Fig 4-80: Fresnel losses at a dielectric/air interface

Total Fresnel losses affecting TF_1

	Transmission (T) at Boundaries				
Incident Angle	1	2	3	4	Total (%)
0	95.7	99.8	100	96	92
10	95.7	99.8	100	96	92
20	95.7	99.8	100	96	92
30	95.6	99.7	100	96	92
40	95.2	99.8	99.9	96	92

c) Variations in TF_2

TF_2 is the critical factor in determining the performance of the solar shade as it represents the attenuation of the direct sunlight by the system. In addition to the losses through the array that result in TF1, further losses are experienced at the obturation array. These are:

- The exclusion of light by the obturations.
- Light that is not blocked by the obturation experiences fresnel reflectances from the glass substrate between the obstructions.

In opposition to this reduction in transmission, there are mechanisms that increase TF_2. Both of these will now be described in greater detail.

i) Losses

As with dilute lens array there are fresnel losses at the front and back surface of the obturation array which is on glass. From the discussion of the previous interfaces, it can be said that the reduced power lens array approximates to a series of plane interfaces. Treating it as such, the exit angle from the back surface of the array can be calculated and therefore the losses at both interfaces of the obturation array which are identical.

Incident Angle (°)	Rs (%)	Rp (%)	R (%)	Ts (%)	Tp (%)	T (%)
0	4.3	4.3	4.3	95.7	95.7	95.7
10	4.4	4.1	4.3	95.6	95.9	95.7
20	5	3.6	4.3	95	96.4	95.7
30	6.1	2.7	4.4	93.8	97.3	95.6
40	8.1	1.6	4.8	91.9	98.4	95.2

Thus the total fresnel losses within the system are:

	Fresnel Losses (%)			
Incident Angle (°)	Dilute lens array	Obturation Array surface 1	surface2	Total
0	92	95.7	95.7	84
10	92	95.7	95.7	84
20	92	95.7	95.7	84
30	92	95.6	95.6	84
40	92	95.2	95.2	83

20	5	3.6	4.3	95	96.4	95.7
30	6.1	2.7	4.4	93.8	97.3	95.6
40	8.1	1.6	4.8	91.9	98.4	95.2

Thus the total fresnel losses within the system are:

	Fresnel Losses (%)			
Incident Angle (°)	Dilute lens array	Obturation Array surface 1	surface2	Total
0	92	95.7	95.7	84
10	92	95.7	95.7	84
20	92	95.7	95.7	84
30	92	95.6	95.6	84
40	92	95.2	95.2	83

Between 0° and 40°A traditional window would reflect 4% at the each air/glass interface (from Fig 4-80). Therefore the total losses are equivalent to double glazing.

c) Gains

In opposition this reduction in transmission, there is an increase in transmitted flux due to increased aberrations.

Aberrations in the image plane cause the broadening of the point spread function at the focus and increase with the incident angle of the source. Consequently, the energy in a single image is spread over a much larger area and less is blocked by the obturation. Spherical aberration, coma and astigmatism all increase with incident angle, reducing the attenuation by the obturations. In addition chromatic and longitudinal chromatic aberration become more significant off-axis, along with the field curvature and distortion. Field curvature is most evident in Fig 4-49 to Fig 4-57, where the distance to the image plane decreases with incident angle and therefore produces a curved image plane.

Using irradiance distribution from SOLSITS TF_2 has been evaluated for the five obturation diameters used in the practical experiments:133μm, 230μm, 246μm, 430μm, 454μm and for solar elevation angles between 0° and 40°.

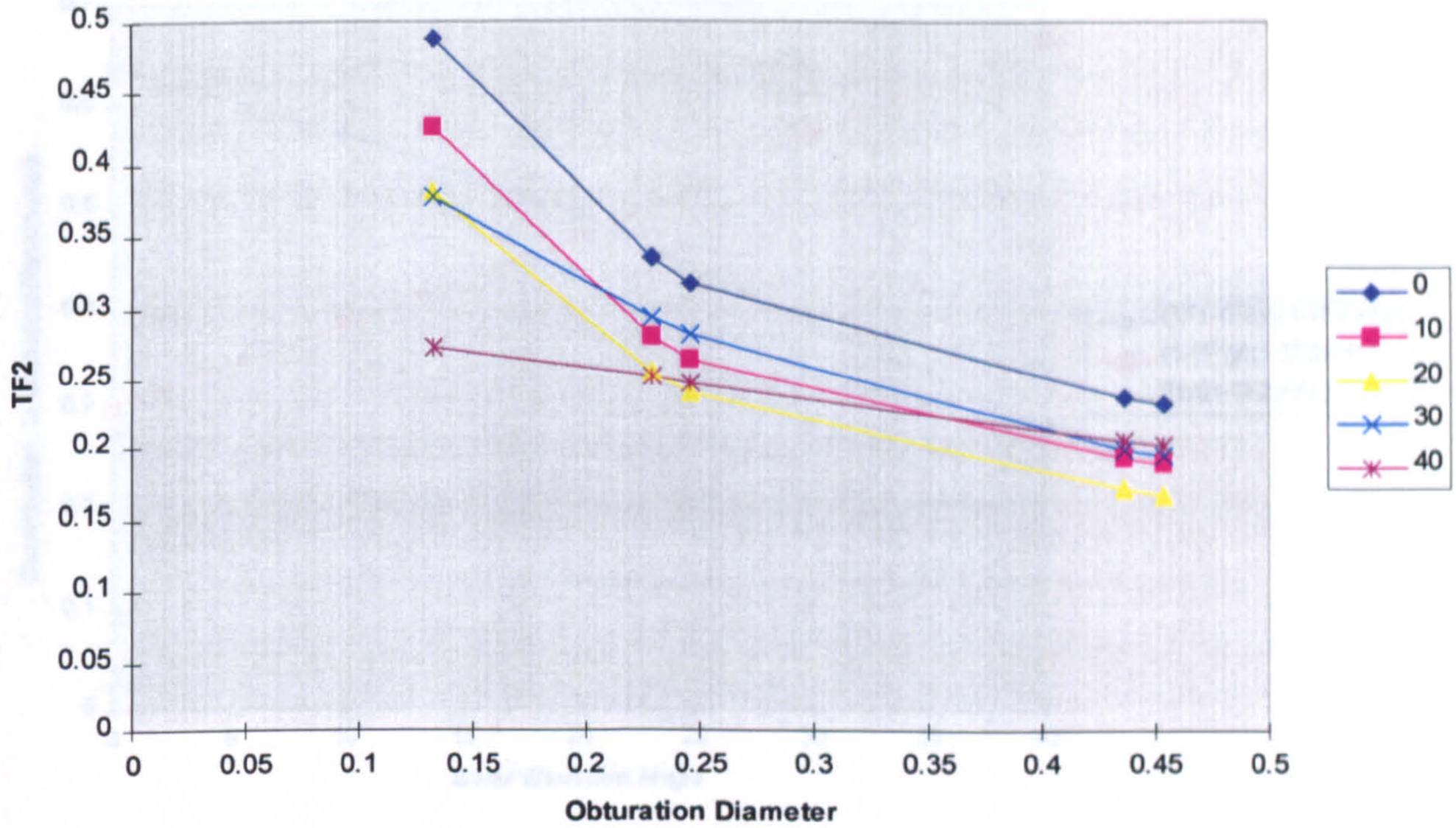

Graph 4-10: Variation in TF2 with Solar Elevation Angle.

According to Graph 4-10 the minimum transmission possible with this solar shade arrangement is 22% which is significantly higher than the target of 5%.

As the fresnel reflections are constant over this angular range, the transmittance TF_2 is dependent on the aberrations and the effective aperture of the lenses. The former increases with incident angle, the latter decreases. At normal incidence, although the aberrations are minimised, the effective lens aperture is reduced only by discontinuities between lenses. Therefore for a given obturation diameter it has the highest transmission. At 20° TF_1 has decreased by 20% but the image remains relatively unaffected by the aberrations (Fig 4-74), so it has the lowest transmission.

The relative importance of the various loss mechanisms can be simply calculated:

Total excluded illuminance= $1-TF_2+FL= (TF_1-TF_2)+(1-TF_1)+FL$

where (TF_1-TF_2) is the attenuation by the obturations

$(1-TF_1)$ is the attenuation by the reduction in aperture size

FL are the fresnel losses

The relative contribution of each is shown in Graph 4-11 to Graph 4-15.

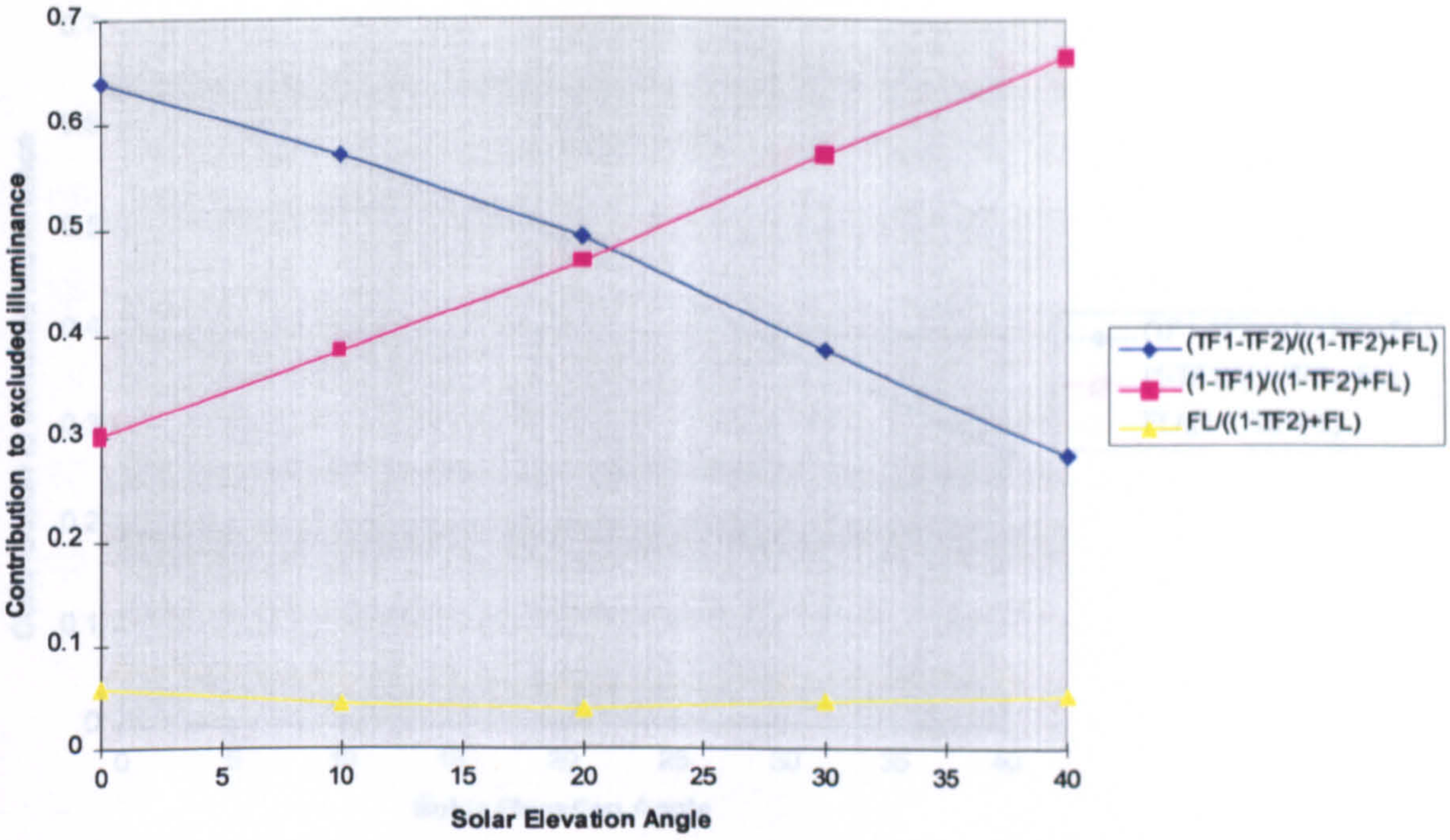

Graph 4-11: Relative contribution of loss mechanisms in solar shade with 0.454mm diameter obturation.

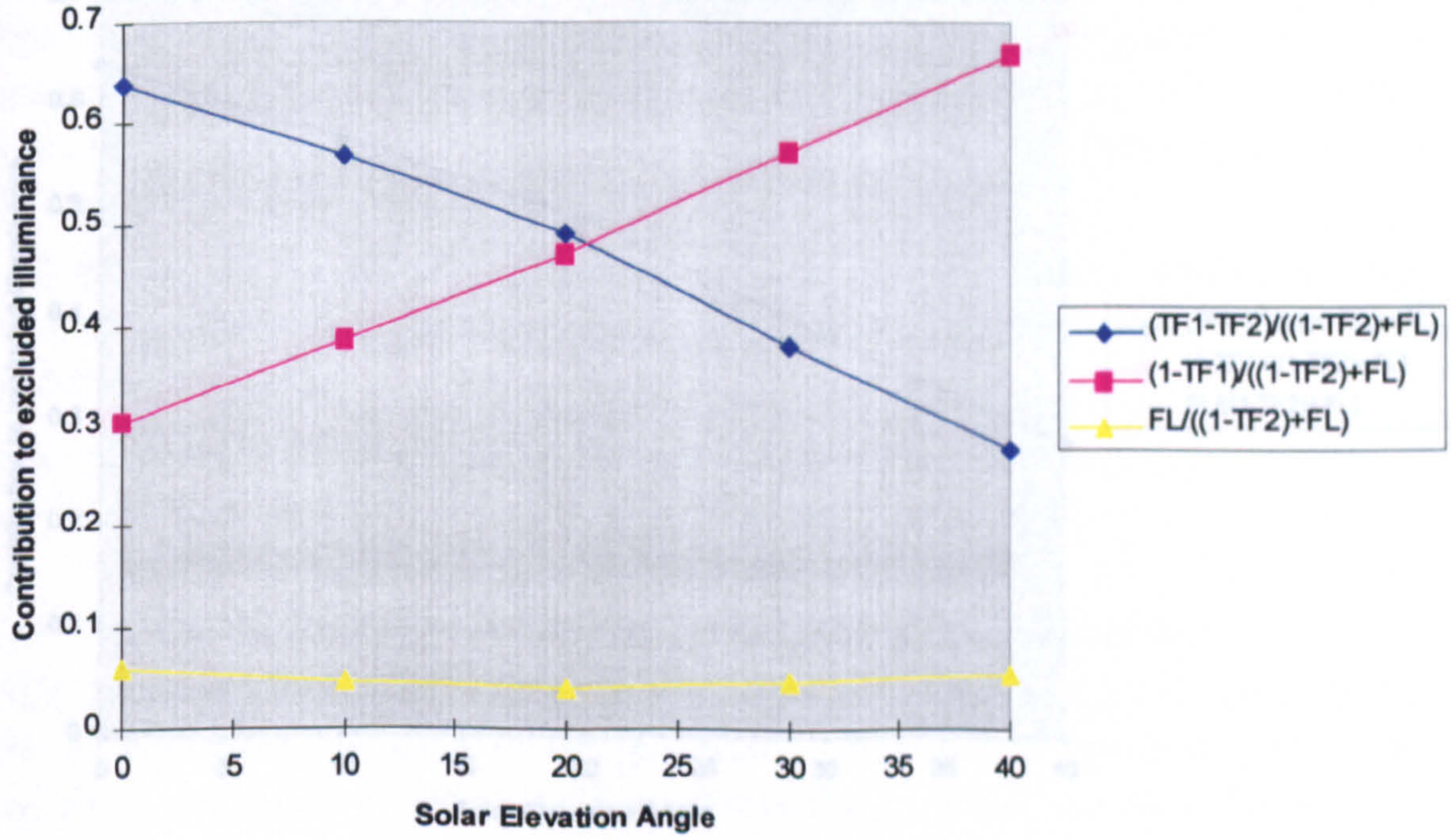

Graph 4-12: Relative contribution of loss mechanisms in solar shade with 0.436mm diameter obturation.

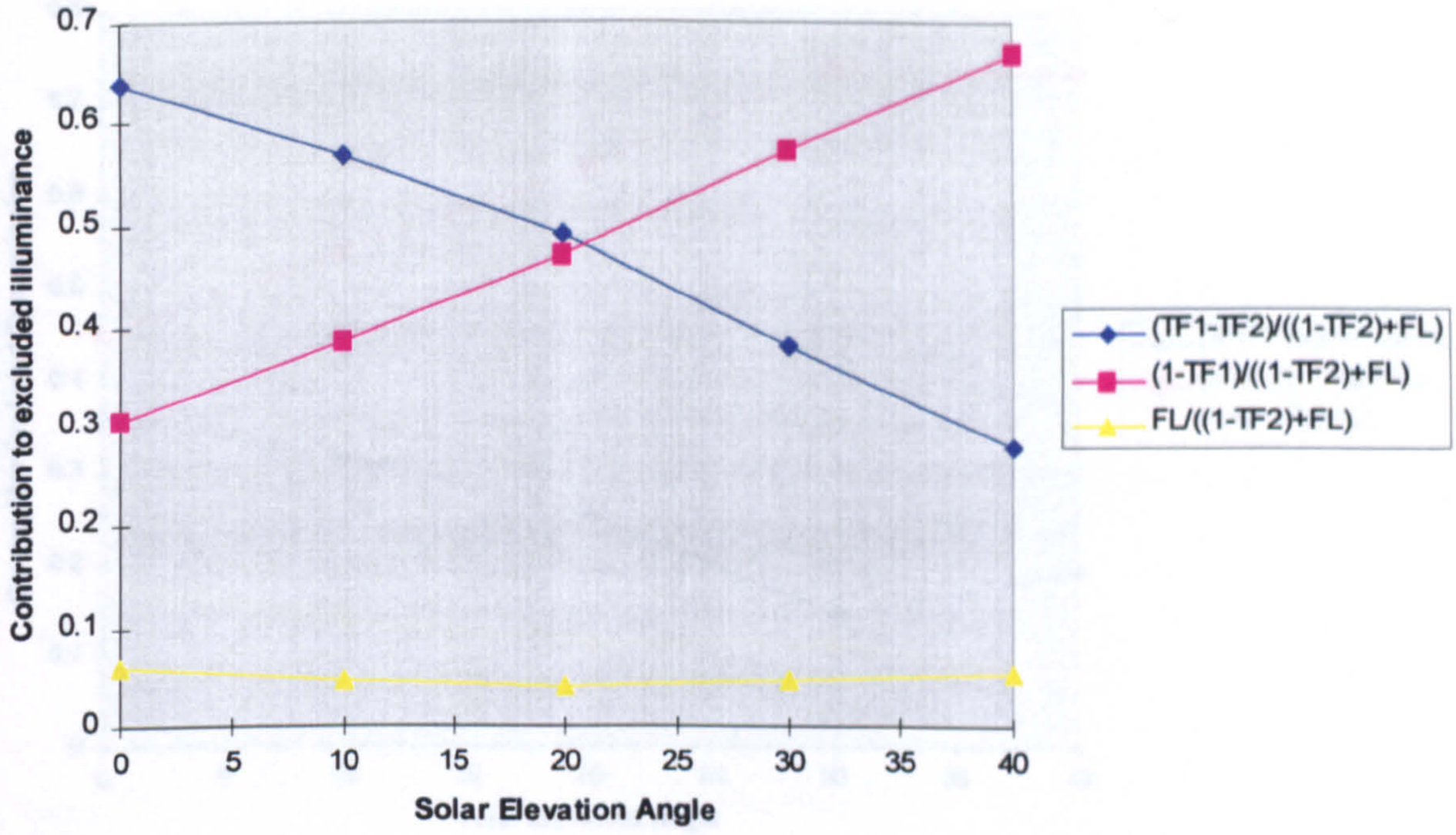

Graph 4-13: Relative contribution of loss mechanisms in solar shade with 0.246mm diameter obturation.

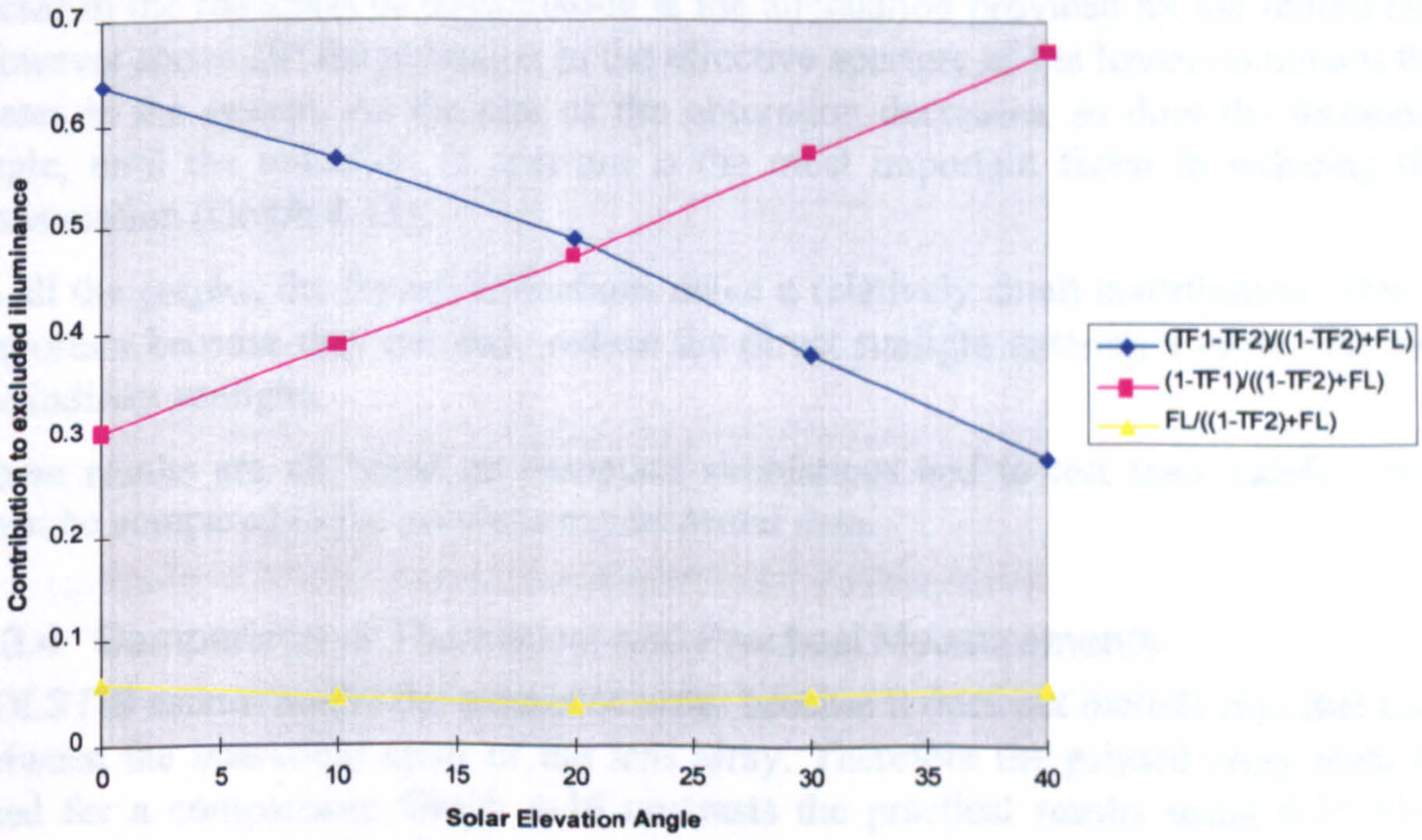

Graph 4-14: Relative contribution of loss mechanisms in solar shade with 0.230mm diameter obturation.

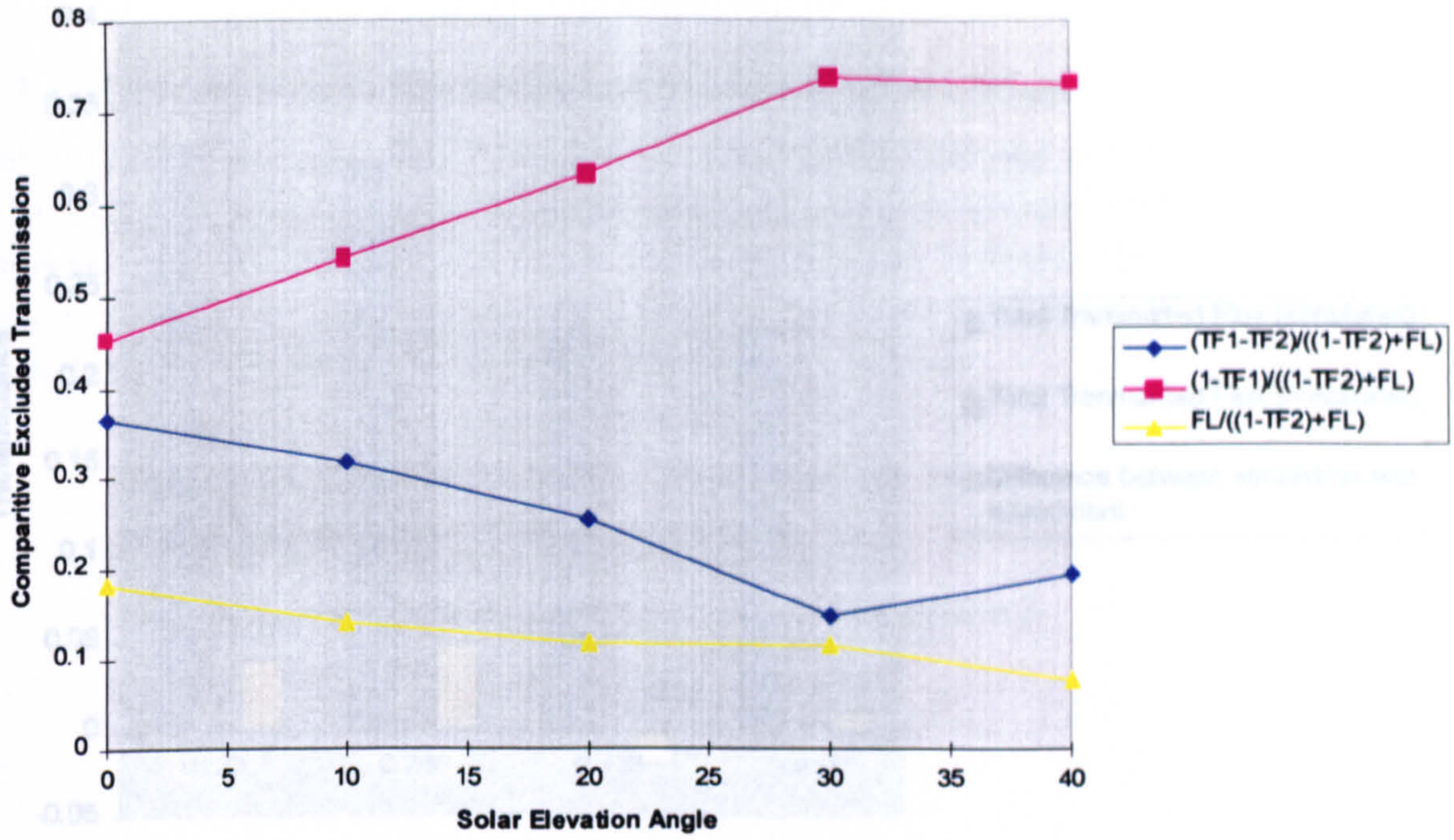

Graph 4-15: Relative contribution of loss mechanisms in solar shade with 0.133mm diameter obturation.

Below 20° and for the range of obturation diameter tested above, the most significant factor in the reduction of transmission is the attenuation provided by the obturation. However above 20° the reduction in the effective aperture of the lenses dominates the losses in the system. As the size of the obturation decreases, so does the threshold angle, until the reduction in aperture is the most important factor in reducing the transmission (Graph 4-15).

In all the graphs, the fresnel reflections make a relatively small contribution. This is important because they not only reduce the direct sunlight entering a room, but also the indirect sunlight.

These results are all based on computer simulations and to test their validity they must be compared to the previous experimental data.

4.3.4 Comparison of Theoretical and Practical Measurements

SOLSTIS cannot model the unpainted array because it does not include rays that pass between the interstitial areas of the lens array. Therefore the painted array must be used for a comparison. Graph 4-16 contrasts the practical results using 0.5° fibre source and the computer simulation.

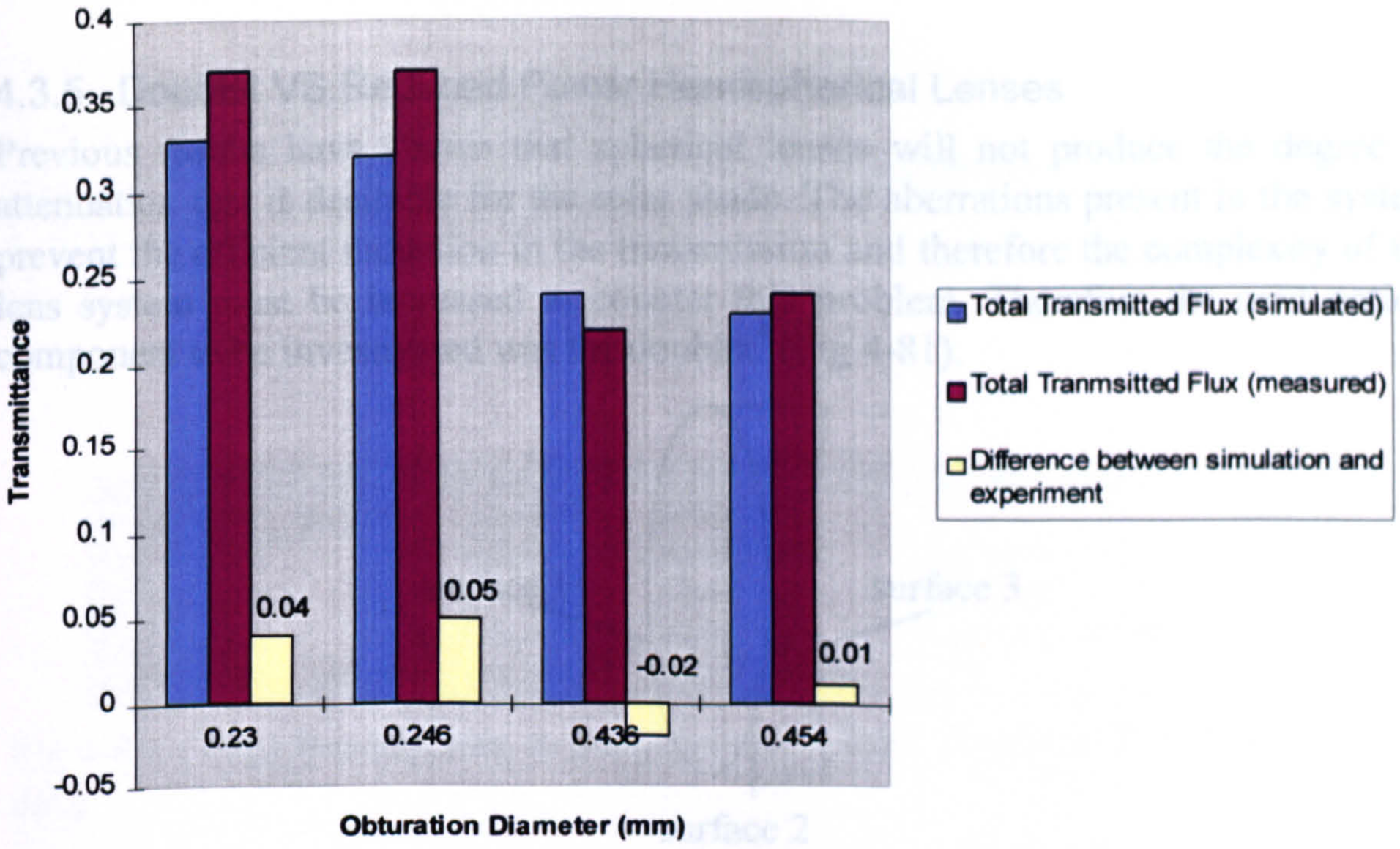

Graph 4-16: Comparison of computer generated and experimental data for source at 0° incidence.

For the computer model the total excluded illuminance is calculated as the fresnel reflections plus (1- TF_2). In the experiments this value is measured directly.

The data shows a good fit, with the difference between the experimental and theoretical data being less than 5% for all obturations. It demonstrates that improving the collimation, manufacturing the stops in situ etc, could not have improved the performance of the system significantly. The results from the first experiment with the fibre source were sufficiently accurate to be used for analysis.

Further verification of the validity of the computer model can be gained by examining irradiance distribution in a single image formed by both the simulation and the experiment. The data for Graph 4-17 was obtained from sections 4.2.6 (empirical readings) and 4.3.2 (simulated measurements). Both sets of data were normalised against themselves, assuming a unit cell in the image plane, equal to the radius of a single lens. All the light from one lens was assumed to be contained within this cell.

4.3.5 Doublet VS Reduced Power Hemispherical Lenses

Previous results have shown that spherical lenses will not produce the degree of attenuation that is desirable for the solar shade. The aberrations present in the system prevent the efficient reduction in the transmission and therefore the complexity of the lens system must be increased to counter this problem. Therefore the next optical component to be investigated was the doublet[4] (Fig 4-81).

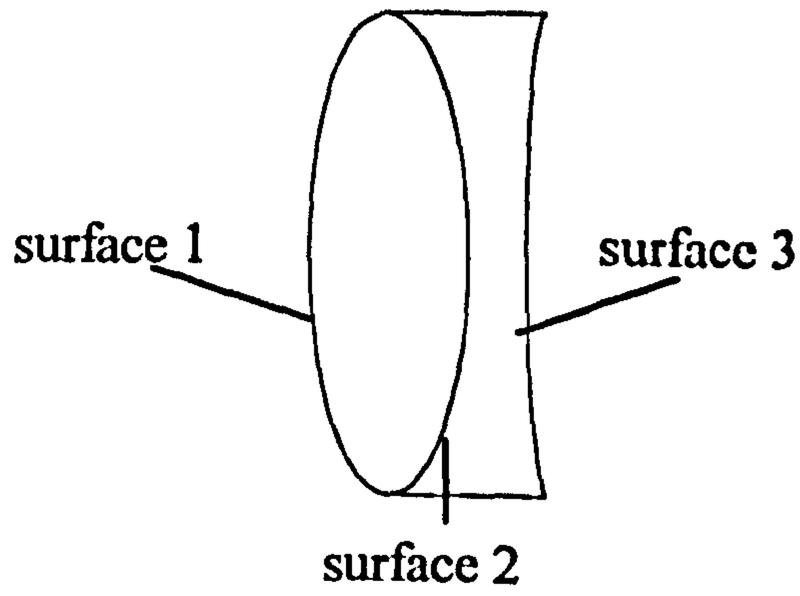

Fig 4-81: Doublet lens

An array of doublets would be technically more difficult to produce than the singlets, but discussions with NPL's Optical Workshop concluded that such a system could be manufactured. Possible manufacturing methods include:

1. Using a bull-nosed cutter on a computer numerically controlled (c-n-c) milling machine to create two curved surfaces (surfaces 2 and 3) on either side of a transparent media such as perspex. A step and repeat process to create a whole array of these singlet lenses. Next a resin could be poured over surface 2 and cured, thus assuming its radius of curvature. Once hardened the resin could be polished into surface 1.
2. An ultrasonic vibrating tool-bit in an abrasive slurry could be used to create surfaces 2 and 3, then surface 1 produced as described in (1).
3. For mass production the two elements of the doublet could be manufactured separately by hot-pressing then joined with an optical cement.

However no doublet arrays were available at NPL and therefore the following analysis relied solely on computer modelling.

[4] Adapted from examples in SOLSTIS software.

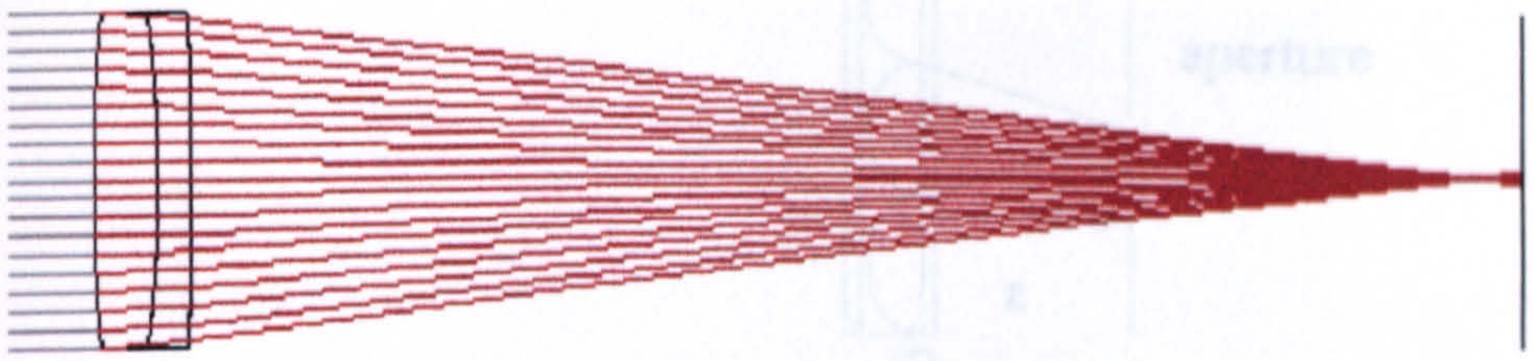

n°	Surface	Radius	Parameter	Aperture	Glass	Index	Dispersion	Thickness
OB	SPHERE	Infinite	c=0.0000	2.600	AIR	1.000000	Infinite	Infinite
1	SPHERE	7.881	c=0.0000	2.600	BK7	1.516798	64.17	0.650
2	SPHERE	-5.763	c=0.0000	2.600	SF5	1.672694	32.21	0.325
3	SPHERE	-17.240	c=0.0000	2.600	AIR	1.000000	Infinite	12.540
IM	SPHERE	Infinite	c=0.0000	2.600	IMAGE			

Fig 4-82: (Top) Doublet lens in polychromatic light. (Bottom) Doublet system data.

The doublet is well-corrected for coma, spherical and chromatic aberrations. The focused image of the doublet is contrasted to that of the reduced-power spherical lens in Fig 4-83.

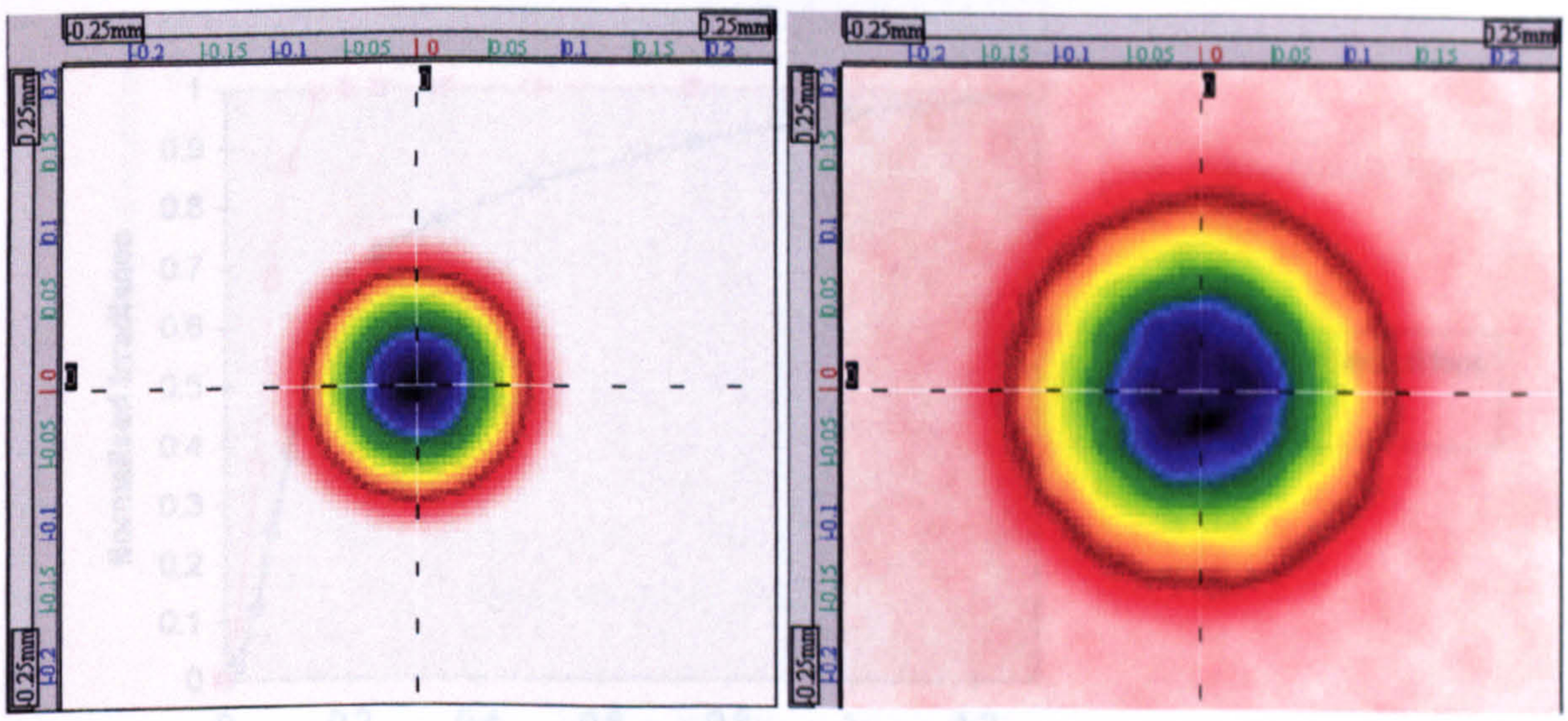

Fig 4-83: (Left) Image formed by doublet lens. (Right) Image formed by dilute spherical lens.

The doublet produces an image that is approximately 200 micrometers in diameter, in contrast to the power weakened spherical lens which produces an image that extends beyond 500 micrometers. This, however, occurs at normal incidence that is not the most important scenario for this application. Consequently the two were compared over a range of incident angles.

The nature of the comparison was by simulating the effect of placing an aperture at the image plane and measuring the transmission (see Fig 4-84).

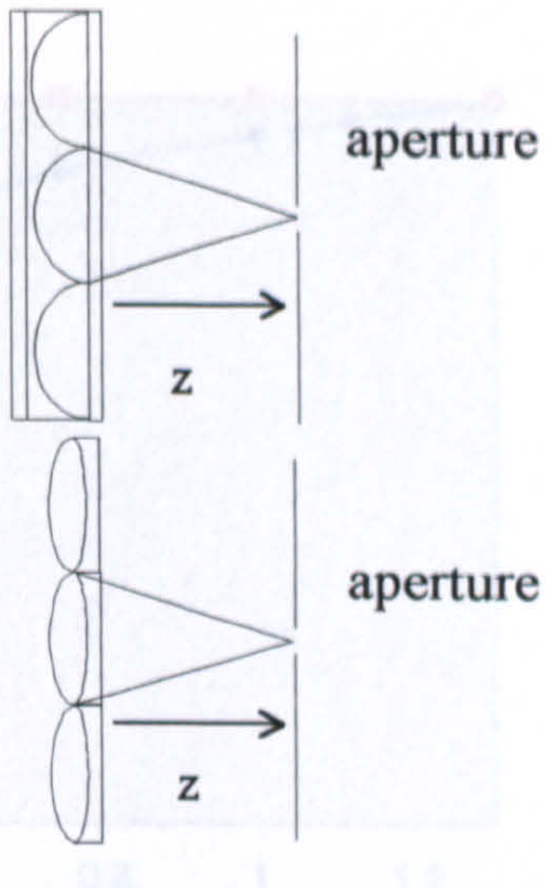

Fig 4-84: Transmission through aperture of radius r, where 0<r<1.3mm.

The aperture was centred on the central element of the array (thus negating any vignetting effects) and its radius varied between 0 and 1.3mm (the radius of a single lens). The transmission through the aperture over the range of radii revealed the irradiance distribution in a single image. The process was repeated over a range of incident angles and for both arrays. The results are shown below.

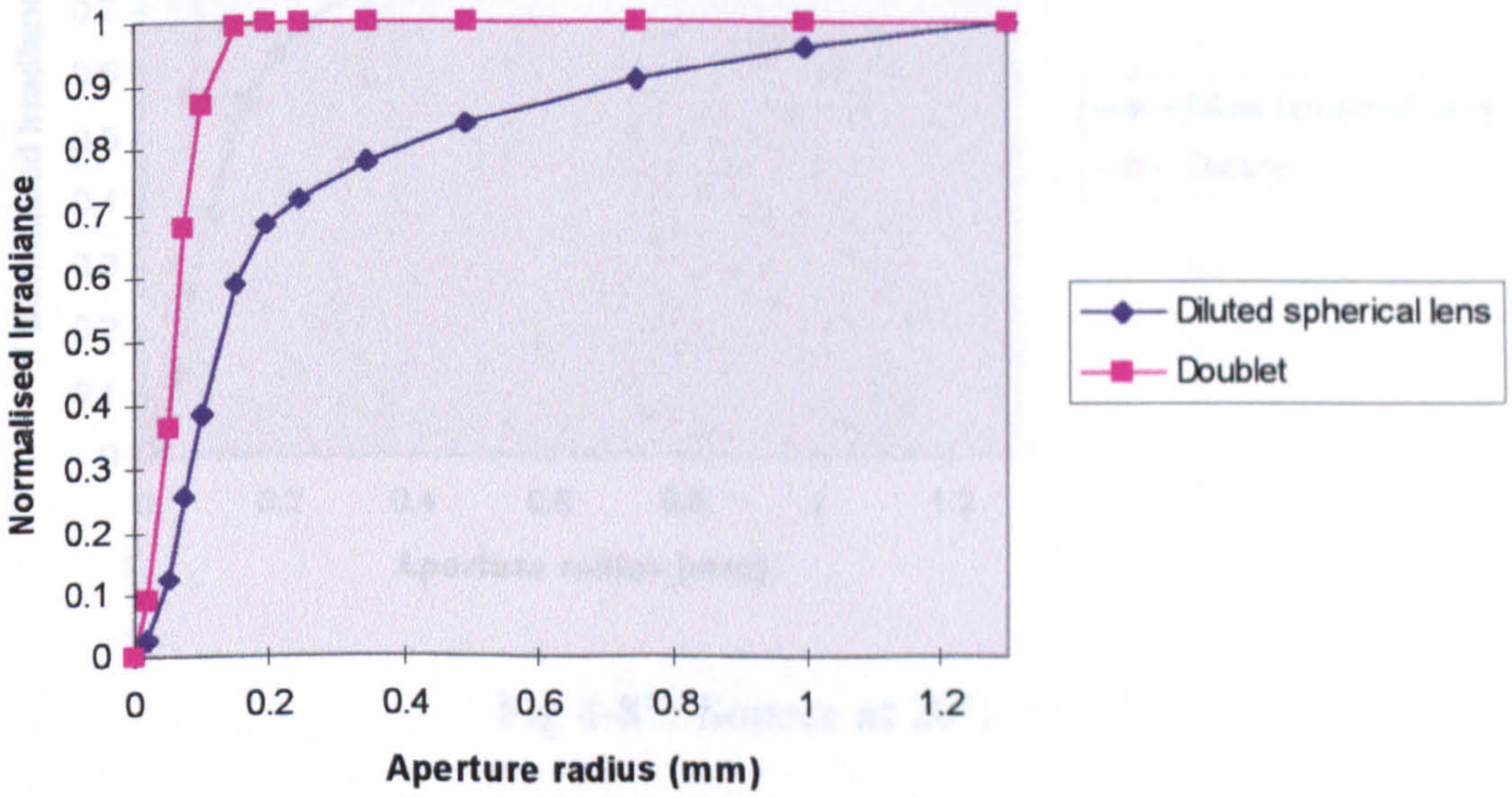

Fig 4-85: Source at 0°.

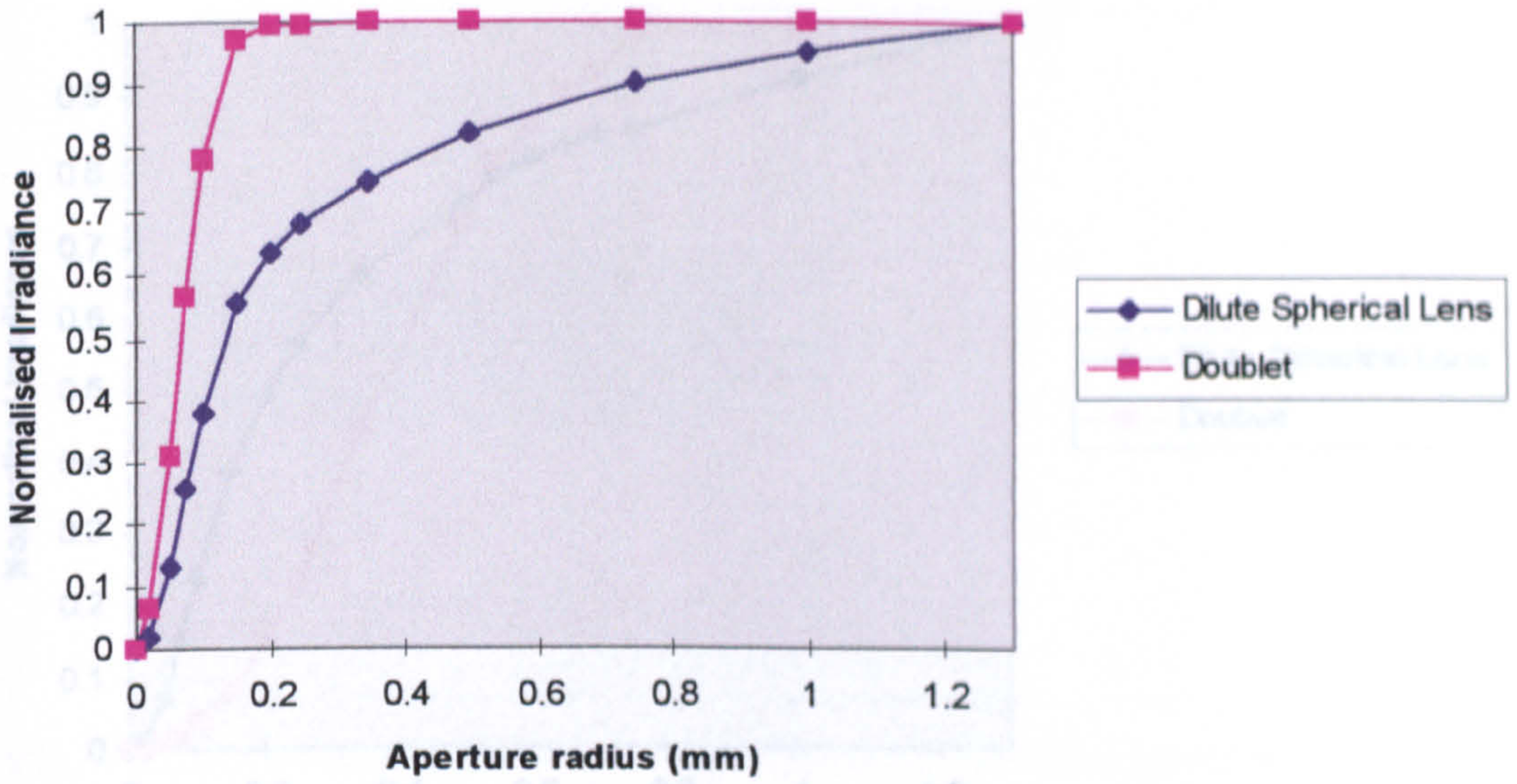

Fig 4-86: Source at 10°.

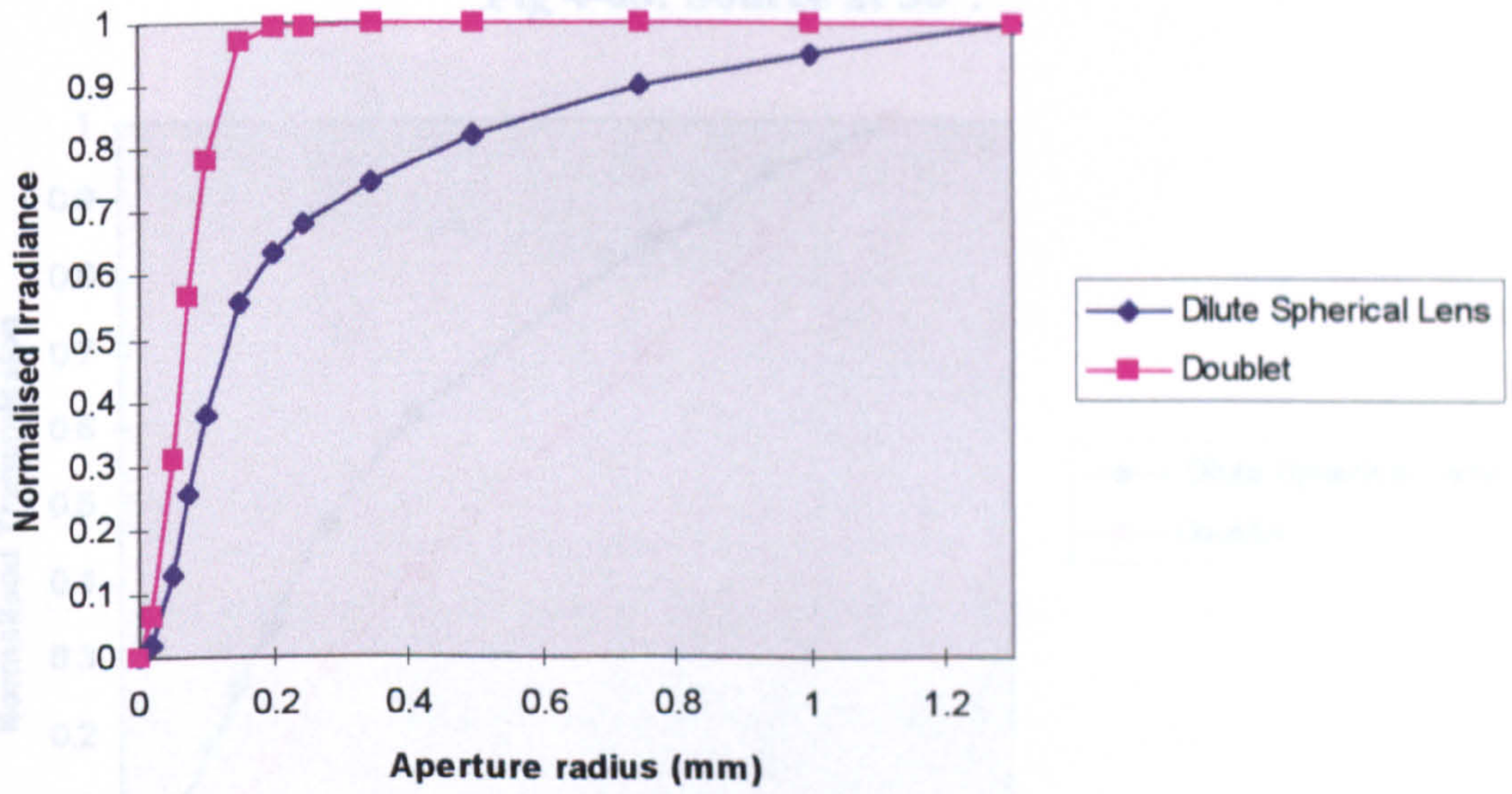

Fig 4-87: Source at 20°.

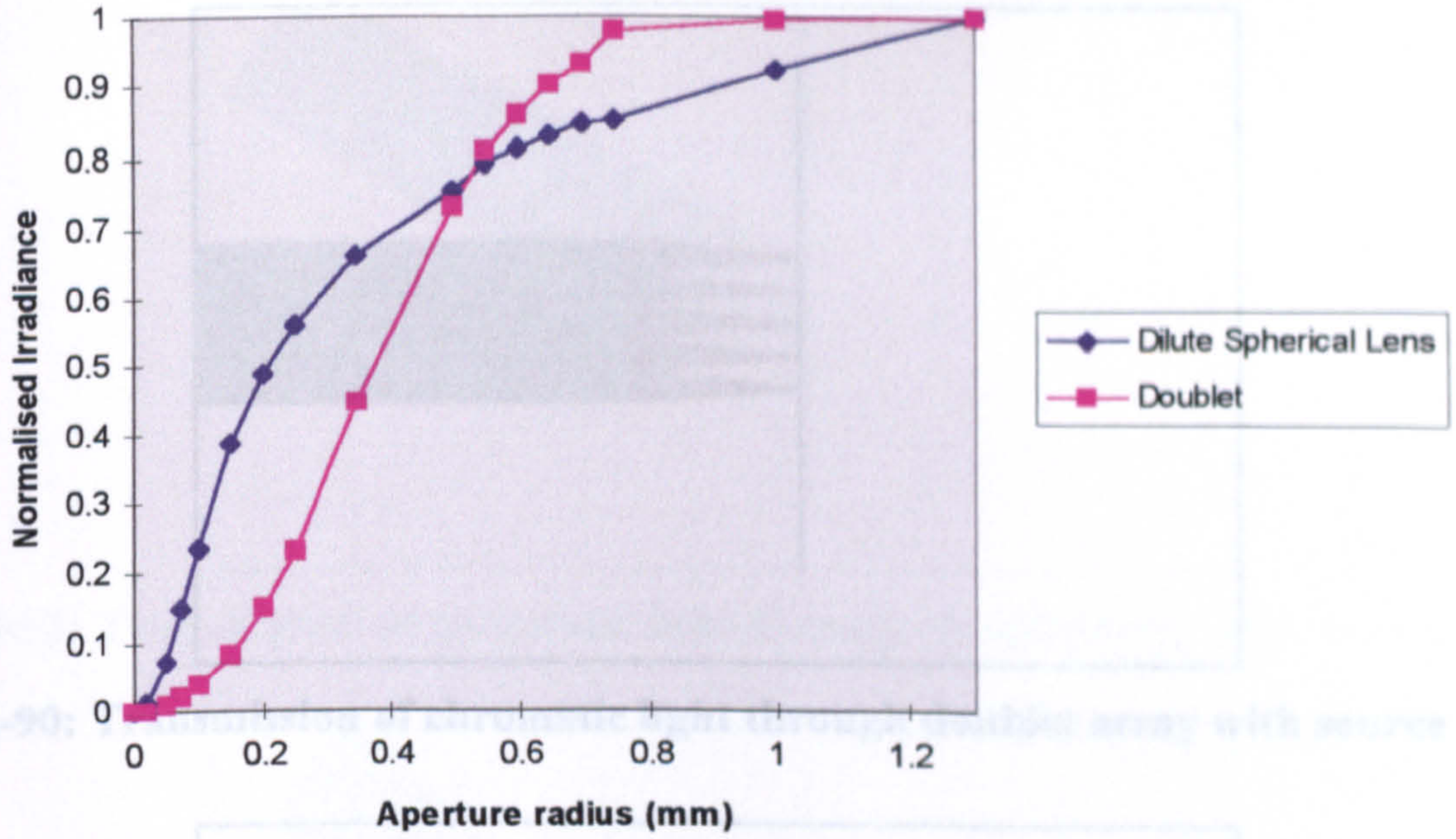

Fig 4-88: Source at 30°.

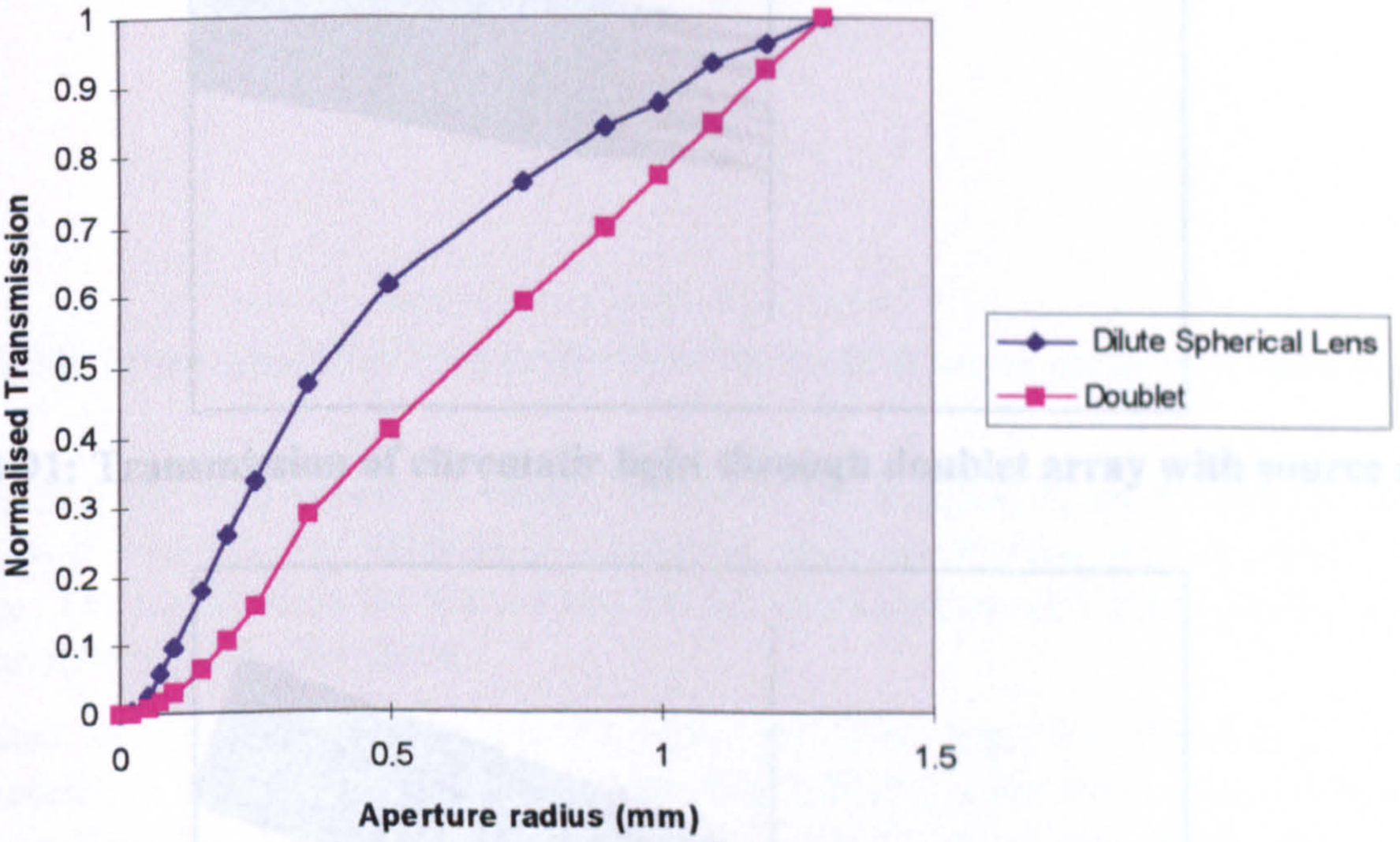

Fig 4-89: Source at 40°.

The results show that between 0° and 20°, the doublet as expected produces a higher quality image than the spherical lenses. The largest diameter obturation tested in the preceding experiments (0.454 mm) would achieve 100% attenuation. However, at 30° and 40°, the aberrations become more significant and the image diffuse. Furthermore at 40°, the attenuation would be worse for the doublet than for the spherical lenses. Although the doublet corrects for aberrations of sharpness, it does not address aberrations such as field curvature or distortion and these can be significant off-axis.

The increase in field curvature is obvious in the ray-traces shown below (Fig 4-90 to Fig 4-94). Best focus is significantly closer to the back surface at 40° than at normal incidence to the array.

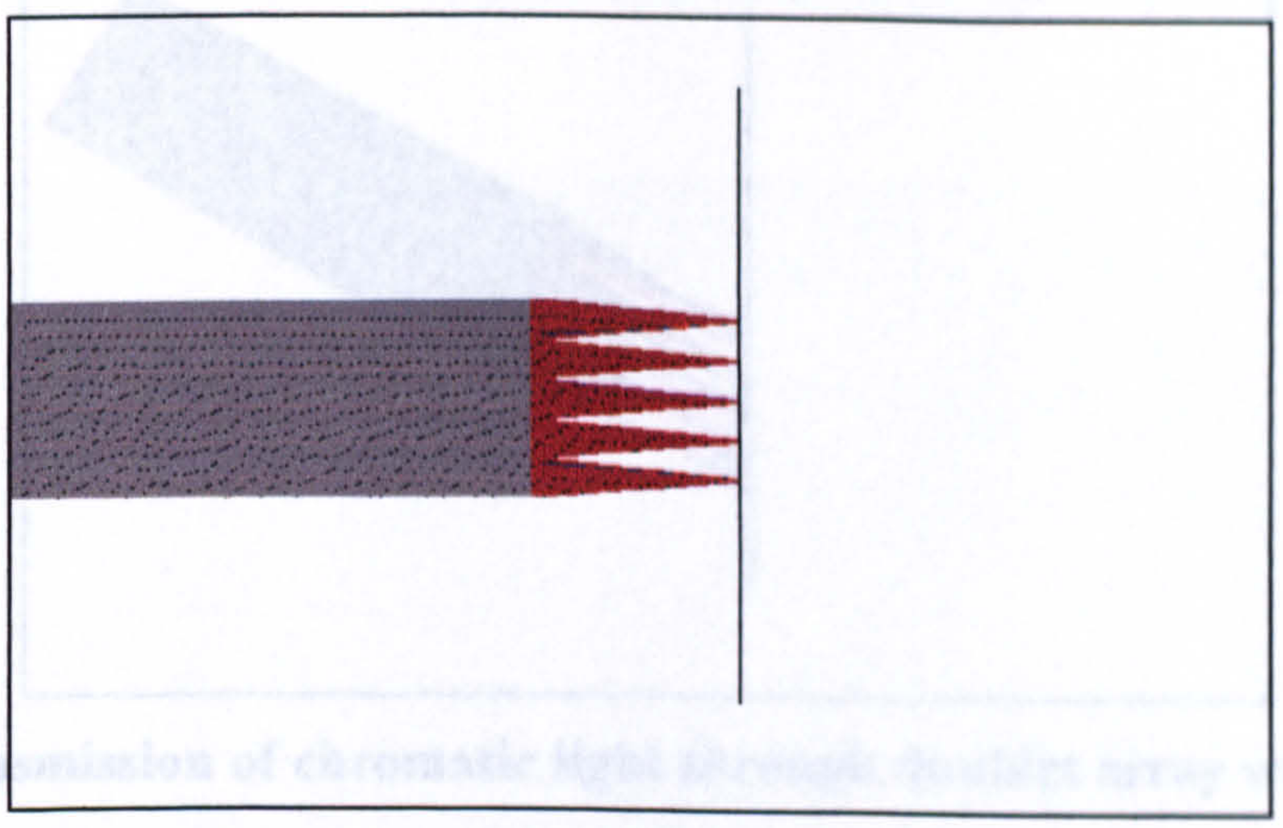

Fig 4-90: Transmission of chromatic light through doublet array with source at 0°.

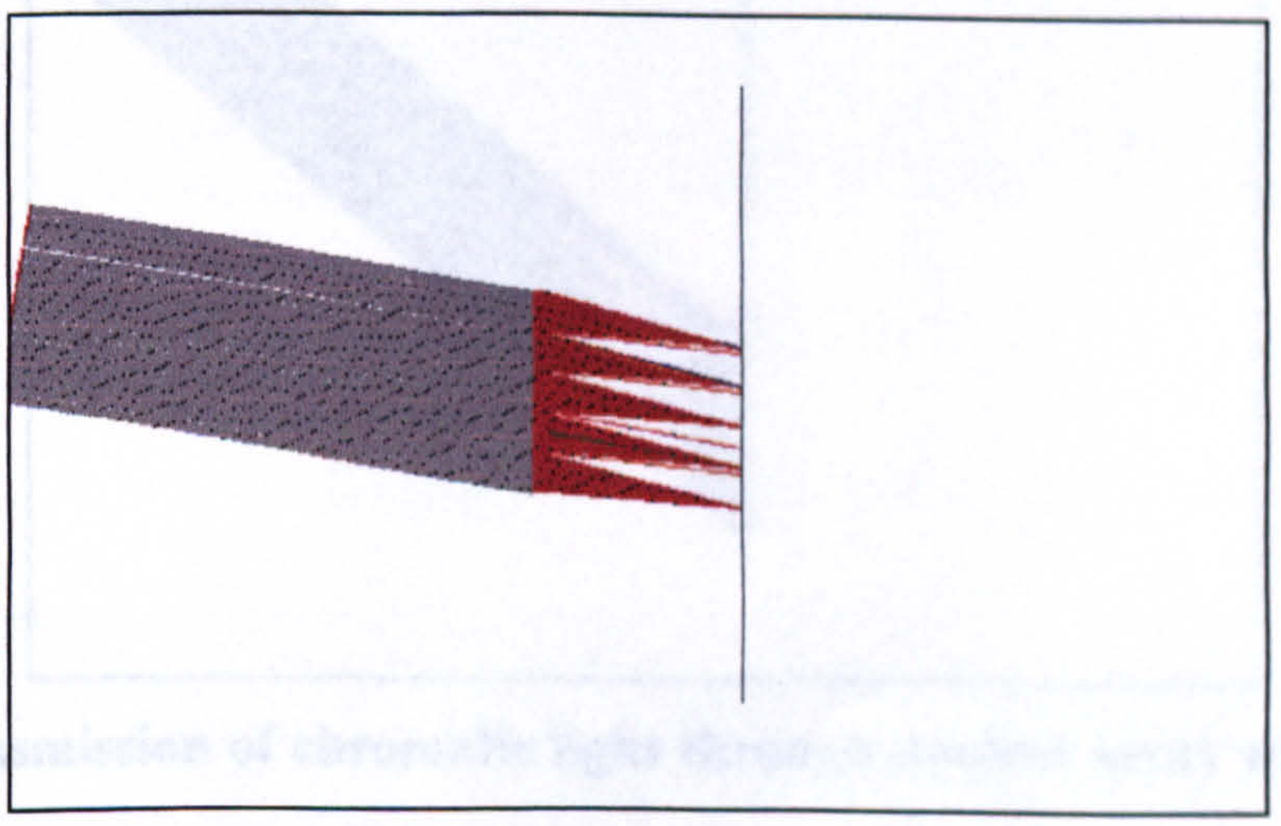

Fig 4-91: Transmission of chromatic light through doublet array with source at 10°.

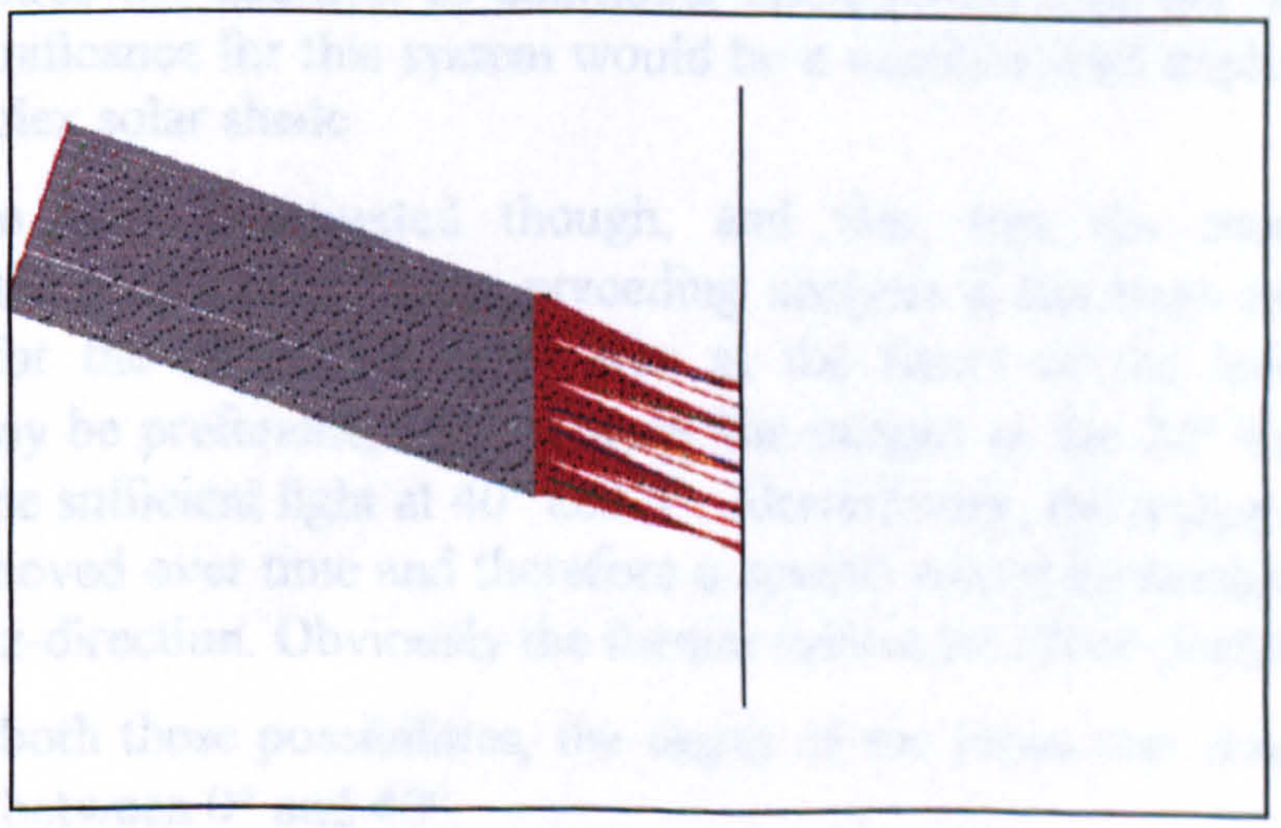

Fig 4-92: Transmission of chromatic light through doublet array with source at 20°.

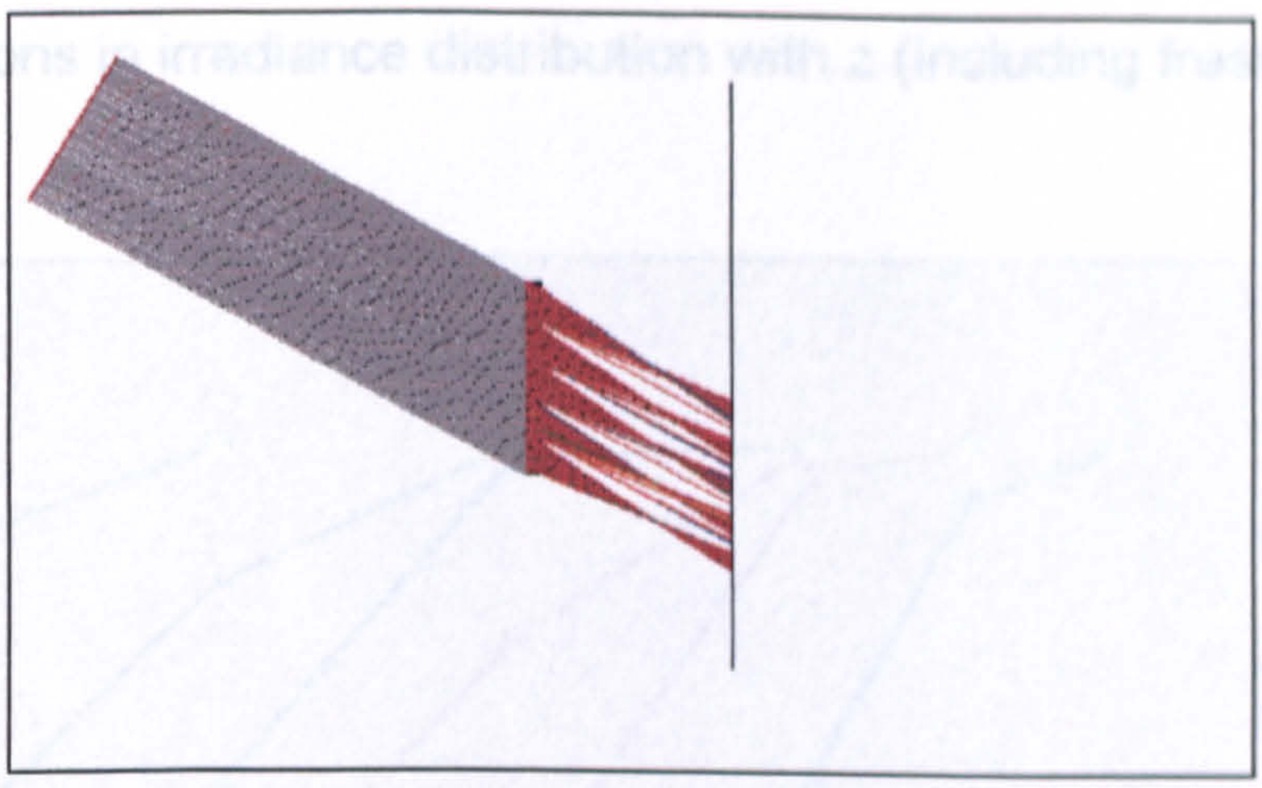

Fig 4-93: Transmission of chromatic light through doublet array with source at 30°.

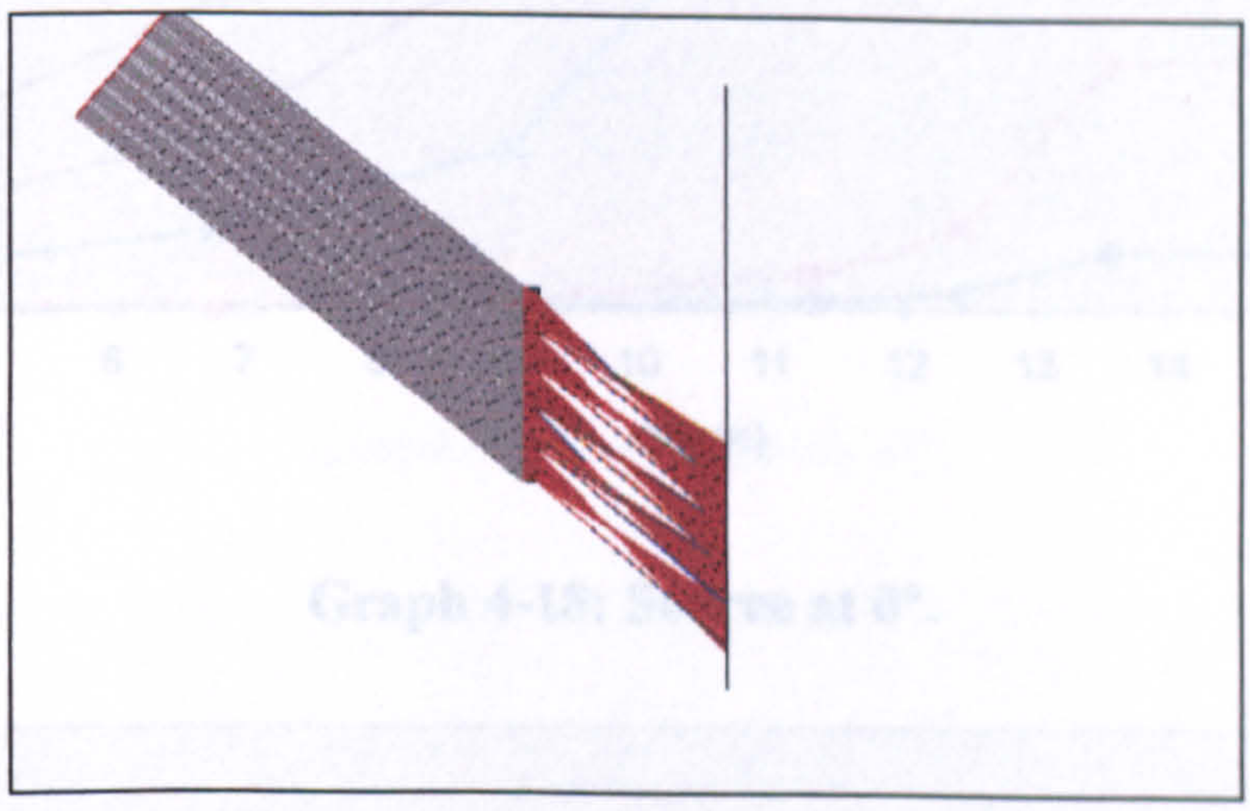

Fig 4-94: Transmission of chromatic light through doublet array with source at 40°.

Correcting for field curvature usually increases the complexity of an optical system because it requires the addition of additional components that are separated by air spaces. The significance for this system would be a window with triple glazing and an extremely complex solar shade.

Another option was investigated though, and that was the translation of the obturations in the z direction. In the preceding analysis it has been assumed that the best position for the obturation array was at the focus of the lenses for normal incidence. It may be preferable, say, to block the images at the 20° best focus which may also exclude sufficient light at 40° and 0°. Alternatively, the image plane may have to be actively moved over time and therefore a system would be needed that translates in the x, y **and** z-direction. Obviously the former option would be preferable.

To investigate both these possibilities, the depth of the focus was determined for the incident angles between 0° and 40°.

4.3.6 Variations in irradiance distribution with z (including fresnel reflections[5])

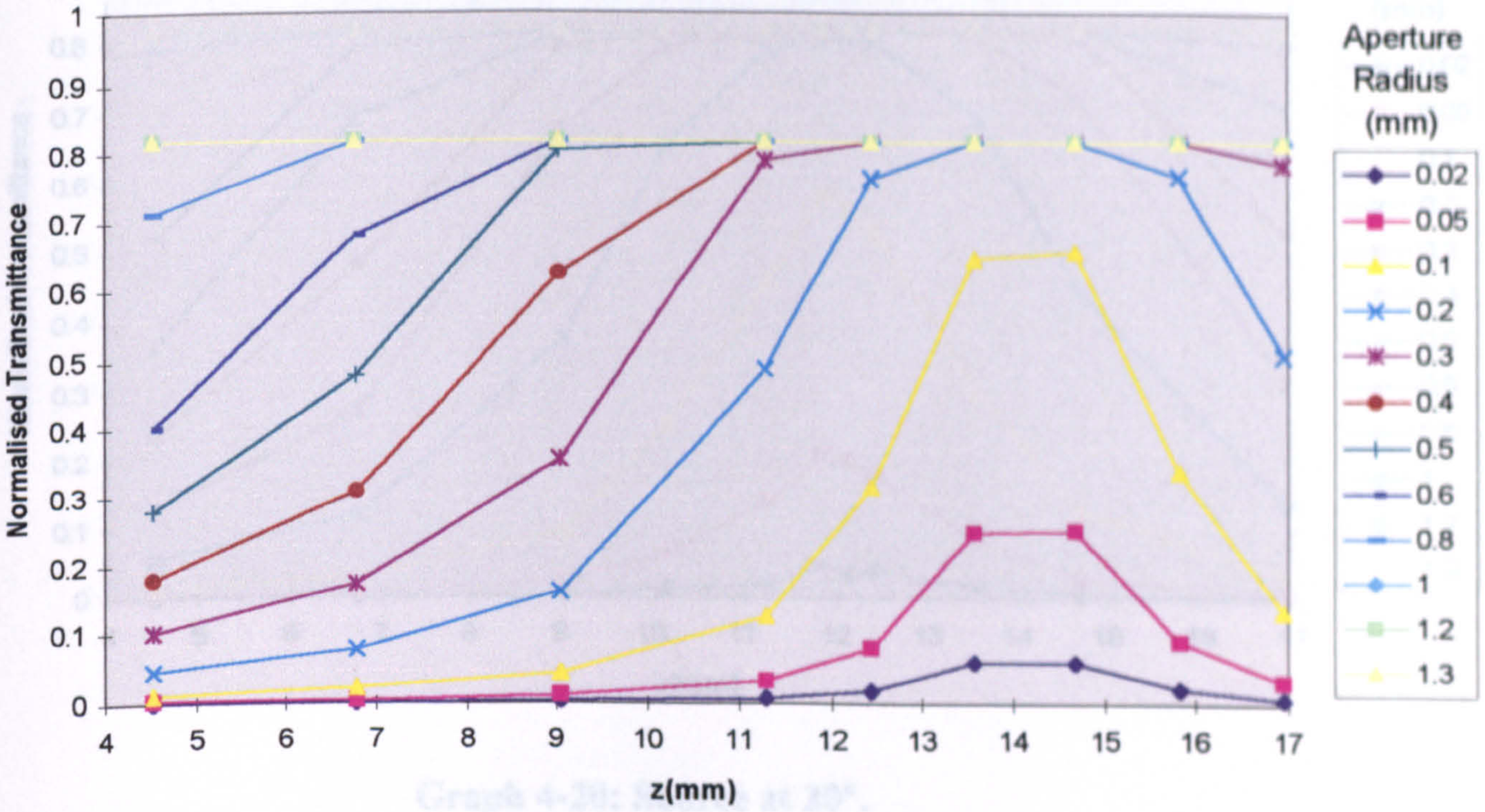

Graph 4-18: Source at 0°.

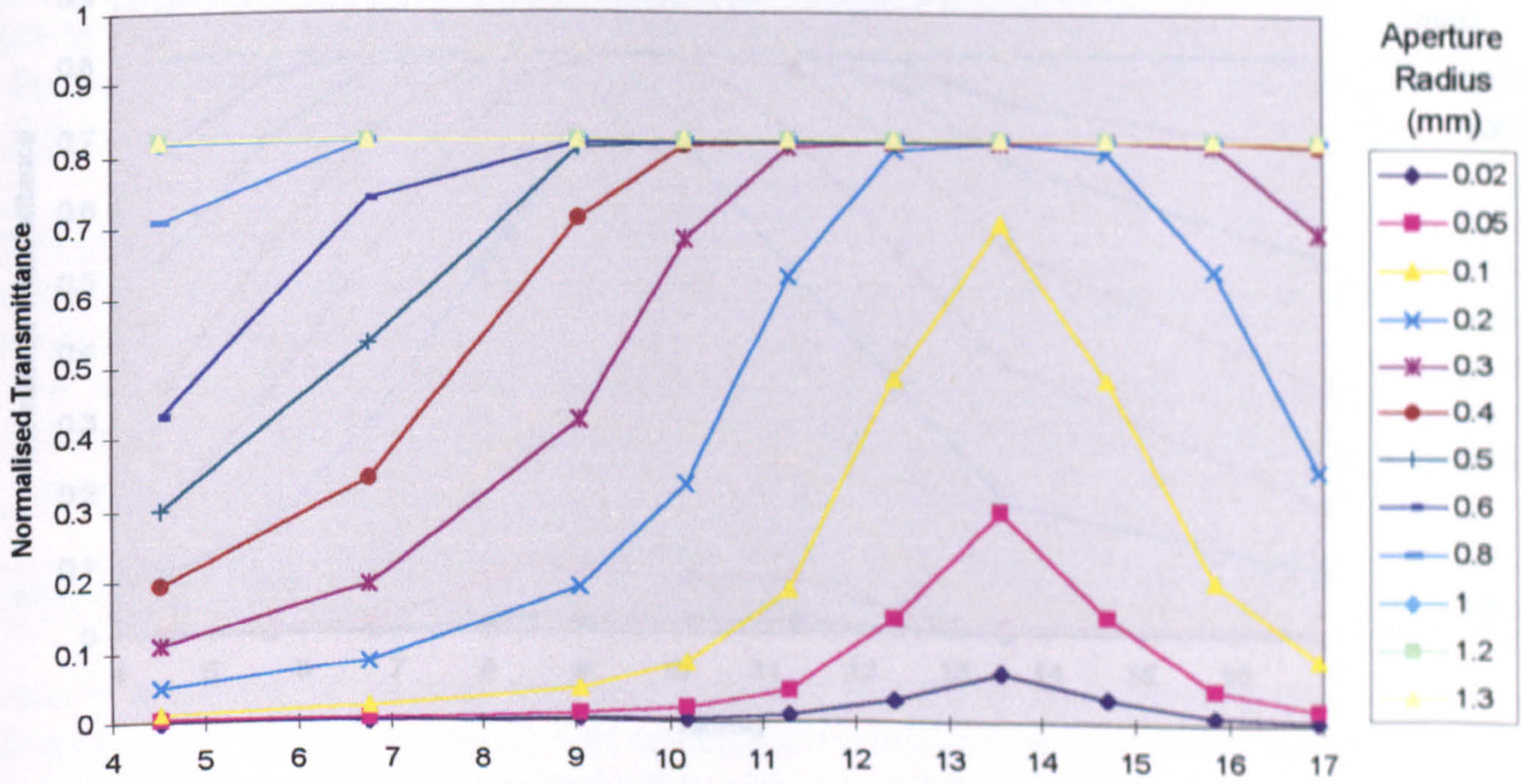

Graph 4-19: Source at 10°.

---

[5] In section 4.3.3 (b) (iii) it was shown that the fresnel losses for hemispherical lenses approximate well to those of a plane surface. As the doublet considered here has much lower radii of curvature at each media interface, then the fresnel losses could be calculated on the basis of plane interfaces as well.

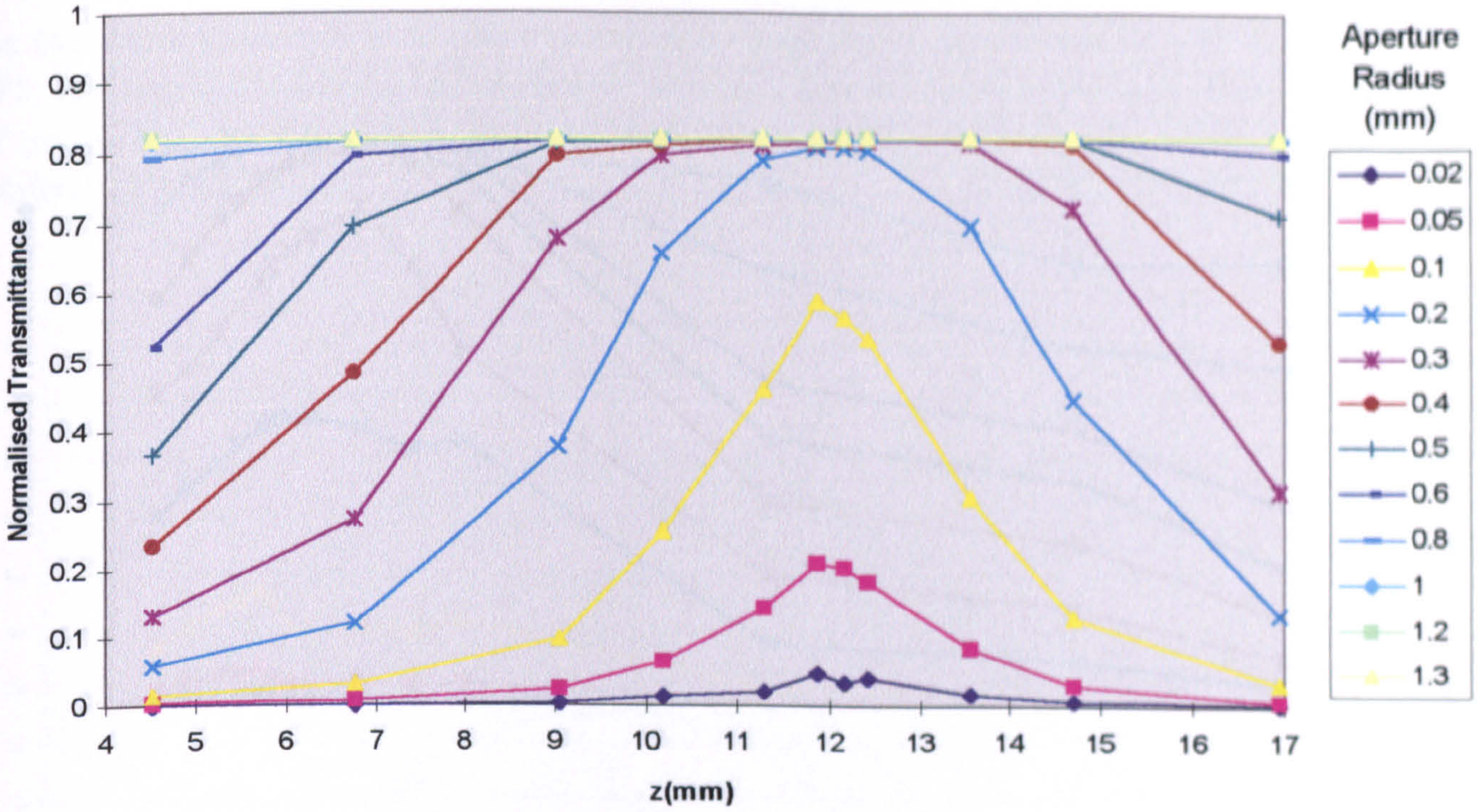

Graph 4-20: Source at 20°.

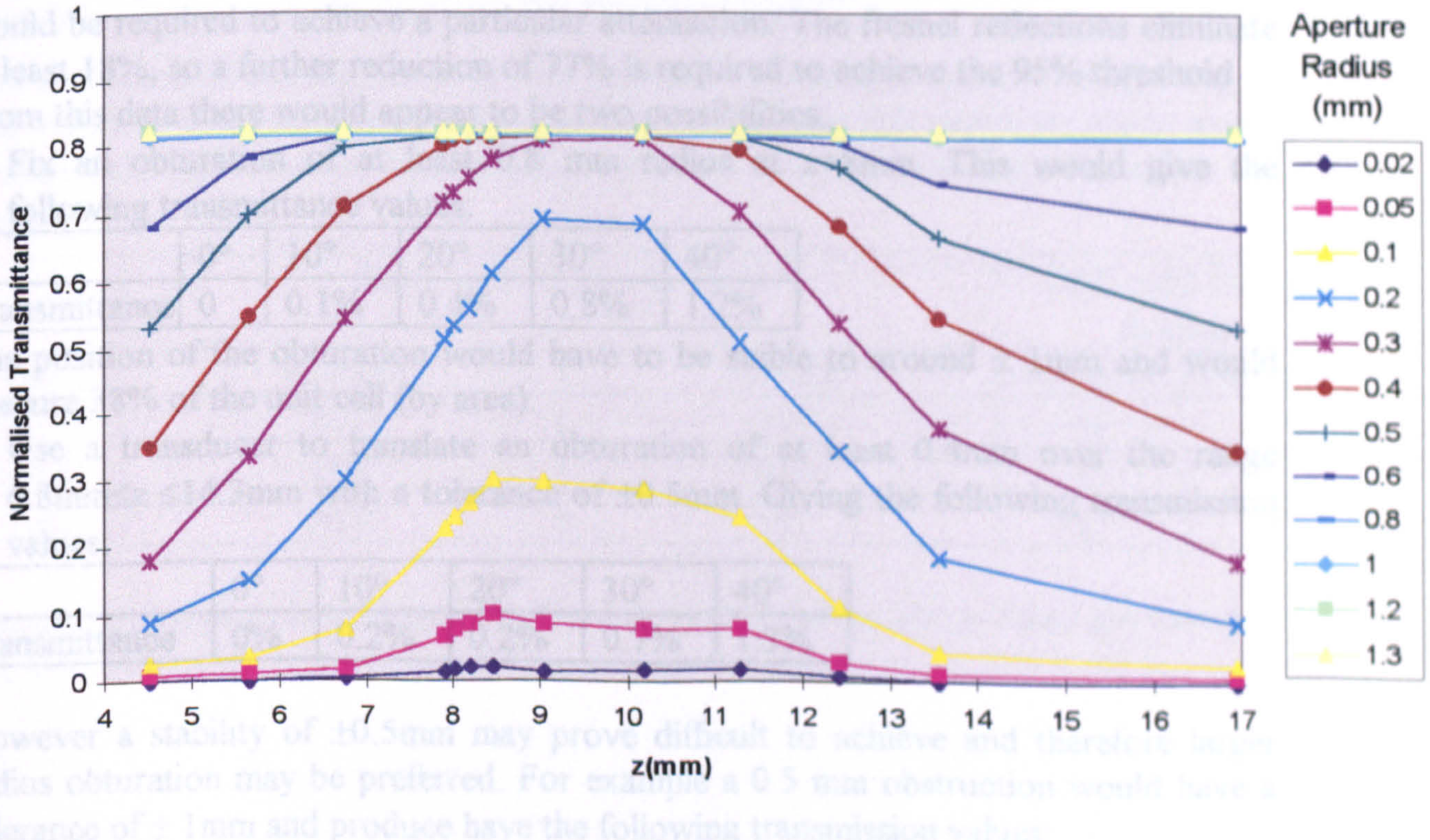

Graph 4-21: Source at 30°.

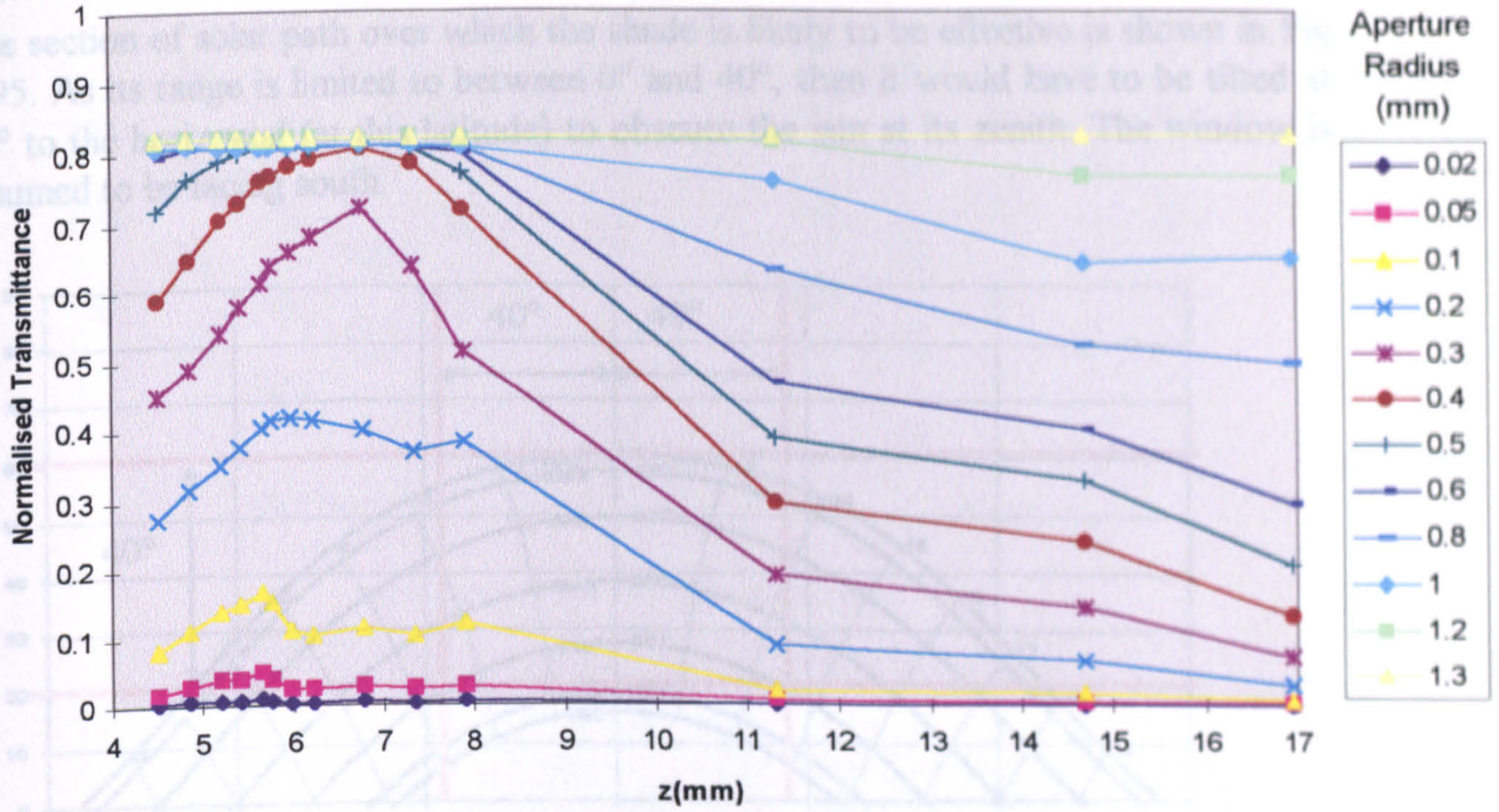

Graph 4-22: Source at 40°.

The above graphs can be used to determine the size and position of an obturation that would be required to achieve a particular attenuation. The fresnel reflections eliminate at least 18%, so a further reduction of 77% is required to achieve the 95% threshold From this data there would appear to be two possibilities:

- Fix an obturation of at least 0.8 mm radius at z=8mm. This would give the following transmittance values:

	0°	10°	20°	30°	40°
Transmittance	0	0.1%	0.4%	0.8%	1.2%

The position of the obturation would have to be stable to around ± 1mm and would obscure 38% of the unit cell (by area).

- Use a transducer to translate an obturation of at least 0.4mm over the range 6.8mm≤z ≤14.3mm with a tolerance of ±0.5mm. Giving the following transmission values:

	0°	10°	20°	30°	40°
Transmittance	0%	0.2%	0.2%	0.7%	1.3%

However a stability of ±0.5mm may prove difficult to achieve and therefore larger radius obturation may be preferred. For example a 0.5 mm obstruction would have a tolerance of ± 1mm and produce have the following transmission values:

	0°	10°	20°	30°	40°
Transmittance	0%	0.1%	0.2%	0.7%	1.1%

It would though increase the obscuration of the unit cell from 9% to 14%.

Of the two options, the static obturation array is to be preferred because it would be technically easier to achieve in practice.

4.3.7 Doublet Array

The section of solar path over which the shade is likely to be effective is shown in Fig 4-95. As its range is limited to between 0° and 40°, then it would have to be tilted at 20° to the horizontal (at this latitude) to obscure the sun at its zenith. The window is assumed to be facing south.

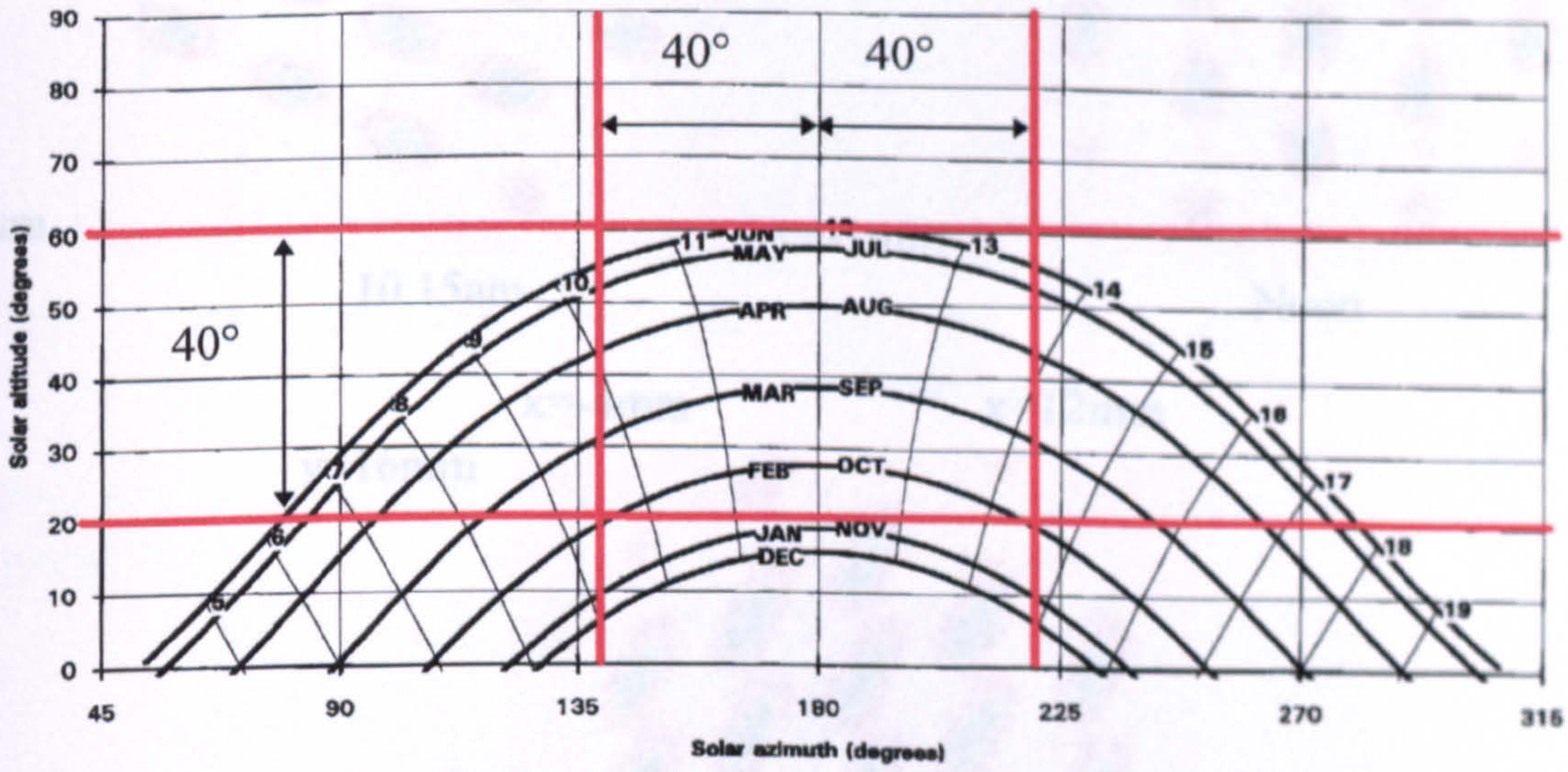

Fig 4-95: Solar path diagram[xvi] for a latitude of 52° (the location of NPL) showing the range of effectiveness for the solar shade.

The simulation of the doublet array was limited to the path of the sun during June, as this would be when the direct sunlight is strongest. During this month the shade would attenuate the light between 10.15pm and 1.45pm. Three points were chosen within this region:

	Angle with respect to Earth		Angle with respect to array	
Time	Azimuth	Altitude	Azimuth	Altitude
10.15am	140°	55°	40°	15°
noon	180°	60°	0°	40°
1pm	207°	59°	-27°	39°

Images formed at a plane 8mm from the back surface, at the above times are shown in Fig 4-96.

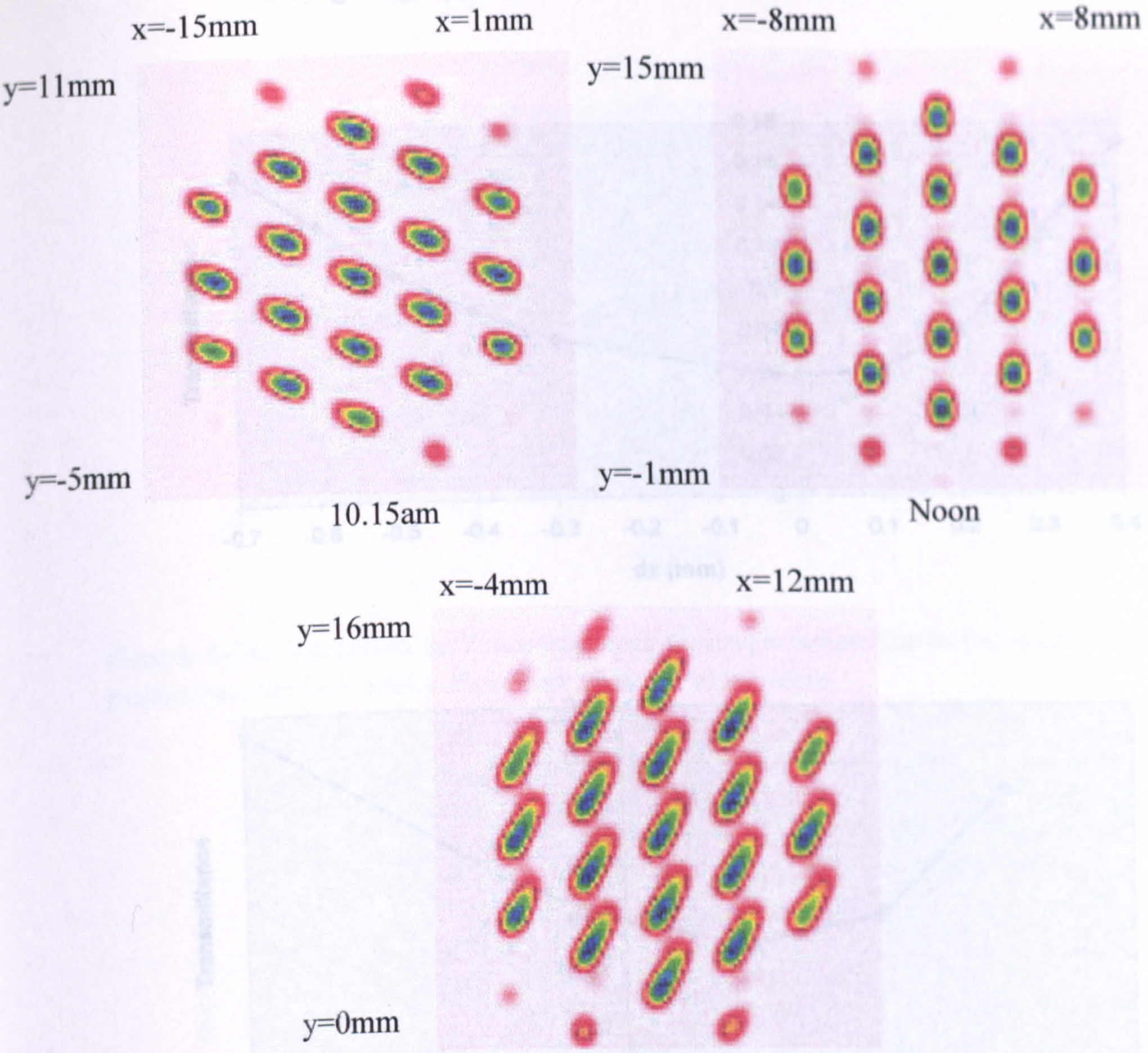

Fig 4-96: Images formed by the doublet lens array at a plane 8 mm from the lens array.

An array of obturations was then centred on the images and incrementally translated to minimise the transmission. Graph 4-23 to Graph 4-25 show the variation in transmission for small perturbations of the obturation array. All figures exclude fresnel reflectances.

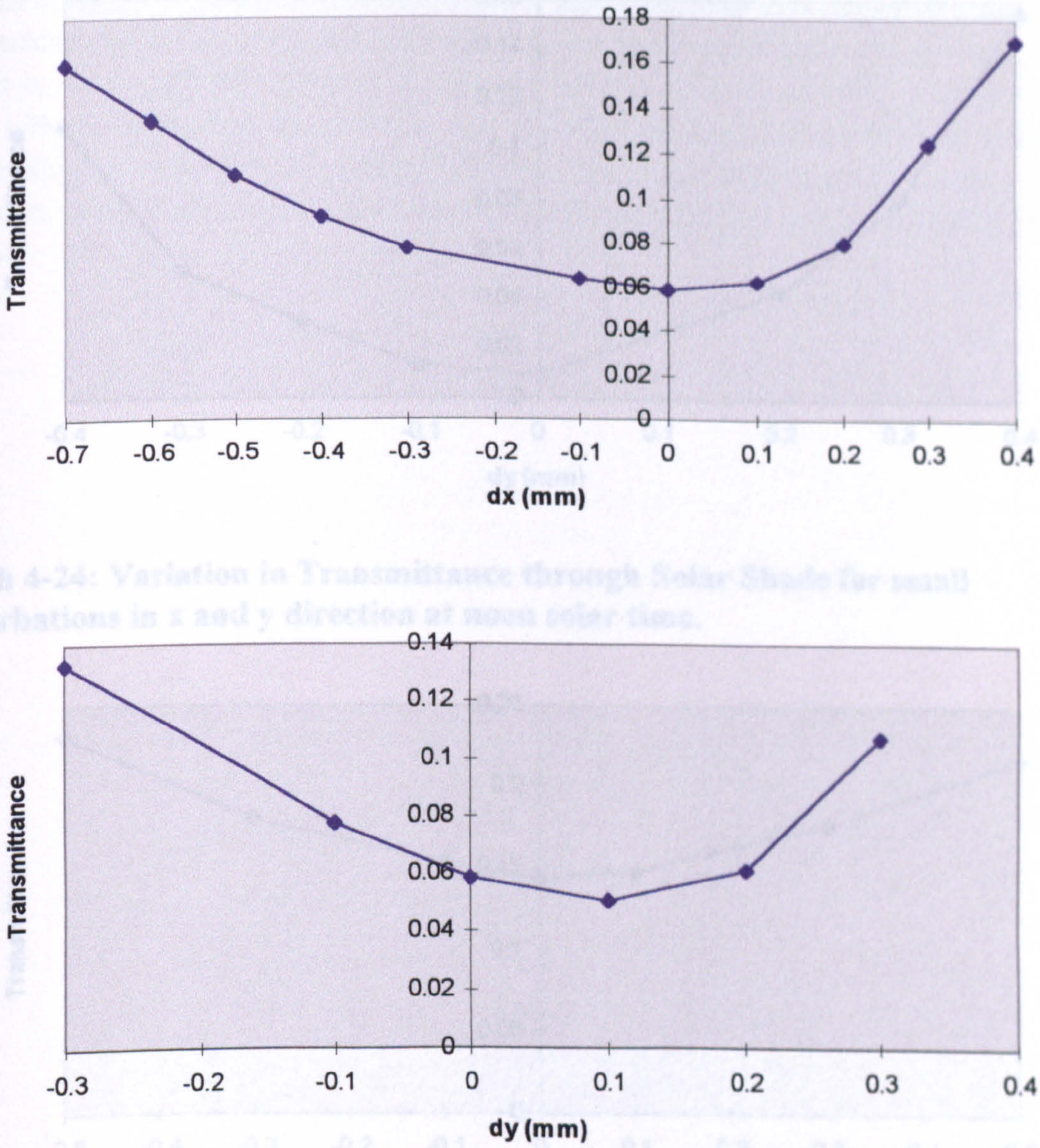

Graph 4-23: Variation in Transmittance through solar shade for small perturbations in x and y direction at 10.15 a.m. solar time.

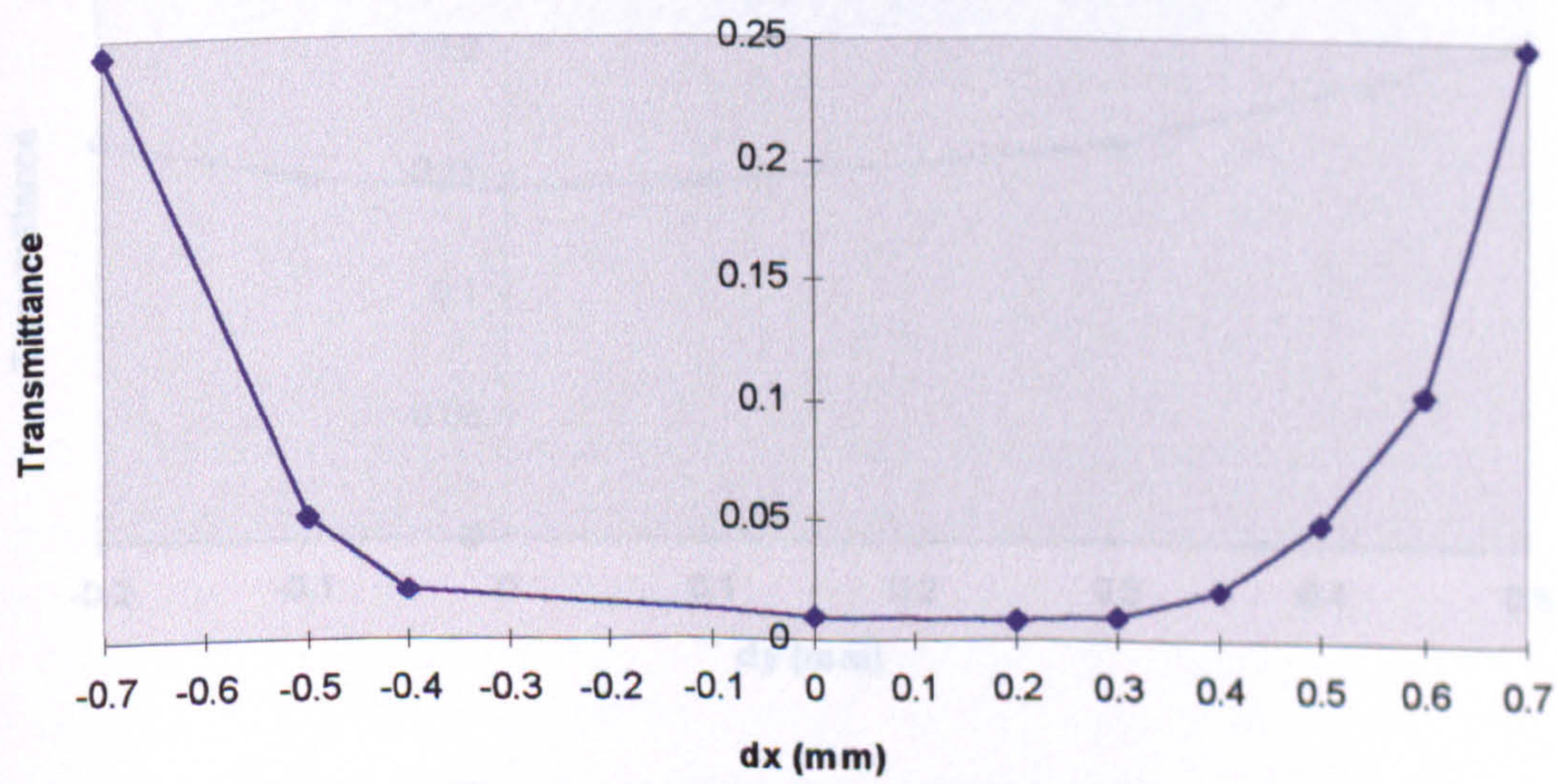

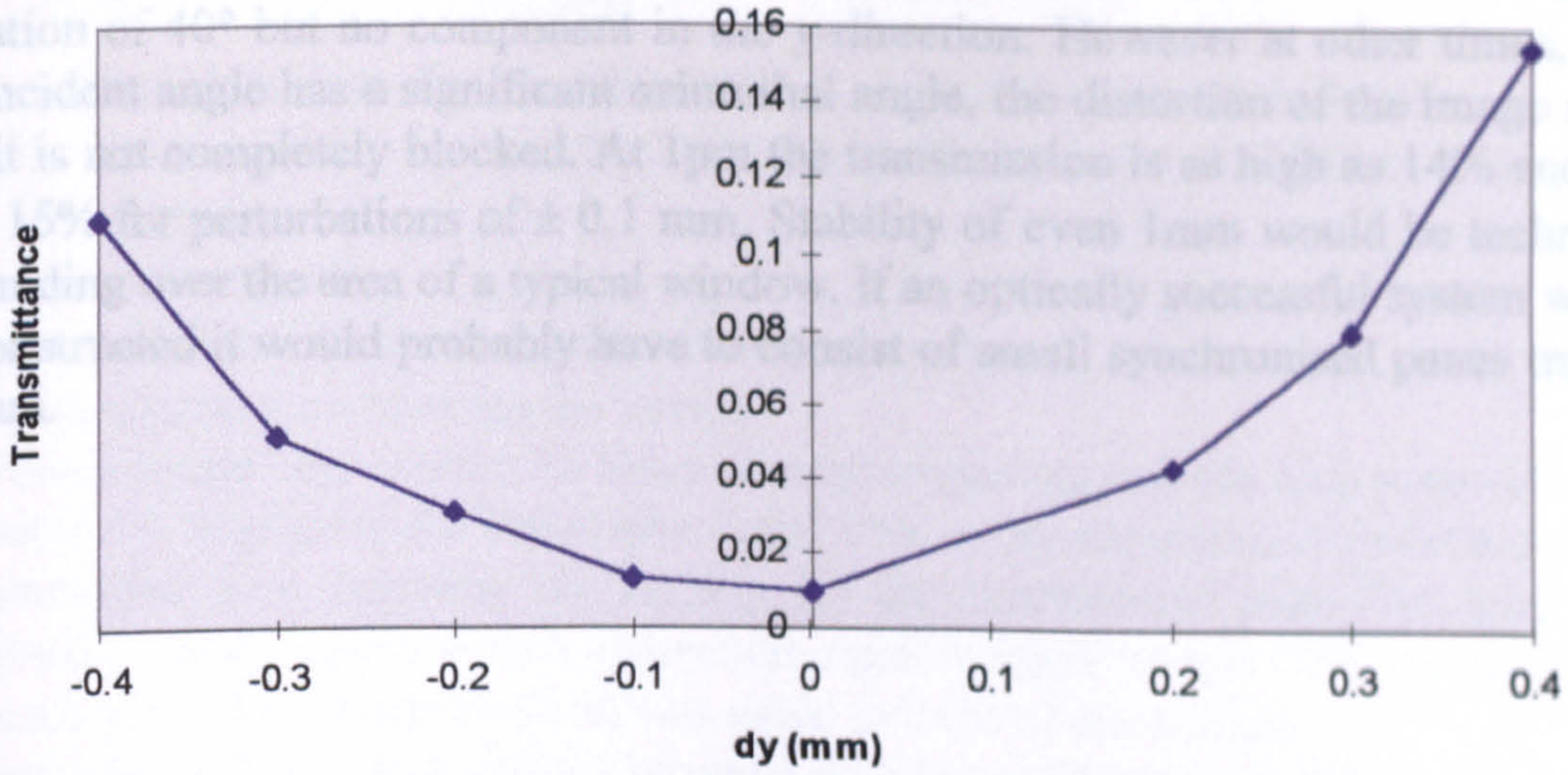

Graph 4-24: Variation in Transmittance through Solar Shade for small perturbations in x and y direction at noon solar time.

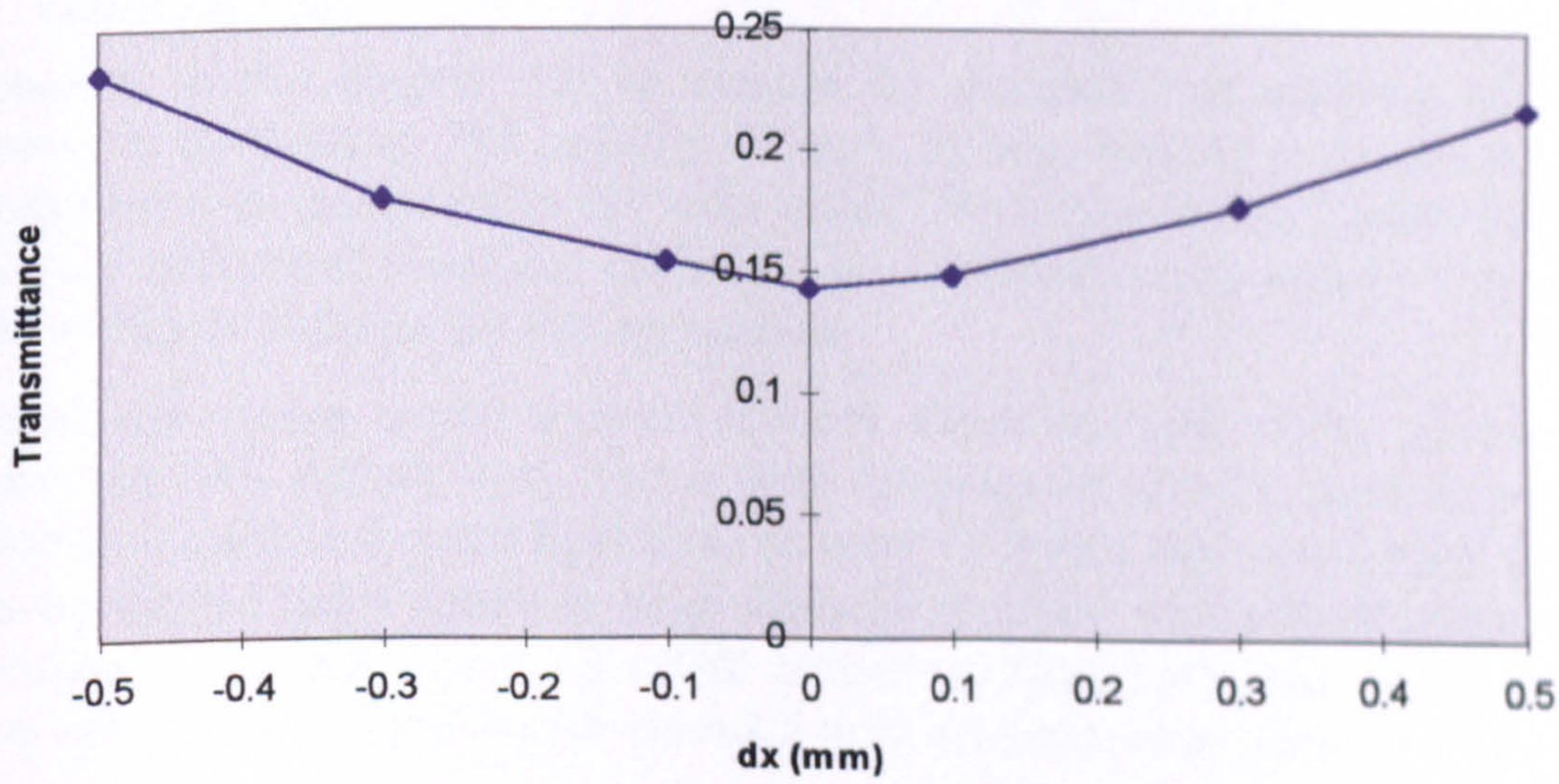

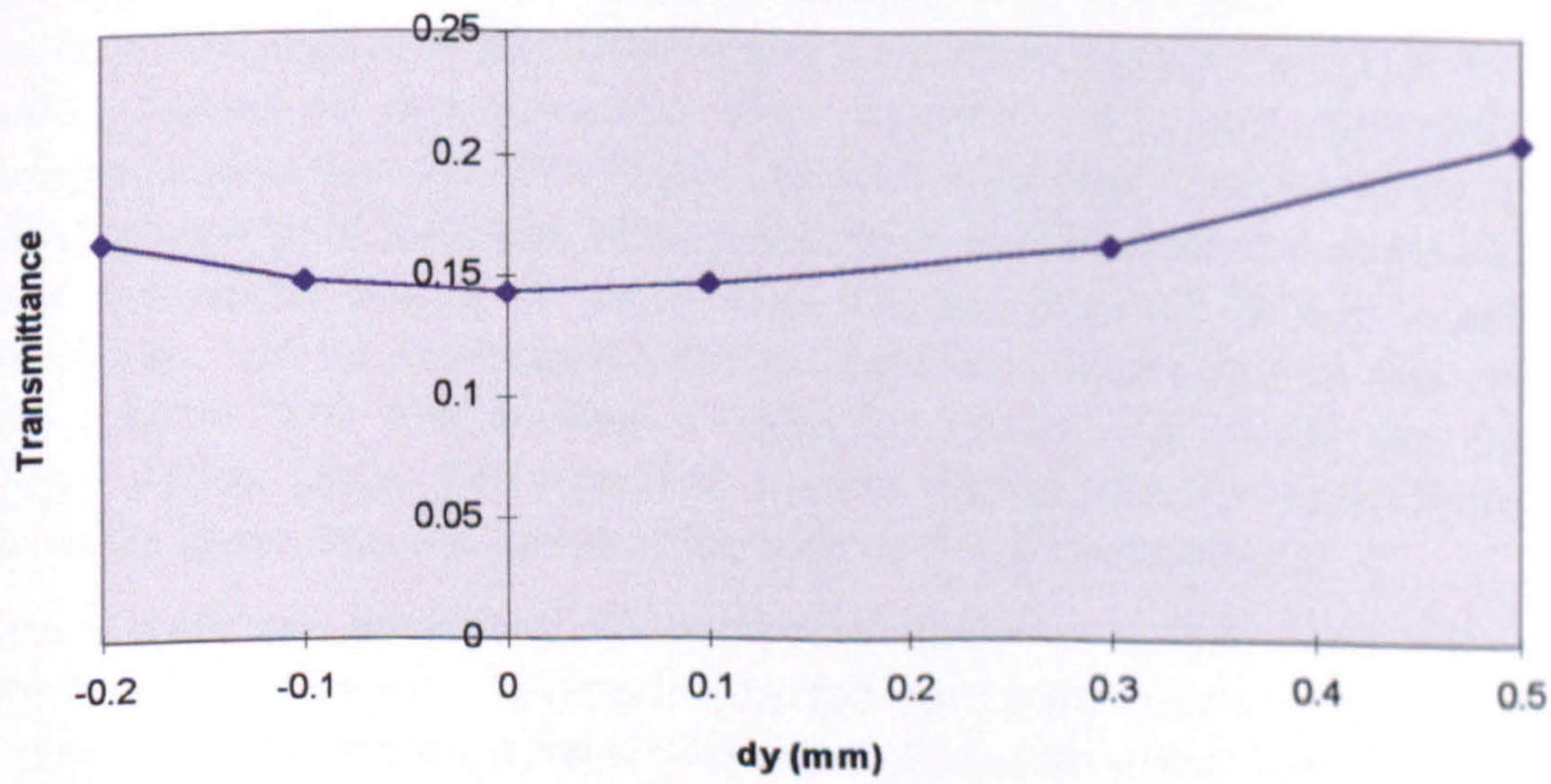

Graph 4-25: Variation in Transmittance through Solar Shade for small perturbations in x and y direction at 1pm solar time.

The obturations efficiently exclude direct sunlight at noon, when the sun has an elevation of 40° but no component in the y-direction. However at other times, when the incident angle has a significant azimuthal angle, the distortion of the image means that it is not completely blocked. At 1pm the transmission is as high as 14% and rises over 15% for perturbations of ± 0.1 mm. Stability of even 1mm would be technically demanding over the area of a typical window. If an optically successful system were to be constructed it would probably have to consist of small synchronised panes tracking the sun.

4.3.8 Diffuse Light transmission

All the research has so far been directed at minimising the transmission of direct sunlight, however there are mechanisms that will attenuate the diffuse daylight as well. These are:

- Fresnel reflectances
- Unfocused light illuminating the obturation array
- The interstitial area between the lenses

The fresnel losses approximate to those of double glazing and the area covered by the obturations is negligible for unfocused light. The major reduction is therefore due to the interstitial area between the lenses. In the photometry plots the lens were hexagonally close packed with a separation equal to their period. This represents the minimum 'dead' interstitial area and was equal to 24% of the surface.

Assuming the diffuse transmittance of clean double glazing to be 0.7[xvi], the theoretical limit for the solar shade would be 53%. This is comparable to the target of 55% for thin films (see page 4-12). It is also significantly higher than the minimum acceptable transmittance for glazing of 38% established by Boyce[xii].

4.4 Conclusions

The purpose of this chapter was to explore the possibility of applying microlens technology to daylighting. The majority of the work was directed at the development of transparent solar protection or the 'solar shade'. Two other systems were examined briefly (the cylindrical microlens diffuser and the afocal beam-steerer) but neither showed sufficient potential for this application.

The ideal solar shade would transmit 0%-5% direct sunlight whilst allowing the admission of 80% diffuse light. The system investigated at NPL used an array of obturations to exclude focused light from an array of lenses that would track the sun. The lenses chosen had a relatively large diameter (2.6mm) with a focal plane on the back surface of the lens. The power of the lenses was therefore reduce with a layer of silicone rubber and the focal length extended from approximately 4 mm to 14 mm.

Initial experiments showed that the system would only reduce the transmission of direct sunlight to 42% with 0.454 mm obturations at 0° incidence. To improve the attenuation of the light, the interstitial areas were made opaque, which reduced the attenuation further to approximately 20%. Visually the image appeared to be significantly smaller than the obturations The remaining laboratory work was directed at locating the source of this light. Measurements on the obturations demonstrated that they were sufficiently opaque for the system. The alignment of the lens images with the obturations was the investigated but no significant improvement was achieved over the original 20% transmission. Finally the energy distribution was analysed revealing a diffuse image that extended 4 times further than its visual appearance. This extended image was the source of the relatively high transmission.

Subsequent work was performed via computer simulation to determine if the shade was theoretically possible. Differences in the simulated to measured attenuation values were less than 5% for a range of obturation diameters and therefore the model was considered to representative of the system. As the angle of incidence increases, photometry plots showed that the individual images become indistinct after 40°. Therefore to prevent glare at higher angles the array would have to be tilted. Analysis

of the losses within the system demonstrated that below a threshold angle Θ, the obturations cause the major losses within the system. However above this angle it is the reduction in the aperture that causes the greatest attenuation.

To improve on this system an array of doublet lenses was considered. The doublet produced an image of less than 0.2mm diameter, compared to the diffuse image of the power reduced array that has a diameter> 1.2mm. As the angle of incidence increases, the image diameter increases until at 40° the doublet is producing a larger image the power-reduced lens.

Ray-tracing showed that a contributor to the image enlargement was field curvature. In optical systems, the presence of this aberration leads to a greater number of individual optical elements. In the solar shade this would mean triple glazing. Changing the position of the obturation array from the focus at normal incidence (14 mm from the back surface) to 8mm behind the array meant that transmittance values of less than 1.2% were achievable (for 0.8mm obturations).

However, the work had so far assumed that the solar azimuth was 0°. By changing the source position to match points on the solar path it was shown that attenuation is critically dependent on the azimuthal value. At 1pm for example the position of the obturations would have to be stable to ±0.1mm to maintain a 15% transmission value (excluding fresnel losses).

The solar shade described above does improve on the transparent protection provided by thin films in the visible spectrum (see section 4.2). The target transmission value for a thin film is 20% compared to the 15% provided by the tilted doublet array. The films though do not suffer from the tight mechanical tolerances that are required when the solar shade is tracking the sun.

Future research should centre designing an optical system with a superior off-axis performance. Reducing the size of the focused image will also reduce the mechanical tolerances on the system. This will dictate the nature of the tracking device. In addition the period of the arrays should be considered. Increasing the size of the lenses may allow more sophisticated optics to be used and also reduce the number of obturations required. Consequently the transmission of diffuse light could be optimised, whilst still attenuating the direct light. This will also have implications for any mechanical tracking system.

The work described in this chapter could be the beginning of an effective solar shade that significantly reduces glare discomfort for room occupants.

i Daly D, Stevens R F, Hutley M C, Davies N, 'The Manufacture of Microlenses by the Melting of Photoresist', Measurement Science and Technology vol 1, no. 8, August 1990, p759-66.

ii Goltsos W, Holz M, 'Agile Beam Steering Using Binary Optics Microlens Arrays', Optical Engineering, vol 29, (11), pp1392-1397 (1990).

iii Smith G B, Dligatch S, Sullivan R, Hutchins M G, 'Thin Film Angular Selective Glazing', Solar Energy, vol 62, part3, pp229-244, (1998).

iv Aizlewood M E, 'Innovative Daylighting Systems: an Experimental Evaluation', Lighting Research and Technology 22 (1) pp141-152 (1993).

v Littlefair P J 'Light shelve: Computer Assessment of Daylighting Performance' Lighting Research and Technology 27 (2) pp79-91 (1993).

vi Lee E S, DiBartolomeo D I, Selkowitz S E, 'Thermal and Daylighting Performance of an Automated Venetian Blind and Lighting System in a Full-Scale Private Office', Energy and Buildings, vol 29, pp47-63, (1998).

vii Smith G B, Dligatch S and Ng M W 'Low Emittance Angular Selective Window Systems' Proc. SPIE vol 253 pp317-325 (1995).

viii Smith G B, Dligatch S, Jahan F, 'Thin Film Angular Selective Glazing', Renewable Energy, vol 15 part 1-4, pp183-188 (1998).

ix Bell J,'Intelligent Windows will Challenge Building Firms', Opto and Laser Europe, Issue 37, February 1997, pp 21-25.

x Green M, 'WO3- Based Electrochromic Windows- Problems and Status,' Institute of Ionics, vol 5, part 3-4, pp 161-170, (1999).

xi Georg A, Graf W, Schweiger D, Wittver W, Nitz P, Wilson H R, 'Switchable Glazing with a Large Dynamic Range in Total Solar Energy Transmittance', Solar Energy, vol.62, no. 3, pp 215-228, (1998).

xii Boyce P, Eklund N, Magnum S, Saalfield C, Tang L 'Minimum Acceptable Transmittance of Glazing', Lighting research Technology 27 (3) 145-152 (1995).

xiii Chauvel P, Collins J B, Dogniaux R, Longmore L, 'Glare from Windows: Current Views of the Problem', Lighting Research and Technology, 14 (1), pp 31-46 (1982)

xiv Bhatia R, Hutley M C, Gombert A, 'Daylighting Applications of Microlens Arrays', EOS Topical Meeting: Microlens Arrays, May 1997, National Physical Laboratory, pp 98-100 (1997).

xv Hecht E 'Optics, Second Edition', Addison Wesley, (1987).

xvi Littlefair P J, 'Designing with Innovative Daylighting', Building Reserch Establishment Report, (1996).

5. Thesis Conclusions

The purpose of this thesis was to develop novel optical devices that could improve interior illumination and reduce the energy bill in a variety of buildings. The aim was to exploit existing industrial technology to manufacture a low-cost daylighting system. Several methods have been explored in this research, however the two principle devices were an array of microprisms and an array of microlenses.

Much time was spent on exploring the optical properties of the microprisms, however the critical aspect of their performance was measured in large scale testing in an office. Significant improvements in the internal illumination were accompanied by very strong glare and therefore would be unacceptable to the occupants. There was not sufficient diffusion by the imperfections in the structure to mitigate the glare discomfort. It is doubtful that any structure that relies on refraction could produce sufficient deviation over a wide range of solar angles. It is equally unlikely that any system that directs sunlight towards occupants could negate glare through surface roughness alone. It is the author's opinion therefore that a structure of the nature described in this thesis would not be successful.

Reflective systems would certainly be more capable of achieving the desired deviation angle: either through a mirrored surface or through total internal reflection. The latter is to be preferred over the former as it does not cause the lengthening of the incident illumination on reflection and consequently avoids infrared heating effects. It is very easy when designing such systems to rely on ray-tracing techniques that mimic the solar position. However, completely clear skies are a rarity in northern Europe and therefore the development process must place a great emphasis on diffuse sky conditions.

The second micro-textured surface explore in this thesis was the microlens array. Unlike the prisms, its purpose was to exclude sunlight and thereby reduce glare by tracking the sun and blocking its focused image with obturations. Such a system would not cause darkening of the room (and the use of electric lighting) as skylight would still be admitted.

Direct sunlight is very intense and therefore requires a high degree of attenuation, which requires a precise alignment between lens array and obturation. It was unlikely that such precision would be achieved with microlenses and therefore lenses on the millimetre scale were explored instead. Such lenses could not be produced using the same process as the microprisms because of the change in size and therefore would be more expensive.

The system tested in the research used spherical lenses, which are the optically simple and easy to mass-produce. Despite reducing the power of the lenses to reduce aberrations and blocking the interstitial areas, the desired level of attenuation (95%) was not obtainable. Modelling of the system with a ray-tracing package showed that to achieve such a low transmission would require an obturation with a diameter that would exclude nearly all of the diffuse as well as the direct sunlight.

In order to produce a smaller solar image, a more complex lens system was sought. The doublet lens investigated improved on the singlet at low solar angles, but produced a more aberrated image at the higher angles. Furthermore, when the two-dimensional solar path was considered, the mechanical tolerances required for the tracking system to maintain the alignment between the obturation and the array would

be extremely demanding. Achieving a stability of 0.1 mm over a large glazed area in any weather conditions is unlikely to say the least.

To improve the system a lens system would have to be designed specifically for extreme, off-axis sources. Such a device is likely to be complex, involve triple glazing and be considerably more expensive than the methods described in this thesis. It is doubtful that this would be achievable with lenses other than those on the macroscopic scale.

Appendix A

The determination of errors in the thesis uses the student-t statistical method. The error at the 95% confidence level for n measurements is given by:

$$\sigma_{95\%} = \sigma_{n-1}(t/n^{1/2})$$

where:

σ_{n-1}= standard deviation
and t is obtained from the table below*

n	t
(1)	(12.7)
2	4.3
3	3.18
4	2.78
5	2.57
6	2.45
7	2.37
8	2.31
9	2.26
10	2.23
15	2.13
20	2.09
30	2.04
50	2.01
100	1.98
200	1.97
∞	1.96

* Campion P J, Burns J E, Williams A, 'A Code of Practice for the Detailed Statement of Accuracy', Her Majesty's Stationary Office, London (1973).

Appendix B

Given below is the product data obtained for the 3M prisms tested in Chapter 2.

3M™ Brightness Enhancement Film (BEF) II

A brilliant solution for improved backlight efficiency

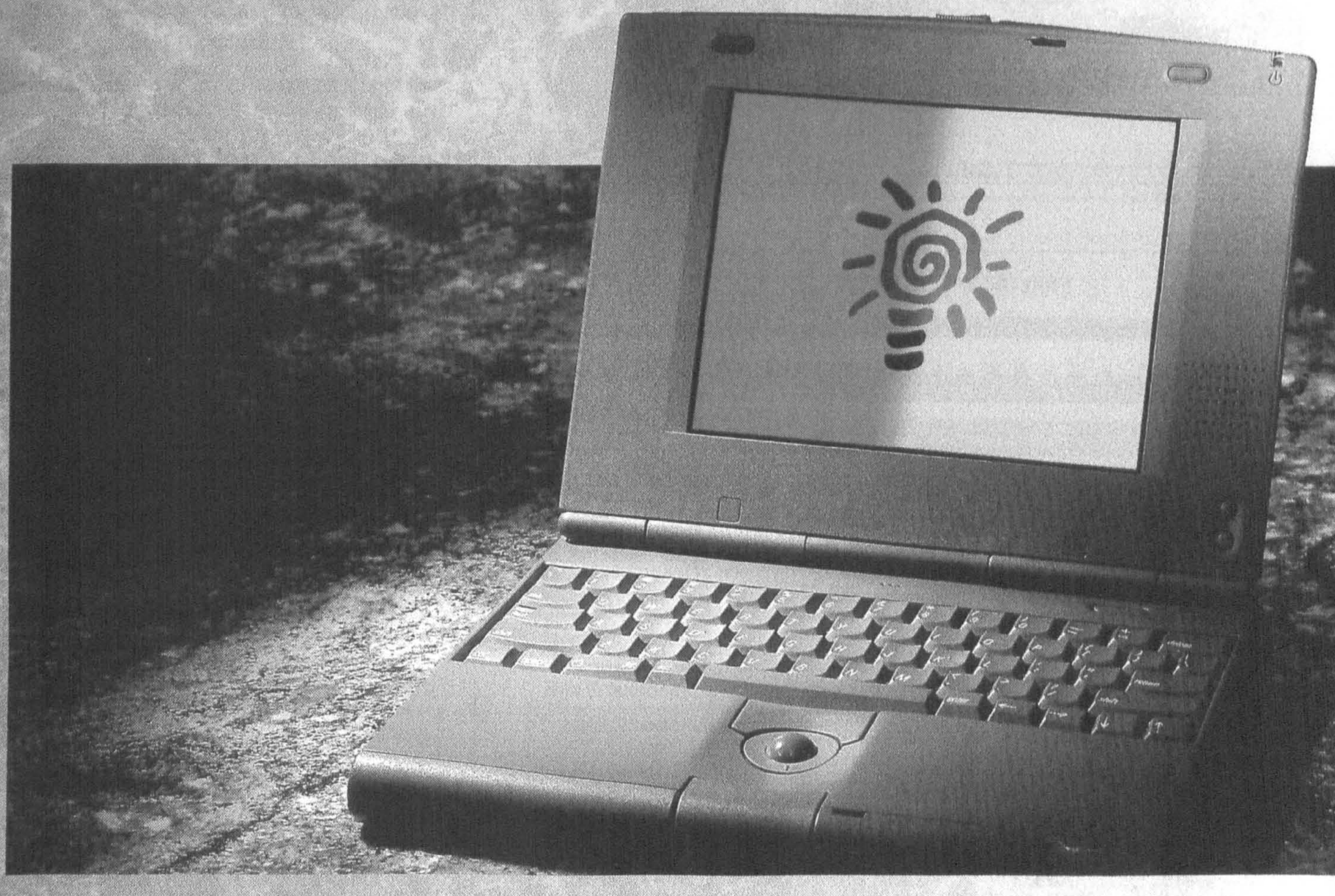

Get more out of your displays

3M Brightness Enhancement Film (BEF) II is a transparent optical composite that improves backlight efficiency by controlling the exit angle of light using a micro-fine prismatic pattern. 3M BEF II can make your LCD displays up to 120% brighter.

3M BEF II is the second generation of 3M Brightness Enhancement Film. Manufactured by an improved process, BEF II is thinner than 3M's industry-leading BEF I, and has an optimal prism pitch and angle. The prismatic structure of 3M BEF II increases brightness while reducing moiré patterns.

Enhanced screen brightness

Improved battery and lamp life

Even the latest, most efficient laptop computers consume much of their nominal operating power simply lighting the display. By incorporating 3M BEF II into your displays, you can reduce backlight power requirements — and increase useful battery life between recharging. Reducing power to the lamp also lowers the heat load placed on the electrode, extending its usable life.

Increased power efficiency

Proprietary 3M optical technology

The key technologies involved in making BEF II are proprietary to 3M. No other film offers the efficiency of 3M BEF II.

Easy to incorporate into your manufacturing process

Incorporating 3M BEF II into your displays is easy. It's available in precut custom sizes. 3M BEF II requires no lamination and works with almost every backlight or light guide. At less than 0.006″ thick, 3M BEF II adds virtually no weight or thickness to your display.

Works in a variety of applications

3M BEF II is designed for use with almost any diffuse light source. Applications include LCDs, electroluminescent panels, laptop computers, word processors, personal TVs, camcorders, mobile communication devices, automotive and avionic displays, and more.

3M *Innovation*

3M™ Brightness Enhancement Film (BEF) II

How it works

3M BEF II employs two principles — refraction and reflection — to increase the efficiency of your backlight. 3M BEF II refracts light within the viewing cone (up to 35 degrees off the perpendicular) toward the viewer. Light outside this angle is reflected back and recycled until it exits at the proper angle.

In addition, 3M BEF II is designed to prevent optical coupling with adjacent sufaces.

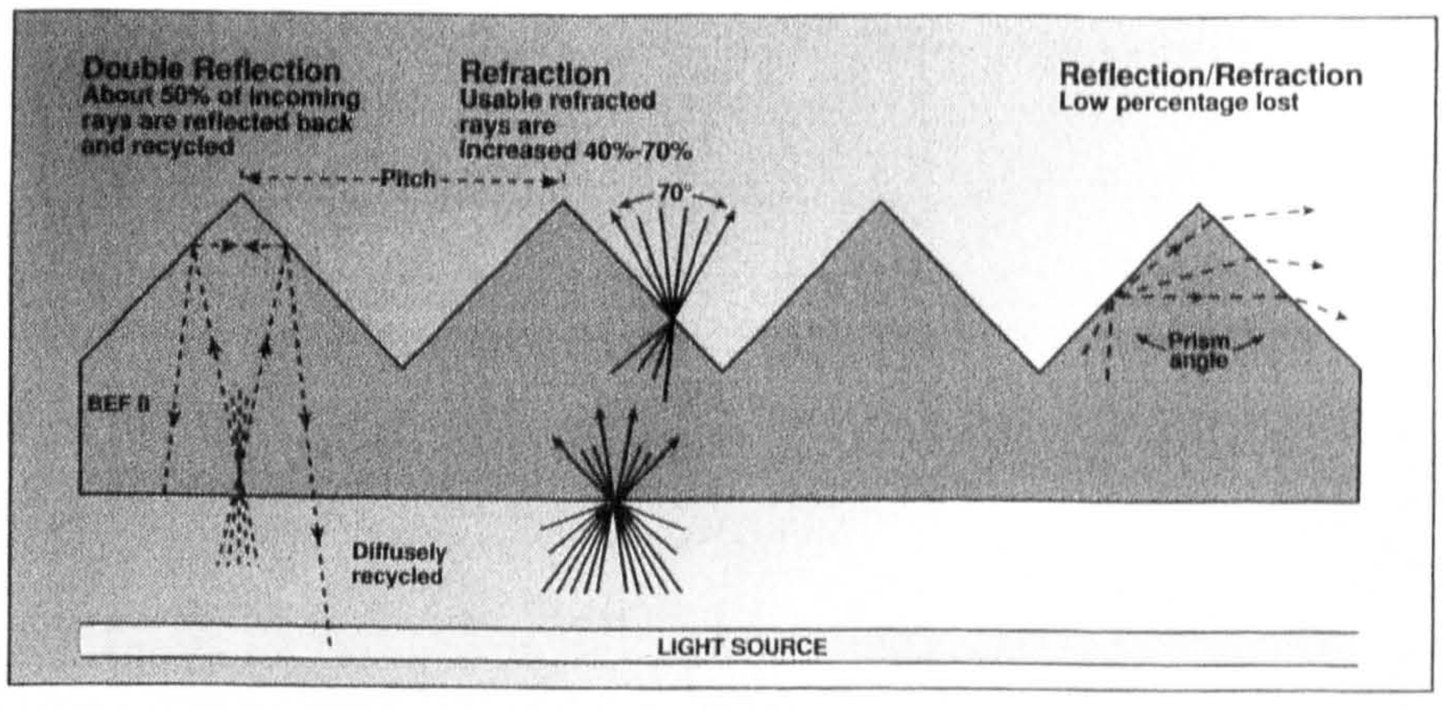

3M BEF II in a typical backlight application

A layer of 3M BEF II channels light from the backlight into a viewing cone for maximum effectiveness. Almost all of the light is emitted in this zone — toward a viewer in front of the display — instead of to the sides.

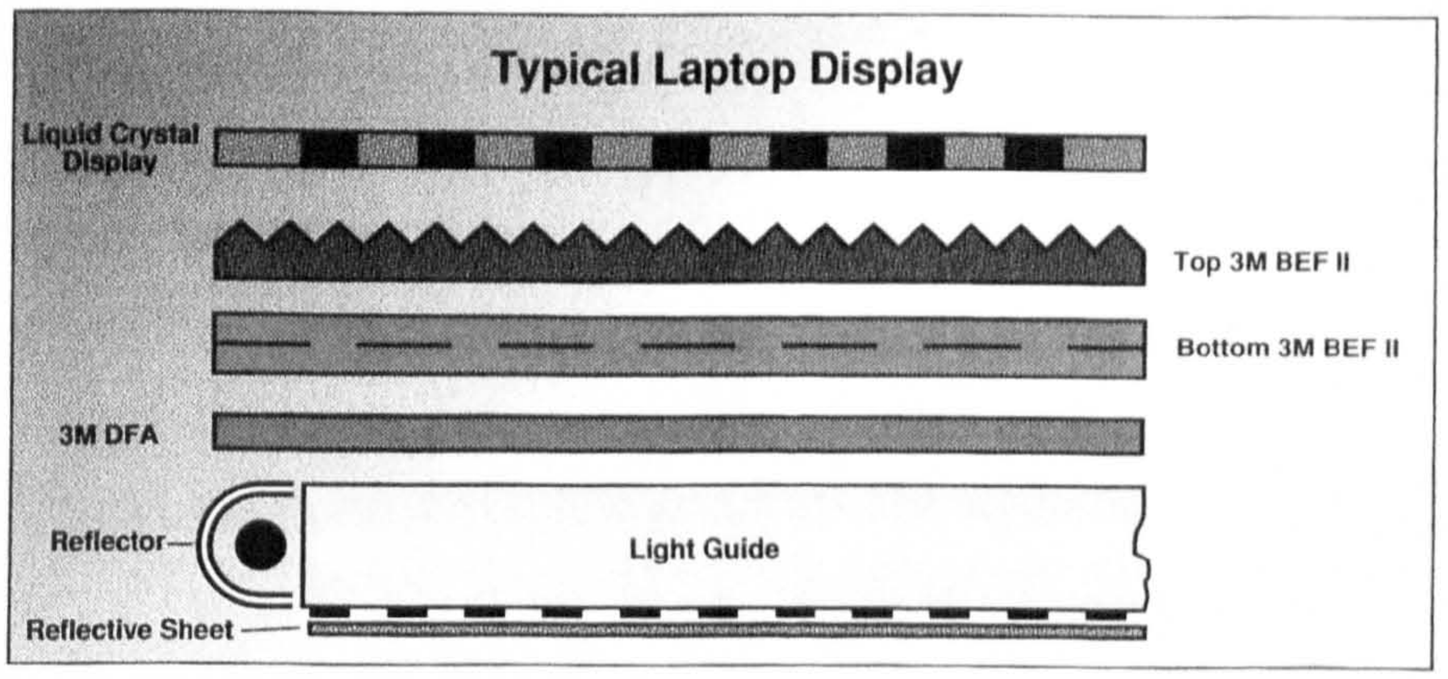

Film combination options

3M Brightness Enhancement Films can be interchanged in crossed configurations. Combining BEF II 90/50 with 90/24 provides maximum on-axis brightness while reducing moiré interference. Different film combinations provide options for power savings and viewing angle brightness.

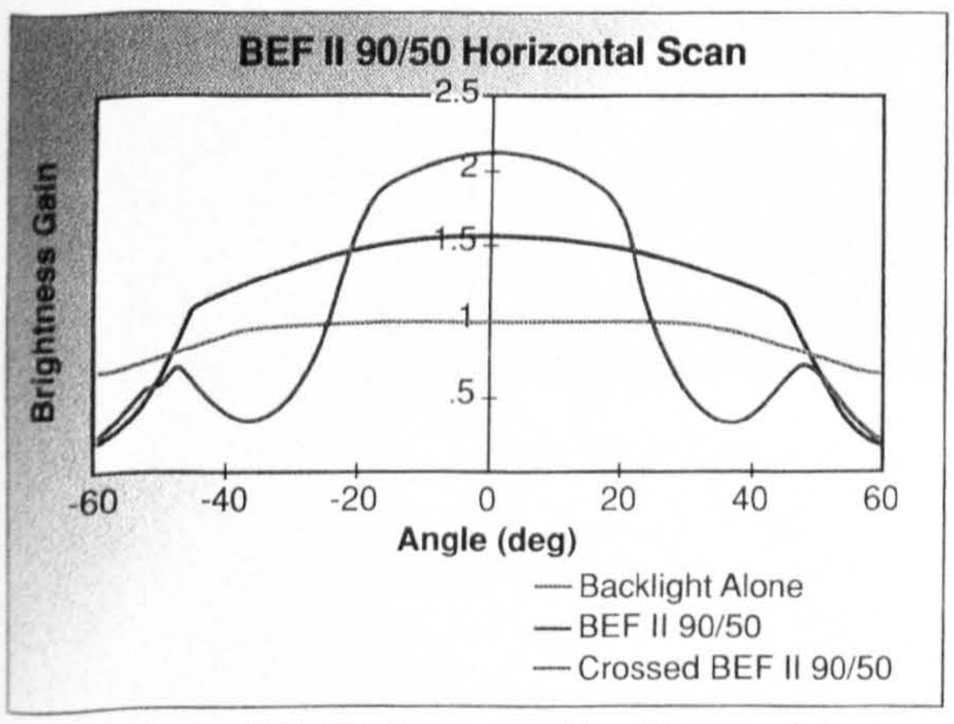

A single sheet of 3M BEF II increases the efficiency of display backlighting up to 60%. Two sheets, crossed at a 90° angle, give an increase of up to 120%.

Film Properties	BEF II 90/50	BEF II 100/31	BEF II 90/24
Repeating Microreplicated Prism			
• Prism Angle	90°	100°	90°
• Prism Pitch	50µm	31µm	24µm
• Prism Replication	99.5%	99.5%	99.5%
Brightness Enhancement* Peak Brightness Gain			
• Single Film	59%	50%	56%
• Crossed Film	116%	93%	109%
Half Brightness for Full Viewing Angle* (Top BEF II, Horizontal Prism)			
• Single Film Vertical/Horizontal	70°/98°	76°/110°	71°/101°
• Crossed Film Vertical/Horizontal	44°/47°	63°/63°	49°/51°
Material			
• Prismatic Structure	Modified Acrylic Resin	Modified Acrylic Resin	Modified Acrylic Resin
• Substrate Backing	Polyester	Polyester	Polyester
Physical Characteristics			
• Form	Film	Film	Film
• Nominal Thickness	155µm	140µm	140µm
Product Size Offering			
• Custom Sizes	Specified to Display Dimensions	Specified to Display Dimensions	Specified to Display Dimensions

*3M BEF II brightness gain depends on the backlight material composition, design and overall lighting efficiency.

The technical data for the products described are typical, based on information accumulated during their life, and are not to be used in the generation of purchase specifications which define property limits rather than typical performance.

For technical specification sheets about 3M Brightness Enhancement Film II, or for more information about other 3M™ Optical Enhancement Films, please call:

1-800-328-7098, Ext. 1

3M

Electronic Display Lighting

3M Center, Building 225-4N-14
St. Paul, MN 55144-1000

Recycled paper
40% pre-consumer
10% post-consumer

Litho in U.S.A. with 3M film, proofing systems and offset plates.

75-0500-1690-8

3M™ Transmissive Right Angle Film (TRAF) II

All the right angles to do two jobs

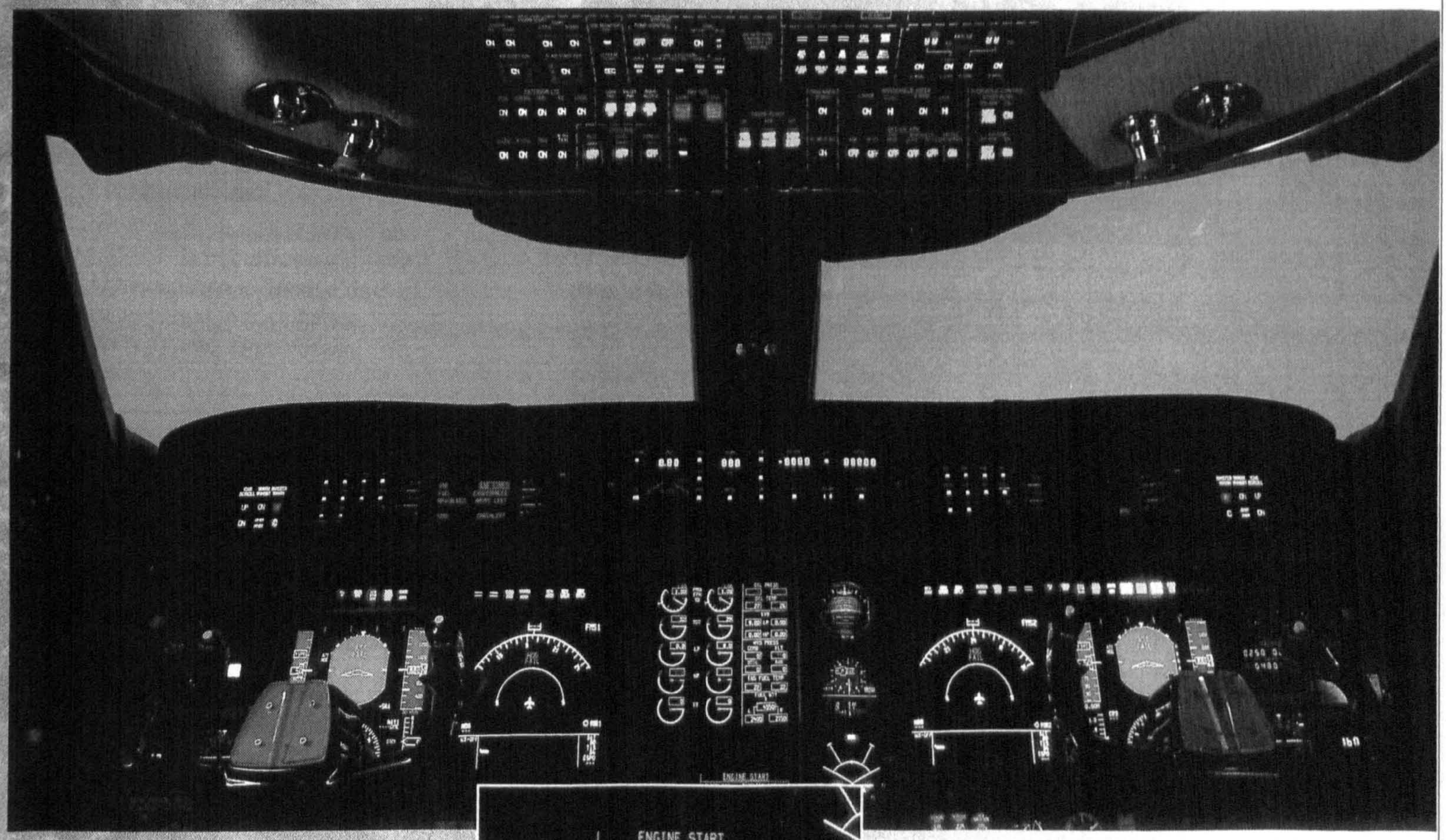

It's like two films in one

3M Transmissive Right Angle Film (TRAF) II is a dual-purpose, transparent optical composite.

In edge-lit systems, you can use it to redirect light coming in from the side back toward the on-axis viewer. While in displays with multiple or serpentine light sources, you can use 3M TRAF II as a beam splitter to create a more uniform light source. In this configuration, the prisms are directed toward the light source, where they split the incoming light rays.

Proprietary technologies

Thirty years of microreplication technologies — many of them proprietary to 3M — stand behind 3M TRAF II. These technologies, which allow for flexibility in prismatic structures, have led to the development of 3M's other optical enhancement films, such as our revolutionary 3M™ Brightness Enhancement Films.

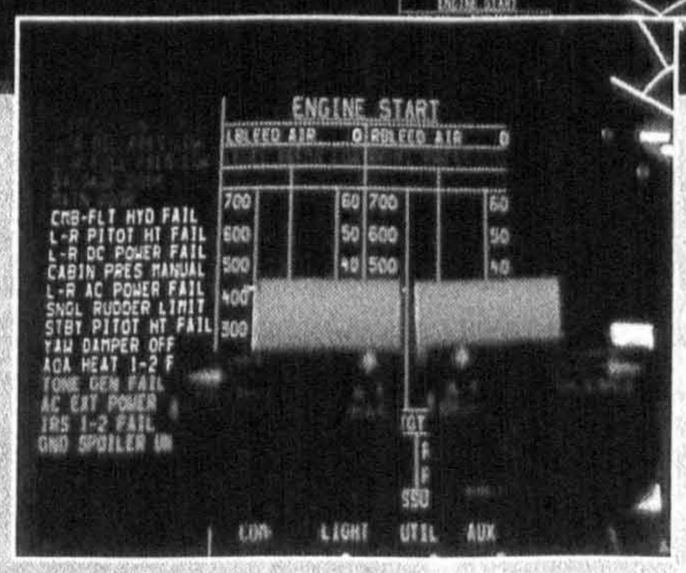

Unbeatable combinations

You can easily combine 3M TRAF II with other 3M™ Optical Enhancement Films for even more dramatic gains in display lighting efficiency. For example, you can team the film with 3M™ Diffusing Film Alternative in a beam splitter application and virtually eliminate display hot spots. Or combine it with a sheet of 3M BEF to significantly increase overall display brightness. Add two sheets of 3M BEF, crossed at 90 degrees, and you can boost screen brightness by up to 120%.

Optimum viewing angle

Easy to incorporate in any flat panel system

Incorporating 3M TRAF II into your displays is easy. It's available in precut custom sizes and requires no lamination (for greater rigidity, it can also be laminated to other surfaces). In addition, at less than 0.006″ thick, 3M TRAF II adds virtually no weight or thickness to your display.

Applications include avionics and automotive displays, instrumentation, and most edge-lit, multiple or serpentine lighting systems.

3M *Innovation*

3M™ Transmissive Right Angle Film (TRAF) II

How it works

The diagram at right illustrates how 3M TRAF II works both in an edge-lit system and as a beam splitter. In an edge-lit system, light enters the film at an angle of 0° to 20° off the horizontal and is turned at an angle of roughly 90 degrees back toward the viewer. In a multiple or serpentine lighting system, light enters the grooved side of 3M TRAF II and the beams are split into multiple rays. The result is a much more uniform light source.

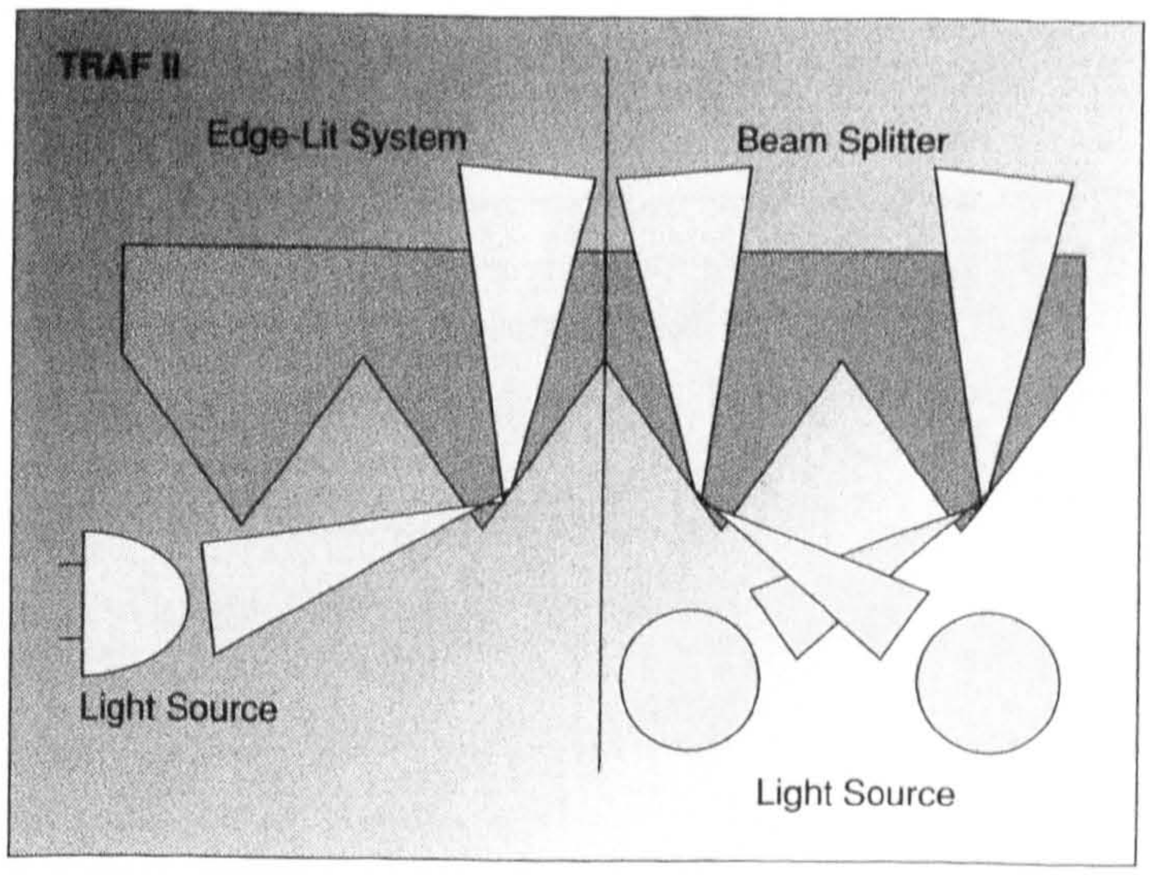

3M TRAF II in a typical avionics application

The diagrams at right illustrate how you can use 3M TRAF II in conjunction with other 3M™ Optical Enhancement Films to increase display brightness, enhance lighting uniformity and improve the angle of view.

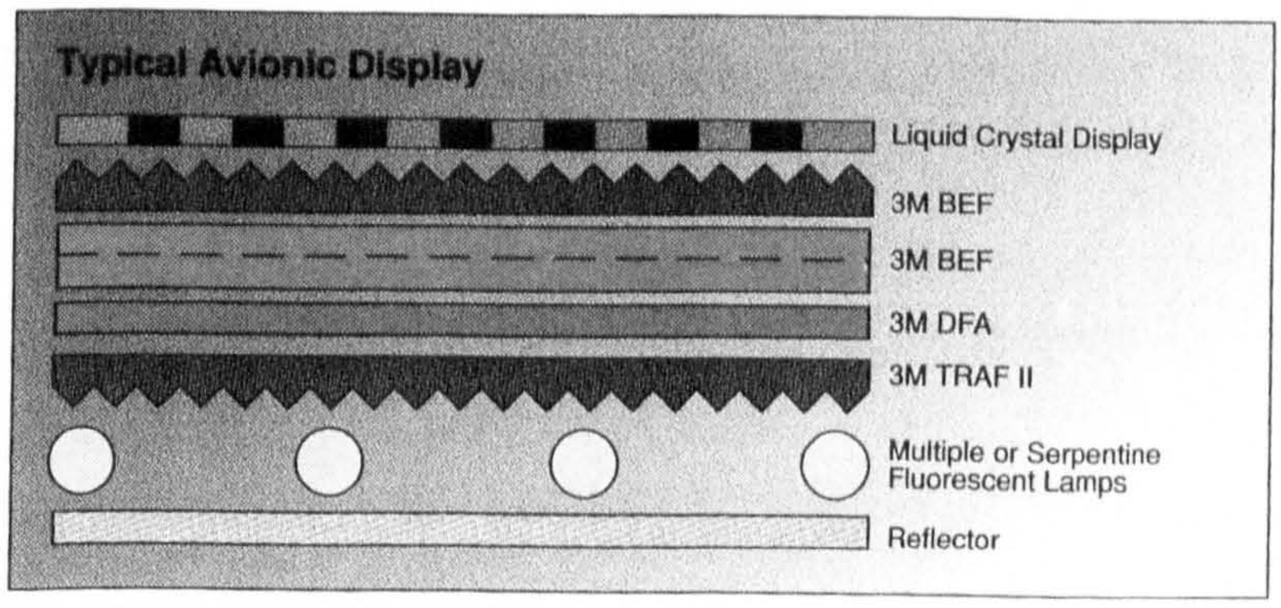

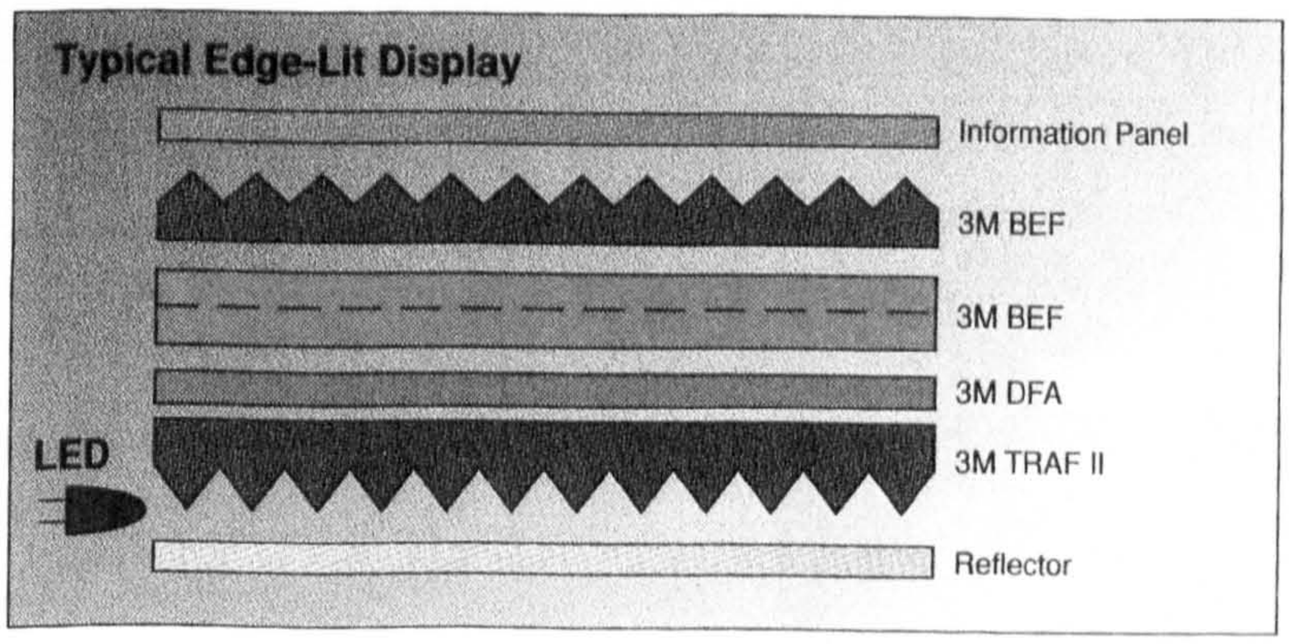

Film Properties	TRAF II
Repeating Microreplicated Prism • Prism Angle • Prism Pitch • Prism Replication	 71° 50µm 99.5%
Material • Prismatic Structure • Substrate Backing	 Modified Acrylic Resin Polyester
Acceptance Angle of Light	0° - 20°
Physical Characteristics • Form • Nominal Thickness	 Film 155µm
Product Size Offering • Custom Sizes	 Specified to Display Dimensions

The technical data for the products described are typical, based on information accumulated during their life, and are not to be used in the generation of purchase specifications which define property limits rather than typical performance.

For more information about other 3M Optical Enhancement Films, please call:

1-800-328-7098, Ext. 1

3M

Electronic Display Lighting

3M Center, Building 225-4N-14
St. Paul, MN 55144-1000

Recycled paper
40% pre-consumer
10% post-consumer

Litho in U.S.A. with 3M film, proofing systems and offset plates.

 75-0500-1689-0

3M™ Image Directing Film (IDF) II

Sending light off in the right direction

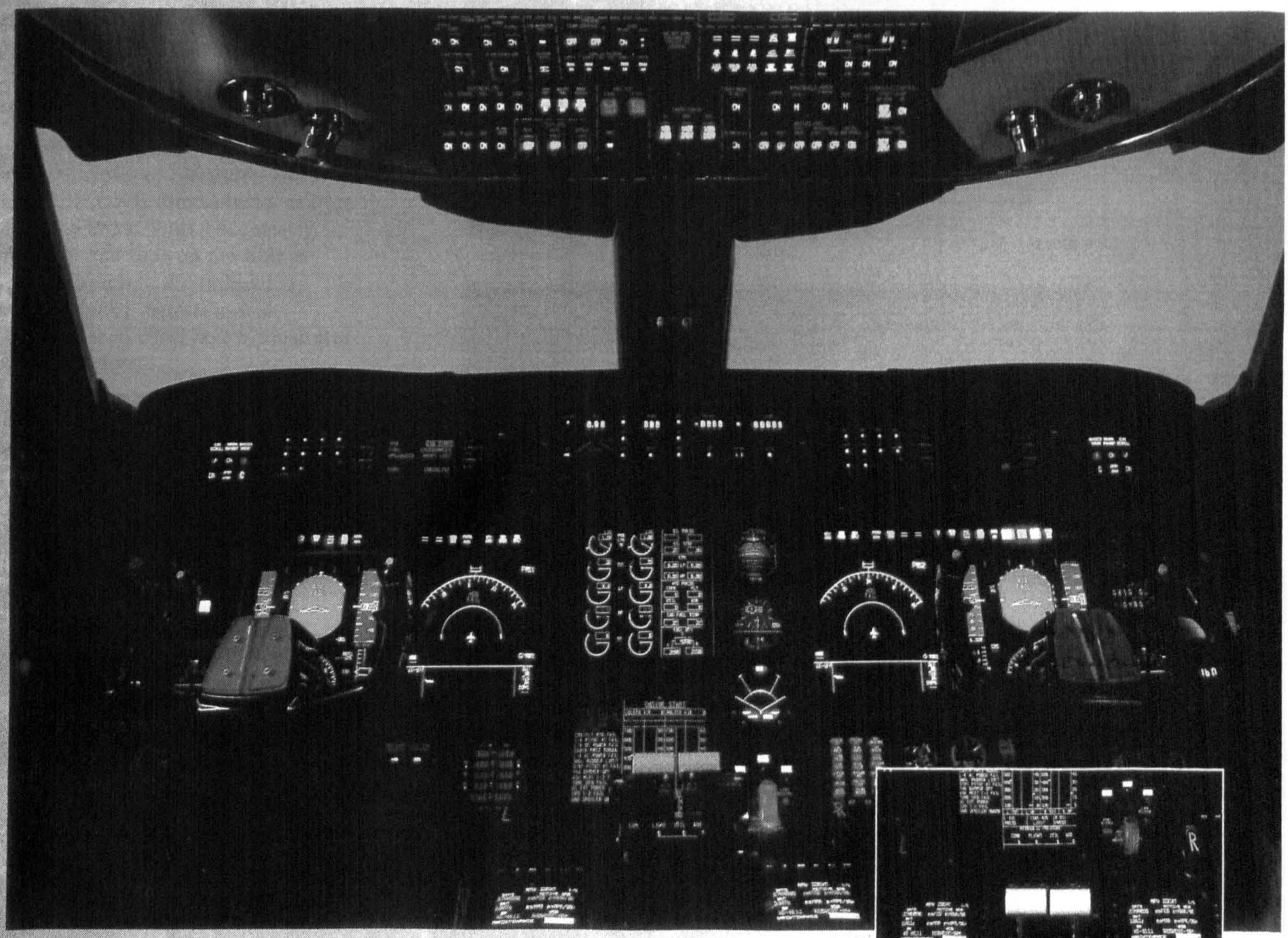

Direct your image to the viewer

For a variety of reasons, many flat panel displays do not naturally transmit their images at the best angle for the viewer. 3M Image Directing Film (IDF) II can help. A transparent optical composite, 3M IDF II takes the images created by your flat panel displays and redirects them to the optimum viewing angle.

Optimum viewing angle

Proprietary technologies

Thirty years of microreplication technologies — many of them proprietary to 3M — stand behind 3M IDF II. These technologies have led to the development of other 3M™ Optical Enhancement Films, such as our revolutionary 3M™ Brightness Enhancement Films.

Easy to use

Incorporating 3M IDF II into your displays is easy. It can be used either within the lighting system or above the display.

When used in the lighting system, 3M IDF II is simply inserted into the backlight or laminated to another material for rigidity. The film is less than 0.006″ thick and therefore adds virtually no weight or thickness to your display.

Combine and conquer

You can use 3M IDF II to direct the image on almost any flat panel display. And you can combine it with other 3M Optical Enhancement Films to boost screen brightness, improve lighting uniformity and cut power consumption, as well.

Applications include LCDs, avionics and automotive displays, instrumentation, point-of-sales devices, gaming and arcade machines, and more. The film works equally well in both production and retrofit environments.

3M *Innovation*

3M™ Image Directing Film (IDF) II

3M IDF II in a typical display application

The diagrams at right illustrate how you can use 3M IDF II in conjunction with other 3M™ Optical Enhancement Films to increase screen brightness, enhance screen uniformity and improve the angle of view.

How it works

Using the principles of refraction and reflection, 3M IDF II directs incident light at a controlled angle. And since nearly all of the light that falls on the film is transmitted through it, the redirected images are virtually distortion-free. The horizontal scan chart below illustrates how the film performs.

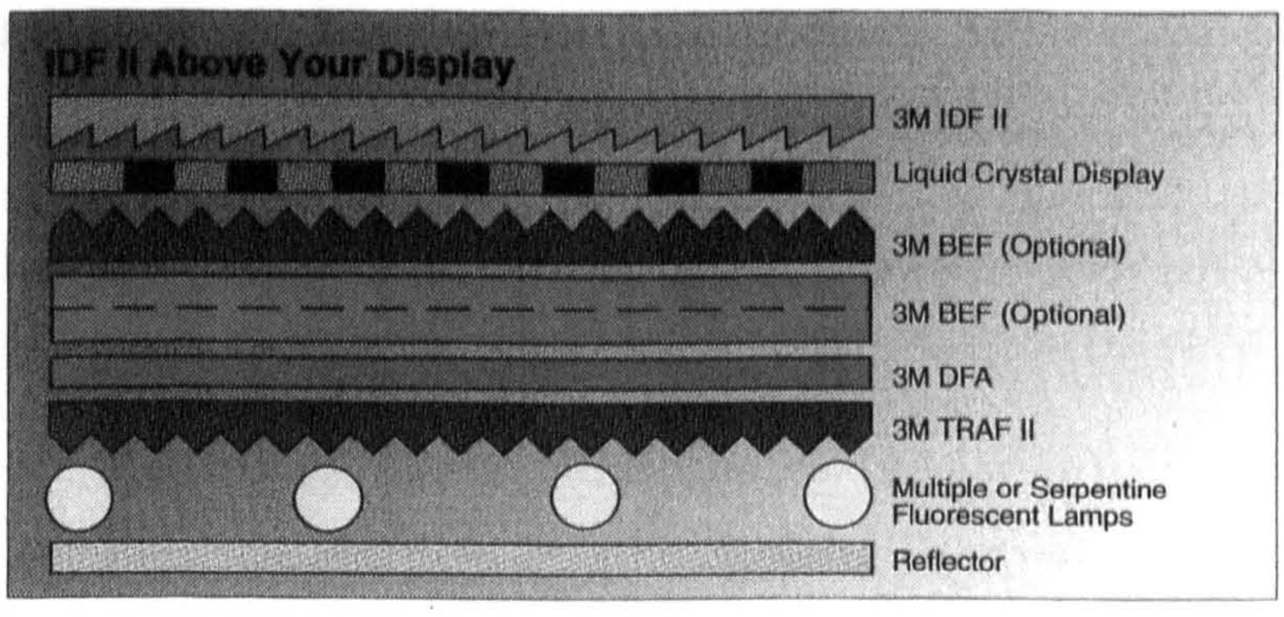

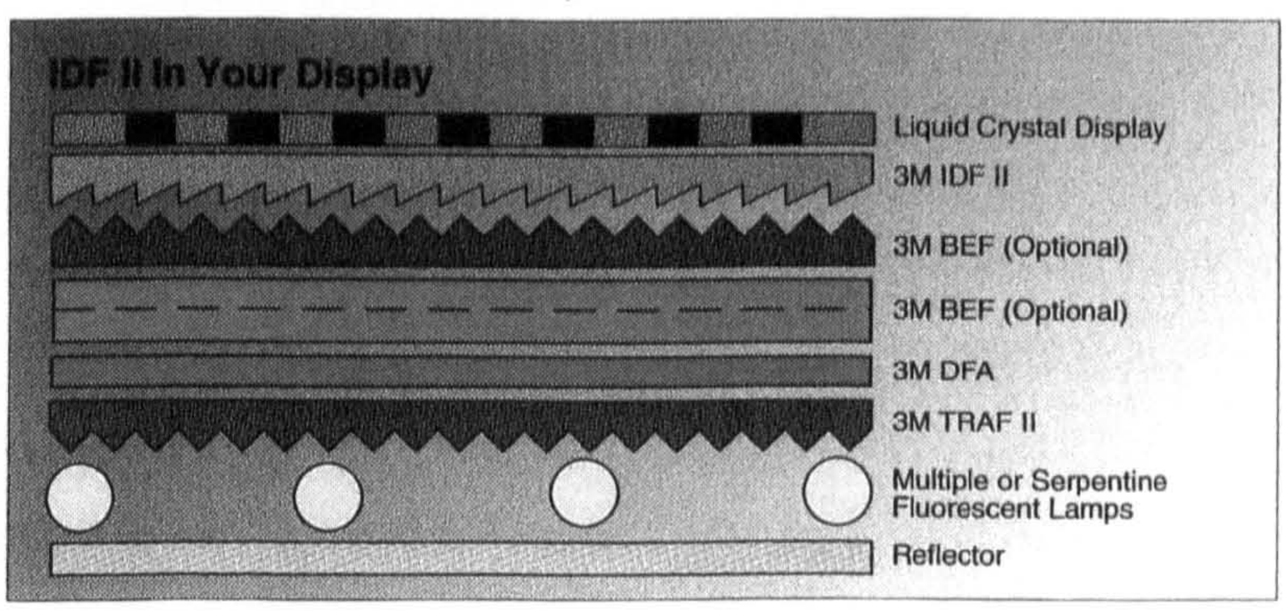

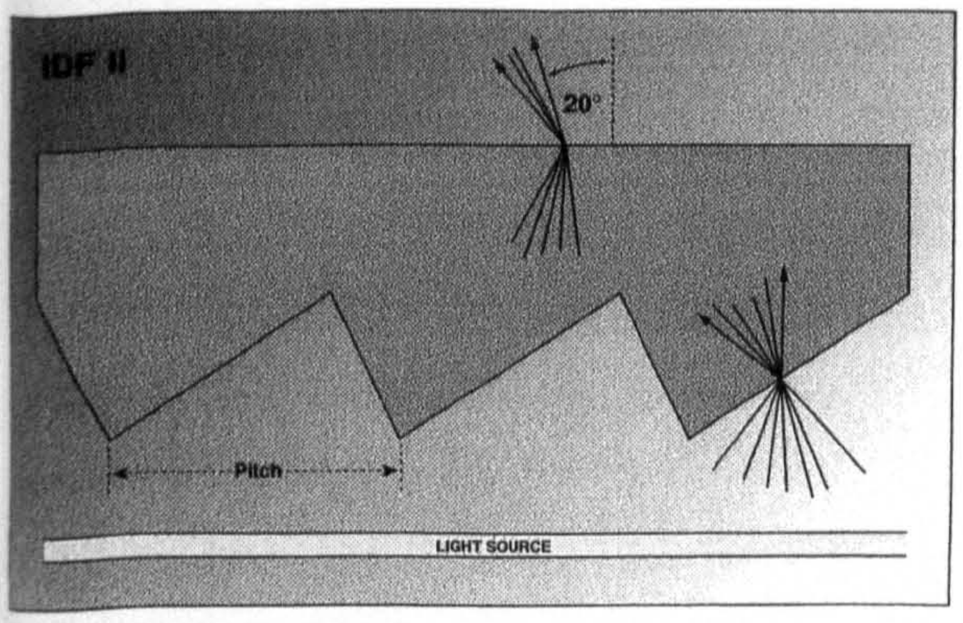

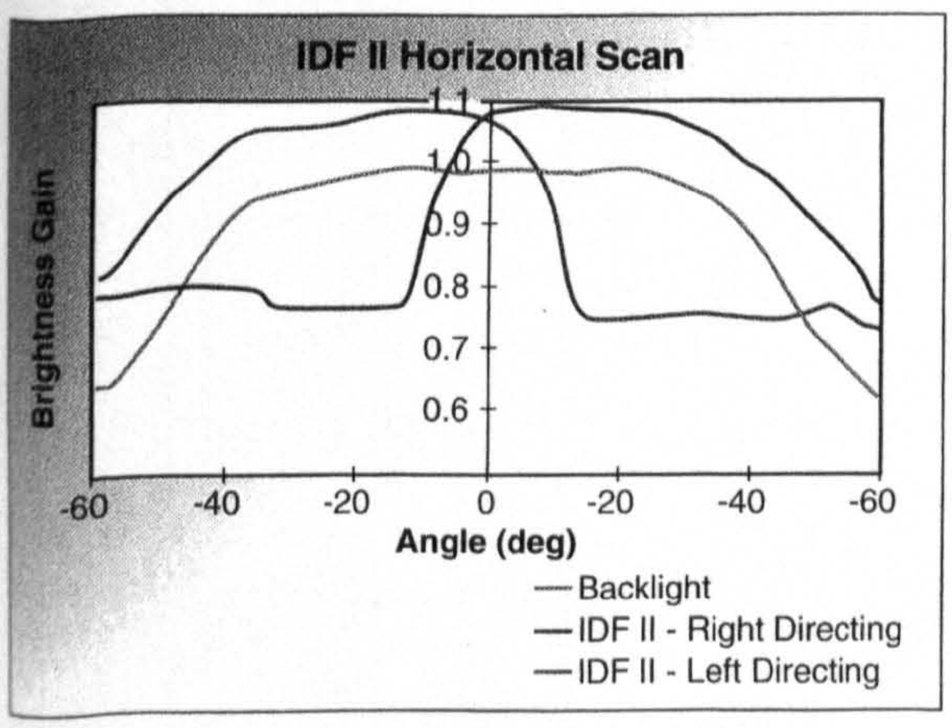

Film Properties	IDF II 20
Repeating Microreplicated Prism • Prism Pitch • Prism Replication • Deviation Angle	 50µm >99.5% 20°
Material • Prismatic Structure • Substrate Backing	 Modified Acrylic Resin Polyester
Physical Characteristics • Form • Nominal Thickness	 Film 155µm
Product Size Offering • Custom Sizes	 Specified to Display Dimensions

The technical data for the products described are typical, based on information accumulated during their life, and are not to be used in the generation of purchase specifications which define property limits rather than typical performance.

Important Notice to Purchaser

The following is made in lieu of all warranties, express or implied, including any implied warranties of merchantability or fitness for a particular purpose. 3M will replace or refund the purchase price of such quantity of the product found to be defective in materials or manufacture. 3M shall not be liable in contract or in tort for any injury, loss, or damage, whether direct, indirect, incidental, special or consequential, arising out of the use of or the inability to use the product. **The remedies set forth herein are exclusive.**

For more information about other 3M Optical Enhancement Films, please call:

1-800-328-7098, Ext. 1

3M

Electronic Display Lighting
3M Center, Building 225-4N-14
St. Paul, MN 55144-1000

40% pre-consumer
10% post-consumer

Printed in U.S.A.

 75-0500-1692-4

Appendix C

Given below is the product data obtained for the 'Llumar' thin film product.

A clear perspective on solar protection.

LLumar® WINDOW FILM

Why Window Film?

Llumar® Window Film is a microthin film composed of polyester and metallized coatings bonded by adhesives that is installed onto glass surfaces to provide significant solar protection. It screens out heat, blocks out 99% of the sun's damaging ultraviolet rays and deflects harsh, uncomfortable glare while allowing glare-controlled sunlight to pass through. Llumar adapts to the changes in the seasons, reflecting the hot sun in the summer, and with Low E films to reradiate heat in the winter, you can be comfortable all year long.

Llumar is so ruggedly constructed that it resists scratching and is backed by the best warranty in the industry.

Use our E Mail for more information or call us at 1-800-2-LLUMAR.

Take the Llumar Bright Test and see if you need LLumar Window Film

Residential Applications

LLumar WINDOW FILM

Llumar® Window Film.
The clear answer to lasting beauty for your home.

Fade protection from the sun.
Over time, the rays of the sun fade whatever is in their path. But professionally installed Llumar Window Film blocks out 99% of the damaging ultraviolet rays that ordinary windows allow in. That means that draperies, wood furniture, upholstery and carpeting will last longer.

Keep temperature and glare under control.
Llumar Window Film reflects the hot sun in the summer and keeps you comfortable all year round. Plus, Llumar deflects annoying glare while reading or watching television.

A durable, scratch-resistant coating.
Llumar comes with the industry's toughest and most durable surface: the patented SR coating. This hard surface can be cleaned with most everyday household window cleaners as well.

Designer shades.
Available in a beautiful palette of designer shades, Llumar offers a range of tints to coordinate with any room, including neutral.

A protective barrier.
Ordinary glass will break and splinter, but having Llumar on your windows can reduce the likelihood of injury because Llumar helps hold fragments of shattered glass in place.

Commerical Applications

LLumar® WINDOW FILM

Llumar® Window Film. The clear answer for business.

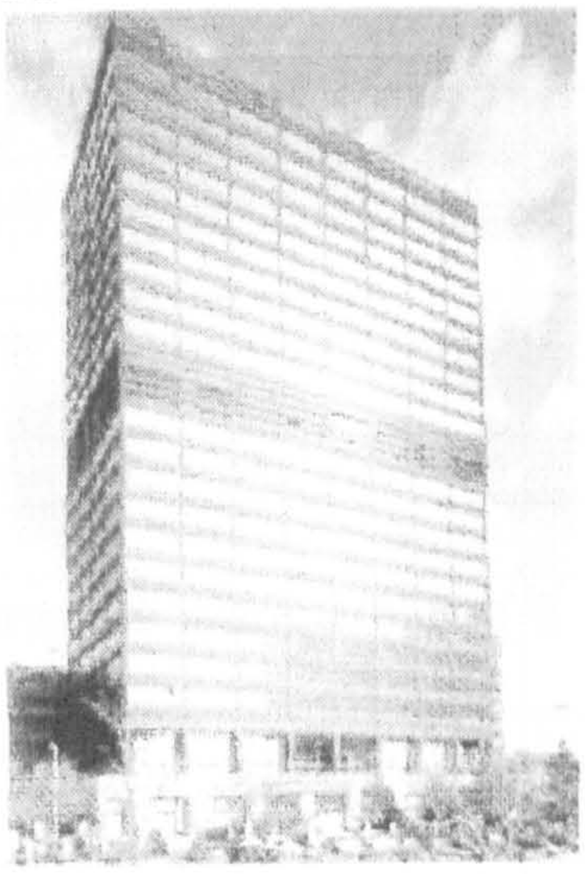

Today's buildings utilize more glass than ever before. The trend toward open floor plans, high ceilings and extensive use of glass has become the preferred standard. But glass windows are notorious energy wasters, making building owners and managers increasingly concerned about excessive glare, heat build-up and higher energy costs.

Llumar provides comfort. Reduces glare.

Llumar is a retrofit product installed directly to the interior side of the glass. It helps correct temperature imbalances between sunny and shady areas and it deflects harsh, uncomfortable glare reducing eye strain that is common while doing paperwork or viewing computer screens. Employees are more comfortable and more productive!

Llumar saves energy. Protects furnishings.

Llumar can reject up to 79% of the incoming solar energy, cutting power bills. And, with 99% ultraviolet rejection, fading of interiors will be reduced and furnishings will last longer...a small investment to protect your big investments!

Llumar beautifies windows. With easy maintenance.

From the inside, Llumar has a pleasant, glare and distortion-free view and from the outside it has a uniform appearance that complements the building's design. And, Llumar is available in a range of designer shades, including neutral. Llumar's patented, scratch-resistant (SR) coating resists scratches, keeping the film looking as new as the day it was installed assuring carefree maintenance with most conventional methods of window cleaning.

A warranty that lasts.

Appendix D: Results of Questionnaire

Time 9:00 am, Sky: Clear Completed Questionnaires: 3

	Questionnaires				
	1	2	3	Average	SD
Switch the lights on? (Yes=1 No=2)	2	2	2	2	0
Pull the blinds? (Yes=1 No=2)	2	2	2	2	0
Room is evenly lit?	2	2	2	2	0
Room front is too dark?	5	5	5	5	0
Room front is too bright?	5	5	5	5	0
Room back is too dark?	5	4	3	4	1
Room back is too bright?	5	5	4	4.7	0.6
Prism window source of glare? (Yes=1 No=2)	2	2	2	2	0
Glare rating (Very Strong=1, Very Weak=5)					
Normal window source of glare? (Yes=1 No=2)	2	2	2	2	0
Glare rating (Very Strong=1, Very Weak=5)					
First text (Strongly agree=1, Strongly disagree=5)					
Easy to read words?	2	1	2	1.7	0.6
Strain eyes?	5	5	4	4.7	0.6
Turn on light	5	5	5	5	0
Second text (Strongly agree=1, Strongly disagree=5)					
Easy to read words?	1	1	1	1	1
Strain eyes?	5	5	5	5	0
Turn on light	5	5	4	4.7	0.6
Third text (Strongly agree=1, Strongly disagree=5)					
Easy to read words?	1	1	1	1	1
Strain eyes?	5	5	5	5	0
Turn on light	5	5	5	5	0

Time 9:00 am, Sky: Broken Cloud Completed Questionnaires: 9

	Questionnaires										
	1	2	3	4	5	6	7	8	9	Average	SD
Switch the lights on? (Yes=1 No=2)	1	2	2	2	2	2	2	2	2	1.9	0.3
Pull the blinds? (Yes=1 No=2)	2	2	2	2	2	2	2	2	2	2.0	0
Room is evenly lit?	4	2	2	2	2	2	3	2	4	2.6	0.9
Room front is too dark?	4	5	5	5	5	3	5	4	5	4.6	0.7
Room front is too bright?	2	5	5	5	5	3	5	3	5	4.2	1.2
Room back is too dark?	2	5	5	5	5	3	5	4	4	4.2	1.1
Room back is too bright?	4	5	5	5	5	3	5	4	5	4.6	0.7
Prism window source of glare? (Yes=1 No=2)	2	2	2	2	2	2	2	2	2	2	0
Glare rating (Very Strong=1, Very Weak=5)											
Normal window source of glare? (Yes=1 No=2)	2	2	2	2	2	2	2	2	2	2	0
Glare rating (Very Strong=1, Very Weak=5)											
First text (Strongly agree=1, Strongly disagree=5)											
Easy to read words?	3	1	1	1	1	1	2	1	2	1.4	0.7
Strain eyes?	5	5	5	5	5	5	4	5	4	4.8	0.4
Turn on light	2	5	5	5	5	5	5	5	5	4.7	1.0
Second text (Strongly agree=1, Strongly disagree=5)											
Easy to read words?	2	1	1	1	1	1	1	1	2	1.2	0.4
Strain eyes?	3	5	5	5	5	5	5	5	4	4.7	0.7
Turn on light	3	5	5	5	5	5	5	5	2	4.4	1.1
Third text (Strongly agree=1, Strongly disagree=5)											
Easy to read words?	1	1	1	1	1	1	1	1	2	1.1	0.3
Strain eyes?	4	5	5	5	5	5	5	5	5	4.9	0.3
Turn on light	4	5	5	5	5	5	5	5	3	4.7	0.7

Time: 1.00pm, Sky: Clear, Completed Questionnaires: 6

	Questionnaire							
	1	2	3	4	5	6	Average	SD
Switch the lights on? (Yes=1 No=2)	1	2	2	2	2	2	1.8	0.4
Pull the blinds? (Yes=1 No=2)	2	1	2	1	1	1	1.3	0.5
Room is evenly lit?	2	2	2	3	3	3	2.5	0.6
Room front is too dark?	3	5	4	5	5	5	4.5	0.84
Room front is too bright?	3	5	3	5	4	4	4.0	0.9
Room back is too dark?	3	5	4	5	4	5	4.3	0.8
Room back is too bright?	3	5	3	5	4	3	3.8	1.0
Prism window source of glare? (Yes=1 No=2)	2	1	1	1	1	1	1.2	0.4
Glare rating (Very Strong=1, Very Weak=5)		1	1	1	2	1	1.2	0.5
Normal window source of glare? (Yes=1 No=2)	2	2	2	2	2	2	2.0	0
Glare rating (Very Strong=1, Very Weak=5)								
First text (Strongly agree=1, Strongly disagree=5)								
Easy to read words?	3	1	1	1	1	1	1.3	0.8
Strain eyes?	3	5	5	5	5	5	4.7	0.8
Turn on light	2	5	4	5	5	5	4.3	1.2
Second text (Strongly agree=1, Strongly disagree=5)								
Easy to read words?	3	1	2	1	1	1	1.5	0.8
Strain eyes?	3	5	4	5	5	5	4.5	0.8
Turn on light	2	5	2	5	5	5	4.0	1.6
Third text (Strongly agree=1, Strongly disagree=5)								
Easy to read words?	2	1	2	1	1	1	1.3	0.5
Strain eyes?	4	5	4	5	5	5	4.7	0.5
Turn on light	3	5	3	5	5	5	4.3	1.0

Time: 1.00pm, Sky: Broken Cloud, Completed Questionnaires: 10

	Questionnaire											
	1	2	3	4	5	6	7	8	9	10	Av.	SD
Switch the lights on? (Yes=1 No=2)	2	1	2	2	2	2	2	2	1	2	1.8	0.4
Pull the blinds? (Yes=1 No=2)	2	2	2	1	1	2	1	1	2	2	1.6	0.5
Room is evenly lit?	1	4	2	2	2	2	4	2	4	2	2.5	1.1
Room front is too dark?	5	2	5	5	5	5	5	5	5	5	4.7	1.0
Room front is too bright?	3	5	5	5	4	5	4	5	4	5	4.5	0.7
Room back is too dark?	5	2	5	5	5	5	5	2	2	4	4	1.4
Room back is too bright?	3	5	5	5	5	5	4	4	5	4	4.5	0.7
Prism window source of glare? (Yes=1 No=2)	1	2	2	1	1	1	1	1	2	1	1.3	0.5
Glare rating (Very Strong=1, Very Weak=5)	5	0	0	2	1	4	1	4	0	4	2.3	1.9
Normal window source of glare? (Yes=1 No=2)	2	2	2	2	2	2	2	2	2	2	2	0.0
Glare rating (Very Strong=1, Very Weak=5)												
First text (Strongly agree=1, Strongly disagree=5)												
Easy to read words?	1	2	1	1	1	1	1	1	4	1	1.4	1.0
Strain eyes?	5	3	5	5	5	5	5	5	3	5	4.6	0.8
Turn on light	5	2	5	5	5	5	5	5	2	5	4.4	1.3
Second text (Strongly agree=1, Strongly disagree=5)												
Easy to read words?	1	2	1	1	1	1	1	1	4	1	1.4	1.0
Strain eyes?	5	4	5	5	5	5	5	5	3	5	4.7	0.7
Turn on light	5	3	5	5	5	5	5	5	2	5	4.5	1.1
Third text (Strongly agree=1, Strongly disagree=5)												
Easy to read words?	1	2	1	1	1	1	1	1	2	1	1.2	0.4
Strain eyes?	5	4	5	5	5	5	5	5	4	5	4.8	0.4
Turn on light	5	4	5	5	5	5	5	5	3	5	4.7	0.7

Time 1.00 p.m., Sky: Overcast, Completed Questionnaires: 7

	Questionnaire								
	1	2	3	4	5	6	7	Average	SD
Switch the lights on? (Yes=1 No=2)	1	1	1	1	1	1	1	1	0
Pull the blinds? (Yes=1 No=2)	2	2	2	2	2	2	2	2	0
Room is evenly lit?	5	3	4	3	3	4	5	3.9	0.9
Room front is too dark?	5	3	4	4	5	3	5	4.1	0.9
Room front is too bright?	5	5	4	1	2	5	3	3.6	1.6
Room back is too dark?	2	2	2	2	4	2	1	2.1	0.9
Room back is too bright?	5	5	5	5	4	5	5	4.9	0.4
Prism window source of glare? (Yes=1 No=2)	2	2	2	2	1	2	2	1.9	0.4
Glare rating (Very Strong=1, Very Weak=5)		0	0		5			1.7	2.9
Normal window source of glare? (Yes=1 No=2)	2	2	2	2	1	2	2	1.9	0.4
Glare rating (Very Strong=1, Very Weak=5)					3				
First text (Strongly agree=1, Strongly disagree=5)									
Easy to read words?	1	1	2	1	1	2	1	1.3	0.5
Strain eyes?	5	4	4	4	4	3	4	4.0	0.6
Turn on light	1	3	3	3	2	2	4	2.6	1.0
Second text (Strongly agree=1, Strongly disagree=5)									
Easy to read words?	1	2	1	1	2	2	1	1.4	0.5
Strain eyes?	5	5	5	4	2	4	3	4.0	1.2
Turn on light	2	3	3	3	1	2	4	2.6	1.0
Third text (Strongly agree=1, Strongly disagree=5)									
Easy to read words?	1	1	1	1	1	1	1	1	0
Strain eyes?	5	5	5	5	5	5	4	4.9	0.4
Turn on light	1	5	5	5	5	1	5	4.3	1.5

Time 4.00 p.m., Sky: Clear, Completed Questionnaires: 4

	Questionnaire					
	1	2	3	4	Average	SD
Switch the lights on? (Yes=1 No=2)	1	2	2	2	1.8	0.5
Pull the blinds? (Yes=1 No=2)	2	2	1	2	1.8	0.5
Room is evenly lit?	2	3	2	3	2.5	0.6
Room front is too dark?	3	5	5	4	4.3	1.0
Room front is too bright?	3	4	5	4	4	0.8
Room back is too dark?	3	3	5	2	3.3	1.3
Room back is too bright?	3	3	5	5	4	1.2
Prism window source of glare? (Yes=1 No=2)	2	2	2	2	2	0
Glare rating (Very Strong=1, Very Weak=5)						
Normal window source of glare? (Yes=1 No=2)	2	2	2	2	2	0
Glare rating (Very Strong=1, Very Weak=5)						
First text (Strongly agree=1, Strongly disagree=5)						
Easy to read words?	3	2	1	2	2	0.8
Strain eyes?	3	5	5	5	4.5	1
Turn on light	2	4	5	4	3.8	1.3
Second text (Strongly agree=1, Strongly disagree=5)						
Easy to read words?	3	1	1	1	1.5	1
Strain eyes?	3	5	5	5	4.5	1
Turn on light	2	5	5	5	4.3	1.5
Third text (Strongly agree=1, Strongly disagree=5)						
Easy to read words?	2	1	1	1	1.3	0.5
Strain eyes?	4	5	5	5	4.8	0.5
Turn on light	3	5	5	5	4.5	1

Time: 4.00 p.m., Sky: Broken Cloud, Completed Questionnaires: 5

	Questionnaire						
	1	2	3	4	5	Average	SD
Switch the lights on? (Yes=1 No=2)	2	2	2	2	2	2	0
Pull the blinds? (Yes=1 No=2)	2	2	2	2	2	2	0
Room is evenly lit?	2	2	2	2	2	2	0
Room front is too dark?	4	5	5	5	4	4.6	0.5
Room front is too bright?	5	5	5	4	5	4.8	0.4
Room back is too dark?	5	4	5	3	4	4.2	0.8
Room back is too bright?	5	5	5	5	4	4.8	0.4
Prism window source of glare? (Yes=1 No=2)	2	2	2	1	2	1.8	0.4
Glare rating (Very Strong=1, Very Weak=5)				5			
Normal window source of glare? (Yes=1 No=2)	2	2	2	2	2	2	0
Glare rating (Very Strong=1, Very Weak=5)							
First text (Strongly agree=1, Strongly disagree=5)							
Easy to read words?	1	2	1	2	1	1.4	0.5
Strain eyes?	5	5	5	5	5	5	0
Turn on light	5	3	5	2	4	3.8	1.3
Second text (Strongly agree=1, Strongly disagree=5)							
Easy to read words?	1	1	1	1	1	1	0
Strain eyes?	5	5	5	5	5	5	0
Turn on light	5	5	5	5	5	5	0
Third text (Strongly agree=1, Strongly disagree=5)							
Easy to read words?	1	1	1	1	1	1	0
Strain eyes?	5	5	5	5	5	5	0
Turn on light	5	5	5	5	5	5	0

Time: 4.00 p.m., Sky: Overcast, Completed Questionnaires: 7

	Questionnaire								
	1	2	3	4	5	6	7	Average	SD
Switch the lights on? (Yes=1 No=2)	1	2	1	1	1	1	1	1.1	0.4
Pull the blinds? (Yes=1 No=2)	2	2	2	2	2	2	2	2	0
Room is evenly lit?	5	3	4	3	5	4	4	4	0.8
Room front is too dark?	5	4	5	1	1	2	3	3	1.7
Room front is too bright?	1	5	5	5	5	4	5	4.3	1.5
Room back is too dark?	1	4	2	1	1	2	1	1.7	1.1
Room back is too bright?	5	5	5	5	5	4	5	4.9	0.4
Prism window source of glare? (Yes=1 No=2)	2	2	2	2	2	2	2	2	0
Glare rating (Very Strong=1, Very Weak=5)									
Normal window source of glare? (Yes=1 No=2)	2	2	2	2	2	1	2	1.9	0.4
Glare rating (Very Strong=1, Very Weak=5)						3			
First text (Strongly agree=1, Strongly disagree=5)									
Easy to read words?	2	1	1	2	2	2	4	2	1
Strain eyes?	3	5	5	4	4	2	4	3.9	1.1
Turn on light	1	4	1	1	4	2	1	2	1.4
Second text (Strongly agree=1, Strongly disagree=5)									
Easy to read words?	3	1	1	2	2	2	4	2.1	1.1
Strain eyes?	2	5	5	4	4	3	2	3.6	1.3
Turn on light	1	5	1	2	5	2	1	2.4	1.8
Third text (Strongly agree=1, Strongly disagree=5)									
Easy to read words?	3	1	1	1	1	2	4	1.9	1.2
Strain eyes?	2	5	5	4	3	3	2	3.4	1.3
Turn on light	1	5	3	3	5	2	1	2.9	1.7

Comparison of lighting conditions, with and without prisms. Completed questionnaires: 4

	Questionnaire									
	1			2			3			4	
	prisms	no prisms		prisms	no prisms		prisms	no prisms		prisms	no prisms
Yes=1 No=2											
Switch the lights on?	1	1		2	1		2	2		1	1
Pull the blinds?	2	2		2	2		2	2		2	2
Room is evenly lit?	4	5		2	5		2	4		4	5
Room front is too dark?	5	4		5	4		5	5		5	5
Room front is too bright?	5	5		5	5		2	2		5	5
Room back is too dark?	2	1		2	1		3	2		2	2
Room back is too bright?	5	5		2	5		4	5		5	5
Prism window source of glare?	2	2		2	2		2	2		2	2
Glare rating											
Normal window source of glare?	2	2		2	1		2	2		2	2
Glare rating					3						
First text											
Easy to read words?	1	2		2	3		1	2		1	1
Strain eyes?	5	4		4	2		5	5		5	5
Turn on light	2	1		4	1		4	4		1	1
Second text											
Easy to read words?	1	2		1	1		1	1		1	1
Strain eyes?	5	4		5	5		5	5		5	5
Turn on light	2	1		5	4		5	5		2	2
Third text											
Easy to read words?	1	1		1	1		1	1		1	1
Strain eyes?	5	5		5	5		5	5		5	5
Turn on light	3	3		5	5		5	5		4	1

Acknowledgements

Thanks must go to the following people:

- *Mum and Dad for all their love and support throughout the 4 years.*
- *My sister for constructing a fantastic turkey costume and tremendous set flares for me, and her soon-to-be husband (Adam) for assisting in their fitting.*
- *'Los noberos', Senora Moreno and Herr Hembd. The former for consistently wupping me at tennis, and the latter for showing me dried mangos and the application of ruthless German efficiency.*
- *My unofficial supervisors Dr Richard Stevens and Prof Mike Downs who have taken the time and trouble to read over my thesis.*
- *Nick Turner for his assistance as a section head and as a good friend.*
- *Ian Garbutt and Rob Ferguson for preventing me from accidentally killing myself in the workshop.*
- *All the other inmates of Building 45 who have helped me, many of which have escaped and now run-free. These include: John Nunn, Bob Ward, Gordon Rodgers, Anne Kierney, John Baines, Mike McCarthy, Dave Putland, Lurch, Andy Parker and Dan Daly.*

In addition to working at NPL I have also been fortunate enough to spend time at the Fraunhofer Institute in Freiburg and the ENTPE in Lyon. Therefore the following people also deserve a mention:

- *Andreas Gombert for providing assistance in the lab and getting me appallingly drunk outside of it. His ability to consume vast amounts of alcohol without any noticeable after effects is an exceptional talent.*
- *Richard Mitanchey, Pierre Laforgue at the ENTPE. Not only for their help in getting results but also for their good humour and strong cheeses.*

Finally, I would like to thank Prof. Miles Padgett for his invaluable assistance in completing the corrections after the viva examination.